Indian Institute of Chemical Engineers

IIChE-CHEMCON 2023

LECTURE NOTES ON ENERGY TRANSITION: CHALLENGES AND OPPORTUNITIES

Editors:

Dr. Avijit Ghosh
Prof. Sunil Baran Kuila
Prof. Madhu Agarwal
Prof. N. Balasubramanian

Book Chapter

ISBN: 978-93-100-0071-9

LIST OF CHAPTERS

15	Title: Nuclear Waste Management Authors: Gagana M B
16	Title: Screening of Symbiotic Bacteria for Biodiesel Production in Algae Growth Authors: Chelladurai Chellamboli, Raguraman Dhinesh Kanna, Muthiah Perumalsamy
17	Title: Advanced Energy Storage Solutions: Innovative Approaches to Microencapsulation of Phase Change Materials Authors: Naveen Jose, Menon Rekha Ravindra, Deb Prasad Ray
18	Title: Hydrogen Geo-storage - A Review on Storage and Recovery from Carbonate Reservoirs Authors: Vishnu Chandrasekharan Nair, Anooja Sara Mathew
19	Title: Machine Learning-Guided Optimization of Biofuel Blends for Enhanced Engine Efficiency and Emission Reduction Authors: Sandip Kumar Lahiri, Prithwish Das, Aniket Biswas, Srijan Sardar, Bitopama Modak, Fahim Ahmed, Ananya Pal
20	Title: Photocatalytic Performance of Aluminum-Doped Graphene-like ZnO (g-AZO) Monolayer Authors: Divya Somvanshi, Sayantika Chowdhury
21	Title: Characterization and Adsorption Performance Evaluation of Waste Char Authors: Aparna Ray Sarkar, Arka Sanyal, Manoj Kumar Sonthalia, Abhijit Kundu
22	Title: Preparation, Characterization and Application of Mixed Clay Based Low Cost Ceramic Membrane in Treatment of Oil-in-Water Emulsions Authors: Kanchapogu Suresh, Amish Gour, Mukesh Kumar Yadav, Vidhi Jani
23	Title: Synthesis, Characterization and Degradation of Boron, Cerium and Silver Ternary Doped Titanium Dioxide Photocatalyst via EDTA Citrate Method using Ampicillin Antibiotic under Sunlight Authors: Yash Mishra, Dr. Hari Mahalingam
24	Title: Intelligent Techniques for Wastewater Treatment: A Technical Review Authors: Swati Sharma, Mita K. Dalal
25	Title: How Does Climate Change Impact Water Sources, Affecting Quality and Availability, and What Are the Resulting Consequences for Water Treatment and Infrastructure? Authors: Rajarshi Ray, Rupam Khowash, Bidripta Mondal, Saswata Saha
26	Title: Optimization of Novel Symbiotic Bacteria in Algae Growth Authors: Chelladurai Chellamboli, Muthiah Perumalsamy, Udayar Kabil Dev
27	Title: Effects of Indoor Plants on Occupants' Perceptions of Indoor Climate, Sick Building Syndrome (SBS), Emotional State, Self-Assessed Performance, and Overall Space Satisfaction: A Systematic Review Authors: Mukesh Budaniya, Mani Sankar Dasgupta
28	Title: Replacement of Coal by RDF (Refused Derived Fuel) Authors: Sunil Baran Kuila, Soumyadip Das, Ritu Thakur, Subrata Dasgupta, Sankalan Das, Biswajit Mandal

https://doi.org/10.36375/prepare_u.iiche.a384

Emerging Techniques of Carbon Capture and Storage (CCS): A Review

Dr. Monal Dutta [1*], Moinak Halder [2], Souvik Nath [3], Sankhadeep Ghosh[4]
[1,2,3,4*] *Department of Chemical Engineering, Calcutta Institute of Technology, Howrah, India*
**Email: soniairin@gmail.com*

Abstract

The typical process of Carbon Capture and Storage (CCS) mainly involves the capture of carbon dioxide (CO_2) emissions from various industrial processes or from the flue or stack gas which is generated as a result of burning of fossil fuels. Therefore, the main processes of Carbon Capture and Storage (CCS) basically categorized as post-combustion carbon capture, pre-combustion carbon capture and oxy-fuel combustion systems. The first method is specially used in various steel and power plants whereas the pre-combustion carbon capture process is mainly employed in different industrial processes. Apart from these techniques, Direct Air Capture and Storage (DAC) method is also used in order to capture CO_2 directly from ambient air. The main characteristics of the CCS process includes capturing CO_2 from the point sources of where it is been produced such as, smokestacks of iron and steel factories and then transporting the captured CO_2 to the storage site for subsequent sequestration. The captured CO_2 is firstly compressed to a liquid form and then it is being transported via ship or in a pipeline to store beneath the ground where it is geologically sequestrated by injecting it into porous rock formations in geological basins.

Keywords: *Carbon Capture and Storage (CCS); Pre-combustion carbon capture process; Post-combustion carbon capture; Direct Air Capture and Storage (DAC); Carbon Sequestration; Geological Basins.*

1. Introduction

In the recent era Carbon Capture and Storage (CCS) technologies have successfully resolved the major challenges associated with greenhouse gas emissions from industrial combustion processes. In this typical process carbon dioxide (CO_2) is been captured before it is released into the atmosphere. The captured CO_2 is then stored underground in various geological formations. As Carbon capture and storage (CCS) captures the CO_2 emissions from various potential sources so it in-turn reduces global warming to a greater extent. The process basically comprises off three-step namely capturing of the CO_2, transportation and storage. The considerable amount of CO_2 could be captured from various industrial sources such as from power generation which contributes approximately 40% of total CO_2 emissions [1]. Carbon capture and storage technologies comprises of a set of techniques that are used to reduce greenhouse gas emissions from various point and nonpoint sources including industrial processes and power generation units [2, 3]. The main process of CO_2 capture can be done in various stages like at pre-combustion stage, at post-combustion stage, at oxy-fuel combustion stage and direct air capture stage [4, 5]. The storage process is followed by Carbon transportation which is widely done through pipeline transportation, shipping transportation, and road and rail transportation etc [6, 7]. Once the captured carbon is being transported to a specific site then that carbon can be further utilized in various fields such as, in the field of oil/gas recovery, chemicals and fuels utilization and agriculture utilization.

Through these technologies captured CO_2 is being converted into valuable products which promoting a circular carbon economy [8]. In order to prevent further emission CO_2 is stored through geological storage, mineral carbonation storage, terrestrial storage, and ocean [9, 10]. Therefore as a whole CCS technologies offer a combination of techniques that can be widely used to reduce greenhouse gas emissions from various potential sources. But apart from these advantages there are some economic and regulatory challenges associated with this technology. In the present review paper a complete overview of various recent advancements associated with CCS technologies are discussed in details.

2. Effect of Carbon dioxide emissions on atmosphere

The emission of carbon dioxide (CO_2) from various sources is responsible for global warming [11]. Due to burning of fossil fuels, deforestation and increasing urbanization have significantly increased the concentration of CO_2 in the atmosphere [12]. Therefore, it is very necessary to implement various CO_2 capturing technologies which generally capture CO_2 from stationary and large industrial processes, such as power generation. These technologies are known as carbon capture and storage (CCS) and when it is coupled with the effective utilization of captured carbon then it is called as carbon capture utilization and storage (CCUS) [13]. In addition to reducing the CO_2 concentration in the atmosphere CCUS also helps to reduce emissions of other GHG pollutants. It also uses hydrogen as a carbon-free fuel as a reliable low carbon energy supply. But CCUS mainly focuses on carbon storage and it is less effective for utilizing the captured CO_2 for beneficial applications [14]. The CO_2 capture process includes effective capture technologies, transportation and storage of CO_2. The whole process offers several economical benefits like alternative power generation coupled with enhanced oil recovery for in bio-fuel production. Inspire of having so many advantages CCUs have several challenges like various risks and safety issues related to its transportation and storage.

3. Description of the carbon capture technologies

As discussed earlier, combustion of fossil fuels in industrial processes contributes most of the CO_2 emissions. The other sources may include emissions from various electricity generations and burning of residual food crops in the agricultural process especially during inter season. In the recent decade, different types of carbon capture technologies namely Pre-combustion which is generally used in steel and cement plants [15], Post-combustion and oxygen-enriched combustion are used widely in the power industries to reduce carbon concentration in the atmosphere. Apart from these, chemical extraction is also employed to separate CO_2 in coal. As an advanced method the extraction of CO_2 is also practiced from industrial process streams through chemical extraction process [16]. The last practiced CO_2 capture method involves capturing of CO_2 directly from air which is termed as Direct Air Capture (DAC) [17].

3.1 Pre-combustion Process

In this process CO_2 is mainly captured from fossil fuel feed stocks before they are burned to produce energy. This process is specially used for coal gasification and various gas-reforming. In this process, the captured gases are converted to water gas which comprises of H_2, CO, and CO_2. After this CO_2 is being separated from the captured as mixtures through different technologies. At the end of the process, H_2 is obtained as the clean-fuel product. The concentration of the CO_2 obtained through Pre-combustion Process is relatively high. The major advantage of this process is it involves low energy consumption costs but the CO2 separation step is expensive [18].

3.2 Post-combustion Process

Post-combustion process separates CO_2 directly from flue gases and it produces a

mixture of CO_2, oxygen, and N_2 compounds. The post-combustion carbon capture may be done in various ways. One of such technologies can be described through temperature-vacuum-swing adsorption process where silica is used as an adsorbent for adsorption of aqueous monoethanolamine (MEA). The said process is widely used for separating CO2 from natural gas, hydrogen, and flue gases [19]. This post combustion technology has been adapted to a greater extent mainly in cement and steel industry where the GHG emissions are considered from a point-source [20]. The advantage of Post-combustion Process includes low investment cost and the original combustion process [21].

3.3 Direct Air Capture (DAC)

Direct air capture (DAC) method involves extraction of CO_2 directly from the atmosphere at any location. This process generally captures CO_2 from steel plant. After effective capturing of atmospheric CO_2 DAC it is stored in deep geological formations or used for a variety of applications. The process typically uses some adsorbent materials which are suitable for CO_2 adsorption. Once the as is being adsorbed then it is extracted from the absorbents through a desorption process via heat treatment [22]. But this method is quite costly.

3.4 Other treatment technologies

The other CO_2 separation technologies are mainly gas absorption processes which uses various solid and liquid solvents for absorbing CO_2 from as stream. Apart from above mentioned methods, CO_2 can also be separated through various methods such as, temperature swing and pressure swing adsorption, membrane separation, electrochemical methods and membrane absorption techniques etc [23]. In the membrane separation technique a micro porous membrane is use for gas separation.

3.5 Amine-based capture processes

Apart from other conventional techniques for CO_2 removal the amine-based solvent process is implemented to absorb CO_2 directly from flue gas. The major advantage of this method is cost effectiveness [24].

4. Carbon transport technologies

Once the carbon is being effectively captured from its potential source then the captured carbon is transported from its sources to desired storage sites through various means like pipeline transportation, shipping transportation, and road and rail transportation etc. Among all these methods, pipeline transportation is the most common and cost-effective method for transporting large volumes of CO_2 over long distances [25].

5. Carbon storage technologies

Generally the captured carbon is stored in various geological formations to prevent it from being released into the atmosphere [26]. This kind of storage facility mainly includes geological storage, mineral carbonation storage, terrestrial storage, and ocean storage etc. But among all these techniques, geological storage is the most important technology for mitigating climate change by storing carbon dioxide (CO_2) deep underground in geological formations [27]. One of such storage method is storing of CO_2 in different types of volcanic rocks which are typically known as basalts. The storage of CO_2 can also be done through stratigraphic trapping where it is injected into a trap surrounded by rocks boundaries. Then the injected CO_2 penetrates though the void spaces of the rocks until it reaches the impermeable layers of rocks. Due to the variation of pore diameters some CO_2 is unable to come out of the void spaces [28]. Another suitable alternative is to store CO_2 by dissolving it into water which offers the advantage of reducing the corrosive properties of the injected gas. But on the other hand, due to the increased solubility of injected CO_2 in the rock formations it alters the pH of the system and makes the solution more acidic. The trapped CO_2 can also react with various minerals which are already stored in the earth's core and subsequent reactions with these mineral

materials leads to formation of carbonate minerals. Besides all the above mentioned methods another type of geological storage of CO_2 is through saline formations in various geological structures beneath the Earth's surface. But there are several challenges associated with this storage method like chances of leakage and fractures in the rock structures which may lead to earthquake [29]. Sometimes, naturally deposited layers in the sea floor enable the escaping of trapped CO_2 into the atmosphere [30]. In addition CO_2 can also be stored in fossil-fuel reservoirs for long periods. Examples of such reserves may be onshore reserves which are mostly located near the point sources to reduce the transport costs [31]. The enhanced oil recovery (EOR) or enhanced gas recovery (EGR) during CO_2 capturing process is mainly done through injection, production, and recycling of injected fluids [32]. But in the EGR process CO_2 is injected in the geological formations with the presence of natural gas.

6. Carbon utilization technologies

Proper utilization of carbon technologies offers an effective way to transform carbon dioxide (CO_2) and other carbon-containing waste streams either into valuable products or materials [33]. Converting waste materials into reusable products also enhances the carbon economy. Some of the widespread uses of carbon utilization technologies lies in the field of enhanced oil/gas recovery (EOR and EGR). In addition to these, the captured CO_2 can also be utilized in biomass power-generation plants. Here, CO_2 is absorbed from the atmosphere by various plants. The CO_2 storage efficacy can also be enhanced by burying various bio-char and biomass materials [34].

7. Conclusions

From this review work it can be concluded that in the present decade, carbon capture utilization and storage method offers an attractive alternative to reduce carbon footprints from atmosphere. Although various techniques are available to capture the CO_2 from the atmosphere but the economic feasibility of the process depends upon the type of method used and partly on the transportation cost. The said economy can further be enhanced by utilizing the captured CO_2 for various purposes such as power generation, biofuel production and enhanced oil and gas recovery. Apart from storing in various reservoirs, the main storage method of CO_2 is storing through formations. But the major challenges associated with geological storage are chances of leakage of stored CO_2. Whereas, in comparison to the geological storage CO_2 storage in various off shore preservers offers the advantage of low cost by reducing the transportation cost.

Acknowledgments

The authors would like to acknowledge the help and support of Chemical engineering department of Calcutta institute of Technology. We had not used any financial support from anywhere although we are thankful to our Respected Director Academics for his constant encouragements throughout the project.

References

1. Sovacool BK. (2017) Contestation, contingency, and justice in the Nordic low-carbon energy transition. Energy Pol. 102:569–82. doi.org/10.1016/j.enpol.2016.12.045.

2. Klein T, Anderegg W (2021). A vast increase in heat exposure in the 21st century is driven by global warming and urban population growth. Sustain. Cities Soc. 73: 103098. https://doi.org/10.1016/j.scs.2021.103098.

3. McQueen N, Kelemen P, Dipple G, Renforth P, Wilcox J (2020) Ambient weathering of magnesium oxide for CO_2 removal from air. Nat. Commun. 11 (1): 3299. https://doi.org/10.1038/s41467-020-16510-3.

4. Rosa L, Sanchez DL, Realmonte G, Baldocchi D, D'Odorico P (2021) The water footprint of carbon capture and storage technologies. Renew Sustain Energy Rev.

138:110511. https://doi.org/10.1016/j.rser.2020.110511.
5. Realmonte G, Drouet L, Gambhir A. et al. (2019) An inter-model assessment of the role of direct air capture in deep mitigation pathways. Nat Commun 10:3277. https://doi.org/10.1038/s41467-019-10842-5.
6. Rode D, Anderson J, Zhai H, Fischbeck P (2022) Many hands make light work: widening the U.S. path forward from COP26. Environ. Sci. Technol. 56:10.https://doi.org/10.1021/acs.est.1c07965.
7. Noothout P, Wiersma F, Hurtado O, Macdonald D, Kemper J, van Alphen K (2014) CO_2 pipeline infrastructure – lessons learnt. Energy Proc. 63:2481–92. https://doi.org/10.1016/j.egypro.2014.11.271.
8. Shu DY, Deutz S, Winter BA, Baumgärtner N, Leenders L, Bardow A (2023) Renewable Sustain. Energy Rev.178:113246. https://doi.org/10.1016/j.rser.2023.113246.
9. Adu E, Zhang Y, Liu D (2019) Current situation of carbon dioxide capture, storage, and enhanced oil recovery in the oil and gas industry. Can J Chem Eng.97:1048–76. https://doi.org/10.1002/cjce.23393.
10. Khatiwala S, Primeau F, Hall T (2009) Reconstruction of the history of anthropogenic CO_2 concentrations in the ocean. Nature.462:346–9. https://doi.org/10.1038/nature08526.
11. Liang J, Lupien R, Xie H, Vachula R, Stevenson M, Han B, Lin Q, He Y, Wang M, Liang P, Huang Y (2021) Lake ecosystem on the Qinghai–Tibetan Plateau severely altered by climatic warming and human activity. Palaeogeogr. Palaeoclimatol. Palaeoecol. 576:110509. https://doi.org/10.1016/j.palaeo.
12. Luderer G, Vrontisi Z, Bertram C, Edelenbosch OY, Pietzcker RC, Rogelj Jet al (2018) Residual fossil CO_2 emissions in 1.5–2 ◦C pathways. Nat Clim Chang.8(7):626–633.10.1038/s41558-018-0198-6.
13. Al-Shargabi M, Davoodi S, Wood DA, Rukavishnikov VS, Minaev KM (2022) Carbon Dioxide Applications for Enhanced Oil Recovery Assisted by Nanoparticles: Recent Developments. ACS Omega. 7(12): 9984–94. https://doi.org/10.1021/acsomega.1c07123.
14. Bui M, Adjiman CS, Bardow A, Anthony EJ, Boston A, Brown S, et al. (2018) Carbon capture and storage (CCS): the way forward. Energy Environ Sci; 11(5):1062–176. DOI: 10.1039/c7ee02342a rsc.li/ees.
15. Dziejarski B, Krzyzynska R, Andersson K (2023) Current status of carbon capture, utilization, and storage technologies in the global economy: a survey of technical assessment. Fuel. 342:127776. https://doi.org/10.1016/j.fuel.2023.127776.
16. Ivanov Y, Pyatnichko O, Zhuk H, Onopa L, Soltanibereshne M. 2017. Extraction of carbon dioxide from gas mixtures with amines absorbing process. Energy Procedia.128:240–247. 10.1016/j.egypro.2017.09.062.
17. Erans M, Sanz-Pérez ES, Hanak DP, Clulow Z, Reiner DM, Mutch GA (2022) Direct air capture: process technology, techno-economic and socio-political challenges. Energy Environ Sci. 15:1360-1405. DOI: 10.1039/d1ee03523a rsc.li/ees
18. Chao C, Deng Y, Dewil R, Baeyens J, Fan X (2021) Post-combustion carbon capture. Renew Sustain Energy Rev. 138:110490. https://doi.org/10.1016/j.rser.2020.110490.
19. Borhani TN, Wang M (2019) Role of solvents in CO_2 capture processes: The review of selection and design methods. Renewable Sustain. Energy Reviews. 114:109299. https://doi.org/10.1016/j.rser.2019.109299.
20. Jayarathna SA, Lie B, Melaaen MC (2013) Amine based CO_2 capture plant: Dynamic modeling and simulations. Int J Greenhouse Gas Control. 14:282–90. https://doi.org/10.1016/j.ijggc.2013.01.028.
21. Mukherjee A, Okolie JA, Abdelrasoul A, Niu C, Dalai AK (2019) Review of post combustion carbon dioxide capture technologies using activated carbon. J Environ Sci. 83:46–63. https://doi.org/10.1016/j.jes.2019.03.014
22. Castro-Mu˜noz R, Zamidi Ahmad M, Malankowska M, Coronas J (2022) A new relevant membrane application: CO2 direct air capture (DAC). Chem Eng J. 446:137047. https://doi.org/10.1016/j.cej.2022.137047.

23. Ahmad AL, Sunarti AR, Lee KT, Fernando WJN (2010) CO_2 removal using membrane gas absorption. Int. J. Greenhouse Gas Contol. 4(3):495-498. https://doi.org/10.1016/j.ijggc.2009.12.003.
24. Aghel B, Janati S, Wongwises S, Shadloo MS (2022) Review on CO_2 capture by blended amine solutions. 119: 103715. Int. J. Greenhouse Gas Control. https://doi.org/10.1016/j.ijggc.2022.103715.
25. Lu H, Ma X, Huang K, Fu L, Azimi M (2020) Carbon dioxide transport via pipelines: a systematic review. J Clean Prod.266:121994. https://doi.org/10.1016/j.jclepro.2020.121994.
26. Aminu MD, Nabavi SA, Rochelle CA, Manovic V (2017) A review of developments in carbon dioxide storage. Appl Energy. 208:1389–419. https://doi.org/10.1016/j.apenergy.2017.09.015 .
27. Ajayi T, Gomes JS, Bera A (2019) A review of CO_2 storage in geological formations emphasizing modeling, monitoring and capacity estimation approaches. Pet Sci.16(5):1028–63.DOI:10.1007/s12182-019-0340-8.
28. Feng D, Li X, Wang X, Li J, Zhang X (2018) Capillary filling under nanoconfinement: The relationship between effective viscosity and water-wall interactions. Int J Heat Mass Transf. 118:900–910. https://doi.org/10.1016/j.ijheatmasstransfer.2017.11.049.
29. Wei N, Li X, Liu S, Lu S, Jiao Z (2021) A strategic framework for commercialization of carbon capture, geological utilization, and storage technology in China. Int J Greenhouse Gas Control. 110:103420. https://doi.org/10.1016/j.ijggc.2021.103420.
30. Connelly DP, Bull JM, Flohr A, Schaap A, Koopmans D, Blackford JC, et al. (2022) Assuring the integrity of offshore carbon dioxide storage. Renew Sustain Energy Rev.166:112670. https://doi.org/10.1016/j.rser.2022.112670.
31. Roussanaly S, Hognes ES, Jakobsen JP (2013) Multi-criteria analysis of two CO_2 transport technologies. Energy Proc 2013;37:2981–8. https://doi.org/10.1016/j.egypro.2013.06.184.
32. Zhao N, Xu T, Wang K, Tian H, Wang F (2018) Experimental study of physical-chemical properties modification of coal after CO_2 sequestration in deep unmineable coal seams. Greenhouse Gases Sci Technol. 18:8(3): 510–28. https://doi.org/10.1002/ghg.1759.
33. Lamberts-Van Assche H, Compernolle T (2022) Using real options thinking to value investment flexibility in carbon capture and utilization projects: a review. Sustain. 14:2098. https://doi.org/10.3390/su14042098.
34. Schaffer S, Pr¨oll T, Al Afif R, Pfeifer C (2019) A mass- and energy balance-based process modelling study for the pyrolysis of cotton stalks with char utilization for sustainable soil enhancement and carbon storage. Biomass Bioenergy.120:281–90. https://doi.org/10.1016/j.biombioe.2018.11.019.

https://doi.org/10.36375/prepare_u.iiche.a385

[International Conference on Energy Transition: Challenges and Opportunities at Chemical Engineering Congress (CHEMCON-2023) – On the occasion of Platinum Jubilee Year of Indian Institute of Chemical Engineers]

Biopolymer Supported ZnO Bionanocomposites Film and Their Application in Environmental Remediation and Controlling of Contagious Diseases

Rebika Baruah[a,b*], , Karishma Talukdar[a,b], Vekuno Cukhamu[a], Archana Moni Das[a,b]

[a]*CSIR-North East Institute of Science and Technology, Jorhat-785006, Assam, India*

[b]*Academy of Scientific and Innovative Research (AcSIR), Ghaziabad- 201002, India*

**Corresponding Author's Name: Rebika Baruah,*

Email: baruahrebika9@gmail.com,

Phone number: 9476626581

Abstract

Abstract ID: ANN OP-1
Mention Abstract Theme: Advanced Nano-Materials & Nanotechnology (ANN)

Bionanocomposites are innovative sustainable materials that possess multifunctional attractive nature in various fields. Cellulose/chitosan/ ZnO bionanocomposites (CCZBC) films were synthesized by utilizing water extracts of *Livistona jekinsiana* as reducing as well as capping agents to synthesize ZnO NPs impregnated chitosan/cellulose bionanocomposites thin film. X-ray diffraction pattern of CCZBCC revealed the wurtzite structure of ZnO nanoparticles. Fourier transform infrared spectroscopy revealed the presence of plant extracts, cellulose, and chitosan in CCZBC. Scanning Electron Microscope (SEM) images provided information about the morphology of the surface of CCZBC. The elemental composition of CCZBC was determined by Energy Dispersive X-ray (EDX) analysis. Transmission Electron Microscope (TEM) provided the shape and size of CCZBC. CCZBC possessed efficient photocatalytic degradative properties in the remediation of two anthropogenic dyes, Eosin blue and Bromocresol green, potential antimicrobial activity against *Escherichia coli* (*E. coli*) and *Staphylococcus aureus* (*S. aureus*)., and antioxidant property in DPPH assay. Therefore, the chitosan/cellulose/Ag NPs bionanocomposites film can be considered an efficient material for biomedical and environmental applications.

Keywords: Bionanocomposites; ZnO nanoparticles; Cellulose; Chitosan; Thin Film

1. Introduction

Environmental pollution is a great challenge for human civilization in the 21st century (Khan *et al.* 2018). Water pollution is the main threat to surviving a healthy life in the world (Ahmed *et al.* 2017). Due to the technical evaluation, much wastage is drained off to the water bodies that cause detrimental effects on the aquatic lives (Ahmed *et al.* 2017; Baruah *et al.* 2021). It is an urgent need to develop an innovative and novel technique to remediate water pollutants and make water safe for drinking

(Rashid *et al.* 2021; Baruah *et al.* 2022). Many methods were developed to degrade harmful chemicals in wastewater. Most of them have disadvantages of high pressure, temperature, cost, longer time, larger area, production of byproducts, etc. (Baruah *et al.* 2021). Photocatalysis is the most efficient method that can be applied in wastewater treatment (Rashid *et al.* 2021). This method is a very cost-effective, simple, and eco-friendly method (Vardhan *et al.* 2019; Rashid *et al.* 2021). Photocatalysis in the presence of nanoparticles (NPs) is an ideal alternative to conventional methods (Vardhan *et al.* 2019). Due to the large surface to volume ratio, extra small-size NPs can scavenge organic pollutants within a short period to the larger extent (Goswami *et al.* 2018; Vardhan *et al.* 2019; Liu *et al.* 2019; Rashid *et al.* 2021).

ZnO is an n-type semiconductor belonging to group III-IV family (Baruah *et al.* 2019). ZnO is a universally recognized photocatalyst due to its wide band gap (3.37 eV), high photosensitivity, low cost, and environment-friendly nature (Mishra *et al.,* 2016; Matinise *et al.* 2017; Goswami & Das, 2019; Baruah *et al.* 2023). ZnO efficiently degraded rhodamine B (RhB) (Yadav *et al.* 2018), methyl orange (MO) (Baruah *et al.* 2021), congo red (CR) (Baruah *et al.* 2019), methylene blue (MB) (Baruah *et al.* 2021), and acid red 18 (Kumar *et al.* 2018). Because of its bio-safety, biocompatibility, and biodegradability, it is an important material in pharmaceutical and pro-ecological systems (Stan *et al.* 2015). Therefore, many works have been published in several book reviews and papers regarding the synthesis and application of ZnO. But still, people try to extract the novel character of this promising particle by altering the method of preparation due to its multitasking nature (Varadavenkatesan *et al.* 2019; Golmohammadi *et al.* 2020; Baruah *et al.* 2021).

Synthesis of nanoparticles by green methods is the best solution to the problems arising from the physical and chemical ones (Lu *et al.,* 2019). The interaction of nanoparticles with biomaterials is a demanding area of research (Hassan *et al.* 2015). The green synthesis of nanoparticles includes biologically originated systems. Among them, plants are the most preferable (Fowsiya *et al.* 2016; Singh *et al.* 2019). The secondary metabolites present in the plants act both as reducing and stabilization agents (Rajakumar *et al.* 2018; Agarwal & Shanmugam, 2020; Kamarajan *et al.* 2022). Plants mediated synthesis leads to stable and uniformly shaped and size nanoparticles (Zbair *et al.* 2018; Hadjltaief *et al.*2018; Ong *et al.,* 2018). Many plants are used for the synthesis of nanoparticles like *Livistona jenkinsiana* (Baruah *et al.* 2021), *Alpinia nigra* (Baruah *et al.* 2019), *Hibiscus sabdariffa* (Baruah *et al.* 2023), *Azadirachta indica* (Sharma *et al.* 2021), *Aloe vera* (Sadiq *et al.* 2021), etc.

Phragmites australis is a common reed that belongs to wetland species. The plant is a perennial, widely distributed emergent macrophyte with vigorous growth. It possesses remarkably high amplitude of tolerance. It is the dominant plant species in many watercourses and often forms huge reed beds along many shallow lakes and freshwater canals, especially in Egypt. Phytochemical analysis reveals its abundance of bioactive compounds such as tannins, phenolic compounds, flavonoids, terpenoids, and glycosides (Hosny *et al.,* 2021). These phytochemicals can easily reduce and stabilize the NPs by electrostatic stabilization. This plant

shows potential antibacterial and antioxidant activities (Hosny *et al.*, 2021). *Phragmites australis* mediated Au, Ag, and Cu NPs were reported, but the synthesis of ZnO NPs was reported in this paper for the first time.

In this work, the synthesis of ZnO NPs was carried out using aqueous extracts. *Phragmites australis*. ZnO NPs were characterized by UV-Visible, FTIR, XRD, SEM, TEM, DLS, and zeta potential analysis. Photocatalytic activity of ZnO NPs was screened in the degradation of MO, and MB under solar irradiation. The antibacterial activity of ZnO NPs was studied against *Staphylococcus aureus*, *Escherichia coli, Bacillus subtilis, and Klebsiella pneumonia* by agar well diffusion method. The antioxidant ability of ZnO NPs was also evaluated by using a DPPH scavenging assay.

2. Experimental

2.1. Materials

All the chemicals were used as received without further purification. Chemicals were purchased from Sigma Aldrich and Merk chemicals, Rankem, Himedia, SRL, and LobaChemie. Double-distilled H_2O was used to prepare all the reagent solutions.

2.2. Analytical methods

UV-Vis spectrophotometer (Hitachi Model No –U-3900) was used to observe the characteristics absorption peak of ZnO NPs. FTIR spectroscopy (Perkin-Elmer FT-IR-2000 spectrometer) confirmed the involvement of phytochemicals in the synthesis of ZnO NPs. The crystalline nature and morphology of ZnO NPs were determined by XRD (Rigaku Ultima IV diffractometer) and SEM (ZEISS, SIGMA instrument). Elemental analysis of the NPs was recorded by EDS spectrum. TEM (JEM-2100 Plus) determined the phase, shape, and size of the ZnO NPs. Zeta potential and DLS values were measured by Nano ZS Zetasizer (Malvern) instrument to evaluate the size distribution, polydispersity index (PDI), and electric charge of the nanoparticles. Photocatalytic degradation of MB and MO and scavenging of DPPH by ZnO NPs were examined by a UV-Visible spectrophotometer. The zone of inhibition of harmful pathogens in antibacterial activity was measured using an Antibiotic Zone Scale. Origin Pro 9, Chem Draw 15, and Image J software were used to plot graphs, draw chemical structures, and determine the size of ZnO NPs respectively.

2.3. Preparation of plant extract

Phragmites australis were collected from Holmora Village, North West Jorhat, Assam, India. The plant was washed with double distilled water to remove impurities. Thereafter, the plant was cut into small pieces of 1-2 cm size and dried under sunlight to make them moisture free. Dried small pieces were converted into fine powder by grinding and stored in a zipper bag for further studies.

10 gm of leaves was added to an Erlenmeyer flask containing 100 ml of double distilled. The mixture was treated at 45°C for 60 minutes under stirring. Clear plant extracts were collected by filtration of the mixture followed by centrifugation at 5000 rpm for 30 min. The extract was refrigerated at 4°C for future applications.

2.4. Synthesis of Phragmites australis fabricated ZnO NPs (PA@ZnO NPs)

30 ml of plant extract and 10 mM of $ZnCl_2$ solution were mixed in an Erlenmeyer flask. 10 ml of 1 M NaOH solution was added to the mixture dropwise to make the pH of the mixture 7. Then the mixture was constantly stirred at

https://doi.org/10.36375/prepare_u.iiche.a385

60°C for 3 h to prepare a deep yellow color solution. The formation of PA@ZnO NPs was preliminarily confirmed by observing UV-Vis spectra of ZnO NPs and the color change of the reaction mixture. Then the colloidal solution was sonicated for 1h at 50°C, centrifuged at 6000 rpm for 15 min and washed with 50% C_2H_5OH and H_2O solution. Impurity-free segregated pellets were dried in an oven at 60°C for 12 hours and converted to fine powder form by grinding with mortar and pestle. Obtained PA@ZnO NPs were stored in a vacuum desiccator for different characterization and potent application.

2.5. Photocatalytic activity of the PA@ZnO NPs

Methylene Blue and Methyl Orange were considered as the model dye to examine the photocatalytic activity of PA@ZnO NPs. 2.5 mg of the photocatalyst and 25 ml of each dye solution were mixed (1mg/ml) and kept in dark under stirring conditions for 30 minutes to attain the adsorption-desorption equilibrium. After that, each mixture of dye and NPs was subjected to sunlight under continuous stirring. 2 ml aliquots of each suspension of MB and MO were collected after every 5 minutes and measured the absorption of the mixture at 665 and 463 nm respectively. Thus the time dependant photo degradative effect of the PA@ZnO NPs towards MB and MO dye was examined with the help of a UV-Vis spectrophotometer. The complete degradation of dyes was achieved in 60 minutes.

2.6. Antioxidant activity of PA@ ZnO NPs

DPPH (2, 2-diphenyl-1-picrylhydrazyl) was used as a model free radical in the examination of the antioxidant activity of the PA@ZnO NPs. Ascorbic Acid (AA) and pure DPPH solution were considered as positive and negative standards respectively. Different concentrations (20, 40, 60, 80 & 100µg/ml) of AA and PA@ZnO NPs were prepared in double-distilled water. 1 ml of water was added to each concentration of AA and NPs. 1 ml of DPPH (.1mM of 20 ml ethanolic solution) was also added to them. The prepared solutions were incubated in dark conditions at room temperature for 30 min. The absorbance of each solution was measured at 517 nm against the 30% ethanolic aqueous solution. IC50 value was calculated by plotting the extract concentration on the X-axis versus the corresponding percentage of scavenging effect on the Y-axis in the log dose inhibition curve by using the following formula:

% scavenging = [Absorbance of control - Absorbance of test sample/Absorbance of control] X 100

2.7. Antibacterial activity of PA@ZnO NPs

Bacillus subtilis (MTCC 441) and *Escherichia coli* (ATCC 11229) were selected to screen the antibacterial activity of PA@ZnO NPs by using agar well diffusion method. Fresh bacterial cultures were prepared in Mueller Hinton broth medium, where 10 µl cultures of *E. coli* and *S. aureus* were inoculated separately, and incubated for 18 hours at 37°C, in a shaker until the turbidity resembled with McFarland 0.5 turbidity standard. 100 µl of each pathogen was spread on Petri dishes separately containing sterilized Mueller Hinton agar using a sterilized spreader. Then the wells (6 mm) were made in agar plates by the sterilized well borer and each concentration of PA@ZnO NPs (20, 40, 60, 80, and 100 µg/ml) were added to the respective marked wells and kept at 37°C for 24 h for incubation. The positive control of this experiment was neomycin. The zone of inhibition

https://doi.org/10.36375/prepare_u.iiche.a385

of bacteria was measured in millimeters (mm) by an antibacterial zone measuring scale. The test was performed three times and the results were shown as mean ± standard deviation.

3. Results and Discussions

3.1. UV-Visible spectroscopy

Optical properties of PA@ZnO NPs were studied by UV-Visible spectroscopy in the range of wavelength 200-700 nm. ZnO NPs showed the characteristics absorption peak at 340 nm with the blue shift from the absorption peak of bulk ZnO at 378 nm [Figure 1]. The characteristics absorption peak of ZnO NPs was due to surface Plasmon resonance and the blue shift from the bulk value was due to the quantum confinement effect (Vinayagam *et al.*, 2020). Mie's theory states that one absorption peak reveals the uniform spherical shape of nanoparticles. NPs exhibit more than a single SPR band due to the anisotropicity of the particles. The symmetry of NPs is inversely proportional to the number of SPR (Baruah *et al.* 2021; Baruah *et al.* 2022). Band gap PA@ZnO NPs was calculated by the formula E_g=1240/λ. The band gap was found to be 3.65 eV that value reinforced the semiconducting property of the material. Reported results have similarities with literature like *Livistona jekinsiana* and nanocellulose mediated ZnO NPs showed characteristic absorption peaks at 332 and 368.33 nm respectively (Baruah *et al.* 2021; Baruah *et al.* 2023).

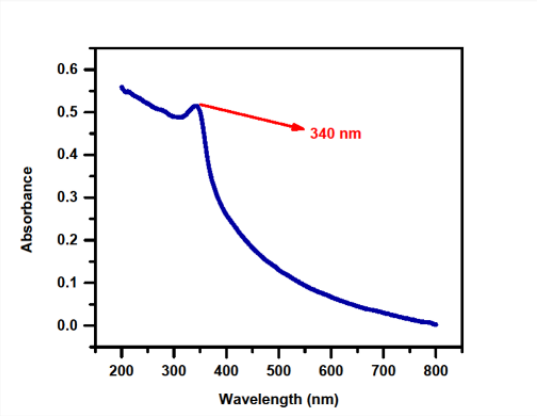

Figure 1: UV-visible spectrum of PA@ZnO NPs.

3.2. FT-IR Analysis

The involvement of phytochemicals in the synthesis and stabilization of PA@ZnO NPs and the chemical composition of ZnO NPs was studied by FTIR analysis [Figure 2]. Different phytoconstituents like phenolic compounds, steroids, flavonoids, terpenoids, alkaloids, etc. are responsible for the fabrication of ZnO NPs (Baruah *et al.* 2019). The band that appeared at 3354 and 2919 cm^{-1} were due to the O–H stretching and the C-H asymmetric and symmetric stretching respectively (Baruah *et al.* 2023). The peak at 1633 cm^{-1} pointed out the –C=C – stretching vibrations of the aromatic compounds (Rajakumar *et al.* 2018). The absorption band at 1470 and 1371 cm^{-1} were due to the C-N stretching vibrations and O-H banding of phenolic compounds (Goswami *et al.* 2018). The absorption band at 888 cm^{-1} was caused by the bending of primary/secondary amines. The sharp band that appeared at 569 cm^{-1} elucidated the stretching vibrations of the Zn-O metallic bond of ZnO NPs (Baruah *et al.* 2021; Baruah *et al.* 2023).

https://doi.org/10.36375/prepare_u.iiche.a385

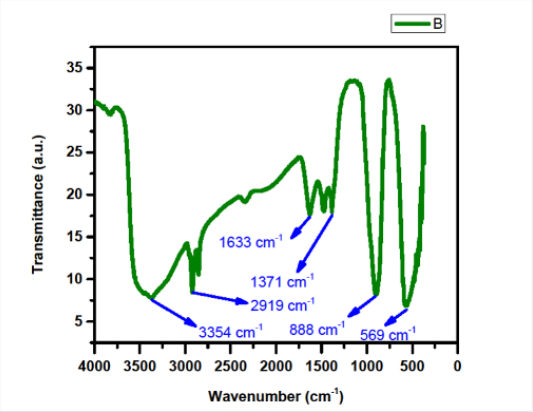

Figure 2: FTIR spectrum of PA@ZnO NPs.

3.3. XRD Analysis

The crystalline nature of PA@ZnO NPs was established by the XRD pattern of ZnO NPs. The characteristic peaks in the plane (100), (002), (101), (102), (110), (103), (112) appeared at 2θ = 31.64°, 34.57°, 36.38°, 47.65°, 56.64°, 62.95°, 67.91° respectively [Figure 3] corresponding with JCPDS (Card Number 36-1451) (Hosny *et al.*, 2021). These peaks revealed the wurtzite structure of ZnO NPs. The comparatively greater peak intensity of the (101) plane was observed which represented preferred growth in the (101) direction (Baruah *et al.* 2021; Baruah *et al.* 2023).

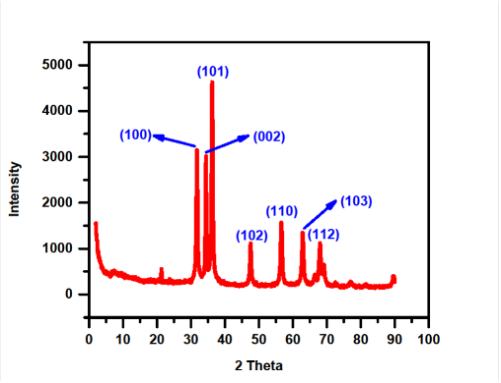

Figure 3: XRD pattern of PA@ZnO NPs.

3.4. FESEM and EDX analysis

Morphology of the surface of PA@ZnO NPs was studied by FESEM of ZnO NPs. SEM images revealed the spherical shape of the ZnO NPs [Figure 4 [A]]. The NPs were uniformly distrusted with lower agglomeration. The agglomeration was due to the high surface energy of ZnO NPs due to the stabilization of biomaterials of the plant extracts.

The elemental composition of PA@ZnO NPs was determined by EDX analysis. The EDX data of ZnO NPs showed signals for Zn and O [Figure 4 [B]], revealing the presence of Zn and O in the ZnO NPs. Other elements C, Cu, Cl, and Si in the EDX spectrum were due to the presence of different phytoconstituents of plant extracts. The SEM and EDX data were in accordance with the literature (Baruah *et al.* 2021; Baruah *et al.* 2023).

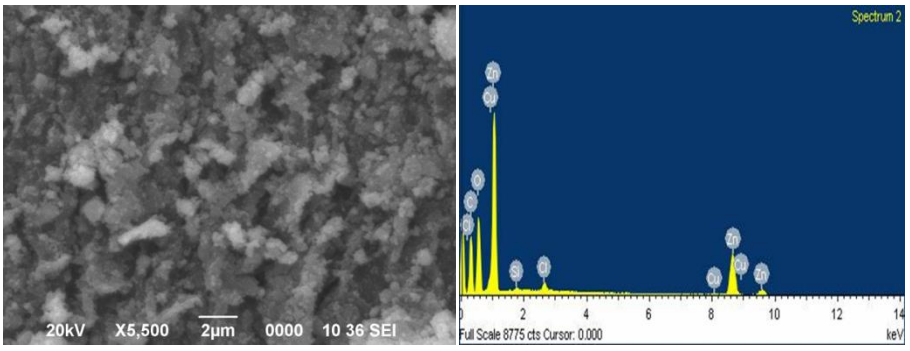

[A] **[B]**

Figure 4: SEM images [A] and EDX spectrum [B] of PA@ZnO NPs.

https://doi.org/10.36375/prepare_u.iiche.a385

3.5. TEM analysis

TEM images of PA@ZnO NPs assigned the shape and size of NPs. The shape of the ZnO NPs was found to be different like spherical, oval, and hexagonal [Figure 5 [A]]. The agglomeration of nanoparticles was observed due to the aqueous medium of the synthesis. The average size of the ZnO NPs was 23 nm with a standard deviation of 2.874 [Figure 5[D]]. The SAED pattern correlated the planes (002), and (110) that the planes resembled the XRD patterns of ZnO NPs [Figure 5 [C]]. The fringe spacing in HRTEM of ZnO NPs was 0.25 nm which corresponded to the (002) plane of the ZnO NPs [Figure 5 [B]]. The TEM results revealed the uniformly dispersed and evenly shaped nature of the ZnO NPs (Baruah *et al.* 2021; Baruah *et al.* 2023).

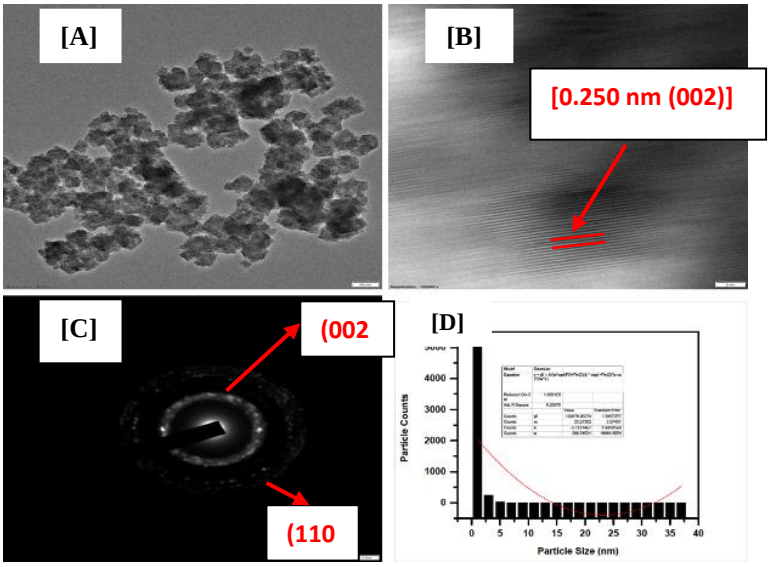

Figure 5: TEM image [A], HRTEM image [B], SAED pattern [C], and average particle size distribution [D] of PA@ZnO NPs.

3.6. Colloidal properties

Zeta potential revealed the colloidal behavior of nanoparticles by providing information about the density of the electric charge on the surface of the particles. The average zeta potential of ZnO NPs was −11.66 mV with a standard deviation of 3.4 [Table 1]. DLVO theory stated that the density of the electric discharge on the surface of the particles is directly proportional to the repulsive force of the static electricity between the particles. This force is responsible for the higher stability of the nanoparticles (Baruah *et al.* 2021; Baruah *et al.* 2023). The reported zeta potential value confirmed that PA@ZnO NPs were stable NPs that were useful for their catalytic application in dye degradation.

DLS analysis determined the hydrodynamic diameter of PA@ZnO NPs and which was in the range of 100-1000 nm [Figure 6]. The hydrodynamic diameter of ZnO NPs was greater that the size of NPs given by TEM analysis due to the solvation effect. The Polydispersity Index (PDI) of ZnO NPs was found to be 0.203 with a standard deviation of 0.894. The results confirmed that the reported eco-friendly method was the successful one to synthesize the stable ZnO NPs.

https://doi.org/10.36375/prepare_u.iiche.a385

Zeta potential and DLS analysis data were similar to the previous literature (Baruah *et al.* 2021; Baruah *et al.* 2023).

Record	Type	Sample Name	T	ZP	Mob	Cond	Wall Zeta Potential
			°C	mV	µmcm/Vs	mS/cm	mV
1	Zeta Potential	PA@ZnO NPs	25	-9.18	-0.7193	199	0
2			25	-12.2	-0.96	205	0
3			25	-13.6	-1.062	206	0

Table 1. Zeta potential of PA@ZnO NPs.

			Size (d.n...	% Intensity:	St Dev (d.n...
Z-Average (d.nm):	1434	**Peak 1:**	587.3	100.0	**76.49**
PdI:	0.720	**Peak 2:**	0.000	0.0	**0.000**
Intercept:	**0.894**	Peak 3:	**0.000**	**0.0**	**0.000**

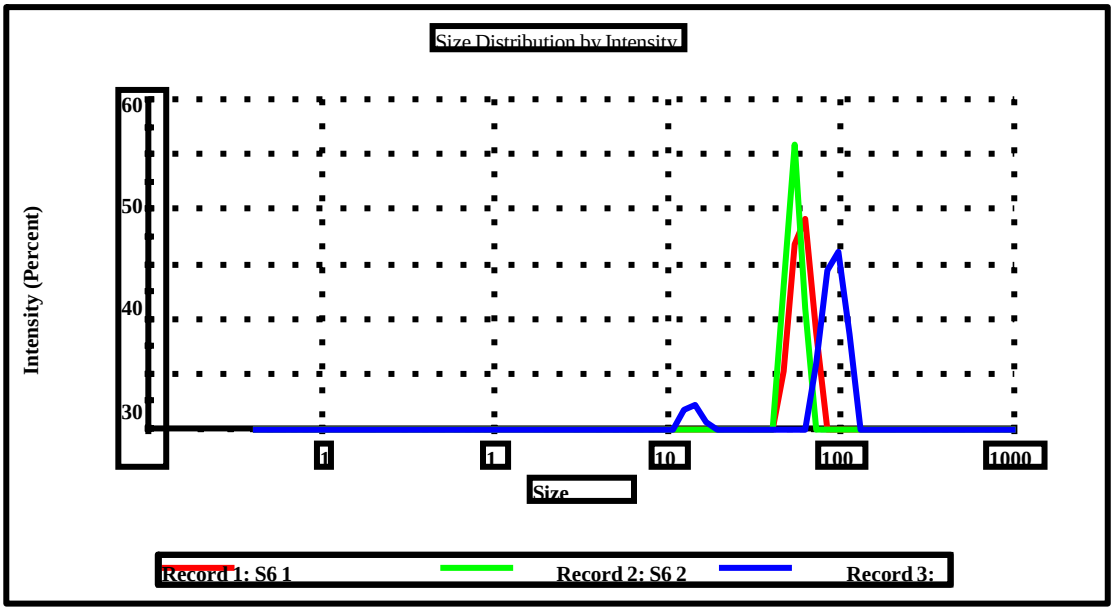

Figure 6: DLS Analysis of PA@ZnO NPs.

3.7. Photocatalytic activity of PA@ZnO NPs

ZnO NPs degraded dye molecules in the presence of photons. Under solar irradiation, the electron (e−) of the valence bond excites to the conduction band and hole (h+) generates in the valance band [eq. (a)]. The hole reacts with adsorbed water molecules and surface-bound hydroxyl groups (OH−) and generates hydroxyl radicals (OH•) [(b) and (c)]. Electron reduces the oxygen molecule present in the solution and produces superoxide radical anion (O2•−) [(d)]. The degradation of MB and MO was proposed to

https://doi.org/10.36375/prepare_u.iiche.a385

take place through a disproportion of the produced free radicals during the reactions [(e)].

The following equations are illustrated to describe the photocatalytic activities of ZnO NPs in the degradation of MB and MO dye:

$$\mathbf{ZnO + h\upsilon \rightarrow e^{-}(CB) + h^{+}(VB)\ (a)}$$

$$\mathbf{h^{+}(VB) + H_2O \rightarrow H^{+} + OH^{\bullet}\ (b)}$$

$$\mathbf{h^{+}(VB) + OH^{-} \rightarrow OH^{\bullet}\ (c)}$$

$$\mathbf{e^{-}(CB) + O2 \rightarrow O2^{\bullet -}\ (d)}$$

$$\mathbf{OH^{\bullet} + O2^{\bullet -} + Dye \rightarrow Degraded\ product\ (e)}$$

3.7.1. Degradation of Methyl Orange and Methylene Blue

PA@ZnO NPs degraded MO in 60 min up to 80% under sunlight. The intensity of the maximum absorption peak of the MO was measured at 463 nm and it was decreased with increasing the irradiation time [Figure 7[A]]. The degradation of MB was also observed in presence of PA@ZnO NPs under solar irradiation. The intensity of the maximum absorption of the MB was measured at 665 nm and decreased with time. Degradation MB was observed for 60 min and the dye degraded up to 82% [Figure 7[B]]. The results were in accordance with the literature. As time proceeded the degradation of the dye increased due to the higher surface energy of PA@ZnO NPs. ZnO NPs degraded harmful dyes to environment-friendly products like H_2O and CO_2 [Figure 8] (Baruah *et al.* 2021; Baruah *et al.* 2023).

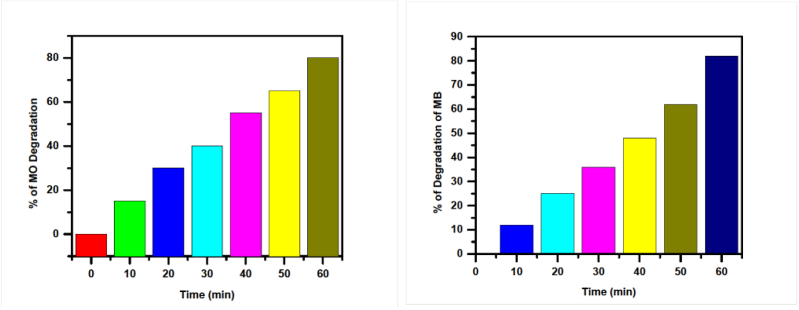

[A] **[B]**

Figure 7: % of Degradation of MO [A] and MB [B].

https://doi.org/10.36375/prepare_u.iiche.a385

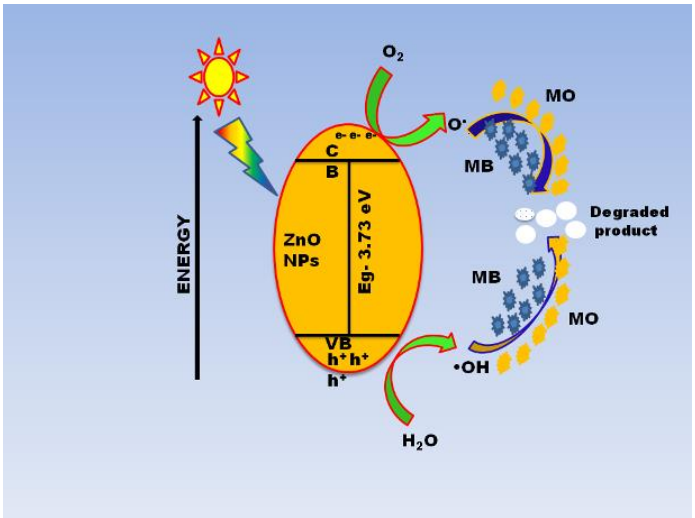

CB – conduction band, VB – Valance band, e^- - electrons, h^+ - holes, $O_2^{-\bullet}$ - superoxide anion radical and •OH – hydroxyl radical

Figure 8: Mechanism of Photodegradation effect of PA@ZnO NPs under solar irradiation.

3.8. Biomedical application of PA@ZNO NPs

3.8.1. Antioxidant activity

The antioxidant activity of PA@ZnO NPs was studied by considering DPPH as a model free radical. Characteristics maximum absorption peak of this radical at 517 nm decreased with the increasing concentration of ZnO NPs. The purple-colored DPPH reacts with an antioxidant in the presence of a hydrogen donor and becomes paired off yellow-colored DPPHH (Stan *et al.* 2015). The IC50 value AA and ZnO NPs were found to be 60.00 and 85.05µg/ml respectively [Figure 9]. Due to the high surface area to volume ratio, ZnO NPs efficiently interacted with DPPH and reduced it (Baruah *et al.* 2021; Baruah *et al.* 2023). IC50 values have resembled literature. Therefore, it is possible to propose an Equation below:

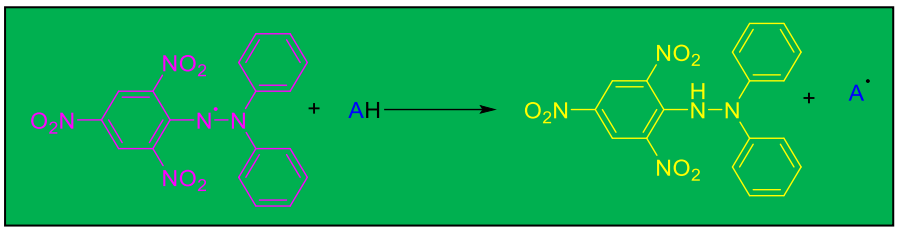

DPPH **DPPHH**

https://doi.org/10.36375/prepare_u.iiche.a385

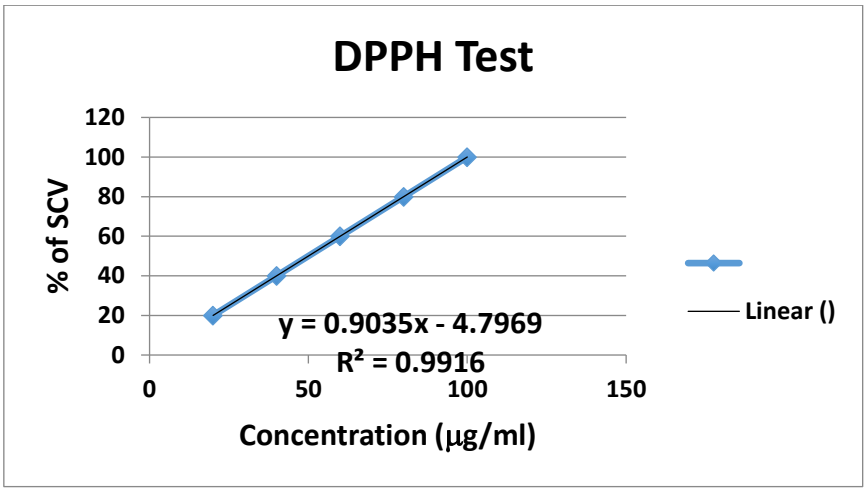

[A]

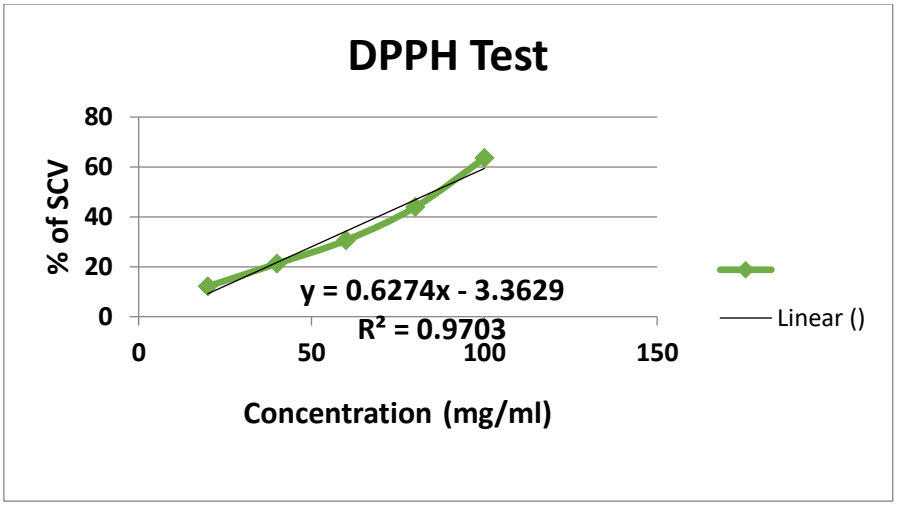

[B]

Figure 9: Antioxidant activity of Ascorbic acid [A], and PA@ZnO NPs [B].

3.8.2. Antimicrobial activity of PA@ZnO NPs

PA@ZnO NPs were applied against gram-positive *S. aureus* and gram-negative *E. coli* and they behaves as broad-spectrum antibiotics. The diameter of the inhibition zone was listed in Table 2. The zone of inhibition (mm) against *S. aureus* measured 10 ± 0.50, 12 ± 0.20, 14 ± 0.40, and 16 ± 0.10; against *E. coli* measured 9 ± 0.40, 10 ± 0.70, 11 ± 0.30, and 13 ± 0.40 mm; for concentrations at 30, 60, 90 and 120 µg/ml, respectively. The inhibition zone of bacteria increased as the concentration of ZnO NPs increased [Fig. 10]. ZnO NPs could more efficiently inhibit the growth of gram-positive bacteria than that of gram-negative ones. The different structural components of the cell wall of both bacteria are the reason for this selectivity. The cell wall of gram-positive bacteria is composed of peptidoglycan (80%). Teichoic acids and proteins and lipopolysaccharide compose the other portion of the cell wall and outer membrane respectively. The cell wall of gram-negative bacteria is composed of only 10% peptidoglycan and the outer membrane contains 50% lipopolysaccharides, 35% phospholipids, and 15%

https://doi.org/10.36375/prepare_u.iiche.a385

lipoproteins and gives resistance to the bacteria towards antibiotics (Baruah *et al.* 2021; Baruah *et al.* 2022). The results were similar to literature (Baruah *et al.* 2023).

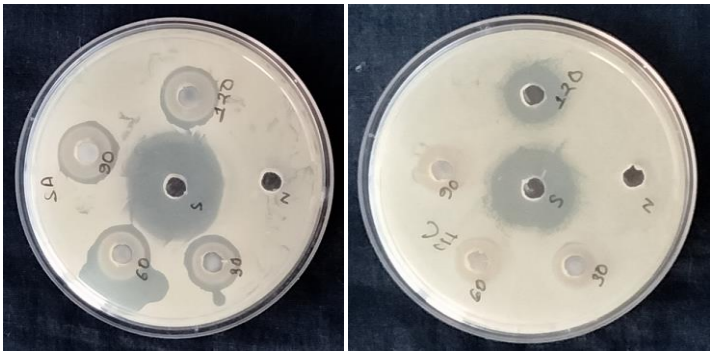

[A] **[B]**

Figure 10: Inhibition zone of *S. aureus* [A], and *E. coli.* [B] in presence of PA@ZnO NPs.

S No.	Test Organisms	Zone of Inhibition (in mm) for different concentrations of ZnO NPs				Neomycin (Standard) (ZI)[b]
		1	2	3	4	
11	*S. aureus*	10± 0.50	12± 0.20	14± 0.40	16± 0.10	26± 0.50
22	*E. coli*	9± 0.40	10± 0.70	11± 0. 30	13± 0.40	22± 0.60

Table 2. Diameter of inhibition zone (in mm) of tested bacteria in the presence of PA@ZnO NPs

4. Conclusion

Phragmites australis fabricated ZnO NPs were synthesized via a mild and simple method for the first time. The contribution of phytochemicals in the synthesis and stabilization of PA@ZnO NPs was confirmed by the FTIR spectrum. The characteristics absorption peak of ZnO NPs appeared at 340 nm in the UV-visible spectrum due to the SPR of ZnO NPs. The hexagonal wurtzite structure of ZnO NPs was confirmed by the XRD pattern of NPs. SEM and TEM images determined the morphology, shape, and size of the ZnO NPs and the size of the nanoparticles was 23 nm with a standard deviation of 2.874. The stability of the nanoparticles was determined by zeta potential with a value of −11.66 mV with a standard deviation of 3.4. The size, size distribution, and polydispersity index of the nanoparticles were analyzed by DLS value that was in the range of 100-1000 nm. EDS provides information on the elemental composition and purity of ZnO NPs. PA@ZnO NPs efficiently photocatalyzed the degradation of MO and MB under solar irradiation up to 80% and 82% respectively. ZnO NPs showed broad-spectrum antibiotics against *S. aureus* and *E. coli*. ZnO NPs also showed potent antioxidant activity with an IC50 value of 85.05 μg/ml. Hence,

Phragmites australis fabricated ZnO NPs is a new efficient, and environmentally friendly candidate to overwhelm water pollution and infectious diseases.

Acknowledgments

The authors were sincerely grateful to the Director of CSIR-North East Institute of Science and Technology, Jorhat, Assam for his valuable guidance to perform our research with excellent facilities. R. B. acknowledged the Department of Science and Technology, New Delhi, for the Fellowship grants.

Conflict of Interest: There is no conflict of interest

References

[1] Khan, S. A., Noreen, F., Kanwalc, S., Iqbal, A., & Hussain, G. (2028). Green synthesis of ZnO and Cu-doped ZnO nanoparticles from leaf extracts of *Abutilon indicum, Clerodendrum infortunatum, Clerodendrum inerme* and investigation of their biological and photocatalytic activities. *Materials Science & Engineering: C, 82,* 46–59. https://doi.org/10.1016/j.msec.2017.08.071

[2] Ahmed, S., Chaudhry, S. A., & Ikram, S. (2017). A review on biogenic synthesis of ZnO nanoparticles using plant extracts and microbes: A prospect towards green chemistry. *Journal of Photochemistry and Photobiology B: Biology, 166,* 272-284. https://doi.org/10.1016/j.jphotobiol.2016.12.011

[3] Baruah, R., Yadav, A., & Das, A. M. (2021). *Livistona jekinsiana* fabricated ZnO nanoparticles and their detrimental effect towards anthropogenic organic pollutants and human pathogenic bacteria. *Spectrochimica Acta Part A: Molecular and Biomolecular Spectroscopy, 251,* 119459. https://doi.org/10.1016/j.saa.2021.119459

[4] Baruah, R., Yadav, A., & Das, A. M. (2022). Evaluation of the multifunctional activity of silver bionanocomposites in environmental remediation and inhibition of the growth of multidrug-resistant pathogens†. *New Journal of Chemistry, 46,* 10128-10153. 10.1039/D1NJ06198D

[5] Vardhan, K. H., Kumar, P. S., & Panda, R. C. (2019). A review on heavy metal pollution, toxicity and remedial measures: Current trends and future perspectives. *Journal of Molecular Liquids, 290,* 111197. https://doi.org/10.1016/j.molliq.2019.111197

[6] Rashid, T., Sherf, F., Hazafa, A., Hashmi, R. Q., Zafar, A., Rasheed, T., & Hussain, S. (2021). Design and feasibility study of novel paraboloid graphite based microbial fuel cell for bioelectrogenesis and pharmaceutical wastewater treatment. *Journal of Environmental Chemical Engineering, 9 (1),* 104502. https://doi.org/10.1016/j.jece.2020.104502

[7] Liu, Y., Zhang, Q., Xu, M., Yuan, H., Chen, Y., Zhang, J., Luo, K., Zhang, J., & You, B. (2019). Novel and efficient synthesis of Ag-ZnO nanoparticles for the sunlight-induced photocatalytic degradation. *Applied Surface Science, 476,* 632–640. https://doi.org/10.1016/j.apsusc.2019.01.137

[8] Goswami, M., Baruah, D., & Das, A. M. (2018). Green synthesis of silver nanoparticles supported on cellulose and their catalytic application in the scavenging of organic dyes. *New Journal of Chemistry, 42,* 10868-10878. 10.1039/C8NJ00526E

[9] Baruah, D., Yadav, R.N.S., Yadav, A., & Das, A.M. (2019). *Alpinia nigra* fruits mediated synthesis of silver nanoparticles and their antimicrobial and photocatalytic activities. *Journal of Photochemistry & Photobiology B: Biology, 201,* 111649.

https://doi.org/10.1016/j.jphotobiol.2019.111649

[10] Goswami, M. & Das, A. M. (2019). Synthesis and Characterization of a Biodegradable Cellulose Acetate-Montmorillonite Composite for Effective Adsorption of Eosin Y. *Carbohydrate Polymers, 206,* 863-872. https://doi.org/10.1016/j.carbpol.2018.11.040

[11] Mishra, P., Singh, Y. P., Nagaswarupa, H. P., Sharma, S. C., Vidya, Y. S., Prashantha, S. C., Nagabhushana, H., Anantharaju, K. S., Sharma, S., & Renuka, L. (2016). *Caralluma fimbriata* extract induced green synthesis, structural, optical and photocatalytic properties of ZnO nanostructure modified with Gd. *Journal of Alloys and Compounds, 685,* 656-669. https://doi.org/10.1016/j.jallcom.2016.05.044

[12] Matinise, N., Fuku, X. G., Kaviyarasu, K., Mayedwa, N., & Maaza, M. (2017). ZnO nanoparticles via *Moringa oleifera* green synthesis: physical properties & mechanism of formation. *Applied Surface Science, 406,* 339-347. https://doi.org/10.1016/j.apsusc.2017.01.219

[13] Baruah, R., Goswami, M., Das, A. M., Nath, D., & Talukdar, K. (2023). Multifunctional ZnO Bionanocomposites in the Treatment of Polluted Water and Controlling of Multi-drug Resistant Bacteria. *Journal of Molecular Structure, 1283,* 35251. https://doi.org/10.1016/j.molstruc.2023.135251

[14] Yadav, L. S. R., Raghavendra, M., Manjunath, K., & Nagaraju, G. (2018). Photocatalytic, biodiesel, electrochemical sensing properties and formylation reactions of ZnO nanoparticles synthesized via eco-friendly green synthesis method. *Journal of Materials Science: Materials in Electronics, 29,* 8747-8759. https://doi.org/10.1007/s10854-018-8891-9

[15] Kumar, K. H. S., Dhananjaya, N., & Yadav, L. S. R. (2018). *E. Tirucalli* plant latex mediated green combustion synthesis of ZnO nanoparticles: structure, photoluminescence and photo-catalytic activities. *Journal of Science: Advanced Materials and Devices, 3(3),* 303-309. https://doi.org/10.1016/j.jsamd.2018.07.005

[16] Stan, M., Popa, A., Toloman, D., Dehelean, A., Lung, I., & Katona, G. (2015). Enhanced Photocatalytic Degradation Properties of Zinc Oxide Nanoparticles Synthesized by Using Plant Extracts. *Materials Science in Semiconductor Processing, 39,* 23-29. https://doi.org/10.1016/j.mssp.2015.04.038

[17] Varadavenkatesan, T., Lyubchik, E., Pai, S., Pugazhendhi, A., Vinayagam, R., & Selvaraj, R. (2019). Photocatalytic Degradation of Rhodamine B by Zinc Oxide Nanoparticles Synthesized Using the Leaf Extract of Cyanometra Ramiflora. *Journal of Photochemistry and Photobiology B: Biology, 199,* 111621. https://doi.org/10.1016/j.jphotobiol.2019.111621

[18] Golmohammadi, M., Honarmand, M., & Ghanbari, S. (2020). A Green Approach to Synthesis of ZnO Nanoparticles Using Jujube Fruit Extract and Their Application in Photocatalytic Degradation of Organic Dyes. *Spectrochimica Acta Part A: Molecular and Biomolecular Spectroscopy, 229,* 117961. https://doi.org/10.1016/j.saa.2019.117961

[19] Lu, J., Batjikh, I., Hurh, J., Han, Y., Ali, H., Mathiyalagan, R., Ling, C., Ahn, J. C., & Yang, D. C. (2019). Photocatalytic Degradation of Methylene Blue Using Biosynthesized Zinc Oxide Nanoparticles from Bark Extract of Kalopanax Septemlobus. *Optik, 182,* 980-985. https://doi.org/10.1016/j.ijleo.2018.12.016

[20] Hassan, S. S. M., Azab, W. I. M. E., Ali, H. R., & Mansour, M. S. M. (2015). Green Synthesis and Characterization of ZnO

Nanoparticles for Photocatalytic Degradation of Anthracene. *Advances in Natural Sciences: Nanoscience and Nanotechnology, 6(4),* 045012. 10.1088/2043-6262/6/4/045012

[21] Singh, K., Singh, J., Rawat, M., Green Synthesis of Zinc Oxide Nanoparticles Using Punica Granatum Leaf Extract and Its Application towards Photocatalytic Degradation of Coomassie Brilliant Blue R-250 Dye. *SN Applied Sciences, 1,* 1-8. https://doi.org/10.1007/s42452-019-0610-5

[22] Fowsiya, J., Madhumitha, G., Al-Dhabi, N. A., & Arasu, M. V. (2016). Photocatalytic Degradation of Congo Red Using Carissa Edulis Extract Capped Zinc Oxide Nanoparticles. *Journal of Photochemistry and Photobiology B: Biology, 162,* 395-401. https://doi.org/10.1016/j.jphotobiol.2016.07.011

[23] Kamarajan, G., Anburaj, D. B., Porkalai, V., Muthuvel, A., & Nedunchezhian, G. (2022). Green Synthesis of ZnO Nanoparticles Using Acalypha Indica Leaf Extract and Their Photocatalyst Degradation and Antibacterial Activity. Journal of the Indian Chemical Society, 99, 100695. https://doi.org/10.1016/j.jics.2022.100695

[24] Rajakumar, G., Thiruvengadam, M., Mydhili, G., Gomathi, T., & Chung, I. M. (2018). Green approach for synthesis of zinc oxide nanoparticles from *Andrographis paniculata* leaf extract and evaluation of their antioxidant, anti-diabetic, and anti-inflammatory activities. *Bioprocess and Biosystems Engineering, 41,* 21-30. https://doi.org/10.1007/s00449-017-1840-9

[25] Agarwal, H., & Shanmugam, V. K. (2020). A review on anti-inflammatory activity of green synthesized zinc oxide nanoparticle: Mechanism-based approach. Bioorganic Chemistry, 94, 103423. https://doi.org/10.1016/j.bioorg.2019.103423

[26] Zbair, M., Anfar, Z., Ait Ahsaine, H., Alem, N. E., & Ezahri, M. (2018). Acridine orange adsorption by zinc oxide/almond shell activated carbon composite: Operational factors, mechanism and performance optimization using central composite design and surface modeling. Journal of Environmental Management, 206, 383-397. https://doi.org/10.1016/j.jenvman.2017.10.058

[27] Hadjltaief, H. B., Ameur, S. B., Costa, P. D. Zina, M. B., & Galvez, M. E. (2018). Photocatalytic decolorization of cationic and anionic dyes over ZnO nanoparticle immobilized on natural Tunisian clay. *Applied Clay Science, 152,* 148-157. https://doi.org/10.1016/j.clay.2017.11.008

[28] Ong, C. B., Ng, L. Y., & Mohammad, A. W. (2018). A Review of ZnO Nanoparticles as Solar Photocatalysts: Synthesis, Mechanisms and Applications. Renewable and Sustainable Energy Reviews, 81, 536-55. https://doi.org/10.1016/j.rser.2017.08.020

[29] Sharma, J. L., Dhayal, V., & Sharma, R. K. (2021). White-rot fungus mediated green synthesis of zinc oxide nanoparticles and their impregnation on cellulose to develop environmental friendly antimicrobial fibers. *3 Biotech, 11,* 269. https://doi.org/10.1007/s13205-021-02840-6

[30] Sadiq, H., Sher, F., Sehar, S., Lima, E. C., Zhang, S., Iqbal, H. M. N., Zafar, F., & Nuhanović, M. (2021). Green Synthesis of ZnO Nanoparticles from Syzygium Cumini Leaves Extract with Robust Photocatalysis Applications. *Journal of Molecular Liquids, 335,* 116567. https://doi.org/10.1016/j.molliq.2021.116567

[31] Hosny, M., Fawzy, M., El-Borady, O. M., & Mahmoud, A. E. D. (2021). Comparative study between Phragmites australis root and rhizome extracts for mediating gold nanoparticles synthesis and their medical and environmental applications. *Advanced Powder*

Technology, *32*, 2268-2279. https://doi.org/10.1016/j.apt.2021.05.004

[32] Vinayagam, R., Selvaraj, R., Pugazhendhi, A., & Varadavenkatesan, T. (2020). Synthesis, characterization and photocatalytic dye degradation capability of Calliandra haematocephala-mediated zinc oxide nanoflowers, Journal of Photochemistry & Photobiology, B: Biology, 203, 111760. https://doi.org/10.1016/j.jphotobiol.2019.111760

https://doi.org/10.36375/prepare_u.iiche.a386

XRD analysis of nanosized silicon derived from broken glassware

Moulie Ghosh[a], Snigdha Khuntia[a], Sridhar Dalai[a*]
[a]*School of Engineering and Applied Science, Ahmedabad University, Ahmedabad, Gujarat 380009, India*
*Email: sridhar.dalai@ahduni.edu.in

Abstract

Recently silicon (Si) nanomaterial has drawn substantial interest owing to its versatility in chemical, and physical characteristics. The reduced size, and high surface area, unlike the bulk Si, has made it appropriate for diverse applications. There are numerous sources reported so far responsible for the production of nanostructured Si. However, the advantage of using broken glassware is that it doesn't require to undergo any purification process such as pre-heating or pre-acid leaching. Herein, we describe the synthesis of silicon nanomaterial from broken glassware collected from the laboratory employing the magnesiothermic reduction method. To explore the structure-property relationship, X-ray diffraction (XRD) patterns act as the fingerprint of the material. XRD study has been performed to qualitatively and quantitatively analyze the synthesized nanomaterial. From the qualitative analysis, the diffraction pattern observed after heat treatment has exhibited the formation of Si along with magnesium oxide (MgO) and magnesium silicate (Mg_2SiO_4). Whereas after the subsequent HCl and HF leaching, peaks for only Si have been observed. Incorporating Scherrer's Equation on the intense (111) plane, the crystallite size of Si has been estimated to be 49 nm. Using Rietveld analysis, the weight percentage of Si has been found to increase gradually with each treatment step.

Keywords: *Laboratory glass; Silicon; Nanomaterial; XRD; Rietveld analysis; Crystalline solid*

1. Introduction

The application of Silicon (Si) nanomaterial has made a tremendous impact on a broad range of fields including energy, sensors, catalysis, optoelectronics, photonics and biology (Chan et al. 2008; Betty 2008; perrone donnorso et al. 2012; Peng et al. 2013; Priolo et al. 2014; Wang and He 2017; Chandra Muduli and Kale 2023). It has been a widely used semiconducting material because of the attractive merits such as the rich abundance, and favourable biocompatibility (Kuang et al. 2015; Pakuła et al. 2023). Additionally it is worth pointing out the attractive features such as the controllable surface, excellent physical, chemical, mechanical, optical, electronic and catalytic properties, large surface to volume ratio which makes it a promising candidate for various application (Betty 2008; He et al. 2010; Falk et al. 2019). As a result, it has motivated to investigate and develop various nanostructures to meet the increasing demand of Si based applications. Several methods to produce crystalline Si nanostructures have been developed such as laser induced pyrolysis of Silane, chemical vapor deposition of Silane, metal assisted chemical etching of electronic grade crystalline silicon wafers, electrochemical anodization of crystalline wafers, oxidation of metal silicides, microemulsion technique and the convention carbothermal reduction (Kumar et al. 2012; Favors et al. 2015). However, many of these methods lack the scalabilty due to the involvement of expensive set up, intensive energy consumption and high cost and toxic precursor. Si can be found in many natural sources as it exists in oxide form as Silicon

dioxide (Si). Also, SiO_2 can be found in many industrial wastes as well. These nanostructures of Si can be prepared from wide range of inexpensive SiO_2 sources such as clay minerals, sand, coal, rice husk, bamboo leaves, sugarcane bagasse, and some indurtial sources like LCD, glass fibre, windshield (Favors et al. 2015; Ryu et al. 2016; Silviana and Bayu 2018; Furquan et al. 2018; Choi et al. 2018; Kang et al. 2019, 2020; Falk et al. 2019). Among many of the SiO_2 sources waste glassware could be an attractive source for Si production. Making effective use of discarded glassware can contribute in an excellent way to the solid waste management. The SiO_2 content in the glassware can be directly reduced to Si nanomaterial via magnesiothermic reduction method without undergoing any pre-treatment (Bao et al. 2007; Entwistle et al. 2018; Ghosh et al. 2022; Bristogianni and Oikonomopoulou 2022).

For understanding the sizes, shapes, and morphology of any nanomaterial various characterization techniques are required for the measurement. X- ray diffractometry (XRD) is one of the techniques adopted for the characterization of the nanomaterials and hence considered to be the fingerprint of the substance. It is a nondestructive and non- contact analytical technique. For accurate quantification of the interfacial atomic arrangements, the XRD intensities can be measured. The principle of XRD is based upon the Bragg's Law ($\lambda = 2d\sin\theta$) that relates the wavelength (λ) of the incident radiations to the distance between the two adjacent planes (d) and the diffraction angle (θ) (Rao and Biswas 2009; Sharma et al. 2012; Boddolla).

The present work aims to investigate the potential use of glass as an alternative source of SiO_2 and its reduction to Si using the XRD analysis. The XRD results have also been supported by the other characterization techniques such as Raman spectroscopy, Scanning Electron Microscopy, and Transmission Electron Microscopy.

2. Materials and methods

2.1 Materials

All the chemicals were used without further purification. Magnesium powder, Hydrochloric acid, and Hydrofluoric acid were purchased from Merck India Pvt. Ltd. The feed waste glassware was collected from the Laboratory and then crushed followed by grinding into fine powder.

2.2 Methods

2.2.1 Synthesis of Si Nanomaterial

Glass powder and Magnesium powder with 1:1 wt. ratio was homogeneously mixed using the mortar pestle and transferred to a crucible. The crucible filled with the mixture of glass powder and Mg powder was kept in the muffle furnace. The muffle furnace was heated with a heating ramp rate of 5 $^oCmin^{-1}$ and maintained at 650 ^oC for 5 h. After naturally cooling to room temperature, the heat-treated sample was collected and leached with 5 M of hydrochloric acid followed by subsequent washing with deionized water. Then the sample was dried in a hot air oven at 80 ^oC for 12 h. The obtained sample was then immersed in hydrofluoric acid (HF) for 1 h and repeatedly washed with deionized water. The product was finally dried at 80 ^oC for 12 h in a hot air oven. After drying the sample was collected and labelled GM_BH, GM_AH, GM_HCl, SiNM where G and M stand for Glass and Magnesium respectively, BH, AH, HCl stand for Before heat treatment, After heat treatment, HCl treated samples respectively and the final product has been denoted as SiNM which indicates the Silicon nanomaterial. These samples were further used for characterization.

2.2.2 Characterization of Material Properties

https://doi.org/10.36375/prepare_u.iiche.a386

The formation of the sample was confirmed by subjecting it different characterization techniques.

The crystal structure and phase evolution of the samples were investigated by powder X-ray diffractometry. The patterns were recorded on Rigaku Miniflex 600, using Cu K□ source having radiation of wavelength 1.54Å operated at 40 kV and 15 mA. This has been operated within an angular scan range (2□□ from 10º - 80º at a scanning speed of 2ºmin^{-1} and a step size set to 0.02º. The crystalline phases present in the samples were determined by comparing the peak positions and intensities with those listed in the Powder Diffraction File (PDF 2) data base. To further confirm the structural information and purity Raman spectroscopy was employed by using a Labram HR 10 Confocal Micro- Raman spectrometer at an excitation wavelength of 532 nm. The morphology of the prepared material was determined by JEOL JSM 7600 F Field Emission Gun-Scanning Electron Microscope (FEG-SEM) equipped with Energy Dispersive X-ray (EDX). The High-Resolution Transmission Electron Microscopy (HRTEM) Micrograph was obtained using Talos F200i S/TEM operated at 200 kV.

3. Results and discussions

The Si nanomaterial has been synthesized via magnesiothermic reduction of waste glassware collected from the laboratory in a muffle furnace. In order to clearly identify the phase transformation of amorphous glass to crystalline Si, the powder XRD analysis has been performed and shown in Fig. 1. The diffraction patterns of the feed glass (WG), reducing agent magnesium (Mg) along with the samples after every treatment steps (GM_AH, GM_HCl) and product (SiNM) have been compared in Fig. 1a. Every diffractogram has been measured in the angular range of 2θ between 10º - 80 º. The feed glass exhibited a noticeable broad hump near 22 º that corresponds to the amorphous phase of the SiO_2. The reducing agent Mg powder exhibited sharp crystalline peaks at 2Ɵ 32.1º, 34.3 º, 36.5 º, 47.7 º, 57.3 º, 63 º, 68.6 º, and 70 º that is attributed to the hexagonal crystal system of Mg phase (PDF card no. 01-071-4618). After heat treatment of the glass and Mg powder mixture, the reduced coarse sample (GM_AH) showed the sharp peaks of Si along with the phases of Magnesium oxide (MgO) and Magnesium silicate (Mg_2SiO_4). The XRD pattern of the reduced sample has been well matched with the PDF card of the Si (PDF card no. 00-005-0565), MgO (PDF card no. 01-076-2583) and Mg_2SiO_4 (PDF card no. 01-077-9267) shown in Fig. 1b and in Fig. 1c and 1d exhibits the attribution of Si, MgO phases to the cubic crystal structure whereas Fig. 1e reveals the orthorhombic crystal structure of Mg_2SiO_4. The missing of the broad hump near 22 º and the peaks corresponding to the Mg phase suggests the effective reduction of SiO_2 to Si and conversion of Mg to Mg- byproducts. Further on treatment with HCl acid, the sample (GM_HCl) shown the distinct five peaks of Si, which is attributed to the dissolving of MgO and Mg_2SiO_4 using HCl and removal of the Mg salts after subsequent washing with deionized water. The XRD analysis performed on the final product (SiNM) exhibited five obvious peaks which can be indexed to the cubic phase of Si. The XRD peaks obtained at 2θ of 28.8º, 47.8º, 56.7º, 69.7ºand 77.1º are correspond to the hkl (111), (220), (311), (400), and (331) respectively. The sharp peaks obtained are attributed to the formation of crystalline Si. However, it has been observed that the crystallinity has not been affected of the final product after etching with HF acid.

https://doi.org/10.36375/prepare_u.iiche.a386

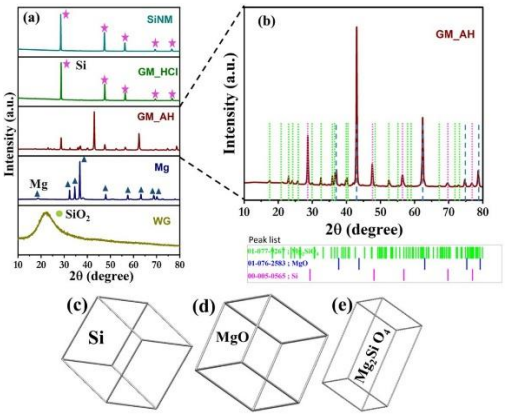

Fig. 1 XRD pattern (a) waste glass (WG, bottom), Mg powder (Mg), After heat treated sample (GM_AH), After HCl leached (GM_HCl), Final Product (SiNM); (b)magnified After heat treated sample (GM_AH) along with peak matching; Crystal Structure of phases (c)Si ; (d) MgO ; (e) Mg_2SiO_4

The XRD results has been corroborated with the phase quantification performed using the Rietveld method. Using the Rietveld analysis, the phase distribution has been measured and demonstrated in Fig. 2. It is clearly observed from the Fig. 2a, the Si content increased from 19.1% to 96.7 % in comparison with the other two phases (MgO and Mg_2SiO_4). It is also evident that the formation of Mg_2SiO_4 phase is almost negligible. However most of the MgO produced after heat treatment, eventually gets lowered after two step acid leaching. This again suggests the proper removal of the Mg byproduct after acid leaching and also the less favouring of the side reaction between MgO formed at the interface and the unreacted SiO_2 to form Mg_2SiO_4.

The diffraction pattern of SiNM has been further analyzed by Rietveld refinement program. The XRD profile correspond to the cubic phase structure along with the space group

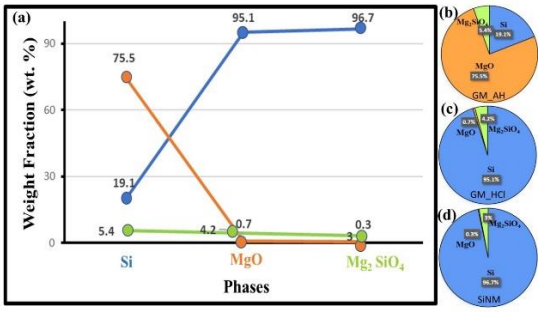

Fig. 2 (a) Quantitative phase analysis using Rietveld Method; Pie chart for the phase distribution (b) GM_AH, (c) GM_HCl, (d) SiNM

of Fd-3m. The Rietveld refinement parameter values obtained as profile R-factor (Rp): 4.21%, weighted profile R-factor (R_{wp}): 6.51%, expected R-factor (R_{exp}): 2.71%, and goodness of fit (χ^2): 7.39%. The fitted parameter values agree with the crystallographic model and the experimental XRD data. The primary crystallite size of SiNM has been found to be in the range of 45 nm - 50 nm, determined by the Debye Scherrer's Equation (Eq.1) and considering the FWHM correspond to the intense peak assigned to (111) plane.

$$\mathbf{D} = \frac{\mathbf{k\lambda}}{\mathbf{\beta cos\theta}} \qquad \text{Eq.1}$$

where D is the crystallite size, k is the shape factor, λ is the wavelength, β is the FWHM, 2Θ is the Bragg's angle.

The interplanar distance related to the (111) plane and the lattice parameter a for the cubic phase of Si has been estimated using the Bragg;s Equation (Eq.2) and found to be 3.137Å and 5.43 Å respectively.

$$\mathbf{n\lambda = 2dsin\theta} \qquad \text{Eq.2}$$

Furthermore, as a complement to XRD analysis, both the crystallinity and purity has been confirmed by the Raman analysis shown in Fig. 3 The Raman spectrum

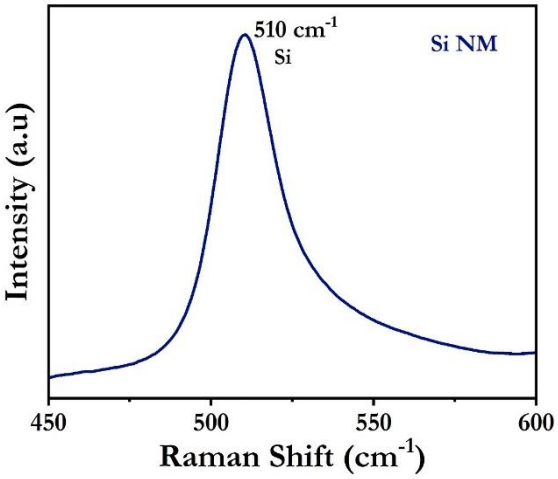

Fig. 3 Raman Spectroscopy of SiNM

of the final product (SiNM) after HF treatment depicted a clear peak at 510 cm^{-1}

that corresponds to the crystalline Si. Additionally, the absence of amorphous peak of Si at 480 cm^{-1} implies the crystalline phase of Si. The distinct peak at 510 cm^{-1} which is much lower than the bulk Si at 520 cm^{-1} suggests the formation of nano-scaled Si.

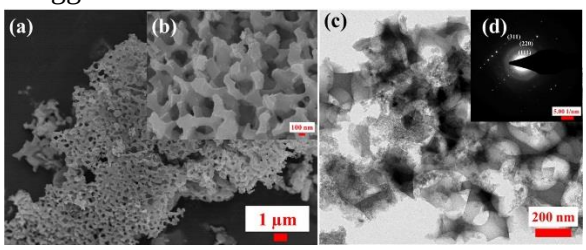

Fig. 4 SEM image of SiNM (a) low magnification, (b) high magnification (inset); (c) HRTEM image of SiNM, (d) SAED pattern of SiNM (inset)

The morphology of the product (SiNM) after magnesiothermic reduction and two step acid leaching process has been investigated by FESEM and HRTEM shown in Fig.4. The FESEM image in Fig 4a and 4b revealed the highly porous matrix of crystalline Si nanomaterial. The porosity can be attributed to the selective elimination of the imbedded Mg by-products such as MgO and Mg_2SiO_4 phases. The HRTEM image in Fig. 4c has also confirmed the formation of the porous network. The selected area electron diffraction pattern shown in Fig. 4d (inset) exhibited the (111), (220) and (311) is also in consistent with the XRD pattern of SiNM and moreover the dots observed in the pattern confirms the polycrystallinity of the material. The SiNM produced using the waste laboratory glassware found to be pure as determined by the XRD, Raman, SEM and TEM analysis.

4. Conclusion

In summary, Si nanomaterial was fabricated through magnesiothermic reduction using waste laboratory glassware as an alternative source of SiO_2. To confirm the formation of the material the present study was concerned to retrieve the important information related to the phase transformation, phase content, crystallographic structure, space group, lattice parameter, interplanar distance, crystallite size using the X-ray Diffractometry Analysis. The study revealed the conversion of amorphous SiO_2 contained in the waste glass feed to crystalline Si nanomaterial through the XRD patterns. The wt % of the cubic phase Si coupled with cubic phase of MgO and orthorhombic Mg_2SiO_4 phase have been observed where Si content found to be higher with negligible amount of Mg_2SiO_4 and reduced content of MgO. The average domain size of SiNM was found to range between 45- 50 nm. The Raman, FESEM and HRTEM analysis further complimented the XRD results and confirmed the formation of pure Si nanomaterial from waste laboratory glassware.

Acknowledgment

The authors express their gratitude to School of Engineering and Applied Science, Ahmedabad University for offering the laboratory and instrumental facilities. The authors would also like to acknowledge the financial support received by Ahmedabad University under seed grant through Grant no. URBSEASI22A1/SG/22-23/05_SD_10.23. Authors are also thankful to sophisticated analytical instrument facilities at SAIF, IIT Bombay and Sophisticated Instrumentation Centre for Applied Research & Testing (SICART), Anand, Gujarat for providing the sophisticated analytical instrumental facilities of FEG-SEM and HRTEM.

References

1. Bao Z, Weatherspoon MR, Shian S, et al (2007) Chemical reduction of three-dimensional silica micro-assemblies into microporous silicon replicas. Nature 446:172–175. https://doi.org/10.1038/nature05570
2. Betty C (2008) Porous Silicon: A Resourceful Material for Nanotechnology. NANOTEC 2:128–136. https://doi.org/10.2174/187221008784534514

3. Boddolla S A review on Characterization techniques of Nanomaterials. International Journal of Engineering
4. Bristogianni T, Oikonomopoulou F (2022) Glass up-casting: a review on the current challenges in glass recycling and a novel approach for recycling “as-is” glass waste into volumetric glass components. Glass Struct Eng. https://doi.org/10.1007/s40940-022-00206-9
5. Chan CK, Peng H, Liu G, et al (2008) High-performance lithium battery anodes using silicon nanowires. Nat Nanotechnol 3:31–35. https://doi.org/10.1038/nnano.2007.411
6. Chandra Muduli R, Kale P (2023) Silicon nanostructures for solid-state hydrogen storage: A review. International Journal of Hydrogen Energy 48:1401–1439. https://doi.org/10.1016/j.ijhydene.2022.10.055
7. Choi M, Kim J-C, Kim D-W (2018) Waste Windshield-Derived Silicon/Carbon Nanocomposites as High-Performance Lithium-Ion Battery Anodes. Sci Rep 8:960. https://doi.org/10.1038/s41598-018-19529-1
8. Entwistle J, Rennie A, Patwardhan S (2018) A review of magnesiothermic reduction of silica to porous silicon for lithium-ion battery applications and beyond. J Mater Chem A 6:18344–18356. https://doi.org/10.1039/C8TA06370B
9. Falk G, Shinhe GP, Teixeira LB, et al (2019) Synthesis of silica nanoparticles from sugarcane bagasse ash and nano-silicon via magnesiothermic reactions. Ceramics International 45:21618–21624. https://doi.org/10.1016/j.ceramint.2019.07.157
10. Favors Z, Wang W, Bay HH, et al (2015) Scalable Synthesis of Nano-Silicon from Beach Sand for Long Cycle Life Li-ion Batteries. Sci Rep 4:5623. https://doi.org/10.1038/srep05623
11. Furquan M, Raj Khatribail A, Vijayalakshmi S, Mitra S (2018) Efficient conversion of sand to nano-silicon and its energetic Si-C composite anode design for high volumetric capacity lithium-ion battery. Journal of Power Sources 382:56–68. https://doi.org/10.1016/j.jpowsour.2018.02.011
12. Ghosh M, Khuntia S, Dalai S (2022) Effect of Molar Ratio of Feed on the Facile Synthesis of Silicon Nanosheets from Laboratory Waste Glass. In: Mukherjee K, Layek RK, De D (eds) Tailored Functional Materials. Springer Nature, Singapore, pp 131–140
13. He Y, Fan C, Lee S-T (2010) Silicon nanostructures for bioapplications. Nano Today 5:282–295. https://doi.org/10.1016/j.nantod.2010.06.008
14. Kang W, Kim J-C, Kim D-W (2020) Waste glass microfiber filter-derived fabrication of fibrous yolk-shell structured silicon/carbon composite freestanding electrodes for lithium-ion battery anodes. Journal of Power Sources 468:228407. https://doi.org/10.1016/j.jpowsour.2020.228407
15. Kang W, Kim J-C, Noh JH, Kim D-W (2019) Waste Liquid-Crystal Display Glass-Directed Fabrication of Silicon Particles for Lithium-Ion Battery Anodes. ACS Sustainable Chem Eng 7:15329–15338. https://doi.org/10.1021/acssuschemeng.9b02654
16. Kuang L, Mitchell BS, Fink MJ (2015) Silicon nanoparticles synthesised through reactive high-energy ball milling: enhancement of optical properties from the removal of iron impurities. Journal of Experimental Nanoscience 10:1214–1222. https://doi.org/10.1080/17458080.2014.989552
17. Kumar SM, Murugan K, Chandrasekhar SB, et al (2012) Synthesis and characterization of nano silicon and titanium nitride powders using atmospheric microwave plasma technique. J Chem Sci 124:557–563. https://doi.org/10.1007/s12039-012-0256-y
18. Pakuła D, Marciniec B, Przekop RE (2023) Direct Synthesis of Silicon Compounds—From the Beginning to Green Chemistry Revolution. AppliedChem 3:89–109. https://doi.org/10.3390/appliedchem3010007
19. Peng F, Wang J, Ge G, et al (2013) Photochemical reduction of CO2 catalyzed by silicon nanocrystals produced by high energy ball milling. Materials Letters 92:65–67.

https://doi.org/10.1016/j.matlet.2012.10.059
20. perrone donnorso M, Miele E, De angelis F, et al (2012) Nanoporous silicon nanoparticles for drug delivery applications. Microelectronic Engineering 98:626–629. https://doi.org/10.1016/j.mee.2012.07.095
21. Priolo F, Gregorkiewicz T, Galli M, Krauss TF (2014) Silicon nanostructures for photonics and photovoltaics. Nature Nanotech 9:19–32. https://doi.org/10.1038/nnano.2013.271
22. Rao CNR, Biswas K (2009) Characterization of Nanomaterials by Physical Methods. Annual Rev Anal Chem 2:435–462. https://doi.org/10.1146/annurev-anchem-060908-155236
23. Ryu J, Hong D, Choi S, Park S (2016) Synthesis of Ultrathin Si Nanosheets from Natural Clays for Lithium-Ion Battery Anodes. ACS Nano 10:2843–2851. https://doi.org/10.1021/acsnano.5b07977
24. Sharma R, Bisen DP, Shukla U, Sharma BG (2012) X-ray diffraction: a powerful method of characterizing nanomaterials. Recent Research in Science and Technology
25. Silviana S, Bayu WJ (2018) Silicon Conversion From Bamboo Leaf Silica By Magnesiothermic Reduction for Development of Li-ion Baterry Anode. MATEC Web Conf 156:05021. https://doi.org/10.1051/matecconf/201815605021
26. Wang H, He Y (2017) Recent Advances in Silicon Nanomaterial-Based Fluorescent Sensors. Sensors 17:268. https://doi.org/10.3390/s17020268

https://doi.org/10.36375/prepare_u.iiche.a387

Funtionalization of Titanium Metal Oxide Nanoparticles with Synthetic Polymer

Mansi Tiwari[a*], S.V.A.R.Sastry[b], Sandeep Kumar[c]
[a]*Research Scholar, Department of Chemical Engineering,*
Harcourt Butler Technical University, Kanpur, U.P., India. Pin-208002.
[b]*Associate Professor, Department of Chemical Engineering,*
& Associate Dean, Research & Development,
Harcourt Butler Technical University, Kanpur, U.P., India. Pin-208002.
[c]*Scientist 'E' & Deputy Director,*
Defence Materials and Stores Research and Development Establishment, Kanpur, U.P., India.
Corresponding author- tiwariman21220@gmail.com

Abstract
Functionalization of titanium dioxide (TiO_2) nanoparticles with synthetic polymers is an important area of research due to the wide range of potential applications in fields such as catalysis, sensors, drug delivery, and photovoltaics. The process involves modifying the surface of TiO_2 nanoparticles with synthetic polymers to improve their stability, dispersibility, and interaction with other materials. This abstract elucidates the rationale behind this dynamic field, encompassing the enhancement of TiO_2 nanoparticle stability, surface modification for tailored reactivity, controlled release mechanisms, and improved photocatalytic properties. With applications spanning from catalysis to drug delivery and photovoltaics, the functionalization of TiO_2 nanoparticles offers transformative potential. Characterization techniques such as Transmission Electron Microscopy, FTIR Spectroscopy analysis are essential for understanding the resulting nanoparticle-polymer hybrid materials structural and physicochemical properties. This process involves modifying the surface characteristics of TiO2 nanoparticles through the integration of synthetic polymers, thereby imparting diverse functionalities and enhancing their utility in a myriad of applications.

Keywords: nanoparticles; titanium metal oxide; synthetic polymers.

1. Introduction

The remarkable mechanical qualities, resistance to corrosion, and biocompatibility of titanium and its alloys have earned them great respect across a wide range of industries, including chemical, aerospace, and biomedical engineering. However, obtaining the best possible functionality and surface qualities is frequently a crucial prerequisite in these applications. One extensively researched method for improving titanium's performance and customizing its surface properties is surface modification. The use of synthetic polymers, such as polyethylene glycol (PEG) and polyvinyl alcohol (PVA), has become apparent as a potential strategy among the various surface modification techniques available[1]. For a number of reasons, the functionalization of TiO_2 surfaces using artificial polymers like PEG and PVA is very interesting. First off, it makes it possible to create surfaces for biomedical implants that are bioactive and fouling-resistant, as well as improve the tribological characteristics of aerospace components[2]. Second, based on the particular application and functionalization method used, these polymers' adaptability enables a broad range of surface attributes to be created. Thirdly, PVA and PEG are both advantageous due to their biocompatibility and simplicity of handling, which makes them ideal for a range of uses[3,4]. This study compares and examines the functionalization of TiO_2 surfaces using

https://doi.org/10.36375/prepare_u.iiche.a387

synthetic polymers, PEG and PVA. Through an examination of the procedures, outcomes, and consequences of these adjustments, we want to clarify the benefits and constraints of every polymer in terms of surface functionalization. This work intends to advance the fields of surface science and material engineering by providing a thorough analysis of how PEG and PVA might be used to optimize titanium surfaces for various engineering and biomedical applications[5].

2. **Materials and Methods:** Ethyl acetate, polyethylene glycol (PEG 6000), poly vinyl alcohol, sodium lauryl sulfate, distilled water, titanium oxide and HCl.

2.1 Equipment and Method: Ultrasonicator (Model: AB-34, Make: Digital pro+) and Solvent Evaporation.

2.2 Parameters varied*:* Temperature (30-80^0C)

In this paper, Solvent Evaporation methods are used to form nanoparticles with selective raw materials such as PVA and PEG.

2.3 Formation of TiO_2-NPs via solvent evaporation method

Phase I was prepared as follows: 30 ml water was placed in a beaker, and 2 gm of surfactant was thoroughly mixed in it. Phase II was prepared as follows: 5.5 gm of titanium oxide was dispersed in 25 ml of solvent (HCL). Two phases are prepared that are immiscible. Emulsification and mixing were performed by using an ultrasonicator at 80°C for 90 min. The nanoparticles formed were placed in a desiccator at room temperature for 24 hrs for moisture removal.

2.4 Ultrasonication:

Use an ultrasonicator to further disperse the nanoparticles in the PEG and PVA solution at 80^0C for 2 hours. Ultrasonication helps break up any nanoparticle agglomerates and ensures a homogenous dispersion. Ultrasonicate the mixture for a sufficient amount of time, depending on the nanoparticle size and the equipment used.

2.5 Functionalizing titanium oxide nanoparticles with PEG :

Functionalizing TiO_2 nanoparticles with Polyethylene Glycol (PEG) typically involves a series of steps to ensure effective coating and stabilization of the nanoparticles. Below are the general steps for functionalizing TiO_2 nanoparticles with PEG:

Preparation of PEG Solution: PEG is a water-soluble polymer and is available in various molecular weights use (PEG6000). Dissolve 50gm of PEG6000 mol.wt. in 100ml water. A PEG solution is prepared by dissolving PEG in a suitable solvent, such as water to create a stable and homogenous solution.

Mixing Titanium Nanoparticles with PEG Solution: Take 0.5 gm of synthesized TiO_2 nanoparticles are mixed with the PEG solution. The mixing can be achieved through ultrasonication at 80^0C for 2 hours to ensure the uniform dispersion of the nanoparticles within the PEG solution.

Surface Adsorption or Ligand Exchange: The functionalization of TiO_2 nanoparticles with PEG can occur through surface adsorption or ligand exchange leave the solution for 24 hours. In surface adsorption, PEG molecules adsorb onto the surface of the TiO_2 nanoparticles, forming a protective coating. In ligand exchange, existing surface ligands on the nanoparticles are replaced by PEG molecules.

Reaction and Coating Formation: The mixture of TiO_2 nanoparticles and PEG solution is allowed to react under controlled conditions, which may involve heating or other specific parameters. During this process, the PEG

https://doi.org/10.36375/prepare_u.iiche.a387

molecules bind to the surface of the nanoparticles, forming a stable and uniform coating.

Removal of Excess PEG: After functionalization, any excess PEG that has not bound to the TiO_2 nanoparticles needs to be removed. This is typically done through purification step i.e precipitation. Purification ensures that only PEG-functionalized TiO_2 nanoparticles are retained.

2.6 Functionalizing titanium oxide nanoparticles with PVA:

Functionalizing TiO_2 nanoparticles with a polyvinyl alcohol (PVA) solution is a common method to improve their dispersion and stability in various applications, such as in nanocomposite materials or coatings. Here's a general guide on how to functionalize TiO_2 nanoparticles with a PVA solution:

Preparation the PVA Solution: Dissolve 50gm the PVA powder in 100 ml of distilled water to create a PVA solution. The concentration of PVA can vary, but a concentration of 1-5% PVA in water is typically suitable for functionalization. Use a container and stir the solution until the PVA is fully dissolved.

Mixing of PVA Solution and titanium oxide Nanoparticles: Add the prepared PVA solution to the 0.5gm of TiO_2 nanoparticles. The amount of PVA should be carefully chosen based on the desired functionalization and dispersion level. Stir the mixture to ensure even coating of the nanoparticles.

Drying of Functionalized Nanoparticles from the PEG and PVA solutions: functionalized TiO_2 nanoparticles from the PEG and PVA solution. Allow them to air-dry at room temperature. Rinse the functionalized nanoparticles with deionized water to remove any residual PEG and PVA solution.

3. Characterization of TiO_2 Nanoparticles:

The functionalized TiO_2 nanoparticles can be characterized to confirm the successful functionalization. Characterization techniques such as transmission electron microscopy (TEM), scanning electron microscopy (SEM), dynamic light scattering (DLS), and Fourier-transform infrared spectroscopy (FTIR) can be used to analyze the size, structure, and presence of PEG on the nanoparticle surface.

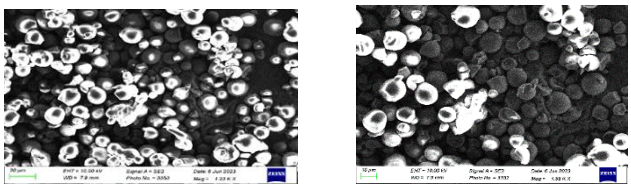

Figure. 1 FESEM images of Functionalized TiO2 NPs with PEG

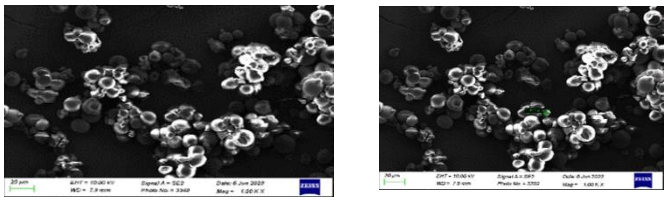

Figure. 2 FESEM images of Functionalized TiO2 NPs with PVA

Stability Testing: The stability of the PEG-functionalized TiO_2 nanoparticles is assessed under various conditions to ensure their long-term stability and dispersibility. Stability testing provides valuable insights into how PVA-functionalized TiO_2 nanoparticles perform under various conditions and can help ensure the nanoparticles' suitability for your intended use.

4. Results

The functionalization of TiO_2 nanoparticles with PEG shown in (Figure 1) improves their stability, biocompatibility, and dispersibility in both aqueous and non-aqueous environments. PEG-functionalized TiO_2 nanoparticles find applications in various fields, including drug delivery, imaging, and biomedical research. The specific parameters and conditions for functionalization may vary based on the desired properties and applications of the functionalized TiO_2 nanoparticles. Optimization of the process is crucial to achieve the desired results.

The functionalization of TiO_2 nanoparticles with PVA (Figure 2) improves their film formation, biodegradability, film thickness supports ecofriendly. PVA have their unique advantages and are suitable for various applications. The choice between them will depend on the specific characteristics. If you need a stable film, controllable film thickness, or biodegradability, PVA could be the better choice.

5. Conclusion

Studies on the functionalization of TiO_2 with PVA and PEG on the utilization of solvent evaporation technique for the demonstrated their potential in advancing the field of automotive and biomedical applications. Both offer distinct advantages and can be tailored to achieve functionalization of TiO_2 however, the functionalization of titanium metal oxide nanoparticles with polyethylene glycol (PEG) and polyvinyl alcohol (PVA) polymers represents a significant advancement in the field of nanomaterials and materials science. This research has demonstrated the successful modification of titanium metal oxide nanoparticles with these biocompatible polymers, which has opened up a wide range of potential applications in various fields.

References

1. S. V. Jadhav, D. S. Nikam, V. M. Khot, S. S. Mali, C. K. Hong, and S. H. Pawar, “PVA and PEG functionalised LSMO nanoparticles for magnetic fluid hyperthermia application,” *Mater. Charact.*, vol. 102, pp. 209–220, Apr. 2015, doi: 10.1016/j.matchar.2015.03.001.
2. S. Metanawin, P. Panutumron, A. Thongsale, and T. Metanawin, “The functionalization of hybrid titanium dioxide by miniemulsion polymerization technique,” *Mater. Today Proc.*, vol. 5, no. 3, pp. 9651–9657, 2018, doi: 10.1016/j.matpr.2018.01.133.
3. A. A. Roslan, S. N. A. Zaine, H. Mohd Zaid, M. Umar, and H. G. Beh, “Nanofluids stability on amino-silane and polymers coating titanium dioxide and zinc oxide nanoparticles,” *Eng. Sci. Technol. an Int. J.*, vol. 37, p. 101318, Jan. 2023, doi: 10.1016/j.jestch.2022.101318.
4. S. Rahim, M. Sasani Ghamsari, and S. Radiman, “Surface modification of titanium oxide nanocrystals with PEG,” *Sci. Iran.*, vol. 19, no. 3, pp. 948–953, Jun. 2012, doi: 10.1016/j.scient.2012.03.009.
5. Z. Noroozi and O. Bakhtiari, “Preparation of amino functionalized titanium oxide nanotubes and their incorporation within Pebax/PEG blended matrix for CO2/CH4 separation,” *Chem. Eng. Res. Des.*, vol. 152, pp. 149–164, Dec. 2019, doi: 10.1016/j.cherd.2019.09.030.

https://doi.org/10.36375/prepare_u.iiche.a388

Biocompatible Approaches in Synthesis of Polymeric Nanoparticles

Mansi Tiwari[a*], S.V.A.R.Sastry[b], Sandeep Kumar[c]

[a]Research Scholar, Department of Chemical Engineering,
Harcourt Butler Technical University, Kanpur, U.P., India. Pin-208002.
[b]Associate Professor, Department of Chemical Engineering,
& Associate Dean, Research & Development,
Harcourt Butler Technical University, Kanpur, U.P., India. Pin-208002.
[c]Scientist 'E' & Deputy Director,
Defence Materials and Stores Research and Development Establishment, Kanpur, U.P., India.
Corresponding author- tiwariman21220@gmail.com

Abstract

Polymeric nanoparticles have shown immense potential in different applications due to their biocompatibility, tuneable properties, and versatile functionalities. As the demand for safe and effective nanoparticles continues to rise, researchers have been exploring innovative synthesis techniques to develop biocompatible polymeric nanoparticles with enhanced therapeutic efficacy and reduced toxicity. This article aims to present an overview of the latest emerging trends in the synthesis of biocompatible polymeric nanoparticles. Each trend is explored in terms of its potential advantages, challenges, and applications in different nanofields. Furthermore, the article highlights the importance of considering biocompatibility, toxicity, and regulatory considerations in the development of these advanced polymeric nanoparticles. The article concludes with future prospects and potential directions for research in the field of biocompatible polymeric nanoparticles synthesis.

Keywords: Biocompatible; Characterization; Polymer; Polymeric nanoparticles; Synthesis.

Introduction

PNPs are so tiny and helpful in polymer-based nanoparticles. They are the colloidal organic compounds in nano size with polymeric material which produced polymer nanoparticles (PNPs) within size range of 1-1000 nm. The polymeric core of the active compounds can be loaded moreover surface-adsorption as well as internally.

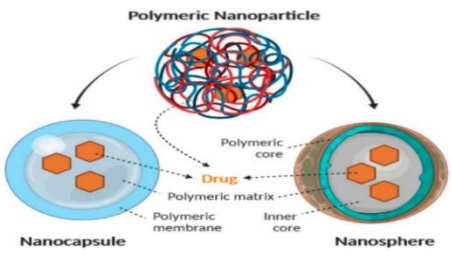

Fig.1 Diagram of the structure of nanocapsules and nanospheres by PNPs[1]

Preparation Techniques of Polymeric Nanoparticles

Techniques define specific solvent contain specific emulsification. These techniques are Solvent Diffusion, Nanoprecipitation, Solvent Evaporation, Reverse Salting-Out.

Emulsification/Solvent Diffusion

The technique involves creating an oil-in-water emulsion by mixing water miscible solvent containing both the drug and polymer [1], with a solution containing surfactant. In this emulsion technique, the internal phase of the emulsion is composed of a hydro miscible solvent, like ethyl acetate. This step is crucial in ensuring the formation of stable emulsions, which is important for the successful synthesis of PNPs. Upon dilution with a huge quantity of water; the droplets dispersed in the emulsion undergo solvent diffusion into the external aqueous phase. This process ultimately leads to formation of colloidal particles that consist of the polymer.

Nanoprecipitation

https://doi.org/10.36375/prepare_u.iiche.a388

This technique allows the production of nanoparticles with controlled size, shape, and surface properties. Nanoprecipitation can be used to synthesize nanoparticles with a variety of polymers, including biodegradable and biocompatible polymers [8]. These polymers have unique physical and chemical properties that make them useful for various applications. This is a versatile and effective method for the synthesis of polymeric nanoparticles with various applications in medicine, energy, and agriculture. Continued research and development in this field could lead to significant progressions in science and technology, improving the quality of life and addressing some of the most pressing global challenges.

Solvent evaporation

It is a simple and versatile method that involves the dissolution of a polymer and a drug or other active agent in an organic solvent [3]. The resulting solution is then added dropwise to a surfactant-containing aqueous phase, while stirring at high speeds to form an emulsion. The solvent is then evaporated under reduced pressure, which causes the polymer to precipitate and form nanoparticles.

Emulsification/Reverse Salting-Out

This is a technique that relies on the separation of a hydrophilic solvent from aqueous solution via salting-out effect, which can lead to the creation of nanospheres [4]. The hydrophobic drug is then added to the organic phase, and the solvent is removed by evaporation under reduced pressure. The resulting nanospheres are stabilized by a surfactant, which prevents particle aggregation. This method is simple and fast, and it allows for the production of monodisperse nanospheres with a narrow size distribution dimensions ranging from 170 to 900 nm.

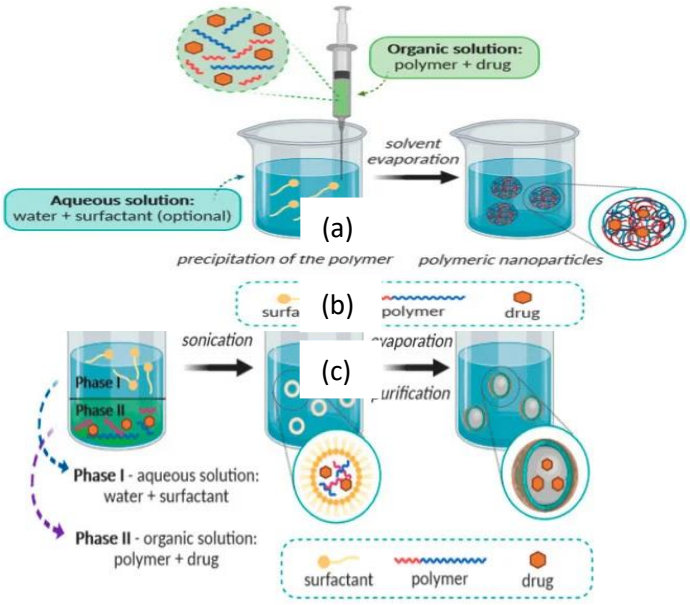

(d)

Fig.2 (a) solvent diffusion method, (b)solvent evaporation, (c) nanoprecipitation method, (d) reverse salting-out method.

Characterization

Characterization techniques are essential for the study and evaluation of PNPs. Some of the commonly used characterization techniques for PNPs are Dynamic Light Scattering (DLS), Transmission Electron Microscopy (TEM), Atomic Force Microscopy (AFM), Fourier Transform Infrared Spectroscopy (FTIR), X-ray Photoelectron Spectroscopy (XPS), Differential Scanning Calorimetry (DSC), Zeta Potential Analysis. These techniques can help

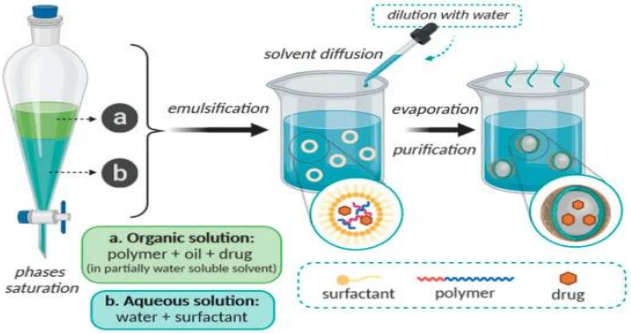

https://doi.org/10.36375/prepare_u.iiche.a388

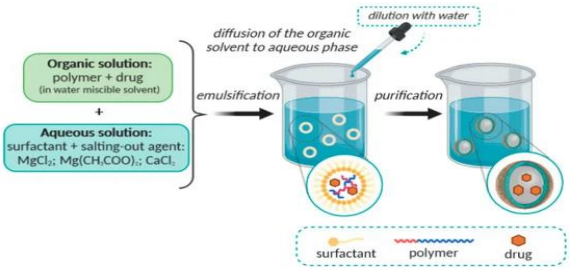

in the development of new applications for these materials [5-7].

Prominent applications of PNPs

The latest advancements in the integration of inorganic nanoparticles into polymers have allowed for the alteration of the physical and chemical properties of polymers.

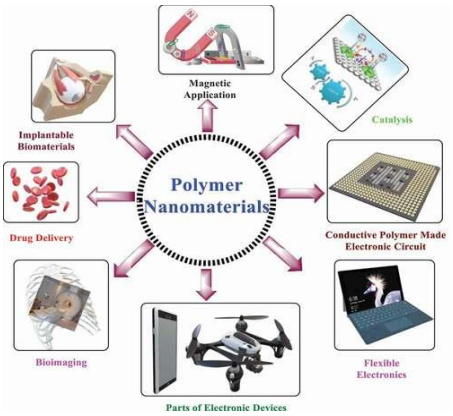

Fig. 3 Applications of polymeric nanoparticles

Magnetic application

Due to versatile nature of PNPs, the use of magnetic polymeric nanoparticles in these areas has expanded significantly, leading to rapid growth in research to develop novel magnetic nanoparticles with improved properties.

Flexible electronics

Manufacturing of electronic devices polymeric nanoparticle plays important role in it to make it light in weight, easy to use, easy to carry.

Drug delivery

Polymer-based medication transport phenomena are of great interest for both theoretical research and clinical applications which focus on the development of nanocarriers with diagnostic and therapeutic objectives [2,6].

Bioimaging

Polymer nanoparticles have emerged as a valuable tool for bioimaging, with various techniques such as computerized tomography (CT), magnetic resonance imaging (MRI), positron emission tomography (PET) and ultrasound imaging, being developed for biological systems imaging.

Medicinal applications

Polymer nanoparticles have found numerous applications in medical science which shows significant attention from scientists for their potential applications in medical science, owing to their desirable properties such as biocompatibility, biodegradability, low cytotoxicity, and others [7].

Conclusions

This paper explained about the different preparation techniques of polymeric nanoparticles and the significant methods used for characterization of polymeric nanoparticles using Electron microscopy, FTIR and DSC. At room temperature, the polymer nanoparticle solutions exhibited a maximum absorption spectrum within the nanometer range. The properties of polymeric nanoparticles can be engineered to further include biocompatibility and biodegradability.

References

1. Souto E.B., Souto S.B., Campos J.R., Severino P., Pashirova T.N., Zakharova L.Y., Silva A.M., Durazzo A., Lucarini M., Izzo A.A., et al. Nanoparticle Delivery Systems in the Treatment of Diabetes Complications. Molecules. 2019; 24:4209. doi: 10.3390/molecules24234209.
2. Vasile C. Polymeric Nanomaterials in Nanotherapeutics. Elsevier; London, UK: 2018.
3. Szczęch M., Szczepanowicz K. Polymeric Core-Shell Nanoparticles Prepared by Spontaneous Emulsification Solvent Evaporation and Functionalized by the Layer-by-Layer

Method. Nanomaterials. 2020;10:496 . doi: 10.3390/nano10030496.
4. Krishnamoorthy K., Mahalingam M. Selection of a suitable method for the preparation of polymeric nanoparticles: Multi-criteria decision making approach. Adv. Pharm. Bull. 2015;5:57.
5. Crucho C.I.C., Barros M.T. Polymeric nanoparticles: A study on the preparation variables and characterization methods. Mater. Sci. Eng. C Mater. Biol. Appl. 2017;80:771–784. doi: 10.1016/j.msec.2017.06.004.
6. Bohrey S., Chourasiya V., Pandey A. Polymeric nanoparticles containing diazepam: Preparation, optimization, characterization, in-vitro drug release and release kinetic study. Nano Converg. 2016;3:1–7. doi: 10.1186/s40580-016-0061-2.
7. Vasile C. Polymeric Nanomaterials in Nanotherapeutics. Elsevier; London, UK: 2018
8. Martinez Rivas C.J., Tarhini M., Badri W., Miladi K., Greige-Gerges H., Nazari Q.A., Galindo Rodriguez S.A., Roman R.A., Fessi H., Elaissari A. Nanoprecipitation process: From encapsulation to drug delivery. Int. J. Pharm. 2017;532:66–81. doi: 10.1016/j.ijpharm.2017.08.064.

https://doi.org/10.36375/prepare_u.iiche.a389

Enhancing Irrigation Efficiency Through The Integration Of Potassium-Based Hydrogel In Ldpe Mulch Film For Sustainable Agriculture

Rathna NR[a], Karthick S[a] , Badhrinath S[a] ,Keerthivasan C[a] , Hemanth Kumar B[a] , Aakash M[a]
aDepartment of Plastics Technology, CIPET: Institute of Petrochemicals Technology (IPT), Guindy, Chennai -600032, Tamil Nadu, India

Abstract

Irrigation plays an important role on our daily basis. All consumable green plants are being irrigated under manual supervision. A proper level of water and sunlight (humid condition) is the basic necessity for proper growth and health of the crops. Mulching is the process being followed in places with extreme climate conditions where scarcity of water is high. On the other hand, on recent growth the hydrogels are being used on large scale for agriculture purpose for their tendency to absorb and preserve water.

Thus, using both the concepts, the hydrogels are being incorporated in the mulching film to increase their usage in the field of plasticulture. Mulching film is prepared using Low Density Polyethylene (LDPE) by extrusion process. Potassium based hydrogels are used to improve the production and to maintain the pH of the soil. Thus, mulching film incorporated with potassium-based hydrogels can improvise the production of crops and minimize the usage of surplus water maintaining the nutrition of the soil.

Keywords: Potassium based Hydrogel; Development in irrigation; Improvisation of mulch film; Polymers in agriculture; LDPE with hydrogel; Advancement of polymer in agriculture.

INTRODUCTION :

Objective of the work

The mulching technique has been followed in the arid climatic conditions where water availability is scarce and evaporation is to be avoided. Also, hydrogels are recently used directly on the field which helps to absorb water and deliver it to the crop when required. Thus, instead of using two different techniques, the project focuses on interlocking hydrogels in the mulch film so that a single process can be done. The hydrogel incorporated mulch film helps in conserving evaporation as well hydrogels help to conserve water usage.

1. **Introduction**

Low density polyethylene is the majorly used commodity plastic used by all common people. It is mainly preferred for its easy availability and low cost.

1.2.1 Mulching Process

Mulch is a layer of material applied to the surface of soil. It is a layer of organic or inorganic material placed over the root zone of a plant to benefit the roots and the soil. Organic materials may include wood chips, bark, pine needles, and straw, leaves, or grass clippings. These materials will eventually decompose, adding organic matter to the soil and need to be supplemented or replaced on a regular basis. Inorganic materials typically do not

https://doi.org/10.36375/prepare_u.iiche.a389

decompose, need replacement only occasionally, are often more expensive, and include rock or pebbles, landscape fabric, newspaper, plastic or even shredded rubber tires for playground areas.

Mulching is the process or practice of covering the soil/ground to make more favourable conditions for plant growth, development and efficient crop production. Mulch technical term means 'covering of soil'. While natural mulches such as leaf, straw, dead leaves and compost have been used for centuries, during the last 60 years the advent of synthetic materials has altered the methods and benefits of mulching. The research as well as field data available on effect of synthetic mulches make a vast volume of useful literature. When compared to other mulches plastic mulches are completely impermeable to water; it therefore prevents direct evaporation of moisture from the soil and thus limits the water losses and soil erosion over the surface. In this manner it plays a positive role in water conservation. The suppression of evaporation also has a supplementary effect; it prevents the rise of water containing salt, which is important in countries with high salt content water resources.

Fig 1. Mulching film

Advantages on using plastic mulch

- To supress weed growth

Sunlight helps foster the growth of weeds by compacting soil; plastic mulch blocks sunlight from reaching the soil around the plant, thus preventing weeds from appearing. Black polyethylene and other opaque films in particular are useful for this purpose, blocking a wider range of weeds than organic mulches. The only exception is clear plastic, which lets sunlight in. The presence of fewer weeds also reduces the necessity for mechanical cultivation, leading to less root damage.

- To conserve water in crop production and landscaping

Plastic film with its moisture barrier properties does not allow the soil moisture to escape Water

https://doi.org/10.36375/prepare_u.iiche.a389

that evaporates from the soil surface under mulch film, condenses on the lower surface of the film and falls back as droplets. Thus moisture is preserved for several days and increases the period between two irrigations. The irrigation water or rainfall either moves into the soil thru holes on the mulch around the plant area or through the un-mulched area.

- Better moisture retention

Mulching facilitates even distribution of water and hence soil can retain water for a longer time. It ensures each single crop gets enough water for its well growth.

- Minimized fertilizer leaching

Plastic mulches prevent an excess of water from going into the soil, helping to limit the loss of plant nutrients through leaching. Because the mulch is restrictive in this sense, it is most ideal to use it in conjunction with the drip irrigation method, which allows the addition of water and fertilizer in small amounts.

- Higher crop quality

Plastic mulch helps crops avoid direct contact with soil; this results in the plants being cleaner, which is desirable for fruits such as strawberries. It also works to prevent rot as mud from irrigation is not splashed on the crops.

- Reduction in root damage

The use of plastic mulch creates a practically weed free area around the plant, removing the need for cultivation except between the rows of plastic. Root damage associated with cultivation is therefore eliminated. Due to these factors, the use of plastic mulch can lead to an improvement in the overall growth of the plant.

According to the survey, there are different types of mulch film:

A wide range of plastic films based on different types of polymers have all been evaluated for mulching at various periods in the 1960s. LDPE, HDPE and flexible PVC have all been used and although there were some technical performance differences between them, they were of minor nature. Owing to its greater permeability to long wave radiation which can increase the temperature around plants during the night times, polyethylene is preferred. Today the vast majority of plastic mulch is based on LLDPE because it is more economic in use.

Basic properties of mulch film

a. Air proof so as not to permit any moisture vapour to escape.

b. Thermal proof for preservation of temperature and prevention of evaporation

c. Durable at least for one crop season

Importance of parameters of the plastic film

(a)Thickness

Normally the thickness of the film does not affect the mulching effect except when it is used for solarisation. But some of the recent references do indicate the impact of film thickness on crop yield. Since it is sold by weight it is advantageous to use as thin a film as possible

https://doi.org/10.36375/prepare_u.iiche.a389

but at the same time due consideration should be given for the longevity of the film. The early mulch film used was of 60-75 micron (240-300 gauges) thickness, and today it is possible to have 15 micron thick film due to advent of film extrusion technology. These films are mechanically weak, as shown by their easy tearing when pulled tension.

b) Width

This depends upon the inter row spacing. Normally a one to one and half meter width film can be easily adopted to different conditions.

c) Perforations

The perforations may be advantageous under some situations and disadvantageous for some other situation. The capillary movement of water and fertilizer distribution will be better and more uniform under unperforated condition. But for prevention of water stagnation around the plants, perforation is better. But it has got the disadvantages of encouraging weed growth.

d) Mulch colour

The colour of the mulch affects

i. Soil temperature

ii. Temperature of air around the plants

iii. Soil salinity

a. Due to lesser quantity of water used

b. Due to reduction in evaporation and prevention of upward movement of water.

Transparant film - Deposits more salt on soil surface

Black film - Restricts water movement and upward movement of salt is reduced.

iv. Weed flora - Black film

v. Insect control - Opaque while film acts as golden colour and attracts insects

Mulch Laying Techniques

i. Mulch should be laid on a non-windy condition
ii. The mulch material should be held tight without any crease and laid on the bed
iii. The borders (10 cm) should be anchored inside the soil in about 7-10 cm deep in small furrows at an angle of 45°.

Pre planting mulch:

The mulch material should be punctured at the required distances as per crop spacing and laid on the bed. The seeds/seedlings should be sown/transplanted in the holes.

Precautions for Mulch Laying

• Do not stretch the film very tightly. It should be loose enough to overcome the expansion and shrinkage conditions caused by temperature and the impacts of cultural operation.

• The slackness for black film should be more as the expansion, shrinkage phenomenon is maximum in this color.

• The film should not be laid on the hottest time of the day, when the film will be in expanded condition.

Removal of mulch

In case the mulch film needs to be used for more than one season (thicker film) the plant is cut at its base near the film and the film is removed and used. By compounding appropriate additives into the plastics it is possible to produce a film, which, after exposure to light (solar radiation) will start to breakup at a pre determined time and eventually disintegrated into very small friable fragments. The time period can be 60, 90, 120 or 150 days and for maize a 60-day photodegradable mulch is used. However there are still some further problems to resolve. It has been observed that the edges of the mulch, which are buried to secure the mulch to the soil, remain intact and become a litter problem when brought to the surface during the post-harvest ploughing.

https://doi.org/10.36375/prepare_u.iiche.a389

Thus to overcome these problems, the mulch sheet is being replaced after every harvest. On the other hand, bio-degradable mulch sheet are also in use. But the major problem is that, the broken parts of the film lead to soil pollution. Thus these are the challenges that are to be overcome.

2. **Hydrogel in Agriculture**

Hydrogels are hydrophilic cross-linked polymers that form three dimensional molecular networks which can absorb and hold great amounts of water. Hydrogel agriculture technology uses insoluble gel forming polymers to improve the water-holding properties of different soils. This can increase water-holding and water use, improve soil permeability, reduce the need for irrigation, reduce compaction, soil erosion, and leaching, and improve plant growth.

Hydrogel Agriculture (Super Absorbent Polymer for Agriculture) is potassium based nontoxic polymer capable of absorbing and retaining water up to 300 — 500 times of its own size. When mixed with soil and sown at the roots of a plant, it spares 65 – 95% of water utilized. Its application is basic yet effective. It was created to develop farming in extreme climates, whether excessively hot, excessively parched, and so forth. It assists with: dry season, desertification, poor soil quality, and treatment. Rather than day by day watering, Super Absorbent Polymers permit watering once per week, sparing time, money, and water.

Super absorbent polymer for Agriculture can assimilate and hold a great degree of water in respect to their own particular mass. Water-retaining polymers, which are delegated hydrogels when cross-connected, absorb fluids through hydrogen bonding with water. A SAP's capacity to retain water is an element of the ionic concentration of the watery arrangement.

Super Absorbent Polymer(SAP) for Agriculture is effective for water utilization in agricultural and horticultural crops in areas with little or negligible amount of rainfall and under limited irrigation conditions. It offers huge economic viability to cultivations and is a boon to dry states and the future generation of farming.

Hydrogel polymers/ Super Absorbent polymers (SAP) are a system of polymer chains hydrophilic in nature with water as the dispersion medium. Hydrogel polymer is capable of storing more than 90% water and has a level of adaptability same as natural tissues, because of their huge water content.

Hydrogel polymer is a water absorption agent that once added to soil or substrate will absorb and hold vast amounts of water and supplements, nearly up to 400 times of its own particular weight. Hydrogel polymers formed through cross linking polymer chains (physical, ionic or shared bonding) and are well known for their ability to absorb water. Hydrogels are mostly homogeneous in nature. Super Absorbent Polymers, which are delegated hydrogels, retain watery arrangements through hydrogen bonding with water atoms. In de-ionized and de-mineralized water, a SAP may assimilate 300 times its weight (from 30 to 60 times its own volume).

Potassium based Super Absorbent Polymer (SAP)

Potassium Polyacrylate is a polymer of a potassium cation and acrylamide with an Absorption Capacity Index in the scope of 30-100. This polyacrylate helps in the germination of seedlings, with plants or for transportation of plants or seedlings. It is nontoxic, harmless, and non-polluting.

$$\text{Absorption Capacity Index (ACI)} = \frac{\left(\text{Weight of water saturated gel polymer}\right) - \left(\text{Dry weight of polymer}\right)}{\text{Polymer dry weight}}$$

https://doi.org/10.36375/prepare_u.iiche.a389

Amid dry periods, sodium polyacrylate has a tendency to gather and form cross links that repress re-swelling when it is re-wetted. With a limited number of wet/dry cycles, sodium polyacrylate hinders plant development. This inhibition emerges because sodium particles in the sodium polyacrylate system are easily replaceable and these particles are absorbed by the soil particles or have a tendency of exchange with the cations on the surface of plant roots. The result is a condition that is different from an alkaline soil, which tends to affect and inhibit plant growth and soil hardening.

Hydrogels can be used in all type of agriculture such as

Open Field & Protective Cultivation

Hydrogel is mixed with soil around the root zones of common trees and plants, providing water and nutrients stably over a period of time. While depending on young to fully grown trees, hydrogel amount differs from 20 – 100 gms mixed with the soil matrix per tree.

Terrace Farming, Home grown Gardens, and Vertical Farming

Super Absorbent Polymer can be mixed with soil matrix, for indoor and open air pots, growers, window boxes, porches, terraces, hanging, greenhouses and city scene. Using SAP proves beneficial to water usage, time, labour and lessening drought and wilting risks which come into light if the plant is not watered for long, enabling a greener and bloomer period.

Arboriculture

Arboriculture incorporates social techniques such as selection, planting, preparing, bug and pathogen control, pruning, molding, and evacuation. It is principally centered on individual woody plants and trees kept up for landscape and amenity purposes, ordinarily in gardens, parks, etc. under the

Potassium Acrylate

https://doi.org/10.36375/prepare_u.iiche.a389

general umbrella of agriculture. Hydrogel reduces mortality rate due to transplantation shocks and enhances root development. A hole is dug about three times the volume of the root, at the plantation site, and 1 - 2 kgs of this product per m3 of soil is mixed. The plant is placed the bottom of the hole and is evenly filled with the treated soil. The top surface is covered with 5 cm of untreated soil so as to prevent UV degradation of the product.

Bare Root Dipping

To prevent desiccation of the roots of seedlings during transplanting or transportation, 1 kg of potassium polyacrylate is mixed in 150 - 200 liters of water with/ without an additional fungicide/ bactericide, and allowing it to stand for 15 minutes. It finds a great use in flower preservation during transportation; fresher flowers which in turn increase their market value.

Hydro Seeding

Hydro seeding is a planting procedure that uses a mixture of seed and mulch, used as an erosion control system on construction destinations, and as another option to the conventional procedure of sowing dry seeds. Hydrogel mixed with cellulose mulch is used to stabilize newly graded soils, maintaining a minimum surface area, helping in sprouting of seedlings even in dry areas.

Fertilizers

Hydrogel polymers can be dry mixed into fertilizer preparations. It is able to absorb large volumes of liquids that can be released over a long time reducing leaching of essential soil nutrients. Therefore, this substrate was used for the slow release of fertilizers alone or in combination with a water-holding gel, dosed at 1 to 5kg by weight.

Hydroponics/ Soil less media

Hydroponics is a technique of growing plants using only mineral supplement solutions, in water, without soil. Plants might be grown with their roots in the mineral solution only, or in a dormant/ inert medium. Hydrogel mixed with hydroponics media reduces the water stress.

1.2.3 Work principle of hydrogel

Hydrogel polymer comes in crystal or powder, which jellifies upon contact with water or other liquids. These particles may be taken as mini water reservoirs in soil. It soaks up and stores water inside, with the capacity of absorbing nearly 400 – 600 times its own weight. Water from these reservoirs is released upon root demand through osmotic pressure difference. In arid areas, the use of hydrogel in sandy soils (macro porous medium) increases the water holding capacity, which significantly improves the quality of plants. Hydrogel Polymer can influence soil permeability, density, structure, texture, and evaporation rate of water through the soil. Hydrogel with excellent water absorption quality is an exceptionally helpful green and eco-friendly item for farming and agriculture fields. It can be used for farms and forestry services, sparing water for homestead and garden and enhancing trees' surviving ratio.

This aqua absorbent act as a reservoir of water and will only use the reserved resource at the time of need, allowing a better agricultural yield. Super Absorbent Polymers have a unique mechanism to absorb and retain water; discharging it only when the crop demands for it otherwise it does not lose out on the moisture level.

2.1 LITERATURE SURVEY

The project is a basic try in the field of PLASTICULTURE where the plastic is being used in the field of agriculture to overcome the drawbacks. As in the introductory part, the mulching art is being incorporated with hydrogels for better water retention by crops.

Irrigation water is becoming scarce and the world is looking for water-efficient agriculture. Increasing food demand and declining water resources are challenges for food security (Kreye et al. 2009). With decreasing water availability,

https://doi.org/10.36375/prepare_u.iiche.a389

rice production is needed to be switched towards water saving production systems. In the system of aerobic rice, especially adapted aerobic rice cultivars are grown under non-flooded or aerobic soils with supplementary irrigation (Bouman 2001, Bouman et al. 2005).

Hydrogel is a synthetic polymer, which is able to absorb and hold 80–180 times its volume of water for a long time (Wang and Gregg 1990). Hydrogel acts as a reservoir to store and release a steady stream of water and nutrients which plants need to grow. Plant roots are able to absorb water from the crystal bead of hydrogel. Several previous studies showed that these are very useful under limited water conditions to cope with plant water needs (Henderson and Hensley 1985, Ingram and Yeager 1987, Wang and Gregg 1990).

Johnson (1984) reported that addition of hydrogel at the rate of 2 g/kg improved the water holding capacity of sand from 171% to 402%. Application of hydrogel decreases the irrigation requirements of several crops by improving water holding capacity resulting in delay and onset of permanent wilting percentages under intense evaporation. An increase in water holding capacity due to hydrogel amendment significantly reduced the irrigation requirement of many plants (Taylor and Halfacre 1986).

Mulching reduces the deterioration of soil by way of preventing the runoff and soil loss, minimizes the weed infestation and checks the water evaporation. Thus, it facilitates for more retention of soil moisture and helps in control of temperature

fluctuations, improves physical, chemical and biological properties of soil, as it adds nutrients to the soil and ultimately enhances the growth and yield of crops. Further, reported that mulching boosts the yield by 50-60 per cent over no mulching under rain fed situations. (Patil shirish.S, 2013).

William (1993) reported that although a variety of vegetables can be grown successfully using plastic mulches. Muskmelons, honeydews, watermelons, squash, cucumbers, tomatoes, peppers, eggplant, okra, sweet corn, and cole crops have shown significant increases in earliness, total yield, and quality. Jaiswal et al. (1997) found that mulching of carrots was effective and root yield was increased by 34.6 % compared with no mulching. Islam et al. (2002) investigated the effect of planting time, mulching and irrigation on the growth and yield of cabbage cv. Atlas-70. Mulching and irrigation significantly affected the growth and yield of cabbage. The highest gross yield (71.85 kg/plot) was obtained from the black polyethylene mulch followed by water hyacinth mulch (65.99 kg/plot). Considering marketable yield, both black polyethylene mulch (103.01 t/ha) and water hyacinth mulch (90.99 t/ha) exerted statistically similar effects followed by irrigation at 15 days interval (85.85 t/ha), whereas non-mulching and non-irrigated plots (control) exhibited the lowest marketable yield (38.87 t/ha).

EXPERIMENTAL WORK

3.1 Material Used

3.1.1 Low Density Polyethylene

Low density polyethylene is a thermoplastic made from monomer ethylene. It is not reactive at room temperature, except by strong oxidising agents and solvents. It is flexible and tough and is either translucent or opaque. They are majorly semi crystalline. It contains the chemical components carbon and hydrogen.

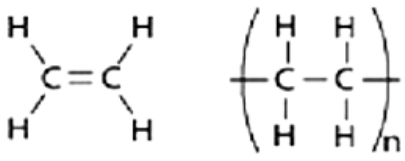

https://doi.org/10.36375/prepare_u.iiche.a389

Plastic film is a thin continuous polymeric material. These thin plastic membranes are used to separate areas or volumes, to hold items, to act as barrier or as printable surfaces. Plastic films are used in a wide variety of applications. These include: packaging, plastic bags, labels, building construction, landscaping, electrical fabrication, photographic film, film stokes for movies, video tape etc. On the other hand various colour mulches are produced based on their usage.

Generally the thickness of mulch does not majorly affect the efficiency of the mulch film. It's only the colour and additives that play a major role. But generally the thickness is in the range of 7 microns to 100 microns depending on the type of plant and its growth duration.

Selection of mulch

The selection of mulches depends upon the ecological situations and primary and secondary aspects of mulching

Rainy season	Perforated mulch
Orchard and plantation	Thicker mulch
Soil solarisation	Thin transparent film
Weed control through solarisation	Transparent film
Weed control in cropped land	Black film
Sandy soil	Black film
Saline water use	Black film
Summer cropped land	White film
Insect repellent	Silver colour film
Early germination	Thinner film

Table 1. Selection of mulch

3.1.2 Carbon Black

Carbon black is an important and versatile ingredient for plastics compounders. It can contribute colour, opacity, electrical conductivity and protection from ultra-violet degradation. The choice of carbon black is dependent on the final product requirements. In this regard, particle size and structure (degree of permanent particle aggregation) are the two most important characteristics of a carbon black in determining its performance.

Carbon black is typically used in thermoplastics to impart at least one the properties below

- Colour
- UV Protection
- Conductivity

Since most thermoplastics are rigid at the end use temperature, the reinforcing effects of the carbon black have to be balanced with desired end use mechanical properties. In addition, the carbon black contaminants such as grit, ash and sulfur have a more crucial impact on the thermoplastic's mechanical properties and the processing of these materials. For plastics applications involving color and UV protection, carbon black is typically dispersed into a plastic master batch at a high dosage, 25 to 40% by weight.

The key performance criteria of carbon black products important to molded plastics applications are:

- Color Strength
- Blue Tone
- Effect on Master batch Viscosity
- UV Stability
- Dispersibility

3.1.3 HYDROGEL

The hydrogel was purchased from CHEMZEST Enterprises Pvt., Ltd. The hydrogel purchased was potassium based as it improves and stimulates the growth of the plant and also is non-toxic for the soil. The other type is sodium based but is said to damage the soil on continuous usage

https://doi.org/10.36375/prepare_u.iiche.a389

and longer run. Thus the hydrogel purchased is "potassium polyacrylate".

The hydrogel is directly available in the market is being used in the agricultural field. Thus this hydrogel was purchased to calculate its water absorbency. It was identified to absorb a minimum of 50% of its own weight and when left to dry it turned dark brown and shrinked. Thus it does not damage the field when left to dry.

Analysis	**Unit**	**Specification**
Appearance		White , granular
Particle size	Mm	Granular MS: 1.0-2.0
Odor		Imperceptible
Moisture	%	10 Max
Ph		7.0 – 8.0
Free Acrylamide content	Ppm	500 max
Bulk Density	g/cm3	0.80
Water Solubility		Insoluble
Toxicity In soil		None
Shelf life	Years	5
Degradability in Soil	Years	1-5
Absorbency	g/g	
Deionized Water		300-400
0.9% NaCl		100-150
Soil		150-200

Table 2 Specification of Hydrogel

The hydrogel was heated upto 200°C in the hot air oven and then crushed to bring it to the powder form for easy miscibility. The crushed and powdered hydrogel was subjected to mesh analysis as to distinguish the sizes. The mesh numbers of mesh100, mesh200 and mesh350 was used to disintegrate the minimum of the size. The hydrogel was then stored in air tight packs for further preservation.

3.2 PROCESSING

3.2.1TWIN SCREW EXTRUSION

https://doi.org/10.36375/prepare_u.iiche.a389

Twin screw extrusion is used extensively for mixing, compounding, or reacting polymeric materials. The flexibility of twin screw extrusion equipment allows this operation to be designed specifically for the formulation being processed. For example, the two screws may be co-rotating or counter-rotating, intermeshing or non-intermeshing. In addition, the configurations of the screws themselves may be varied using forward conveying elements, reverse conveying elements, kneading blocks, and other designs in order to achieve particular mixing characteristics.

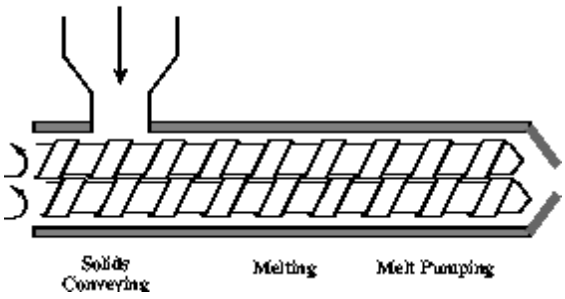

Fig 2. Twin screw extrusion process

The Low Density Polyethylene (LDPE) was blended with hydrogel using twin screw extrusion process. The temperature was maintained in a range of 110°C to 190°C and the composition of different components are as follows

Components	Weight (gms)
LDPE Virgin granules	60
Potassium based hydrogel	30gms
Carbon black	5 gms
Compatibilizer	2 gms

Table 3 Components used in extrusion process

The extrudate was water cooled and then dried in hot air oven at 80°C for a period of half an hour. Thus, the collected extrudate was cut in small sizes using a pelletizer. The pellets were then used in blown film extrusion to obtain a film.

3.2.2 BLOWN FILM EXTRUSION

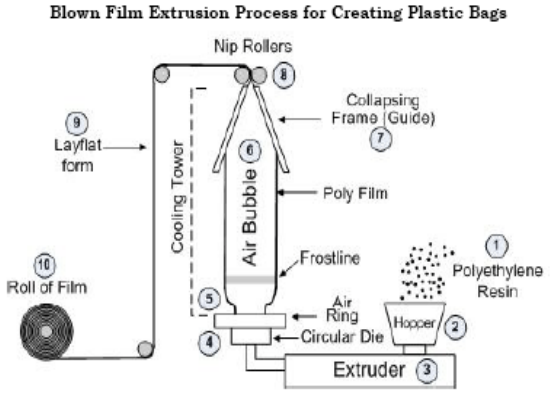

Fig 3 Blow film extrusion process

The LDPE incorporated with hydrogel was air dried at 80°C for a period of 1 hour and then was extruded as film. The thickness of the film was maintained in the range of 1.5 – 2 cm. The temperature was maintained at 180°C. The obtained film was tested for color variation and presence of bubbles.

3.3 Testing Procedure

3.3.1 Fourier Transform Infrared Spectroscopy (FTIR)

FTIR spectrometers (Fourier Transform Infrared Spectrometer) are widely used in organic synthesis, polymer science, petrochemical engineering, pharmaceutical industry and food analysis. In addition, since FTIR spectrometers can be hyphenated to chromatography, the mechanism of chemical reactions and the detection of unstable substances can be investigated with such instruments. The range of Infrared region is 12800 ~ 10 $cm^{-1}$and can be divided into near-infrared region (12800 ~ 4000 cm^{-1}), mid-infrared region (4000 ~ 200 cm^{-1}) and far-infrared region (50 ~ 1000 cm^{-1}). The discovery of infrared light can be dated back to the 19th century. Since then, scientists have established various ways to utilize infrared light. Infrared transform spectroscopy is the method

https://doi.org/10.36375/prepare_u.iiche.a389

which scientists use to determine the structures of molecules with the molecules characteristic absorption of infrared radiation. Infrared spectrum is molecular vibrational spectrum. When exposed to infrared radiation, sample molecules selectively absorb radiation of specific wavelengths which causes the change of dipole moment of sample molecules. Consequently, the vibrational energy levels of sample molecules transfer from ground state to excited state. The frequency of the absorption peak is determined by the vibrational energy gap. The number of absorption peaks is related to the number of vibrational freedom of the molecule. The intensity of absorption peaks is related to the change of dipole moment and the possibility of the transition of energy levels. Therefore, by analyzing the infrared spectrum, one can readily obtain abundant structure information of a molecule. Most molecules are infrared active except for several homonuclear diatomic molecules such as O_2, N_2 and Cl_2 due to the zero dipole change in the vibration and rotation of these molecules. What makes infrared absorption spectroscopy even more useful is the fact that it is capable to analyze all gas, liquid and solid samples. The common used region for infrared absorption spectroscopy is 4000 ~ 400 cm^{-1} because the absorption radiation of most organic compounds and inorganic ions is within this region. FTIR spectrometers are the third generation infrared spectrometer. FTIR spectrometers have several prominent advantages: (1) The signal-to-noise ratio of spectrum is significantly higher than the previous generation infrared spectrometers. (2) The accuracy of wavenumber is high. The error is within the range of ± 0.01 cm^{-1}. (3) The scan time of all frequencies is short (approximately 1 s). (4) The resolution is extremely high (0.1 ~ 0.005 cm^{-1}). (5) The scan range is wide (1000 ~ 10 cm^{-1}). (6) The interference from stray light is reduced. Due to these advantages, FTIR Spectrometers have replaced dispersive IR spectrometers.

FTIR Spectrometers

The Components of FTIR Spectrometers

A common FTIR spectrometer consists of a source, interferometer, sample compartment, detector, amplifier, A/D convertor, and a computer. The source generates radiation which passes the sample through the interferometer and reaches the detector. Then the signal is amplified and converted to digital signal by the amplifier and analog-to-digital converter, respectively. Eventually, the signal is transferred to a computer in which Fourier transform is carried out. **Figure 4** is a block diagram of an FTIR spectrometer.

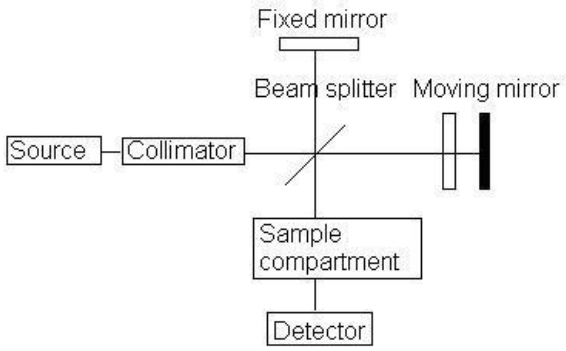

Figure 4. Block diagram of an FTIR spectrometer

The major difference between an FTIR spectrometer and a dispersive IR spectrometer is the Michelson interferometer. Fourier transform infra-red spectroscopy (FTIR) is a technique which is used to obtain an infra-red spectrum of absorption, emission, photoconductivity or Raman scattering of a solid, liquid or gas. An FTIR spectrometer simultaneously collects high spectral resolution data over a wide spectral range. This confers a significant advantage over a dispersive spectrometer which measures intensity over a narrow range of wavelengths at a time. The goal of any absorption spectroscopy is to measure how well a sample absorbs light at each wavelength. The best method is by "dispersive spectroscopy" technique is to shine a

https://doi.org/10.36375/prepare_u.iiche.a389

monochromatic light beam at a sample, how much of the light is absorbed and repeat for each different wavelength.

This FTIR was used to analyse the structural characteristics of the polyethylene film subjected to microbial action. The wave number ranges from 400 cm^{-1} to 4000 cm^{-1}. The films were analysed using NICOLET 6700 USA. A change in the structural characteristics was noticed that is discussed in results.

3.3.2 SCANNING ELECTRON MICROSCOPE (SEM)

Introduction:

The development of Scanning Electron Microscopy (SEM) in the early 1950's brought with it new areas of study in the medical and physical sciences because it allowed examination of great variety of specimens. As in any microscope, the main objective is magnification and focus for clarity. An optical microscope uses lenses to bend an electron beam, which is used to bend the light waves, and the lenses are adjusted for focus. In the SEM, electromagnets are used to bend an electron beam, which is used to produce the image on a screen. By using electromagnets an observer can have more control in how much magnification it obtains. The electron beam also provides greater clarity in the image produced. The SEM is designed for direct studying of the surfaces of solid objects. The SEM is a type of electron microscope capable of producing high-resolution images of sample surface. Due to the manner in which the image is created, SEM images have characteristic three-dimensional appearance and are useful for judging the surface structure of the sample.

SEMs are patterned after reflecting light microscopes and yields similar information:

Topography: The surface features of an object.

Morphology: The shape, size and arrangement of the particles making up the object that are lying on the surface of the sample.

Crystallographic Information: The arrangement of atoms in the specimen and their degree of order; only useful on single crystal particles>20 micrometers.

Working Principle:

The instrument can be simplified into three major sections: a) electron-optical 'column'; b) vacuum system and c) electronics and display system. A tungsten filament is heated to 2700 K, which produces electron gun, having stream of monochromatic electrons (energy ranging from a hundred ev to 50kev.) that are accelerated towards the anode disc. The stream is condensed by the first condenser lens to control the diameter and current of the beam. The beam is then constricted by the condenser aperture, eliminating some high-angle electrons. The second condenser lens forms the electrons into a thin, tight, coherent beam and usually controlled by the 'fine probe current knob'. A set of coils then scan or sweep the beam in a grid fashion dwelling on points for a period of time determined by the scan speed .

The final lens, the objective, focuses the scanning beam onto the part of the specimen desired. A cathode-ray display tube is scanned synchronously with the electron beam. The brightness of the display tube is modulated by the signal, which arises from the interaction of the beam with the surface element, which is probed. The strength of this signal is translated into image contrast. Secondary electrons, which the beam probe liberates from the specimen surface, are collected and used as the contrast signal. The yield of collected electrons depends on the nature of the specimen surface and on its inclination with respect to the probing beam. Consequently, one obtains pictures with a high perspective appearance.

https://doi.org/10.36375/prepare_u.iiche.a389

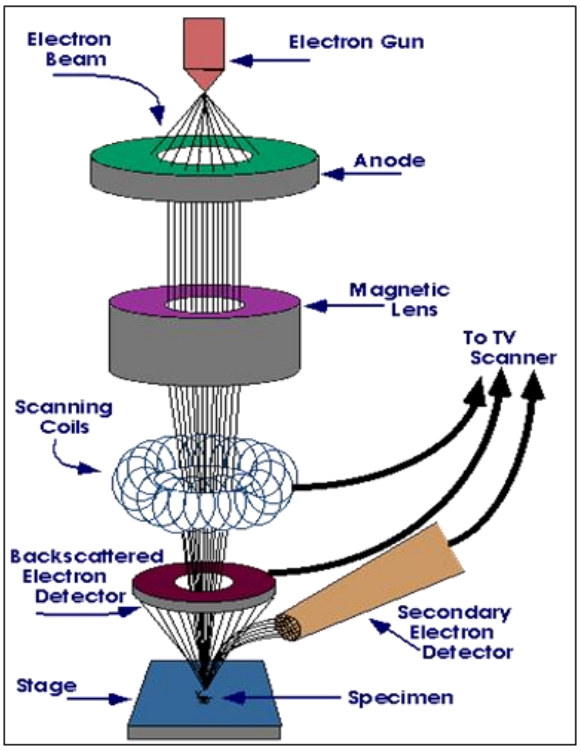

Fig 5 Schematic representation of SEM

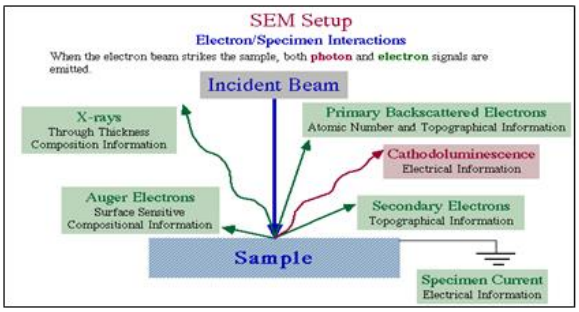

Fig 6 SEM set-up electron specimen interaction

Backscattered electrons produced by an incident electron colliding with an atom in the specimen, which is nearly normal to the incident's path. The incident electron is then scattered "backward" 180 degrees. The production of backscattered electrons varies directly with the specimen's atomic number or “specimen interaction volume”. Specific interaction volume is the volume inside the specimen in which interactions occur while being struck with an electron beam. The differing production rates cause higher atomic number elements to appear brighter than lower atomic number elements. This interaction is utilized to differentiate parts of the specimen that have different average atomic number. These elastically scattered electrons usually called 'backscattered electrons' are used for SEM imaging.

Resolution of the SEM:

The spatial resolution of the SEM depends on the size of the electron spot, which in turn depends on both the wavelength of the electrons and the magnetic electro-optical system which produces the scanning beam. The resolution is also limited by the size of the interaction volume, or the extent to which the material interacts with the electron beam. The spot size and the interaction volume both might be large compared to the distances between atoms, so the resolution of the SEM is not high enough to image individual atoms, as is possible in the shorter wavelength (i.e. higher energy) transmission electron microscope (TEM). The SEM has compensating advantages, though, including the ability to image a comparatively large area of the specimen; the ability to image bulk materials (not just thin films or foils); and variety of analytical models are available for measuring the composition and nature of the specimen. Depending on the instrument, the resolution can fall somewhere between less than 1 nm and 20 nm. Resolution is 0.4nm at 30Kv and 1.6nm at 1Kv. In general, SEM images are easier to interpret than TEM images.

Test Procedure:

In the present investigation the morphology of the nanocomposites was observed using SEM-JSM-6390 (JEOL Ltd, Japan) with 15 kV accelerating voltage at 5mm resolution. Specimens are platinum coated at low temperature. Ultra-thin specimens of 100μm thickness were cut from fractured surface of tensile specimen using Reichert ultra-cut microtome. The specimens were collected on a

https://doi.org/10.36375/prepare_u.iiche.a389

trough filled with water and placed on a 200 – mesh grids.

Scanning electron microscope (SEM) is a type of electron microscope that produces images of a sample by scanning it with a focused beam of electrons. SEM was used to analyse visually the changes on the surface of the polyethylene film subjected to microbial action. Polyethylene being non-conducting in nature was subjected to gold sputtering before subjecting it to the action of electron beams. The magnification in the range of 1000X to 4000X was analysed. Significant changes were observed on the surface of the polyethylene film which proved microbial degradation.

3.3.3 WATER ABSORPTION TECHNIQUE

The test was carried out using the procedure ASTM D570. Moisture absorption (also known as water absorption) is the capacity of a material to absorb moisture from its environment. Plastics absorb water to a limited degree. The degree of moisture absorption depends on the type of plastic and the ambient conditions such as temperature, humidity and contact time. Not only can dimensions change due to moisture absorption, but also material properties, such as mechanical strength, electrical conductivity and the dielectric loss factor, can be also affected.

The moisture absorption leads to changes in dimensions of finished products, a reduction in strength and also changes in electrical insulating characteristics. Various polymeric materials are susceptible to water absorption during its life exposure. This may cause dimensional instability with property degradation and ultimately lead to failure. This test was designed to evaluate materials by exposing specimens to water for different time & temperature profiles. Testing is conducted on specimens that are submersed in water and a before & after weight change is documented. Depending on the application of the product, certain levels of moisture are accepted. Certain materials require small amounts of moisture for ultimate field performance. However, it is generally accepted that the lower the number, the better, especially during molding or extrusion. Most polymers are dried @ 500°C in an Air Circulated Oven for 24 hours and re-weighed to the nearest 0.001 gms. High Engineered grades (filled or hi-temp.) may require higher drying profiles, but the time is generally the same.

Polyamides (nylons) generally show higher water absorption than other engineering plastics. The only polymer with zero water absorption is PTFE. Plastics with very low water absorption are PEEK, PPS, PPSU, PVDF, PET, PPE, PP and PE. Furthermore, low water absorption is exhibited by POM, PA12, PC and ABS.

The result shall be either increase or decrease in weight depending on the composition and types of ingredients being used. The results are calculated as follows

$$\text{Increase in weight \%} = \frac{Wet\ weight - Conditioned\ weight}{Conditioned\ weight} \text{ X } 100$$

In case of soluble substances being present the weight decreases and the result is calculated using the formula,

$$\text{Soluble matter, lost \%} = \frac{Conditioned\ weight - Reconditioned\ weight}{Conditioned\ weight} \text{ X } 100$$

3.3.5 DENSITY

https://doi.org/10.36375/prepare_u.iiche.a389

Fig 9 METLER TOLEDO weighing balance

Density is the mass per unit volume of a material. Specific gravity is a measure of the ratio of mass of a given volume of material at 23°C to the same volume of deionized water. Specific gravity and density are especially relevant because plastic is sold on a cost per pound basis and a lower density or specific gravity means more material per pound or varied part weight. There are two basic test procedures- Method A and Method B. The more common being Method A, can be used with sheet, rod, tube and molded articles. For Method A, the specimen is weighed in air then weighed when immersed in distilled water at 23°C using a sinker and wire to hold the specimen completely submerged as required. Density and Specific Gravity are calculated. The density measurement was done following the ASTM D792 method. The METLER TOLEDO analytical and precision balance was used to perform the density measurement. LDPE having density lesser than that of water, benzene was used as the liquid medium. The density was calculated using the formula

$$\text{Density(g/cc)} = \frac{Weight\ in\ air - Weight\ in\ liquid}{Weight\ in\ liquid} \text{X density of liquid}$$

The major advantages of the machine are

- High flexibility to accommodate individual process needs
- Automatic density calculations for solids and liquids including temperature adjustment of the reference liquid
- Statistic evaluation of multiple samples
- All results, including User, Sample ID, Lot Number, Time and Date can either be printed or saved on a USB stick.

Thus, using density test method, the variations in density can be observed and further improvisation required can be altered in materials as such.

RESULTS AND DISCUSSIONS

4.1 Fourier Transform Infrared Spectroscopy (FTIR)

FTIR is a technique used to obtain an infra-red spectrum of absorption. This FTIR was used to analyse the structural characteristic of the films subjected to microbial action.The FTIR was taken for both low density polyethylene (LDPE) and hydrogel. The results obtained are as follows

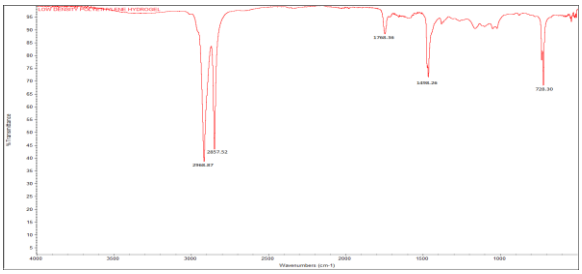

Fig 4.1 The FTIR spectrum of LDPE

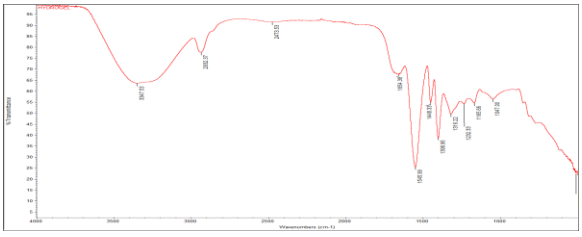

https://doi.org/10.36375/prepare_u.iiche.a389

Fig 4.2 The FTIR spectrum of hydrogel

4.2 SCANNING ELECTRON MICROSCOPE (SEM)

The SEM was performed to analyse the structural changes on the surface of the film. The test was performed based on before and after usage in soil. The results are observed as follows

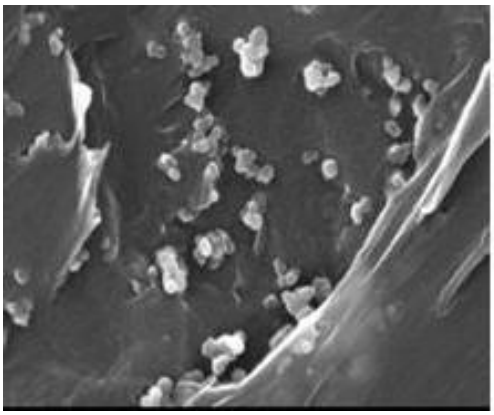

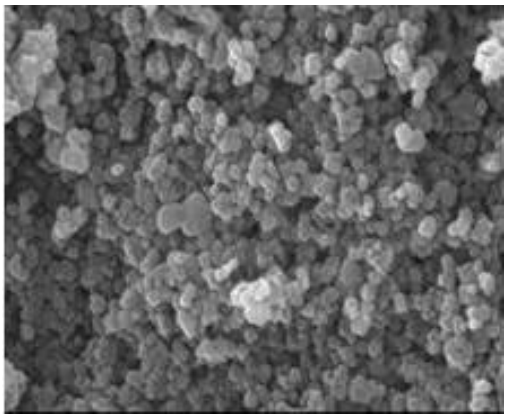

Fig 12 The SEM micrograph of LDPE with hydrogel after blending process (a) 15000X (b) 20000X

The film was then subjected to continuous alternate sunlight and water as in case of agriculture. The film was then subjected to SEM analysis to observe the changes in the surface. It was clearly seen the hydrogel particles been eroded and the film was cracked open in several areas indicating the hydrogels being dissolved into the soil surface. The obtained results are as follows

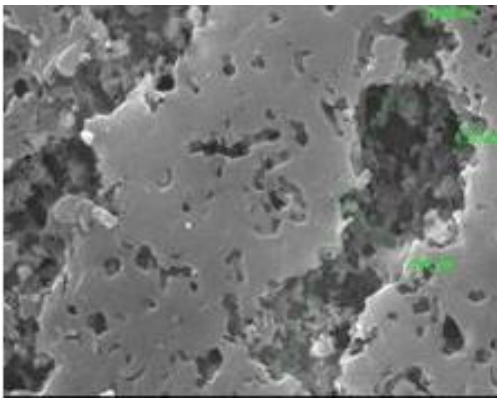

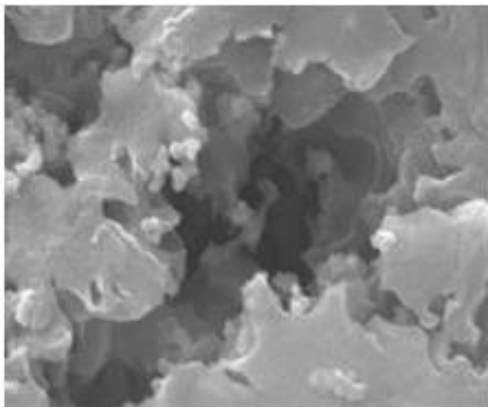

The SEM micrograph of LDPE with hydrogel after usage as mulch film (a) 15000X (b) 20000X

This supports the fact that weight loss being observed in the water absorption analysis. Thus, the hydrogel particles have got lossen away from the LDPE film surface and thus leaving holes and cracks on them. This clearly indicates that hydrogel being mixed with the soil and acts as water storage units.

4.3 WATER ABSORPTION ANALYSIS

For this technique the film was cut into small pieces of 5X5 cm and weighed before being

https://doi.org/10.36375/prepare_u.iiche.a389

suspended in water. The test was carried out in four different ceramic bowls and weight analysis was carried out in time interval of 24 hours for seven days. The results are as follows

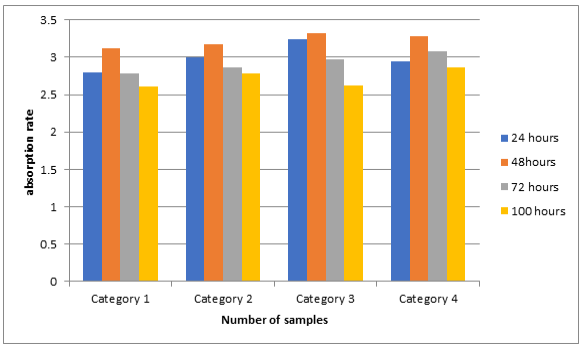

The results observed was that initially there was an increase in weight, but after 48 hours the weight dropped down on daily basis and at the end of 100 hours a constant weight was observed. This indicates that initially, the water was being absorbed by the hydrogels been present in the film, which caused an increase in weight. Later, with the proof of SEM analysis, the hydrogel particles were seen to drift away from the film and been mixed with water.

Fig 14 Weight analysis of four different samples

The same analysis was done using soil instead of water, as in case of being used in agriculture. The film was cut to a size of 10X5 cm and a plastic bowl was taken. Two such bowls were filled with soil and the soil was covered with mulch film. On a daily basis, the soil was watered every day and weight analysis was done to the film. The same was observed where the weight of the film increased on 24 hours basis and later decreased gradually indicating loss of hydrogel particles.

Fig 15 The mulch film with soil for weight analysis

The changes in weight was observed as following

amples	4 hours	8 hours	2 hours	00 hours
ample1 10 gms)	1.28	0.54	.86	.2
ample 2 10 gms)	1.62	1.06	0.84	.68

Table 4 Changes in weight on water absorption

Thus, the samples weight decreased and was seen to be constant after a span of 100 hours. The both samples were subjected to SEM analysis to observe the morphological changes.

4.4 DENSITY

As LDPE, having a density lesser than water, benzene was used as medium having a density of 0.875 g/cc. The test was carried out using

https://doi.org/10.36375/prepare_u.iiche.a389

METLER TOLEDO analytical balance. The results obtained are as follows

Samples	Density (g/cc)
Sample 1	0.948
Sample 2	0.942
Average	0.945

Table 5 Density variation

Thus, the density has slightly increased when compared to LDPE virgin film being only 0.938 g/cc. Thus, the hydrogel have contributed to an instant increase in weight.

CHAPTER V

CONCLUSION

The LDPE was blended with hydrogel using twin screw extruder at around 180°C and then film was extruded using blow film extrusion at a temperature of about 200°C. The film was then subjected to water absorption using four different samples and an average rate of absorption was calculated. Then the film was subjected to coverage with soil as in case of being used in agriculture.

The hydrogels were seen to dissolve into the soil, as a result the water absorption was increased. The results were proven using changes observed in morphological unit using Scanning Electron Microscope (SEM), Water absorption technique and density. The FTIR result was taken for both hydrogel and Low density Polyethylene to identify the miscibility possibilities. Also, by capillary method, the melting point for hydrogel was calculated. It did not melt or degrade till a temperature range of 340°C. Only change is the colour turning from white to light brownish shade.

The scanning electron microscope (SEM) proved the miscibility of Low density polyethylene with that of potassium based hydrogel. The hydrogel being in nano particle size, they were blended with LDPE easily and thus , this has been proven by the magnification. On usage with soil, the film was washed and analysed further, the disappearance of hydrogels were noticed and further the cracks have been developed on the surface of the film. Thus, this proves that hydrogels has been leached out on to the soil.

The water absorption technique proves the rate of water absorption. The average percentage of absorption is around 26% and drip irrigation method has been used. But the fluctuations in absorption has also been observed. This technique further analyses that using different types of irrigation the absorption rate varies.

The density test was made to analyse the changes in density of the mulch film. The film showed an increase in density as compared to that of virgin Low density polyethylene. Also, morphological changes were noticed. The film was easily ruptured, hence mechanical analyses were difficult to be made. Also, the film has to be degraded after a period of 6 months, hence analysis were made by blending mulch film with that of poly lactic acid to make it degradable easily.

Thus , when being blended the hydrogels shows a higher rate of disposal into the soil when compared to that of being dispersed directly into the soil. Also by this method, the consumption of hydrogels can be effectively increased. Thus, this helps in saving of water consumption and that the calculated amount of water absorption takes place.

CHAPTER VI

FUTURE WORK

https://doi.org/10.36375/prepare_u.iiche.a389

Though the potassium based hydrogel incorporated mulch film proves a boon on water storing capacity, the major concern relies on the disposal after usage. Once, the harvesting period is over, the mulch film has to be removed and replaced with a new one. The problem arises with that of degradation. So , the future work has to be concentrated on making it more of bio-degradable after serving its purpose.

Also, on degradation, the film should either provide nutrients to the soil or on other hand should not cause soil pollution. Thus, the following has to be improvised on the next stage

- The mulch film on disposal should not create soil pollution.
- The film should be made bio-degradable.
- On being bio-degradable, the degradation should start only after harvest period and the ingredients should not affect the plant growth.

Thus, the further improvisation shall lead to more of commercialization with further improved properties.

CHAPTER VII

REFERENCE

1. Influence of cell size, hydrogel, and drought stress on bell pepper transpiration, water usage, and growth – Robert.J.Dufault and William H Nair.

2. Effect of hydrogel on the performance of aerobic rice sown under different techniques.- A. Rehman, R. Ahmad, M. Safdar.

3. Water-efficient management strategies in rice production. International Rice Research Notes. - Bouman B.A.M. (2001)

4. Yield and water use of irrigated tropical aerobic rice systems. Agricultural Water Management. - Bouman B.A.M., Peng S., Castaneda A.R., Visperas R.M. (2005)

5. Water absorption by synthetic polymer (Aquasorb) and its effect on soil properties and tomato yield. International Journal of Agriculture and Biology. - Hayat R., Ali S. (2004)

6. Innovative soil conditioning and mulching techniques for forest restoration in mediterranean conditions. - Coello-Gomez Jaime, Fuentes-Boix Carla, Pique Míriam (2015)

7. The effect of a soil-amending hydrogel on Eucalyptus grand is establishment practices in the Zululand forestry region. - Viero P.W.M. (2002)

8. Hydrogels from radiation crosslinked blends of hydrophilic polymers and fillers. - Steven N Yen, Frederick D Osterholtz (1975)

9. Polymers in agriculture – a review. –Franseco puoci, Francesa Iemma, Giussepe criollo (2008)

10. A long-term experiment to study the role of mulches in the physiology and macro-nutrition of strawberry grown under water stress**.** - Halil Kirnak, Cengiz Kaya, David Higgs and Sinan Gercek (2001).

11. Improving agricultural water use efficiency in arid and semiarid areas of China.- XiPingDeng , LunShan , HepingZhang, Neil C.Turner.

12. Effect of mulching on soil and plant water status, and the growth and yield of wheat (*Triticum aestivum* L.) in a semi-arid environment. ShanthaNagarajan PramilaAggarwal , V.K.Gupta , R.K.Tomar , R.N.Garg, R.N.Sahoo , A.Sarkar , U.K.Chopra , K.S. SundaraSarma , N.Kalra.

ACKNOWLEDEMENT

It has been a great privilege, and good learning experience for me to be a part of CIPET-Chennai. It gives me great pleasure to acknowledge with deep sense of gratitude and appreciation to all those who have guided,

https://doi.org/10.36375/prepare_u.iiche.a389

inspired, motivated and extended their cooperation throughout the period of my project.

We would like to express our sincere gratitude to the following individuals for their invaluable support and guidance,which have a played a pivotal role in shaping our academic journey:

- **Mr. S.ILANGOVAN, Principal Director & Head , CIPET, Chennai** for letting students venture and explore the laboratory facilities and for immense help in project work.
- **Dr.SYED AMANULLA, Principal, CIPET,Chennai** for his visionary leadership,commitment to educational excellence for our educational pursuits.
- **Dr.RADHASHYAM GIRI, Vice principal, CIPET,Chennai** for his valuable insights,mentorship,and for fostering an environment of academic excellence.
- **Mr. Y.HIDAYATHULLAH, Head of Department- Plastics Technology** course in charge of who was kind enough to approve the project.

I am greatly indebted to staffs in **Plastic Testing Centre (PTC)** for helping me with all support & their valuable suggestions and constant motivation.

I would like to convey my deep regards and gratitude to all the **Staff members of CIPET-Chennai** associating me to various sections of the concern for facilities and foregoing guidance for completing this project.

And I wish to express my sincere thanks to my **family** and my **friends** for supporting, encouraging me all through my life. It would not be possible without their encouragement to complete this project successfully.

https://doi.org/10.36375/prepare_u.iiche.a390

[International Conference on Energy Transition: Challenges and Opportunities at Chemical Engineering Congress (CHEMCON-2023) – On the occasion of Platinum Jubilee Year of Indian Institute of Chemical Engineers]

QUANTITATIVE COMPARISON OF DIETARY FIBRES FOR VITAMIN B12 ENCAPSULATION

Anirudh Rishikesh URS[1*], Manish Danda[1], Priyanka Rajesh Bhargav[1], Shreya Shanbhog[1], Ganganna Vijaya Kumar[2], Halebeedu Gurusiddappa Ashok Kumar[2], Sumathra Manokaran[2], Trilokchandran Bodhireddy[2]

Author 1 Anirudh Rishikesh URS, BE student, Department of Biotechnology, RV College of Engineering, Mysore Rd, RV Vidyaniketan, Post, Bengaluru, Karnataka, India 560059. anirudhrurs.bt21@rvce.edu.in*

Author 2 Manish Danda, BE student, Department of Biotechnology, RV College of Engineering, Mysore Rd, RV Vidyaniketan, Post, Bengaluru, Karnataka, India 560059. manishdanda.bt21@rvce.edu.in

Author 3 Priyanka Rajesh Bhargav, BE student, Department of Biotechnology, RV College of Engineering, Mysore Rd, RV Vidyaniketan, Post, Bengaluru, Karnataka, India 560059. priyankarb.bt21@rvce.edu.in

Author 4 Shreya Shanbhog, BE student, Department of Biotechnology, RV College of Engineering, Mysore Rd, RV Vidyaniketan, Post, Bengaluru, Karnataka, India 560059. shreyas.bt21@rvce.edu.in

Author 5 Ganganna Vijaya Kumar, PhD in Biotechnology, Department of Biotechnology, RV College of Engineering, Mysore Rd, RV Vidyaniketan, Post, Bengaluru, Karnataka, India 560059. vijayakg@rvce.edu.in

Author 6 Halebeedu Gurusiddappa Ashok Kumar, PhD in Botany, Department of Biotechnology, RV College of Engineering, Mysore Rd, RV Vidyaniketan, Post, Bengaluru, Karnataka, India 560059. hgashok@rvce.edu.in

Author 7 Sumathra Manokaran, PhD in Biochemistry, Department of Biotechnology, RV College of Engineering, Mysore Rd, RV Vidyaniketan, Post, Bengaluru, Karnataka, India 560059. sumathram@rvce.edu.in

Author 8 Trilokchandran Bodhireddy, PhD in Biotechnology, Department of Biotechnology, RV College of Engineering, Mysore Rd, RV Vidyaniketan, Post, Bengaluru, Karnataka, India 560059. trilokc@rvce.edu.in

https://doi.org/10.36375/prepare_u.iiche.a390

ABSTRACT

Vitamin B12, also referred to as Cobalamin, is an essential nutrient for the human body. DNA synthesis, neurological functions, and haematopoiesis are a few of the vital roles vitamin B12 plays. However, it is concerning that a significant 47% of the Indian population is grappling with a deficiency in this vital nutrient. Vitamin B12 supplements in the form of capsules and tablets serve to solve this problem. We hereby explore a solution which is not only efficient but also sustainable, namely, Vitamin B12 encapsulation in environmentally friendly matrices via ionotropic gelation. Dietary fibres have been explored especially well in the food industry as encapsulating matrices and are known to have the potential for controlled release of bio actives in the pharmaceutical industry. This research work provides a comparison of the concentrations of different dietary fibres, namely alginate, pectin and cellulose required to encapsulate Vitamin B12. It serves as a starting point to discovering the full potential of these capsules in helping to solve the pressing issue of vitamin B12 deficiency.

Keywords: Vitamin B12, encapsulation, dietary fibre matrices

1. Introduction

1.1) Vitamin B12

Vitamin B12, scientifically termed cobalamin, is abundantly found in animal-derived foods like meat, fish, poultry, eggs, and dairy products. It is an essential water-soluble nutrient crucial for maintaining human health (Green et al., 2017d).

The importance of vitamin B12 spans various dimensions of human health. It plays key roles in red blood cell production, DNA synthesis, and maintaining optimal nervous system functionality. Additionally, it actively participates in the metabolism of carbohydrates, fats, and proteins, contributing to cognitive function and overall brain health. It is known to have potential in mitigating conditions like megaloblastic anaemia, pernicious anaemia, and cardiovascular diseases, emphasising its multifaceted role in human physiology (Weissbach & Taylor, 1969c) (Ling & Chow, 1954).

Vitamin B12 deficiency poses a prevalent health concern with multifaceted causes. Insufficient dietary intake is significant, particularly in individuals following vegetarian or vegan diets with limited natural sources. Compounding the issue is impaired absorption in the small intestine, often associated with gastrointestinal disorders like Crohn's disease and celiac disease, increasing the risk of deficiency. Extrinsic variables, such as excessive alcohol consumption, various malabsorption syndromes, specific medications, and the natural ageing process with associated physiological changes, contribute to the

https://doi.org/10.36375/prepare_u.iiche.a390

complexity of vitamin B12 deficiency. These diverse factors underscore the need for comprehensive assessment and management in clinical and public health contexts (Stabler, 2013) (Pawlak et al., 2013) (Ward et al., 2015).

Proactive intervention becomes imperative for individuals facing vitamin B12 deficiency challenges, leading healthcare practitioners to prescribe vitamin B12 injections or high-dose oral supplements as effective strategies. These therapeutic interventions are indispensable tools in mitigating the consequences of deficiency, ensuring the sustained provision of this essential nutrient, especially when conventional dietary sources or natural absorption mechanisms prove insufficient. The clinical deployment of these interventions emphasises their clinical significance and tailored use in managing vitamin B12 deficiency (Cyran, 2002).

1.2) Encapsulation

Encapsulation has emerged as a highly efficient tool for the targeted and precise delivery of sensitive biological compounds, proving to hold high potential in tackling vitamin B12 deficiency. This methodology offers a versatile means to govern the distribution, action, and metabolic fate of the encapsulated substances, thereby rendering it an asset across diverse domains, notably within the realms of pharmaceuticals and functional foods. The increasing popularity of encapsulation is associated with its intrinsic potential to optimise therapeutic or functional outcomes and to meet the contemporary demand for tailored and effective delivery systems (Klojdová et al., 2023).

The substances enveloped within protective matrices, whether they are individual pure compounds or intricate mixtures, are variably referred to by terms such as coated materials or core materials, among others. In contrast, the materials employed to envelop and safeguard these substances encompass a diverse nomenclature, encompassing designations such as shells, capsules, or membranes (Madene et al., 2005).

Capsules have established themselves as a ubiquitous and versatile encapsulation system, distinguished by their precisely tailored composition. This composition is meticulously designed to fulfil a dual role: safeguarding the integrity of the encapsulated sensitive compounds and enabling their deliberate release at precise locations within the intricate milieu of the gastrointestinal tract (Varankovich et al., 2015).

Ionotropic gelation is one of the methodologies used to encapsulate biologically active compounds. This technique relies on the cross-linking between polymer chains with the help of ions (Gadziński et al., 2022).

Hydration gelation is another process involved in the formation of gel matrices through the absorption of water. Initially the polymer is either exposed to a hydrated environment or water is introduced into it. This forms a protective matrix around the polymer substrate.

https://doi.org/10.36375/prepare_u.iiche.a390

1.3) Dietary fibres

Dietary fibres represent a significant component of plant-derived foods, characterised by their resilience to enzymatic digestion within the human gastrointestinal system. These fibrous materials are abundantly present in a spectrum of natural sources, notably encompassing whole-grain cereals, nuts, seeds, and an array of fruits and vegetables. Notable examples of dietary fibres include cellulose, pectin, alginate, lignin, among others. These compounds form a substantial component of the human diet, exerting diverse physiological effects and imparting essential health benefits.

The applications of dietary fibres span a multitude of dimensions, significantly impacting various aspects of human health. The several key applications of dietary fibres, elucidating their diverse and vital roles are digestive health and constipation prevention, facilitation of weight loss, maintenance of gut microflora and metabolites.

In our research, we are endeavouring to harness the potential of dietary fibres as encapsulating agents for vitamin B12 capsules. This approach involves the utilisation of distinct dietary fibres, namely Alginate, Cellulose, and Pectin as encapsulation matrices. These dietary fibres, renowned for their diverse physiological effects and health benefits, hold promise as suitable carriers for the encapsulation of vitamin B12, offering a range of possibilities for the controlled delivery and release of this essential micronutrient, combining the benefits of tackling vitamin B12 deficiency and the numerous advantages the fibres pose.

1.3.1) Alginate

Alginate, a naturally occurring polysaccharide derived from brown seaweeds, is a widely recognized dietary fibre with versatile applications in various industries, including food, pharmaceuticals, and biotechnology (Anderson et al., 2018). It is a linear polymer consisting of blocks of (1,4) - linked-β-D-mannuronate(M) and α-guluronate(G). The blocks are made up of consecutive G residues, consecutive M residues or alternating G and M residues. Its remarkable gelling and thickening properties make it a favoured choice for encapsulation purposes.

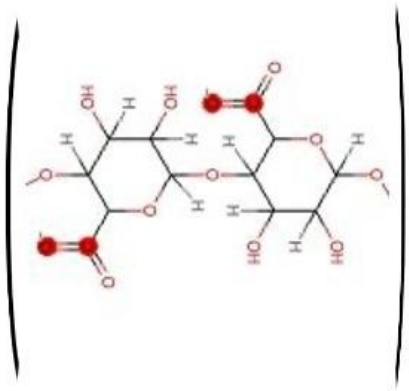

Figure1. Alginate structure

1.3.2) Cellulose

Cellulose, an abundant structural component in plant cell walls, is known for its insolubility and

https://doi.org/10.36375/prepare_u.iiche.a390

resistance to digestion by human enzymes. It has been employed in encapsulation due to its biocompatibility and the ability to provide a physical barrier for controlled release applications. It is a linear polysaccharide consisting of β-(1,4)-linked glucose units.

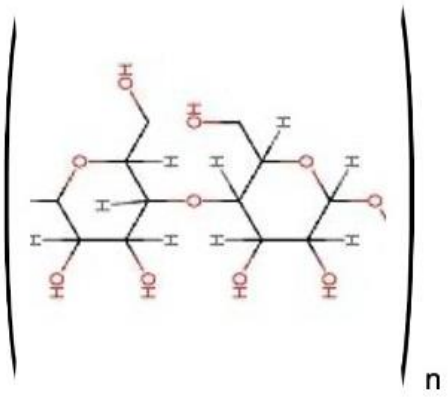

Figure2. Cellulose structure

1.3.3) Pectin

Pectin, another plant-derived polysaccharide, predominantly found in fruits, possesses excellent gelling properties attributed to its highly branched structure. It is an acidic polysaccharide that consists of 150 - 500 α-(1,4)-D-galacturonic acid (Lara-Espinoza et al., 2018). Pectin's unique gelling ability has made it a valuable candidate for encapsulation, enabling the development of controlled-release systems in the pharmaceutical and food industries.

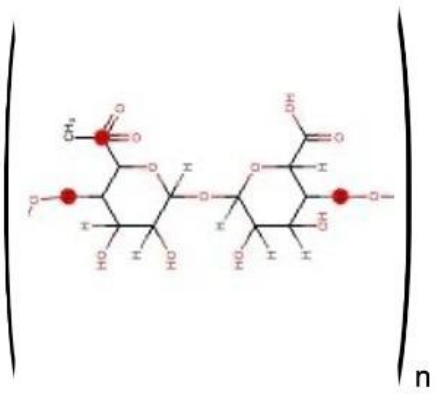

Figure3. Pectin structure

These dietary fibres, Alginate, Cellulose, and Pectin, collectively represent a rich resource for encapsulation technologies, offering diverse functionalities and potential applications in tackling vitamin B12 deficiency.

2. Methodology

*(All concentrations are expressed as weight/volume %)

2.1) Preparation of Cross-linking solution:

A 100 mM solution of calcium chloride was prepared in distilled water to serve as the cross-linking agent for the fibre encapsulation of Vitamin B12 via ionotropic gelation.

2.2) Encapsulations of Vitamin B12 at 2% concentration of Dietary fibres:

https://doi.org/10.36375/prepare_u.iiche.a390

Sodium alginate, pectin, and hydroxypropyl methylcellulose, each of which was weighed to 2 grams and dissolved in 100 ml distilled water to obtain the 2% solutions.

Vitamin B12 powder corresponding to the recommended concentration of 2.4 micrograms was added to each and mixed well (Office of Dietary Supplements - Vitamin B12, n.d.).

The mixture was pipetted out dropwise into the prepared calcium chloride solution.

2.3) Encapsulations of Vitamin B12 at 3%, 4%, 5%, 6%, 7% concentrations of Dietary fibre:

The previous steps were repeated for higher concentrations of the fibres in increments of 1 % (3%, 4%, 5%, 6%, 7% and 8%) with corresponding weights of alginate, pectin, and cellulose in distilled water as long as the capsules were obtained.

The obtained bead capsules were washed with distilled water to remove excess calcium chloride.

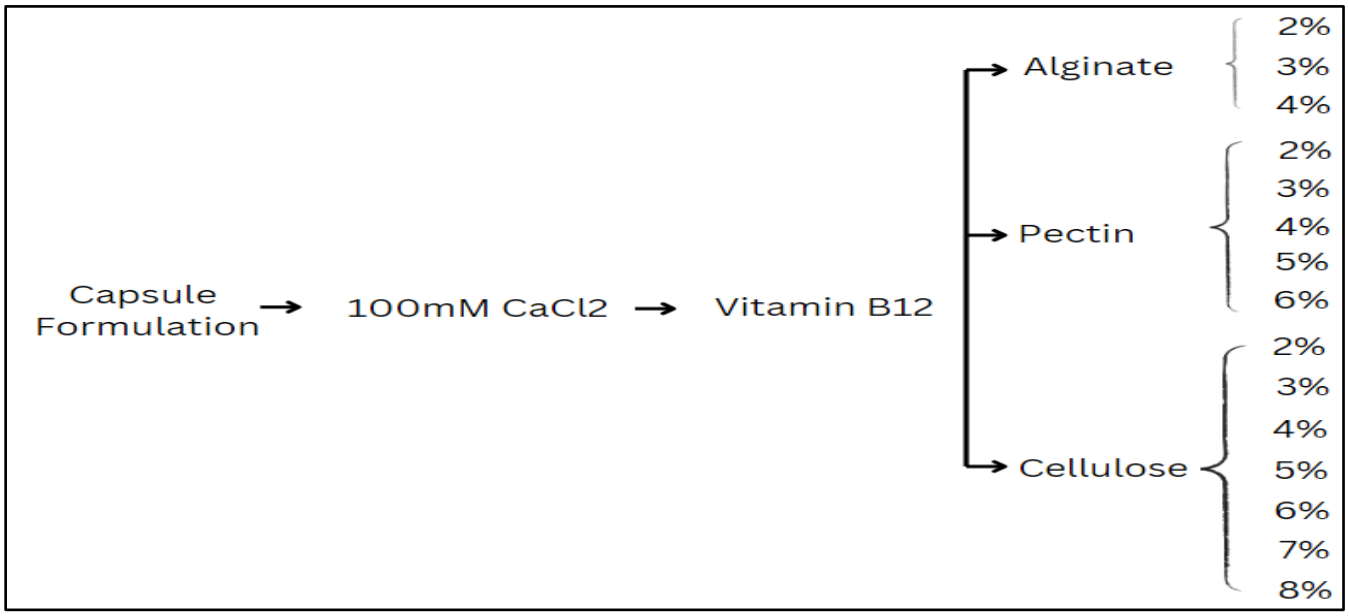

Figure 4. Experimental design for vitamin B12- dietary fibre encapsulate formulation.

https://doi.org/10.36375/prepare_u.iiche.a390

3. Results and Discussion

Figure 5. Encapsulation of Vitamin B12 with 4% Alginate

Figure 6. Encapsulation of Vitamin B12 with 6% Pectin

Bead capsules of Vitamin B12 were obtained in alginate at 4% concentration.

Bead capsules of Vitamin B12 were obtained in pectin at 6% concentration.

Bead capsules of Vitamin B12 were not obtained in cellulose up to a concentration of 8%, following which the matrix turned very thick making it unsuitable for obtaining capsules.

The wet laboratory observations can be potentially justified as follows.

Alginate and Pectin follow the gelation mechanism of ionotropic gelation whereas Cellulose follows the simple mechanism of hydration for encapsulation rather than ionotropic gelation. Ionotropic gelation involves cross linking of the fibre material with divalent calcium ions which results in it being a stronger gelation approach than hydration, wherein the material absorbs water due to its hydrophilicity and swells up forming jelly capsules. This probably explains the reason as to why alginate and pectin could form capsules of vitamin B12 at lower concentrations unlike cellulose (Smrdel et al., 2008) (Aguilar et al., 2015) (Smyth et al., 2018).

Next, within alginate and pectin, the higher threshold concentration of pectin can be explained as follows.

Pectin is a complex polymer of galacturonic acid with a higher degree of methyl esterification of the carboxyl groups compared to that in alginate, a linear polysaccharide of guluronic acid and mannuronic acid. This higher extent of esterification of the carboxyl groups in pectin compared to alginate leads to lower availability of free carboxyl groups for interaction with the calcium ions, thus resulting in a much higher concentration of pectin being required for

https://doi.org/10.36375/prepare_u.iiche.a390

encapsulating vitamin B12 compared to alginate via ionotropic gelation (Shen et al., 2022).

Table 1: Comparison of concentrations % of different dietary fibres required to obtain capsules of Vitamin B12

Concentration (w/v)	*Alginate*	*Pectin*	*Cellulose*
2%	**-**	**-**	**-**
3%	**-**	**-**	**-**
4%	**+**	**-**	**-**
5%		**-**	**-**
6%		**+**	**-**
7%			**-**
8%			**-**

LEGEND:

+	**Obtained Capsules**
-	**Capsules Not Obtained**

4. Conclusion

The concentration of Alginate that is required to encapsulate vitamin B12 is 4%. On the other hand, the concentration of Pectin required to encapsulate vitamin B12 is 6% and no capsules were obtained with cellulose. Correspondingly, the order of quantity of each of the three dietary fibres required for encapsulating vitamin B12 using a fixed volume of distilled water is Alginate followed by Pectin, with no vitamin B12 capsulation observed with cellulose as a matrix.

Thus, the conclusion drawn is that alginate would be the best suited matrix material among the three for vitamin B12 encapsulation based on the quantity of the dietary fibres required alone, as a sole parameter of comparison.

5. Acknowledgement

We express our sincere gratitude to R V College of Engineering and Rashtreeya Sikshana Samithi Trust, for having provided us with the requisite facilities to conduct our research.

6. References

1) Klojdová, I., Milota, T., Smetanová, J., & Stathopoulos, C. (2023). Encapsulation: A Strategy to Deliver Therapeutics and Bioactive Compounds? *Pharmaceuticals*, *16*(3), Article 3. https://doi.org/10.3390/ph16030362

2) Singla, R., Garg, A., Surana, V., Aggarwal, S., Gupta, G., & Singla, S. (2019). Vitamin B12 Deficiency is Endemic in Indian Population: A Perspective from North India. *Indian Journal of Endocrinology and Metabolism*, *23*(2), 211–214. https://doi.org/10.4103/ijem.IJEM_122_19

3) Smith, A. D., Warren, M. J., & Refsum, H. (2018). Chapter Six—Vitamin B12. In N. A. M. Eskin (Ed.), *Advances in Food and Nutrition Research* (Vol. 83, pp. 215–279). Academic Press. https://doi.org/10.1016/bs.afnr.2017.11.005

4) National Institutes of Health, Office of Dietary Supplements. (n.d.). Vitamin B12. Retrieved January 14, 2024, from https://ods.od.nih.gov/factsheets/VitaminB12-HealthProfessional/

5) Lee, Kuen Yong, Mooney, David J(2012). Alginate: properties and biomedical applications.(Vol. 37, 106-126)

6) Lara-Espinoza, Claudia, Carvajal-Millán, Elizabeth, Balandrán-Quintana, René, López-Franco, Yolanda, Rascón-Chu, Agustín.(2018), Pectin and Pectin-Based Composite Materials: Beyond Food Texture.(Vol. 23, Issue 4)

7) Khatun, Bably, Das, Jonali, Rizwana, Shagufta, Maji, T.K.(2023), Biodegradable polymers- a greener approach for food packaging(Green Sustainable Process for Chemical and Environmental Engineering and Science, 317-369)

8) Madene, A., Jacquot, M., Scher, J., & Desobry, S. (2005). Flavour encapsulation and controlled release – a review. *International Journal of Food Science & Technology*, *41*(1), 1–21. https://doi.org/10.1111/j.1365-2621.2005.00980.x

9) Varankovich, N., Khan, N. H., Nickerson, M. T., Kalmokoff, M., & Korber, D. R. (2015). Evaluation of pea protein–polysaccharide matrices for encapsulation of acid-sensitive bacteria. *Food Research International*, *70*, 118–124. https://doi.org/10.1016/j.foodres.2015.01.028

10) Gadziński, P., Froelich, A., Jadach, B., Wojtyłko, M., Tatarek, A., Białek, A., Krysztofiak, J., Gackowski, M., Otto, F., & Osmałek, T. (2022). Ionotropic gelation and chemical crosslinking as methods for fabrication of Modified-Release GELLAn Gum-Based drug delivery systems. *Pharmaceutics*, *15*(1), 108. https://doi.org/10.3390/pharmaceutics15010108

11) Green, R., Allen, L. H., Bjørke-Monsen, A. L., Brito, A., Guéant, J. L., Miller, J. W., Molloy, A. M., Nexø, E., Stabler, S. P., Toh, B. H., Ueland, P. M., & Yajnik,

C. S. (2017d). Vitamin B12 deficiency. *Nature Reviews Disease Primers*, *3*(1). https://doi.org/10.1038/nrdp.2017.40

12) Weissbach, H., & Taylor, R. T. (1969c). Metabolic role of vitamin B12. In *Vitamins and hormones* (pp. 395–412). https://doi.org/10.1016/s0083-6729(08)60763-3

13) Ling, C. T., & Chow, B. F. (1954). THE INFLUENCE OF VITAMIN B12 ON CARBOHYDRATE AND LIPIDE METABOLISM. *Journal of Biological Chemistry*, *206*(2), 797–805. https://doi.org/10.1016/s0021-9258(19)50851-1

14) Stabler, S. P. (2013). Vitamin B12Deficiency. *N Engl J Med 2013; 368:149-160*, *368*(2), 149–160. https://doi.org/10.1056/nejmcp1113996

15) Pawlak, R., Parrott, J. S., Raj, S., Cullum-Dugan, D., & Lucus, D. (2013). How prevalent is vitamin B12deficiency among vegetarians? *Nutrition Reviews*, *71*(2), 110–117. https://doi.org/10.1111/nure.12001

16) Ward, M., Kariyawasam, V. C., Mogan, S. B., Patel, K., Pantelidou, M., Sobczyńska-Malefora, A., Porté, F., Griffin, N., Anderson, S., Sanderson, J., Harrington, D. J., & Irving, P. (2015). Prevalence and Risk Factors for Functional Vitamin B12 Deficiency in Patients with Crohn's Disease. *Inflammatory Bowel Diseases*, *21*(12), 2839–2847. https://doi.org/10.1097/mib.0000000000000559

17) Cyran, E. M. (2002). Vitamin B12 deficiency: Recognition and Management. *Primary Care Case Reviews*, *5*(2), 53–60. https://doi.org/10.1097/00129300-200206000-00001

18) Lee, Kuen Yong, Mooney, David J(2012), Progress in polymer science 37(1) 106-126 https://doi.org/10.1016/j.progpolymsci.2011.06.003

19) Richards, Heidi Lynn, Baker, Priscilla G. L., Iwuoha, Emmanuel,(2012), Metal Nanoparticle Modified Polysulfone Membranes for Use in Wastewater Treatment: A Critical Review, 02(03) 183-1933 **https://doi.org/10.3390/molecules23040942**

20) Smrdel, P., Bogataj, M., & Mrhar, A. (2008). The influence of selected parameters on the size and shape of alginate beads prepared by ionotropic gelation. *Scientia Pharmaceutica*, *76*(1), 77–89. https://doi.org/10.3797/scipharm.0611-07

21) Aguilar, K. C., Tello, F., Bierhalz, A. C. K., Romo, M. P., Martínez-Flores, H. E., & Grosso, C. R. F. (2015). Protein adsorption onto alginate-pectin microparticles and films produced by ionic gelation. *Journal of Food Engineering*, *154*, 17–24.

https://doi.org/10.1016/j.jfoodeng.2014.12.020

22) Smyth, M., M'Bengue, M., Terrien, M., Picart, C., Bras, J., & Foster, E. J. (2018). The effect of hydration on the material and mechanical properties of cellulose nanocrystal-alginate composites. *Carbohydrate Polymers*, *179*, 186–195. https://doi.org/10.1016/j.carbpol.2017.09.002

23) Shen, B., Guo, Z., Huang, B., Zhang, G., Peng, F., & Hu, S. (2022). Preparation of hydrogels based on pectin with different esterification degrees and evaluation of their structure and adsorption properties. *International Journal of Biological Macromolecules*, *202*, 397–406. https://doi.org/10.1016/j.ijbiomac.2021.12.160

https://doi.org/10.36375/prepare_u.iiche.a391

Development and Analysis of a Dietary Fiber-rich Food Supplement for the Elderly: An Initial Work

Sambaran Mondal[a], Mala Dey[a], Sweety Bardhan[a], Sayantika Saha[a], Neepa Banerjee[b], Shankarashis Mukherjee[a]

[a]*Public Health Analytics Unit, Department of Food and Nutrition, West Bengal State University, Kolkata 700126,India*
[b]*Bhairab Ganguly College, Kolkata 700056,India*

Abstract

Population aging is a predominant phenomenon worldwide. Aging increases the vulnerability of the body and results in the occurrence of health issues. The increasing adaptation of sedentarism in the elderly complicates the situation further. As people are now getting concerned about a healthy diet, the need for the consumption of adequate dietary fiber has been felt for its nutraceutical properties, especially the production of short-chain fatty acids by the gut microbiota. In this backdrop, an attempt is being made to develop a dietary fiber-rich food supplement for the elderly and analyze its properties. Several edible cereals and other edible ingredients were used for the formulation of the supplement. Preparatory and evaluatory methods and techniques were applied. An investigation of the possible mechanisms between the beneficial nutrient molecules and bodily effects has been taken into consideration. The outcome indicates that the supplement is a good source of dietary fiber and can be used for the geriatric diet.

Keywords: Elderly food supplement; fiber-rich supplement; elderly health; dietary fiber; physiochemical properties.

1. Introduction

The world is experiencing a rapid increase in the elderly population. In the year 2020, the world consists of around 100 crores of elderly people (aged ≥60 years), which is estimated to reach about 140 crores by 2030 and will be doubled i.e., will reach 210 crores by the year 2050 [1]. Significant improvements in technology and healthcare facilities lead to a longer lifespan for people worldwide [2]. India, as one of the most populous countries, has also observed a steady rise in its elderly population; the Census 2011 revealed the country consisted of 10.3 crores of elderly persons at that time, which is projected to reach about 23 crores in 2036 and 31.9 crores by 2050 [3,1]. Aging is the inherent irreversible deterioration of body functions over time, which decreases functional ability, causes adjusted quality of life, and leads to death. [4,5]. With aging, physiological functions decrease and the human body becomes prone to the development of diseases and disorders [6,7,8]. The changing lifestyle pattern over decades promoted the adaption of secondary behavior (i.e., activities like sitting or reclining that involve energy expenditure of less than 1.5 metabolic equivalents) and imbalanced dietary intake among the elderly [9], which in turn increases the prevalence of noncommunicable diseases (NCDs), neurodegenerative diseases, all-cause mortality and reduced cognitive function [10-15] and become a threat to the process of healthier aging. The widespread distribution and increment of lifestyle diseases; led people to accommodate different strategies including dietary adaptation of nutraceuticals, especially the addition of dietary fiber to daily diet [16,17,18]. Dietary fiber is composed of Soluble Dietary Fibers (SDFs) (like inulin, pectin, gum, arabic gum, galactomannan, beta-glucans), and insoluble dietary fibers (like

https://doi.org/10.36375/prepare_u.iiche.a391

cellulose, hemicelluloses, lignin), which are able to suppress the occurrence of NCDs and acts as a functional nutrient, as they possess intense physiochemical properties i.e., Water Holding Capacity (WHC), Water Swelling Capacity (WSC), Oil Holding Capacity (OHC), Glucose Absorption Capacity (GAC), Cholesterol Absorption Capacity and Viscosity, have beneficial effect on physiological functions of the human body [19,20,21]. Another recent perspective has been focused over a period i.e., the gut microbiome modulation by the SDFs [22].
SDFs are utilized and metabolized by the gut microbiota to produce beneficial end products, especially the Short Chain Fatty Acids (SCFAs), which plays an important role in reducing the occurrence of gastrointestinal diseases e.g., inflammatory bowel disease, irritable bowel disease, functional constipation, diverticular disease and colorectal cancer [23,24,25]. In this backdrop, an attempt was made to develop a dietary fiber-rich food supplement for the elderly and analyze its physiochemical properties.

2. Experimental

2.1 Materials

Edible cereals like maize and wheat, psyllium husk, and dextrose were used as basic ingredients for the formulation of the food supplement.

2.2 Analytical methods

Several processing techniques such as the application of dry heat, grinding, and mixing were used. No preservative or color was used. Microscopic observations of granules were made. pH was measured using a digital pH meter. Tests for WHC and WSC were performed using standard procedures [19,26,27]. The sensory tests were carried out using the 9-point hedonic scale by 18 consenting nonsmoking, non-alcoholic elderly persons aged 60-65 years, who did not have any oral disease and/or were taste compromised. Nutrient contents were calculated using IFCT, 2017. A preliminary cost calculation was also carried out.

3. Results and Discussions

The structure of the granules of the supplement has been observed under a microscope with 400X magnification.

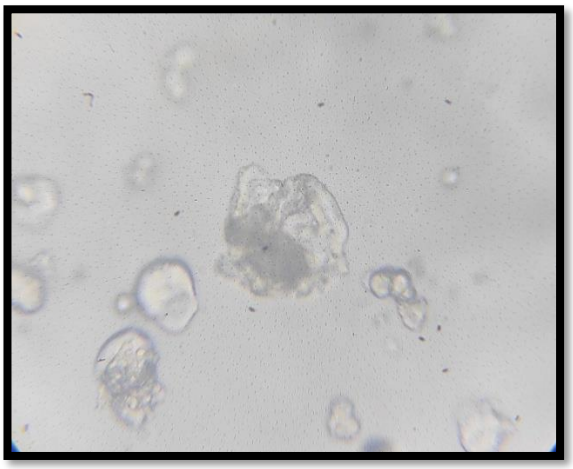

Fig.1: Molecular structure of the molecules under the microscope (400X)

The Physical characteristics in both solid state and after addition of water of the food supplement have been shown in table 1.

Table 1: Physical characteristics of the food supplement

Characteristics	Solid state	After water addition
Texture	Coarse granules	Gel-like structure
Flavor	Sweet	Less sweet
Taste	Sweet	Slightly sweet
Appearance	Yellowish	Yellowish
Smell	Pleasant	No smell

The physiochemical properties of the supplement have been presented in Table 2.

Table 2: Physiochemical properties of the supplement

Properties	Value
pH	6.3- 6.5
WHC *(g/g)*	2.60 ± 0.03
WSC *(ml/g)*	2.40 ± 0.10

https://doi.org/10.36375/prepare_u.iiche.a391

The scores of the sensory tests conducted using the food supplement (solid state) has been presented in Fig. 2.

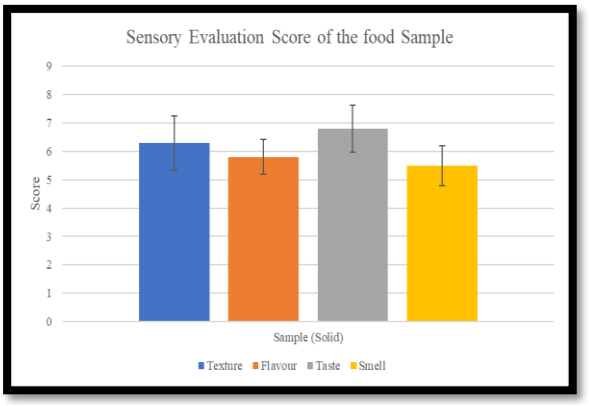

Fig.2: Sensory Evaluation Score (mean) of the food sample (solid)

The calculated nutritive value of the food supplement has been presented in Table 3.

Table 3: Nutritive value (calculated) of the food supplement

Nutrients	Amount *(g)*
Dietary fiber	14.9
Carbohydrate	62.8
Protein	7.7
Fate	2.4
Energy	1290 *(kJ)*

The calculated preliminary cost of the food supplement is INR 19.78, which can increase to INR 22.78 after the inclusion of packaging and labeling costs.

The prevalence of noncommunicable diseases is a global burden and has become the biggest threat to the progress of Healthy Aging worldwide [28]. Dietary fiber possesses significant beneficial characteristics, that help in the prevention of noncommunicable diseases [29]. Dietary fibers like cellulose, hemicellulose, inulin, pectin, etc prevent pathogenic infestation, which is responsible for the stimulation of human immune system, as well as gut barrier function and also helps in production of SCFAs (like acetate, butyrate, propionate) [30].
In vivo studies reported that acetate was responsible for reduction in levels of IL-1β and IL-18 production and increase in NLRP3-inflammasome ubiquitination [31]; the latter is responsible for regulation of NLRP3-inflammasome, a immune system component that increases inflammation and helps in the progression of diseases like atherosclerosis, Alzheimer's, and Inflammatory Bowel Disease [32]. Butyrate increases acetylation, and along with propionate, it regulates glucose homeostasis with the regulation of G-Protein Coupled Receptor-43 (GPR43) AMP-activated protein kinase (AMPK) [33,34]. The food supplement being developed is rich in dietary fiber, and hence expected to provide the health benefits associated with dietary fiber. Microscopic observation of the granules indicated that the molecules of the supplement are capable of holding sufficient water, and physiochemical properties, assessed quantitatively supported it. WHC and WSC help in intestinal peristalsis and motility [35]. Although the texture was coarse in the solid state; when dissolved in lukewarm water, it formed a gel-like structure, and a small change has also been observed in taste. The pH of the supplement on addition of lukewarm water, after bringing down to room temperature is in the range of 6.3 to 6.5, and hence close to neutral. There are several fiber-rich supplements available in Indian market, but they have scope for improvement especially with regard to taste. As with aging, the functions of taste buds decrease, an initial attempt was made and the results of sensory tests performed by elderly individuals confirmed a slight better. The nutritive value calculation shows that the supplement contains about 15g of dietary fiber per 100 g of the supplement, which may able to fulfill half of the recommended daily intake for the elderly as recommended by ICMR. On the basis of the characteristics discussed, it may be concluded that the developed food supplement is rich in dietary fiber, which may be helpful for elderly persons.

Acknowledgements

The authors acknowledge study participants, UGC and West Bengal State University.

References

1. United Nations Department of Economic and Social Affairs. 2022. World Population Prospect 2022:

release note about major differences in total population estimates for mid-2021 between 2019 and 2022 revisions. New York. Population Division; [accessed 2023 Nov 2]. https://population.un.org/wpp/Publications/Files/WPP2022_Release-Note-rev1.pdf.

2. Ananthakrishnan, A.N., Kaplan, G.G., Ng, S.C. 2020. Changing global epidemiology of inflammatory bowel diseases: sustaining health care delivery into the 21st century. *Clinical Gastroenterology and Hepatology*, 18, 1252-1260. Doi: 10.1016/j.cgh.2020.01.028.

3. Government of India, Ministry of Health and Family Welfare. 2020. Population Projections for India and States 2011 – 2036. New Delhi. National Commission on Population; [accessed 2023 Nov 2]. https://main.mohfw.gov.in/sites/default/files/Population%20Projection%20Report%202011-2036%20-%20upload_compressed_0.pdf.

4. Cai, Y., Song, W., Li, J., et al. 2022. The landscape of aging. *Sci. China Life Sci.* 65, 2354–2454. Doi: 10.1007/s11427-022-2161-3.

5. Banerjee, N., Chatterjee, S., Bardhan, S., Mukherjee, S. 2022. Impact of select design characteristics in food packaging on consumer behavior: A study on Elderly population in Kolkata. *Ergonomics for Design and Innovation*, p. 1045-1057, (Springer Nature, Singapore). Doi: 10.1007/978-3-030-94277-9_89.

6. Amorim, J.A., Coppotelli, G., Rolo, A.P., et al. 2022. Mitochondrial and metabolic dysfunction in ageing and age-related diseases. *Nat Rev Endocrinol*., 18, 243–258. Doi: 10.1038/s41574-021-00626-7.

7. Li, Z., Zhang, Z., Ren, Y., et al. 2021. Aging and age-related diseases: from mechanisms to therapeutic strategies. *Biogerontology*, 22(2), 165-187. Doi: 10.1007/s10522-021-09910-5.

8. Chatterjee, A., Chatterjee, S., Banerjee, N., Mukherjee, S. 2020. A Study to Assess Relationship between Different Obesity Indices and Musculoskeletal Discomfort Score in Agricultural Workers in Southern Districts of West Bengal, India. *Open Acc J Comp & Alt Med*., 2, 171-180.

9. Alessy, S.A., Malkin, J.D., Finkelstein, E.A., et al. 2023. Effectiveness of Interventions Promoting Physical Activity and Reducing Sedentary Behavior in Community-Dwelling Older Adults: An Umbrella Review with Application to Saudi Arabia. *J Epidemiol Glob Health*, 13, 361–373. Doi: 10.1007/s44197-023-00111-6.

10. Banerjee, N., Santra, T., Bardhan, S., De, S., Mukherjee, S. 2022. Impact of practicing Bharatnatyam dancing on obesity status in terms of adiposity indices in human resources engaged in white collar jobs: A study in Bangalee Females. In: ChakrabartiD, Karmakar S, Salve UR. (eds) Ergonomics for Design and Innovation. Proceedings of HWWE 2021; 2021 Dec 1-3; Guwahati, India. Springer Nature. p. 1521-1529. Doi: 10.1007/978-3-030-94277-9_130.

11. Banerjee, N., Chatterjee, S., Chatterjee, S., Bhattacharjee, S., De, S., Mukherjee, S. 2021. Relation between Occupational Sitting Duration and Central Obesity? A Study in Bengalee Female Human Resources Engaged in Sedentary Occupation. In: Muzammil M, Khan AA, Hasan F. (eds) Ergonomics for Improved Productivity. Proceedings of HWWE 2017; 2017 Dec 8-10; Aligarh, India. Springer Nature. p. 911-920. Doi: 10.1007/978-981-15-9054-2.

12. Banerjee, N., Biswas, P., Chatterjee, S., Santra, T., Chatterjee, S., Mukherjee, S. 2021. Impact of Bharatnatyam Dancing on Obesity and Diabetes Risk Status: A Study in Bengalee Female Human Resources

Engaged in Sedentary Occupations. In: Muzammil M, Khan AA, Hasan F. (eds) Ergonomics for Improved Productivity. Proceedings of HWWE 2017; 2017 Dec 8-10; Aligarh, India.Springer Nature. p. 921-929. Doi: 10.1007/978-981-15-9054-2.

13. Ruiz-Gonzalez, D., Hernandez-Martinez, A., Valenzuela, P.L., Morales, J.S., Soriano-Maldonado, A. (2021). Effects of physical exercise on plasma brain-derived neurotrophic factor in neurodegenerative disorders: a systematic review and meta-analysis of randomized controlled trials. *Neuroscience & Biobehavioral Reviews*, 128, 394-405. Doi: 10.1016/j.neubiorev.2021.05.025.

14. Santra, T., Chatterjee, S., Chatterjee, S., Bardhan, S., Banerjee, N., Pal, B., Gangopadhyay, S., Mukherjee, S. 2022. Assessing Lung Functions Status in Male Human Resources engaged in Wood Processing Works: Using Surrogate Markers. In: Chakrabarti D, Karmakar S, Salve UR. (eds) Ergonomics for Design and Innovation. Proceedings of HWWE 2021; 2021 Dec 1-3; Guwahati, India. Springer Nature. p. 1423–1433. Doi: 10.1007/978-3-030-94277-9_122.

15. Bhattacharjee, S., Santra, T., Chatterjee, A., Chatterjee, S., Banerjee, N., Chatterjee, S., Mukherjee, S. 2022. Cognitive Status of Adult Bengalee Male Individuals Undergoing Training in Football.In: Chakrabarti D, Karmakar S, Salve UR. (eds) Ergonomics for Design and Innovation. Proceedings of HWWE 2021; 2021 Dec 1-3; Guwahati, India. Springer Nature. p. 1303-1311. Doi: 10.1007/978-3-030-94277-9_111.

16. Chatterjee, S., Banerjee, N., Chatterjee, S., Bardhan, S., Saha, S., Mukherjee, S. 2022. Cognitive Ability improvement in Indian Classical Dancing: A Study in Bengalee Female.In: Chakrabarti D, Karmakar S, Salve UR. (eds) Ergonomics for Design and Innovation. Proceedings of HWWE 2021; 2021 Dec 1-3; Guwahati, India. Springer Nature. p. 727–737. Doi: https:10.1007/978-3-030-94277-9_62.

17. Bhattacharjee, S., Santra, T., Chatterjee, S., Biswas, P., Banerjee, N., Mukherjee, S. 2021. A Study on flexibility and fitness status of adult Bengalee males undergoing training in football. In: Muzammil M, Khan AA, Hasan F. (eds) Ergonomics for Improved Productivity. Proceedings of HWWE 2017; 2017 Dec 8-10; Aligarh, India. Springer Nature. p. 869-881.Doi: 10.1007/978-981-15-9054-2_102.

18. Chanda, S., Tiwari, R.K., Kumar, A., Singh, K. 2019. Nutraceuticals inspiring the current therapy for lifestyle diseases. *Advances in Pharmacological and Pharmaceutical Sciences*, 2019, 6908716. Doi: 10.1155/2019/6908716.

19. He, Y., Wang, B., Wen, L., Wang, F., et al. 2022. Effects of dietary fiber on human health. *Food Science and Human Wellness*, 11(1), 1-10. Doi: 10.1016/j.fshw.2021.07.001

20. Huang, J.Y., Liao, J.S., Qi, J.R., Jiang, W.X., Yang, X.Q. 2021. Structural and physicochemical properties of pectin-rich dietary fiber prepared from citrus peel. *Food Hydrocolloids*, 110, 106140. Doi: 10.1016/j.foodhyd.2020.106140.

21. Soliman, G.A. 2019. Dietary fiber, atherosclerosis, and cardiovascular disease. *Nutrients*, 11(5), 1155. Doi: 10.3390/nu11051155.

22. Spencer, C.N., McQuade, J.L., Gopalakrishnan, V., McCulloch, J.A., et al. 2021. Dietary fiber and probiotics influence the gut microbiome and melanoma immunotherapy response. *Science*, 374(6575), 1632-1640. Doi: 10.1126/science.aaz7015.

23. Guan, Z.W., Yu, E.Z., Feng, Q. 2021.

Soluble dietary fiber, one of the most important nutrients for the gut microbiota. *Molecules*, 26(22), 6802. Doi: 10.3390/molecules26226802.

24. Gill, S.K., Rossi, M., Bajka, B., Whelan, K. 2021. Dietary fibre in gastrointestinal health and disease. *Nat. Rev. Gastroenterol. Hepatol*., 18, 101–116. Doi: 10.1038/s41575-020-00375-4.

25. Koh, A., De Vadder, F., Kovatcheva-Datchary, P., Backhed, F. 2016. From Dietary Fiber to Host Physiology: Short-Chain Fatty Acids as Key Bacterial Metabolites. *Cell*, 165, 1332–1345. Doi: 10.1016/j.cell.2016.05.041.

26. Robertson, J.A., Monredon, D.F., Dysseler, P., et al. 2000. Hydration Properties of Dietary Fibre and Resistant Starch: a European Collaborative Study. *LWT - Food Science and Technology*, 33, 72-79. Doi: 10.1006/fstl.1999.0595.

27. Boulos, N.N., Greenfield, H., Wills, R. 2000. Water holding capacity of selected soluble and insoluble dietary fibre. *International Journal of Food Properties*, 3, 217-231. Doi: 10.1080/10942910009524629.

28. World Health Organization. 2023. Noncommunicable diseases. Geneva. [accessed 2023 Nov 4]. https://www.who.int/news-room/fact-sheets/detail/noncommunicable-diseases.

29. Khan, J., Khan, M.Z., Ma, Y., et al. 2022. Overview of the composition of whole grains' phenolic acids and dietary fibre and their effect on chronic non-communicable diseases. *International Journal of Environmental Research and Public Health*, 19, 3042. Doi: 10.3390/ijerph19053042.

30. Kumar, J., Rani, K., Datt, C. 2020. Molecular link between dietary fibre, gut microbiota and health. *Molecular Biology Reports*, 47, 6229-6237. Doi: 10.1007/s11033-020-05611-3.

31. Chen, Y., Ye, X., Escames, G., et al. 2023. The NLRP3 inflammasome: contributions to inflammation-related diseases. *Cell Mol Biol Lett*., 28, 51. Doi: 10.1186/s11658-023-00462-9.

32. Xu, M., Jiang, Z., Wang, C., et al. 2019. Acetate attenuates inflammasome activation through GPR43-mediated Ca2+-dependent NLRP3 ubiquitination. *Experimental &Molecular Medicine*, 51, 1-13. Doi: 10.1038/s12276-019-0296-1.

33. Kibbie, J.J., Dillon, S.M., Thompson, T.A., et al. 2021. Butyrate directly decreases human gut lamina propria CD4 T cell function through histone deacetylase (HDAC) inhibition and GPR43 signaling. *Immunobiology*, 226, 152126. Doi: 10.1016/j.imbio.2021.152126.

34. Yoshida, H., Ishii, M., Akagawa, M. 2019. Propionate suppresses hepatic gluconeogenesis via GPR43/AMPK signaling pathway. *Archives of Biochemistry and Biophysics*, 672, 108057. Doi: 10.1016/j.abb.2019.07.022.

35. Zhuang, Z., Chen, M., Niu, J., et al. 2019. The manufacturing process of kiwifruit fruit powder with high dietary fiber and its laxative effect. *Molecules*, 24(21), 3813. Doi: 10.3390/molecules24213813.

https://doi.org/10.36375/prepare_u.iiche.a391

https://doi.org/10.36375/prepare_u.iiche.a392

[International Conference on Energy Transition: Challenges and Opportunities at Chemical Engineering Congress (CHEMCON-2023) – On the occasion of Platinum Jubilee Year of Indian Institute of Chemical Engineers]

An Up-To-Date Review of Microbially-induced Carbonate Precipitation Process and its Applications

Aneena Sharaf, Anju Das, Jyothika C, Riya P.R, Biju Jacob*

Sree Chitra Thirunal College of Engineering, Pappanamcode, Thiruvananthapuram, Kerala, India -695018

**Corresponding author email: bijujacob@sctce.ac.in*

Abstract

Microbially-induced carbonate precipitation (MICP) is a natural process wherein microbes alter the environment and cause the creation of carbonate minerals. MICP is quicker than typical mineralization owing to the involvement of microbial enzymes. It is economical, sustainable, and environmentally friendly. MICP has many applications, including reinforcing soil and building materials, mending concrete cracks, capturing CO_2, and producing bio-composites. This review seeks to understand the physiology of the MICP process, along with its applications in sustainable construction. Research progress made in this area over the past one decade is lucidly presented. Focus is placed on bio-concrete, which through microbial self-healing, effectively combats concrete's vulnerability to cracking in a durable and practical fashion. Use of the ureolytic bacterium, *Lysinibacillus sphaericus* is explored in the context of self-healing concrete formulation, with focus on its merits over other microbial species with carbonate precipitating potential.

Keywords: Microbially-induced carbonate precipitation; self-healing; bio-concrete; *Lysinibacillus sphaericus*

Introduction

Microbially-induced calcite Precipitation (MICP) is a biomineralization process in which microorganisms, typically certain types of bacteria, facilitate the precipitation of calcium carbonate ($CaCO_3$) minerals from calcium-rich solutions. This method is environmentally friendly and sustainable in terms of cost-effectiveness. Several bacterial species that are capable of carbonate precipitation in natural environments (such as *Sporosarcina pasteurii, Bacillus megaterium,* etc.*)* have been extensively studied. Using enzymes such as urease, these bacteria manipulate their environment leading to calcite precipitation. MICP is seen as a novel technology that comes under the framework of sustainable development goals. Two of the best-known applications of MICP are Bioaugmentation (which involves introducing ureolytic bacteria like *Sporosarcina pasteurii* or *Bacillus species* into soil, concrete, or other matrices where calcium carbonate precipitation is desired) and Biogrouting (which creates calcium carbonate cementation, improving soil cohesion and load-bearing capacity for applications like slope stabilization and foundation reinforcement). This review focuses on one prime application of the MICP process i.e. in the preparation of bio- concrete (also known as self-healing concrete or microbial concrete), a product which is expected to revolutionize tomorrow's construction industry. The uses and applications of the MICP process continue to evolve and expand as researchers explore new ways to leverage the potential of microbial carbonate precipitation in diverse fields.

Microbially-induced carbonate precipitation: the underlying mechanism

Selective cementation has great significance in various fields like petroleum, civil, and geological engineering where microorganisms have been shown to remediate cracks in natural environments. Microbially-induced Carbonate Precipitation (MICP) utilizes different metabolic pathways:

https://doi.org/10.36375/prepare_u.iiche.a392

1. **Urea Hydrolysis**: Bac[4]teria break down urea, releasing carbonate ions and raising the pH, which encourages the precipitation of calcium ions. This method is commonly employed in MICP [3]for bio- concrete development.
2. **Denitrification**: Denitrifying bacteria use nitrate instead of oxygen, resulting in nitrate reduction to nitrite and creating an alkaline environment favorable for calcium carbonate precipitation. Denitrification is beneficial in low-oxygen conditions like concrete cracks.
3. **Dissimilatory Sulfate Reduction**: Sulfate-reducing bacteria metabolize sulfate ions, generating sulfide ions that can react with calcium ions to form calcium carbonate. While less commonly used, dissimilatory sulfate reduction offers another potential pathway for MICP.

Although these three pathways are in use, urea hydrolysis has been widely employed due to its high energy efficiency, low cost, controllable reaction process, and direct separation and harvest procedure. Kinetic studies have shown that the rate of calcite precipitation depends on the concentration of bacterial cells, the ionic strength of the medium, and the pH.

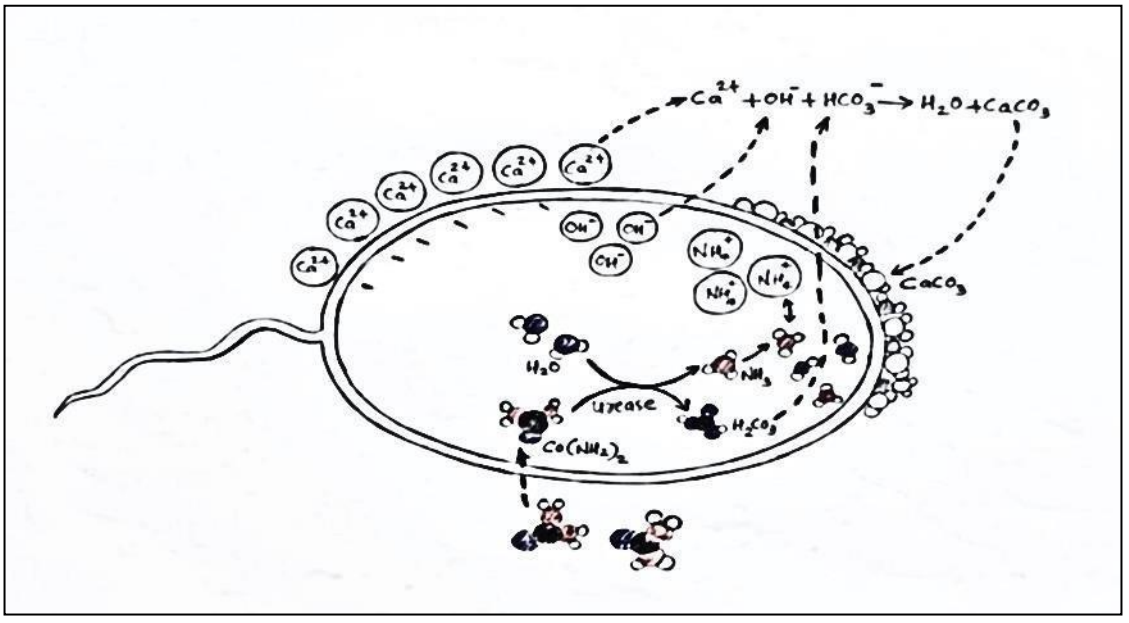

Fig 1 **. Biochemical mechanism of MICP**

Urea (NH_2CONH_2) hydrolyzed by urease enzyme produced by the bacteria results in the production of ammonium ions (NH_4^+) and bicarbonate (H_2CO_3):

$$NH_2\text{-}CO\text{-}NH_2 + H_2O \rightarrow 2NH^+ + H_2CO_3$$

The bicarbonate formed is then reduced to carbonate ions:

$$H_2CO_3 \rightarrow CO^{2-} + 2H^+$$

Microorganisms with a net negative cell surface charge can attract and bind cations, including calcium ions (Ca^{2+}), from their surrounding environment.

$$Cells + Ca^{2+} \rightarrow Cells\text{-}Ca^{2+}$$

The bound calcium ions (Ca^{2+}) on the cell surface react with the carbonate ions (CO_3^{2-}) available in the vicinity to form solid calcium carbonate (calcite) as a precipitate at the nucleation site:

https://doi.org/10.36375/prepare_u.iiche.a392

$$Cells\text{-}Ca^{2+} + CO_3^{2-} \rightarrow Cells\text{-}CaCO_3$$

This process plays a crucial role in biomineralization and can have various environmental and engineering applications.

Current trends and methodologies in self-healing concrete

The self-healing concrete field is rapidly advancing with innovative methods to improve structure durability and sustainability. It has the potential to extend the structure life span and reduce maintenance costs, thus offering promising prospects for the future of infrastructure. Various microorganisms have been utilized in recent studies on bio-concrete to investigate its self-healing properties. These studies focused on exploring the effectiveness of different bacteria and their biomineralization capabilities. Comparative studies on some notable microorganisms such as *Bacillus subtilis, Brevibacillus sp., Bacillus megaterium and Microvirga sp.* led to the conclusion that *B. subtilis*- based bio-concrete yielded the highest compressive strength of 50.37 N/mm^2 . (Vanjinathan, 2023).

Several researchers have focused on investigating the effects of different nutrient sources on the growth of microorganisms and, subsequently, their impact on the properties of bio-concrete. The use of corn steep liquor (an industrial by-product) as a nutrient source for cultivating *S. pasteurii* , a bacterium employed for remediating cracks and fissures in building materials and structures has yielded notable results. Urease activity and calcite production were significantly higher in the CSL-urea medium due to additional nitrogen sources. Calcite constituted 30.12% of sand samples in the CSL-urea medium. Incorporating *S. pasteurii* from the CSL-urea medium into mortar cubes led to a 35% increase in compressive strength. This approach holds the potential for enhancing the longevity and durability of construction materials and structures using industrial by-products like CSL (Achal, 2010).

Another study demonstrated the use of the dairy industry by-product, lactose mother liquor (LML), as a growth medium for *Sporosarcina pasteurii*, showcasing notable urease activity and calcite precipitation. Calcite constituted 24.0% of treated sand samples, with urease production reaching 353 U/ml in LML. Data analysis and conclusion emphasized the application of microbial calcite as a sealing agent for structural imperfections in both artificial and natural settings, with LML as a viable growth medium alternative (Achal 2008)

Investigations have been done on the impact of biomineralization in concrete by introducing ureolytic bacteria (*B. megaterium, B. pasteurii etc.*) without substrate and non-ureolytic bacteria (*B. cohnii*) without chemical feed. The research revealed a novel mineralization pathway that enhanced mechanical properties, reduced water absorption (by approximately 22%), decreased void volume (by around 24%), and lowered sulfate ion concentration at 180 days (by roughly 26%). Bacteria induced thick mineral deposition at the interfacial transition zone (ITZ) and accelerated the formation of hydrated products, resulting in a densified microstructure and improved macro properties of bacterial concrete. The results demonstrated a substantial enhancement of mechanical and durability properties due to the presence of bacteria in the concrete (Chaurasia, 2018)

Bacterial strain *Bacillus licheniformis AK01* isolated from loamy soils demonstrated significant calcite precipitation abilities. AK01 strain showed promising potential for improving concrete properties.The healing capability of AK01 was compared with three other competent bacteria: *Sporosarcina pasteurii DSM-33, Pseudomonas aeruginosa MA01,* and *Bacillus subtilis TRPC2*. The study evaluated the effects of these bacteria on compressive strength and water absorption in mortar specimens (Vahabiab, 2014).

The introduction of microorganisms into bioconcrete can be achieved through different methods, including percolation and direct mixing. These methods serve distinct purposes and can be chosen based on the specific goals and requirements of the bio-concrete project. Studies explored the use of microbiologically induced carbonate precipitation (MICP) for *in situ* soil reinforcement. Surface percolation was employed to immobilize bacteria along the entire length of a 1-meter sand column. The resulting biologically induced cementation exhibited homogeneity, and the efficiency of calcite crystal formation was linked to pore water content. Lower water content led to better strength, with crystals positioned at bridging points between sand grains. These findings suggest that optimizing conditions for crystal precipitation can reduce the cost of MICP technology, making it more feasible for large-scale applications (Chaurasia, 2018). Microorganisms are directly incorporated into the concrete mixture during the initial mixing stage, which ensures consistent microbial presence in the concrete.

A calcite-precipitating bacteria isolated from alluvial soil in Solan, India (identified *Lysinibacillus sp*. I13) is a promising strain. When incorporated into M20 concrete mixtures, *Lysinibacillus sp.* significantly enhanced

compressive strength, showing a 1.5-fold increase compared to *Bacillus megaterium MTCC 1684* after 28 days of curing (Vashishta, 2017).

In the pursuit of self-healing concrete technologies, researchers explored the use of denitrifying bacterial cultures to induce calcium carbonate precipitation within cracks, blocking the ingress of harmful agents and preventing corrosion of steel reinforcement. This approach benefits from microbial nitrate reduction, which occurs when organic matter is oxidized using nitrate (NO^{3-}) instead of oxygen (O_2) as an electron acceptor. Notably, this process enables precipitation in oxygen-limited environments within concrete cracks. Additionally, nitrate reduction produces nitrite (NO^{2-}), a known corrosion inhibitor for steel in concrete. Using an in-house non-axenic culture called "activated compact denitrifying core" (ACDC), the passivation of steel in chloride-containing solutions was achieved, surpassing the performance of protected axenic cultures in various conditions. Researchers tested the use of two axenic NO^{3-}reducing cultures, *Pseudomonas aeruginosa* and *Diaphorobacter nitroreducens*, for microbial self-healing in concrete using denitrification. These bacteria were encapsulated within expanded clay particles (0.5-2mm) and tested on mortar specimens with cracks ranging from 100-500 µm under wet and wet/humid conditions (Ersan, 2013).

It is important to note that the selection of microorganisms, their stage, and the timing of their introduction should be carefully planned and optimized to achieve the desired results while considering factors like the concrete's curing conditions, environmental factors, and the form in which microbes are added (i.e. spore or vegetative form). The inclusion of *Sporosarcina pasteurii* vegetative cells in cement-based materials had several notable effects. It significantly delayed the hydration process, indicating an influence on the material's setting time. Moreover, the bacterial presence promoted increased precipitation of calcium carbonate, especially in the form of calcite. Most importantly, the compressive strength of the bacterial mortar matched or exceeded that of the regular mortar after just one day of hydration. These findings suggest the potential of *Sporosarcina pasteurii* in contributing to the self-healing properties of cement-based materials, thus enhancing their durability and strength (Bundur, 2014).

Another study explored the potential of certain alkali-resistant, spore-forming bacteria from the *Bacillus* genus to serve as self-healing agents in concrete. The research revealed that when bacterial spores were directly added to the cement paste mixture, they remained viable and active for an extended period of up to 4 months. This finding is significant because it demonstrates the potential for these microorganisms to survive in the harsh environment of cement. A noteworthy observation was the decrease in pore size diameter as the cement stone underwent setting. As pore widths reduced to less than 1 micron (the typical size of *Bacillus* spores), the spores' life span decreased (Jonkers, 2008).

Seminal work by several other research groups have been reviewed and the conclusions drawn from each of them are summarized in table 1.

MICP has multiple engineering applications in the fields of geotechnical, geological, hydraulic, geo- environmental and structural engineering, some of which are exemplified as follows:

Geotechnical Engineering

a. **Soil Stabilization**: MICP improves strength and stability of loose soils, thereby enhancing their load bearing capacity.
b. **Foundation Improvement**: In areas of challenging soil conditions, MICP can strengthen foundation soils, mitigate settlement issues and increase bearing capacity of foundations.
c. **Slope Stabilization**: MICP can stabilize slopes to prevent erosion, landslides and slope failures by enhancing its resistance to surface run off and rainfall.

Geological Engineering

a. **Mine Shaft and Tunnel Support**: By consolidation of surrounding geological materials, MICP can enhance the stability of mine shafts and tunnels.
b. **Erosion Control**: MICP can be employed to stabilize soil in erosion-prone areas, preventing soil loss due to water flow or wind erosion.
c. **Heritage Conservation***:* It helps preserve historical buildings and monuments by reinforcing deteriorating stone or mortar with calcium carbonate, maintaining their structural integrity.

Hydraulic Engineering:

a. **Seepage Control**: MICP can reduce soil permeability, effectively controlling seepage and ensuring the structural integrity of critical facilities such as dams and levees.

https://doi.org/10.36375/prepare_u.iiche.a392

b. **Riverbank and Coastal Protection**: It prevents erosion and offers protection against flooding by strengthening riverbanks and coastal structures (which includes shoreline protection, reef restoration and creation of artificial reefs).

Geo-environmental Engineering:

a. **Contaminated Soil Remediation**: It can improve the soil quality at contaminated sites and can immobilize heavy metals and contaminants in soil through calcite precipitation.
b. **Waste Containment**: It can be used to strengthen liners and caps of landfills and waste containment facilities by enhancing their integrity and prevent leachate migration.

Structural Engineering:

a. Concrete Crack Repair: MICP can repair cracks in concrete structures by introducing bacteria having calcium carbonate precipitation capabilities along with nutrient solution. This helps in self-healing of concrete and increases its service life.
b. Structural Strengthening: MICP can be used to enhance the durability and strength of existing concrete and masonry structures within cracks and walls.

Table 1: Review of contemporary literature on bacterial concrete

Sl. No.	Author (Year)	Microorganism(s) used	Key observations/Conclusions
1	Shannon Stocks-Fischer (1999)	*Bacillus pasteurii*	At the pH where calcium precipitation was favorable, the urease activity and its affinity to urea are significantly high.
2	V. Ramakrishnan (2000)	*Bacillus pasteurii, Sporosarcina* sp.	The chosen microorganism grew more efficiently in the presence of oxygen. Hence, microbial repair was more successful in surface cracks.
3	Sookie S. Banga (2001)	*Bacillus pasteurii ATCC 11859*	The effects on elastic modulus and tensile strength of polymer was studied, increased compressive strength of concrete cubes was also observed.
4	Qian Chunxiang (2008)	*Bacillus pasteurii*	Water penetration resistance of a bio-concrete specimen surface was greatly improved by adding Ca^{2+} before urea.
5	Henk M. Jonkers (2008)	*Bacillus cohnii DSM 6307, Bacillus halodurans DSM 497 Bacillus pseudofirmus DSM 8715.*	Addition of Manganese to bio-concrete, induced the formation of bacterial spores.
6	Henk M. Jonkers (2008)	*Bacillus pseudofirmus DSM8715, B. cohnii DSM6307*	Bacterial spores remain viable for a period of 4 months when added to cement paste mixtures.
7	Varenyam Achal (2010)	*Sporosarcina pasteurii*	35% increase compressive strength was observed. Urease activity and calcium production were also enhanced.
8	S.S. Bang (2010)	*Sporosarcina pasteurii ATCC 1832*	*S. pasteurii* cells were immobilized on porous glass beads. The overall performance increased with treatment by microbial calcite.
9	Mousumi Biswas (2010)	*Thermophilic bacteria BKH1*	Compressive and tensile strength of cement-paste and mortar increased. Durability and quality of concrete were also enhanced.

https://doi.org/10.36375/prepare_u.iiche.a392

Sl. No.	Author (Year)	Microorganism(s) used	Key observations/Conclusions
10	Varenyam Achal (2010)	*Bacillus sp. CT-5*	36% increase compressive strength and enhanced durability of building materials.
11	J. Y. Wang (2011)	*Bacillus sphaericus*	Increased water penetration resistance of cracked specimens were observed.
12	Liang Cheng (2012)	*Ureolytic bacteria*	Homogeneous cementation was observed due to calcite crystal formation.
13	S.A. Abo-El-Enein (2012)	*S. pasteurii NCIMB 8841*	The amount of precipitated calcium carbonate, degree of crystallity and strength were increased.
14	Yusuf Cagatay Ersan (2013)	*Pseudomonas aeruginosa, Diaphorobacter nitroreducens*	It was found that the denitrification pathway is an effective and environment-friendly method for self-healing.
15	Ali Vahabiab (2014)	*Bacillus licheniformis AK01*	The compressive strength was improved to 15% and water absorption of mortar was reduced by 25%.
16	J. Y. Wang (2014)	*Bacillus sphaecus LMG 22557*	Hydrogel-encapsulated spores showed a high superiority in self-healing and water permeability decreased by 68%.
17	Wasim Khaliq (2015)	*Bacillus subtilis*	Bacterial immobilization in graphite nanoparticles gave significant enhancement in compressive strength on pre-cracked specimens.
18	Huaicheng Chen (2016)	*Bacillus mucilaginous L3 and Brewer's yeast JCS 05*	The use of ceramsite with immobilized bacteria and nutrients enhanced the flexural strength and self-healing power.
19	Jianyun Wang (2017)	*Bacillus sphaericus LMG 22257*	The bacterium had good tolerance and could survive at highly alkaline pH. The spores were able to germinate at low temperature and revived the ureolytic activity slowly.
20	Rajneesh Vashisht (2017)	*Lysinibacillus species*	Compressive strength increased by 1.5-fold along with higher calcite precipitation activity.
21	Jiaguang Zhang (2017)	*Bacillus cohnii*	Expanded perlite-immobilized bacteria were more efficient in crack healing than expanded clay-immobilized bacteria.
22	A F Alshalif (2018)	*Bacillus pasteurii, Pseudomonas aeruginosa, B. alkalinitrilicus, B. sphaericus, B. subtilis, Enterococcus faecalis, Shewanella sp. and S. pasteurii*	The resilience to survive in the harsh environment of concrete was confirmed from the extreme pH values of the samples taken. Self-healing process was also enhanced.
23	Leena Chaurasia (2018)	*Bacillus megaterium, Bacillus pasteurii, Bacillus cohnii*	Improved the mechanical properties, reduced water absorption and lowered sulfate ion concentration.
24	Yusuf Ç. Erşan, Nico Boon and Nele De Beli (2018)	*Aerobic heterotrophic bacteria (ureolytic strains)*	Calcium carbonate precipitation was enhanced, simultaneous corrosion inhibition was achieved.
25	Nuraiffa Syazwi Adzami, (2018)	*Bacillus sphaericus*	100% pure calcite was produced by calcium carbonate precipitation using calcium nitrate.
26	Wiboonluk Pungrasmi (2019)	*Bacillus sphaericus LMG 22257*	Freeze drying had a high bacterial spore survival rate and high potential as a microencapsulation technique.

https://doi.org/10.36375/prepare_u.iiche.a392

Sl. No.	Author (Year)	Microorganism(s) used	Key Observations/Conclusions
27	Atreyee Sarkara (2019)	*Alkaliphilic bacterium BKH4*	Due to the alkaliphilic nature, there was an enhancement in strength and durability.
28	B. Madhu Sudana Reddy (2019)	*Bacillus sphaericus*	Addition of the bacteria reduced the weakening (loss of strength) of concrete.
29	Z M Hussein (2019)	*Bacillus subtilis*	Deposition of calcium carbonate in the voids and subsequent closure of cracks were observed.
30	Minyoung Hong (2021)	*Bacillus miscanthi strain AK13*	The initial compressive strength of cement mortar was increased by the nitric acid treatment of oyster shell powder from which calcium nitrate was obtained. Increased bacterial survival and crack sealing were observed.
31	Adharsh Rajasekar(2021)	*Bacillus megaterium, Pseudomonas nitroreducens, Bacillus species, Bacillus licheniformis*	Good compressive strength was obtained. Reduced application cost and less environmental concern.
32	Shiren O. Ahmed (2021)	*Bacillus subtilis, Bacillus megaterium*	A novel concrete using selected Egyptian microorganisms had improved physical and mechanical properties.
33	Islam M. Riad (2022)	*Sporosarcina pasteurii DSM 33, Bacillus sphaericus DSM 396*	Compressive strength of concrete was tremendously increased, reduced chloride penetration, improved resistance to sulphate ingress.
34	Amal A. Nasser (2022)	*Bacillus pasteurii, Bacillus sphaericus*	Compressive strength increased by 28- 50% and so did the flexural strength.
35	Faisal Mahmood (2022)	*Bacillus subtilis*	Iron oxide particles were found to be ideal as carrier material to keep the cells alive until fracture formation.
36	J. Vanjinathan(2023)	*Bacillus subtilis, Brevibacillus sp., Bacillus megaterium, Microvirga sp.*	Higher compressive strength was observed in bio-concrete.
37	S. Udhaya (2023)	*Bacillus subtilis*	Flexural strength was found to be increased by 30%; tensile and compressive strength were also enhanced.

Conclusions

Microbially-induced Calcium Precipitation (MICP) represents a promising and sustainable approach for enhancing the durability and self-healing properties of concrete structures. Technologies based on MICP process utilize specially engineered microorganisms and metabolic processes to induce the precipitation of calcium carbonate, effectively sealing cracks and reinforcing concrete material. The efficiency of the self-healing process depends on various factors such as bacterial strain, nutrient source, environmental conditions, and crack width. Extensive research has been done on bio-concrete, aiming at understanding the multifaceted influences of various factors on its performance and exploring the avenues to enhance its efficiency. Aggregating this knowledge enables us to customize bio-concrete formulations for precise applications thus maximizing their self-healing effectiveness.

References

1. A F Alshalif, J M Irwan, N Othman, A Al-Gheethi .2018. New Medium for Isolation of Bacteria From Cement Kiln Dust with a Potential to Apply in Bio-Concrete. 140 : 012155 doi:10.1088/17551315/140/1/012155**.**
2. Adharsh Rajasekar, Charles K. S. Moy, Stephen Wilkinson, Raju Sekar (2021) Microbially induced calcite precipitation performance of multiple landfill indigenous bacteria compared to a commercially available bacteria in porous media. 16(7): e0254676. https://doi.org/10.1371/journal.
3. Ali Vahabiab, Ali Akbar Ramezanianpourb & Kambiz Akbari Noghabi. 2014. A preliminary insight into the revolutionary new line in improving concrete properties using an indigenous bacterial strain *Bacillus licheniformis AK01*, as a healing agent .19:5, 614-627, DOI: 10.1080/19648189.2014.960951.
4. Amal A. Nasser, Noha M. Sorour, Mohamed A. Saafan, Rateb N. Abbas. 2022. Microbially-Induced-Calcite- Precipitation (MICP): A biotechnological approach to enhance the durability of concrete using *Bacillus pasteurii and Bacillus sphaericus.* https://doi.org/10.1016/j.heliyon.2022.e09879.
5. Atreyee Sarkara, Avishek Chatterjee, Saroj Mandal, and Brajadulal Chattopadhyay 2019. Evaluation of Self- Healing Attribute of an Alkaliphilic Microbial Protein in Cementitious Mortars. DOI:10.1061/(ASCE)MT.1943-5533.0004197.
6. B. Madhu Sudana Reddy, D. Revathi. 2019. An experimental study on the effect of *Bacillus sphaericus* bacteria in crack filling and strength enhancement of concrete. *Materials Today: Proceedings*, *19*, 803–809. https://doi.org/10.1016/j.matpr.2019.08.135.
7. Faisal Mahmood, Sardar Kashif Ur Rehman, Mohammed Jameel, Nadia Riaz, Muhammad Faisal Javed, Abdelatif Salmi and Youssef Ahmed Awad. 2022. Self-Healing Bio-Concrete Using Bacillus subtilis Encapsulated in Iron Oxide Nanoparticles.15: 7731. https://doi.org/10.3390/ma15217731.
8. Henk M. Jonkers & Erik Schlangen. 2008. Development of a bacteria-based self-healing concrete. DOI:10.1201/9781439828410.CH72.
9. Henk M. Jonkers, Arjan Thijssena, Gerard Muyzer, Oguzhan Copuroglua, Erik Schlangena 2008. Application of bacteria as self-healing agent for the development of sustainable concrete. 36:230-235. doi: 10.1016/j.ecoleng.2008.12.036. 126 (2016) 297–303. https://doi.org/10.1016/j.conbuildmat.2016.09.023.
10. Huaicheng Chen, Chunxiang Qian, Haoliang Huang. 2016. Self-healing cementitious materials based on bacteria and nutrients immobilized respectively. 126:297-303 doi:10.1016/j.conbuildmat.2016.09.023
11. Islam M. Riad, Ahmed A. Elshami, Mohamed M. Yousry Elshikh. 2022. Infuence of concentration and proportion prepared bacteria on properties of self Healing concrete in sulfate environment. DOI:10.1007/s41062-021-00670-2.
12. J. Vanjinathan, V. Sampathkumar, N. Pannirselvam, Ragi Krishnan, M. Sivasubramanian, S. Kandasamy, S. D. Anitha Selvasofia & M. Kavisri .2023. Microbially-induced self-healing bioconcrete for sustainable development. DOI:10.1007/s13399-023-04640-9.
13. J. Y. Wang, D. Snoeck, S. Van Vlierverghe, W. Verstraete, N. De Belie. 2014. Application of hydrogel encapsulated carbonate precipitating bacteria for approaching a realistic self-healing in concrete. 68:110–119. https://doi.org/10.1016/j.conbuildmat.2014.06.018.
14. J. Y. Wang, N. De Belie, W. Verstraete 2011. Diatomaceous earth as a protective vehicle for bacteria applied for self-healing concrete. 39:567–577. DOI 10.1007/s10295-011-1037-1.
15. Jiaguang Zhang, Yuanzhen Liu, Tao Feng, Mengjun Zhou, Lin Zhao, Aijuan Zhou, Zhu Li. 2017. Immobilizing bacteria in expanded perlite for the crack self-healing in Concrete, 148: 610- 617. http://dx.doi.org/10.1016/j.conbuildmat.2017.05.021.
16. Jianyun Wang, Henk M. Jonkers, Nico Boon, Nele De Belie. 2017. Bacillus sphaericus LMG 22257 is physiologically suitable for self-healing concrete. 101(12):5101-5114. doi: 10.1007/s00253-017-8260-2. PMID: 28365797.
17. Leena Chaurasia, Vishakha Bisht, L.P. Singh, Sanjay Gupta. 2018. A novel approach of biomineralization for improving micro and macro-properties of concrete. 195 (2019) 340–351. https://doi.org/10.1016/j.conbuildmat.2018.11.031.
18. Cheng L, Cord-Ruwisch R. Selective enrichment and production of highly urease

active bacteria by non- sterile (open) chemostat culture. 40(10):1095-104. doi: 10.1007/s10295-013-1310-6. PMID: 23892419.

19. Marcondes, Carlos Gustavo Nastari, Oliveira, Isaac Aguiar, Anjos, Juliane Cristine Santos, Medeiros, Marcelo Henrique Farias. 2020. *Lysinibacillus sphaericus* as a self-healing agent for cement-based materials: a preliminary investigation DOI: https://doi.org/10.37118/ijdr.21078.02.2021 .
20. Minyoung Hong, Indong Jang, Yongjun Son, Chongku Yi and Woojun Park. 2021. Agricultural by-products and oyster shell as alternative nutrient sources for microbial sealing of early age cracks in mortar. https://doi.org/10.1186/s13568-020-01166-5.
21. Mousumi Biswas, Sudipta Majumdar, Trinath Chowdhurya, Brajadulal Chattopadhyaya, Saroj Mandal, Umesh Halder, Shinji Yamasaki. 2010. 46:581–587. doi: 10.1016/j.enzmictec.2010.03.005.
22. Nuraiffa Syazwi Adzami, Miskiah Fadilah Ghazali, Amira Hidayati Ramli, Husnul Azan Tajarudin, Zawawi Daud. 2018. a new potential of calcium carbonate production induced by *bacillus sphaericus* in batch fermentation. https://doi.org/10.30880/ijie.2018.10.09.024 .
23. Qian Chunxiang, Wang Jianyun, Wang Ruixing, Cheng Liang. 2008. Corrosion protection of cement-based building materials by surface deposition of CaCO3 by *Bacillus pasteurii.* doi: 10.1016/j.msec.2008.10.025.
24. Rajneesh Vashisht, Sampan Attri, Deepak Sharma, Abhilash Shukla, Gunjan Goel. 2017. Monitoring biocalcification potential of *Lysinibacillus sp*. isolated from alluvial soils for improved compressive strength of concrete. 207:226–231. https://doi.org/10.1016/j.micres.2017.12.010.
25. S. Udhaya a, V. Vandhana Devi b, J. Philips b, R.L. Lija b. 2023. Experimental study on bio-concrete for sustainable construction .https://doi.org/10.1016/j.matpr.2023.03.676.
26. S.A. Abo-El-Enein, A.H. Ali, Fatma N. Talkhan, H.A. Abdel-Gawwad .2012. Utilization of microbial induced calcite precipitation for sand consolidation and mortar crack remediation. 8:3, 185-192, DOI: 10.1016/j.hbrcj.2013.02.001.
27. S.S. Bang, J.J. Lippert, U. Yerra, S. Mulukutla and V. Ramakrishnan. 2010. Microbial calcite, a bio-based smart nanomaterial in concrete remediation. 1:1, 28-39, DOI: 10.1080/19475411003593451.
28. S.S. Banga, J.J. Lipperta, U. Yerra, S. Mulukutla and V. Ramakrishnan .2010. Microbial calcite, a bio-based smart nanomaterial in concrete remediation. DOI:10.1080/19475411003593451.
29. Shannon Stocks-Fischer, Johnna K. Galinat, Sookie S. Bang .1999. Microbiological precipitation of CaCO 31:1563-1571.https://doi.org/10.1016/S0038-0717(99)00082-6.Shiren O. Ahmed,
30. Sookie S. Banga, Johnna K. Galinata, V. Ramakrishnan. 2000. Calcite precipitation induced by polyurethane- immobilized *Bacilluspasteurii*.https://doi.org/10.1016/S0141-0229(00)00348-3.
31. V. Ramakrishnan, K. P. Ramesh and S. S. Bang. 2000. Bacterial concrete doi: 10.1117/12.424404.
32. Varenyam Achal, Abhijit Mukherjee, M. Sudhakara Reddy. 2010. Biocalcification by *Sporosarcina pasteurii* using corn steep liquor as nutrient source.https://doi.org/10.1089/ind.2010.6.170.
33. Varenyam Achal, Xiangliang Pan, Nilüfer Özyurt. 2010. Improved strength and durability of fly ash- amended concrete by microbialcalciteprecipitation 37:554-559.https://doi.org/10.1016/j.ecoleng.2010.11.009.
34. Wasim Khaliq, Muhammad Basit Ehsan. 2015. Crack healing in concrete using various bio influenced self- healing techniques. 102:349–357. https://doi.org/10.1016/j.conbuildmat.2015.11.006.
35. Wiboonluk Pungrasmi, Jirapa Intarasoontron, Pitcha Jongvivatsakul, and Suched Likitlersuang. 2019. Evaluation of Microencapsulation Techniques for MICP Bacterial Spores Applied in Self-Healing Concrete. 9:12484 | https://doi.org/10.1038/s41598-019-49002-6.
36. Yusuf Ç. Erşan, Nico Boon and Nele De Beli. 2018. Granules with activated compact denitrifying core (ACDC) for self-healing concrete with corrosion protection functionality. Volume: 2: 475-484.
37. Yusuf Cagatay Ersan, Nico Boon, Nele De Belie. 2013. Microbial Self-Healing Concrete: Denitrification as an Enhanced and Environment-Friendly Approach. Abstract ID: 43 ICSHM2015.
38. Z M Hussein, A H Abedali and A S Ahmead 2019. Improve ment Properties of Self -Healing Concrete by Using Bacteria doi:10.1088/1757-899X/584/1/012034.

https://doi.org/10.36375/prepare_u.iiche.a393

Sustainable Sequestration Of Carbon Dioxide – A Review

Sangita Bhattacharjee[1], Trina Dutta[2]

[1]Assistant Professor, Chemical Engineering Department, Heritage Institute of Technology, Kolkata - 700107
[2] Assistant Professor, Department of Chemistry, JIS College of Engineering, Kalyani, West Bengal – 741235

Abstract

Among various GHG gases causing global warming, the contribution by CO_2 alone is about 60%. Post combustion carbon capture is most viable technique compared to pre-combustion and oxy-fuel combustion CO_2 capture techniques used for conventional coal based thermal power plants. Cryogenic separation, chemical absorption, adsorption, membrane based separation etc. belong to post combustion carbon sequestration technology however these methods have some or other disadvantages. Ocean injection results in lowering of pH of sea water thus affecting bacteria zooplankton and benthos species. Moreover following a considerable period of time, the stored CO_2 can leak. Controlled addition of CO_2 in ready-mix concrete, as produced in the United States, Canada and Singapore improves the compressive strength without sacrificing performance or durability. Microalgae consumes substantial quantity of carbon dioxide (1 Kg dry algae biomass consumes about 1.83 Kg CO_2) and hence very effective in bio-fixation of CO_2 waste as well as in improvement of air quality. Accumulation of oil (about 20 to 50% weight of dry biomass) and fast growth of microalgae make microalgae cultivation a commercially interesting and promising technology to mitigate global warming problem and generation of bio-fuel alongwith other benefits namely production of nutrient dense foods, chemicals and fertilizer.

Keywords: Greenhouse gases; ready-mix concrete, sustainable; microalgae; biomass; bio-fixation

Introduction

Still now, thermal power plants mostly are fulfilling the rising energy demand and thus constitute major cause of CO_2 emission. Rapid industrialization including installation and commissioning of various chemical manufacturing plants, urbanization, deforestation and increased automobile exhaust emission constitute increasing release of carbon dioxide. Due to these human activities,CO_2 concentration in atmosphere has risen upto 380 ppm from 280 ppm (parts per million) with a span of last50 years [1]. Due to this, various detrimental effects such as rise in sea level, melting of floating iceberg, and global warming warn the subsistence and growth of humankind. Hence it is utmost important to design suitable methodologies to efficiently collect CO_2 and transform into industrially suitable materials.

From the flue gas CO_2 is to be removed and then it is required to be stored for subsequent use and thus the negative impacts of carbon dioxide release could be reversed. The concept of circular carbon economy (CCE) deals with various technologies associated to capture carbon at emission site and store for subsequent use for manufacture of fire extinguishers, plastic components, fuels, fertilizers, soda ash, food and drinks, building materials etc.[2]. The paper has been undertaken to discuss different latest methods required to be adapted for controlling and solving the critical issue of

global warming arising due to increased concentration of CO_2 in the environment.

Various approaches of Carbon-Di-oxide sequestration:

Till date the Carbon Capturing and Storage (CCS) has been viewed as the most favorable option for CO_2 sequestration directly from emissions, the large stationary sources [3]. CO_2 can be captured directly from its source of formation before polluting the atmosphere [4,5]. For the storage, the confined CO_2 can be compressed, transferred, and injected within underground reserve area [6,7]. The captured CO_2 can be recycled by different industries like cement, oil, food processing, power plants, iron & steel industries [8]. For the transportation of CO_2 over a long distance, the structure and pipelines are to be properly configured. It must be configured in proper dimension to hold out against the velocity and pressure of the fluid. The USA confirms the CO_2 transportation around 50 to 60 million tons/year over long distances [4]. In the indirect method of carbon capturing, CO_2 can be trapped by plants during photosynthesis. This process is not only environment-friendly also capable of trapping CO_2 into the soil [9].

Carbon capturing approaches:

There are three major processes for Carbon capturing namely post-combustion, pre-combustion and oxy-fuel combustion [10].

Several capturing techniques such as absorption, adsorption, biological technique, extraction ,membrane technology as well as hybrid technique have been explored to address the ever-growing Global warming issue [11,12].

Although absorption is considered as the most common, it is highly energy demanding. Additionally, the used solvent may be corrosive for the vessel depending on its nature. Currently Membrane-based CO_2 separation becomes a promising alternative for traditional chemical absorption technology.

In this review, techniques like short term injection, utilization of carbon dioxide in ready-mix concrete, absorption, membrane technology have been discussed. Various advanced techniques based on different advanced materials such as ionic liquids, porous organic polymers, zeolites, metal-organic frameworks and covalent organic frameworks also have been discussed. Sequestration of CO_2 using photosynthetic reactions, one of the best ways for sustainability, also has been reviewed in detail.

Short-term sequestration:

Carbon-dioxide can be injected directly into sinks instantaneously. But most sinks leak the sequestered CO_2 in the remote future. However, CCUS in geothermal storage is very important due to relative increment of CO_2 emission and highly attractive alternative in geothermal power generation [14].

Ocean Injection:

Though ocean injection can bring down global warming issue instantaneously but that can leak the sequestered CO_2 in distant future. Moreover, this way of sequestration would result in lowering of pH of sea water thus affecting the species like bacteria; zooplankton; and benthos [15]. To resolve the issue, the delocalized CO_2 can be used for ocean fertilization. In this case the photosynthetic organisms absorb CO_2 during photosynthesis; their growth accelerated with nutrients and dead organisms enrich ocean fertility by remineralization. On the contrary, the marine ecosystem is affected by alteration in phytoplankton structure. Moreover, anaerobic decomposition under ocean may liberate methane, nitrogen monoxide and create disadvantages of greenhouse gases again [16].

https://doi.org/10.36375/prepare_u.iiche.a393

Geologic injection:

Geologic injection refers Mineral carbonation; coal seams; and Enhanced oil recovery (EOR).

Mineral carbonation: -In this process, silicates are converted into carbonates with following reaction [15].

$$(Ca, Mg)_xSi_yO_{x+2y} + xCO_2 \rightarrow x(Ca, Mg)CO_3 + ySiO_2$$

This is a long-term natural process that occurs by chemical weathering. The rate of reaction may be accelerated with the solubilization of mineral ions in strong acids or running under high pressure of CO_2. But discharge of strong acids harms the system and surroundings, and high pressure will increase operating cost [16,17]. The mechano-chemical process was also studied. In these method, various forms of natural silicates were ground repeatedly to absorb gaseous CO_2. But the carbon fixation yield was not significant compared to energy requirement for grinding action [18]. The surface activation [19] and involvement of biological catalyst [20] also investigated to enhance rate of reaction. However mineral carbonation technology has not much scope as it impacts mineral industries for a huge requirement of metal oxides [16].

Coal seams: - This case permanent CO_2 retention is possible with replacement of methane gas present in porous coal beds. If methane replacement is done by absorbing CO_2, the permanent retention of carbon is possible [21]. This methane recovery process is highly efficient along with CO_2 sequestration [22].

EOR: - In this process the oil movement and its extraction in reservoirs are enforced by captured CO_2. The CO_2 can again be recycled for reuse. However, the process is economically not viable for huge energy requirement to remove CO_2. To resolve the issue a plant for CO_2 recovery can be combined with enhanced oil recovery to decrease the conveyance expenses. In spite of that this remains too costly [15].

Pre, post & Oxy-fuel combustion:

In Pre-Combustion technique, syngas (a mixture of H_2 and CO) is derived from fossil fuel by partial oxidation or gasification. The reaction is preceded by water gas formation by steam pursued by water-gas shift reaction before the actual combustion takes place [23]. Carbon dioxide gas is separated from the synthesis gas using physical/chemical absorption process generating H_2 concentrated stream. This H_2 may be reused as a gaseous fuel and utilized for power generation. Thus CO_2 emission can be eliminated in pre-combustion with consecutive steps [24, 25]. The pre-combustion becomes easy at higher concentrations & pressure and decrease energy requirement about10% to 16% [3]. As for example during ammonia processing, both hydrogen and carbon dioxide gases are produced but CO_2 is removed prior to synthesis ammonia synthesis [26].

But commercial application is the major barrier for gasification in pre-combustion technique. Although CO_2 concentration is high in pre-combustion, but the cost of equipment is higher and extensive supporting systems are required [27].Additionally, the pre-combustion gas stream containing CO and CH_4 create great concern having toxic effect of CO and greenhouse effect of CH_4. Moreover, the existence of H_2S even in trace amounts creates a serious hazard especially for the stability of metal-organic frameworks if it is used to separate CO_2 [24, 28]. Overall the pre-combustion technique is not a good option for high cost, low efficiency and high-temperature demands [29].

Oxy-combustion CO_2 capturing process is one of the effective ways for CO_2 elimination [30]. In this process combustion takes place with

nearly pure oxygen instead air [10]. In consequence the flue gas contains mainly water vapour & concentrated CO_2. The CO_2 purification obtained easily by condensation of water vapors [3]. This process can integrate the pre-combustion and the post-combustion both in case of fuel gasification taking place almost pure oxygen environment [28]. But oxy-combustion is not cost effective for the requirement of large amount of cryogenic O_2 production. This method may be practiced to newly build or reconstructed plants [27].

In Post-combustion, after complete combustion carbon dioxide gas is captured from the flue gas and before it pollutes the atmosphere [31]. This is Retrofit technology option [27].

In comparison the oxy-fuel combustion is associated with newly constructed power plants while for gasification units the pre-combustion capture is more suitable [32]. However, in traditional power plants, the direct combustion occurs. So being an "end-of-pipe" technology, post-combustion is most recommended among all [33]. Figure 1 represents the CO_2 capture schemes.

Technical approach:

Chemical absorption:

Among various post-combustion techniques referred above, the most acceptable and feasible for implementation is the chemical absorption [34]. Chemical absorption can be combined with various solvents (amines [33–36], nanofluids [37, 38], ionic liquids [41–43], amino acid salt solutions [44, 45], etc. Monoethanolamine (MEA) is most acceptable among different amines [46].

Currently, various companies are implementing larger-scale power plants by chemical absorption process in collaboration with research organizations. As for example the first post-combustion capture pilot plant with CO_2-scrubbing plant contracted in July, 2009 at Niederaussem in Germany [47]; CO_2 capture plant of Dong power plant situated in Denmark [48] are mentionable. The first and largest commercial CCS project is SaskPower's Boundary dam, integrated with Carbon Capture and storage [49] and by July, 2016 it captured about 1 million ton CO_2 successfully.

Although the absorption (chemical) process is an established technology but is not cost effective as it is energy intensive. Optimization can be done by modification of parameters, process and solvents [50].

Membrane technology:

To remove CO_2 from a gas stream using membrane separation, the part of CO_2 permeates across the membrane known as permeate and the residual flue gas has been known as retentate. After certain time, the permeate sideCO_2 concentration becomes higher. The compressor & vacuum pump need to be used to enhance the pressure gradient among feed side & permeate side so as to maintain the required driving force for membrane separation [51,52].

The degree of separation is influenced by selectivity & permeability of membrane. It depends on membrane materials and module. Among various membrane materials such as organic (polymeric), inorganic (e.g. ceramic), and combined (mixture of organic & inorganic) membranes are commonly used. Among various configuration of membrane module, spiral wound [53, 54], hollow fiber [55],& envelope [56] are primarily accepted.

As per research findings, membrane technology has no added advantage over Chemical absorption process [6], but in combination of these two processes can optimize the cost and energy requirement [14].

Use of CO_2 in ready-mix concrete:

Use of captured CO_2 in concrete, has been practiced by producers of ready-mix concrete (RMC) in Canada the USA and Singapore. The Concrete is widely used and has been the most

https://doi.org/10.36375/prepare_u.iiche.a393

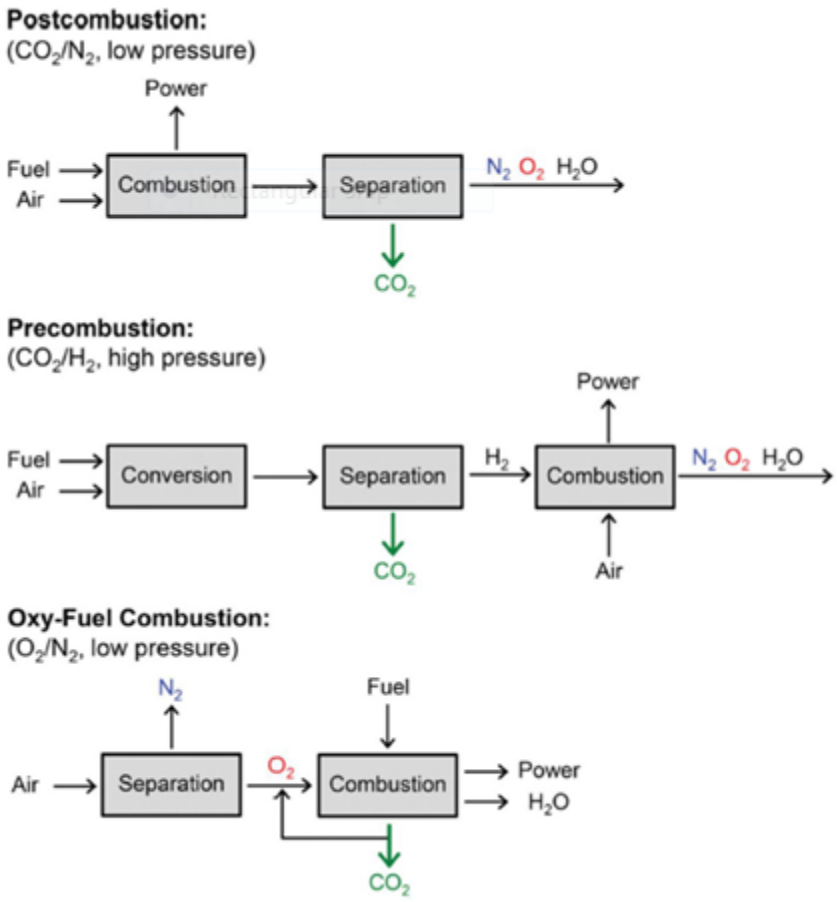

Fig.1. Basic Schemes of different CO_2 Capture Processes **[1].**

important construction material. According to requirement, RMC is manufactured batch wise and subsequently, used at the particular site. Compared to various other materials, concrete is less energy intensive and has lower carbon footprint. Portland cement that is used to produce concrete emits large quantities of CO_2. During cement production, limestone ($CaCO_3$) is converted to reactive calcium silicate wherein CO_2 is a by-product [57,58]. It has been reported that manufacturing of cement is accountable for 8% of planet warming CO_2release which is substantially higher than global carbon release from aviation [59].

According to the International Energy Agency, for cement industry, it has been aimed to reduce CO_2 emission to 1.55 gigatonne in the 2050 [60], while during the same time cement production has been anticipated to enhance by about 50%. To implement the said target of reducing CO_2 emissions, few approaches were decided to be followed. Reduction of CO_2 emission through enhanced use of alternative and suitable raw materials, taking measures so as to enhance the energy efficiency of cement kilns and capturing of carbon dioxide released from such plants are the required approaches.

Researchers have studied the impact of injection of carbon dioxide in batching and mixing. It is reported [60] that the idea of CO_2 utilization can create lower carbon concrete products. The injection of CO_2 was found to improve of the

concrete in terms of compressive strength. Sean Monkman and Mark McDonald [61] have studied the outcome of the injection of CO_2 during batching after concrete was produced. Using a metering device, the flow of pressurized liquid $CO_2$was controlled into the concrete via a discharge conduit during batching. The liquid, upon reaching the atmosphere, after getting discharged undergoes phase transition with the formation of CO_2 snow which is fine particles of solid carbon dioxide and CO_2 gas. During investigation, controlled supply of carbon dioxide was made to flow intermittently into freshly prepared concrete for a particular duration. CO_2, upon mixing with fresh, wet cement, react with calcium ions to form calcium carbonate and thus gets solidified and bound chemically with the concrete. The fresh concrete thus produced was undergone standard tests such as ASTM C231 which is a standardized test method to determine for Air Content of fresh concrete, ASTM C143, which is a standardized test method for Slump of hydraulic-cement Concrete. Furthermore, another test, ASTM C39 was also carried for evaluating compressive strength of hardened concrete cylinders. Investigation showed that addition of CO_2 could bring improvement of compressive strength of concrete.

Quantification of direct absorption in concrete is a difficult task. Generally carbon dioxide applied in concrete consisted of 50% solid and 50% gas. The combined overall efficiency is estimated as approx. 60%. So though the dosage in the study has been specified as 482 gm / m^3 of concrete, actually 289 g ofCO_2 was actually fixed. Therefore an estimated 14.4 tonnes of CO_2 was actually absorbed over $50x10^3$ m^3 of concrete produced. In terms of compressive strength, a drop of about 11-13% was observed in air entrained reduced binder batches. However addition of CO_2 was found to enhance the reduced binder concrete strength, the increase was evaluated to 10% at seventh day and approx. 13% at twenty eighth day. Following CO_2 addition, the strength of this reduced binder batch, was found to be almost equal to the strength obtained from the standard mix [61].

Sequestration of CO_2 UsingMOF (Metal organic Framework): These pertain to a class of polymer having permanent porosity. In these materials, coordination of metal ions/clusters to organic ligands to form one, two, or three-dimensional structure occur.

In MOFs, crystalline porous frameworks are obtained due to joining of polynuclear metal clusters by organic linkers. Two dimensional structure of MOFs such as sheets, plates, rings, membranes disc, flakes, walls etc. having large surface area and increased surface / volume value. MOF of erenormous structural diversities and possibilities for design of materials with customized characteristics. Owing to the characteristics of high pore volume, specific surface area, ability to be functionalized and stability render MOFs these good candidates for gas separation. The formation of a MOF has been shown pictorially in Fig.2 [62,63].

One of the deeply researched area is the cyclo-addition of carbon dioxide with epoxides in MOF-catalyzed CO_2 conversion reactions [64]. MOF composites formed by combining MOFs along with other materials, found to be suitable for sequestration of CO_2. Recently MOF-based materials are efficiently utilized for transforming CO_2 into different products using methods such as electrocatalytic reduction, photocatalytic reduction, hydrogenation etc.[64].

Recently emerged electro-chemical reduction reaction of carbon dioxide has become a promising technology which uses green energy to manufacture fuels and valuable chemicals including ethylene, carbon monoxide, methanol, ethanol, formic acid, oxalic acid etc. from CO_2.

https://doi.org/10.36375/prepare_u.iiche.a393

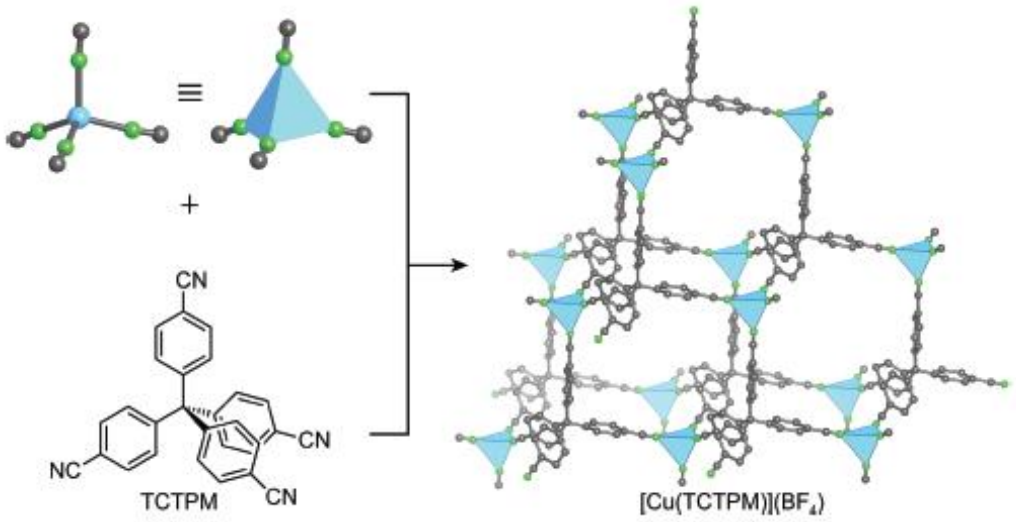

Fig.2.Cationic coordination network crystal structure [Cu(TCTPM)](BF_4)]

(TCTPM =tetracyanotetraphenylmethane].[63].

Recent researches have shown that multicarbon products can be formed from CO_2 using Cu and Cu based modified nanoparticles. In the field of catalysis, copper based metal-organic frameworks have been achieving increasing importance among various other copper-based nanoparticles, due to their electrical, topological their textural properties[65].

Removal of CO_2 using Ionic Liquids:

To overcome various disadvantages of aqueous amine used for scavenging CO_2 owing to several disadvantages of using costly, corrosive amine such as high volatility, considerable energy utilization, the need for choiceof a new solvent had become primarily important [66]. The non-volatility, structure-turnability, relative non-flammability, recyclability, designability and high carbon dioxide absorbing capacity make ionic liquids one of the most suitable materials for capturing carbon dioxide, that can be subsequently transformed into valuable, fine chemicals. ILs are actually salts having lower melting points (less than 100^0C). These consist of cations such as pyrrolidinium, pyridinium, imidazolium, amine etc. and anions such as azolate, carboxylate, thionate, thionate, halide, hexafluorophosphateetc. [67,68]. ILs can be tailor made to achieve optimum CO_2 solubility.

High viscosity of ILs is one of the major disadvantages of using these as scrubbing agent, however viscosity can be reduced by adopting suitable mean. ILs, having both the properties of catalyst as well as solvent, can be utilized in the transformation of carbon dioxide molecules to different organic compounds including formic acid/formats, methanol, carbon mono-oxides etc.[69].

During the last decade, Rosen *et.al*.[70] had investigated the ability of Room Temperature Ionic liquid (RTIL) in the electrochemical conversion of carbon dioxide to carbon. An electrochemical conversion of CO_2 to CO in

18% aqueous 1-ethyl-3-methylimidazolium tetrafluoroborate was achieved.

Photosynthetic sequestration of carbon dioxide:

0.05% of annual absorption of more than 3800 zetta joules solar energy by Earth, is utilized in photosynthesis by plants to produce biomass [71].Generation of renewable energy instead of full dependence on conventional energy obtained from fossil fuels have been explored in recent years. Generation of biofuel from biomass obtained using photosynthesis not only lowers eet etc. cultivated in agricultural field, hence to make the production of biofuel more sustainable, the second generation biofuels are obtained from non-edible plants and thus are not in direct competition with food production.

Various techniques of biofuel production as well as carbon dioxide sequestration from micro / macro algae have been investigated by researchers across the globe. Algal biofuel, obtained through various conversion processes from the oil-rich algae are third generation advanced renewable fuels. Algae can be multicellular (macro algae) or unicellular(micro algae), exists in 3000 breeds. Increased efficiency related to fermentation/ hydrolysis is achieved in case of algae due to lesser content of hemicelluloses and the absence of lignin [72]. A particular type of algae, microalgae is capable of fixing CO_2 in presence of solar light ten times more compared to terrestrial plants [73]. From algal biomass various types of fuel can be obtained using different routes such as biodiesel through transesterification, biogas following anaerobic digestion, bioethanol through fermentation, bio-oil, bio-char and biogas through pyrolysis, also energy can be obtained from direct combustion of algae.

Other uses of algae include feedstock for aquaculture, pharmaceuticals, cosmetics, chemicals, biofertilizers, systhetic substitutes atmospheric CO_2 levels as a result of photosynthetic reactions, also creates far lower emission than burning fossil fuels. Though the first generation fuel ethanol, produced from starch/ sugar-based crop, has shown the possibility of manufacturing liquid fuels from renewable sources, but had the disadvantages of low energy-conversion efficiency, almost halved energy density compared to oil-based fuels and increased cost. Moreover during conversion of biomass to ethanol by fermentation, considerable CO_2 is also emitted in environment. Moreover first generation biofuels are obtained directly from crops namely cane, sugar b ,hydrocolloids etc. Strict regulation for food safety only permits some health and food products based on *Dunaliella*, *Chlorella*, *Spirulina* species for human consumption [74].

Different groups of algae such as *Chlorophyta*, *Rhodophyta* and *Phaeophyta* are found in a natural habitats such as deep oceans, in rocky shores as well as in freshwater too. Rapid growth potential of microalgae, its high oil content upto 50% dry weight of biomass as well as high CO_2 biofixation (about 1.83 Kg CO_2 per Kg biomass of microalgae) - altogether make microalgae cultivation very beneficial commercially as well as in terms of improvement of air quality and balancing CO_2 level in environment. [75,76,77]. Furthermore, effluent from agro-food industry, if utilized for cultivation of microalgae as a growth medium, will be very much beneficial as it can provide the useful nutrients to algae as well as pave a way to solve effluent discharge problems.[78].

In the past, algae cultivation was be carried out in open ponds- natural or artificial. Shallow and stagnant ponds favor algal growth due to more penetration of sunlight and warm water. However for large-scale production of algae, U shaped raceway ponds with circulation facility are used.

[75].

https://doi.org/10.36375/prepare_u.iiche.a393

Natural cultivation and artificial cultivation (using photobioreactor) of algae has been depicted in Fig.3[79]. For obtaining high productivity of algae in a controlled as well as closed environment, photobioreactor (PBRs) are fed with all growth requirements of algae. Proper control of various parameters namely optimum temperature & pH, culture density, required light exposure, supply of CO_2 and water, mixing type is possible in PBRs.

Bitog et. al in 2011 performed a study on CO_2biofixation taking two species of green algae namely *chlorella vulgaris* and *Nannochloropsis Graditana* in a a tubular reactor at 25^0C temperature with two different initial CO_2 concentrations of 4 and 8 vol% respectively using simulated light enhanced photosynthesis. A greater CO_2 uptake rate of more than 1.70 gm./(lit.day) was found in case of *N. Graditana* at 8 vol% CO_2 concentrations. A cell concentration of $1.7x10^7$ cells / ml was reported on the 10^{th} day of cultivation [79].

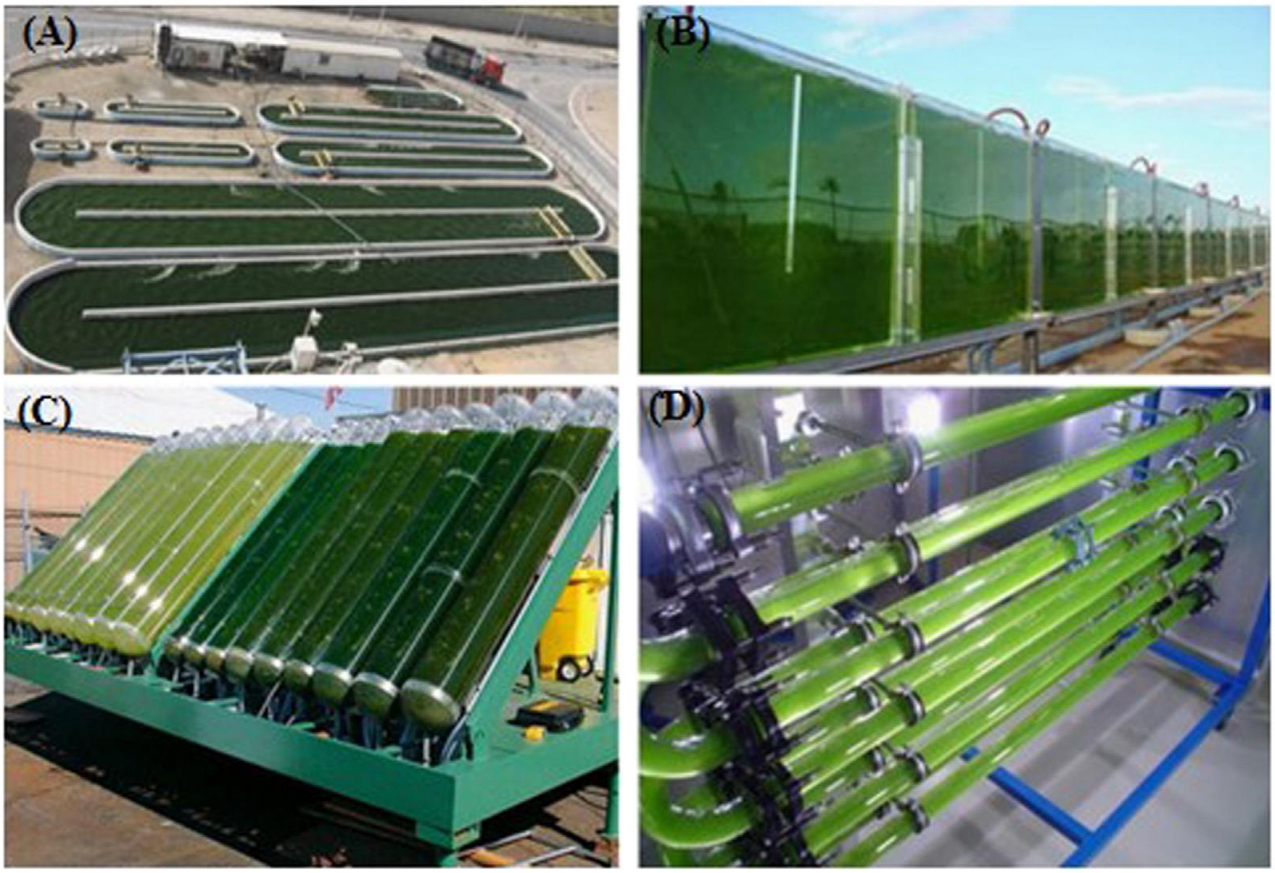

Fig. 3. Cultivation methods for algae (A) natural (B) Cultivation in flat plate photo-bioreactor (C) Cultivation in tubular photo-bioreactor, (D) Cultivation in column photo-bioreactor [79].

https://doi.org/10.36375/prepare_u.iiche.a393

CO_2 fixation with wastewater treatment:

Algae production in wastewater is a useful, constructive and sustainable technique in combating environmental pollution. Cultivation of microalgae in wastewater not only sequesters CO_2 from environment as well as solve wastewater discharge related problems partially but also produce various important nutraceuticals , such as β-carotene which can be obtained from the biomass of *Dunaliella* and *Spirulina* species. With an aim to eliminateCO_2 gas from a flue gas stream as well as ammonia from wastewater economically, cultivation of *Dunaleilla, Chlorella Vulgaris*were carried out using steel making plant effluent. A CO_2 fixation rate of 26 g. /(m^3.h) and ammonia removal rates of 0.92 gm. NH_3/(m^3.h) were observed when the wastewater was supplemented with 46.0gm PO_4/m^3 at 15% (v/v) CO_2 and with no control of pH condition [80].It has been reported that in Tampa,Howard F. Curren Advanced Wastewater Treatment Plant, and in the city of Lakeland, Florida, the Wetland Treatment System are capable of generating algal biomass of about 71 tons /(ha. year) , liquid biofuel of about 2.7x10^5 gal /hr, and methane of about 4.15x10^6 kg/ yr. [81].

References:

[1] https://pubs.usgs.gov/fs/2008/3097/pdf/CarbonFS.pdf

[2] https://www.investindia.gov.in/team-india-blogs/carbon-capture-utilization-and-storage-ccus-indias-leap-towards-green-energy

[3] Younas, M., Rezakazemi, M., Daud, M., Wazir, M. B., Ahmad, S., Ullah, N., & Ramakrishna, S. (2020). Recent progress and remaining challenges in post-combustion CO2 capture using metal-organic frameworks (MOFs). Progress in Energy and Combustion Science, 80, 100849.

[4] Babarinde, F., &Adio, M. A. (2020). A review of carbon capture and sequestration technology. Journal of Energy Technology and Environment, 2.

[5] Rubin, E. S., Mantripragada, H., Marks, A., Versteeg, P., &Kitchin, J. (2012). The outlook for improved carbon capture technology. Progress in energy and combustion science, 38(5), 630-671.

[6] Wang, Y., Zhao, L., Otto, A., Robinius, M., &Stolten, D. (2017). A review of post-combustion CO2 capture technologies from coal-fired power plants. Energy Procedia, 114, 650-665.

[7] Wang, M., &Oko, E. (2017). Special issue on carbon capture in the context of carbon capture, utilisation and storage (CCUS). International Journal of Coal Science & Technology, 4, 1-4.

[8] Suliestyah, S., & Sari, I. P. (2021, March). Effect of temperature and time of carbonization on coal-based activated carbon adsorption. In IOP Conference Series: Materials Science and Engineering (Vol. 1098, No. 6, p. 062020). IOP Publishing. https://doi.org/10.1088/1757-899x/1098/6/062020

[9] Odunlami, O. A., Vershima, D. A., Oladimeji, T. E., Nkongho, S., Ogunlade, S. K., &Fakinle, B. S. (2022). Advanced techniques for the capturing and separation of CO2–a review. Results in Engineering, 15, 100512.

[10] Zhang, S., Liu, L., Zhang, L., Zhuang, Y., & Du, J. (2018). An optimization model for carbon capture utilization and storage supply chain: A

case study in Northeastern China. Applied Energy, 231, 194-206.

[11] Azzouz, A., Platon, N., Nousir, S., Ghomari, K., Nistor, D., Shiao, T. C., & Roy, R. (2013). OH-enriched organo-montmorillonites for potential applications in carbon dioxide separation and concentration. Separation and Purification Technology, 108, 181-188. https://doi.org/10.1016/j.seppur.2013.02.006

[12] Roussanaly, S., Anantharaman, R., Lindqvist, K., Zhai, H., & Rubin, E. (2016). Membrane properties required for post-combustion CO2 capture at coal-fired power plants. Journal of membrane science, 511, 250-264.

[13] Shao, R., &Stangeland, A. (2009). Amines Used in CO2 Capture. Oslo, Norway: The Bellona Foundation.

[14] Dutta, T., Bhattacharjee, S., & Chakraborty, J. (2020). Sustainable Carbon Di-Oxide Sequestration Using Photosynthetic Reactions.

[15] Stewart, C., &Hessami, M. A. (2005). A study of methods of carbon dioxide capture and sequestration—the sustainability of a photosynthetic bioreactor approach. Energy Conversion and management, 46(3), 403-420.

[16] Yang, H., Xu, Z., Fan, M., Gupta, R., Slimane, R. B., Bland, A. E., & Wright, I. (2008). Progress in carbon dioxide separation and capture: A review. Journal of environmental sciences, 20(1), 14-27.

[17] Maroto-Valer, M. M., Fauth, D. J., Kuchta, M. E., Zhang, Y., &Andrésen, J. M. (2005). Activation of magnesium rich minerals as carbonation feedstock materials for CO2 sequestration. Fuel Processing Technology, 86(14-15), 1627-1645.

[18] Nelson, M. G. (2004). Carbon dioxide sequestration by mechanochemical carbonation of mineral silicates. University of Utah (US).

[19] Maroto-Valer, M. M., Tang, Z., & Zhang, Y. (2005). CO2 capture by activated and impregnated anthracites. Fuel Processing Technology, 86(14-15), 1487-1502.

[20] Liu, N., Bond, G. M., Abel, A., McPherson, B. J., & Stringer, J. (2005). Biomimetic sequestration of CO2 in carbonate form: Role of produced waters and other brines. Fuel processing technology, 86(14-15), 1615-1625.

[21] Herzog, H. (2001). What future for carbon capture and sequestration?. Environmental Science and Technology-Columbus, 35(7), 148A.

[22] Beecy, D. J., &Kuuskraa, V. A. (2001). Status of US geologic carbon sequestration research and technology. Environmental Geosciences, 8(3), 152-159.

[23] Zhang Z, Borhani TNG, El-naas MH. Chapter 4.5 –carbon capture. Elsevier; 2020. doi: 10.1016/B978- 0-12- 813734- 5.0 0 056-1.

[24] Sumida, K., Rogow, D. L., Mason, J. A., McDonald, T. M., Bloch, E. D., Herm, Z. R., ... & Long, J. R. (2012). Carbon dioxide capture in metal–organic frameworks. Chemical

reviews, 112(2), 724-781.doi: 10.1021/cr2003272.

[25] Li, H., Wang, K., Sun, Y., Lollar, C. T., Li, J., & Zhou, H. C. (2018). Recent advances in gas storage and separation using metal–organic frameworks. Materials Today, 21(2), 108-121.doi: 10.1016/j.mattod.2017.07.006

[26] Kajama, M. N., Nwogu, N. C., &Gobina, E. (2014). Experimental study of carbon dioxide separation with nanoporous ceramic membranes. WIT Transactions on Ecology and the Environment, 186, 625-633. 10.2495/ESUS140551

[27] Figueroa, J. D., Fout, T., Plasynski, S., McIlvried, H., & Srivastava, R. D. (2008). Advances in CO2 capture technology—the US Department of Energy's Carbon Sequestration Program. International journal of greenhouse gas control, 2(1), 9-20.

[28] Rezakazemi, M., Niazi, Z., Mirfendereski, M., Shirazian, S., Mohammadi, T., & Pak, A. (2011). CFD simulation of natural gas sweetening in a gas–liquid hollow-fiber membrane contactor. Chemical Engineering Journal, 168(3), 1217-1226. https://doi.org/10.1016/j.cej.2011.02.019

[29] Ge, X., & Ma, S. (2020). CO2 capture and separation of metal–organic frameworks. Materials for carbon capture, 5-27. https://doi.org/10.1002/9781119091219.ch2

[30] Tomioka, T., Sakai, T., & Mano, H. (2013). Carbon dioxide separation technology from biogas by "membrane/absorption hybrid method". Energy Procedia, 37, 1209-1217.https://doi.org/10.1016/j.egypro.2013.05.219

[31] Shafie, S. N. A., MdNordin, N. A. H., Bilad, M. R., Misdan, N., Sazali, N., Putra, Z. A., ... & Man, Z. (2021). [emim][tf2n]-modified silica as filler in mixed matrix membrane for carbon dioxide separation. Membranes, 11(5), 371.https://doi.org/10.3390/membranes11050371

[32] Wang, Y., Zhao, L., Otto, A., Robinius, M., &Stolten, D. (2017). A review of post-combustion CO2 capture technologies from coal-fired power plants. Energy Procedia, 114, 650-665. https://doi.org/10.1016/j.egypro.2017.03.1209

[33] Merkel, T. C., Lin, H., Wei, X., & Baker, R. (2010). Power plant post-combustion carbon dioxide capture: An opportunity for membranes. Journal of membrane science, 359(1-2), 126-139.

[34] Rao, A. B., & Rubin, E. S. (2002). A technical, economic, and environmental assessment of amine-based CO2 capture technology for power plant greenhouse gas control. Environmental science & technology, 36(20), 4467-4475.

[35] Zhang, Z., Zhao, S., Rezakazemi, M., Chen, F., Luis, P., & Van der Bruggen, B. (2017). Effect of flow and module configuration on SO2 absorption by using membrane contactors. Global NEST Journal, 19(4), 716-725.

[36] Rezakazemi, M., Heydari, I., & Zhang, Z. (2017). Hybrid systems: Combining membrane and absorption technologies leads to more efficient acid gases (CO2 and H2S) removal from natural gas. Journal of CO2 utilization, 18, 362-369. https://doi.org/10.1016/j.jcou.2017.02.006

[37] Shirazian, S., Marjani, A., &Rezakazemi, M. (2012). Separation of CO 2 by single and mixed aqueous amine solvents in membrane contactors: fluid flow and mass transfer modeling. Engineering with Computers, 28, 189-198. https://doi.org/10.1007/s00366-011-0237-7

[38] Fasihi, M., Shirazian, S., Marjani, A., &Rezakazemi, M. (2012). Computational fluid dynamics simulation of transport phenomena in ceramic membranes for SO2 separation. Mathematical and Computer Modelling, 56(11-12), 278-286. https://doi.org/10.1016/j.mcm.2012.01.010

[39] Hajilary, N., & Rezakazemi, M. (2018). CFD modeling of CO2 capture by water-based nanofluids using hollow fiber membrane contactor. International Journal of Greenhouse Gas Control, 77, 88-95. https://doi.org/10.1016/j.ijggc.2018.08.002

[40] Rezakazemi, M., Darabi, M., Soroush, E., &Mesbah, M. (2019). CO2 absorption enhancement by water-based nanofluids of CNT and SiO2 using hollow-fiber membrane contactor. Separation and Purification Technology, 210, 920-926. https://doi.org/10.1016/j.seppur.2018.09.005

[41] Razavi, S. M. R., Rezakazemi, M., Albadarin, A. B., &Shirazian, S. (2016). Simulation of CO2 absorption by solution of ammonium ionic liquid in hollow-fiber contactors. Chemical Engineering and Processing: Process Intensification, 108, 27-34. https://doi.org/10.1016/j.cep.2016.07.001

[42] Mesbah, M., Shahsavari, S., Soroush, E., Rahaei, N., &Rezakazemi, M. (2018). Accurate prediction of miscibility of CO2 and supercritical CO2 in ionic liquids using machine learning. Journal of CO2 Utilization, 25, 99-107. https://doi.org/10.1016/j.jcou.2018.03.004

[43] Dashti, A., Harami, H. R., Rezakazemi, M., &Shirazian, S. (2018). Estimating CH4 and CO2solubilities in ionic liquids using computational intelligence approaches. Journal of Molecular Liquids, 271, 661-669. https://doi.org/10.1016/j.molliq.2018.08.150

[44] Soroush, E., Shahsavari, S., Mesbah, M., &Rezakazemi, M. (2018). A robust predictive tool for estimating CO2 solubility in potassium based amino acid salt solutions. Chinese Journal of Chemical Engineering, 26(4), 740-746. https://doi.org/10.1016/j.cjche.2017.10.002

[45] Soroush, E., Mesbah, M., Hajilary, N., &Rezakazemi, M. (2019). ANFIS modeling for prediction of CO2 solubility in potassium and sodium based amino acid Salt solutions. Journal of Environmental Chemical Engineering, 7(1), 102925. https://doi.org/10.1016/j.jece.2019.102925

[46] Luis, P. (2016). Use of monoethanolamine (MEA) for CO2 capture in a global scenario: Consequences and alternatives. Desalination, 380, 93-99. https://doi.org/10.1016/j.desal.2015.08.004

[47] Brochure CO2 Scrubbing - Ultra-modern climate protection for coal-fired power plants. http://www.rwe.com/web/cms/en/213186/rwepower-ag/innovations/coal-innovation-centre/co2-scrubbing/ (accessed 22.09.2016).

[48] Well, W. v. In An Overview of the CASTOR Pilot Plant-Carbon capture and storage (CCS) in power production, Topsøe Catalysis Forum, Munkerupgaard, Munkerupgaard, 27-28 August 2008.

[49] Boudaray dam carbon capture project. http://saskpowerccs.com/ccs-projects/boundary-dam-carbon-capture-project/ (accessed 12.09.2016).

[50] Abu-Zahra, M. R., Schneiders, L. H., Niederer, J. P., Feron, P. H., &Versteeg, G. F. (2007). CO2 capture from power plants: Part I. A parametric study of the technical performance based on monoethanolamine. International Journal of Greenhouse gas control, 1(1), 37-46.

[51] Metz, B., Davidson, O., De Coninck, H. C., Loos, M., & Meyer, L. (2005). IPCC special report on carbon dioxide capture and storage. Cambridge: Cambridge University Press.

[52] Zhao, L., Riensche, E., Menzer, R., Blum, L., &Stolten, D. (2008). A parametric study of CO2/N2 gas separation membrane processes for post-combustion capture. Journal of membrane science, 325(1), 284-294. https://doi.org/10.1016/j.memsci.2008.07.058

[53] Zhao, L., Riensche, E., Weber, M., &Stolten, D. (2012). Cascaded Membrane Processes for Post-Combustion CO2 Capture. Chemical engineering & technology, 35(3), 489-496. https://doi.org/10.1002/ceat.201100462

[54] Microdyn Nadir. http://www.microdyn-nadir.com/fileadmin/user_upload/downloads/catalogue.pdf (accessed 07.09.2016).

[55] Esposito, E., Clarizia, G., Bernardo, P., Jansen, J. C., Sedláková, Z., Izák, P., ... &Tasselli, F. (2015). Pebax®/PAN hollow fiber membranes for CO2/CH4 separation. Chemical Engineering and Processing-Process Intensification, 94, 53-61. https://doi.org/10.1016/j.cep.2015.03.016

[56] Borsig membrane technology. Membrane technology for processes and environment. Vol. 2016.

[57] Barcelo, L., Kline, J., Walenta, G., & Gartner, E. (2014). Cement and carbon emissions. Materials and structures, 47(6), 1055-1065. https://doi.org/10.1617/s11527-013-0114-5

[58] https://www.cbsnews.com/news/cement-industry-co2-emissions-climate-change-brimstone/

[59] Barman, A., Bhattacharjee, S., Dutta, T., Pal, S., Chatterjee, S., Karmakar, P., & Mondal, S. (2022, July). Biofuel from organic waste-a

smart solution to conserve nonrenewable resources–A review. In *Journal of Physics: Conference Series* (Vol. 2286, No. 1, p. 012028). IOP Publishing.
DOI 10.1088/1742-6596/2286/1/012028

[60] Zhang, D., Ghouleh, Z., & Shao, Y. (2017). Review on carbonation curing of cement-based materials. Journal of CO2 Utilization, 21, 119-131.https://doi.org/10.1016/j.jcou.2017.07.003

[61] Monkman, S., & MacDonald, M. (2017). On carbon dioxide utilization as a means to improve the sustainability of ready-mixed concrete. Journal of Cleaner Production, 167, 365-375. https://doi.org/10.1016/j.jclepro.2017.08.194

[62] Nivetha, R., Sharma, S., Jana, J., Chung, J. S., Choi, W. M., &Hur, S. H. (2023). Recent Advances and New Challenges: Two-Dimensional Metal–Organic Framework and Their Composites/Derivatives for Electrochemical Energy Conversion and Storage. International Journal of Energy Research, 2023(1), 8711034.

https://doi.org/10.1155/2023/8711034

[63] https://application.wiley-vch.de/books/sample/3527345027_c01.pdf

[64] Al-Rowaili, F. N., Zahid, U., Onaizi, S., Khaled, M., Jamal, A., & AL-Mutairi, E. M. (2021). A review for Metal-Organic Frameworks (MOFs) utilization in capture and conversion of carbon dioxide into valuable products. Journal of CO2 Utilization, 53, 101715.https://doi.org/10.1016/j.jcou.2021.101715.

[65] Kang, X., Fu, G., Fu, X. Z., & Luo, J. L. (2023). Copper-based metal-organic frameworks for electrochemical reduction of CO2. Chinese Chemical Letters, 34(6), 107757.

https://doi.org/10.1016/j.cclet.2022.107757

[66] Shao, R., and Stangeland, A. (2009). Amines Used in CO2 Capture–Health and Environmental Impacts. Oslo: The Bellona Foundation.

[67] Goodrich, B. F., de la Fuente, J. C., Gurkan, B. E., Zadigian, D. J., Price, E. A., Huang, Y., et al. (2011). Experimental measurements of amine-functionalized anion-tethered ionic liquids with carbon dioxide. Ind. Eng. Chem. Res. 50, 111–118. doi: 10.1021/ie101688a

[68] Niedermaier, I., Bahlmann, M., Papp, C., Kolbeck, C., Wei, W., Calderon, S. K., et al. (2014). Carbon dioxide capture by an amine functionalized ionic liquid: fundamental differences of surface and bulk behavior. J. Am. Chem. Soc. 136, 436–441. doi: 10.1021/ja410745a

[69] Alvarez-Guerra, M., Albo, J., Alvarez-Guerra, E., and Irabien, A. (2015). Ionic liquids in the electrochemical valorisation of CO2. Energy Environ. Sci. 8, 2574–2599. doi: 10.1039/C5EE01486G

[70] Rosen, B. A., Salehi-Khojin, A., Thorson, M. R., Zhu, W., Whipple, D. T., Kenis, P. J. A., et al. (2011). Ionic liquid–mediated selective conversion of CO2 to CO at low overpotentials. Science 334, 642–643. doi: 10.1126/science

[71] Lewis, N. S., &Nocera, D. G. (2006). Powering the planet: Chemical challenges in solar energy utilization. Proceedings of the National Academy of Sciences, 103(43), 15729-15735. https://doi.org/10.1073/pnas.0603395103

[72] Saqib, A., Tabbssum, M. R., Rashid, U., Ibrahim, M., Gill, S. S., &Mehmood, M. A. (2013). Marine macroalgae Ulva: a potential feed-stock for bioethanol and biogas production. Asian J AgriBiol, 1(3), 155-163.

[73] Wang, X., Hao, C., Zhang, F., Feng, C., & Yang, Y. (2011). Inhibition of the growth of two blue-green algae species (Microsystisaruginosa and Anabaena spiroides) by acidification treatments using carbon dioxide. BioresourceTechnology, 102(10), 5742-5748. https://doi.org/10.1016/j.biortech.2011.03.015

[74] Gao, Y., Gregor, C., Liang, Y., Tang, D., & Tweed, C. (2012). Algae biodiesel-a feasibility report. Chemistry Central Journal, 6, 1-16. https://doi.org/10.1186/1752-153X-6-S1-S1

[75] Chisti, Y. (2007). Biodiesel from microalgae. Biotechnology advances, 25(3), 294-306. https://doi.org/10.1016/j.biotechadv.2007.02.001

[76] Metting, F. B. (1996). Biodiversity and application of microalgae. Journal of industrial microbiology, 17, 477-489. https://doi.org/10.1007/BF01574779

[77] Essaki, K., Nakagawa, K., Kato, M., &Uemoto, H. (2004). CO_2 absorption by lithium silicate at room temperature. Journal of Chemical Engineering of Japan, 37(6), 772-777. https://doi.org/10.1252/jcej.37.772

[78] Cantrell, K. B., Ducey, T., Ro, K. S., & Hunt, P. G. (2008). Livestock waste-to-bioenergy generation opportunities. Bioresource technology, 99(17), 7941-7953. https://doi.org/10.1016/j.biortech.2008.02.061

[79] Bitog, J. P., Lee, I. B., Lee, C. G., Kim, K. S., Hwang, H. S., Hong, S. W., ... & Mostafa, E. (2011). Application of computational fluid dynamics for modeling and designing photobioreactors for microalgae production: A review. Computers and electronics in agriculture, 76(2), 131-147. https://doi.org/10.1016/j.compag.2011.01.015

[80] Adamczyk, M., Lasek, J., &Skawińska, A. (2016). CO_2 biofixation and growth kinetics of *Chlorella vulgaris* and *Nannochloropsis gaditana*. Applied biochemistry and biotechnology, 179, 1248-1261. https://doi.org/10.1007/s12010-016-2062-3

[81] Yun, Y. S., Lee, S. B., Park, J. M., Lee, C. I., & Yang, J. W. (1997). Carbon dioxide fixation by algal cultivation using wastewater nutrients. Journal of Chemical Technology & Biotechnology: International Research in Process, Environmental and Clean Technology, 69(4), 451-455.

https://doi.org/10.36375/prepare_u.iiche.a394

Photobioreactors for production of biofuels from microalgae: a concise review

[1]Arpit Mondal, [1]Arijit Seth, [1]Debjit Seth, [2]Devyani Thapliyal, [1*]Pramita Sen, [2]Raj Kumar Arya

*Corresponding Author name: Pramita Sen

Email: pramita.sen@gmail.com Phone number: 9831088581

[1]Department of Chemical Engineering, Heritage Institute of Technology Kolkata-700107, India

[2]Department of Chemical Engineering, Dr. B.R. Ambedkar National Institute of Technology, Jalandhar 144011, India

Mention Abstract Theme: Energy and Environment (EE)

Abstract

Microalgal strains are potential cell factories capable of producing valuable biochemicals including biofuels. Photobioreactors are closed systems capable of producing large quantities of microalgae and high yields of biofuel under optimal operating conditions, namely, light, temperature and pH. The design configurations of these systems are horizontal or serpentine tube, flat plate, bubble column and stirred tank of which tubular and flat plate bioreactors show promising results in biofuel production. However, the separation of algal biomass from the treated wastewater poses a major challenge in the use of algae for wastewater treatment. To overcome this problem, biofilm-based photobioreactor, an immobilized algal cultivation reactor, has emerged as a promising strategy. In the present study, we discuss the different types of photobioreactors, the distinct advantages of using these reactors over the open pond technology, the microalgal growth dynamics, reaction kinetics, diffusional limitations, and challenges faced during reactor scale-up. The review finally tries to provide a perspective on how further developments can be made in this reactor technology for setting up an economical, controllable and efficient method of microalgae cultivation and biofuel generation.

Keywords: microalgae; photobioreactor; kinetics; diffusional limitations

https://doi.org/10.36375/prepare_u.iiche.a394

1. Introduction

In modern science developments in microalgal culture technology have played a role to a considerable extent. They have been producing various types of chemicals and bulk products from microalgae. Bio polyesters, lipids, carbohydrates, proteins, pigments, colors, and antioxidants, are all known as several biological derivatives [1-4]. They are all viable options for clean energy extraction and bioremediation [5]; recognized as feedstock for third-generation renewable biofuels and energy (e.g., biodiesel, bioethanol, biobutanol, biohydrogen, etc.). CO_2 can biofixate or attenuate bioelectricity [6-9], and clear the flue of hazardous substances such as wastewater [10] treatment, nitric, and sulfur oxides gas [11,12]. Microalgae do in fact hold a superior to their terrestrial plants, they have tremendous potential as cell factories.

The global energy demand for microalga has been steadily enhanced, and the yearly production rate is estimated at ca. 20,000 tons [4,13]. Nevertheless, the full potential of microalgae is still constrained by the existence of still less expensive alternatives in the market.

Photoautotrophic cultivation is currently the most widely used mode for producing microalgae, and the only workable strategy at present to obtain biomass at a large scale [5,14]; this is because sunlight is a free, renewable, and clean source of energy. Used to grow microalgae, there are different cultivation methods, depending on the desired product and available species. They result in higher costs. Open systems, such as circular and raceway ponds, are the most used industrial devices and account for 90% of the overall microalga annual production [15]. For the high rate of demand and interest in microalgae, closed cultivation systems known as photobioreactors (PBRs) have been developed. While open systems are relatively cheap and easy to operate, PBRs tend to be more complex and expensive. Open systems used for microalgae cultivation have certain drawbacks such as poor mass transfer rate and high-water evaporation, instability of culture conditions, susceptibility to contamination, and need for a large land surface [5,12,16]. On the other hand, a closed photobioreactor offers better control over the growth environment, including nutrients, temperature, pH, and lighting. This allows for the cultivation of single species of microalgae for longer periods, reducing the risk of external contamination [8,17]. Several types of photobioreactors have been developed to isolate and cultivate green microalgae. These reactors are used at small and pilot scales, in laboratories as well as outdoors [14,18,19]. The conventional closed PBR configurations include a few standard designs [20], including flat-plate [21-23], tubular (horizontal) [14,21,22,24], and column-type [10,11,17]. The column-type reactors are further divided into stirred tank-type PBR and aerated columns (bubble column or airlift). Scaling up capital costs presents major difficulties [25]. The choice of PBR geometry and operational methods depends on the intrinsic features of the microalga selected (in terms of energy demand and growth kinetics), the intended bio-compounds or by-products, and local conditions [16,26].

2. Photobioreactors

Due to the limitations of open pond systems, extensive research has been carried out to find an alternative. Photobioreactors have emerged as a feasible option for cultivating algae due to their high rate of production and generation of quality

https://doi.org/10.36375/prepare_u.iiche.a394

algal cells. A photobioreactor is an enclosed vessel that uses light and CO2 to facilitate the rapid propagation of the cells (Tan et al., 2018). compared to open pond cultivation, photobioreactors require less space. Various types of photobioreactors have been developed such as tubular, bubble, flat, horizontal, foil, and porous photobioreactors. Among them, tubular and flat panel photobioreactors are the most widely used and efficient closed culture systems for the commercial cultivation of microalgae (Suparmaniam et al., 2019). Fig.-1 Represents the Design and applications of photobioreactors.

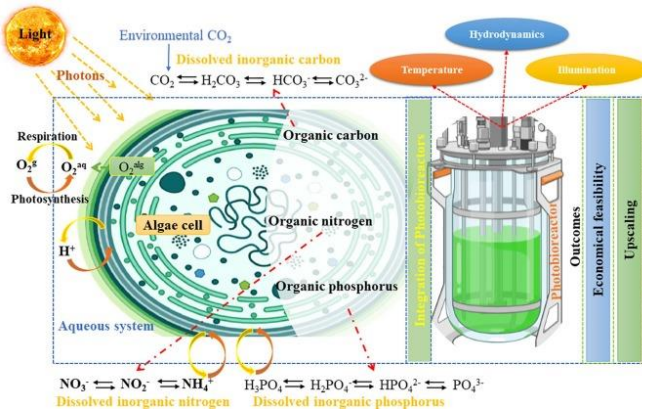

Fig. 1 Applications of photobioreactor

3. *Different types of PBRs & their Design Configuration:*

3.1 Flat-plate PBR:

The flat plate photobioreactor (FP- PBR) has been used since the 1950s and can be used indoors and outdoors [26]. However, there has been a high risk of photoinhibition, especially in outdoor cultures or at the early stage of growth. When exposed to high levels of light, cells become inhibited due to light over-saturation, which can severely affect photosynthesis and cellular metabolism. This can ultimately lead to the collapse of the culture [40]. The FP-PBR can be oriented vertically or inclined at a tilt angle to maximize incident light and increase biomass productivity. Agitation can be provided through either a pump lift over-driven or airlift method, with baffles included to improve mixing efficiency. Oxygen buildup is usually not a problem since there is an effective open gas disengagement system, except when a vertical alveolar panel is used [43]. A design of scalable airlift flat panel photobioreactor for microalgae cultivation is shown in Fig.- 2.

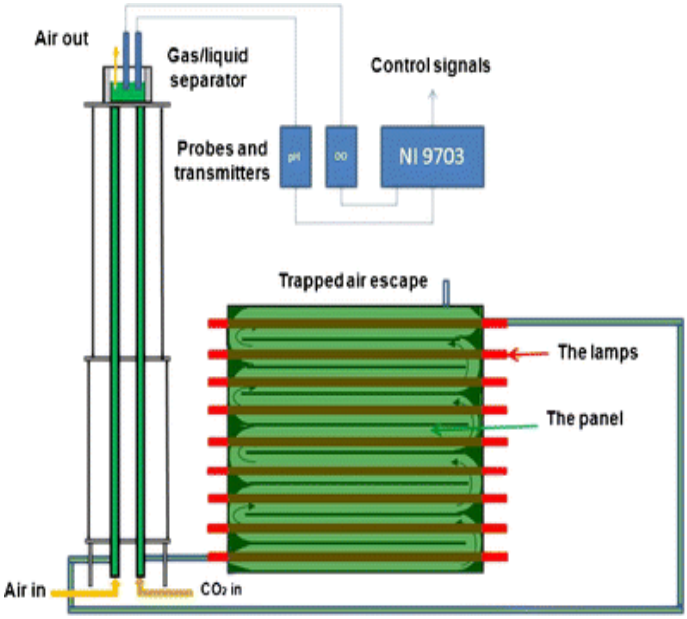

Fig.- 2 Airlift flat panel photobioreactor

3.2 Biofilm-based photobioreactor

A biofilm-based photo bioreactor is a specialised system designed to cultivate photosynthetic microorganisms, such as algae and cyanobacteria, in the form of biofilms. A biofilm is a complex, three-dimensional community of microorganisms that adhere to surfaces and grow together in a matrix of extracellular polymeric substances. In the context of photobioreactors the microorganisms grow on the solid substrate or surface and form a biofilm structure while being exposed to light for photosynthesis.

https://doi.org/10.36375/prepare_u.iiche.a394

3.3 Tubular PBR:

Transparent tubing, either made of glass or polyethylene is used to create conservative tubular PBRs. The most common configuration is a serpentine loop arranged in a single plane, which is usually displayed horizontally and is a popular choice for outdoor mass culturing [27]. Apart from the tube arrangement, tubular PBRs differ in tube length and diameter, flow velocity, form of recirculation, and geometric shape of the light receiver. The tubes used are typically between 0.1 and 0.6 cm in diameter [28], while their lengths can be several hundred meters long. The tube length is determined by the photosynthesis activity and the distance between liquid degassing points [29].

Tubular photobioreactors (PBRs) are considered as solar collectors since they use microalgae flow through a large surface area exposed to sunlight. The "lens effect" or "focusing effect" ensures that the incident light is evenly distributed, as it flows radially and is diluted along the circumference, which focuses it on the axis of the tube. This effect reduces the mutual shading and increases radiation intensity, which in turn reduces photo-inhibition [30]. One of the significant advantages of this configuration is the high surface-to-volume ratio, which is particularly suitable for efficient light harvesting while minimizing photo-inhibition [31-33].

3.4 Vertical column PBR:

Vertical column PBRs can be categorized into stirred-tank vessels and aerated columns, such as bubble columns or airlifts. the central regions of these types of reactors typically appear as dark or dimly lit environments, limiting cell exposure to light along the axis, which can negatively affect photosynthetic efficiency and microalga biomass production and productivity [34,35]. In general, the relatively low ratio of surface area to volume (A/V ratio) hampers scale-up [15,36]. For a better understanding of the advantages and drawbacks of both stirred tank and aerated column PBRs, please refer to [Table 1].

3.5 Stirred-tank type PBR:

Stirred tank PBRs are commercial bioreactors that are commonly made of steel, glass, or organic glass. They are often used in the industry to produce fine chemicals or pharmaceutical products. These systems are particularly useful for the heterotrophic growth of microalgae using appropriate organic carbon sources [26]. The main advantage of this apparatus is the precision, control accuracy of every operating parameter, and the minimization of contamination by heat sterilization. By using wall transparent arrangements, they can also be used for phototrophic cultivation, photomixotrophic, and photoheterotrophic modes if an external light source is provided (e.g., fluorescent lamp, LED, or even sunlight). Although it has a quite low A/V ratio, this configuration is useful for optimization processes at a laboratory scale (indoors) [37]. Fig.3 shows Façade integrated photobioreactors for building energy efficiency.

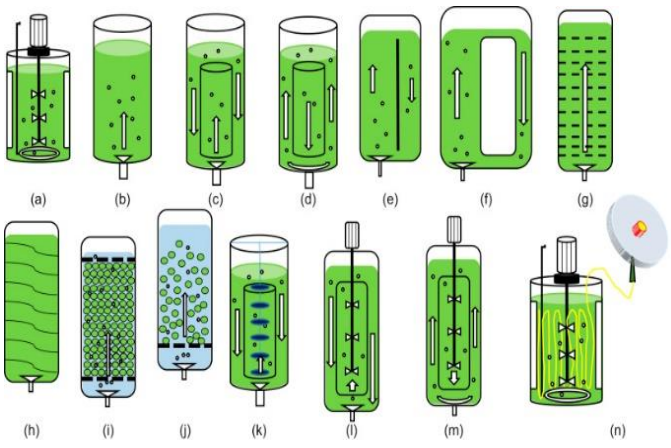

Fig.- 3 Façade integrated photobioreactor

https://doi.org/10.36375/prepare_u.iiche.a394

3.6 Aerated columns-PBR:

A common type of photobioreactor is the aerated column-PBR, which is typically made of transparent glass or plastic and has a vertical cylinder shape. To avoid shading effects caused by a high cell concentration, smaller radii have been suggested. However, the core regions of these reactors are often dimly lit or dark, which limits the exposure of cells to light along the axis and reduces photosynthesis efficiency [33]. Scale-up problems can also occur due to the relatively low AA/V ratio [6,38]. Aerated columns can be classified as bubble columns or airlift reactors, depending on their mode of liquid motion [39]. In both cases, agitation, gas, or CO2 is sparged at the bottom of the PBR to provide agitation and mixing, which ensures good overall mixing and sufficient gas transfer rates [36,40].

4. Designing Equation of Photobioreactor:

Designing a photobioreactor requires considering several factors, such as reactor geometry, the availability of light, temperature regulation, and the requirements of the microorganisms or algae you plan to grow. There I no single "design equation" for a photobioreactor since the design will be influenced by your specific objectives and limitations. However, some equations are commonly used in the design and operation of photobioreactors:

4.1 Light Intensity and Distribution:

4.1.1 Beer-Lambert Law:

This law is used to calculate light attenuation through a culture medium, which is important for determining the required light intensity.

$$\log\left(\frac{I0}{I}\right) = A = \in lC$$

- A is the absorbance
- ε is the molar attenuation coefficient or absorptivity of the attenuating species
- ℓ is the optical path length
- C is the concentration of the attenuating species

4.1.2 Mass Transfer and Oxygen Transfer:

Oxygen Transfer Rate (OTR): OTR is crucial for microorganism growth. It can be calculated using equations like oxygen transfer coefficient (Kla) and Henry's law.

Kla Equation: This equation relates the volumetric mass transfer coefficient (Kla) to the reactor design and operating conditions.

4.1.3 Hydrodynamic and Mixing Considerations:

Reynold's Number (Re): It is used to assess the flow regime inside the reactor, whether it's laminar or turbulent.

Mixing time: This is a measure of the time required to achieve good mixing in the reactor. It can be estimated based on the reactor geometry and agitation rate.

4.1.4 Temperature Control:

https://doi.org/10.36375/prepare_u.iiche.a394

Heat Transfer Equations: Depending on the design, heat transfer equations can be used to determine the cooling or heating requirements for maintaining the desired temperature.

4.1.5 Biomass growth kinetics:

Monod Equation: This equation describes the specific growth rate of microorganisms as a function of substrate concentration.

$$\mu = \mu_{max} * ([S])/(K_s + [S])$$

where: μ is the specific growth rate.

- μ_{max} is the maximum specific growth rate.
- S is the substrate concentration.
- Ks is the half-saturation constant.

Reactor Sizing:

- You will need to perform mass and energy balances to size the reactor appropriately based on your target biomass production.

Light Source Design:

- Depending on the type of light source (natural sunlight, artificial light), you'll need to design the lighting system to provide adequate and controlled light intensity

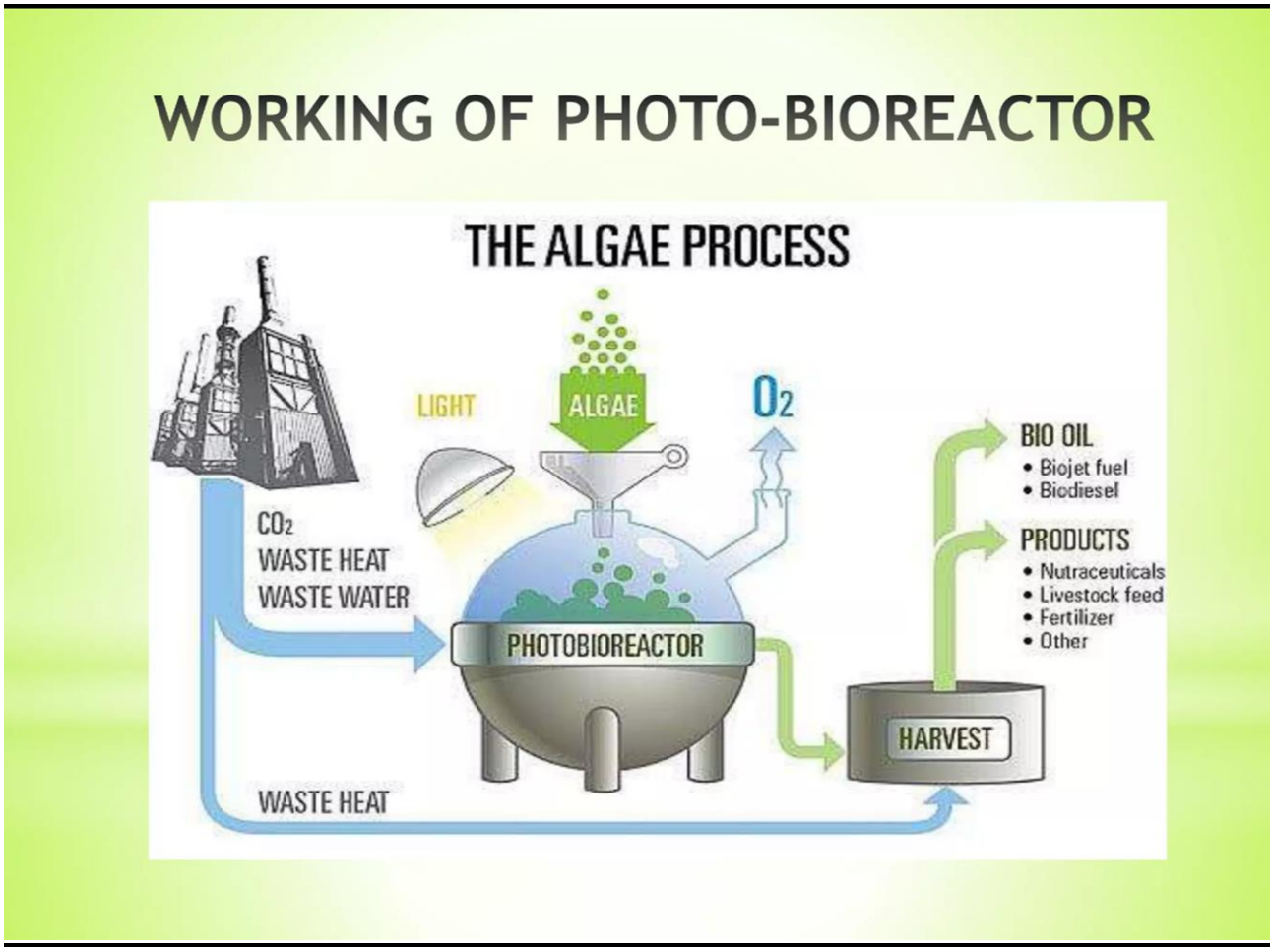

Fig.- 4 Working of photobioreactors

Figure 4 Represents the working of Photo-Bioreactors

6. Comparison between most common enclosed photobioreactor configuration for microalga cultivation system. (Adapted from [35,37,40]):

https://doi.org/10.36375/prepare_u.iiche.a394

Types of photobioreactor	Advantages	Limitations	Applicability/observations
Flat-plate	-High area-to-surface ratio -Large, illuminated surface area. -Good light path -Moderate biomass yields	-Expensive construction materials -Easily subjected to photo-inhibition -Hard temperature control -Scale-up problems	-Suitable for outdoor and indoor -Application to algal strains with high lipid content
Tubular (horizontal)	-High S/V ratio -Effective in the capture of solar radiation -Relatively low cost to build	-Poor mass transfer -High risk of pH gradient and O2 build-up -Risk of photo-inhibition or photo-oxidation -Risk of overheating -High land surface area required	-Well suited for cultivation outdoors -Well suited for industrial cultivation of most common microalgae species
Column (vertical) Stirred tank	-Precise monitoring of each culture parameter -Used for optimization studies. -Cheap and compact -Low maintenance cost	-Low area-to-volume ratio -Poor efficiency in light conversion -Low productivity	-Ideal for producing added value compounds. -Cultivation of biomass for wastewater treatment -Limited to heterotrophic microalgae
Aerated columns (bubble columns and airlift)	-Good mixing -Efficient CO2 supply and O2 removal -Low fouling -Low land requirements	-Risk of high shear stress on cultures -Photo-inhibition problems -Small illumination area -Deficient scale-up	-Unstable for microalgae prone to flotation and/ or species highly sensitive to shear stress

https://doi.org/10.36375/prepare_u.iiche.a394

7. General parameters affecting PBR performance:

The performance of a photobioreactor is influenced by a variety of factors, including physicochemical parameters like temperature, pH, dissolved oxygen, CO2 availability, shearing, and nutrient availability, as well as physical and operational factors. Light requirements surface area to volume ratio, mixing and agitation patterns, exchange rates of Co2 and O2, nutrients provisions and renewal temperature and pH control, the quality of construction material, and biofouling all play a crucial role in the proper operation of a PBR. Some of these parameters interact with one another, which makes designing an effective PBR as a cultivation system a complicated task [41].

7.1 Temperature:

Temperature control is a significant operational parameter in PBR performance; it greatly influences the growth rate of microalgae [42]. The efficiency of photosynthesis depends on a balance between light and temperature [43]. Microalgae hold an optimum temperature interval – that should be sought a priori. This is essential to promote effective light harnessing and CO2 biofixation, and thus reach high biomass productivity. Optimum temperatures typically range within 20–24 ◦C. Nevertheless, most microalgae can tolerate temperatures between 16 and 35 ◦C [44-46].

7.2 pH:

Maintaining an optimal pH level is crucial for the performance of photobioreactors (PBRs). Any deviation from the optimum range can severely impact the microalgal cell's ability to absorb CO2 and other essential nutrients like iron, thereby affecting overall the health of the culture [47]. The pH level is primarily controlled by balancing the supply and mass transfer of the CO2 in the liquid phase and the uptake by the microalgal cells. The total dissolved inorganic carbon (DIC) in the medium plays a significant role in controlling the pH level. If the DIC appears mainly in the form of CO2, it can cause acidic pH shifts (<7). Conversely, frequent alkaline pH shifts occur when the main form of DIC is carbonate (i.e., CO3 2-) [40].

7.3 Light and surface area-to-volume ratio

Achieving effective photoautotrophic cultivation of microalgae requires an efficient light supply and the appropriate wavelength range. During photosynthesis, most microalgae process energy within the 400–700 nm range, also known as photosynthetically active radiation (PAR). Solar light is often used as a cost-effective source of energy for microalgae growth in common outdoor mass cultivation systems.

The Surface area-to-volume ratio (S/V ratio) plays a vital role in the performance of PBRs. The distribution of light over the PBR surface depends on the total transparent surface area available, in general, which in turn is affected by the S/V ratio. Generally, the higher the S/V ratio, the higher the percentage of light presenting the PBR surface, leading to an improvement in photosynthetic efficiency, and higher productivity of biomass and metabolite productivities [16,20,48].

https://doi.org/10.36375/prepare_u.iiche.a394

7.4 Mixing and agitation

In microalga cultivation systems, the cells are typically suspended in the broth medium. As a result, mixing is a crucial factor that helps to ensure that the culture is homogenized and to prevent the cells from settling or clumping together on the walls of[the PBRs, particularly in horizontal tubular PBRs [36]. Proper mixing also helps to distribute the nutrients evenly and reduces temperature and pH gradients. If mixing is poor, the nutrients and pH may accumulate in undesired gradients, leading to biofouling on the walls of the PBRs, as well as an increase in oxygen levels in the medium [49]. To improve mixing, baffles or static mixtures can be used inside the reactors [43,50].

7.5 Gas exchange

The ability to exchange gasses (such as removing O2 and adding CO2) is an important feature of PBRs for cultivating microalgae [45]. However, the process of delivering CO2 is limited by mass transfer, which can be a problem for open systems due to the low atmospheric pressure of CO2. This means that microalgae cannot directly use gaseous CO2, but instead require it to be dissolved in a liquid phase for enhanced mass transfer rates [51].

8. Process of Microalgae to Biofuel Production:

8.1 Harvesting:

The development of a cost-effective microalgal biodiesel industry requires the use of minimum energy harvesting techniques. However, the small size of microalgal cells, negative charges on their surface, their density near water, and their suspension in dilute media present some hindrances in the development of a low cost harvesting approach (Muhammad et al., 2020). There are many harvesting techniques available, including centrifugation, filtration, flocculation, electrophoresis, gravitational sedimentation, and flotation. Centrifugation is the most widely used technique on a laboratory scale, but it is highly energy-demanding and may lead to cell damage, thus not being applicable to large-scale biodiesel production (Morais Junior et al., 2020).

8.2 Lipid extraction:

To produce biodiesel, it is essential to extract lipids from the cells. However, the extraction process requires a suitable technique. For optimal lipid extraction, pretreatment of harvested and dried cells is necessary. This pretreatment involves mechanical disruption of cells using mortar and pestle, bead mills, ultra-sonication, etc (Zheng et al., 2011; Greenly and Tester, 2015; Rivera et al., 2018). Alternatively, methods such as microwaving, acid/based treatment, and enzyme treatment can be used to break down cell structure (Zuorro et al., 2016). Additionally, pulsed electric field (PEF) and high voltage electric discharge (HVED) are efficient approaches for cell lysis.

8.3 Transesterification:

The transesterification reaction is a process where one mole of triglyceride and three moles of alcohol react to produce a simple ester (biodiesel) in the presence of a catalyst. This method is widely accepted as one of the best approaches for biodiesel production (Tabatabaei et al., 2019). The catalyst plays a crucial role in determining the ease of converting triglycerides to ester (Pathak et al., 2018; Changmai et al., 2020).

https://doi.org/10.36375/prepare_u.iiche.a394

9. Determination of algal growth rate kinetics

The algal growth rate was determined by measuring the growth of microalgae using a spectrophotometer. Briefly, samples were withdrawn, and the algal growth was measured by recording the absorbance at 680 nm. For the determination of biomass, the algal suspension was centrifuged at 15,000 rpm for 10 min and dried at 55 °C for 60 min in a hot air oven. The relation between the growth rate and the biomass was estimated using a liner regression equation (eq:2) and specific growth rate (eq:3) (Tamil Selvan et al. 2020):

$$\mathbf{Y = 0.8754X - 0.3645} \quad (2)$$

where, X—optical density at 680 nm and N—dry biomass weight (gmL−1)

$$\boldsymbol{\mu = \frac{\ln(N_1 - N_0)}{t_1 - t_0}} \quad (3)$$

Were, μ—Specific growth rate and Ln—Linear regression.

9.1 Determination of CO2 utilization kinetics:

The CO2 biosorption ability and the biofixation efficiency rate (BCO2) of the selected microalgal algal species were calculated using the modified methodology of De Morais and Costa (2007). The bio fixation efficiency rate, percentage of CO2 removal, and consumption rate were calculated as mentioned below: The BCO2 (Eq:4) and CO2 removal (%) (Eq:5) were estimated based on the equations, given as the determination of bio fixation efficiency rate:

$$\boldsymbol{B_{CO2} = X_C * P(\frac{Z_{CO2}}{Z_C})} \quad \mathbf{(4)}$$

where, Xc % of carbon content from the given microalgal cell, P is the biomass productivity expressed in terms of mg mL−1d−1, ZC is the molecular weight Carbon (C) and ZCO2 is the molecular weight carbon dioxide (CO2). The determination of CO2 removal (%):

$$\boldsymbol{R_{CO2} = \left(\frac{total\ CO_2 biofixed(V)}{total\ CO_2 input(V)}\right) * 100} \quad \mathbf{(5)}$$

where RCO2 is carbon dioxide (CO2) removal in terms of percentage and V is the volume of CO2.

9.2 Determination of heavy metals biosorption capacity:

To study the biosorption ability of heavy metals using microalgae, 50 mL of the effluent treated with algae was filtered using a nylon Millipore membrane filter. The filtered microalgal cells were collected and utilized for biosorption capacity studies using atomic adsorption spectroscopy. The kinetics studies of heavy metals biosorption using microalgae were evaluated by kinetic models such as the Langmuir and Freundlich model (Tamil Selvan et al. 2020) as mentioned below.

For the Langmuir model, the biosorption ability was calculated using the following equation:

$$\boldsymbol{\frac{C_e}{q_e} = \left(\frac{1}{bq_{max}}\right) + \left(\frac{C_e}{q_{max}}\right)} \quad \mathbf{(6)}$$

where q_e is Algal biosorption capacity at equilibrium (mg g−1), Ce is the Concentration of metals at equilibrium (mg L−1),q_{max} is Maximum

biosorption capacity (mg g−1), and is Langmuir constant (L g−1).

For the Freundlich model, the biosorption ability was calculated using the following equation:

$$q_e = K_F * C_e^{1/n} \quad (7)$$

where K_F is the Freundlich constant,1/n is Adsorption intensity, q_e is Algal biosorption capacity at equilibrium (mg g−1) and C_e is the Concentration of metals at equilibrium (mg L−1).

10. Challenges and Opportunities:

10.1 Biofouling:

Biofouling is a major issue in PBRs, especially in closed ones. This happens when cells aggregate and stick to the inner walls of the system, the biomass concentration decreases, and the system's performance is negatively affected [52]. Choosing the right construction material and geometry is crucial to prevent biofouling. Designs like flat plate PBRs with a more cuboidal shape and are easier to clean and maintain than tubular reactors. PBRs that have continuous turbulent regimes due to random stirring or gas bubbling are less prone to biofouling. Additionally, fluid radial flow patterns like those cylindrical vessels achieved via rotation stirring are better than axial flow only [54].

Many unconventional designs for photobioreactors (PBRs) have been suggested to overcome the major challenges of classical configurations. These modifications have improved light conduction, hydrodynamic patterns, mass transfer, and controllability. However, there are still several obstacles to be addressed.

PBR configurations designed to reduce light path (and increase the surface area to volume ratio) show promising advances in improving light distribution inside the system, which is a major issue when dealing with high-density microalgae culture. However, optical fibers and light guide devices in column vessels and compact systems are difficult to scale in terms of both cost-effectiveness and long-term performance [36,42].

LED-based lighting technologies have become important in novel PBRs and supporting technologies have experienced significant advancement in recent years. Enhancing hydrodynamics with tailor-made internal flow patterns and developing effective flashing light effects and light/dark cycles have proven useful in improving microalgae biomass productivity. Active mixing has been found to enhance microalgae performance when exposed to intercalated illumination and dark cycles [41,53]. Many low-cost plastics favour the transmittance of light into the microalga cultures, yet photo-limitation may be induced. Less expensive, yet more fragile materials are more susceptible to leakage and contamination. They can undergo photo-degradation when exposed to UV-radiation (combined with exposure to high temperatures) [32], thus compromising plastic optical properties and eventually impairing regular microalgae growth and performance.

Overall, the development of novel PBRs still faces several challenges as unconventional configurations for microalgae cultivation, especially in view of the high construction and operational costs incurred in scaling up. Nevertheless, investigation and development in this field offer a major opportunity to combine empirical experience and theoretical fundamentals in attempting to produce economically more

feasible and environmentally sustainable systems [54].

10. Conclusion:

We've developed a profitable and sustainable biodiesel production method using carefully selected microalgae species. Hybrid bioreactors are effective for mass-producing algae, and combining different types of bioreactors may help develop appropriate bioreactors for mass algal culture. To produce large quantities of algal biomass, we suggest using photobioreactors with photonics and biotechnologies. However, more economic assessments are needed to compete with petroleum-derived fuels.

11. Acknowledgement:

We would like to express our gratitude to our mentor, (Prof. Dr. Pramita Sen), for her innovative ideas and guidance, which greatly helped us to fulfill this project.

12. References:

1. T.M. Mata, A.A. Martins, N.S. Caetano, Microalgae for biodiesel production and other applications: A review, Renew, Sustain. Energy Rev 14 (2010) 217–232, https://doi.org/10.1016/j.rser.2009.07.020.
2. L. Brennan, P. Owende, Biofuels from microalgae—a review of technologies for production, processing, and extractions of biofuels and co-products, Renew. Sust. Energ. Rev. 14 (2010) 557–577, https://doi.org/10.1016/j.rser.2009.10.009. F. García-Camacho, J.J. Gallardo-Rodríguez, A. Sanchez-Mir ´ on, ´ M.C. Ceron- ´ García, E.H. Belarbi, Y. Chisti, E. Grima-Molina, Biotechnological significance of toxic marine dinoflagellates, Biotechnol. Adv. 25 (2007) 176–194, https://doi. org/10.1016/j.biotechadv.2006.11.008.
3. J. Assunçao, ˜ A. Catarina Guedes, F. Xavier Malcata, Biotechnological and pharmacological applications of biotoxins and other bioactive molecules from dinoflagellates, Mar. Drugs. 15 (2017) 1–43, https://doi.org/10.3390/ md15120393. T.M. Mata, A.A. Martins, N.S. Caetano, Microalgae for biodiesel production and other applications: A review, Renew, Sustain. Energy Rev 14 (2010) 217–232, https://doi.org/10.1016/j.rser.2009.07.020.
4. M.K. Lam, K.T. Lee, A.R. Mohamed, Current status and challenges on microalgaebased carbon capture, Int. J. Greenh. Gas Control. 10 (2012) 456–469, https:// doi.org/10.1016/j.ijggc.2012.07.010.
5. C.Y. Chen, K.L. Yeh, R. Aisyah, D.J. Lee, J.S. Chang, Cultivation, photobioreactor design and harvesting of microalgae for biodiesel production: a critical review, Bioresour. Technol. 102 (2011) 71–81, https://doi.org/10.1016/j. biortech.2010.06.159 Y. Chisti, Biodiesel from microalgae beats bioethanol, Trends Biotechnol. 26 (2007) 126–131, https://doi.org/10.1016/j.tibtech.2007.12.002.
6. Y. Chisti, Biodiesel from microalgae beats bioethanol, Trends Biotechnol. 26 (2007) 126–131, https://doi.org/10.1016/j.tibtech.2007.12.002.

7. R.P. John, G.S. Anisha, K.M. Nampoothiri, A. Pandey, Micro and macroalgal biomass: a renewable source for bioethanol, Bioresour. Technol. 102 (2011) 186–193, https://doi.org/10.1016/j.biortech.2010.06.139.
8. R.N. Singh, S. Sharma, Development of suitable photobioreactor for algae production - a review, Renew. Sust. Energ. Rev. 16 (2012) 2347–2353, https://doi.org/10.1016/j.rser.2012.01.026.
9. P.L. Show, M.S.Y. Tang, D. Nagarajan, T.C. Ling, C.W. Ooi, J.S. Chang, A holistic approach to managing microalgae for biofuel applications, Int. J. Mol. Sci. 18 (2017) 1–34, https://doi.org/10.3390/ijms18010215.
10. A. S´anchez-Miron, ´ M.C. García-Ceron, ´ F. García-Camacho, E. Molina-Grima, Y. Chisti, Mixing in bubble column and airlift reactors, Chem. Eng. Res. Des. 82 (2004) 1367–1374, https://doi.org/10.1205/cerd.82.10.1367.46742.
11. T.M. Mata, A.A. Martins, N.S. Caetano, Microalgae for biodiesel production and other applications: A review, Renew, Sustain. Energy Rev 14 (2010) 217–232, https://doi.org/10.1016/j.rser.2009.07.020.
12. M.K. Lam, K.T. Lee, A.R. Mohamed, Current status and challenges on microalgaebased carbon capture, Int. J. Greenh. Gas Control. 10 (2012) 456–469, https://doi.org/10.1016/j.ijggc.2012.07.010.
13. M. Płaczek, A. Patyna, S. Witczak, Technical evaluation of photobioreactors for microalgae cultivation, in: E3S Web Conf., 2017, p. 02032, https://doi.org/10.1051/e3sconf/20171902032.
14. E. Molina Grima, J. Fern´ andez, F.G. Aci´en, Y. Chisti, Tubular photobioreactor design for algal cultures, J. Biotechnol. 92 (2001) 113–131, https://doi.org/10.1016/S0168-1656(01)00353-4.
15. Y. Chisti, Biodiesel from microalgae, Biotechnol. Adv. 25 (2007) 294–306, https://doi.org/10.1016/j.biotechadv.2007.02.001.
16. P.L. Gupta, S.M. Lee, H.J. Choi, A mini review: photobioreactors for large scale algal cultivation, World J. Microbiol. Biotechnol. 31 (2015) 1409–1417, https://doi.org/10.1007/s11274-015-1892-4.
17. A.P. Carvalho, L.A. Meireles, F.X. Malcata, Microalgal reactors: a review of enclosed system designs and performances, Biotechnol. Prog. 22 (2006) 1490–1506, https://doi.org/10.1021/bp060065r.
18. C.Y. Chen, K.L. Yeh, R. Aisyah, D.J. Lee, J.S. Chang, Cultivation, photobioreactor design and harvesting of microalgae for biodiesel production: a critical review, Bioresour. Technol. 102 (2011) 71–81, https://doi.org/10.1016/j.biortech.2010.06.159
19. M.K. Lam, K.T. Lee, A.R. Mohamed, Current status and challenges on microalgaebased carbon capture, Int. J. Greenh. Gas Control. 10 (2012) 456–469, https://doi.org/10.1016/j.ijggc.2012.07.010.
20. M.S.A. Rahaman, L.-H. Cheng, X.-H. Xu, L. Zhang, H.-L. Chen, A review of carbon dioxide capture and utilization by membrane integrated microalgal

cultivation processes, Renew. Sust. Energ. Rev. 15 (2011) 4002–4012, https://doi.org/10.1016/j.rser.2011.07.031.

21. M. Płaczek, A. Patyna, S. Witczak, Technical evaluation of photobioreactors for microalgae cultivation, in: E3S Web Conf., 2017, p. 02032, https://doi.org/10.1051/e3sconf/20171902032.
22. A.P. Carvalho, L.A. Meireles, F.X. Malcata, Microalgal reactors: a review of enclosed system designs and performances, Biotechnol. Prog. 22 (2006) 1490–1506, https://doi.org/10.1021/bp060065r.
23. A.P. Carvalho, L.A. Meireles, F.X. Malcata, Microalgal reactors: a review of enclosed system designs and performances, Biotechnol. Prog. 22 (2006) 1490–1506, https://doi.org/10.1021/bp060065r.
24. J.J. Gallardo-Rodríguez, A. S´ anchez-Miron, ´ F. García-Camacho, L. Lopez-rosales, ´ Y. Chisti, E. Molina-Grima, Bioactives from microalgal dinoflagellates, Biotechnol. Adv. 30 (2012) 1673–1684, https://doi.org/10.1016/j.biotechadv.2012.07.005.
25. G. Olivieri, P. Salatino, A. Marzocchella, Advances in photobioreactors for intensive microalgal production: configurations, operating strategies and applications, J. Chem. Technol. Biotechnol. 89 (2014) 178–195, https://doi.org/10.1002/jctb.4218.
26. C.N. Dasgupta, J. Jose Gilbert, P. Lindblad, T. Heidorn, S.A. Borgvang, K. Skjanes, D. Das, Recent trends on the development of photobiological processes and photobioreactors for the improvement of hydrogen production, Int. J. Hydrog. Energy 35 (2010) 10218–10238, https://doi.org/10.1016/j.ijhydene.2010.06.029.
27. M.R. Tredici, Mass production of microalgae: Photobioreactors, in: A. Richmond (Ed.), Handb. Microalgal Cult. Biotechnol. Appl. Phycol, Blackwell Publishing Ltd, Oxford, UK, 2007, pp. 178–214, https://doi.org/10.1002/9780470995280.ch9.
28. A. Karemore, D. Ramalingam, G. Yadav, G. Subramanian, R. Sen, Photobioreactors for Improved Algal Biomass Production: Analysis and Design Considerations, in: Algal Biorefinery an Integr, Springer International Publishing, Cham, Approach, 2015, pp. 103–124, https://doi.org/10.1007/978-3-319- 22813-6_5.
29. J. Degen, A. Uebele, A. Retze, U. Schmid-Staiger, W. Trosch, A novel airlift photobioreactor with baffles for improved light utilization through the flashing light effect, J. Biotechnol. 92 (2001) 89–94, https://doi.org/10.1016/S0168-1656(01)00350-9.
30. Z. Yang, J. Cheng, X. Xu, J. Zhou, K. Cen, Enhanced solution velocity between dark and light areas with horizontal tubes and triangular prism baffles to improve microalgal growth in a flat-panel photo-bioreactor, Bioresour. Technol. 211 (2016) 519–526, https://doi.org/10.1016/j.biortech.2016.03.145.

31. I.S. Suh, C.-G. Lee, Photobioreactor engineering: design and performance, Biotechnol. Bioprocess Eng. 8 (2003) 313–321, https://doi.org/10.1007/BF02949274.
32. J. Doucha, F. Straka, K. Lívanský, Utilization of flue gas for cultivation of microalgae Chlorella sp. in an outdoor open thin-layer photobioreactor, J. Appl. Phycol. 17 (2005) 403–412, https://doi.org/10.1007/s10811005-8701-7.
33. A. Juneja, R.M. Ceballos, G.S. Murthy, Effects of environmental factors and nutrient availability on the biochemical composition of algae for biofuels production: a review, Energies. 6 (2013) 4607–4638, https://doi.org/10.3390/en6094607.
34. D.A. Pereira, V.O. Rodrigues, S.V. Gomez, ´ E.A. Sales, O. Jorquera, Parametric sensitivity analysis for temperature control in outdoor photobioreactors, Bioresour. Technol. 144 (2013) 548–553, https://doi.org/10.1016/J.BIORTECH.2013.07.009.
35. 36. A.P. Carvalho, L.A. Meireles, F.X. Malcata, Microalgal reactors: a review of enclosed system designs and performances, Biotechnol. Prog. 22 (2006) 1490–1506, https://doi.org/10.1021/bp060065r.
36. A.P. Carvalho, L.A. Meireles, F.X. Malcata, Microalgal reactors: a review of enclosed system designs and performances, Biotechnol. Prog. 22 (2006) 1490–1506, https://doi.org/10.1021/bp060065r.
37. M.E. Huntley, Z.I. Johnson, S.L. Brown, D.L. Sills, L. Gerber, I. Archibald, S. C. Machesky, J. Granados, C. Beal, C.H. Greene, Demonstrated large-scale production of marine microalgae for fuels and feed, ALGAL (2015) 24–26, https://doi.org/10.1016/j.algal.2015.04.016.
38. M.E. Iniguez, ˜ J.A. Conesa, A. Fullana, Recyclability of four types of plastics exposed to UV irradiation in a marine environment, Waste Manag. 79 (2018) 339–345, https://doi.org/10.1016/j.wasman.2018.08.006.
39. C. Strümpel, M. McCann, G. Beaucarne, V. Arkhipov, A. Slaoui, V. Svr ˇ ˇcek, C. del Canizo, ˜ I. Tobias, Modifying the solar spectrum to enhance silicon solar cell efficiency-an overview of available materials, Sol. Energy Mater. Sol. Cells 91 (2007) 238–249, https://doi.org/10.1016/j.solmat.2006.09.003.
40. Zuorro, A., Mafei, G., Lavecchia, R., 2016. Optimization of enzyme assisted lipid extraction from Nannochloropsis microalgae. J. Taiwan Inst. Chem. Eng. 67, 106–114. https://doi.org/10.1016/j.jtice.2016.08.016.
41. Zheng, H., Yin, J., Gao, Z., Huang, H., Ji, X., Dou, C., 2011. Disruption of Chlorella vulgaris cells for the release of biodiesel-producing lipids: a comparison of grinding, ultrasonication, bead milling, enzymatic lysis, and microwaves. Appl. Biochem. Biotechnol. 164, 1215–1224.

https://doi.org/10.1007/s12010-011-9207-1.

42. A comprehensive review on cultivation and harvesting of microalgae for biodiesel production: environmental pollution control and future directions. Bioresour. Technol. 301 (1), 1–19, 122804. https://doi.org/10.1016/j.biortech.2020.122804.
43. J. Degen, A. Uebele, A. Retze, U. Schmid-Staiger, W. Trosch, A novel airlift photobioreactor with baffles for improved light utilization through the flashing light effect, J. Biotechnol. 92 (2001) 89–94, https://doi.org/10.1016/S0168-1656(01)00350-9.
44. Z. Yang, J. Cheng, X. Xu, J. Zhou, K. Cen, Enhanced solution velocity between dark and light areas with horizontal tubes and triangular prism baffles to improve microalgal growth in a flat-panel photo-bioreactor, Bioresour. Technol. 211 (2016) 519–526, https://doi.org/10.1016/j.biortech.2016.03.145.
45. I.S. Suh, C.-G. Lee, Photobioreactor engineering: design and performance, Biotechnol. Bioprocess Eng. 8 (2003) 313–321, https://doi.org/10.1007/BF02949274.
46. J. Doucha, F. Straka, K. Lívanský, Utilization of flue gas for cultivation of microalgae Chlorella sp. in an outdoor open thin-layer photobioreactor, J. Appl. Phycol. 17 (2005) 403–412, https://doi.org/10.1007/s10811005-8701-7.
47. A. Juneja, R.M. Ceballos, G.S. Murthy, Effects of environmental factors and nutrient availability on the biochemical composition of algae for biofuels production: a review, Energies. 6 (2013) 4607–4638, https://doi.org/10.3390/en6094607.
48. D.A. Pereira, V.O. Rodrigues, S.V. Gomez, ´ E.A. Sales, O. Jorquera, Parametric sensitivity analysis for temperature control in outdoor photobioreactors, Bioresour. Technol. 144 (2013) 548–553, https://doi.org/10.1016/J.BIORTECH.2013.07.009.
49. H. Zheng, Z. Gao, F. Yin, X. Ji, H. Huang, Effect of CO2 supply conditions on lipid production of Chlorella vulgaris from enzymatic hydrolysates of lipid-extracted microalgal biomass residues, Bioresour. Technol. 126 (2012) 24–30, https://doi.org/10.1016/j.biortech.2012.09.048.
50. M.E. Iniguez, ˜ J.A. Conesa, A. Fullana, Recyclability of four types of plastics exposed to UV irradiation in a marine environment,Waste Manag. 79 (2018) 339–345, https://doi.org/10.1016/j.wasman.2018.08.006.
51. C. Strümpel, M. McCann, G. Beaucarne, V. Arkhipov, A. Slaoui, V. Svr ˇ ˇcek, C. del Canizo, ˜ I. Tobias, Modifying the solar spectrum to enhance silicon solar cell efficiency-an overview of available materials, Sol. Energy Mater. Sol. Cells 91 (2007) 238–249, https://doi.org/10.1016/j.solmat.2006.09.003.
52. Zuorro, A., Mafei, G., Lavecchia, R., 2016. Optimization of enzyme assisted lipid

extraction from Nannochloropsis microalgae. J. Taiwan Inst. Chem. Eng. 67, 106–114. https://doi.org/10.1016/j.jtice.2016.08.016.

53. Zheng, H., Yin, J., Gao, Z., Huang, H., Ji, X., Dou, C., 2011. Disruption of Chlorella vulgaris cells for the release of biodiesel-producing lipids: a comparison of grinding, ultrasonication, bead milling, enzymatic lysis, and microwaves. Appl. Biochem. Biotechnol. 164, 1215–1224. https://doi.org/10.1007/s12010-011-9207-1.
54. A comprehensive review on cultivation and harvesting of microalgae for biodiesel production: environmental pollution control and future directions. Bioresour. Technol. 301 (1), 1–19, 122804. https://doi.org/10.1016/j.biortech.2020.122804.

https://doi.org/10.36375/prepare_u.iiche.a395

Trend analysis of precipitation under climate change scenario

Trina Dutta[a] * (0000-0003-3909-6153), Hirok Chaudhuri[b] (0000-0002-3925-4257)

[a]Department of Chemistry, JIS College of Engineering, Kalyani, Nadia, West Bengal 741235, India.
[b]Department of Physics and Center for Research on Environment and Water, National Institute of Technology Durgapur, West Bengal 713209, India.

**Corresponding author's email ID: trina.d80@gmail.com, Mobile No.:9830531385*

Abstract

The climate change is a natural phenomenon. But it has been hastened by anthropogenic activities. As an obvious consequence, extreme weather events like cyclones, heavy rainfall, and floods have increased. On the contrary, desertification also taking place in other parts of the country. So, disaster management and water management are essential for each part of the country even in the areas not affected still now. This paper analyses the June-July-Aug-Sep (JJAS) rainfall pattern over 117 years (1901-2017) for six meteorological subdivisions in East & North-East India. A rainfall trend with polynomial curve fitting has been shown for individual regions. The descriptive analysis was also done to compare the overall rainfall and variations over the periods.

Keywords: Climate change; JJAS Rainfall; Trend analysis; Descriptive analysis

https://doi.org/10.36375/prepare_u.iiche.a395

Graphical Abstract

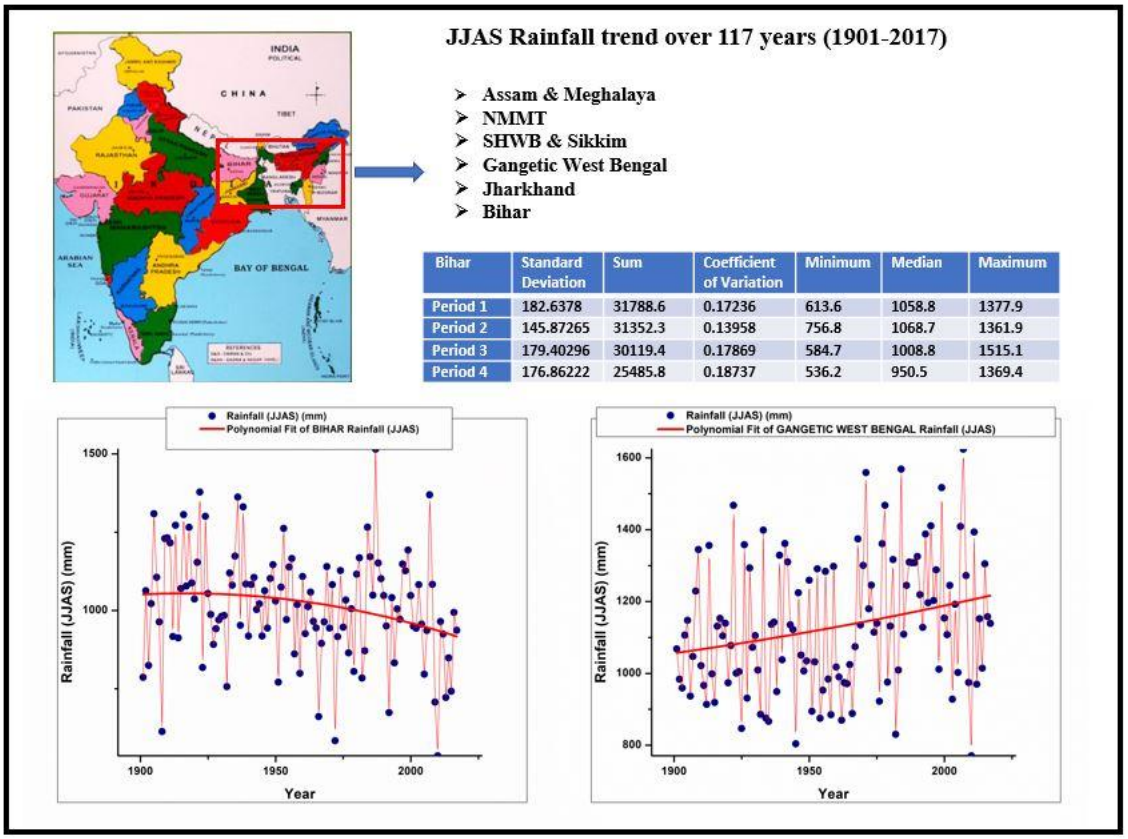

Bihar	Standard Deviation	Sum	Coefficient of Variation	Minimum	Median	Maximum
Period 1	182.6378	31788.6	0.17236	613.6	1058.8	1377.9
Period 2	145.87265	31352.3	0.13958	756.8	1068.7	1361.9
Period 3	179.40296	30119.4	0.17869	584.7	1008.8	1515.1
Period 4	176.86222	25485.8	0.18737	536.2	950.5	1369.4

1. Introduction

In the latest years, large-scale economic loss, lives & property damage took place due to the inconsistent and unpredictable nature of the monsoons. Also, the destruction caused to the farmlands and environment. For example, the economy and life loss in major metro cities like Mumbai, Bangalore, and Chennai happened in 2005 for heavy rainfall (Goswami et al. 2006; Rajeevan et al. 2008). Additionally, the unpredictable nature of rainfall generates food insecurity issues. Thus, the prediction of monsoon rainfall patterns got important in many Asian countries (Reuter et al. 2013).

Not only that, the non-uniform variation in rainfall, is also a major concern of recent decades. Even the variation is not dependent on Latitude-longitude. Such as whether most of the locations in Gujrat (11 from 16) getting increased Summer Monsoon Rainfall (SMR), the Jharkhand getting decreased rainfall although it is in the same latitude.

Furthermore, the monsoon core zone is currently showing a decreasing trend in SMR rainfall (Kulkarni 2012; Guhathakurta et al. 2015). Northeast India, popular for homogeneous and huge rainfall, also experienced a notable rainfall reduction after 1950 (Guhathakurta et al. 2015). The “dry becomes drier and wet becomes wetter” paradigm is not universal. Rather the High Rainfall Zone (HRZ) experiencing less rainfall and Low Rainfall Zone (LRZ) experiencing higher rainfall (Barde et al. 2021a). The Indian Monsoon Sparse Zone (IMSZ) is showing a Counter-clockwise epochal shift (Barde et al. 2021b).

In this regard, the rainfall trend analysis is very important to predict flood-prone or drought-prone areas which can reduce agricultural loss,

https://doi.org/10.36375/prepare_u.iiche.a395

water stress, and economic loss as well. This paper observed the Indian summer monsoon (ISM) which is highly crucial for India as a larger part of employment is agriculture based (Gadgil et al. 2019; Ministry of Finance 2018). Generally, the duration of monsoon in India is from June to September (Wang et al. 2006). Even a small variation in the amount and timing of rainfall brings a significant impact on agricultural productivity and the economy as well.

In this study, the researchers observed the century-long trend (1901-2017) for six meteorological subdivisions in East & North-East India. The regions are Assam & Meghalaya; Nagaland Manipur Mizoram and Tripura (NMMT); Sub Himalayan West Bengal (SHWB) & Sikkim; Gangetic West Bengal; Jharkhand and Bihar respectively. From the descriptive statistics the Mean; Median; Standard Deviation; Maximum; Minimum; Coefficient of Variation were also analyzed to understand changing patterns properly. This is highly essential to take preventive measures for extreme weather events.

2. Data & Methodology

In this study the rainfall data considered from 1901 to 2017. The kharif, the monsoon crop of India requires a lot of water along with hot and humid weather. In this study the investigators considered Monsoon season, June-July-August-September (JJAS) for east and North-east India. The study includes six stations Assam & Meghalaya; Madhya Maharashtra; Sub Himalayan West Bengal & Sikkim; Gangetic West Bengal; Jharkhand and Bihar. The data was collected from Open Government Data (OGD) Platform India (OGD 2021).

Starting from year 1901, JJAS rainfall data in mm unit considered for 117 years. The polynomial curve fitting done for individual zone. The duration 1901-1930, 1931-1960, 1961-1990 and 1991-2017 represented as period 1; period 2; period 3; and period 4 respectively. For each zone, mean, median, maximum, minimum, sum, Standard Deviation (SD), and Coefficient of Variation (CV) have been calculated for the individual period.

3. Results and Discussions

Assam & Meghalaya:

In case of Assam & Meghalaya, overall rainfall trend is slightly decreasing, shown in Fig. 1. The overall JJAS rainfall gradually decreased from period 1 to period 4, as sum decreased from 52909.6 mm to 44172.8 mm [table 1]. Highest Maximum rainfall and highest minimum rainfall both observed highest in period 1 respectively 2442.5 mm and 2169 mm. The average deviation from the mean value is lowest in period 2 (147.70323) and Coefficient of Variation is close to zero (0.08524).

Nagaland Manipur Mizoram and Tripura (NMMT):

In case of NMMT the JJAS rainfall has a decreasing trend over the years as shown in Fig.2. The overall rainfall decreases gradually from 49572.7 mm to 37661.4 mm. The lowest value for mean, median, minimum, maximum observed in period 4. Rainfall variation increasing and notable rainfall fluctuations observed during period 3 [table 2].

Sub Himalayan West Bengal & Sikkim (SHWB & Sikkim):

In case of Sub Himalayan West Bengal & Sikkim (SHWB & SIKKIM) the JJAS rainfall has a decreasing trend over the years (Figure 3). The sum of rainfall is maximum in period 1 (64989.8 mm) and minimum in period 4 (54432.7 mm) as shown in table 3. Average deviation from the mean value over the periods varies up to around 331 mm. The highest rainfall variation takes place in period 4 as the coefficient of variation observed highest (0.16419) in this duration.

Gangetic West Bengal:

In the case of Gangetic West Bengal JJAS rainfall has an increasing trend over the years, shown in Figure 4. Although the overall rainfall

https://doi.org/10.36375/prepare_u.iiche.a395

was reduced in period 4, but the mean, median, and maximum rainfall was observed highest in period 4. Maximum rainfall fluctuation was observed in period 3 [Table 4].

Jharkhand:

In case of Jharkhand the JJAS rainfall has a decreasing trend as observed in figure 5. Overall rainfall is decreasing gradually from 33809.4 mm to 27796.3 mm. Additionally the rainfall fluctuations observed highest for period 4. That creates problems for overall management in all sectors including agriculture [table 5].

Bihar:

In case of Bihar the JJAS rainfall showing a decreasing trend over the periods as shown in fig. 6. Overall rainfall decreasing gradually over the periods from 31788.6 mm to 25485.8 mm. The mean, minimum, median, maximum observed lowest for period 4. Moreover, the highest rainfall fluctuations observed in 4th period which requires shift in planning in all sectors including agriculture [table 6].

Table 1. Descriptive Statistics of Assam & Meghalaya from 1901-2017

Period	N total	Mean	Standard Deviation	Sum	Coefficient of Variation	Minimum	Median	Maximum
Period 1	30	1763.65333	206.33952	52909.6	0.117	1465	1714.9	2442.5
Period 2	30	1732.82333	147.70323	51984.7	0.08524	1424.6	1705.65	2001
Period 3	30	1728.91333	73.63629	51867.4	0.15827	1261.7	1693.7	2356.3
Period 4	30	1636.02963	254.01362	44172.8	0.15526	1172.9	1683.9	2169

https://doi.org/10.36375/prepare_u.iiche.a395

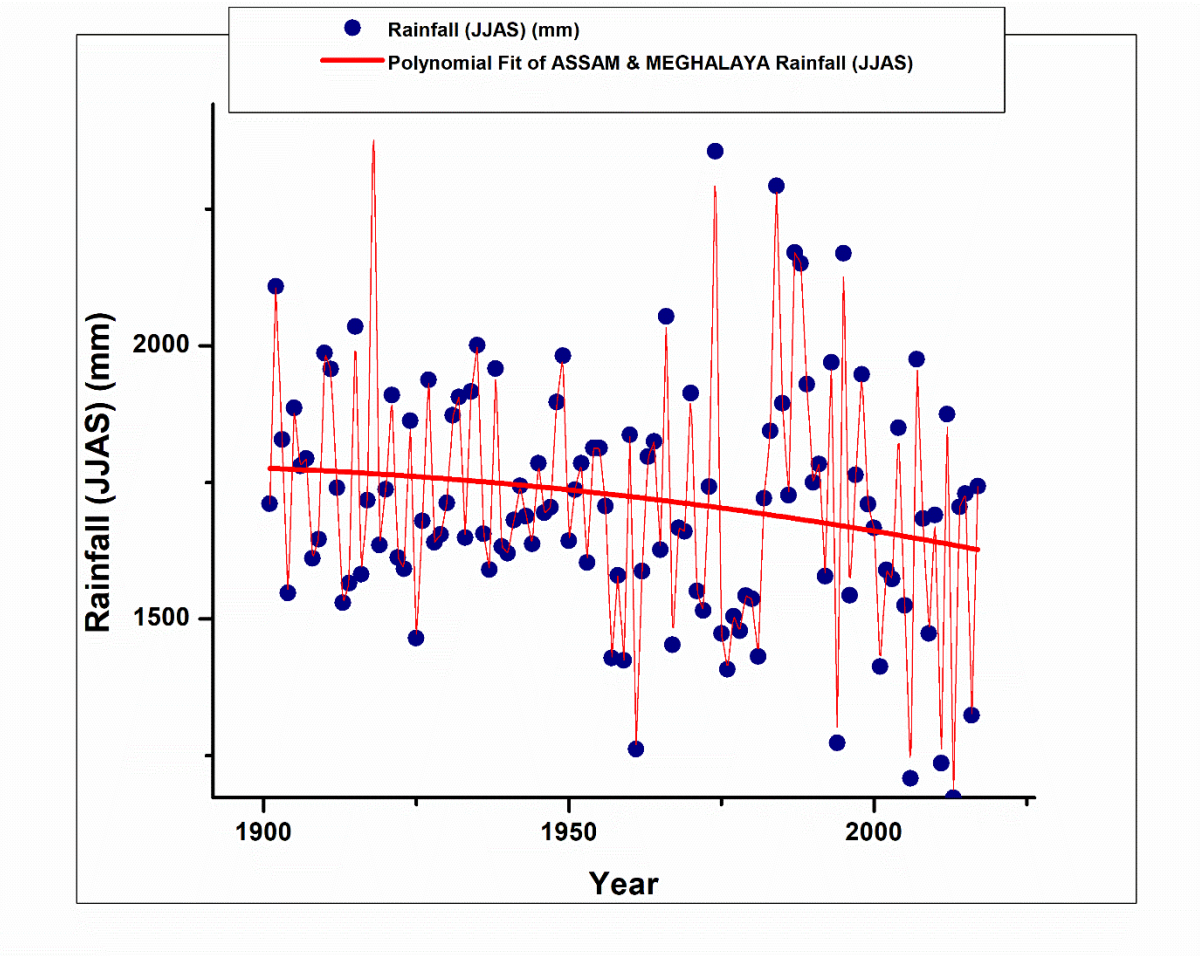

Figure 1: JJAS rainfall in mm for Assam & Meghalaya from 1901-2017

Table 2: Descriptive Statistics of NMMT from 1901-2017

Period	N total	Mean	Standard Deviation	Sum	Coefficient of Variation	Minimum	Median	Maximum
Period 1	30	1652.42333	162.34117	49572.7	0.09824	1394.9	1598.7	2145.5
Period 2	30	1786.65333	236.71944	53599.6	0.13249	1119	1810.9	2271.1
Period 3	30	1578.94667	453.22196	47368.4	0.28704	898.7	1415.05	3050.2
Period 4	30	1394.86667	208.26415	37661.4	0.14931	995.2	1367.9	1829.8

https://doi.org/10.36375/prepare_u.iiche.a395

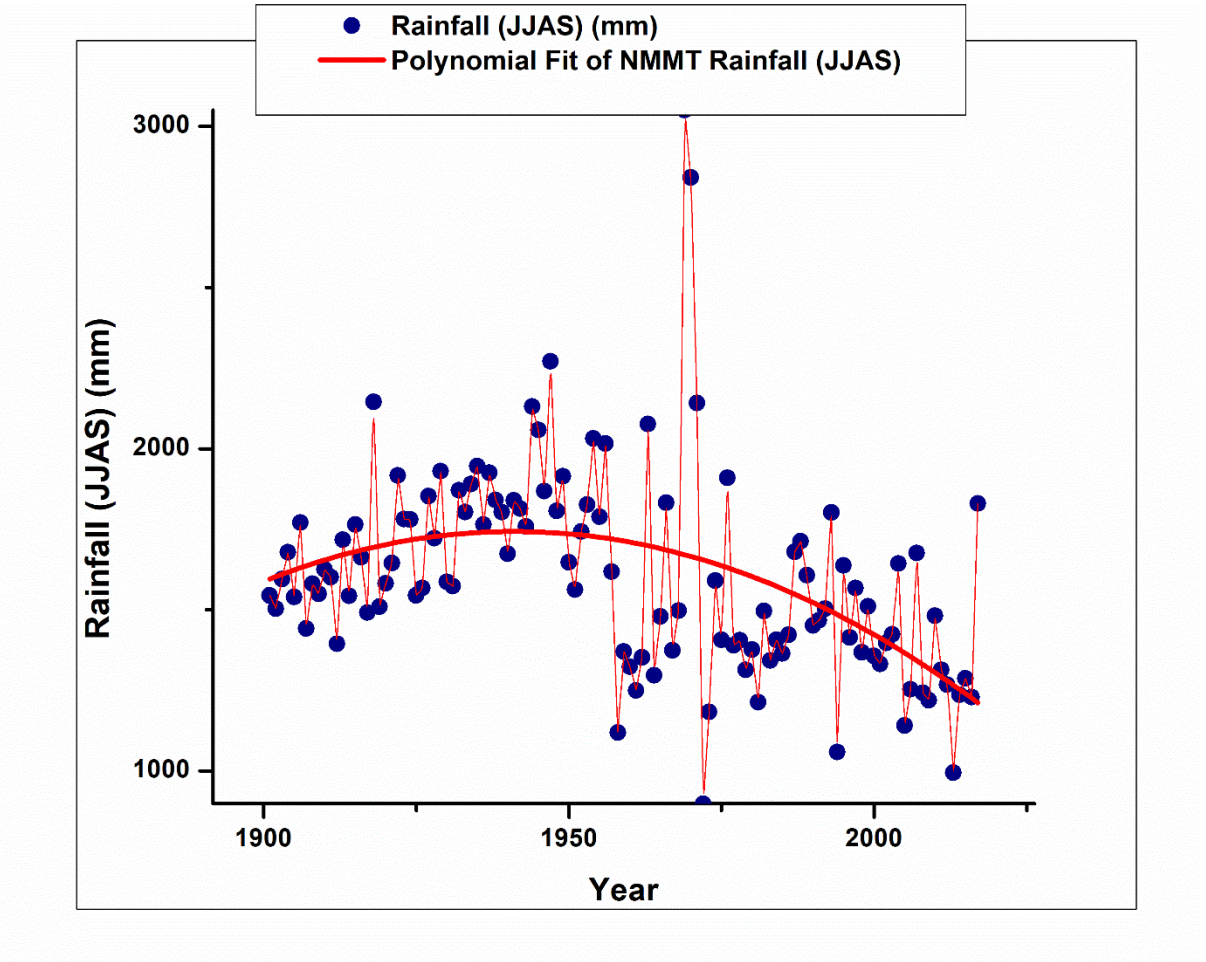

Figure 2: JJAS rainfall in mm for NMMT from 1901-2017

Table 3: Descriptive Statistics of SHWB & Sikkim from 1901-2017

Period	N total	Mean	Standard Deviation	Sum	Coefficient of Variation	Minimum	Median	Maximum
Period 1	30	2166.32667	320.71873	64989.8	0.14805	1503.7	2173.25	2756.6
Period 2	30	2140.05	232.26804	64201.5	0.10853	1734.2	2092.1	2596.9
Period 3	30	2165.51333	279.81689	64965.4	0.12922	1711.1	2144.2	2726
Period 4	30	2016.02593	331.01083	54432.7	0.16419	1443.6	1980.1	2846.8

https://doi.org/10.36375/prepare_u.iiche.a395

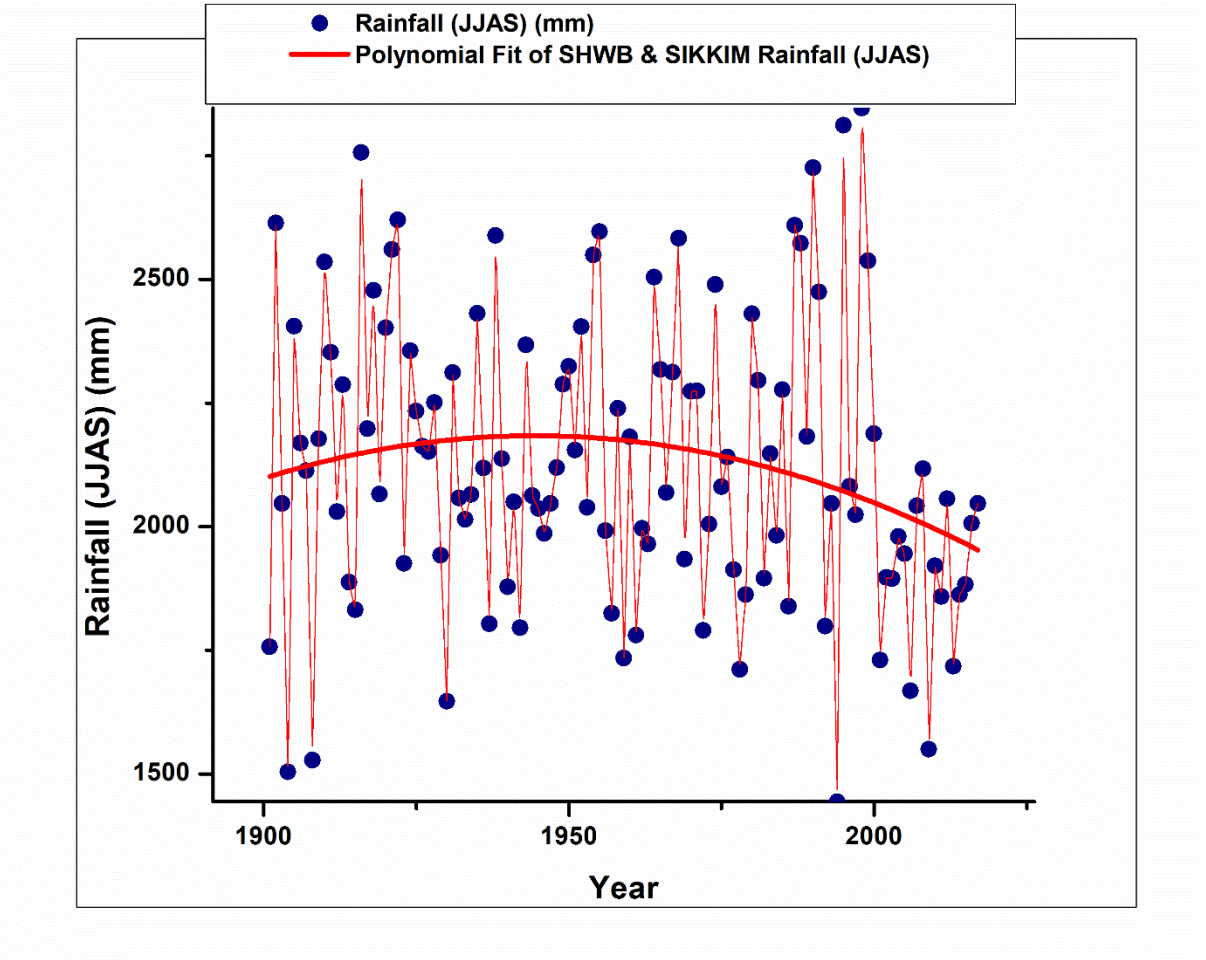

Figure 3: JJAS rainfall in mm for SHWB & Sikkim from 1901-2017

Table 4: Descriptive Statistics of Gangetic West Bengal from 1901-2017

Period	N total	Mean	Standard Deviation	Sum	Coefficient of Variation	Minimum	Median	Maximum
Period 1	30	1088.72	153.0395	32661.6	0.14057	847	1070.15	1467.7
Period 2	30	1081.86333	173.50835	32455.9	0.16038	804.3	1036.45	1398.9
Period 3	30	1167.68667	200.78115	35030.6	0.17195	830.4	1136.9	1568.4
Period 4	30	1191.63704	192.18705	32174.2	0.16128	770.7	1192.3	1624.2

https://doi.org/10.36375/prepare_u.iiche.a395

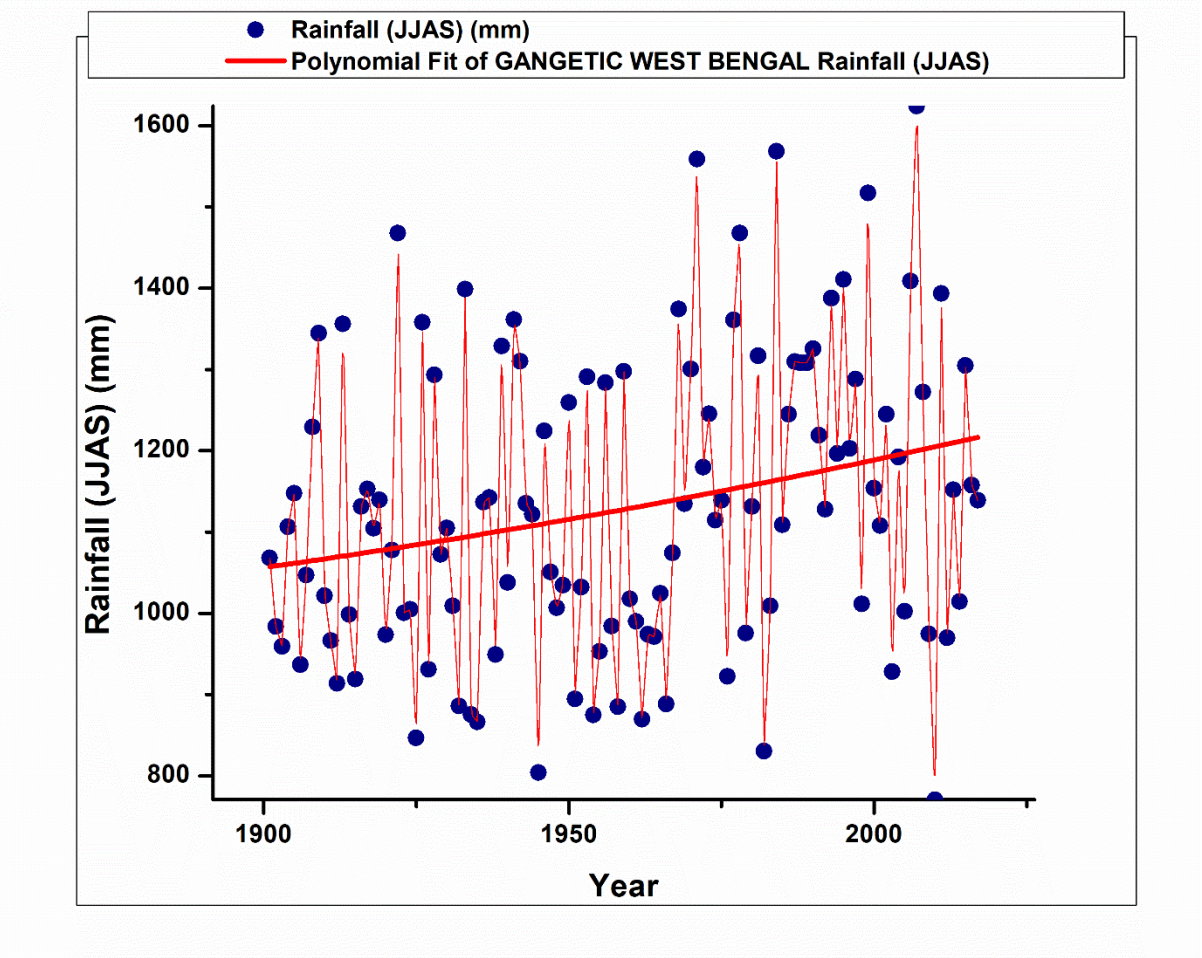

Figure 4: JJAS rainfall in mm for Gangetic West Bengal from 1901-2017

Table 5: Descriptive Statistics of Jharkhand from 1901-2017

Period	N total	Mean	Standard Deviation	Sum	Coefficient of Variation	Minimum	Median	Maximum
Period 1	30	1126.98	137.75901	33809.4	0.12224	819.3	1119.5	1325.9
Period 2	30	1126.16	143.05744	33784.8	0.12703	880.7	1129.7	1412.3
Period 3	30	1047.44667	176.61591	31423.4	0.16862	724.3	1008.05	1539
Period 4	30	1029.49259	191.47207	27796.3	0.18599	578.4	1031.5	1366.3

https://doi.org/10.36375/prepare_u.iiche.a395

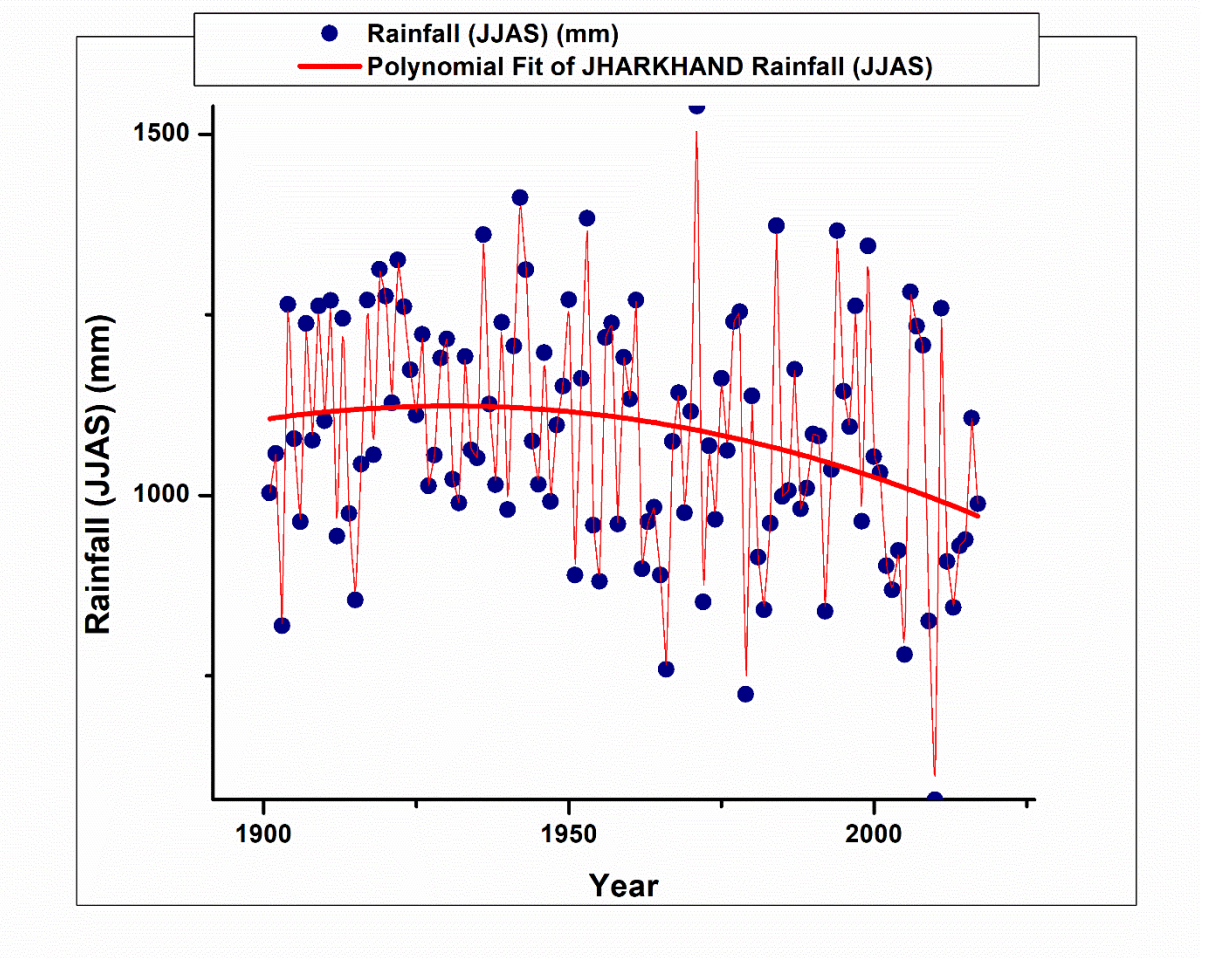

Figure 5: JJAS rainfall in mm for Jharkhand from 1901-2017

Table 6: Descriptive Statistic of Bihar from 1901-2017

Period	N total	Mean	Standard Deviation	Sum	Coefficient of Variation	Minimum	Median	Maximum
Period 1	30	1059.62	182.6378	31788.6	0.17236	613.6	1058.8	1377.9
Period 2	30	1045.07667	145.87265	31352.3	0.13958	756.8	1068.7	1361.9
Period 3	30	1003.98	179.40296	30119.4	0.17869	584.7	1008.8	1515.1
Period 4	30	943.91852	176.86222	25485.8	0.18737	536.2	950.5	1369.4

https://doi.org/10.36375/prepare_u.iiche.a395

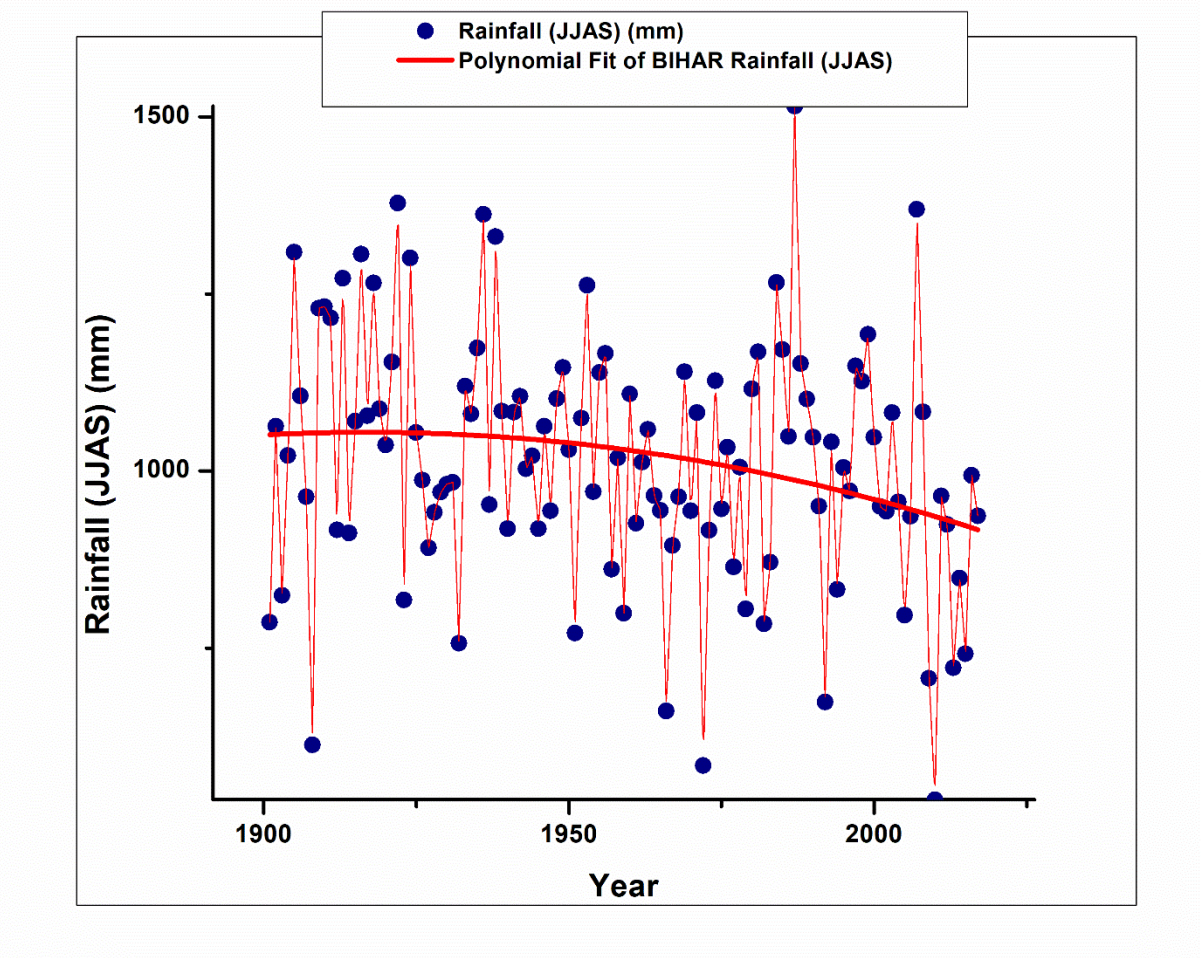

Figure 6: JJAS rainfall in mm for Bihar from 1901-2017

4. Conclusion

In this study the JJAS rainfall trend studied for six meteorological subdivisions of East and North-East India over 117 years (1901-2017). The regions are Assam & Meghalaya, NMMT, Sub Himalayan West Bengal (SHWB) & Sikkim; Gangetic West Bengal; Jharkhand & Bihar respectively. Among these six regions rainfall trend decreases except Gangetic West Bengal. It is not a matter about either increasing or decreasing. It is all about variations and unpredictability. Even a small variation affect agriculture a lot especially the SMR is highly important for Kharip crops. As observed here the Coefficient of Variation (CV) increasing during period 3 and period 4. Only the low CV observed during period 2 for Assam & Meghalaya; period 1 for NMMT; very high CV observed in case of Gangetic West Bengal and Jharkhand. The highest CV was observed for Bihar which is a major concern. So, water management needs to be increased systematically for socio-economic well-being.

Acknowledgments

Thankful to Dr. Palash Sinha, Scientist, School of Earth, Ocean and Climate Sciences, IIT, Bhubaneswar. Also thankful to JIS College of

Engineering, Kalyani, and National Institute of Technology Durgapur for their support.

References

Barde, V., Sinha, P., Mohanty, U. C., & Panda, R. K. (2021a). Reversal nature in rainfall pattern over the Indian heavy and low rainfall zones in the recent era. Theoretical and Applied Climatology, 146, 365-379. https://doi.org/10.21203/rs.3.rs-298721/v1

Barde, V., Sinha, P., Mohanty, U. C., Zhang, X., & Niyogi, D. (2021b). Counter-clockwise epochal shift of the Indian Monsoon Sparse Zone. Atmospheric Research, 263, 105806. https://doi.org/10.1016/j.atmosres.2021.105806

Gadgil, S., Francis, P. A., & Vinayachandran, P. N. (2019). Summer monsoon of 2019. Current Science, 117(5), 783-793.

Goswami, B. N., Venugopal, V., Sengupta, D., Madhusoodanan, M. S., & Xavier, P. K. (2006). Increasing trend of extreme rain events over India in a warming environment. Science, 314(5804), 1442-1445.

Guhathakurta, P., Rajeevan, M., Sikka, D. R., & Tyagi, A. (2015). Observed changes in southwest monsoon rainfall over India during 1901–2011. International Journal of Climatology, 35(8), 1881-1898.

Kulkarni, A. (2012). Weakening of Indian summer monsoon rainfall in warming environment. Theoretical and Applied Climatology, 109, 447-459.

Ministry of Finance, Government of India (2018) Climate change and Agriculture in Economic Survey 2017-2018, chapter 6, 82–101. Government of India. URL http://mofapp.nic.in:8080/economicsurvey/pdf/082-101 Chapter 06 ENGLISH Vol 01 2017-18.pdf.

Open Government Data (OGD) Platform India (https://data.gov.in/)

Rajeevan, M., Bhate, J., & Jaswal, A. K. (2008). Analysis of variability and trends of extreme rainfall events over India using 104 years of gridded daily rainfall data. Geophysical research letters, 35(18).

Reuter, M., Kern, A. K., Harzhauser, M., Kroh, A., & Piller, W. E. (2013). Global warming and South Indian monsoon rainfall—lessons from the Mid-Miocene. Gondwana Research, 23(3), 1172-1177. http://dx.doi.org/10.1016/j.gr.2012.07.015

Wang, B., Ding, Y., & Sikka, D. R. (2006). Synoptic systems and weather. The asian monsoon, 131-201.

https://doi.org/10.36375/prepare_u.iiche.a396

Carbon Footprint Reduction from Construction Industry: A Review

Sohel Baidya[1*]

[1*]*Department of Chemical Engineering, Calcutta Institute of Technology,*

Howrah-711316, India

**Contact number: 033 2661 0736, Email: sohelbaidya22@gmail.com*

Abstract

The building sector is one of the largest contributors to greenhouse gas emission in urban areas. Quantitative assessment of the carbon footprint of urban buildings is needed for advance research and policy debates on building carbon emission reduction and sustainable architectural planning. Businesses are now attempting to reduce their negative effects on the environment by incorporating environmental considerations into their supply chain processes. The review emphasizes the significance of optimizing construction processes to minimize energy consumption and waste generation. The use of low-carbon materials such as recycled and locally sourced materials, as well as the implementation of energy-efficient designs, can significantly reduce carbon emissions. Additionally, the incorporation of renewable energy sources, such as solar and wind power, can further minimize the environmental impact. With a variety of problems faced by designers and planners, the practices taken to reduce carbon footprints are very diverse. As global concerns about environmental sustainability grow, there is an urgent need to reduce the carbon footprint associated with construction activities. This review explores various strategies and technologies that have been employed to mitigate carbon emissions throughout the construction lifecycle. By adopting sustainable practices and technologies, the construction industries can play a vital role in carbon footprint reduction.

Keywords: Greenhouse gases; Carbon footprint; Construction Lifecycle; Supply Chain Operations; Low-carbon materials.

1. Introduction

https://doi.org/10.36375/prepare_u.iiche.a396

The global construction sector plays a pivotal role in shaping society's infrastructure and buildings but is accompanied by a significant environmental impact, consuming substantial amounts of non-renewable energy and contributing to elevated carbon dioxide (CO_2) emissions [1]. Increased greenhouse gas emissions in the industrial age, caused primarily by human activities, pose a serious threat to the global environment Due to the use of fossil fuels and desertification increased, these emissions, especially carbon dioxide (CO_2), contribute to climate change. As CO_2 levels rise, broader environmental risks, agricultural instability, and potential public health challenges intensify [2]. The relentless growth in worldwide average atmospheric temperature, attributed to human-driven emissions of heat-trapping greenhouse gases, has resulted inside the pervasive phenomenon of global warming. Urbanization, a key contributor to this anthropogenic affect, has appreciably propelled CO_2 emissions inside the constructing quarter. As a vital aspect of economic and social improvement, the constructing region, spanning creation to operation, has emerged as a major environmental problem, accounting for a tremendous component of global CO_2 emissions [3]. This paper gives an assessment of the challenges, environmental affects, and mitigation strategies critical for curbing CO_2 emissions inside the dynamic realm of urban improvement and construction.

2. Literature Review

Globally, construction and building operations contribute significantly to environmental issues, responsible for 33% of greenhouse gas (GHG) emissions and 40% of global energy consumption. The increasing urban population is expected to fuel future construction, intensifying GHG emissions. Policies like building codes can effectively reduce emissions, but criticisms include complexity and lack of flexibility. Alternatively, a carbon tax, with lower administrative costs, appeals to stakeholders for its simplicity. However, setting an appropriate tax rate is challenging, and public opposition may hinder its effectiveness [4]. The sustainable advancement of the building sector faces a critical challenge with the substantial carbon dioxide (CO_2) emissions from non-sustainable energy sources during planning, construction, and operations. The reliance on fossil fuels, constituting 40% of global greenhouse gas emissions in

construction, overshadows the 6% contribution from renewable energy sources. Efforts to reduce the CO_2 footprint in high-density urban areas remain insufficient. Indirect CO_2 emissions from electricity use dominate, accounting for 85% globally, while direct emissions constitute 14%. Meeting the 2030 Climate and Energy Framework goals necessitates addressing low productivity and efficiency through detailed evaluations of construction and operation processes across the building's life cycle [3]. This escalating emission of greenhouse gases, particularly carbon dioxide (CO_2), surpasses agreed-upon safe levels, posing severe threats such as disruptive weather disasters, agricultural instability, and public health challenges. The concept of a carbon footprint, originating in the 1990s, measures the cumulative greenhouse gas emissions, expressed in tons of CO_2 equivalents per year, produced by individuals, companies, or activities. Greenhouse gases, encompassing various compounds, including CO_2 and methane, stem from diverse processes like fossil fuel combustion, manufacturing, land-use practices, and transportation, with associated pollutants impacting living organisms [5].

3. Carbon Emissions in Construction Industry

The global construction sector contributes 5.5% of total CO_2 emissions, with 99.5% of its direct energy use derived from fossil fuels, mainly for on-site construction operations. Improving energy efficiency and optimizing construction machine operations offer significant potential for reducing direct carbon emissions. Indirect carbon emissions, dominated by non-renewable energy resources (85%) and non-energy use (14%), highlight the importance of addressing materials in the construction sector. Imported inputs, especially from higher carbon-intensity countries, contribute to carbon embodied in domestic construction. Strategies to mitigate carbon emissions include enhancing energy efficiency, adopting a renewable energy mix, and encouraging innovation, particularly in emerging economies like China, which plays a crucial role in the global construction sector's carbon mitigation efforts. Cement production, a major source of non-energy use CO_2 emissions, requires strategies like energy saving, carbon separation, and carbon capture and storage for decarbonization. Policy development is essential to overcome barriers

and challenges, especially economic factors and legislation, in implementing carbon capture and storage solutions [1]. Despite proposed innovative methods for mitigating carbon footprints, especially in dense urban areas, the issue persists. A critical factor is the direct correlation between non-sustainable energy use and environmental impact, with construction activities emitting CO_2 both directly and indirectly. Addressing this challenge involves meticulous evaluation and optimization of construction and operation processes throughout a building's life cycle, aiming to enhance productivity and efficiency while aligning with global sustainability targets [3]. Managing carbon emissions is crucial across various stages of a building's life cycle. The product stage involves upstream emissions from raw material extraction, manufacturing, and transportation. Building lifespan significantly impacts embodied emissions, with longer lifespans correlating to lower emissions. Material nature, such as cement and steel, plays a pivotal role, with virtual and physical carbon considerations. The choice of energy in manufacturing also influences embodied emissions. Construction stages involve emissions from material transportation and on-site activities, with fossil fuel use being a primary contributor. The operational phase contributes the majority of CO_2 emissions, influenced by factors like energy source and user behavior. Additionally, end-use and demolition phases have minimal green-house gas contributions, with recycling presenting a potential for further emission reduction [6].

4. Technological Innovations and Sustainable Practices

Carbon footprint management is a critical process aimed at mitigating the environmental impact of human activities, particularly in the construction industry. Many countries have implemented strategic policies to reduce carbon emissions and energy consumption. Green building practices, such as sustainable construction and the use of eco-friendly materials, are key strategies for achieving emission reduction targets. Various rating systems, like LEED and BREEAM, play a crucial role in setting standards and promoting sustainable building efficiencies globally. The construction sector's significant contribution to greenhouse gas emissions underscores the need for innovative solutions. Utilizing low-carbon cement, recyclable materials, and

implementing efficient waste management practices are highlighted as effective strategies. Furthermore, reducing transportation-related emissions, optimizing energy usage, and incorporating green land conservation practices contribute to a more sustainable construction industry. Despite efforts in developed countries, there's a slower adoption of green building concepts in developing nations, emphasizing the importance of global collaboration in advancing technological innovations and sustainable practices for a greener future [5]. Technological innovation plays an important role in reducing the environmental impact of the construction industry on the environment in pursuit of sustainable construction practices One prominent approach is to incorporate or replace traditional clinker materials for cement production, reducing energy consumption and CO_2 emissions, and new clinker chemistry offers an environmentally friendly alternative than conventional Portland cement. By incorporating additives such as fly ash and silica fume, lightweight concrete not only improves the quality of buildings but also contributes to a significant reduction in CO_2 emissions Furthermore, materials a reused-materials, such as recycled asphalt pavement and recycled concrete aggregates promote sustainable development in construction. The adoption of energy-efficient technologies, like fluidized bed kilns and oxy-fuel technologies, demonstrates a commitment to lowering energy consumption and emissions in cement production. Moreover, innovations in building materials, such as magnesium oxide as an alternative to calcium-based binders in clay bricks, contribute to lower carbon footprints. The focus extends beyond the construction phase, emphasizing the importance of efficient building operations through energy-efficient HVAC systems, water-saving technologies, and renewable energy integration. The construction project aims to create a resilient and environmentally friendly built environment while recognizing these sustainable practices and technological advancements [4].

5. Conclusion

In conclusion, this review paper explores the critical concept of reducing carbon footprints within the construction industry. It gives a brief evaluation of various strategies for promoting sustainable improvement. The construction sector, acknowledged for its great

contribution to worldwide carbon emissions, is at a crossroads that demands transformative measures. The paper highlights key techniques which include the use of green materials, modern construction techniques, and the inclusion of renewable energy sources as possible pathways to scale down carbon footprints. Additionally, it underscores the significance of adopting life cycle tests to gauge the general environmental effects. The review emphasizes the need for collaborative efforts among policymakers, industry professionals, and stakeholders to strengthen sustainable practices. The potential blessings amplify past environmental conservation, encompassing economic viability, public health, and societal well-being. Embracing sustainable practices is portrayed not simply as an ethical preference however as a crucial step toward carbon footprint reduction and environmentally responsible future within the ever-evolving creation landscape.

Acknowledgments

The author would like to acknowledge the help and support of Department of Chemical Engineering of Calcutta Institute of Technology. I have not used any financial support from anywhere although I am thankful to our Respected Director Academics for his constant encouragements throughout the project.

Statements & Declarations

Funding

"The author declares that no funds, grants, or other support were received during the preparation of this manuscript."

Competing Interests

"The author has no relevant financial or non-financial interests to disclose."

Author Contributions

"All authors contributed to perform the literature survey and to find the appropriate research gap for the present review study and literature survey was performed by [Sohel Baidya]. The first draft of the manuscript was written by [Sohel Baidya] and all authors commented on previous versions of the manuscript. All authors read and approved the final manuscript."

References

1. Huang, L., Krigsvoll, G., Johansen F., Liu, Y., Zhang, X., (2017). Carbon emission of global construction sector. *Renewable and Sustainable Energy Reviews (2017).* http://dx.doi.org/10.1016/j.rser.2017.06.001.

2. Labaran, YH., Mathur, VS., Farouq, MM., (2021). The carbon footprint of construction industry: A review of direct and indirect emission. *Journal of Sustainable Construction Materials and Technologies. 6. 101-115.* http://dx.doi.org/10.29187/jscmt.2021.66.
3. Ahmed, Ali, K., Ahmad, MI., Yusup, Y., (2020). Issues, Impacts, and Mitigations of Carbon Dioxide Emissions in the Building Sector. *Sustainability, 12, 7427.* https://doi.org/10.3390/su12187427.
4. Sizirici, B., Fseha, Y., Cho, C.-S., Yildiz, I., Byon, Y.-J., (2021). A Review of Carbon Footprint Reduction in Construction Industry, from Design to Operation. *Materials, 14, 6094.* https://doi.org/10.3390/ma14206094.
5. Labaran, YH., Mathur, VS., Muhammad, SU., Musa, AA., (2022). Carbon footprint management: A review of construction industry. *Cleaner Engineering and Technology, Volume 9, 100531, ISSN 2666-7908.* https://doi.org/10.1016/j.clet.2022.100531.
6. Fenner, AE., Kibert, CJ., Woo, J., Morque, S., Razkenari, M., Hakim, H., Lu, X., (2018). The carbon footprint of buildings: A review of methodologies and applications. *Renewable and Sustainable Energy Reviews, Volume 94, Pages 1142-1152, ISSN 1364-0321.* https://doi.org/10.1016/j.rser.2018.07.012.

https://doi.org/10.36375/prepare_u.iiche.a397

An Efficient method to produce Green Hydrogen by Electrolysis Method

Aryan Saha[a], Diya Mukherjee[a], Avijit Ghosh[a]

[a]*Heritage Institute of Technology, Anadapur, Kolkata 700107, India*

Abstract

Green hydrogen is called the fuel of the future as it has the ability to power the hard to electrify sectors like industries, transportation and building contributing around 65% of yearly greenhouse gas emission. The process by which Green Hydrogen is produced is called Water Electrolysis. The technique involves "breaking" of the water molecules using electricity in an electrolyser to extract the dihydrogen (H2). The electricity used must be carbon-free to consider the hydrogen produced as green. Green hydrogen is a clean energy source that emits only water vapor and leaves behind no residue in the air, like coal and oil. The produced hydrogen is ready for use in direct applications like transport and steel production and in direct power applications like fuels, fertilizers and is a great replacement for natural gas. India is well positioned to be a major green hydrogen production center considering the ample amount and the low-cost of the renewable resources that would allow for some of the lowest green hydrogen prices in the world.

Keywords: Green hydrogen; electrolysis; renewable; dihydrogen; electricity; electrolyser

1. Introduction

In the early decades of the 21st century, the world finds itself at a crossroad, where the confluence of escalating climate concerns and the escalating demands for energy drives us to explore innovative, sustainable solutions. Traditional fossil fuels, the lifeblood of our industrialized societies continue to deplete and the consequences of greenhouse gas emissions become increasingly apparent, the need for innovative and sustainable energy solutions has never been more pressing. In this transformative moment, Green hydrogen, often referred to as "the fuel of the future," a versatile and promising energy carrier, has emerged as a frontrunner in the pursuit of a cleaner and more sustainable energy future. We delve deeply into the enigmatic realm of electrolysis, unravelling its inner workings that may drive green hydrogen toward economic viability and scalable implementation. In an epoch defined by the necessity to confront climate change, green hydrogen shines as a symbol of innovation and a cornerstone of a sustainable future. Moreover, we survey the landscape of its applications, from fuelling zero-emission transportation to forming the linchpin of integrated energy ecosystems in a world that increasingly values environmental stewardship.

Nevertheless, the voyage of green hydrogen is not without its share of challenges and opportunities. This paper thoroughly investigates the economic facets, assessing the investment requirements for a hydrogen-based future, the cost dynamics of renewable energy integration, and the policy frameworks required to facilitate this transformation. Concurrently, we delve into the manifold environmental dividends of green hydrogen, from its role in mitigating

greenhouse gas emissions to its potential to enhance global energy security.

Our aim for this research has been to produce Green Hydrogen through the electrolysis of water which splits water molecules into hydrogen and oxygen using renewable energy sources, creating a clean energy carrier with a multitude of applications. It holds the potential to revolutionize the global energy landscape. This versatile energy vector not only serves as a means to store and transport renewable energy but also provides a clean alternative for sectors traditionally reliant on fossil fuels, such as heavy industry, transportation, and energy storage. Its role in reducing greenhouse gas emissions and mitigating climate change cannot be overstated.

This research paper seeks to explore the multifaceted realm of green hydrogen, delving into its production technologies, applications, economic viability, and environmental benefits. Through a comprehensive examination of the current state of green hydrogen research, this paper aims to shed light on the opportunities and challenges that lie ahead. By understanding the science and engineering behind green hydrogen production, assessing its potential applications, and evaluating its economic feasibility, we can better appreciate its role in a sustainable, low-carbon future**.**

In a world increasingly beset by the consequences of unchecked carbon emissions, green hydrogen is more than a novel concept; it is a pivotal catalyst for change.

2. Methods to produce Green Hydrogen:

Green hydrogen is hydrogen produced through a process that generates little to no greenhouse gas emissions. It is considered a key element in the transition to a sustainable energy future. Various methods for green hydrogen production are being researched and developed. Here is an in-depth overview of some of the most prominent methods for green hydrogen production:

***i. Water Electrolysis*:** Electrolysis is the most widely used and accepted method for producing green hydrogen. In this process, water with the help of electricity is split into hydrogen and oxygen. There are three main types: alkaline electrolysis, solid oxide electrolysis and proton exchange membrane (PEM) electrolysis.

***ii. Alkaline Electrolysis*:** Alkaline electrolysis uses an alkaline electrolyte solution, often potassium hydroxide (KOH), to facilitate the electrolysis process. It operates at a higher temperature than PEM electrolysis, typically around 70-100°C. Alkaline electrolyzers are known for their durability, and they have been used in industrial applications for decades. They are often chosen for their ability to produce large quantities of hydrogen.

***iii. Solid Oxide Electrolysis*:** Solid oxide electrolysis operates at much higher temperatures, typically above 800°C. These high temperatures enable faster reaction kinetics and higher efficiency. Solid oxide electrolyzers are particularly well-suited for integration with high-temperature heat sources, such as concentrated solar power or advanced nuclear reactors. This technology is efficient but also more complex and typically requires specialized materials.

***iv. Proton Exchange Membrane (PEM) Electrolysis*:** In PEM electrolysis, a solid

https://doi.org/10.36375/prepare_u.iiche.a397

polymer electrolyte membrane, often made of a perfluoro sulfonic acid polymer, separates the anode and cathode compartments. The membrane allows the transport of protons (H+ ions) while preventing the crossover of gases. This method operates at relatively low temperatures (typically between 50-80°C), which reduces energy consumption, and is well-suited for smaller-scale applications. PEM electrolyzers are valued for their rapid response time and
ability to adjust to variable loads, making them suitable for applications where responsiveness is critical.

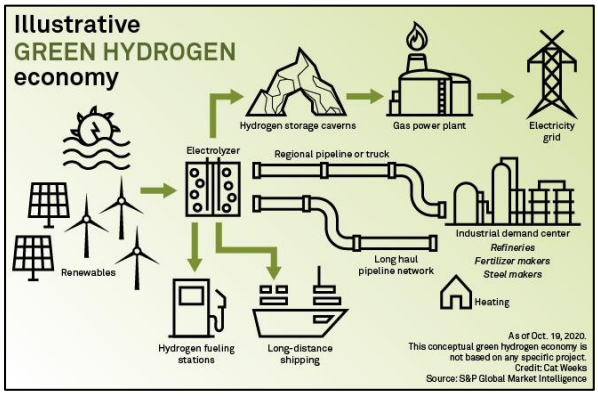

Figure 1: Green hydrogen economy illustration

3. Materials used:

i. 2 Carbon rods (Electrodes)
ii. Beaker
iii. Demarcated test tubes
iv. Power supply source
v. R.O. Water
vi. 98% Concentrated Sulfuric acid
vii. Copper wires

4. Experimental procedure:

i. At first our aim was to bring all the materials together and make a setup with the help of which we could clearly assess the formation of the hydrogen and could also easily replace certain parts if needed.

ii. In the beaker we poured 1000ml of R.O. water and then filled up two 10ml test tubes with R.O. water which we overturned and put in the beaker full of water. Next, we managed to slide in both the carbon rods in each of the test tubes ensuring that no water bubble entered in the test tubes. Before inserting the carbon rods in the test tubes, we had wound one side of a wire to both the carbon rods and with the help of a glue gun, had stuck the wires to the rods. Next, we wound the other sides of the wires to the positive and negative sides of the power supply respectively. This was the initial setup that we had made.

iii. Initially the following readings were taken:
Level of water in both test tubes = 10ml
Water level in beaker = 1000ml

iv. Next, we poured 2ml of 98% conc. Sulfuric acid in the water in the beaker to ensure that the water would conduct the electricity easily because the acid would increase the degree of ionization of water.

v. Now we started doing the experiment with a voltage of 1.5V initially. We conducted experiment with this voltage for 30 minutes. After 30 minutes we observed that 0.3ml of Hydrogen was produced at the cathode.

vi. We conducted the ‘Pop’ test to confirm the presence of Hydrogen and following that also conducted the lime water test to confirm the lack of the presence of carbon. The lack of carbon was needed to be checked to ensure that there was no

https://doi.org/10.36375/prepare_u.iiche.a397

carbon emission which directly ensured the formation of "Green Hydrogen."

vii. The similar test was conducted for different voltages: 3V, 6V, 9V and 12V. Green Hydrogen formed was The similar test was conducted for different voltages: 3V, 6V, 9V and 12V. Green Hydrogen formed was 1ml, 2ml, 2.5ml and 4.7ml respectively. The time for all the other four readings was also set at 30 minutes and all the water of the test tubes and the beaker were replaced (2ml Sulfuric acid was always added to the beaker whenever the water was replaced) before starting the process to take a reading.

viii. From the experiment we can conclude that the generation of the Hydrogen gas is directly proportional to the voltage supplied and plotting which we received almost a linear graph.

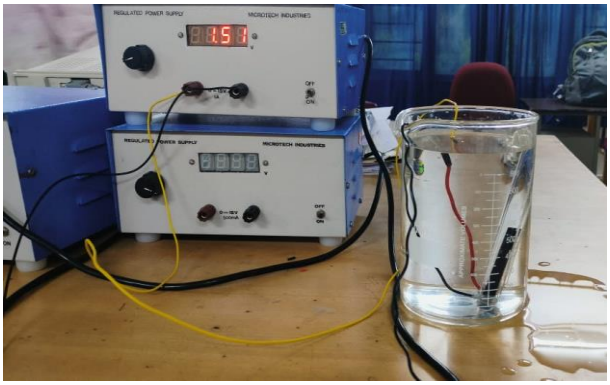

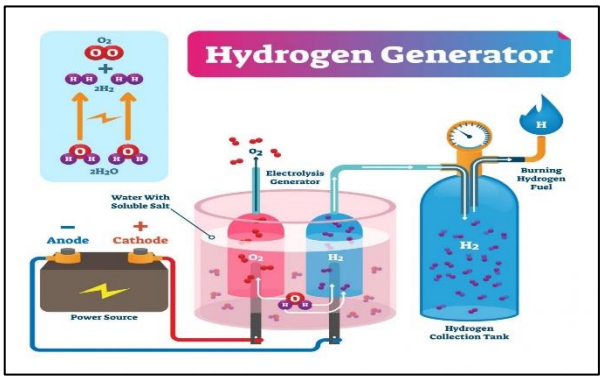

Figure 2: [A] Our Setup **[B]** Representation of our setup

5. Observations:

The following observations were recorded during the experimental procedure:
Time = 30 minutes

Sl. No.	Voltage (V)	Volume of water (ml)	Volume of hydrogen produced (ml)
1.	1.5	1000	0.3
2.	3	1000	1
3.	6	1000	2
4.	9	1000	2.5
5.	12	1000	4.7

Table 1: Volume of Hydrogen produced at different voltages.

https://doi.org/10.36375/prepare_u.iiche.a397

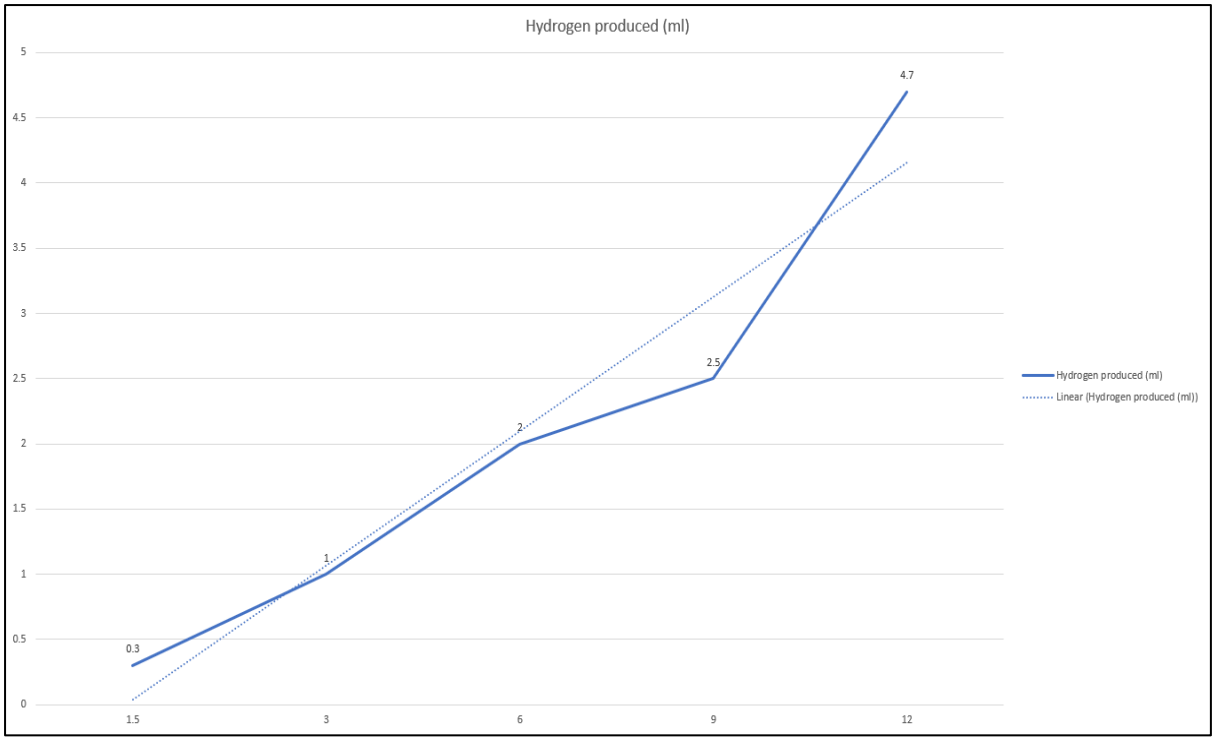

Figure 3: Volume of Hydrogen produced V/s Voltage graph

Confirmatory Test:

For confirmation of Hydrogen: ***Pop Test*** **-** The "pop test" is a simple and qualitative method for confirming the presence of hydrogen gas. It is a rapid and often visually striking way to detect hydrogen. When hydrogen gas comes in contact with an open flame, it rapidly combusts, producing a distinctive "pop" or "explosion" sound. This reaction is due to hydrogen's high flammability and its ability to burn in the presence of oxygen, which is present in the air.

For detection of Carbon: ***The limewater test*** **-** The limewater test, also known as the calcium hydroxide test or the "milkiness test," is a straightforward experiment used to detect the presence of carbon dioxide (CO2) gas by observing a chemical reaction. It relies on the reaction between carbon dioxide and calcium hydroxide (Ca(OH)2) to form calcium carbonate (CaCO3), which is only slightly soluble in water. The result of this reaction is a cloudy or milky appearance in the limewater.

6. **Experimental results:**

A colourless and odourless gas was formed in the cathode (Hydrogen) and another colourless and odourless gas was formed in the anode. On bringing a burning splinter near to the gas in the cathode, the burning splinter got extinguished with a pop sound ensuring the presence of hydrogen gas. But when the extinguished splinter is brought near the gas in the anode, the splinter rekindles ensuring the presence of oxygen gas. Since, our aim is to produce green hydrogen, so it is very important to check that there is no carbon emission in the entire procedure. In the following method that we had opted for, carbon could only be emitted in the form of carbon dioxide gas from the anode because carbon dioxide gas in order to be formed needed depleted carbon and oxygen gas that were only present in the

anode. So, in order to check that no carbon dioxide gas was present, at first we sealed the opening of the anode with a cork and then make a seisure in the cork through which we can pass a tube and the other part of the tube we insert in another test tube which has lime water in it. Now, the gas from the test tube of the cathode flows to the other test tube and there is no effect on the lime water in the other test tube which ensures the lack of the presence of carbon dioxide. If carbon dioxide was present, there would have been a colour change in the lime water, the lime water would have turned milky. The chemical reactions for the electrolysis process are given below:

Reaction at cathode:

$2H (+) + 2e (-) \rightarrow H2$

Reaction at anode:

$H2O \rightarrow 2H (+) + 1/2\ O2 + 2e (-)$

$1/2\ O2 + 1/2\ O2 \rightarrow O2$

7. Efficiency of Green hydrogen:

Increasing the overall efficiency of green hydrogen production involves optimizing various aspects of the process, from the generation of renewable energy to the conversion of that energy into hydrogen. Here are some key strategies to improve the overall efficiency of green hydrogen production:

i. High-Efficiency Renewable Energy Sources: Use of high-efficiency renewable energy sources such as advanced solar panels and wind turbines. Investing in the latest technology can maximize the electrical energy output for a given amount of sunlight or wind.

ii. Load Management: Implementation of load management and smart grid technologies to match hydrogen production with renewable energy availability helps avoid curtailment of excess energy and ensures that the electricity used for electrolysis is generated from renewable sources.

iii. Electrolyzer Selection: Choice of the most efficient electrolysis technology available, such as proton exchange membrane (PEM) or solid oxide electrolyzers. These technologies typically have higher electrical efficiencies compared to older alkaline electrolysis methods.

iv. Operating Conditions: Optimization of the operating conditions of the electrolyzer, including temperature, pressure, and flow rates. Running the electrolyzer under optimal conditions can improve its efficiency.

v. Heat Recovery: Implementation of heat recovery systems to capture and utilization of excess heat generated during the electrolysis process. This can enhance overall efficiency and reduce the energy input required.

vi. Hydrogen Compression and Storage: Selection of efficient methods for hydrogen compression and storage, considering factors like energy losses during compression and the choice of storage materials. Advanced materials and techniques can reduce energy losses during these processes.

vii. Co-Generation and Co-Production: Exploring opportunities for co-generation, where the heat produced during hydrogen production is used for other industrial processes or for district heating. Co-production, where hydrogen production is combined with the production of other

valuable chemicals, can also improve overall process efficiency.

viii. Grid Integration: Integration of green hydrogen production facilities with the local energy grid and other energy systems to optimize energy flow and balance supply and demand.

ix. Life Cycle Assessment: Conducting a life cycle assessment (LCA) to evaluate the environmental impact of the entire hydrogen production and utilization process helps identify areas for improvement and ensures that the overall system is sustainable and efficient.

x. Technological Advancements: Staying informed about the latest advancements in hydrogen production technologies, materials, and system design. Continuously adopting new innovations can lead to efficiency gains.

xi. Regulatory Support: Advocative support from government policies and incentives that encourage green hydrogen production and promote efficiency. Policy measures can include carbon pricing, subsidies, and renewable energy targets.

xii. Economies of Scale: Considerations in scaling up hydrogen production facilities can often lead to cost savings and efficiency improvements.

8. Challenges:

Green hydrogen, produced through the electrolysis of water using renewable energy sources, holds great promise as a clean and sustainable energy carrier. However, there are several challenges that need to be addressed to realize its full potential:

i. High Production Costs: One of the primary challenges is the high cost of green hydrogen production compared to hydrogen produced from fossil fuels. The cost of renewable energy equipment, such as solar panels and wind turbines, as well as the cost of electrolysis equipment, needs to come down significantly to make green hydrogen economically competitive.

ii. Intermittent Renewable Energy: The variability and intermittency of renewable energy sources like wind and solar can lead to fluctuations in green hydrogen production. Addressing this challenge requires effective energy storage and grid management solutions to ensure a stable hydrogen supply.

iii. Electrolyzer Efficiency: Improving the efficiency of electrolysis technology is essential to reduce energy losses during hydrogen production. Researchers are working on developing more efficient and cost-effective electrolyzers.

iv. Scale-up and Infrastructure: Building the necessary infrastructure for green hydrogen production, distribution, and utilization is a massive undertaking. It requires significant investment and coordination among various stakeholders.

v. Hydrogen Transportation and Storage: Developing efficient and safe methods for transporting and storing hydrogen is a challenge. Hydrogen is a low-density gas and can be challenging to transport over long distances. Methods such as pipeline networks, liquefaction, and solid-state storage are being explored.

vi. Competing Technologies: Other clean energy carriers and technologies, such as

batteries for energy storage and direct electrification, are in competition with green hydrogen. Deciding which technology is most suitable for different applications is an ongoing challenge.

vii. Regulatory and Policy Frameworks: The development of supportive policies, regulations, and standards for green hydrogen production and use is critical. Governments need to provide incentives and create a favorable business environment for green hydrogen to thrive.

viii. Public Acceptance and Awareness: Building public support and awareness for green hydrogen can be a challenge, as many people are still not familiar with its benefits and potential applications.

ix. Material Availability: The production of electrolyzers and other hydrogen-related technologies may require specific materials, some of which could face supply challenges. Efforts to diversify material sources and develop alternative technologies are essential.

x. International Collaboration: Collaboration among nations and regions is crucial for scaling up green hydrogen production. Cooperation in research, development, and investment can help overcome the global nature of the challenge.

xi. Environmental Impact: While green hydrogen is cleaner than hydrogen produced from fossil fuels, there are still environmental considerations, such as water usage and land use for renewable energy installations. Sustainable practices must be employed to mitigate these impacts.

Addressing these challenges requires a multi-faceted approach that involves technological innovation, policy support, infrastructure development, and international cooperation. As technology and knowledge continue to evolve, green hydrogen has the potential to play a significant role in the transition to a more sustainable and low-carbon energy future.

9. Environmental impact:
Green hydrogen is often considered an environmentally friendly energy carrier compared to hydrogen produced from fossil fuels. However, its environmental impact can still vary depending on several factors. Here are some key aspects of the environmental impact of green hydrogen:

i. Carbon Emissions Reduction: Green hydrogen is produced using renewable energy sources, such as wind, solar, or hydropower. As a result, the carbon emissions associated with its production are significantly lower compared to hydrogen produced from fossil fuels. This reduction in carbon emissions contributes to mitigating climate change.

ii. Air Pollution Reduction: Since green hydrogen production doesn't involve burning fossil fuels, it doesn't produce air pollutants such as sulfur dioxide (SO2), nitrogen oxides (NOx), and particulate matter, which are associated with respiratory and environmental health problems.

iii. Water Usage: Electrolysis, the process used to produce green hydrogen, requires water. While this is generally a low-impact water usage process, it can become a concern in regions with water scarcity. Efforts to minimize water use and develop

water-efficient electrolysis systems are ongoing.

iv. Land Use: The deployment of renewable energy sources like wind and solar to generate electricity for hydrogen production can impact land use. Large-scale renewable energy installations may require significant land area. Sustainable land management practices are important to minimize land use and protect ecosystems.

v. Materials and Resource Use: The production of electrolyzers and other hydrogen-related technologies may require specific materials. Ensuring a responsible and sustainable supply chain for these materials is important to minimize environmental impacts.

vi. Energy Efficiency: The overall efficiency of green hydrogen production, including energy losses in the conversion process, can impact its environmental footprint. Improving the energy efficiency of the entire hydrogen production chain can reduce resource consumption and associated environmental impacts.

vii. Waste Management: Electrolysis and other hydrogen production processes can generate waste materials. Proper waste management and recycling practices are necessary to minimize environmental harm.

viii. Lifecycle Analysis: To fully understand the environmental impact of green hydrogen, a comprehensive lifecycle analysis is essential. This analysis takes into account all stages, from the production of renewable energy to the end use of hydrogen, and evaluates the environmental effects and resource use at each step.

ix. Environmental Regulations and Standards: Implementing and enforcing environmental regulations and standards for green hydrogen production and utilization can help ensure responsible and sustainable practices are followed.

x. Sustainable Practices: Promoting sustainable practices in the development and deployment of green hydrogen technology, including responsible land use, water use, and materials sourcing, is essential to minimize its environmental impact.

While green hydrogen offers significant environmental benefits when compared to hydrogen produced from fossil fuels, it is not without environmental considerations. The goal is to continually improve the sustainability of green hydrogen through innovation, efficient resource use, and responsible practices, ultimately contributing to a more environmentally friendly and sustainable energy future.

10. Discussion:

Green hydrogen has emerged as a promising solution in the quest for sustainable and clean energy. As the world grapples with the urgent need to reduce greenhouse gas emissions and transition away from fossil fuels, green hydrogen offers a versatile and environmentally friendly alternative. Here is a deeper discussion on green hydrogen:

i. ***Renewable Energy Integration:***

Green hydrogen is produced through electrolysis, a process that splits water into hydrogen and oxygen using electricity. What sets it apart is the source of this electricity—renewable energy. By harnessing power from solar, wind, or

hydropower, green hydrogen ensures a zero-emission production process.

ii. ***Versatility in Applications***:
Green hydrogen's versatility is a key advantage. It can be used in various sectors, including transportation, industry, and energy storage. In transportation, hydrogen fuel cells can power vehicles, offering a clean alternative to conventional fossil fuel-powered cars. In industry, hydrogen is a vital component for sectors like steel and chemical production, offering a green pathway to decarbonization.

iii***. Decarbonizing Difficult Sectors***:
One of the most significant advantages of green hydrogen is its potential to decarbonize sectors that are challenging to electrify directly. Industries such as heavy manufacturing, aviation, and shipping rely on high-energy-density fuels, where green hydrogen presents a viable solution to significantly reduce emissions.

iv. ***Energy Storage and Grid Balancing***:
Green hydrogen can also be used as a form to store energy. Excess energy generated from renewables can be used for electrolysis, creating hydrogen stores that can be converted back to electricity during peak demand periods. This feature makes green hydrogen an essential component in balancing energy grids, especially as renewable sources can be intermittent.

v. ***Global Collaboration and Innovation***:
Countries worldwide are investing in research and development to enhance the efficiency and reduce the costs associated with green hydrogen production. International collaboration and knowledge-sharing are driving innovation, leading to the development of more efficient electrolysis technologies, and increasing the feasibility of large-scale green hydrogen projects.

vi. ***Challenges and Considerations***:
While the potential of green hydrogen is vast, challenges remain. These include the high production costs, efficiency improvements in electrolysis, building necessary infrastructure, and ensuring a sustainable supply chain for raw materials. Overcoming these challenges requires concerted efforts from governments, industries, and researchers.

vii. ***Policy Support and Market Development***:
Government policies play a crucial role in the adoption of green hydrogen. Subsidies, tax incentives, and regulatory frameworks can stimulate investment in green hydrogen projects. Additionally, creating a robust market for green hydrogen encourages private sector involvement and innovation.
In summary, green hydrogen represents a beacon of hope in the transition toward a cleaner and more sustainable energy future. Its potential to decarbonize diverse sectors, coupled with ongoing technological advancements and supportive policies, positions green hydrogen as a vital player in the global efforts to combat climate change and develop a more sustainable world for the generations to come.

10. Conclusion:
The green hydrogen production experiment, it is evident that the use of renewable energy sources, such as wind and solar power, in electrolysis processes is a promising avenue for sustainable hydrogen production. The results demonstrate that the system was able to efficiently convert electrical energy into hydrogen gas, with

minimal environmental impact compared to conventional fossil fuel-based methods.

The experimental setup showcased the feasibility of using electrolysis with renewable energy inputs to generate green hydrogen, contributing to the global efforts to mitigate climate change and transition towards a more sustainable energy economy. The process exhibited good efficiency, and further optimization could potentially enhance the overall yield and reduce costs associated with production.

However, it is important to note that there are still challenges to overcome, such as scalability, cost-effectiveness, and the development of reliable energy storage solutions. Additionally, research should continue to focus on improving the performance of electrolysis technologies and exploring novel catalyst materials to enhance the efficiency of the process.

Overall, this experiment provides valuable insights into the potential of green hydrogen production as a key component of the renewable energy landscape. Further research and development in this field will be crucial to unlocking the full potential of green hydrogen as a clean and sustainable energy carrier.

Furthermore, the experiment underscores the critical role that policy and regulatory frameworks play in accelerating the adoption of green hydrogen technologies. Supportive policies, such as incentives for renewable energy projects and carbon pricing mechanisms, will be instrumental in driving the transition towards a hydrogen-based economy.

Additionally, collaboration between public and private sectors, as well as international cooperation, will be essential in scaling up green hydrogen production and distribution infrastructure. This will help create a robust and interconnected hydrogen ecosystem that can meet the growing demands of various sectors including transportation, industry, and energy storage.

The green hydrogen production experiment represents a significant step forward in realizing a sustainable and decarbonized energy future. It highlights the potential of harnessing renewable resources to produce a clean and versatile energy carrier. With continued innovation, investment, and policy support, green hydrogen can play a pivotal role in achieving global climate goals and ensuring a more sustainable and resilient energy system for generations to come.

Acknowledgement:

We extend our heartfelt gratitude to the individuals and organizations who have been instrumental in the successful completion of this research project.

We would like to express our deep appreciation to Dr. Avijit Ghosh for his unwavering support, invaluable guidance, and mentorship. His expertise and encouragement have been the cornerstone of this research, and we are profoundly grateful for his mentorship.

Our sincere appreciation goes to Mrs. Suparna Banerjee for her technical expertise and support throughout the research. Their assistance in experimental work and data analysis was invaluable.

We acknowledge Heritage Institute of Technology, Kolkata for fostering an environment conducive to academic and research excellence, which significantly contributed to the quality of this work.

We extend our heartfelt thanks to our respective families for their unwavering support, encouragement, and understanding. Their presence provided the motivation and strength needed to complete this endeavor.

https://doi.org/10.36375/prepare_u.iiche.a397

References:

1. Baum ZJ, Diaz LL, Konovalova T, and Zhou QA. 2022. Materials Research Directions Toward a Green Hydrogen Economy: A Review. Ohio: Division of the American Chemical Society. Report License: CC-BY 4.0.

2. Kumar SS, Lim H. 2022. An overview of water electrolysis technologies for green hydrogen production, Ulsan: Carbon Neutrality Demonstration and Research Center. Report License by: CC-BY 4.0.

3. Rezk H, Olabi AG, Abdelkareem MA, Alahmer A, Sayed ET. 2023.Maximizing Green Hydrogen Production from Water Electrocatalysis: Modelling and Optimization. Department of Electrical Engineering.

4. Ali O. 2022. What are the Future Prospects of the Green Hydrogen Market? AZO Cleantech.

5. Symons A. 2022. Green hydrogen: Fuel of the future has 'big potential' but a worrying blind spot, scientists warn, Euro news green.

6. Chatenet M, Pollet BG, Dekel DR. 2022. Water electrolysis: from textbook knowledge to the latest scientific strategies and industrial developments. PuBMed. National Center for Biotechnology Information.

7. Raj K, Lakhina P, Stranger C. 2022. Harnessing Green Hydrogen opportunities for deep decarbonization in India. NITI Aayog.

8. Starace F. 2022. Green hydrogen factbook. Enel Group.

https://doi.org/10.36375/prepare_u.iiche.a398

Nuclear Waste Management

Gagana M B

Affiliation: Gagana M B, Bapuji Institute of Engineering and Technology, Davangere, Karnataka, India.

Abstract

In the recent years the waste management has become a huge challenge to the global community. The nuclear waste which has radioactive components are causing a tough challenge to dispose. In various countries they have adopted methods like dumping the waste in sealing cans and burying in underground or below the sea bed which is very harmful to the environment and habitants. The radioactive waste has to be treated but without the human handling. So we can do it with the help of AIML and data science, where we can program the machinery to carry out the neutralizing process. As there is remains of radiation in the nuclear waste we can use it to form energy resources. Though it's very hard to manage but we still haven't found the safest way and with the current measure taken to dispose are very uncertain and do not ensure complete safety. Why bury it when we can convert it into some form of energy or useful resource.

keywords: Nuclear waste; Radioactive; Energy; Radiation; Technology.

Abbreviations

LLW- Low level waste

HLW- high level waste

AI- Artificial intelligence

AIML- artificial intelligence and machine learning

1. Introduction

The spent nuclear power of a reactor is the nuclear waste. The generation of the waste has been taking place since from 1960-1970. The world has already seen the destruction and harm caused by radioactive elements. The unstable nature of these elements release radiation when the disintegration of atoms takes place. The uranium and plutonium were the major elements which were used in creating nuclear power and weapons. The end product of the nuclear power generation is the nuclear waste which is hazardous and has radiation. The handling of these waste is done in different methods. Mainly the methods of incineration- treating the waste at high temperatures and evaporation techniques. The most widely used method is- sealing the radioactive waste in a multi-layered cans or tanks, which is mostly made of lead and also layering it with concrete and burying these cans in a geo-disposable site. These methods are considered to be safer and reliable, on the other hand some countries like France, Japan, Germany, Belgium and Russia are recycling the used plutonium to generate the electricity. The waste is classified into two levels ie., 1) Low and Intermediate level of waste 2) High level of waste. The high level of waste is very dangerous and is aqueous in state and has 99% of the radioactive radiation. It's a challenging task to handle this level waste and it shouldn't be exposed to living beings and to the atmosphere. There are various action taken to resolve this issue by adopting the methods of deep geological disposals. It is accepted as the safest method of disposal and is implemented.

In recent studies and publications various discoveries has been made and it is shown that LLW can be transformed and has shown its implementations in the field of medical sciences and technology. As there is a lot of undiscovered components left in the HLW. Instead of disposing it can it be transformed into some other form of resources? Or can there be any alternatives methods of handling this waste.

https://doi.org/10.36375/prepare_u.iiche.a398

2. Methods

Nuclear waste management is a critical aspect of the nuclear energy industry and is essential to ensure the safe handling and disposal of radioactive materials.

The emerging nuclear medicine is gaining lots of demand as there is a proof and studies been taking place regarding this topic. The LLW are already finding its implementation in this field but high level waste composition is much complex in its structure and there might be many useful things in this aqueous substance. Though it seems as impossible to experiment with HLW and analyse it more but the current emerging technology makes it possible.

The designing of special safety suits to protect human beings from radiation, temperature and toxic gases produced from the nuclear waste. We are currently using the safety suits designed from the Lead but to be in the environment where the handling of nuclear waste is taking place we need a advanced safety equipment's. The suits have to be experimented by exposing it to various aspects similar to its working conditions. As lead is also harmful to human beings, there creates a need of any other substitute other than lead. Tyvek 10000 and 2000 are currently in use but we need still more advanced to handle HLW. the suits better have GPS and at least some automatic parameter analysing technology.

Building of plants to process HLW. The process system be built in the nuclear power plant. This particular unit can be in small scale or large scale based on the percentage of the HLW produced in that particular plant. The material which it is built with should be corrosion resistant. We can use some technology that we are already implementing while dealing with volcanos and lava. The material of the bucket and ladle can be used as they are high temperature resistant. Some of the countries are converting used plutonium to generate electricity we can try to implement this technology even in case of HLW. if we could find ways in generating electricity as a product of HLW, this can be another source of energy. We can take the assistance of AI to monitor various parameters and AIML to manufacture equipment's, which can carry out the process of handling with HLW. by this we can prevent human beings working in the hazardous environment and reduces the risk of getting exposed to radiations.

Finding an alternative to generate nuclear energy. We are using uranium and plutonium currently to generate nuclear energy. The mining of the uranium is very hazardous and difficult. We have already seen the deformities

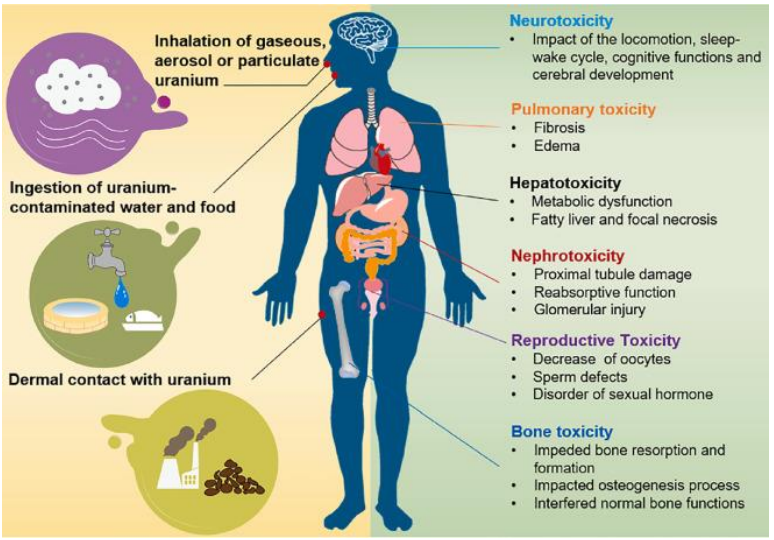

Figure1Emerging health risks and underlying toxicological mechanisms of uranium contamination: Lessons from the past two decades https://www.researchgate.net/figure/The-primary-exposure-routes-and-health-risk

it has caused in the workers who have worked in the mining and uranium is not available abundantly everywhere. we can find some other element which is not harmful and doesn't

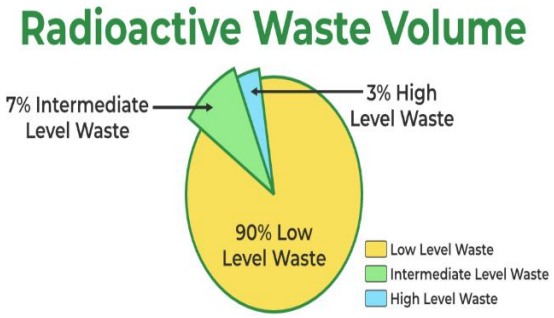

Figure 2 GeeksforGeeks. (2023, February 13). Radioactive waste and pollution. GeeksforGeeks. https://www.geeksforgeeks.org/radioactive-wastes-and-pollution

emit radiations. This element has to be sustainable, economic and available abundantly to generate power. It should be perfect alternative for uranium with no hazardous impacts.

https://doi.org/10.36375/prepare_u.iiche.a398

3. Results

The processing of any material has many processes. The nuclear power plant which can take on HLW should be situated in a isolated and a very ideal conditions of environment. This particular field of research need experts of the various domains to work together to find the solution. There are still several elements which are not discovered and this brings forth

Type of uranium	Composition (%)	
	^{235}U	^{238}U
Natural uranium	0.7	99.3
Slightly-enriched uranium	1.0-1.8	≈98.5
Low-enriched uranium	3	97
Weapon-grade uranium (WGU)	93.5	6.5

Figure 1 [PDF] The long-term nuclear explosives predicament : final disposal of military usable fissile material in nuclear waste from nuclear power and from the elimination of nuclear weapons | Semantic Scholar

a speculation of an element in existence which can help us in finding the solution of the issue.

As the artificial intelligence is finding its implementation in various fields and technology, it can assist us in dealing with the nuclear waste as well and also take on the works that is hazardous for the human beings to involve. We can design the machines in a way where nothing harmful is emitted and gets out of the system to the environment.

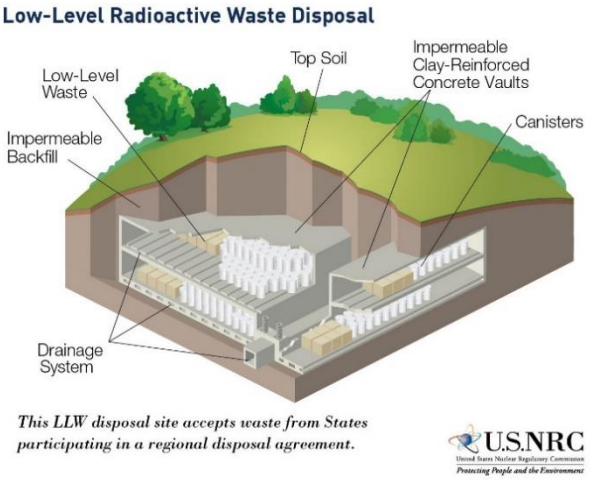

Figure 4 NRC maps of radioactive waste sites. (n.d.). NRC Web. https://www.nrc.gov/reading-rm/doc-collections/maps/radioactive-waste-sites.html

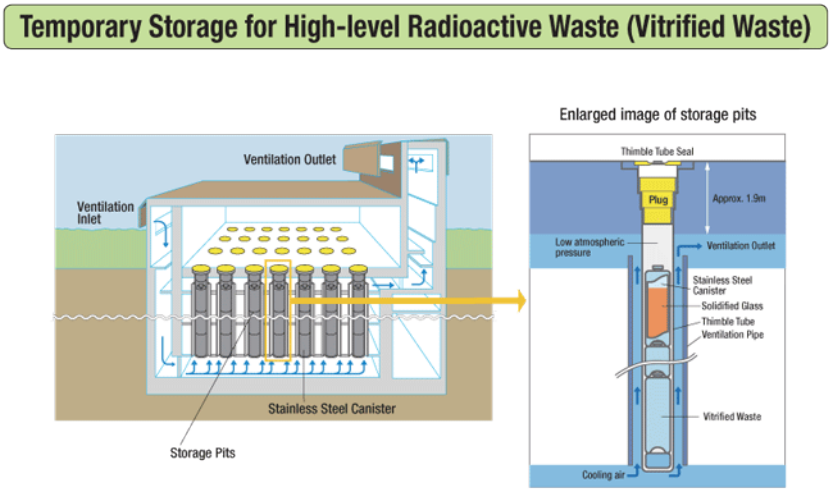

Figure 5 High-level Radioactive Waste (HLW) Management - The Federation of Electric Power Companies of Japan(FEPC). (n.d.). https://www.fepc.or.jp/english/nuclear/waste_management/high-level/index.html

4. Discussions

The present generation is in need of sustainable and reliable form of energy. With ever increasing demand for energy, the fossil fuels are unable to fulfil the demand. The pollution caused and as the coal is near to extinction, we need other forms of energy. We are currently using many available forms of energy but we are in need of high electric power supply with less consumption of resource. When the world was introduced to the energy equation $E=mc^2$, the nuclear energy came into existence and we knew that it could fulfil the energy demand. But the end result of the nuclear energy generation ie., nuclear waste caused the huge problem and debates around the world. If we can find the most suggestable method to handle the nuclear waste then we can nearly overcome the energy crisis. We can try to convert the nuclear waste into some other form of energy or find a absolute no harm disposable method. The geological disposable method can only postpone the effects for now but eventually in the it will cause problems in future. But why dispose it when we still have the room for converting the waste into something useful. Most of the powerful nations which are producing nuclear energy have technology to use the nuclear energy but there is still no invention about how to handle the waste with a success rate of 100%. In recent days, there has been disposable of nuclear waste water(treated) into water bodies which is very concerning as it may contain toxic materials in it. These incidents indicate that there is a need for better disposal method of any state of waste which is associated with the nuclear energy.

Acknowledgement

I'm greatfull to my parents who have supported me to write this paper. Thank you to my father Mr. M. Basavaraja, who motivated me all through the journey.

References

1. Alwaeli, Mohamed, and Viktoria Mannheim. 2022. "Investigation into the Current State of Nuclear Energy and Nuclear Waste Management—A State-of-the-Art Review" *Energies* 15, no. 12: 4275. https://doi.org/10.3390/en15124275

2. Weber, W.J., Navrotsky, A., Stefanovsky, S. *et al.* Materials Science of High-Level Nuclear Waste Immobilization. *MRS Bulletin* **34**, 46–53 (2009). https://doi.org/10.1557/mrs2009.12

3. Niemeyer, I. (2023). Panel: safeguarding nuclear waste management. Safety of nuclear waste Disposal, 2, 205-205. https://doi.org/10.5194/sand-2-205-2023

4. Ringwood, A. (1985). disposal of high-level nuclear wastes: a geological perspective. Mineralogical Magazine, 49(351), 159-176. https://doi.org/10.1180/minmag.1985.049.351.04

5. Jenkins-Smith, H., Silva, C., Nowlin, M., & deLozier, G. (2010). Reversing nuclear opposition: evolving public acceptance of a permanent nuclear waste disposal facility. Risk Analysis, 31(4), 629-644. https://doi.org/10.1111/j.1539-6924.2010.01543.x

6. Noka, V. (2023). The role of nuclear cultural heritage in long-term nuclear waste governance. Safety of nuclear waste Disposal, 2, 227-228. https://doi.org/10.5194/sand-2-227-2023

7. Enderle, S. (2023). Solving problems collectively in nuclear waste governance. Safety of nuclear waste Disposal, 2, 267-267. https://doi.org/10.5194/sand-2-267-2023

8. Ramana, M. (2018). Technical and social problems of nuclear waste. Wiley Interdisciplinary Reviews Energy and Environment, 7(4). https://doi.org/10.1002/wene.289

9. Ewing, R., Whittleston, R., & Yardley, B. (2016). geological disposal of nuclear waste: a primer. Elements, 12(4), 233-237. https://doi.org/10.2113/gselements.12.4.233

10. Birkhölzer, J., Houseworth, J., & Tsang, C. (2012). geologic disposal of high-level radioactive waste: status, key issues, and trends. Annual Review of Environment and Resources, 37(1), 79-106. https://doi.org/10.1146/annurev-environ-090611-143314

11. Frankel, G., Vienna, J., Lian, J., Guo, X., Gin, S., Kim, S., … & Scully, J. (2021). Recent advances in corrosion science applicable to disposal of high-level nuclear waste. Chemical Reviews, 121(20), 12327-12383. https://doi.org/10.1021/acs.chemrev.0c00990

12. Hoyer, E., Kreye, P., Lohser, T., & Rühaak, W. (2021). Preliminary safety assessments in the high-level radioactive waste site selection procedure in germany. Safety of nuclear waste Disposal, 1, 37-38. https://doi.org/10.5194/sand-1-37-2021

13. Näslund, J., Brandefelt, J., & Liljedahl, L. (2013). Climate considerations in long-term safety assessments for nuclear waste repositories. Ambio, 42(4), 393-401. https://doi.org/10.1007/s13280-013-0406-6

14. Segall, G., Grady, E., Fair, J., Ghesani, M., & Gordon, L. (2017). nuclear medicine training in the united states. Journal of nuclear Medicine, 58(11), 1733-1734. https://doi.org/10.2967/jnumed.117.200857

15. Sram, R., Dobiáš, L., Rossner, P., Veselá, D., Veselý, D., Rakusová, R., … & Rericha, V. (1993). Monitoring genotoxic exposure in uranium mines.. Environmental Health Perspectives, 101(suppl 3), 155-158. https://doi.org/10.1289/ehp.101-1521117

16. Zhang, Z., Tang, Z., Liu, Y., He, H., Guo, Z., Feng, P., … & Sui, Q. (2023). Study on the ecotoxic effects of uranium and heavy metal elements in soils of a uranium mining area in northern guangdong. Toxics, 11(2), 97. https://doi.org/10.3390/toxics11020097

17. Kautsky, U., Saetre, P., Berglund, S., Jaeschke, B., Nordén, S., Brandefelt, J., … & Andersson, E. (2016). The impact of low and intermediate-level radioactive waste on humans and the environment over the next one hundred thousand years. Journal of Environmental Radioactivity, 151, 395-403. https://doi.org/10.1016/j.jenvrad.2015.06.025

18. Ojovan, M., Robbins, R., & Garamszeghy, M. (2017). Advances in conditioning of low- and intermediate-level nuclear waste. Mrs Advances, 3(19), 983-990. https://doi.org/10.1557/adv.2017.613

https://doi.org/10.36375/prepare_u.iiche.a405

Screening of Symbiotic Bacteria for Biodiesel Production in Algae Growth

Chelladurai Chellamboli[1*], Muthiah Perumalsamy[2], Raguraman Dhinesh Kanna[3]

[1] Research Scholar, Department of Chemical Engineering, National Institute of Technology, Tiruchirappalli, Tamil Nadu, India.

[2] Associate Professor, Department of Chemical Engineering, National Institute of Technology, Tiruchirappalli, Tamil Nadu, India.

[3]Student, Gnanamani College of Technology, Namakkal, Tamil Nadu, India

Abstract

A novel symbiotic bacterial strain was isolated from the algae culture and further analysed for sequence identification to determine the nature of the species. In this study, 3- to 4-month-old algae were cultured under nonaxenic conditions. Samples were taken to determine the presence of cross contamination, such as bacteria and other species, in the culture system. Microscopic analysis confirmed the presence of *C. pyrenoidosa* and *S. abundans* in the culture system. Additionally, bacterial identification revealed that stable colonies survived in the culture system. Several purifications of two isolated pure colonies were carried out, and growth curves were plotted for the isolated colonies (white and yellow colonies), which had maximum absorbance values of 0.467 and 0.154, respectively, at 660 nm. Moreover, the isolated bacterial colonies were cocultured with pure axenic cultures of *C. pyrenoidosa* and S. *abundans*. Studies have shown that yellow colonies support the growth of algae. Hence, isolated and purified yellow colonies were subjected to morphological, biochemical, 16S rRNA sequencing and FAME analyses via gas chromatography. This analysis confirmed that the isolated symbiotic bacterium was *Stenotrophomonas maltophilia*. The consensus sequence was deposited in the NCBI GenBank KX768757.

Keywords: *Stenotrophomonas maltophilia*; Algae, *Chlorella pyrenoidosa*, *Scenedesmus abundans,* Symbiotic, rRNA

Introduction

Global economic growth depends on the availability of energy to meet demand. This sudden and excessive level of energy consumption has resulted in an energy tragedy for the world, such as the depletion of the finite

supply of fossil fuel sources. Transportation fuels such as gasoline and diesel constitute 27% of all energy produced, in addition to the depletion of fossil fuel resources. Because of the serious environmental risks they pose, including acid rain, global warming, and ozone layer depletion, these fuels are widely acknowledged to be unsustainable (World Energy Outlook, 2007 and Ho et al. 2014). In particular, India imports between 75 and 80% of its petroleum fuel to meet its energy needs. According to statistical reviews, the rate at which fossil fuels are used to produce energy globally could completely disappear in 45 years (Rühl C 2008). Therefore, it is imperative to discover a fossil fuel substitute to lessen the excess shortages of gasoline and diesel and minimize the increase in the price of transportation fuel (Marousek J et al. 2023). Triglycerides (TAGs) are promising substitutes for fossil fuels in energy, according to a number of studies (Khan et al. 2009). The primary benefit of producing eco-friendly biodiesel from biomass is that it will boost the rural economy (Barnwal et al. 2005). Therefore, the creation of biodiesel from biomass was the main focus of this study.

According to Tica et al. (2010) and Zhang et al. (2022), biodiesel is currently used as a sustainable energy source to meet future energy needs because it releases more oxygen into the atmosphere and emits less sulfur, nitrogen, and traces of SOx, NOx, CO, benzene, and toluene. In accordance with Leung et al. (2010) and Vyas et al. (2010), biodiesel is primarily made from vegetable or animal fats and is composed of fatty acid alkyl esters that are produced during the transesterification process by converting triacylglycerols (TAGs) into diacylglycerols (DAGs), free fatty acids (FFAs), and phospholipids (PLs). Because biodiesel is made from edible and nonedible crop residues, first- and second-generation biofuel sources have reduced the production of transportation fuels and have their own limitations (Ulgiati 2001; Chisti 2007 and 2012; Borowitzka 1988; Borowitzka and Moheimani 2013; Pate 2013; Klein-Marcuschamer et al. 2013). Consequently, a third generation of algae-based fuel oil producers emerged through photosynthetic reactions (Chisti 2007, 2013; Hu et al. 2008; Brennan and Owende 2010; Huang et al. 2010). In comparison to other sources, algae offer a cost-effective way to

produce enough biodiesel to partially replace fossil fuels, although this approach is debatable (Malcata 2011; Pate et al. 2011; Klein-Marcuschamer et al. 2013; Pate 2013).

Several studies have reported that various algal species can secrete oils, confirming the capacity of algae to manufacture biodiesel (Banerjee et al. 2002; Chisti 2007; Griffiths and Harrison 2009; Griffiths et al. 2012) by limiting nutrient supplements and stressing cells to produce oil by starvation of some nutrients (Illman et al. 2000; Rodolfi et al. 2009; Griffiths et al. 2012). In addition to TAG, algae oil may also contain other components that are used to produce a high level of energy and carbon, such as non-triglycerides, polar lipids, carotenoids, chlorophyll, and terpenoid hydrocarbons (Banerjee et al. 2002). The energy content of algal crude oil is 35,800 kJ kg^{-1}, or 80% of the average energy found in petroleum fuels (Chisti 2012). Forty percent of the oxygen that has evolved in the atmosphere from 75% of microalgae is due to the growth of algae (Ponnuswamy et al. 2013). Therefore, algal crude oil is recognized as a possible replacement for transportation fuels. Thus, strains that produce a high yield of microalgae were selected for cultivation in this study. Numerous studies have been conducted to improve algae growth, either directly or indirectly, through the use of artificial sources. Furthermore, according to a literature review, triggered natural or artificial sources have several disadvantages, such as a lower yield or a longer time requirement for better lipid production. To address these problems, a novel symbiotic bacterial strain was isolated from the algal culture, and sequence identification was performed to determine the species's innate capabilities. To produce biodiesel, *Stenotrophomonas maltophilia* (*S. maltophilia*) has a symbiotic effect on the growth of algae. Most bacteria can terminate algae growth within a day.

Stenotrophomonas maltophilia for algae evolution

S. maltophilia is a member of the Xanthomonadaceae family. *S. maltophilia*, formerly known as *Pseudomonas maltophilia* or *Xanthomonas maltophilia*, has been designated the sole species within the recently established genus *Stenotrophomonas*. The non-fermentative gram-negative bacillus *S. maltophilia* grows

easily on a variety of bacteriological media (Adegoke et al. 2017). A number of characteristics give *S. maltophilia* its potential as a pathogen, particularly because of its ability to secrete a wide range of extracellular enzymes, such as lipases, fibrolyses, and proteases, which may be important in the colonization process. Molecular typing systems have advanced the understanding of the epidemiology of *S. maltophilia* infection (Gajdács et al. 2019; Brooke et al. 2021). Numerous techniques for typing have been developed, including ribotyping, DNA macro restriction analysis, random amplification of polymorphic DNA, enterobacterial repetitive intergenic consensus-PCR, and multilocus enzyme electrophoresis. Fungal lipases such as Lipozyme TL IM reportedly exhibit decreased activity in regard to the transesterification of various vegetable oils by bacterial lipases, such as *Pseudomonas* lipase. *S. maltophilia* isolated from algal culture itself sustains the algal life cycle. As a result, *S. maltophilia*, a type of symbiotic bacteria, was identified from the algal culture. To understand the symbiotic algae-bacterial growth behaviour for the production of biodiesel, a purified isolated symbiotic bacterial strain was sequentially coupled with various algal species. Many studies have been completed on algae growth enhancement, which may either directly or indirectly depend on artificial sources, but the yield efficiency has not reached a satisfactory level. To overcome this constraint, a novel symbiotic bacterial strain was isolated from the algae culture, and its growth profile was tested under different conditions for biodiesel production.

Methodology

Initially, this study involved collecting samples from algae cultivated for approximately three to four months in culture and grown in the laboratory under atmospheric conditions. This algae culture was grown under non-axenic conditions with good biomass production without additional nutrient supplementation or aeration. Therefore, to determine the culture status, the sample was further analysed for cross-contamination in the culture system. Microscopic analysis confirmed the presence of *C. pyrenoidosa and S. abundans* in the culture system. In addition, bacterial identification techniques such as the streak and pour plate

methods were used to identify stable colonies that survived in the culture system. Several purifications were performed, and two different pure colonies were found. Therefore, these colonies were taken up to construct growth curves. These curves were plotted for isolated colonies (white and yellow colonies), which showed the maximum absorbance value. Moreover, the isolated bacterial colonies were cocultured with a pure axenic culture of *C. pyrenoidosa* and *S. abundans*.

Optical density method

The growth phases of the algal cultures were determined by measuring the absorbance at 660 nm with a UV-2600 Shimadzu, and the corresponding dry weight was calculated from the standard algal growth plot (Chellamboli et al. 2014 and 2016).

Genomic DNA Extraction

Agar plate colonies from a single streak were scraped, suspended in PBS, and centrifuged. After the pellet was evenly distributed, 600 µl of cell lysis buffer (SDS, Tris-EDTA, and *guanidium isothiocyanate*) was added. The mixture was gently stirred for five minutes while the vial was inverted, and the mixture was subsequently incubated for ten minutes until the suspension nearly became transparent. This solution was covered with 600 µl of isopropanol. The two layers were gradually combined until the solution was homogeneous, and white DNA strands were visible. Using a pipette tip, the DNA strands were spooled and placed into a new vial. The spooled DNA was added to 500 µl of 70% ethanol. For ten minutes, the spooled DNA was centrifuged at 10,000 rpm to precipitate the DNA. The supernatants were discarded. The pellet (not allowed to dry completely) was air-dried. After adding 50 µl of 1X TE, the pellet was suspended. The mixture was incubated at 55–60°C for 5 min to improve genomic DNA solubility. A 1% agarose gel was loaded with 5 µl of freshly extracted DNA and 3 µl of gel loading dye, after which electrophoresis was performed (Maha A. Rakaz et al. 2021).

Agarose Gel Electrophoresis

To make 1× TAE, distilled water was mixed with an appropriate amount of 50× TAE buffer. Fifty milliliters of 1X TAE and 0.5 g of 1% agarose were combined in a 250 ml conical flask and heated to a transparent liquid. The gel tank was

washed and cleaned completely. The combs were placed approximately 2 cm away from the center platform wall, facing the black electrode or cathode. The agarose gel was heated to approximately 60°C, at which point 0.5 µg/ml ethidium bromide was added. The mixture was then swirled twice before being carefully poured into the central platform of the gel tank. The agarose was allowed to solidify. The gel was filled with one X TAE buffer until the buffer level was 0.5–0.8 cm above the gel surface. The combs were gently removed. The samples were run at 50 V against voltage, and the power cords were connected. Following the run, the gel was examined using a UV transilluminator (Addgene 2018).

Column purification

After the column was set up in the collection tube, 400 µl of equilibration buffer was added, and the column was centrifuged for one minute at 10,000 rpm. The buffer that was collected was then removed. The DNA samples were mixed with 400 µl of equilibration buffer and then loaded into the column. This process was repeated until the DNA sample was finished. The flow that passed through the column was collected. After adding 500 µl of wash buffer 1, the mixture was centrifuged for one minute at 10,000 rpm, after which the buffer was extracted. After that, 500 µl of wash buffer 2 was added, and the buffer was collected after centrifuging for one minute at 10,000 rpm. An empty collection tube was used to centrifuge the column to fully remove the buffer for two minutes. After the column was placed in a new collection tube, 50 µl of the eluted buffer was added. After the column was placed in a new collection tube, 50 µl of the eluted buffer was added. The eluted sample was collected and examined on the gel after being incubated for two minutes at room temperature and centrifuged for one minute at 10,000 rpm. The amplification conditions are displayed in Table 1.

Table 1 Amplification properties for bacterium identification

Parameters	Quantity/Volume
Double distilled water	36 µl
10x Taq pol assay buffer	5µl
dNTP mix (100 µM each)	2 µl
Forward Primer(100ng/µl)	1 µl
Reverse Primer(100ng/µl)	1 µl
Taq pol (1u/ µl)	1 µl
Template	2 µl
Total Volume	**50 µl**

https://doi.org/10.36375/prepare_u.iiche.a405

Amplification of the 16S rRNA gene was performed using the primers. Forward primer: 5'-AGAGTTTGATCCTGGCTCAG-3' and reverse primer: 5'- ACGGCTACCTTGTTACGACTT-3'. The conditions for PCR, which were carried out in 0.2 ml PCR tubes with a total volume of 50 µl, are listed in Table 2 (Maha A. Rakaz et al. 2021; Weisburget al. 1991).

Table 2 PCR Condition for bacterium identification

Initial Step		**30 Cycles**	**Final Extension**		**Final Step**
Denat		**Anneal**		**Extend**	
HOLD		**CYCLE**	**HOLD**		**HOLD**
94 ˚C	94 ˚C	58 ˚C	72 ˚C	72 ˚C	4 ˚C
2 min	30 sec	30 sec	1 min 30 sec	5 min	∞

Results and Discussions

Screening of *S. maltophilia* as a symbiotic bacterium for algae growth

The screening of the symbiotic bacteria was carried out in the research laboratory. Normally, bacteria destroy algal species within a few days, as occurs for cross-contaminated strains (nonsymbiotic bacteria). However, few organisms may support algae growth via symbiotic pathway signalling. Therefore, bacterial colonies were isolated from several-month-old algae cultures. Initially, serial dilutions and strike plate methods were used to identify the most sustainable bacterial species. Furthermore, the bacterial colonies were purified three times by the repeated strike plate method to ensure that the pure colonies were not contaminated. Finally, the two colonies were isolated on the basis of the sustainability shown in Fig. 1. Subsequently, the bacteria were grown (Erin R. Sanders 2012; Pettipheret al. 2005).

The maximum OD values were approximately 0.467 and 0.154 for yellow and white colonies, respectively, within 12 hr. Bacterial depletion occurs due to a shortage of nutrients in the medium, and the death phase is recorded. Fig. 2 shows the growth curves of both pure colonies. Later, the yellow colony was selected for further analysis.

https://doi.org/10.36375/prepare_u.iiche.a405

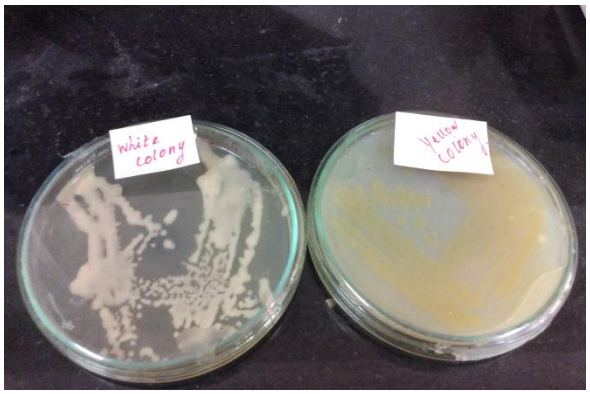

Fig.1 Isolated strains from algae culture a) White colony, b) Yellow colony

The initial growth and activation of algae take a minimum of approximately 12 hr, at which point the activity of symbiotic bacteria is needed. Furthermore, the two isolated colonies were cocultured with algal species. The experimental results showed that the algal species were supported by yellow colony bacteria. Hence, white colonies were excluded from the study, and the screened bacteria were subjected to gene sequence analysis. Studies have proven that yellow colonies support the growth of algae.

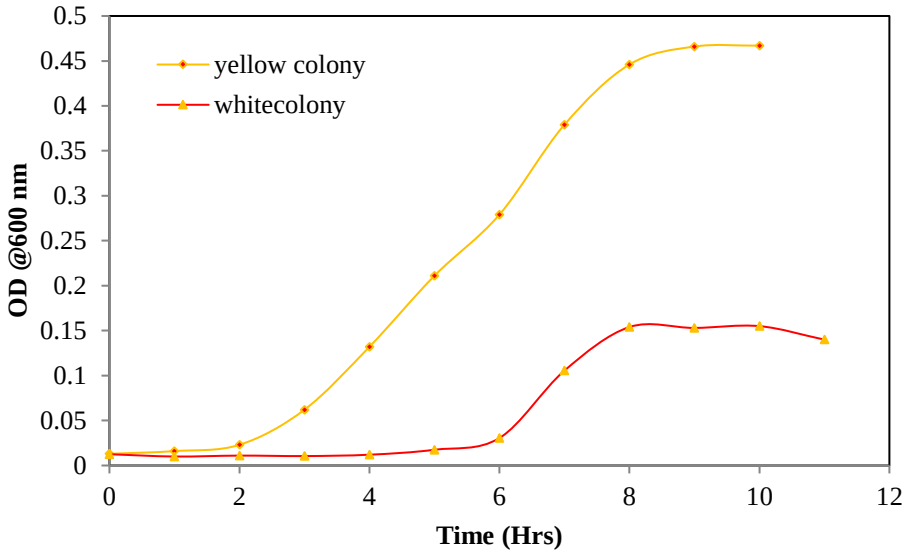

Fig. 2 Bacterial Growth curve for isolated species

Identification of microbial culture products using the 16S rRNA-based molecular technique

To identify the genera and phyla of bacteria in th e gut microbiota, 16S ribosomal RNA (rRNA) s equencing was used for a polymerase chain reaction to amplify a conserved part of the genome of a bacterium (Ranjan R et al., 2016). The 16S rRNA gene sequence was obtained via the base molecular technique used

for identification of enormous numbers of strains. The NCBI GenBank is one of the largest gene deposition databanks for rRNA sequences. The sequences of approximately twenty million genes have been deposited in the genebank, and the gene sequences of unknown microbial strains of the 16S rRNA gene have been compared (Jill E. Clarridge, 2004; Jacquelyn S. Meisel and Elizabeth A. Grice 2017).

Identification of symbiotic bacteria for algae growth

Hence, isolated and purified yellow colonies were subjected to morphological, biochemical, 16S rRNA sequencing and FAME analyses via gas chromatography. This analysis confirmed that the isolated symbiotic bacterium was *Stenotrophomonas maltophilia.* The consensus sequence was deposited in the NCBI GenBank as KX768757. Fig. 3 shows the identification of the bacterial genomic DNA in both isolated colonies. Lane 1 represents an isolated yellow colony, and lane 2 represents an isolated white colony.

Fig. 3 Genomic DNA

Identification of bacterial sequences via gel electrophoresis

The isolated DNA was further subjected to gel electrophoresis, and a single band of 1.5 kb (of 100 ng intensity) was observed. Gel electrophoresis was used to visualize the total RNA extracted from the symbiotic bacteria. Lane 1 shows the 500 bp DNA ladder of 0.5, 1, 1.5, 2.0, 2.5, 3.0, 3.5, 4.0, 4.5 and 5.0 kb. In addition, lanes 2-3 show the 16S rRNA amplification of two different colonies from the study experiments, i.e., the yellow and white colonies shown in Fig.4.

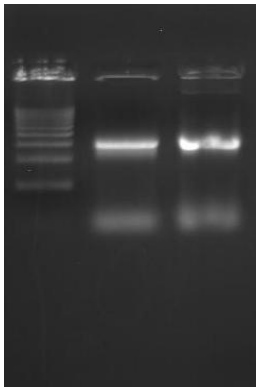

Fig. 4 Electrophoresis of 16s rRNA gene amplification

S. maltophilia STRAIN F-C06 16S ribosomal RNA gene; partial sequence in GenBank

The RNA sequence of *S. maltophilia* isolated from symbiotic bacteria has been deposited in the NCBI GenBank (KX768757). Fig. 5 shows electropherogram plots of DNA fragments from the symbiotic bacteria. The curve shows the relation of time(bps) to the fluorescence intensity of the isolated DNA from the bacteria.

Analysis of *S. maltophilia* via BLAST

BLAST of the gene bank website yielded the most significant result, which was identified by molecular testing. To identify the type of bacteria, GenBank BLAST was used for all bacteria. Several species genus conclusions were drawn from the sequences that produced meaningful alignments. The bacterial isolate was most likely *Stenotrophomonas maltophilia*, for which the maximum identification was above 99%, according to the results of the molecular test. The molecular sequence was 99% identical to the partial sequence of the *S. maltophilia* strain JB5-1 16S ribosomal RNA gene. Similarly, for the *S. maltophilia* AM3-1 16S ribosomal RNA gene, the partial sequence was 99% identical to that of the isolated bacteria. Similarly, the identified bacteria had 99% similarity with other partial sequences of bacteria deposited in GenBank for *Stenotrophomonas sp*., the CV8 16S ribosomal RNA gene, and the *Stenotrophomonas sp*. for the CV6 16S ribosomal RNA gene. *maltophilia* strain CV4 16S ribosomal RNA gene, *S. maltophilia* strain CV1 16S ribosomal RNA gene, *S. maltophilia* strain 257-B 16S ribosomal RNA gene, *Stenotrophomonas sp*. XBGRA2 16S ribosomal RNA gene, *S. maltophilia* strain L1 16S ribosomal RNA gene, *S. maltophilia* strain W8-1 16S ribosomal RNA gene, *S. maltophilia* strain Dh 16S ribosomal RNA gene, and *S. maltophilia* gene for 16S rRNA are shown in Table 3. The use of random primers for *S. maltophilia* was consistent with that of random PCR, which has been shown to be more successful at identifying *S. maltophilia* than gel electrophoresis (GE) and is a significant pathway of choice. PCR is also a much more potent way to demonstrate the degree of reliability of results between two distinct amplification systems (Walt Ream et al. 2013).

https://doi.org/10.36375/prepare_u.iiche.a405

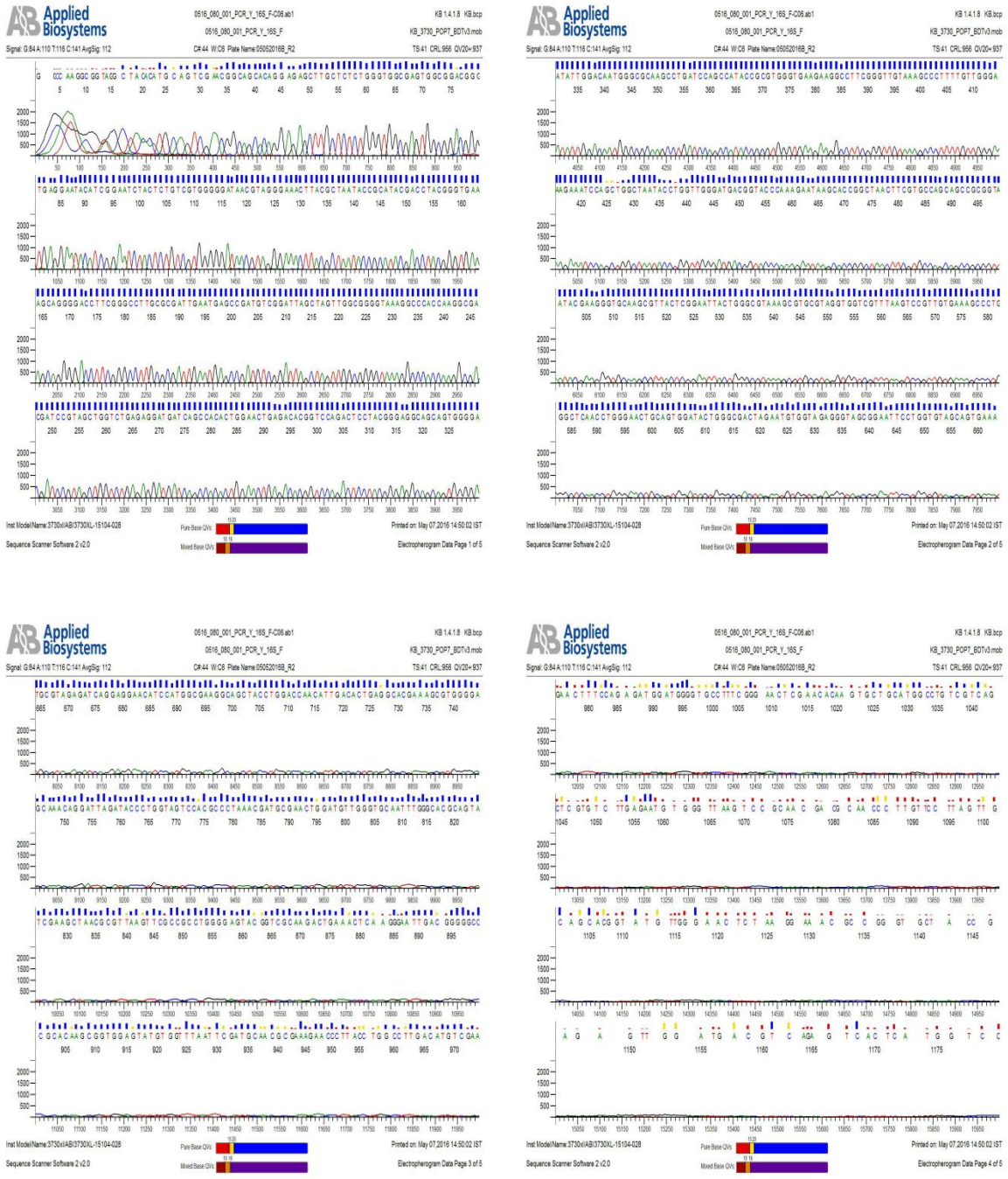

Fig.5 Partial sequence of PCR amplification for *S. Maltophilia*

https://doi.org/10.36375/prepare_u.iiche.a405

Table 3: Sequences producing significant alignments

Description	Max score	Total score	Query cover	E value	Identification	Accession
Stenotrophomonas maltophilia strain JB5-1 16S ribosomal RNA gene, partial sequence	2484	2484	100%	0.0	99%	KT970985.1
Stenotrophomonas maltophilia strain AM3-1 16S ribosomal RNA gene, partial sequence	2484	2484	100%	0.0	99%	KT970982.1
Stenotrophomonas sp. CV8 16S ribosomal RNA gene, partial sequence	2484	2484	100%	0.0	99%	KP895794.1
Stenotrophomonas sp. CV6 16S ribosomal RNA gene, partial sequence	2484	2484	100%	0.0	99%	KP895792.1
Stenotrophomonas maltophilia strain CV4 16S ribosomal RNA gene, partial sequence	2484	2484	100%	0.0	99%	KP895790.1
Stenotrophomonas maltophilia strain CV1 16S ribosomal RNA gene, partial sequence	2484	2484	100%	0.0	99%	KP895787.1
Stenotrophomonas maltophilia strain 257-B 16S ribosomal RNA gene, partial sequence	2484	2484	100%	0.0	99%	KP993216.1
Stenotrophomonas sp. XBGRA2 16S ribosomal RNA gene, partial sequence	2484	2484	100%	0.0	99%	KJ184868.1
Stenotrophomonas maltophilia strain L1 16S ribosomal RNA gene, partial sequence	2484	2484	100%	0.0	99%	KF358247.1
Stenotrophomonas maltophilia strain W8-1 16S ribosomal RNA gene, partial sequence	2484	2484	100%	0.0	99%	JX393000.1
Stenotrophomonas maltophilia strain Dh 16S ribosomal RNA gene, partial sequence	2484	2484	100%	0.0	99%	HQ200414.1
Stenotrophomonas maltophilia gene for 16S rRNA, partial sequence, strain: BL-9	2484	2484	100%	0.0	99%	AB194321.1

Phylogenetic analyses

To further identify the taxonomic position of *Chlorococcum* sp. GD, molecular phylogenetic analysis was carried out. The species used in each phylogenetic analysis were selected on the basis of the data available in the GenBank gene database (Chellamboli and Perumalsamy, 2017). A phylogenetic approach involves the study of relationships between and within groups of organisms, as well as their evolutionary history. Phylogenetic inference techniques, which concentrate on observed

https://doi.org/10.36375/prepare_u.iiche.a405

heritable traits such as DNA sequences, protein amino acid sequences, or morphology, are used to infer these relationships. The results of such an analysis constitute a phylogenetic tree, a diagram with a hypothesis of relationships that represents the evolutionary history of a group of organisms. The phylogenetic analysis tree is displayed in Fig.6. and the first five identities, the sample was determined to be *Stenotrophomonas maltophilia* (Jacquelyn S. Meisel and Elizabeth A. Grice 2017).

Symbiotic bacterial growth of *S. maltophilia* cultivated on different algae

The influence of the different treatments was positive at biomass concentrations of 0.154, 0.43, 0.8, and 0.637 g/L for *S. maltophilia*, *C. pyrenoidosa* cocultured with *S. maltophilia*, *S. abundans* cocultured with *S. maltophilia* and mixed algae cocultured with *S. maltophilia* obtained on the 15th day of culture, respectively. After the 15th day, the growth of algae decreased, as shown in Fig. 7. The biomass concentration of *C. pyrenoidosa* +*S. maltophilia*, *S. abundans* + *S. maltophilia* and mixed algae +*S. maltophilia* were 2.79-, 5.19-, and 4.13-fold greater,

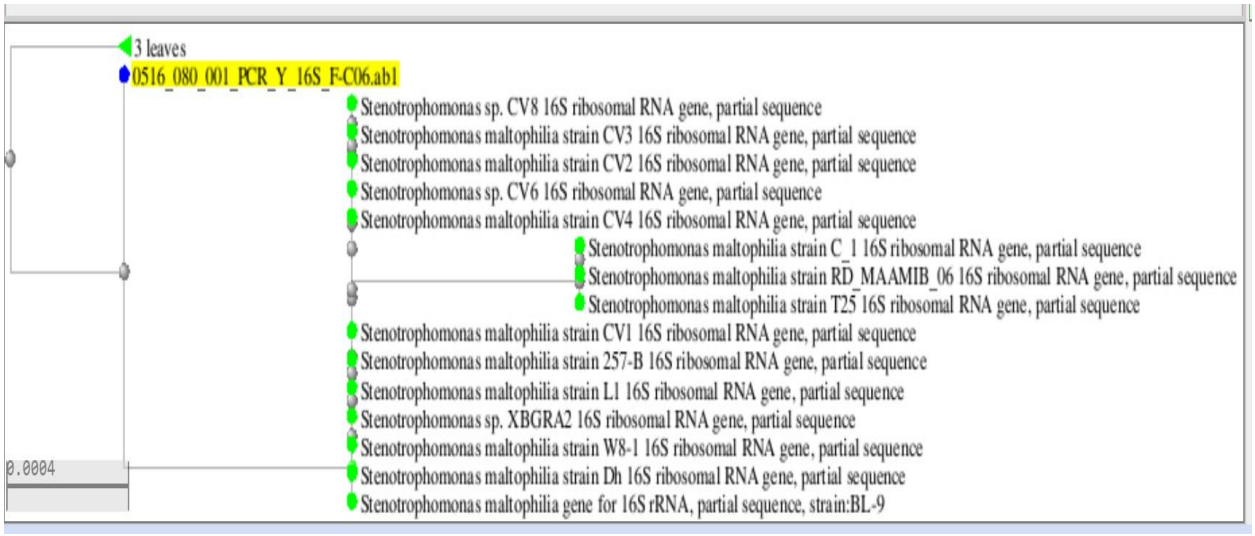

Fig.6 Phylogenic tree of *Stenotrophomonas maltophilia*

https://doi.org/10.36375/prepare_u.iiche.a405

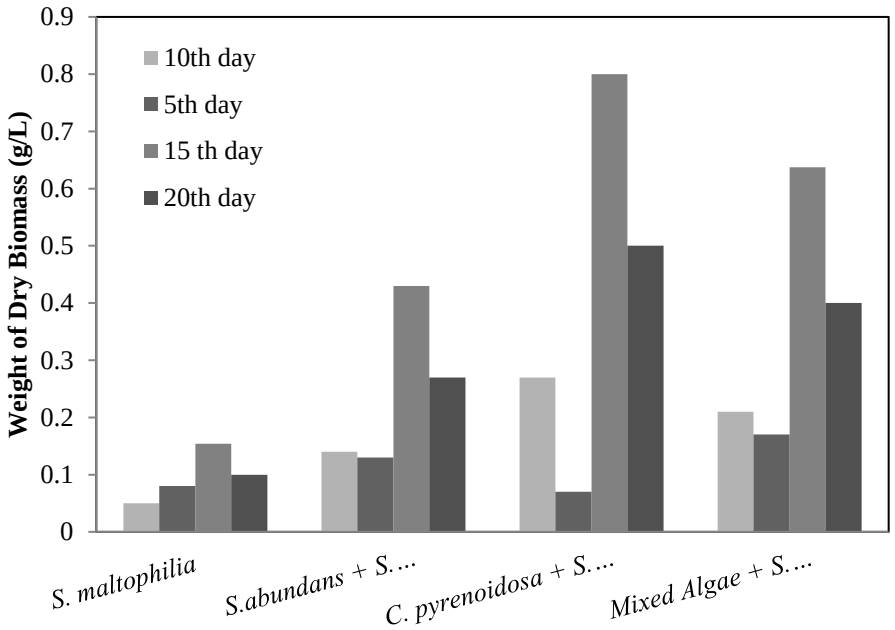

Fig.7. Influence of different treatment conditions such as *S. maltophilia, C. pyrenoidosa*+ *S. maltophilia, S. abundans*+ *S. maltophilia* and mixed algae + Symbiotic bacteria in biomass concentration

respectively. There was evidence that increased biomass production was obtained from *S. abundans* cocultured with *S. maltophilia, as* shown in Fig. 7.

Conclusion

The bacteria isolated from algae culture were subjected to microbial plating methods, and sustainable bacteria were taken for further study of algae cultivation. The standard yellow colony supports the growth of algae biomass production. Therefore, identification of bacterial cultures was performed using the 16S rRNA-based molecular technique. The results showed that 99% of the isolated and sustainable bacterial sequences matched *S. maltophilia.* Furthermore, the strain was deposited in the NCBI database. The increase in biomass production from algae was found for algae mixed with bacteria, and the corresponding lipid production was 4.13-fold. Hence, this study confirmed that *S. maltophilia*is an apt symbiotic bacterium for algae growth and lipid production.

Acknowledgements

The authors are grateful to the National Institute of Technology, Trichy, for providing the

necessary funds and facilities to carry out this research.

Author details

[1]Dr. C. Chellamboli, [2]Dr. M. Perumalsamy, [3]Mr. Dhinesh Kanna R, Bioseparation lab, Department of Chemical Engineering, National Institute of Technology, Tiruchirappalli – 620015, Tamil Nadu, India. Tel: 9489799295; Fax: +91-431-2500133; email:c.chilambu@gmail.com. The electronic supplementary information (ESI) is available: [The native format of the figures has also been uploaded].

Reference

1. Addgene (2018) Protocols, Agarose Gel Electrophoresis. https://www.addgene.org/protocols/gel-electrophoresis/
2. Adegoke AA, Stenström TA, Okoh AI (2017) *Stenotrophomonas maltophilia* as an Emerging Ubiquitous Pathogen: Looking Beyond Contemporary Antibiotic Therapy. Front. Microbiol 8: 2276.
3. Banerjee A, Sharma R, Chisty Y and Banerjee UC (2002) *Botryococcus braunii*: A renewable source of hydrocarbons and other chemicals. Critical Rev. Biotechnol 22(3):245-279.
4. Barnwal BK, Sharma MP (2005) Prospects of biodiesel production from vegetable oils in India. Renew Sust Energ Rev 9:363-398.
5. Borowitzka Armin M, Moheimani Reza N (2013) Algae for Biofuels and Energy Developments in Applied Phycology 5. In: Borowitzka, M.A., Ed., Algae for Biofuels and Energy, Preface, Springer Dordrecht Heidelberg New York London.http://dx.doi.org/10.1007/978-94-007-5479-9
6. Borowitzka MA (1988) Vitamins and fine chemicals from microalgae. In: Borowitzka, M.A, Borowitzka, L.J, editors. Microalgal Biotechnology. Cambridge University Press, Cambridge 153-196 .
7. Brennan L, Owende P (2010) Biofuels from microalgae–a review of technologies for production, processing, and extractions of biofuels and coproducts. Renew Sust Energ Rev 14:557-577.
8. Brooke JS (2021) Advances in the Microbiology of *Stenotrophomonas*

maltophilia. Clin. Microbiol. Rev 34: e0003019

9. Chellamboli C, Perumalsamy M (2014) Application of response surface methodology for optimization of growth and lipids in *Scenedesmus abundans* using batch culture system. RSC Advances 4 (42): 22129-2214.
10. Chellamboli C, Perumalsamy M, (2016) Synergistic Effect of Hormones and Biosolids on *Scenedesmus abundans* for Eliciting Total Biolipids. Water Environment Research 88 (11):2180-2190.
11. Chellamboli C, Perumalsamy M, (2017) *Stenotrophomonas maltophilia* Strain Identification using 16S sequence of rRNA based molecular technique. NCBI GenBank: KX768757. https://www.ncbi.nlm.nih.gov/nuccore/KX768757
12. Chisti Y (2007) Biodiesel from microalgae. Biotech. Adv 25:294-306.
13. Chisti Y (2012) Raceways-based production of algal crude oil. In: Posten, C., Walter, C. (Eds.), Microalgal Biotechnology: Potential and Production. deGruyter, Berlin 113-146.
14. Chisti Y (2013) Constraints to commercialization of algal fuels. J Biotechnol 167: 201-214.
15. Gajdács M, Urbán E (2019) Prevalence and Antibiotic Resistance of *Stenotrophomonas maltophilia* in Respiratory Tract Samples: A 10-Year Epidemiological Snapshot.Health Serv. Res. Manag. Epidemiol 6:2333392819870774.
16. Griffiths MJ, Harrison STL (2009) Lipid productivity as a key characteristic for choosing algal species for biodiesel production. J Appl Phycol 21:493-507.
17. Ho SH, Ye X, Hasunuma T, Chang JS, Kondo A (2014) Perspectives on engineering strategies for improving biofuel production from microalgae — a critical review. Biotechnol. Adv 32 (8):1448–1459.
18. Hu Q, Sommerfeld M, Jarvis E, Ghirardi M, Posewitz M, Seibert M and Darzins A (2008) "Microalgal triacylglycerols as feedstocks for biofuel production: perspectives and advances. Plant J 54:621-639.
19. Huang XF (2016) Culture strategies for lipid production using acetic acid as sole carbon

source by *Rhodosporidium toruloides*. Bioresour. Technol 206:141-149.

20. Illman AM, Scragg AH, Shales SW (2000) Increase in *Chlorella* strains calorific values when grown in low nitrogen medium. Enzyme Microb Technol 27(8): 631-635.
21. Jacquelyn S. Meisel, Elizabeth A. Grice (2017) Chapter 4 - The Human Microbiome. Editor(s): Geoffrey S. Ginsburg, Huntington F. Willard,vGenomic and Precision Medicine (Third Edition),Academic Press 63-77.
22. Jill E. Clarridge, III (2004) Impact of 16S rRNA Gene Sequence Analysis for Identification of Bacteria on Clinical Microbiology and Infectious Diseases. Clin Microbiol Rev. 17(4): 840–862.
23. Khan MS, Zaidi A, Wani PA, Ahemad M, Oves M (2009) Functional diversity among plant growth-promoting rhizobacteria. In: Khan MS, Zaidi A, Musarrat J (eds) Microbial strategies for crop improvement. Springer, Berlin, 105-132.
24. Klein-Marcuschamer D, Chisti Y, Benemann JR, Lewis D (2013) A matter of detail: assessing the true potential of microalgal biofuels. Biotechnol Bioeng 110:2317-2322.
25. Leung DYC, Wu X, Leung MKH (2010) A review on biodiesel production using catalyzed transesterification. Appl. Energy 87:1083-1095.
26. Maha A. Rakaz, Mohammed O. Hussien, Hanan M. Ibrahim (2021) Isolation, Extraction, Purification, and Molecular Characterization for Thermostable α-Amylase from Locally Isolated Bacillus Species in Sudan. Biochem Res Int 6670380.
27. Malcata FX (2011) Microalgae and biofuels: a promising partnership?. Trends Biotechnol 29:542-549.
28. Marousek J, Maroušková A, Gavurová B, Tuček D, Strunecký O (2023) Competitive algae biodiesel depends on advances in mass algae cultivation. Bioresource Technology 374:128802.
29. Pate RC (2013) Resource requirements for the large-scale production of algal biofuels. Biofuels 4:409-435.
30. Pettipher GL, Wang HH (2005) Microbiological Techniques. Editors: Paulworsfold Alan Townshend Colin Poole, In Encyclopedia of Analytical Science

(Second Edition), Elsevier Academic Press, London, pp 16-24.

31. Ponnuswamy I, Soundararajan M, Syed PS (2013) Isolation and characterization of green microalgae for carbon sequestration, waste water treatment and bio-fuel production. Int J Bio-Sci Bio-Techno 5:17-26.
32. Ranjan R, Asha Rani, Ahmed Metwally, Halvor S. McGee, and David L. Perkins (2016) Analysis of the microbiome: Advantages of whole genome shotgun versus 16S amplicon sequencing",Biochem Biophys Res Commun 469(4): 967–977.
33. Rodolfi L, Chini ZG, Bassi N, Padovani G, Biondi N (2009) Microalgae for oil: strain selection, induction of lipid synthesis and outdoor mass cultivation in a low-cost photobioreactor. Biotechnol Bioeng 102:100-112.
34. Rühl C (2008) Bp statistical review of world energy. London*: BP*.
35. Sanders ER (2012) Aseptic Laboratory Techniques: Plating Methods.J Vis Exp 63: 3064.
36. Tica S, Filipovic S, Zivanovic Pand Milovanovic B (2010) Test run of biodiesel in public transport system in Belgrade. Energ Policy 38:7014-7020.
37. Ulgiati S (2001) A comprehensive energy and economic assessment of biofuels: when green is not enough. Crc Crit Rev Plant Sci 20:71-106.
38. Vyas AP, Verma JL, Subrahmanyam N (2010) A review on FAME production processes. Fuel 89:1-9.
39. Walt Ream, Bruce Geller, Janine Trempy, Katharine Field (2013) Molecular Microbiology Laboratory, Second Edition https://doi.org/10.1016/C2011-0-07599-3
40. Walt Ream, Bruce Geller, Janine Trempy, Katharine Field, (2013) Polymerase Chain Reaction and DNA Sequence Analysis of Bacterial Ribosomal RNA Genes. Editor(s): Walt Ream, Bruce Geller, Janine Trempy, Katharine Field, Molecular Microbiology Laboratory (Second Edition), Academic Press, pp 43-70,
41. Weisburg WG, Barns SM, Pelletier DA, Lane DJ (1991) 16S ribosomal DNA amplification for phylogenetic study. Journal of Bacteriology 173(2):697–703. http://doi.org/ 10.1128/jb.173.2.697-703.

42. World Energy Outlook, (2007). The International Energy Agency (IEA).
43. Zafar AM, Javed MA, Aly Hassan A, Mehmood K, and Sahle-Demessie E (2021) Recent updates on ions and nutrients uptake by halotolerant freshwater and marine microalgae in conditions of high salinity. J. Water Process Eng 44:102382
44. Zhang S, Zhang L, Xu G, Li F, Li X (2022) A review on biodiesel production from microalgae: Influencing parameters and recent advanced technologies. Front. Microbiol., Sec. Microbiotechnology 13:970028 doi: 10.3389/fmicb.2022.970028

https://doi.org/10.36375/prepare_u.iiche.a406

Advanced Energy Storage Solutions: Innovative Approaches to Microencapsulation of Phase Change Materials

Naveen Jose[1*], Menon Rekha Ravindra[2], Deb Prasad Ray[3]

[1]*Scientist, C&BP Division, ICAR-National Institute of Natural Fibre Engineering and Technology, Kolkata-700040*
[2]*Principal Scientist, ICAR-National Dairy Research Institute-SRS, Bengaluru-560030*
[3]*Principal Scientist and Head, C&BP Division, ICAR-National Institute of Natural Fibre Engineering and Technology, Kolkata-700040*

*Corresponding author: Naveen Jose, naveenjose50@gmail.com, +919400569023

Abstract

Phase change materials (PCMs) represent a significant innovation in thermal energy storage systems, enabling the controlled absorption and release of energy as needed by a system. PCMs find extensive application across various domains, including but not limited to buildings, textiles, electronic devices, and heat management for batteries. These materials are favored for their remarkable qualities, such as high energy storage density, cost-effectiveness, reusability, minimal interference with the system, and adaptability to a wide range of temperatures. However, the application of PCMs often encounters challenges related to leakage when exposed to different environments. Microencapsulation emerges as a viable technique to safeguard PCMs against external factors and leakage issues, while preserving their thermal energy storage capabilities. Over time, numerous physical and chemical methods have been developed to produce microcapsules with robust mechanical integrity and long-term stability. Nonetheless, none of these methods can deliver Microencapsulated Phase Change Materials (MEPCMs) with all the desired properties. To fully harness the potential of MEPCMs, there is a need for innovative techniques that enhance their structural stability and extend their service life. Existing approaches may require modifications, such as the incorporation of nanoparticles and binding materials, to improve their overall performance. This paper offers an overview of PCM types and shell materials used for encapsulation, common microencapsulation methods, and the characterization techniques employed to

https://doi.org/10.36375/prepare_u.iiche.a406

assess the properties of developed MEPCMs. Furthermore, the paper delves into the limitations and advancements in this field, shedding light on the evolving landscape of PCM encapsulation technology.

Keywords: Microencapsulation, Phase change materials, thermal energy storage, properties

1. Introduction

Phase Change Materials (PCMs) represent one of the most prevalent energy storage systems, where processes like melting, sublimation, and vaporization absorb heat from the surroundings, while solidification or condensation release heat into the system when required. Encapsulation has emerged as a widely employed technique for large-scale PCM applications, as it provides notable benefits such as increased heat transfer area, reduced corrosion, control of volume change during phase transitions, and improved compatibility with the surrounding environment. Depending on the size of the capsules produced, encapsulation is categorized into three classes: Macroencapsulation (1 mm to 1 cm), Microencapsulation (1 μm to 1 mm), and Nanoencapsulation (< 1 μm). Among these, microencapsulation is the most commonly employed method due to its superior stability and ease of preparation when compared to nanoencapsulation. PCMs find applications in a variety of fields, including buildings, textiles, food packaging, and heating and cooling systems. The incorporation of Microencapsulated Phase Change Materials (MEPCMs) into textiles and building materials enhances thermal mass for energy storage without significantly increasing the overall mass of the structure. PCMs are currently being used in absorption refrigeration, air conditioning, and cold energy storage systems for cooling applications in buildings. Microencapsulated Phase Change Material Slurries (MPCS) have also gained prominence, as they involve encapsulated PCMs blended with a carrier fluid, serving as a secondary refrigerant in cooling applications. This innovative approach contributes to increased energy efficiency and reduces the demand for traditional refrigerants, aligning with the imperative for sustainable and environmentally friendly energy practices [1].

https://doi.org/10.36375/prepare_u.iiche.a406

2. Phase Change Materials (PCM)

Phase Change Materials (PCMs) represent the predominant choice among Thermal Energy Storage (TES) systems, effectively absorbing and subsequently releasing energy as needed. Their versatility in storing both latent and sensible heat makes them an ideal component for energy storage. The total heat content stored can be quantified using the formula established by Raj and Goswami (2018, [2]):

$$Q = m\left[\left\{\int_{T_s}^{T_m} C_{ps}dt\right\} + \Delta h_m + \left\{\left\{\int_{T_m}^{T_i} C_{pl}dt\right\}\right\}\right] \quad (1)$$

Phase transitions in PCMs typically occur in response to pressure, strain, light, or heat stimuli and manifest in four distinct forms: Solid-Liquid, Solid-Solid, Solid-Gas, and Liquid-Gas. Solid-solid transitions involve minimal volume changes and do not necessitate encapsulation techniques but are characterized by lower heat transfer efficiency. During these transitions, PCMs may undergo structural changes, such as lattice configuration conversions, with minimal physical alterations, leakage, or supercooling. In the context of building applications, PCMs exhibiting significant volume changes, such as Solid-Gas and Liquid-Gas transitions, are unsuitable as they may compromise the structural integrity of buildings. Additionally, these PCMs may generate high internal pressure, affecting the mechanical stability of the application [3].

PCMs undergoing Solid-Liquid and Solid-Gas transitions are challenging to handle without protective encapsulation, as they may leak into the surrounding system. Ideal PCM characteristics can be categorized into three main requirements: physical, chemical, and economic. The physical prerequisites for a suitable PCM encompass high thermal conductivity (K), a high specific heat capacity (C_p), phase change temperatures within the desired range with minimal supercooling, complete reversibility of the melt/freeze cycle, favorable phase equilibrium, low vapor pressure during operation, and a sufficient rate of crystallization. Key chemical requisites include excellent physical and chemical stability over repeated cycles, low vapor pressure, absence of supercooling and sub-cooling, flame resistance,

https://doi.org/10.36375/prepare_u.iiche.a406

non-hazardous properties, absence of explosive compounds, corrosion resistance when encapsulated, high compatibility with surrounding materials, and non-incongruent melting. From an economic perspective, ideal PCMs should be abundant, cost-effective, reusable, and recyclable [4].

The functionality of PCMs revolves around heat exchange, wherein they absorb and store latent heat energy from the system, subsequently releasing it to the environment during crystallization or reverse cooling [5]. Temperature fluctuations in PCMs during crystallization and melting stages are minimal. The chemical bonds within the PCM material break as they absorb heat from the system during temperature increases, and these bonds are restored during the crystallization process, releasing the absorbed energy [6].

Various methods exist for integrating PCMs into applications, including encapsulation, shape-stabilization, immersion, and direct incorporation. Encapsulation entails containing the PCM within a suitable shell material, while shape stabilization embeds the PCM onto a compatible supporting material. Immersion and direct incorporation methods are more prone to leakage issues.

3. Classification of PCM

PCMs can be generally classified into three broad categories: inorganic, organic and eutectics.

3.1. Inorganic

Inorganic Phase Change Materials (PCMs) are popular alternatives to organic PCMs, offering several key advantages, such as high thermal conductivity, substantial phase change enthalpy, small volume change during phase transition, cost-effectiveness, non-flammability, recyclability, and a high latent heat capacity. However, they do present challenges, including potential corrosiveness to metals, supercooling, phase segregation, toxicity, decomposition, incompatibility with construction materials, dehydration, incongruent melting, limited nucleation ability, and a relatively narrow temperature range of application [7].

https://doi.org/10.36375/prepare_u.iiche.a406

3.1.1. Salt Hydrates: Among inorganic PCMs, salt hydrates stand out as an economical option. They are readily available as by-products from various industrial processes, with minimal volume changes (less than 1%) during phase transition. While they exhibit high density (around 1640 kg/m^3), their heat of fusion can reach up to 296 kJ/kg, and they boast a thermal conductivity of 0.6 W/mK, making them suitable for a wide range of applications. Salt hydrates typically have a transition temperature range of 25-34°C, making them particularly useful in comfort cooling applications. Challenges with salt hydrates include incongruent melting and supercooling, but they demonstrate mechanical and thermal stability during repeated cycling. Techniques like altering chemical composition, mechanical stirring, and introducing nucleating and thickening agents helps to mitigate these issues. While salt hydrates exhibit slightly lower thermal conductivity and a less degree of toxicity, they remain a practical choice. Commonly used salt hydrates include Lithium metaborate octahydrate, Magnesium nitrate hexahydrate, Calcium chloride hexahydrate, and others [8].

3.1.2. Low Melting Point Metals: Low melting point metals and alloys, known for their high thermal conductivity and heat transfer capabilities, are valued for their exceptional heat storage capacity per unit volume due to their inherent high density. Their benefits include non-flammability, minimal volume change during phase transition, high boiling points (>2000°C), reduced vapor pressure, and high latent heat values due to strong intermolecular bonding. However, cost considerations, as well as their elevated thermal and electrical conductivities, which can lead to rapid energy release, can pose challenges. Corrosion with the surrounding environment is another concern. Common low melting point metals include Rubidium, Gallium, and Caesium, while eutectic alloys like Lead, Cadmium, Indium, Bismuth, and Tin are also utilized. These metals find applications in cooling systems for devices such as smartphones, USB flash drives, and laser systems [9].

3.2. Organic

Organic PCMs have gained widespread recognition in contemporary applications. Their

notable advantages include corrosion resistance, low toxicity, good compatibility with building materials, minimal volume changes, reduced issues like super-cooling and phase segregation, and excellent thermal and chemical stability with high thermal energy storage capacity. However, drawbacks include low thermal conductivity, low enthalpy of phase change, volatility, flammability upon heating, higher cost compared to inorganic PCMs, and significant volume changes, especially in the case of paraffin compounds [10].

3.2.1. Paraffin Waxes: Paraffin waxes, among the most economical PCM sources, are frequently used for microencapsulation. They possess self-nucleating ability, no super-cooling effects, a high latent heat of fusion (over 250 kJ/kg), and a density of 0.93 kg/m^3. Paraffin waxes offer a broad melting point range (-5 to 76°C) and maintain their thermal storage ability through repeated cycles, making them suitable for both active and passive cooling of buildings. While their thermal conductivity is low (0.2-0.4 W/mK), this can be advantageous for insulation in building applications [11]. Paraffin's thermal conductivity can be further reduced using shell materials with low thermal conductivity, such as plastic polymers. Fire-resistant shell materials can address the low flash point concern (108-170°C) of paraffin waxes. Paraffin can also be blended with various materials to enhance structural and thermal properties [12,13].

3.2.2. Organic Non-Paraffins (Fatty Acids): Fatty acids are chosen as PCMs due to their abundant natural availability and cost-effectiveness compared to metal PCMs. They exhibit a high heat of fusion (up to 25 kJ/kg) and have a wide melting point range (7.8 to 127.2°C). Their low thermal conductivity (0.14 to 0.17 W/mK) makes them suitable for thermal insulation applications [14]. They typically have minimal super-cooling tendencies and may undergo solid-solid phase transitions in some cases. However, fatty acids have low flash points, making them susceptible to ignition. Impurities can affect their melting points, so pure fatty acids are essential for optimal thermal properties. They are less resistant to oxidizing agents, high temperatures, and flames, and some can be toxic and produce harmful fumes.

https://doi.org/10.36375/prepare_u.iiche.a406

Commonly used fatty acids include stearic acid, palmitic acid, myristic acid, lauric acid, caprylic acid, capric acid, oleic acid, chosen based on specific application requirements [8].

3.3. Eutectics

Eutectic PCMs are typically comprised of a blend of two components with distinct melting points. Each component within this mixture exhibits congruent melting and freezing processes, forming crystals of the compound mixture. A notable advantage of eutectic PCMs is the ability to adjust the mixture's melting point to specific requirements by modifying the composition of each compound. These PCMs are known for their high energy storage density and thermal conductivity, with no congruent phase change and a lack of super-cooling effects. However, they have relatively low specific and latent heat capacities. One significant challenge is their potential for phase separation during repeated cycling, which can impact the thermo-physical properties of the eutectic mixture. Additionally, some eutectic blends may experience super-cooling issues. These materials tend to be relatively costly, and there is limited literature available on their thermo-physical properties [7, 15].

4. General Properties of PCM

Hydrated salts have high thermal conductivity and a high heat of fusion, making them suitable for certain applications. However, they are corrosive, with a melt temperature range from 0 to 100ºC. Metallic PCMs have very high thermal conductivity and medium heat of fusion. They are heavy and stable over thermal cycling, making them suitable for applications requiring stability. However, their high cost can be a drawback. Paraffin PCMs have very low thermal conductivity, but they have a high heat of fusion. They are not corrosive and have a moderate weight, and they are stable over thermal cycling. Paraffins are cost-effective and have a melt temperature range from -20 to 100ºC. Non-paraffin PCMs have low thermal conductivity and a high heat of fusion. They are mildly corrosive and have a moderate weight. While they are stable, they may decompose at high temperatures. However, they tend to be very costly [8].

https://doi.org/10.36375/prepare_u.iiche.a406

5. Microencapsulation of PCM

A significant challenge when using phase change materials (PCMs) in various applications is the potential for leakage during phase transitions, which can reduce the material's effectiveness. Conventional PCMs also encounter issues like sub-cooling, decomposition, and corrosion [16]. To address these problems, encapsulation techniques are commonly employed to shield PCMs from external interactions. Encapsulation can occur at different scales: Macroencapsulation, microencapsulation, and nanoencapsulation. Microencapsulation, in particular, involves covering fine particles or droplets with a coating to create microcapsules. What makes microencapsulation widely accepted is its ability to encapsulate all states of matter (solid, liquid, and gas) using appropriate shell materials [17]. This method simplifies the handling of gases and liquids, making PCMs more versatile in various applications. Microencapsulation offers several advantages, including increased heat transfer area, reduced interactions between PCMs and the environment, and control over the volume changes that occur during phase transitions. The key to successful microencapsulation is the uniform and stable formation of the shell around the core, preventing internal component leakage. While microencapsulation is often used in fields aiming for targeted component release, in the case of microencapsulated PCMs (MEPCMs), the core must remain permanently enclosed within the shell, regardless of external forces [18].

5.1. Core and Shell materials for microencapsulation

The core material of microencapsulated phase change materials (MEPCMs) typically consists of phase change materials that undergo a process of absorbing and releasing energy during phase changes. The selection of the shell material is based on its compatibility with the core material and the surrounding environment. In heat transfer applications, a high thermal conductivity shell material is crucial to enhance heat performance [19]. Generally, inorganic materials exhibit higher mechanical strength and thermal conductivity compared to organic materials. MEPCMs can take on different

https://doi.org/10.36375/prepare_u.iiche.a406

structures depending on the core, shell, and encapsulation method used, including a single core enveloped by a continuous shell, multiple cores within a continuous shell, uniform dispersion of core material within the shell, and core coated with multiple layers of shell material (multi-walled capsules). Shell material stability is crucial for efficient encapsulation, as the shell should be strong enough to withstand stresses and phase change-induced volume changes [17]. Key requirements for shell materials include good barrier properties, protection from external environmental interactions, high-temperature applicability, corrosion resistance, mechanical strength, flexibility, ease of handling, and stable structure. Furthermore, shell materials should provide ample surface area for heat transfer, exhibit good thermal conductivity and diffusivity, remain inert to both the core material and the application environment, and withstand volume changes during phase transitions while remaining readily available, durable, and cost-effective.

Commonly used shell materials fall into several categories [20]:

5.1.1. Metallic Shell Materials: Used in very high-temperature applications, they offer high thermal stability, mechanical strength, and ease of fabrication, remaining intact even at temperatures up to 1000°C. However, they can be costly and susceptible to corrosion.

5.1.2. Organic Shell Materials: Frequently used for microencapsulating phase change materials, these materials are not suitable for heat transfer applications due to their poor thermal conductivity. However, they are widely employed for thermal insulation. Common materials include urea-formaldehyde (UF), melamine-formaldehyde (MF), polyurea, and acrylic resins. Organic shells offer good mechanical stability and resistance to volume changes during phase transitions.

5.1.3. Inorganic Shell Materials: Suitable for high-temperature applications, such as power generation and cement manufacturing, inorganic materials offer good mechanical strength, heat transfer performance, and thermal stability up to 1000°C. They are cost-effective compared to metallic shells. The main drawback is the porosity of the shell, which can lead to internal

https://doi.org/10.36375/prepare_u.iiche.a406

material leakage. Common inorganic shell materials include silica (SiO_2), sodium silicate, titanium dioxide, and calcium carbonate, with silicon dioxide being the most widely used. Surface modification is achievable with silica-based shell materials, and they are useful for controlling the flammable nature of organic core materials.

5.1.4. Hybrid Shell Materials: These materials combine both inorganic and organic elements to create superior stability and thermal conductivity. Incorporating nanoparticles of silver, iron, and silicon nitride into organic shells can enhance their characteristics. However, poor binding between the inorganic and organic components can be an issue, leading to detachment during repeated cycling. Techniques such as chemical hybridization can help mitigate this problem [21].

5.1.5. Plastics: Widely used due to their ease of fabrication and cost-effectiveness, plastics offer various physical and chemical methods for encapsulation. However, their poor thermal conductivity and limited thermal stability, up to a maximum of 400°C, can be limiting factors. Plastics are commonly used in applications like cooling of buildings, paper and food manufacturing, among others.

5.2. Various methods of microencapsulation

Selecting the appropriate core and shell materials and the most suitable method for creating effective microcapsules are crucial in developing high-quality microencapsulated phase change materials (MEPCMs). The choice of microencapsulation method is influenced by various factors, including cost, scalability, regulatory compliance, environmental impact, and health considerations [22]. The most commonly employed methods for microencapsulation include chemical methods, physico-chemical methods, and physico-mechanical methods. These methods often involve two key stages: emulsification and capsule formation. In emulsification, PCMs are finely dispersed in an aqueous phase, impacting the particle distribution and microcapsule size. The subsequent capsule formation stage relies on the cross-linking ability of the shell material surrounding the core. The type and amount of

surfactant play a significant role in determining the size, stability, and formation process of microcapsules [23, 24]. Physical methods are also employed, but they tend to produce larger particles, typically above 100 μm, which may not be suitable for all applications.

5.2.1. Emulsion polymerization: Chemical methods, such as emulsion polymerization, are widely used for producing MEPCMs. For instance, in emulsion polymerization, which is also known as the solvent evaporation technique, the entire process consists of four stages. The core material is initially dispersed in a solvent, which is then emulsified in the presence of a surfactant in an aqueous phase. Subsequently, the solvent is evaporated, resulting in the formation of droplets around solid particles. In the final stage, the obtained solid particles are oven or vacuum dried to yield fine microencapsulated powders. The choice of solvent plays a crucial role, with properties like low toxicity, low boiling point, immiscibility with water, and high volatility being desirable. Dichloromethane has largely replaced the previously used chloroform. The particle size typically ranges from 0.5 to 5 μm, with an encapsulation ratio between 7% and 75% [25].

5.2.2. Dispersion polymerization: It is a straightforward single-stage method where reaction time, monomer and initiator amounts, and stabilizer concentration influence the final product's characteristics. Commonly encapsulated materials via this technique include alcohols, styrene in hydrocarbons, or alcohol mixtures with ether/water. This method allows for the successful encapsulation of hydrophilic core materials, such as PVA [26,27].

5.2.3. Suspension polymerization: This method is known for its cost-effectiveness and improved heat control during the entire process. The process involves mechanisms like monomer diffusion to the interface, secondary nucleation, particle break-up, and coalescence. These mechanisms collectively determine the properties, structure, and size of the resulting microcapsules [28]. The particle size can be estimated using a formula involving factors such as stirring speed, reaction temperature, and shell-to-core material ratio [29]. Parameters like stirring speed, temperature, and shell-to-core

material ratio directly affect the thermal properties of the MEPCM.

5.2.4. Interfacial polymerization: It is a technique where an aqueous phase is prepared by dissolving the core material and various ratios of emulsifiers and stabilizers. The organic phase is then dispersed into the component-rich aqueous phase. This method can produce larger microcapsules, with sizes ranging from 20 to 30 μm in most industrial processes [30]. The solvent used for the core material should be non-reactive, and the first monomer should contain at least two organic compounds. The production parameters are easily controlled, and the maximum temperature reached during the process is around 80°C, which has a minimal impact on the PCMs [31]. However, the process has limitations, as most carrier materials are non-biocompatible and the organic solvents can contaminate the environment.

5.2.5. In situ polymerization: A three-stage process used to create microcapsules with shell materials like melamine-formaldehyde and urea-formaldehyde. This method is ideal for encapsulating a wide range of organic compounds as core materials [18]. The process begins with the formation of an oil-in-water emulsion containing the melted PCMs. Surfactants are added to stabilize the emulsion, and the emulsion is then stirred vigorously at a higher temperature. A cross-linking agent and nucleating agents are incorporated in the later stages. Maintaining a slightly acidic pH initiates the polycondensation reaction. The final microencapsulated material is then processed, cooled, washed, filtered, and dried to produce fine powdered MEPCMs [22, 32]. The size of the microcapsules ranges from 2 to 2000 μm. The reaction time is relatively short for polymers with high inherent reactivity, and this process results in uniformly coated microcapsules [25].

Physico-chemical methods offer a variety of techniques for microencapsulation of phase change materials (PCMs):

5.2.6. Sol-Gel Process: This technology, primarily used for silica shell development around PCMs, involves four stages. PCMs are initially emulsified with surfactants, creating an oil-in-water emulsion. In a separate sol solution, precursor materials for the shell (like

tetraethoxysilane for silica) are dispersed in an acidic environment. The sol solution is slowly added to the emulsion under continuous heating and stirring. Shell formation occurs through polycondensation reactions. The resulting microcapsules are then filtered, washed, and dried. The process yields microcapsules with narrow particle size distribution (0.2-20 μm). While silica and titanium dioxide are common shell materials, high thermal conductivity can pose issues for building applications [25].

5.2.7. Coacervation: This older encapsulation technique includes simple and complex coacervation. In both cases, the process unfolds in three stages: first, core and shell material solutions are emulsified to create an oil-in-water emulsion. Then, oppositely charged colloidal solutions are added, causing the deposition of a polymer coating over the core. Adjusting pH is followed by thermal or chemical cross-linking for shell hardening. The product is cooled for further polymerization, recovered, and harvested as MEPCM. The particle size is efficiently controlled in this process, with factors such as core-to-coating ratio, emulsification time, and cross-linking agent quantity influencing efficiency. However, scaling up to an industrial process can be challenging [33].

***5.2.8. Supercritical CO_2-assisted Process*:** This method, used for essential oil extraction and more recent for encapsulating materials, which involves dynamic and static processes. In dynamic processing, the solution with the core material is premixed with supercritical CO_2 and rapidly expanded in a drying chamber. The static process features continuous mixing in low volume, expanding to atmospheric pressure after passing through a flow restrictor. The rapid expansion results in quick solvent evaporation and drying. This method is environmentally friendly and uses carbon dioxide as a solvent, offering advantages like non-toxicity and cost-effectiveness [34].

5.2.9. Self-Assembly Method: A cost-effective deposition process, the self-assembly method involves shell materials like Cu, Ca, or Na. In this technique, disordered components in a solution self-assemble into an organized structure through precipitation, forming a solid shell around the core. An oil-in-water emulsion, stabilized by mixed surfactants (commonly

anionic and non-ionic), is created. Drop-wise addition of shell material into the emulsion, while maintaining agitation and temperature control, leads to shell deposition. The precipitated MEPCMs are recovered, washed, and vacuum-dried. Key factors in this process are the selection of surfactants that promote shell self-assembly and control over the precipitation and deposition of precursor materials at the oil-water interface [35].

Physico-mechanical methods offer various techniques for large-scale microencapsulation, but limitations in producing microcapsules smaller than 100 μm exist.

5.2.10. Electrospraying: This novel technology allows the creation of smaller microparticles and even nano-encapsulated PCMs. The technique involves spraying liquid shell and PCM materials onto a collector plate with a high electric field. Two separate syringes feed the materials through different nozzles at varying flow rates, with an adjustable voltage applied across the electrode. The resulting materials are collected, cured, washed, and dried to obtain microcapsules with core retention. It offers rapid, high-efficiency encapsulation with particle diameters ranging from 0.5 to 3 μm [36].

5.2.11. Spray Drying: Widely used and suitable for large-scale production, this method pumps a solution containing PCM, shell material, and a dispersing agent to an atomizer in a drying chamber filled with inert gas. Rotary atomization forms a fine spray, allowing solvent evaporation and the production of MEPCMs as fine powders. The method is versatile, cost-effective on a large scale, and easily scalable, with adjustable particle properties. However, high temperatures may damage the core, leading to particle agglomeration [37].

5.2.12. One-Step Method: This technique, known for self-stabilization and ease of industrial scaling, is versatile for various core materials and particle size tuning. It involves self-assembly, as demonstrated in stable MEPCMs with n-nonadecane as the core and silica as the shell. Self-stabilizing amine groups eliminate the need for additional stabilizers. Although it offers scale-up potential, more

research is needed to enhance the final product's properties.

5.2.13. Air Suspension Coating: Similar to spray drying, this method suspends core materials in an upward-flowing airstream, with shell material sprayed over the suspended particles. The process involves handling around 20 variables, offering low production and large-volume handling capabilities, but it requires skilled labour and is mainly applied in food and pharmaceutical industries, with limited application in the PCM field.

5.2.14. Pan Coating: Used for larger capsules (greater than 600 μm), this technique coats solid core materials with atomized or solution-form shell material, then dries them to remove remaining solvent. Particle sizes of MEPCMs produced range from 600 to 5000 μm. The method's advantages include lower equipment costs, but challenges include low encapsulation efficiency and lengthy processing times [38].

5.2.15. Multi Orifice Centrifugal Process: Suitable for solid and liquid core materials, this process uses centrifugal force to pass the core materials through a membrane material, leading to microcapsule formation. Size varies from 5 to 1500 μm, but the high process temperature may affect heat-sensitive materials, and orifice clogging can be a concern.

5.2.16. Fluid Bed Coating: In this highly efficient coating process, shell material solution is sprayed into a hot, fluidized bed containing solid core materials. Two types, top-spray and bottom-spray coaters, are commonly used on an industrial scale. Both produce microcapsules with varied particle sizes. Proper control during drying is essential to prevent agglomeration [39].

5.3. Comparison of Encapsulation Techniques

The choice of encapsulation techniques is largely influenced by the type of core material and the intended application. It has been observed that as the core-to-shell ratio increases, the efficiency of encapsulation decreases. Methods such as complex coacervation and in-situ polymerization are capable of producing larger MEPCM particles with a high core material content, resulting in good encapsulation efficiency. Conversely, the emulsion or mini-

emulsion polymerization technique is suitable for producing smaller MEPCMs. The smaller particle size is achieved by employing high stirrer speeds (ranging from 1000 to 13500 rpm) during emulsion dispersion and oil droplet formation. However, it's important to note that these techniques are relatively energy-intensive and costly. In contrast, the polymerization process typically operates at lower stirrer speeds (ranging from 300 to 600 rpm) and requires more time for particle generation, often up to 24 hours, especially when using silicon shell materials. Ensuring safety measures is essential to prevent interaction with any unreacted reagents after the cross-linking process. Methods such as self-assembly and the sol-gel method can effectively coat organic core materials with inorganic shell materials, resulting in good thermal properties and flame resistance. However, these inorganic shells may be less flexible compared to polymeric shells. MEPCMs with inorganic PCMs as core materials can only be generated through evaporation or solvent extraction methods. From an economic standpoint, MEPCMs with inorganic cores tend to be more expensive than those with organic cores due to the requirement for expensive solvents during synthesis. Furthermore, there is a risk that some solvents trapped inside the shell may leak out during repeated cycling, which is a notable drawback associated with this method.

Table 1. Properties associated with various encapsulation methods

Method of microencapsulation	Encapsulation efficiency (%)	Core content (%)	Diameter (μm)
Interfacial polymerization	71 – 87	29 – 80	0.5 – 1000
Phase separation method	66 – 75	43 – 75	0.5 – 1000
Emulsion polymerization	82.6	28 – 61	0.14 – 2.0
Complex Coacervation	80 – 95	26 – 67	2 – 1200
Phase separation method	66 – 75	43 – 75	0.5 – 1000
Sol-Gel encapsulation	82.0 – 90.7	46 – 74	2 – 30
Mini-emulsion polymerization	80.0 – 82.2	8 – 60	0.1 – 0.5
Solvent extraction/ Evaporation method methods	56 – 64	43 – 53	0.5 – 10

(Source: Su et al., 2015, [8])

https://doi.org/10.36375/prepare_u.iiche.a406

5.4. Problems with microencapsulation of PCM

While microencapsulation is a widely accepted technique, it comes with certain drawbacks. Microencapsulated Phase Change Materials (MEPCMs) face limitations when employed in repeated cycling processes as thermal fluids due to increased viscosity resulting from the incorporation of larger microcapsules [18]. To address this issue, scientists are exploring Nano encapsulation, which produces smaller Nano-capsules. Supercooling is a common challenge in the widespread application of MEPCMs, where the crystallization temperature within the tiny shell material significantly differs from that in the core material within the shell and in the bulk. This disparity is often attributed to the insufficient number of nuclei within the tiny shell material, impacting the stable thermal application [40, 41]. Using organic materials like paraffin as PCMs presents a reduced thermal conductivity issue, which can be partially alleviated by increasing the heat transfer surface area, typically achieved through encapsulation. However, utilizing organic shell materials during encapsulation can further decrease thermal conductivity, making inorganic shell materials a more ideal choice due to their superior thermal conductivity and mechanical strength. Controlling the release of volatile organic compounds is crucial to maintain microsphere stability and ensure air quality, particularly in building applications. Organic PCMs are more susceptible to emitting these compounds, necessitating comprehensive studies before their application. Variations in particle morphology can also affect heat transfer properties, influenced by the type of emulsifiers used. High HLB value emulsifiers tend to result in agglomerated particles, while low HLB emulsifiers may lead to irregular surfaces with cracks or dents [42]. The choice of cross-linking agents can also impact the surface morphology of MEPCMs [43]. When hydrated salts are employed as MEPCMs, there is a risk of compound degradation during repeated cycling due to water gain or loss, considering their high latent heat energy [25]. The absence of standardized techniques for testing mechanical properties is a notable challenge, as it is essential

to assess MEPCM leakage under pressure and external forces.

6. Advances in microencapsulation of PCM

As previously mentioned, overcoming supercooling is a critical challenge in expanding the practical use of Microencapsulated Phase Change Materials (MEPCMs). Researchers have developed various strategies to address this issue. Supercooling can be partially controlled through the addition of nucleating agents, which induce nucleation within the PCMs, and homogeneous nucleation induced by modifying the structure and composition of the shell material to encourage uniform nucleation. Common nucleating agents include nanoparticles, alcohols, and high freezing point paraffin to prevent supercooling. However, it's important to note that the poor thermal characteristics of the shell material can lead to a reduction in the thermal conductivity, impacting MEPCMs' efficiency. To enhance the thermal conductivity of MEPCMs, nanoparticles are added to the shell materials. Inorganic nanoparticles such as Carbon nanotubes, Graphene, TiO_2, Fe_3O_4, have been widely used to improve thermal conductivity [44, 45]. Traditional polymerization processes often involve high temperatures, which can affect the quality of certain PCMs. Modern low-temperature polymerization methods initiated using UV light have been developed to improve the quality of microspheres formed, although further research is needed in this area.

Despite significant advancements in MEPCMs, some challenges require more thorough investigation. While methods to address supercooling and enhance thermal conductivity have been developed, a well-defined and precise solution is still pending. Determining the lifespan of MEPCMs accurately is essential, and methods for extending their service life should be explored. Leakage issues resulting from reduced mechanical strength with repeated use also demand careful examination. In the case of slurries containing dispersed MEPCMs subjected to high shear forces during pumping, their stability during repeated cycling should be studied. Additionally, investigating the use of mixtures with varying melting points in the

microencapsulation process could expand the temperature range and improve melting and solidifying properties [46]. It is crucial to design shell materials with high strength and temperature compatibility for high-temperature applications.

In efforts to mitigate supercooling issues, researchers have introduced nanoencapsulation techniques, which offer enhanced stability compared to microcapsules due to their smaller size and a lack of increased viscosity in the dispersion medium [47,48]. Nano-encapsulated Phase Change Materials (NEPCMs) are typically synthesized using methods like sol-gel, emulsion polymerization, and interfacial polymerization. These approaches have shown promising results in reducing supercooling problems associated with PCMs [49].

7. Conclusion

Microencapsulated Phase Change Materials (MEPCMs) represent an innovative approach to the realm of phase change materials, significantly enhancing their utility across various fields as a stable and effective solution. This technology involves creating stable microspheres that encapsulate core materials, thereby improving thermal, chemical, and physical stability. Common microencapsulation methods for PCMs include complex coacervation, sol-gel processes, in-situ and interfacial polymerization, spray drying, emulsion and suspension polymerization. The selection of a particular method is typically tailored to the specific application, core and shell material types, desired MEPCM size, and required physical, mechanical, and thermal properties. A wide range of materials has been successfully encapsulated using diverse shell materials through these processes, with designs tailored to meet specific application needs. MEPCMs can be applied in both high and low-temperature applications, depending on the choice of core and shell materials. Rigorous testing is essential to ensure that the produced microcapsules maintain quality and stability during repeated cycling. The MEPCM field has been gaining popularity due to its broad applicability, high stability, and extended service life. Various sectors, including waste heat recovery, building heating and cooling systems,

electronics, textiles, packaging materials, heat pumps, and fabrics, benefit from the use of MEPCMs. Challenges such as supercooling and instability need to be addressed systematically to foster sustainable PCM development. Mitigating these issues can be achieved through the incorporation of nanoparticles, the development of nanoencapsulation techniques, and the utilization of multi-phase core materials. It is imperative to focus on continued research and investment in this industry to maximize energy recovery and reuse.

References

1. Zhang, H., Wang, X., & Wu, D. (2010). Silica encapsulation of n-octadecane via sol-gel process: a novel microencapsulated phase-change material with enhanced thermal conductivity and performance. *Journal of Colloid and Interface Science*, *343*(1), 246–255. https://doi.org/10.1016/J.JCIS.2009.11.036
2. Goswami, T. K., & Raj, V. (2018). Use of phase change material (PCM) for the improvement of thermal performance of cold storage. *MOJ Current Research & Reviews* , *Volume 1*(Issue 2), 49–61. https://doi.org/10.15406/MOJCRR.2018.01.00010
3. Akeiber, H., Nejat, P., Majid, M. Z. A., Wahid, M. A., Jomehzadeh, F., Zeynali Famileh, I., Calautit, J. K., Hughes, B. R., & Zaki, S. A. (2016). A review on phase change material (PCM) for sustainable passive cooling in building envelopes. *Renewable and Sustainable Energy Reviews*, *60*, 1470–1497. https://doi.org/10.1016/j.rser.2016.03.036
4. Giro-Paloma, J., Martínez, M., Cabeza, L. F., & Fernández, A. I. (2016). Types, methods, techniques, and applications for microencapsulated phase change materials (MPCM): A review. *Renewable and Sustainable Energy Reviews*, *53*, 1059–1075. https://doi.org/10.1016/j.rser.2015.09.040
5. Farid, M. M., Khudhair, A. M., Razack, S. A. K., & Al-Hallaj, S. (2004). A review on phase change energy storage: Materials and applications. *Energy Conversion and Management*, *45*(9–10), 1597–1615. https://doi.org/10.1016/J.ENCONMAN.2003.09.015
6. Bendkowska, W., & Wrzosek, H. (2009). Experimental study of the thermoregulating properties of nonwovens treated with microencapsulated PCM. *Fibres &*

Textiles in Eastern Europe, *17*(5), 87-91.

7. Silva, T., Vicente, R., & Rodrigues, F. (2016). Literature review on the use of phase change materials in glazing and shading solutions. *Renewable and Sustainable Energy Reviews*, *53*, 515–535. https://doi.org/10.1016/j.rser.2015.07.201
8. Su, W., Darkwa, J., & Kokogiannakis, G. (2015). Review of solid–liquid phase change materials and their encapsulation technologies. *Renewable and Sustainable Energy Reviews*, *48*, 373–391. https://doi.org/10.1016/J.RSER.2015.04.044
9. Kumar, R., Misra, M. K., Kumar, R., Gupta, D., Sharma, P. K., Tak, B. B., & Meena, S. R. (2011). Phase change materials: Technology status and potential defence applications. *Defence Science Journal*, *61*(6), 576–582. https://doi.org/10.14429/DSJ.61.363
10. Huang, X., Alva, G., Jia, Y., & Fang, G. (2017). Morphological characterization and applications of phase change materials in thermal energy storage: A review. *Renewable and Sustainable Energy Reviews*, *72*, 128–145. https://doi.org/10.1016/j.rser.2017.01.048
11. Hough, T.P. (2016) *Solar Energy: New Research*; Nova Publishers: New York, NY, USA, pp 247-287
12. Kheradmand, M., Azenha, M., de Aguiar, J. L. B., & Krakowiak, K. J. (2014). Thermal behavior of cement based plastering mortar containing hybrid microencapsulated phase change materials. *Energy and Buildings*, *84*, 526–536. https://doi.org/10.1016/J.ENBUILD.2014.08.010
13. Jeong, S. G., Jeon, J., Seo, J., Lee, J. H., & Kim, S. (2012). Performance evaluation of the microencapsulated PCM for wood-based flooring application. *Energy Conversion and Management*, *64*, 516–521. https://doi.org/10.1016/J.ENCONMAN.2012.03.007
14. Sharma, A., Tyagi, V. V., Chen, C. R., & Buddhi, D. (2009). Review on thermal energy storage with phase change materials and applications. *Renewable and Sustainable Energy Reviews*, *13*(2), 318–345. https://ideas.repec.org/a/eee/rensus/v13y2009i2p318-345.html
15. Wahid, M. A., Hosseini, S. E., Hussen, H. M., Akeiber, H. J., Saud, S. N., & Mohammad, A. T. (2017). An overview of phase change materials for construction architecture thermal management in hot and dry climate

region. *Applied Thermal Engineering*, *112*, 1240–1259. https://doi.org/10.1016/J.APPLTHERMALENG.2016.07.032

16. Zhao, C. Y., & Zhang, G. H. (2011). Review on microencapsulated phase change materials (MEPCMs): Fabrication, characterization and applications. *Renewable and Sustainable Energy Reviews*, *15*(8), 3813–3832. https://doi.org/10.1016/J.RSER.2011.07.019
17. Gharsallaoui, A., Roudaut, G., Chambin, O., Voilley, A., & Saurel, R. (2007). Applications of spray-drying in microencapsulation of food ingredients: An overview. *Food Research International*, *40*(9), 1107–1121. https://doi.org/10.1016/J.FOODRES.2007.07.004
18. Fang, Y., Kuang, S., Gao, X., & Zhang, Z. (2008). Preparation and characterization of novel nanoencapsulated phase change materials. *Energy Conversion and Management*, *49*(12), 3704–3707. https://doi.org/10.1016/J.ENCONMAN.2008.06.027
19. Fang, Y., Wei, H., Liang, X., Wang, S., Liu, X., Gao, X., & Zhang, Z. (2016). Preparation and Thermal Performance of Silica/n-Tetradecane Microencapsulated Phase Change Material for Cold Energy Storage. *Energy and Fuels*, *30*(11), 9652–9657. https://doi.org/10.1021/ACS.ENERGYFUELS.6B01799
20. Salunkhe, P. B., & Shembekar, P. S. (2012). A review on effect of phase change material encapsulation on the thermal performance of a system. *Renewable and Sustainable Energy Reviews*, *16*(8), 5603–5616. https://doi.org/10.1016/j.rser.2012.05.037
21. Umair, M. M., Zhang, Y., Iqbal, K., Zhang, S., & Tang, B. (2019). Novel strategies and supporting materials applied to shape-stabilize organic phase change materials for thermal energy storage–A review. *Applied Energy*, *235*, 846–873. https://doi.org/10.1016/J.APENERGY.2018.11.017
22. Sarier, N., & Onder, E. (2007). The manufacture of microencapsulated phase change materials suitable for the design of thermally enhanced fabrics. *Thermochimica Acta*, *452*(2), 149–160. https://doi.org/10.1016/J.TCA.2006.08.002
23. Sánchez, L., Sánchez, P., de Lucas, A., Carmona, M., & Rodríguez, J. F. (2007). Microencapsulation of PCMs with a polystyrene shell. *Colloid and Polymer Science*, *285*(12), 1377–1385.

https://doi.org/10.1007/S00396-007-1696-7

24. Salaun, F., Devaux, E., Bourbigot, S., Rumeau, P., Chapuis, P. O., Saha, S. K., & Volz, S. (2008). Polymer nanoparticles to decrease thermal conductivity of phase change materials. *Thermochimica Acta*, *477*(1-2), 25-31.
25. Jamekhorshid, A., Sadrameli, S. M., & Farid, M. (2014). A review of microencapsulation methods of phase change materials (PCMs) as a thermal energy storage (TES) medium. *Renewable and Sustainable Energy Reviews*, *31*, 531–542. https://doi.org/10.1016/J.RSER.2013.12.033
26. Kim, O. H., Lee, K., Kim, K., Lee, B. H., & Choe, S. (2006). Effect of PVA in dispersion polymerization of MMA. *Polymer*, *47*(6), 1953–1959. https://doi.org/10.1016/J.POLYMER.2006.01.025
27. Wang, Y., Xia, T. D., Feng, H. X., & Zhang, H. (2011). Stearic acid/polymethylmethacrylate composite as form-stable phase change materials for latent heat thermal energy storage. *Renewable Energy*, *36*(6), 1814–1820. https://doi.org/10.1016/j.renene.2010.12.022
28. Sánchez-Silva, L., Rodríguez, J. F., Romero, A., Borreguero, A. M., Carmona, M., & Sánchez, P. (2010). Microencapsulation of PCMs with a styrene-methyl methacrylate copolymer shell by suspension-like polymerisation. *Chemical Engineering Journal*, *157*(1), 216–222. https://doi.org/10.1016/J.CEJ.2009.12.013
29. Arshady, R. (1992). Suspension, emulsion, and dispersion polymerization: A methodological survey. *Colloid and Polymer Science*, *270*(8), 717–732. https://doi.org/10.1007/BF00776142
30. Bryant, Y. G. (1999). Melt spun fibers containing microencapsulated phase change material. *ASME-PUBLICATIONS-HTD*, *363*, 225-234.
31. Salaün, F., Bedek, G., Devaux, E., Dupont, D., & Gengembre, L. (2011). Microencapsulation of a cooling agent by interfacial polymerization: Influence of the parameters of encapsulation on poly(urethane-urea) microparticles characteristics. *Journal of Membrane Science*, *370*(1–2), 23–33. https://doi.org/10.1016/J.MEMSCI.2010.11.033
32. You, M., Zhang, X. X., Li, W., & Wang, X. C. (2008). Effects of MicroPCMs on the fabrication of MicroPCMs/polyurethane composite foams. *Thermochimica Acta*, *472*(1-2), 20-24

33. Hawlader, M. N. A., Uddin, M. S., Khin, M. M., Hawlader, M. N. A., Uddin, M. S., & Khin, M. M. (2003). Microencapsulated PCM thermal-energy storage system. *Applied Energy*, *74*(1–2), 195–202. https://EconPapers.repec.org/RePEc:eee:appene:v:74:y:2003:i:1-2:p:195-202
34. Cape, S. P., Villa, J. A., Huang, E. T. S., Yang, T. H., Carpenter, J. F., & Sievers, R. E. (2008). Preparation of Active Proteins, Vaccines and Pharmaceuticals as Fine Powders using Supercritical or Near-Critical Fluids. *Pharmaceutical Research*, *25*(9), 1967. https://doi.org/10.1007/S11095-008-9575-6
35. Gao, F., Wang, X., & Wu, D. (2017). Design and fabrication of bifunctional microcapsules for solar thermal energy storage and solar photocatalysis by encapsulating paraffin phase change material into cuprous oxide. *Solar Energy Materials and Solar Cells*, *168*, 146–164. https://doi.org/10.1016/J.SOLMAT.2017.04.026
36. Yuan, W. J., Wang, Y. P., Li, W., Wang, J. P., Zhang, X. X., & Zhang, Y. K. (2015). Microencapsulation and characterization of polyamic acid microcapsules containing n-octadecane via electrospraying method. *Materials Express*, *5*(6), 480–488. https://doi.org/10.1166/MEX.2015.1268
37. Arpagaus, C., Collenberg, A., Rütti, D., Assadpour, E., & Jafari, S. M. (2018). Nano spray drying for encapsulation of pharmaceuticals. *International Journal of Pharmaceutics*, *546*(1–2), 194–214. https://doi.org/10.1016/J.IJPHARM.2018.05.037
38. Tarun, G., & Murthy, R. S. R. (2011). Patented microencapsulation techniques and its application. *Journal of Pharmacy Research*, *4*(7), 2097-2102.
39. Feng, T., Xiao, Z., & Tian, H. (2009). Recent patents in flavor microencapsulation. *Recent Patents on Food, Nutrition & Agriculture*, *1*(3), 193–202. https://doi.org/10.2174/2212798410901030193
40. Wan, X., Guo, B., & Xu, J. (2017). A facile hydrothermal preparation for phase change materials microcapsules with a pliable self-recovering shell and study on its thermal energy storage properties. *Powder Technology*, *312*, 144–151. https://doi.org/10.1016/J.POWTEC.2017.02.035
41. Zhang, L., Yang, W., Jiang, Z., He, F., Zhang, K., Fan, J., & Wu, J. (2017). Graphene oxide-modified microencapsulated phase change materials with high encapsulation

capacity and enhanced leakage-prevention performance. *Applied Energy*, *197*, 354–363. https://doi.org/10.1016/j.apenergy.2017.04.041

42. Su, W., Darkwa, J., & Kokogiannakis, G. (2017). Development of microencapsulated phase change material for solar thermal energy storage. *Applied thermal engineering*, *112*, 1205-1212.
43. Qiu, X., Song, G., Chu, X., Li, X., & Tang, G. (2013). Preparation, thermal properties and thermal reliabilities of microencapsulated n-octadecane with acrylic-based polymer shells for thermal energy storage. *Thermochimica Acta*, *551*, 136–144. https://doi.org/10.1016/J.TCA.2012.10.027
44. Jiang, X., Luo, R., Peng, F., Fang, Y., Akiyama, T., & Wang, S. (2015). Synthesis, characterization and thermal properties of paraffin microcapsules modified with nano-Al2O3. *Applied Energy*, *137*, 731–737. https://doi.org/10.1016/J.APENERGY.2014.09.028
45. Park, S., Lee, Y., Kim, Y. S., Lee, H. M., Kim, J. H., Cheong, I. W., & Koh, W. G. (2014). Magnetic nanoparticle-embedded PCM nanocapsules based on paraffin core and polyurea shell. *Colloids and Surfaces A: Physicochemical and Engineering Aspects*, *450*(1), 46–51. https://doi.org/10.1016/J.COLSURFA.2014.03.005
46. Peng, G., Dou, G., Hu, Y., Sun, Y., & Chen, Z. (2020). Phase change material (PCM) microcapsules for thermal energy storage. *Advances in Polymer Technology*, *2020*. https://doi.org/10.1155/2020/9490873
47. Sukhorukov, G., Fery, A., & Möhwald, H. (2005). Intelligent micro- and nanocapsules. *Progress in Polymer Science*, *30*(8–9), 885–897. https://doi.org/10.1016/J.PROGPOLYMSCI.2005.06.008
48. Fang, Y., Yu, H., Wan, W., Gao, X., & Zhang, Z. (2013). Preparation and thermal performance of polystyrene/n-tetradecane composite nanoencapsulated cold energy storage phase change materials. *Energy Conversion and Management*, *76*, 430–436. https://doi.org/10.1016/J.ENCONMAN.2013.07.060
49. Wang, Y., Zhang, Y., Xia, T., Zhao, W., & Yang, W. (2013). *Effects of fabricated technology on particle size distribution and thermal properties of stearic-eicosanoic acid/polymethylmethacrylate nanocapsules*. https://doi.org/10.1016/j.solmat.2013.09.028

https://doi.org/10.36375/prepare_u.iiche.a407

[International Conference on Energy Transition: Challenges and Opportunities at Chemical Engineering Congress (CHEMCON-2023) – On the occasion of Platinum Jubilee Year of Indian Institute of Chemical Engineers]

Hydrogen Geo-storage – A Review on Storage and Recovery from Carbonate Reservoirs

Anooja Sara Mathew[a], Vishnu Chandrasekharan Nair[b]

[a]*Research Scholar, Deysarkar Centre of Excellence in Petroleum Engineering, IIT Kharagpur – 721302, India*

[b]*Assistant Professor, , Deysarkar Centre of Excellence in Petroleum Engineering, IIT Kharagpur – 721302, India*

Abstract

Hydrogen has emerged as a promising renewable alternative for addressing our energy needs and advancing towards the goal of achieving net-zero carbon emissions. Large scale generation of hydrogen is a way forward to the storage of renewable energy and securing the energy economy for a future perspective. Within this context, underground hydrogen storage in depleted reservoirs, saline aquifers and salt caverns have garnered increasing attention due to its potential to securely and cost-effectively store hydrogen on a large scale. However, a primary challenge in the domain of hydrogen geo-storage lies in achieving efficient hydrogen extraction from porous media after extended storage periods. In an ideal scenario, the volume of hydrogen recovered should equal the volume initially injected. Due to their abundance and suitability of geological features for storage, formations, once served as a source of fossil fuels are being explored as potential sites for the geo-storage of hydrogen. Although there are many wettability studies on sandstone reservoirs, limited number of studies are available for carbonate rocks. Hence this study provides qualitative insights into the hydrogen trapping efficiency as well as effective recovery from depleted carbonate reservoirs. Also, the challenges associated with the storage phenomena in depleted reservoirs has been addressed here.

Keywords: Hydrogen Geo-storage; Depleted Reservoirs; Carbonate formations; Residual Hydrocarbon Saturation.

1. Introduction

The rising demand for energy due to increase in population along with the policies for decarbonization have pushed the industries and researchers to develop alternate sources of carbon free energies. Hydrogen has evolved from this as a potential carrier of energy as well as means for storage of renewable energy for future. The production and consumption of renewable energies fluctuate and in order to maintain a continuous flow of energy upon varying demands, storage of the same is required. The idea behind green hydrogen is the production of hydrogen from surplus renewable energies through the process of electrolysis. In 2021, hydrogen demand soared to 94 million tonnes (Mt), exceeding the levels before pandemic (91 Mt in 2019) and contributing to about 2.5% of the total energy consumption of the world. As revealed during the recent COP26 summit in Glasgow, hydrogen plays a pivotal role in the global vision for 2050, with nearly 30 countries unveiling their hydrogen roadmaps [1]. For the Indian Government also, the hydrogen economy is an important consideration. In the budget speech of 2021, the finance minister launched the National Hydrogen Mission for producing hydrogen from green power sources [2]. As India aspires to attain energy self-sufficiency by 2047 and reach a state of Net Zero emissions by 2070, we acknowledge the vital significance of Green Hydrogen. India, endowed with abundant renewable energy resources, is well-positioned to manufacture Green Hydrogen on a global scale. The National Green Hydrogen Mission is designed to outline a thorough strategy for building a Green Hydrogen ecosystem and

https://doi.org/10.36375/prepare_u.iiche.a407

stimulating a coordinated approach to address the prospects and hurdles within this emerging sector [3].

The density of hydrogen is approximately 8 times less than that of methane and 22 times less than that of carbon dioxide. This implies that achieving the same mass of hydrogen gas will create the need for more storage space and higher pressure[4]. Once it is massively produced, comes the requirement of large volumes for storage of hydrogen. Hence comes the idea of geo-storage of hydrogen as surface storage methods have practical difficulties. Currently, there are four operational methods for underground natural gas storage: salt caverns, exhausted gas fields, aquifers, and hard rock caverns equipped with linings [1]. These sites are being explored as the potential storage options for hydrogen underground. Fig.1. shows the hydrogen economy including generation, transportation and underground storage of energy from the excess electricity from the renewables and the recovery of hydrogen during peak energy demands.

The chosen criteria for hydrocarbon reservoirs and saline aquifers encompass the following factors: reservoir capacity, the composition of the overlying rock layers, geological activity, depth of occurrence, exploration progress, mineral composition, and the thickness of the overlying rock formations [5]. The lower viscosity of hydrogen compared to methane and carbon dioxide poses a significant challenge for its containment during geological storage. Additionally, the high mobility and extensive diffusion of H_2 result in the reduction of residual amount of H_2 remaining within the porous media during extraction [4]. Even though it is important to highlight that Underground Hydrogen Storage (UHS) can leverage the well-developed technologies and extensive knowledge base associated with geological storage of natural gas and carbon dioxide which have been established over several decades, more experimental investigations have to be done with different combinations of existing and expected reservoir conditions in this area which is still at its infancy to evolve.

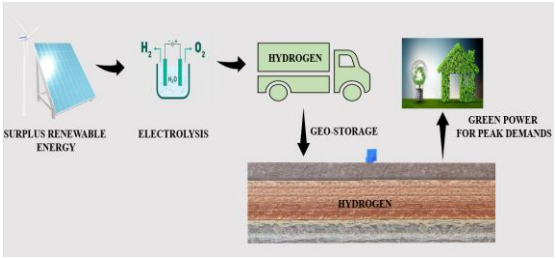

Figure.1: Hydrogen Economy

2. Depleted Reservoirs for Hydrogen Geo-storage

In this era of extensive exploration into large-scale green hydrogen production methods, the quest for viable storage solutions for green hydrogen has also garnered significant interest. Due to the knowledge of existing infrastructure for the extraction of hydrocarbons, depleted hydrocarbon reservoirs serve as the best option among all the practiced geo-storage options for hydrogen. According to the capital cost assessment, depleted oil and gas reservoirs are found to be the most cost-effective storage option, with an estimated cost of approximately $1.29 per kilogram [6].

Oil and gas reservoirs are well known for their vast area, high porosity, reservoir tightness and the presence of impermeable caprock that seals the contained gas. These properties are making them the suitable candidates for underground hydrogen storage [5]–[7]. Geological traps are where natural gas and petroleum deposits are found. Hydrocarbons get stored within the pore spaces of rocks like carbonates or sandstones, which are referred to as reservoirs. The rocks that act as seals for these traps prevent hydrocarbons from migrating excessively. These are the most prevalent types of porous geological underground materials and have good history of natural gas extraction operations over a century [5]. Most of the hydrocarbon reservoirs are sandstone and carbonate reservoirs. Study of different combinations of reservoir conditions and parameters have been conducted on the hydrogen storage in sandstone reservoirs but, there exists a lack of data in the storage of hydrogen in carbonate formations. Hence this paper mainly focuses on the studies conducted on carbonate reservoirs in the context of hydrogen geo-storage.

One of the parameters that plays a pivotal role in the selection of sites for hydrogen storage in

https://doi.org/10.36375/prepare_u.iiche.a407

underground sites is wettability. It's characterized by the ability of the fluid to stay in contact with a solid surface when other immiscible fluids are present. The wettability of hydrogen within reservoir rock relies on the attributes of the reservoir rock, the fluid in the pores, and hydrogen. This wettability can be predicted by assessing the contact angle through measurements [7]. Assessing the potential of hydrogen geo-storage from a wettability perspective is an emerging research area that requires thorough investigation. Due to the lack of literatures to quantify the H_2 wettability of carbonate reservoirs, Hosseini et al.(2022) conducted study on calcite minerals and found out high temperatures, low pressures, low organic acid concentrations and low salinity as the suitable conditions for reducing the risk of hydrogen storage projects in the carbonate reservoirs[8]. Their results also show that at standard conditions, the calcite/hydrogen/water system remained strongly water wet which became intermediately wet with higher physical and thermal conditions. This aligns with the results of the study conducted by Aghaei et al. (2023) where the wettability of carbonate rocks was not altered due to the presence of hydrogen instead the surfaces remained water wet[9]. Their work suggests the future need of studies on geochemical interactions of H_2-rock brine system, snap-off and residual trapping of H_2 that may have influence in the injectivity and recovery efficiencies. Atomistic molecular dynamics simulations were conducted by Yaseri et al. (2023) to investigate the wettability of the hydrogen-water system on quartz and calcite minerals. These simulations were executed using the high-performance open-source software, GROMACS. Sandstone and limestone reservoirs exhibited complete water-wettability (contact angle of 0 degrees) when exposed to hydrogen, irrespective of variations in pressure, temperature, or salinity. They suggested to further validate the wettability outcomes and recommended to explore H_2 core flooding under diverse pressure, temperature, and salinity conditions in future research [10].

The recovery of hydrogen from the underground storage sites upon the varying demand is as much important as its containment. In an ideal condition, the recovered volume of hydrogen should be equal to the injected volume. Losses of different kind can occur during the short - term and long - term storage of hydrogen due to rock-fluid interactions. The interfacial tension (IFT) between the reservoir rock and the fluid governs how the fluid spreads, thereby influencing the interaction between hydrogen and the rock [7]. The measurement of IFT through experimental studies are challenging due to the limitations in measuring the interfacial tension between the rock surface and the liquid or gas fluid phases. Only the IFT between liquid and the gas can be measured in laboratory. Another work of Hosseini et al. (2023) have combined the Neumann's equation and Young's equation to determine the rock – fluid interfacial tension in a carbonate formation. Their studies found out the IFT between calcite/H2/water as a function of temperature, pressure, organic acid concentrations and salinity. The study results emphasize the importance of interfacial tension between the rock and the fluid phases in the context of UHS. The value of IFT was found to decrease with increase in pressure, salinity and organic acid concentration, but increased with temperature [11].

Hou et al. (2023) measured the zeta potential on the surface of carbonate rocks in different salinity solutions in order to find the effect of divalent and monovalent ions on alteration of hydrogen wettability. They also studied the effect of pressure and temperature parameters on the advancing contact angles and receding contact angles in a system of carbonate rock/ hydrogen/ brine [12]. The results indicated the increase in contact angle caused by the divalent ions which showed an increased zeta potential. Also, it was seen that the contact angle increased with pressure and decreased with temperature.

3. Challenges Associated with Hydrogen Geo-storage in Depleted Reservoirs

Many reservoirs which once served as the potential source of hydrocarbons have now been considered as the suitable storage options for hydrogen. Even though the presence of existing gaseous hydrocarbon mixtures in the depleted reservoirs are considered as the beneficial component of cushion gas which maintains the pressure during the injection and withdrawal stages [4] of hydrogen underground, the presence of the same can affect the purity of hydrogen stored. Not every

reservoir identified for underground hydrogen storage needs to be entirely depleted, as some residual gases may persist within it. These native gas remnants within the reservoir have the potential to mix with hydrogen. The degree to which multiphase, multicomponent interactions occur within the reservoir can introduce contaminants into the stored hydrogen. To ensure the secure operation of UHS, it is imperative that the reservoir is devoid of contaminants [5]. However, the residual oil saturations if present in these reservoirs are detrimental as it interacts with the stored hydrogen. The dynamic interaction between the remaining oil saturation and hydrogen storage involves a spectrum of intricate procedures, encompassing factors such as competition for pore space, capillary entrapment, and limitations related to diffusion. Oil fields are prone to exhibit intricate multiphase fluid flow dynamics when interacting with hydrogen, leading to reduced utilization of pore space and increased storage expenses. Additionally, they lack the advantage of pre-existing cushion gas [13]. Hence, the studies considering the effect of oil in UHS are very limited in numbers. Bechara et al. (2023) have conducted studies on the effect of residual oil saturations on unconventional shale reservoirs during the injection, storage and recovery of hydrogen from them. These experimental studies have found out that there is possibility of the production of unwanted amount of oil along with the extraction of hydrogen which indeed creates the need of additional separation procedures for hydrogen. They have also found an additional increase in weight of oil saturated sample on exposure to hydrogen indicating the formation of some chemical compounds [14], [15]. Geochemical aspects of these storage mechanisms have to be properly evaluated under conditions of reservoir temperature and pressure. Also, effects on long term storage of hydrogen has to be studied in future in order to convert depleted oil reservoirs into suitable sites for geo-storage of hydrogen.

Studies conducted by Zeng et al. (2022) on the Majiagou carbonate reservoir in China showed the reduction of hydrogen due to calcite dissolution and geochemical reactions occurring in carbonate rocks. They found out by the geochemical modelling studies that the loss of hydrogen in 0.5 years was about 6.5% and 7.65% at 5 years but, it can reach approximately up to 81.1% over 500 years [17]. This quantifies the suitability of such reservoirs for the short-term storage of hydrogen. Geochemical reactions between rock minerals and the introduced hydrogen may lead to an overestimation of Underground Hydrogen Storage capacity in carbonate formations if not appropriately considered. It is essential to safeguard the stability and integrity of the storage rocks and uphold the formation pressure to guarantee effective hydrogen injection and recovery during peak periods of demand. However, research on the interactions between hydrogen and the reservoir rocks mainly sandstone and carbonate and their impact on the geological storage of hydrogen in these formations is notably scarce. The experimental findings by Yaseri et al. (2023) using micro CT indicated that the expansion of calcite was more pronounced than the dissolution during the initial 75 days of hydrogen injection into carbonate reservoirs, which primarily composed of calcite[16].

The significant impact of hydrogen's subsurface hydrodynamic behavior is a greater concern, particularly when considering depleted reservoirs and aquifers, and it applies universally to all underground hydrogen storage methods. The occurrence of hydrogen in underground areas has also been observed to accelerate geochemical reactions, presenting another concern related to UHS in depleted reservoirs and aquifers [5]. It's important to emphasize that while these capacity assessments are accurate, there's still uncertainty regarding whether hydrogen can be injected into and retrieved from storage reservoirs in a manner similar to natural gas. Consequently, the true hydrogen storage capacity of gas fields remains unconfirmed. Continual effective evaluations of designated storage sites will aid in determining the feasibility of seasonal hydrogen injection and withdrawal. Rigorous risk assessments for abandoned wells and faults, along with thorough dynamic simulations of the hydrogen storage process, can significantly reduce the risk of hydrogen leakage through these potentially vulnerable pathways [13]. However, achieving the effective storage of pure hydrogen in depleted hydrocarbon reservoirs and aquifers has not been accomplished due to the unclear understanding of microbial and

geochemical processes during underground hydrogen storage. The storage capacity, as well as the ability to inject and withdraw H_2, are influenced by the reactions between hydrogen and the rock within the storage formations [16].

4. Conclusion

Hydrogen will continue to increase its demand in the upcoming period of time as a carbon free carrier of energy. With increased demand, increased storage options are also required. Research has identified underground hydrogen storage in depleted reservoirs as a viable and cost-effective choice for hydrogen storage. But due to lack of data in the domains of reactions and interactions of hydrogen under reservoir conditions, it is difficult to predict the efficiency of storage and recovery of hydrogen from UHS sites and it leaves an unclear picture especially in the case of carbonate reservoir. Increased pressure temperature conditions as well as increased periods of storage need to be studied in order to quantify the appropriateness of storage sites. Additionally, residual oil saturations remaining in depleted reservoirs may result in inadvertently retrieving undesirable amounts of oil along with the hydrogen. Thus, understanding the interaction between the remaining oil and stored hydrogen in these reservoirs, and its impact on storage efficiency and subsequent hydrogen recovery, is crucial. Further research in this direction can be expected in future.

Declaration of Competing Interest

The authors declare that they have no known competing financial interests or personal relationships that could have appeared to influence the work reported in this paper.

References

[1] INTERNATIONAL ENERGY AGENCY, “Global Hydrogen Review 2022,” OECD, Oct. 2022. doi: 10.1787/a15b8442-en.

[2] Energy Transition Advisory Committee Ministry of Petroleum & Natural Gas Government of India (ETAC), “THE GREEN SHIFT - The low carbon transition of India’s Oil & Gas sector.”

[3] M. of N. and R. E. Goverment of India, “National Green Hydrogen Mission Ministry of New and Renewable Energy,” no. January, 2023, [Online]. Available: https://www.iea.org/reports/india-energy-outlook-2021

[4] N. S. Muhammed *et al.*, “Hydrogen storage in depleted gas reservoirs: A comprehensive review,” *Fuel*, vol. 337, no. September 2022, p. 127032, Apr. 2023, doi: 10.1016/j.fuel.2022.127032.

[5] H. Bin Navaid, H. Emadi, and M. Watson, “A comprehensive literature review on the challenges associated with underground hydrogen storage,” *Int. J. Hydrogen Energy*, vol. 48, no. 28, pp. 10603–10635, Apr. 2023, doi: 10.1016/j.ijhydene.2022.11.225.

[6] E. I. Epelle *et al.*, “Perspectives and prospects of underground hydrogen storage and natural hydrogen,” *Sustain. Energy Fuels*, vol. 6, no. 14, pp. 3324–3343, 2022, doi: 10.1039/D2SE00618A.

[7] M. S. A. Perera, “A review of underground hydrogen storage in depleted gas reservoirs: Insights into various rock-fluid interaction mechanisms and their impact on the process integrity,” *Fuel*, vol. 334, no. August 2022, p. 126677, Feb. 2023, doi: 10.1016/j.fuel.2022.126677.

[8] M. Hosseini, J. Fahimpour, M. Ali, A. Keshavarz, and S. Iglauer, “Hydrogen wettability of carbonate formations: Implications for hydrogen geo-storage,” *J. Colloid Interface Sci.*, vol. 614, pp. 256–266, May 2022, doi: 10.1016/j.jcis.2022.01.068.

[9] H. Aghaei, A. Al-Yaseri, A. Toorajipour, B. Shahsavani, N. Yekeen, and K. Edlmann, “Host-rock and caprock wettability during hydrogen drainage: Implications of hydrogen subsurface storage,” *Fuel*, vol. 351, no. April, p. 129048, Nov. 2023, doi: 10.1016/j.fuel.2023.129048.

[10] A. Al-Yaseri, S. Abdel-Azeim, and J. Al-Hamad, “Wettability of water-H2-quartz and water-H2-calcite experiment

and molecular dynamics simulations: Critical assessment," *Int. J. Hydrogen Energy*, vol. 48, no. 89, pp. 34897–34905, Nov. 2023, doi: 10.1016/j.ijhydene.2023.05.294.

[11] M. Hosseini, M. Ali, J. Fahimpour, A. Keshavarz, and S. Iglauer, "Calcite–Fluid Interfacial Tension: H 2 and CO 2 Geological Storage in Carbonates," *Energy & Fuels*, vol. 37, no. 8, pp. 5986–5994, Apr. 2023, doi: 10.1021/acs.energyfuels.3c00399.

[12] J. Hou, S. Lin, M. Zhang, and W. Li, "Salinity, temperature and pressure effect on hydrogen wettability of carbonate rocks," *Int. J. Hydrogen Energy*, vol. 48, no. 30, pp. 11303–11311, Apr. 2023, doi: 10.1016/j.ijhydene.2022.05.274.

[13] J. Mouli-Castillo, N. Heinemann, and K. Edlmann, "Mapping geological hydrogen storage capacity and regional heating demands: An applied UK case study," *Appl. Energy*, vol. 283, no. August 2020, p. 116348, Feb. 2021, doi: 10.1016/j.apenergy.2020.116348.

[14] E. Bechara *et al.*, "Effect of Hydrogen Interaction with Crude Oil on the Extraction of Hydrogen if Stored in Depleted Shale Reservoirs: An Experimental Study Analyzing the Outcome of Cyclic Hydrogen Injection into Oil-Saturated Core Samples," in *Day 2 Thu, June 29, 2023*, SPE, Jun. 2023. doi: 10.2118/213851-MS.

[15] E. Bechara, T. Gamadi, A. Hussain, and H. Emadibaladehi, "Effect of Hydrogen Exposure on Shale Reservoir Properties and Evaluation of Hydrogen Storage Possibility in Depleted Unconventional Formations," in *Proceedings of the 10th Unconventional Resources Technology Conference*, Tulsa, OK, USA: American Association of Petroleum Geologists, 2022, pp. 1–15. doi: 10.15530/urtec-2022-3723858.

[16] A. Al-Yaseri, H. Al-Mukainah, N. Yekeen, and A. S. Al-Qasim, "Experimental investigation of hydrogen-carbonate reactions via computerized tomography: Implications for underground hydrogen storage," *Int. J. Hydrogen Energy*, vol. 48, no. 9, pp. 3583–3592, Jan. 2023, doi: 10.1016/j.ijhydene.2022.10.148.

[17] L. Zeng, A. Keshavarz, Q. Xie, and S. Iglauer, "Hydrogen storage in Majiagou carbonate reservoir in China: Geochemical modelling on carbonate dissolution and hydrogen loss," *Int. J. Hydrogen Energy*, vol. 47, no. 59, pp. 24861–24870, Jul. 2022,doi:10.1016/j.ijhydene.2022.05.247.

https://doi.org/10.36375/prepare_u.iiche.a408

Machine Learning-Guided Optimization of Biofuel Blends for Enhanced Engine Efficiency and Emission Reduction

Prithwish Das[1], Aniket Biswas[2], Srijan Sardar[3], Bitopama Modak[4], Fahim Ahmed[5], Dr Sandip Kr Lahiri[*]

[1,2,3,4,5] *Jadavpur University, BE Chemical Engineering, Kolkata-700049, India*
** NIT Durgapur, BE Chemical Engineering, Durgapur-713209, India,*
Email address- ***sklahiri.che@nitdgp.ac.in***

Abstract

India heavily relies on imported foreign crude oil, prompting the need for effective solutions to reduce this dependency. One such solution is the blending of Biodiesel, Palm oil, and Ethanol with original diesel. The crucial concern lies in determining the optimal blending ratio that maximizes Engine Efficiency while maintaining reasonable levels of Oil Consumption and NOx emission. To address this, experimental data are collected from the paper [1] which systematically blends biodiesel. Experimental data involved three input parameters [Load, Palm Biodiesel, Ethanol] and three output parameters [Motor Brake Thermal Efficiency (BTE), Brake Specific Fuel Consumption (BSFC), and Nitrogen Oxides (NOx)], with 40 different runs. The prediction was accomplished using 26 Machine Learning Models, including Gaussian Process Regression, Support Vector regression, ANN, Tree and Linear Regression and others. Among the 26 models considered in the analysis, three models emerged as the top performers. The Stepwise Linear Regression Model [SLRM] yielded the highest Brake Thermal Efficiency (BTE), the Fine Tree Regression Model [FTRM] achieved the lowest Brake Specific Energy Consumption [BSFC], and the Matern 5/2 Gaussian Process Regression Model [MGPRM] demonstrated the lowest Nitrogen Oxide (NOx) emission. These models displayed a range of Root Mean Square Error (RMSE) and R-squared(validation) values: 0.02077–0.02333 and 0.99 for SLRM, 0.03789–0.03907 and 0.98 for FTRM & 0.02184–0.02296 and 0.99 for MGPRM. Moving forward, a multi-objective optimization approach has been undertaken to simultaneously maximize BTE while minimizing both BSFC and NOx emissions. To accomplish this, a Multi Objective Genetic Algorithm [MOGA] is employed to identify the Pareto Optimal Solution. The optimization process [MOGA] resulted in a series of 18 Pareto Optimal Solutions. These solutions provide insights on the appropriate blend ratios of Load, Palm Biodiesel and Ethanol in order to maximize Engine Thermal Efficiency while minimizing Fuel Consumption and NOx emissions.

Keywords: Palm biodiesel; Engine Thermal Efficiency; Machine Learning Model; Multi Objective Genetic Algorithm [MOGA]; Pareto Optimal solutions; Efficient Optimization.

https://doi.org/10.36375/prepare_u.iiche.a408

1. Introduction

The growing demand for fossil fuels and their application in diesel engines, especially in the industrial and automotive sectors, has increased significantly. However, this excessive use of conventional fuels has raised concerns over fuel depletion and the environmentally harmful emissions associated with diesel engines, motivating the exploration of alternative fuels over the past few decades [1,2]. The ongoing global industrial revolution has led to stricter regulations governing the use of diesel engines, largely driven by concerns about environmental pollution. As a response, alternative fuels have gained prominence as a means to mitigate harmful emissions and address global warming [3–5]. Over approximately a century, alternative fuels have been actively pursued as substitutes for traditional fossil diesel. Among these alternatives, biofuels have shown promise, with biodiesel emerging as a leading contender due to its similar properties to conventional diesel fuel [7–9]. Biodiesel is sulphur-free, less toxic, and more environmentally friendly, and it can be produced from a variety of readily available sources. Nevertheless, biodiesel presents some drawbacks, such as higher viscosity, greater density, and poor cold flow properties, which can hinder its effective use in diesel engines [10–12]. In such situations, alcohol-based additives are frequently utilized to modify the characteristics of biodiesel [13]. Notably, among these additives, ethanol, methanol, n-butanol, and diethyl ether are well-known and widely employed [14–18].

Researchers try to conduct experiments with diesel engines to find out at what proportions these additives can be blended so that engine performance, fuel consumptions and NOx emissions from diesel engines can be optimized. A diesel engine's performance is usually measured by three Metrics namely Brake Thermal Efficiency (BTE), Brake Specific Fuel Consumption (BSFC) and NOx (Nitrogen Oxides) emissions. Brake Thermal Efficiency (BTE) is a measure of how efficiently a diesel engine converts the heat energy from fuel into useful mechanical work. It is defined as the ratio of the brake power output to the energy input from the fuel. BTE is typically expressed as a percentage and can be calculated using the following formula: BTE (%) = (Brake Power Output / Fuel Energy Input) × 100.

On the other hand, Brake Specific Fuel Consumption (BSFC) is a measure of the fuel efficiency of a diesel engine. It quantifies the amount of fuel (typically expressed in mass or volume) required to produce one unit of brake power (usually one kilowatt or one horsepower) over a specific period of time. Lower BSFC values indicate better fuel efficiency. BSFC is defined using the following formula*:*

BSFC (g/kWh) = (Fuel Consumption in grams) / (Brake Power Output in kilowatts)

A lower BSFC value indicates that the engine is using less fuel to produce a given amount of power, which is a desirable characteristic for an efficient diesel engine. Engineers and manufacturers work to optimize engine design and operating conditions to minimize BSFC and improve fuel economy. NOx (Nitrogen Oxides) emissions from a diesel engine are a type of air pollution that consists of various nitrogen oxide compounds, primarily nitrogen dioxide (NO2) and nitric oxide (NO). These emissions are a result of the high-temperature combustion process in the diesel engine, which causes nitrogen and oxygen in the air to react and form NOx compounds.

NOx emissions are typically quantified and regulated in terms of concentration or mass per unit volume of exhaust gases. Common units for expressing NOx emissions include parts per million (ppm), grams per kilogram (g/kg), or grams per brake horsepower-hour (g/bhp·hr). The specific method and units used may vary depending on regional regulations and standards.

NOx emissions can be measured using various techniques, including exhaust gas analysers or emissions testing equipment. These measurements are usually taken at the exhaust

outlet of the engine or vehicle to determine the concentration of NOx in the exhaust gases. These values can be used to assess compliance with emissions standards and regulations. Reducing NOx emissions is a significant concern for diesel engine manufacturers and vehicle operators due to their adverse environmental and health effects.

The main problems researchers try to solve is to find the optimum blend ratio of biodiesel and various additives so that the above three conflicting objectives can be optimized.
Traditional methods of conducting engine experiments are now considered time-consuming and costly. As a result, new techniques utilizing computational analysis have been introduced to facilitate faster and more cost-effective experimentation [19–21]. Researchers, such as Krishnamoorthi et al. [22], have conducted experiments to optimize engine performance by varying injection pressure (IP), injection timing (IT), and compression ratio in a diesel engine, ultimately using Response Surface Methodology (RSM) to determine the optimal engine input parameters. They found a compression ratio of 18:1, a fuel injection pressure (FIP) of 250 bar, and an injection timing of 21 degrees before top dead center (bTDC) to be the best settings. Through the application of different design of experiments (DoE) and various RSM models, predictive models for engine responses, such as Brake Thermal Efficiency (BTE), Brake Specific Energy Consumption (BSFC), nitrogen oxides (NOx), hydrocarbons (HC), carbon monoxide (CO), and smoke opacity, have been developed, with coefficient of determination (R2) values for these parameters ranging between 0.9256 and 0.9991 [23–25].

Recent advances in computational analysis of diesel engine performance and emission parameters have introduced Artificial Neural Networks (ANN) as a promising alternative to RSM. ANN models are known for their ability to provide accurate predictions and strong correlations with experimental results. Shivakumar et al. [26] applied separate ANN models to predict engine responses within 8% mean error values (MRE). Taghavifar et al. [27] utilized ANN predictions with a feed-forward backpropagation (BP) learning algorithm and Levenberge-Marquardt transfer function for Computational Fluid Dynamics (CFD) simulated engine outputs, achieving high R2 values of 0.9951, 0.9976, and 0.9995 for NOx, CO2, and soot emissions, respectively. Rao et al. [28] investigated ANN prediction for nine different engine outputs with low error percentages (0.01–0.03) and high R2 values (0.980–0.999). Javed et al. [29] trained an ANN model for predicting engine performance and emissions, achieving an overall R value of 0.99360, Mean Squared Error (MSE) of 0.0011, and Mean Absolute Percentage Error (MAPE) of 4.863001%. Uslu et al. [30] accurately predicted engine responses using ANN models, observing R2 and mean relative error (MRE) values ranging from 0.964 to 0.9878 and 0.51–4.8%, respectively. Furthermore, several comparative studies have been conducted to assess the accuracy of prediction between RSM and ANN models [31,32]. In most cases, ANN models have outperformed RSM models due to their capacity to handle highly nonlinear behaviour during training [33–37]. Uslu et al. [38] developed a prediction model, obtaining an R2 value of 0.9 for RSM and 0.85–0.95 for ANN.

Despite the extensive literature focusing on prediction and optimization using RSM and ANN, and their combined RSM-ANN models, there remains a gap in the investigation of a comparative study between more advanced machine learning models in this domain. An effort has been made in the present study to apply various advanced machine learning models to predict engine performance parameters (BTE, BSFC and NOx) from engine input parameters such as Load %, Palm Biodiesel % and ethanol%. In the present study 2 advanced machine learning models have been applied and the best model is finally selected. After a reliable machine learning model is built,

the second objective is to optimize the blend ratio of Palm Biodiesel % and ethanol% so that a reasonable balance can be found in conflicting 3 objectives like BTE, BSFC and NOx.

The study's goals are bifurcated into two primary components. Firstly, the 26 advanced machine learning models are harnessed for predicting BTE, BSFC, and NOx emissions. Furthermore, diverse error types and correlation analyses have been executed to gauge and contrast the models' precision. On the other hand, leveraging the anticipated responses from the model, a multiobjective genetic algorithm system is effectively employed to determine the optimal engine input parameters and output responses.

2. Materials and Methodology

2.1. Experimental Setup:

In this study experimental data from reference [39] is taken. The reference [39] experimental investigation was carried out on a Kirloskar (TV1) type direct-injected diesel engine with a power rating of 3.5 kW. This engine is a single-cylinder, four-stroke, water-cooled unit with a variable compression ratio. The setup includes an eddy current dynamometer for measuring engine load, a crank angle sensor to monitor engine speed at every 1° crank angle rotation, K-type thermocouples for measuring various temperatures, and a piezoelectric transducer to record in-cylinder pressure. Additionally, a gas analyser was connected to the exhaust pipe to measure exhaust emissions, including NOx, CO, UHC (unburned hydrocarbons), CO2, and O2. Data acquisition and control were facilitated by a computerized system interfaced with specialized software.

2.2. Test Methodology:

The experimental procedure used in [39] for assessing engine performance and emissions involved testing the engine under varying loads, ranging from 20% to 100% in 20% increments, while maintaining a constant speed of 1500 rpm. Fuel consumption was measured using a fuel burette, and environmental conditions were documented. Different blends of diesel, palm biodiesel, and anhydrous ethanol were used in the experiments. 40 experimental runs were carried out at different engine loads, Palm Biodiesel % and ethanol% and 3 metrics of engine performance namely BTE, BSFC and NOx were measured in each run. The data are shown in table 1.

Table 1: Experimental data used for model building [39]

Test Run	Engine Load (%) A	Palm biodiesel (%) B	Ethanol (%) C	BTE	BSFC	NOx
1	40	10	10	0.34	0.51	0.40
2	60	10	5	0.55	0.33	0.60
3	100	15	10	0.81	0.12	0.82
4	40	15	5	0.34	0.55	0.40

https://doi.org/10.36375/prepare_u.iiche.a408

Test Run	Engine Load (%) A	Palm biodiesel (%) B	Ethanol (%) C	BTE	BSFC	NOx
5	60	10	10	0.50	0.34	0.64
6	80	15	10	0.63	0.24	0.74
7	80	15	5	0.69	0.22	0.74
8	40	20	10	0.30	0.55	0.37
9	20	5	5	0.18	0.81	0.12
10	60	15	10	0.48	0.36	0.60
11	100	10	5	0.87	0.12	0.82
12	100	20	10	0.76	0.15	0.78
13	20	10	5	0.17	0.81	0.11
14	20	15	10	0.17	0.77	0.13
15	20	5	10	0.20	0.72	0.11
16	100	20	5	0.90	0.10	0.83
17	80	20	10	0.58	0.27	0.73
18	40	5	5	0.39	0.49	0.37
19	100	5	10	0.86	0.10	0.90
20	60	20	10	0.45	0.38	0.59
21	20	20	5	0.17	0.81	0.10
22	80	5	10	0.69	0.20	0.83
23	80	20	5	0.71	0.21	0.73
24	60	5	5	0.56	0.33	0.56
25	60	20	5	0.53	0.34	0.58
26	80	10	10	0.64	0.23	0.80
27	40	20	5	0.40	0.48	0.38
28	100	15	5	0.87	0.12	0.83
29	100	10	10	0.85	0.11	0.86
30	40	10	5	0.39	0.49	0.39
31	20	20	10	0.10	0.90	0.11
32	40	15	10	0.36	0.49	0.35
33	40	5	10	0.36	0.49	0.45
34	80	10	5	0.73	0.20	0.76
35	80	5	5	0.75	0.19	0.72

https://doi.org/10.36375/prepare_u.iiche.a408

Test Run	Engine Load (%) A	Palm biodiesel (%) B	Ethanol (%) C	BTE	BSFC	NOx
36	20	15	5	0.16	0.84	0.12
37	100	5	5	0.90	0.11	0.84
38	60	15	5	0.51	0.36	0.60
39	20	10	10	0.15	0.81	0.15
40	60	5	10	0.53	0.32	0.68

https://doi.org/10.36375/prepare_u.iiche.a408

2.3. Development Of Machine Learning Model:

Experimental data shown in table 1 is used to develop various machine learning models. First 3 parameters in table-1 namely engine load, Palm Biodiesel % and ethanol%are taken as the input and next 3 engine performance parameters namely BTE, BSFC and NOx are taken as output of machine learning models. At a time one output was taken and 3 different models were built.

In the past decade, a multitude of machine learning models and algorithms have emerged in the literature. The goal is to assess how quickly and accurately these machine learning algorithms can comprehend the intricate nonlinear relationships between input and output data. Each algorithm has its own strengths and weaknesses. Given the absence of prior knowledge about which model suits the data best, this study explores 26 advanced machine learning models.

In this step, pre-processed data are inputted into diverse nonlinear advanced machine learning models such as decision trees, support vector regression, artificial neural regression, and Gaussian process regression. The objective is to evaluate and compare the predictive performance of each algorithm and their accuracy in predicting efficiency (BTE), Brake specific energy consumption (BSFC) and emissions (NOx). Initially, all algorithms were run with their default meta-parameter values in the MATLAB environment. To accurately assess the predictive capabilities of different machine learning models, the dataset was divided into training and validation sets using techniques like k-fold cross-validation. The model's performance was rigorously evaluated on the validation set to ensure its generalizability to unseen data.

Performance metrics, including Coefficient of Determination (R2), Root Mean Square Error (RMSE), and Average Error Percent (AEP), were employed to quantify the accuracy and predictive power of the models. R2 represents the proportion of variance in the dependent variables (output parameters) from the independent variables (input parameters), while RMSE signifies the average deviation between predicted values and actual observations. These metrics offer valuable insights into the model's ability to accurately capture underlying patterns in the data.

2.4. Modelling By Different Machine Learning Algorithms:

For the sake of brevity, a concise introduction to the different machine learning models [40] utilized in this study is provided below.

Linear Regression:

- ***Simple Linear Regression:*** This model involves a linear regression approach with the inclusion of an intercept term and linear predictors. It aims to establish a linear relationship between the predictor variables and the target variable.
- ***Interaction Linear Regression:*** In this linear regression variant, not only the intercept and linear predictors are considered, but also interaction terms among predictors are incorporated. This allows the model to capture more complex relationships between variables.
- ***Robust Linear Regression:*** This type of linear regression is designed to be resistant to the influence of outliers in the data. It incorporates an intercept and linear predictors, but it employs techniques that downplay the impact of extreme data points.
- ***Stepwise Linear Regression:*** This linear regression model employs a stepwise algorithm to determine which predictor variables should be included in the model. It automatically selects variables based on their contribution to the model's performance.

https://doi.org/10.36375/prepare_u.iiche.a408

Decision Trees:

- ***Fine Tree Regression:*** A regression tree with a fine structure, requiring a minimum leaf size of 4. This results in more detailed and potentially overfitted trees that can capture intricate patterns in the data.
- ***Medium Tree Regression:*** This regression tree strikes a balance by requiring a minimum leaf size of 12. It aims to capture meaningful patterns while avoiding excessive complexity that might lead to overfitting.
- ***Coarse Tree Regression:*** In this case, the regression tree is constrained by a minimum leaf size of 36. This promotes a simplified and general representation of the data, suitable for capturing broader trends.

Support Vector Regression:

- ***Linear SVM Regression:*** This support vector machine employs a linear kernel to capture a simple linear relationship in the data. It's relatively interpretable and is suitable for cases where the underlying relationship appears to be linear.
- ***Quadratic SVM Regression:*** Here, a support vector machine is used with a quadratic kernel, enabling the model to capture quadratic relationships between variables.
- ***Cubic SVM Regression:*** Similar to the quadratic variant, this model employs a cubic kernel to capture cubic relationships between variables.
- ***Fine Gaussian SVM Regression:*** This SVM is tailored to capture finely-detailed structures in the data using the Gaussian kernel. The kernel scale is adjusted based on the number of predictors.
- ***Medium Gaussian SVM Regression:*** This version of the SVM captures less intricate patterns in the data compared to the fine Gaussian variant. It still uses the Gaussian kernel but with a kernel scale determined by the number of predictors.
- ***Coarse Gaussian SVM Regression:*** This SVM identifies coarse structures in the data by using a Gaussian kernel with a larger kernel scale, adapted to the number of predictors.

Gaussian Process Regression:

- ***Rational Quadratic GPR:*** This Gaussian process regression model employs the rational quadratic kernel to capture complex relationships with varying scales and magnitudes.
- ***Squared Exponential GPR:*** Using the squared exponential kernel, this model excels at capturing smooth relationships in the data, making it suitable for cases where the underlying relationship is continuous and smooth.
- ***Matern 5/2 GPR:*** This Gaussian process regression model uses the Matern 5/2 kernel, which provides flexibility in capturing both smooth and abrupt changes in the data.
- ***Exponential GPR:*** The exponential kernel is utilized here to capture relationships with a focus on rapidly decaying correlations.

Kernel Approximation Regression:

- ***SVM Kernel Regression:*** In this approach, a Gaussian kernel is applied to perform regression on nonlinear data with numerous observations. The kernel maps predictors to a higher-dimensional space and fits a linear SVM model to the transformed predictors.
- ***Least Square Kernel Regression:*** Similar to the SVM kernel regression, this model uses a Gaussian kernel to regress nonlinear data. However, instead of an SVM, it employs an ordinary least squares linear regression model on the transformed predictors.

https://doi.org/10.36375/prepare_u.iiche.a408

Ensembles of Trees:

- ***Boosted Trees:*** This ensemble method involves combining multiple regression trees using the LS Boost algorithm. It is efficient in terms of time and memory usage, but may require a larger number of ensemble members for optimal performance.
- ***Bagged Trees:*** A bootstrap-aggregated ensemble of regression trees. While it often provides high accuracy, it can be resource-intensive in terms of computation and memory, particularly for large datasets.

Artificial Neural Network:

- ***Narrow ANN Regression:*** This regression neural network consists of a single fully connected layer with 10 neurons, excluding the final fully connected layer used for regression prediction.
- ***Medium ANN Regression:*** With a single fully connected layer containing 25 neurons, this neural network aims to capture moderately complex relationships between predictors and the target.
- ***Wide ANN Regression:*** In this neural network, a single fully connected layer with 100 neurons is used, suitable for capturing broader patterns and relationships in the data.
- ***Bilayered ANN Regression:*** This regression neural network incorporates two fully connected layers (excluding the final regression layer), allowing for more intricate feature extraction and representation.
- ***Trilayered ANN Regression:*** With three fully connected layers (excluding the final regression layer), this neural network aims to capture even more complex hierarchical patterns in the data.

In this study, experimental data of table 1 were applied to all 26 models mentioned above, and a comparison table summarizing their performance was created. Most accurate model (highest R2 and lowest RMSE and AEP) was chosen for further investigation and optimization.

2.5. Optimisation By Multi-Objective Genetic Algorithm:

Once a reliable and accurate model is shortlisted, the next objective of this study is to find the optimum value of 3 input parameters namely engine load, Palm Biodiesel % and ethanol% so that BTE is maximized and BSFC and NOx are minimized simultaneously. Since the 3 objectives are conflicting in nature, a multi-objective genetic algorithm is used here to strike a balance.

Multi-Objective Genetic Algorithms (MOGAs) [41] have emerged as powerful tools in the realm of optimization and decision-making. Unlike traditional single-objective optimization methods, MOGAs are designed to handle complex problems with multiple conflicting objectives, offering a versatile approach to finding a set of diverse and optimal solutions, known as the Pareto front [42]. Leveraging principles from natural evolution, MOGAs employ genetic operators such as selection, crossover, and mutation to iteratively evolve a population of candidate solutions. These algorithms emphasize the exploration of the solution space, balancing the trade-offs between competing objectives. Through generations of evolution, MOGAs guide the search towards the Pareto-optimal front, enabling decision-makers to make informed choices based on a range of optimal solutions rather than a single compromise. (MOGA)s are based on the principle of natural evolution to find optimal methods for problems with multiple conflicting goals. The process begins with initializing a population of solutions to a problem. Each solution is represented as a set, often called chromosomes. These individuals are evaluated using objective functions that

https://doi.org/10.36375/prepare_u.iiche.a408

measure how well they meet the various objectives of the problem. The main elements of MOGA include choice, competition, and change. During the selection period, individuals in the population are selected as parents based on their fitness, determined by the performance. Individuals with more positive goals are more likely to be selected as parents.

During crossover, two parents come together to produce offspring. By applying crossover operators to the parents' chromosomes, genetic information is exchanged to create new solutions. This mimics the process of genetic recombination in natural evolution. After the birth, some candidate solutions may develop mutations in which some of their chromosomes change. Mutations add genetic diversity to the population, preventing premature convergence to optimal solutions. When a new generation of offspring is created, a process called environmental selection is used. This step involves matching parents and offspring and selecting individuals for the next generation. Often, strategies such as elitism are used to ensure that the best available solutions are preserved for future generations. The algorithm repeats this step for several generations or until the fitness improvement is complete.

The goal of MOGA [43] is to strike a balance between exploration and implementation, exploring the overall solution space while using the contract space to converge to Pareto optimality, that is, a set of solutions where no other solution can improve an objective without harming the others.

The result of a multi-objective genetic algorithm is a set of variables that represent trade-offs between conflicting goals. By analysing the Pareto front, decision makers can gain a better understanding of the actual decision-making process by choosing the solutions that best suit their preferences and needs.

3. Results And Discussions:

3 different models are created for BTE, BSFC and NOx. For each model, 26 machine learning algorithms were used and out of them only the one that had the highest R-squared value was selected. Table 2, 3 and 4 summaries Model predictions performance of 26 different algorithms for BTE, BSFC and NOx respectively. The very high value of R2 and low value of RMSE signifies that all 3 models are very accurate.

Table 2: BTE Model predictions performance of different algorithms

Model Number	Model Type	RMSE (Validation)	MSE (Validation)	R-Squared (Validation)	MAE (Validation)
1	Simple Linear Regression	0.03	0.00	0.99	0.02
2	Interaction Linear Regression	0.02	0.00	0.99	0.02
3	Robust Linear Regression	0.03	0.00	0.99	0.02
4	Stepwise Linear Regression	0.02	0.00	0.99	0.02
5	Fine Tree Regression	0.05	0.00	0.97	0.04
6	Medium Tree Regression	0.15	0.02	0.64	0.13

https://doi.org/10.36375/prepare_u.iiche.a408

Model Number	Model Type	RMSE (Validation)	MSE (Validation)	R-Squared (Validation)	MAE (Validation)
7	Coarse Tree Regression	0.25	0.06	0.00	0.21
8	Linear SVM	0.03	0.00	0.99	0.02
9	Quadratic SVM	0.02	0.00	0.99	0.02
10	Cubic SVM	0.03	0.00	0.99	0.02
11	Fine Gaussian SVM	0.24	0.06	0.10	0.20
12	Medium Gaussian SVM	0.07	0.01	0.92	0.06
13	Coarse Gaussian SVM	0.05	0.00	0.96	0.04
14	Boosted Ensemble	0.09	0.01	0.87	0.08
15	Bagged Ensemble	0.09	0.01	0.88	0.07
16	Rational Quadratic GPR	0.02	0.00	0.99	0.02
17	Squared Exponential GPR	0.02	0.00	0.99	0.02
18	Matern 5/2 GPR	0.04	0.00	0.98	0.03
19	Exponential GPR	0.02	0.00	0.99	0.02
20	Narrow ANN	0.04	0.00	0.98	0.03
21	Medium ANN	0.03	0.00	0.99	0.02
22	Wide ANN	0.03	0.00	0.98	0.02
23	Bilayered ANN	0.05	0.00	0.96	0.04
24	Trilayered ANN	0.04	0.00	0.98	0.03
25	SVM Kernel	0.04	0.00	0.97	0.03
26	Least Square Kernel	0.07	0.01	0.92	0.06

Table 3: BSFC Model predictions performance of different algorithms

Model Number	Model Type	RMSE (Validation)	MSE (Validation)	R-Squared (Validation)	MAE (Validation)
1	Simple Linear Regression	0.07	0.00	0.92	0.06
2	Interaction Linear Regression	0.08	0.01	0.91	0.06
3	Robust Linear Regression	0.07	0.00	0.92	0.06
4	Stepwise Linear Regression	0.07	0.00	0.92	0.06
5	Fine Tree Regression	0.03	0.00	0.98	0.03

https://doi.org/10.36375/prepare_u.iiche.a408

Model Number	Model Type	RMSE (Validation)	MSE (Validation)	R-Squared (Validation)	MAE (Validation)
6	Medium Tree Regression	0.13	0.02	0.72	0.12
7	Coarse Tree Regression	0.25	0.06	0.00	0.21
8	Linear SVM	0.08	0.01	0.91	0.05
9	Quadratic SVM	0.04	0.00	0.97	0.03
10	Cubic SVM	0.04	0.00	0.98	0.03
11	Fine Gaussian SVM	0.24	0.06	0.07	0.19
12	Medium Gaussian SVM	0.10	0.01	0.85	0.07
13	Coarse Gaussian SVM	0.10	0.01	0.83	0.07
14	Boosted Ensemble	0.11	0.01	0.82	0.07
15	Bagged Ensemble	0.09	0.01	0.86	0.07
16	Rational Quadratic GPR	0.04	0.00	0.97	0.03
17	Squared Exponential GPR	0.04	0.00	0.98	0.03
18	Matern 5/2 GPR	0.06	0.00	0.95	0.04
19	Exponential GPR	0.04	0.00	0.97	0.03
20	Narrow ANN	0.07	0.01	0.92	0.05
21	Medium ANN	0.05	0.00	0.95	0.04
22	Wide ANN	0.05	0.00	0.97	0.03
23	Bilayered ANN	0.06	0.00	0.94	0.04
24	Trilayered ANN	0.05	0.00	0.95	0.04
25	SVM Kernel	0.06	0.00	0.94	0.04
26	Least Square Kernel	0.08	0.01	0.91	0.05

Table 4: BTE Model predictions performance of different algorithms

Model Number	Model Type	RMSE (Validation)	MSE (Validation)	R-Squared (Validation)	MAE (Validation)
1	Simple Linear Regression	0.06	0.00	0.94	0.06
2	Interaction Linear Regression	0.07	0.01	0.93	0.06
3	Robust Linear Regression	0.06	0.00	0.94	0.06
4	Stepwise Linear Regression	0.07	0.00	0.94	0.06

https://doi.org/10.36375/prepare_u.iiche.a408

Model Number	Model Type	RMSE (Validation)	MSE (Validation)	R-Squared (Validation)	MAE (Validation)
5	Fine Tree Regression	0.03	0.00	0.98	0.03
6	Medium Tree Regression	0.12	0.01	0.80	0.11
7	Coarse Tree Regression	0.27	0.07	0.00	0.24
8	Linear SVM	0.07	0.00	0.94	0.06
9	Quadratic SVM	0.03	0.00	0.98	0.03
10	Cubic SVM	0.03	0.00	0.98	0.03
11	Fine Gaussian SVM	0.25	0.06	0.11	0.22
12	Medium Gaussian SVM	0.07	0.00	0.94	0.05
13	Coarse Gaussian SVM	0.09	0.01	0.88	0.07
14	Boosted Ensemble	0.10	0.01	0.87	0.08
15	Bagged Ensemble	0.10	0.01	0.87	0.08
16	Rational Quadratic GPR	0.02	0.00	0.99	0.02
17	Squared Exponential GPR	0.02	0.00	0.99	0.02
18	Matern 5/2 GPR	0.04	0.00	0.98	0.03
19	Exponential GPR	0.02	0.00	0.99	0.02
20	Narrow ANN	0.03	0.00	0.98	0.02
21	Medium ANN	0.05	0.00	0.97	0.04
22	Wide ANN	0.03	0.00	0.99	0.02
23	Bilayered ANN	0.04	0.00	0.98	0.03
24	Trilayered ANN	0.05	0.00	0.96	0.04
25	SVM Kernel	0.05	0.00	0.96	0.04
26	Least Square Kernel	0.06	0.00	0.94	0.05

As discussed earlier, the model selection is based on 3 features – R-squared value, RMSE (Root Mean Square Error) and MAE (Mean Absolute Error).

All the 3 features for each model have been obtained from the results section of Regression Learner App in Matlab-2023. The model that has displayed the Highest R-squared value, Lowest RMSE value and Lowest MAE value has been selected in each of the cases.

In BTE model, Stepwise Linear Regression algorithm was selected as it gave an R-squared value of 0.99, RMSE value of 0.2234 and MAE value 0.01 which were comparatively the Highest, lowest, and lowest respectively.

https://doi.org/10.36375/prepare_u.iiche.a408

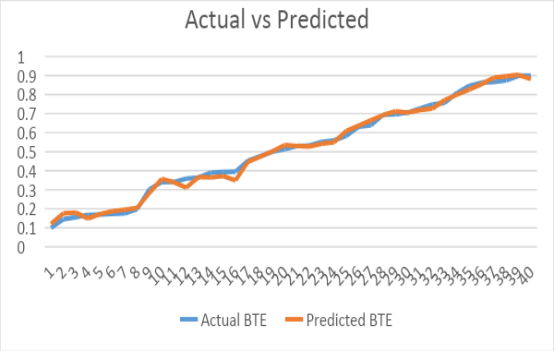

Fig 1. Actual vs model predicted outcome of BTE

In the BSFC model, Tree algorithm was selected as it gave R-squared value of 0.98, RMSE value of 0.034 and MAE value 0.025 which were comparatively the Highest, lowest, and lowest respectively.

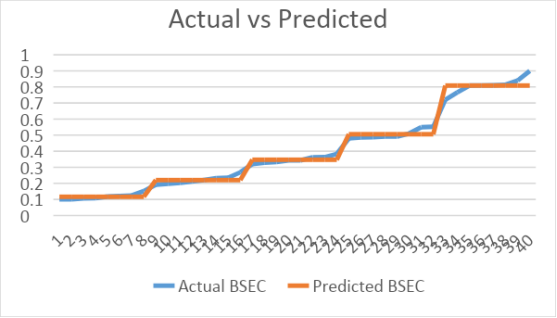

Fig 2. Actual vs model predicted outcome of BSFC

In the NOx model, Gaussian Process Regression-Matern 5/2 algorithm was selected as it gave R-squared value of 0.99, RMSE value of 0.00047 and MAE value 0.016 which were comparatively the Highest, lowest, and lowest respectively.

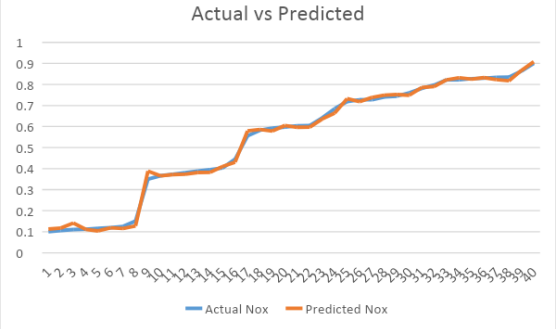

Fig 3. Actual vs model predicted outcome of NOx

Fig 1 ,2 and 3 shows the best model performance, namely experimental data with model predictions and they're almost overlapping for BTE, BSF and NOx respectively.

3.1. Optimization results:

Once a reliable and accurate model is shortlisted, the next objective of this study is to find the optimum value of 3 input parameters namely engine load, Palm Biodiesel % and ethanol% so that BTE is maximized and BSF and NOx are minimized simultaneously. Since the 3 objectives are conflicting in nature, a multi-objective genetic algorithm is used here to strike a balance and create a pareto optimal front.

The Pareto-optimal front, a fundamental concept in multi-objective optimization, represents a set of solutions where no individual solution can be improved in one objective without degrading at least one other objective. In other words, these solutions embody the best possible compromises between conflicting objectives, showcasing the trade-offs inherent in the problem at hand. The Pareto front is not a single solution but a collection of diverse, non-dominated solutions, each offering a unique balance between the competing criteria. Finding these solutions is crucial in decision-making processes where multiple, often conflicting, objectives need to be considered simultaneously. These objectives could be Fuel consumption minimization, Thermal efficiency maximization, or NOx reduction, and the Pareto front reveals the spectrum of solutions that optimally balance these goals. Determining the Pareto front involves utilizing optimization algorithms like Multi-Objective Genetic Algorithms (MOGAs), which iteratively evolve a population of potential solutions, ensuring that no solution dominates another in all objectives. The Pareto-optimal front is invaluable for decision-makers, providing a comprehensive understanding of the solution space and enabling them to make well-informed

https://doi.org/10.36375/prepare_u.iiche.a408

decisions based on the available trade-offs among conflicting objectives.

Fig 4 shows Pareto optimal solutions for BTE vs BSFC, Fig 5 shows Pareto optimal solutions for BTE vs NOx, Fig 6 shows Pareto optimal solutions for BSFC vs NOx

solutions after applying a multi-objective genetic algorithm.

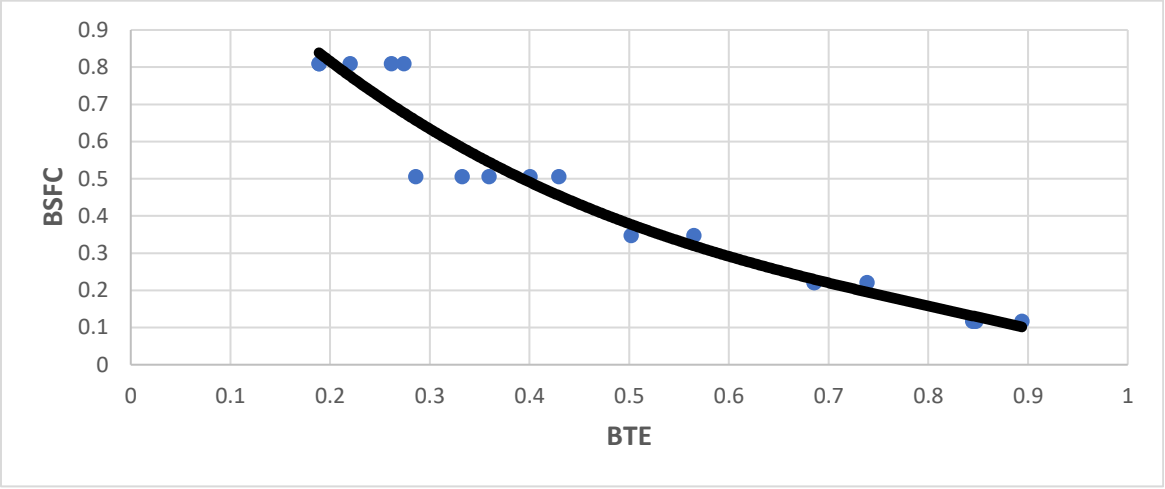

Fig 4: Pareto optimal solutions for BTE vs BSFC

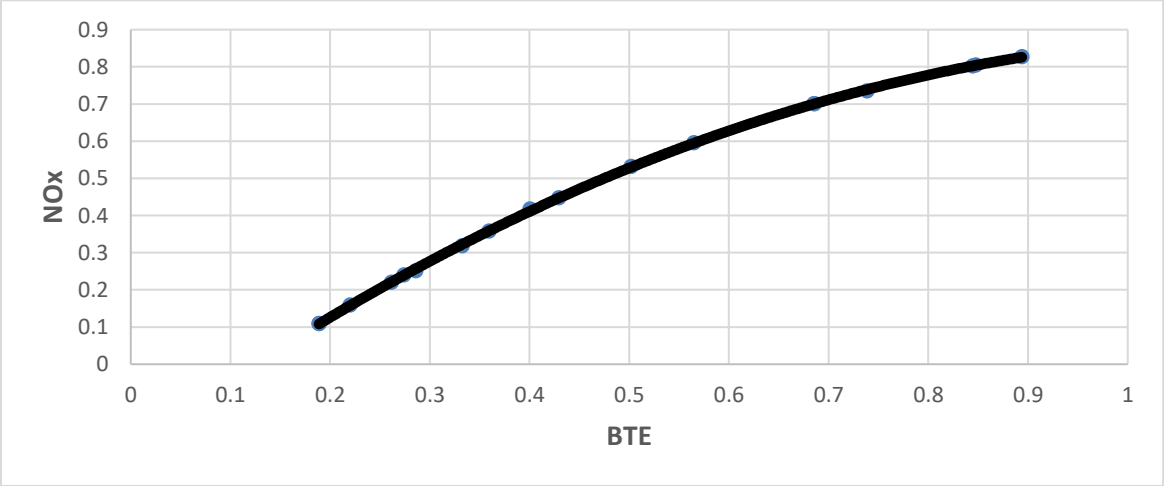

Fig 5: Pareto optimal solutions for BTE vs NOx

Table5 Summarizes the Pareto optimal

https://doi.org/10.36375/prepare_u.iiche.a408

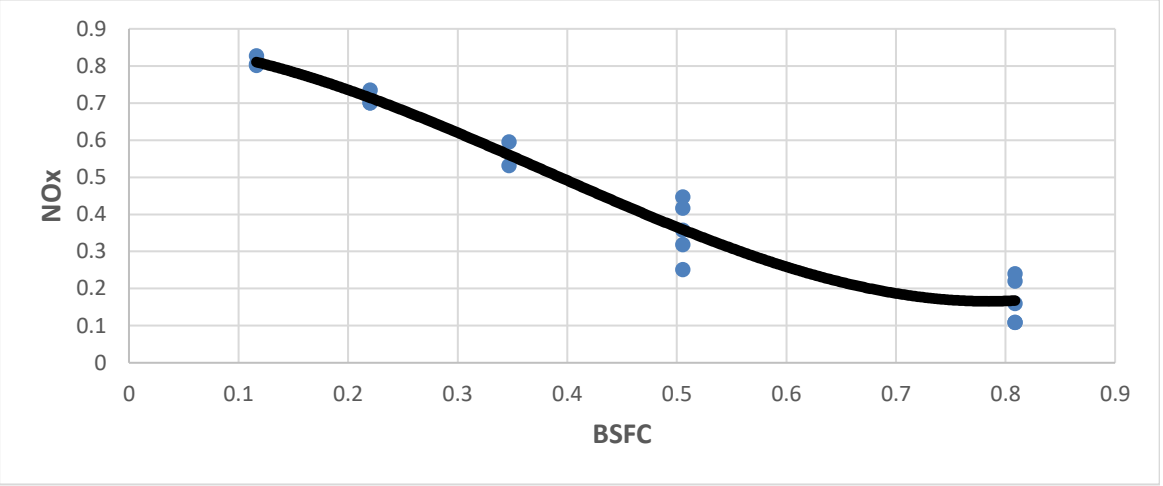

Fig 6: Pareto optimal solutions for BSFC vs NOx

Table 5: Pareto optimal solutions after applying multi-objective genetic algorithm

load% (A)	Palm-biodiesel (B)	Ethanol (C)	BTE	BSFC	NOx
20.00	5.00	5.00	0.19	0.81	0.11
61.89	5.08	5.29	0.57	0.35	0.60
75.34	5.78	5.08	0.69	0.22	0.70
20.00	5.00	5.00	0.19	0.81	0.11
93.46	6.09	5.05	0.85	0.12	0.81
28.11	5.55	5.07	0.26	0.81	0.22
98.75	6.83	5.03	0.89	0.12	0.83
43.71	6.16	5.21	0.40	0.51	0.42
35.98	5.23	5.09	0.33	0.51	0.32
23.47	5.31	5.20	0.22	0.81	0.16
30.79	5.09	5.01	0.29	0.51	0.25
81.15	5.43	5.02	0.74	0.22	0.74
29.55	5.88	5.07	0.27	0.81	0.24
54.97	6.26	5.03	0.50	0.35	0.53
38.98	5.21	5.27	0.36	0.51	0.36
46.85	6.11	5.03	0.43	0.51	0.45
92.97	5.11	5.15	0.85	0.12	0.80
75.39	5.52	5.12	0.69	0.22	0.70

4. Conclusion:

This study aims to determine the optimal proportions of palm biodiesel and ethanol in a biodiesel-ethanol (bio-diesohol) blend. It assesses how load, the shares of palm biodiesel and ethanol, impact Brake Thermal Efficiency (BTE), Brake Specific Energy Consumption (BSFC), and NOx emissions through a multi-objective genetic algorithm. Subsequently, comprehensive 26 machine learning models are established to precisely forecast engine performance. Lastly, a sophisticated hybrid modelling approach is employed to explore the multi-objective genetic algorithm optimization of engine input parameters and response variables.

5. References:

[1] Ghadikolaei MA, Cheung CS, Yung KF. Study of combustion, performance and emissions of diesel engine fueled with diesel/biodiesel/alcohol blends having the same oxygen concentration. Energy 2018;157:258–69. https://doi.org/10.1016/j.energy.2018.05.164.

[2] Agarwal AK, Dhar A. Experimental investigations of performance, emission and combustion characteristics of Karanja oil blends fuelled DICI engine. Renewable Energy2013;52:283–91. https://doi.org/10.1016/j.renene.2012.10.015.

[3] Agarwal AK, Gupta JG, Dhar A. Potential and challenges for large-scale application of biodiesel in automotive sector. Prog Energy Combust Sci 2017;61:113–49. https://doi.org/10.1016/j.pecs.2017.03.002.

[4] Dey S, Deb M, Das PK. Chemical Characterization and Tribological Behavior of Kitchen Chimney Dump Lard (KCDL) as a Bio-lubricant. Revue Des Composites et Des Materiaux Avances 2019;29. 10.18280/rcma.290303.

[5] Aydin H, Ilkiliç C. Effect of ethanol blending with biodiesel on engine performance and exhaust emissions in a CI engine. Appl Therm Eng 2010;30:1199–204. https://doi.org/10.1016/j.applthermaleng.2010.01.037.

7] Dey S, Reang NM, Das PK, Deb M. A comprehensive study on prospects of economy, environment, and efficiency of palm oil biodiesel as a renewable fuel. J Cleaner Prod 2020. https://doi.org/10.1016/j.jclepro.2020.124981.

[8] Guido C, Beatrice C, Napolitano P. Application of bioethanol / RME / diesel blend in a Euro5 automotive diesel engine: potentiality of closed loop combustion control technology. Appl Energy 2013;102:13–23. https://doi.org/10.1016/j.apenergy.2012.08.051

[9] Gulum M, Bilgin A. An experimental optimization research of methyl and ethyl esters production from safflower oil. Environ Climate Technol 2018;22:132–48. https://doi.org/10.2478/rtuect-2018-0009.

[10] Mohiddin MN, Saleh AA, Reddy ANR, Hamdan S. A study on chicken fat as an alternative feedstock: Biodiesel production, fuel characterisation, and diesel engine performance analysis. Int J Automotive and Mech Eng 2018;15:5535–46.10.15282/ijame.15.3.2018.10.0425.

[11] Ali OM, Mamat R, Abdullah NR, Abdullah AA. Analysis of blended fuel properties and engine performance with palm biodiesel-diesel blended fuel. Renewable Energy 2015;86:59–67. https://doi.org/10.1016/j.renene.2015.07.103.

[12] Zaharin MSM, Abdullah NR, Najafi G, Sharudin H, Yusaf T. Effects of physicochemical properties of biodiesel fuel blends with alcohol on diesel engine performance and exhaust emissions: a review. Renew Sustain Energy Rev 2017;79: 475–93.

https://doi.org/10.1016/j.rser.2017.05.035.

[13] Di Y, Cheung CS, Huang Z. Comparison of the effect of biodiesel-diesel and ethanol-diesel on the gaseous emission of a direct-injection diesel engine. Atmos Environ 2009;43:2721–30. https://doi.org/10.1016/j.atmosenv.2009.02.050.

[14] Ren Y, Huang ZH, Jiang DM, Li W, Liu B, Wang XB. Effects of the addition of ethanol and cetane number improver on the combustion and emission characteristics of a compression ignition engine. Proc Inst Mech Eng, Part D: J Automobile Eng 2008;222:1077–87. https://doi.org/10.1243/09544070JAUTO516.

[15] EL-Seesy AI, Kayatas Z, Takayama R, He Z, Kandasamy S, Kosaka H. Combustion and emission characteristics of RCEM and common rail diesel engine working with diesel fuel and ethanol/hydrous ethanol injected in the intake and exhaust port: Assessment and comparison. Energy Conversion and Management 2020;205: 112453. 10.1016/j.enconman.2019.112453.

[16] Dey S, Reang NM, Deb M, Das PK. Study on performance-emission trade-off and multi-objective optimization of diesel-ethanol-palm biodiesel in a single cylinder CI engine: a Taguchi-fuzzy approach ARTICLE HISTORY. Energy Sources Part A 2020;1–21. https://doi.org/10.1080/15567036.2020.1767234.

[17] Yesilyurt MK, Aydin M. Experimental investigation on the performance, combustion and exhaust emission characteristics of a compression-ignition engine fueled with cottonseed oil biodiesel/diethyl ether/diesel fuel blends. Energy Convers Manage 2020;205:112355. https://doi.org/10.1016/j.enconman.2019.112355.

[18] Qi DH, Chen H, Geng LM, Bian YZ. Effect of diethyl ether and ethanol additives on the combustion and emission characteristics of biodiesel-diesel blended fuel engine. Renewable Energy 2011;36:1252–8. https://doi.org/10.1016/j.renene.2010.09.021

[19] Tosun E, Aydin K, Bilgili M. Comparison of linear regression and artificial neural network model of a diesel engine fueled with biodiesel-alcohol mixtures. Alexandria Engineering Journal 2016;55:3081–9.

https://doi.org/10.1016/j.aej.2016.08.011

[20] Atmanli A, Yüksel B, Ileri E, Deniz Karaoglan A. Response surface methodology based optimization of diesel-n-butanol -cotton oil ternary blend ratios to improve engine performance and exhaust emission characteristics. Energy Convers Manage

2015;90:383–94. https://doi.org/10.1016/j.enconman.2014.11.029

[21] Sakthivel R, Ramesh K, Joseph John Marshal S, Sadasivuni KK. Prediction of performance and emission characteristics of diesel engine fuelled with waste biomass pyrolysis oil using response surface methodology. Renewable Energy 2019;136:91–103.10.1016/J.RENENE.2018.12.109.

[22] Krishnamoorthi M, Malayalamurthi R, Mohamed Shameer P. RSM based optimization of performance and emission characteristics of DI compression ignition engine fuelled with diesel/aegle marmelos oil/diethyl ether blends at varying compression ratio, injection pressure and injection timing. Fuel 2018;221: 283–97.

https://doi.org/10.1016/j.fuel.2018.02.070

[23] Fang W, Kittelson DB, Northrop WF. Optimization of reactivity-controlled compression ignition combustion fueled with diesel and hydrous ethanol using response surface methodology. Fuel 2015;160:446–57. https://doi.org/10.1016/j.fuel.2015.07.055

[24] Hirkude JB, Padalkar AS. Performance optimization of CI engine fuelled with waste fried oil methyl ester-diesel blend using response surface methodology. Fuel 2014; 119:266–73. https://doi.org/10.1016/j.fuel.2013.11.039.

[25] Ileri E, Karaoglan AD, Atmanli A. Response surface methodology based prediction of engine performance and exhaust emissions of a diesel engine fuelled with canola oil methyl ester. J Renewable Sustainable Energy 2013;5:033132. https://doi.org/10.1063/1.4811801.

[26] Shivakumar, Srinivasa Pai P, Shrinivasa Rao BR. Artificial Neural Network based prediction of performance and emission characteristics of a variable compression ratio CI engine using WCO as a biodiesel at different injection timings. Applied Energy 2011;88:2344–54.10.1016/j.apenergy.2010.12.030.

[27] Taghavifar HH, Taghavifar HH, Mardani A, Mohebbi A, Khalilarya S, Jafarmadar S. Appraisal of artificial neural networks to the emission analysis and prediction of CO2, soot, and NOx of n-heptane fueled engine. J Cleaner Prod 2016;112:1729–39. https://doi.org/10.1016/j.jclepro.2015.03.035

[28] Prasada Rao K, Victor Babu T, Anuradha G, Appa Rao BV. IDI diesel engine performance and exhaust emission analysis using biodiesel with an artificial neural network (ANN). Egypt J Pet 2017;26:593–600. https://doi.org/10.1016/j.ejpe.2016.08.006

[29] Javed S, Satyanarayana Murthy YV V, Baig RU, Prasada Rao D. Development of ANN model for prediction of performance and emission characteristics of hydrogen dual fueled diesel engine with Jatropha Methyl Ester biodiesel blends. J Natural Gas Sci Eng 2015;26:549–57. doi:10.1016/j.jngse.2015.06.041.

[30] Uslu S, Celik MB. Prediction of engine emissions and performance with artificial neural networks in a single cylinder diesel engine using diethyl ether. Eng Sci Technol Int J 2018;21:1194–201. https://doi.org/10.1016/j.jestch.2018.08.017

[31] Aryasomayajula Venkata Satya Lakshmi SB, Subramania Pillai N, Khadhar Mohamed MSB, Narayanan A. Biodiesel production from rubber seed oil using calcined eggshells impregnated with Al2O3 as heterogeneous catalyst: a comparative study of RSM and ANN optimization. Brazilian J Chem Eng 2020;37: 351–68. https://doi.org/10.1007/s43153-020-00027-9

[32] Hariharan N, Senthil V, Krishnamoorthi M, Karthic SV. Application of artificial neural network and response surface methodology for predicting and optimizing dual-fuel CI engine characteristics using hydrogen and bio fuel with water injection. Fuel 2020;270:117576. https://doi.org/10.1016/j.fuel.2020.117576

[33] Hammoudi A, Moussaceb K, Belebchouche C, Dahmoune F. Comparison of artificial neural network (ANN) and response surface methodology (RSM) prediction in compressive strength of recycled concrete aggregates. Constr Build Mater 2019;209:425–36. https://doi.org/10.1016/j.conbuildmat.2019.03.119

[34] Samuel OD, Okwu MO. Comparison of Response Surface Methodology (RSM) and Artificial Neural Network (ANN) in modelling of waste coconut oil ethyl esters production. Energy Sources Part A 2019;41:1049–61. https://doi.org/10.1080/15567036.2018.1539138.

[35] Astray G, Gullon ´ B, Labidi J, Gullon ´ P. Comparison between developed models using response surface methodology (RSM) and artificial neural networks (ANNs) with the purpose to optimize oligosaccharide mixtures production from sugar beet pulp. Ind Crops Prod 2016;92:290–9. https://doi.org/10.1016/j.indcrop.2016.08.011

[36] Ayoola AA, Hymore FK, Omonhinmin CA, Babalola PO, Fayomi OSI, Olawole OC, et al. Response surface methodology and artificial neural network analysis of crude palm kernel oil biodiesel production. Chem Data Collect 2020;28:100478. https://doi.org/10.1016/j.cdc.2020.100478

[37] Chouaibi M, Daoued K Ben, Riguane K, Rouissi T, Ferrari G. Production of bioethanol from pumpkin peel wastes: comparison between response surface methodology (RSM) and artificial neural networks (ANN). Industrial Crops and Products 2020;155:112822.10.1016/j.indcrop.2020.112822.

[38] Uslu S. Optimization of diesel engine operating parameters fueled with palm oil-diesel blend: Comparative evaluation between response surface methodology (RSM) and artificial neural network (ANN). Fuel 2020;276:117990. https://doi.org/10.1016/j.fuel.2020.117990

[39]. Dey, Suman, Narath Moni Reang, Pankaj Kumar Das, and Madhujit Deb. "Comparative study using RSM and ANN modelling for performance-emission prediction of CI engine fuelled with bio-diesohol blends: A fuzzy optimization approach." Fuel 292 (2021): 120356. https://doi.org/10.1016/j.fuel.2021.120356

[40]. Zheng, M., Wang, F., Hu, X., Miao, Y., Cao, H., & Tang, M. (2022). A Method for Analyzing the Performance Impact of Imbalanced Binary Data on Machine Learning Models. *Axioms*, *11*(11). https://doi.org/10.3390/axioms11110607

[41]. Wang, Z., Zhang, X., Zhang, Z. K., & Sheng, D. (2022). Credit portfolio optimization: A multi-objective genetic algorithm approach. Borsa Istanbul Review, 22(1). https://doi.org/10.1016/j.bir.2021.01.004

[42]. Giordano, P. C., Pereyra, V., Beccaria, A. J., Vero, S., & Goicoechea, H. C. (2020). Application of pareto-optimal front as an option to desirability function for the optimization of a microbiological process. *Microchemical Journal*, *155*. https://doi.org/10.1016/j.microc.2020.104682

[43]. Yu, W., Li, B., Jia, H., Zhang, M., & Wang, D. (2015). Application of multi-objective genetic algorithm to optimize energy efficiency and thermal comfort in building design. *Energy and Buildings*, *88*. https://doi.org/10.1016/j.enbuild.2014.11.063

https://doi.org/10.36375/prepare_u.iiche.a409

Photocatalytic Performance of Aluminum -Doped Graphene-like ZnO (g-AZO) Monolayer

S. Chowdhury[1], and Divya Somvanshi[2*]

[1]*Department of Electronics and Tele-Communication (ETCE) Engineering, Jadavpur University, Kolkata-700032, India*
[2]*Department of Physics, Harcourt Butler Technical University (HBTU), Kanpur-208002, India*
[*]*D. Somvanshi, Email: dsomvanshi@hbtu.ac.in, 8948930652*

Abstract

The graphene-like zinc oxide (g-ZnO) monolayer (ML) is a popular two-dimensional (2D) semiconductor. However, its applications are restricted in the photocatalytic water splitting reaction due to low visible absorption and wide optical band gap. Here, in this work, we studied the electronic structure of Al-doped graphene-like ZnO (g-AZO) ML using Density functional theory (DFT) calculations. The photocatalytic performance parameters such as bandgap, band edge levels, and absorption coefficient of g-AZO ML are studied under the application of biaxial strain varying from -10% to +10%. Our calculations show that g-AZO ML has a suitable band gap, band edge positions, and absorption coefficient in the visible range at ε = +9% and +10% tensile strain for photocatalytic water splitting reaction.

Keywords: Two-dimensional materials; Substitutional doping; biaxial strain; Photocatalysis reaction

I. Introduction

Photocatalytic water splitting is a promising technique for large-scale hydrogen production which uses renewable energy sources and also reduces global warming effects [1, 2]. For water splitting reaction, two conditions must be satisfied, first, the band edge positions must straddle the reduction and oxidation potentials of water.

Secondly, the band gap must exceed the hydrolysis voltage of water (1.23 eV) and be smaller than 3.00 eV [3, 4]. Recently, 2D semiconductors are being investigated for large-scale hydrogen production [4-9]. DFT tools allow the exploration of various external parameters to increase the photocatalytic performance of 2D materials [1, 10, 11]. The g-ZnO ML has high carrier mobility, large surface area, and excellent optical characteristics which enriches its applications in photocatalytic and energy harvesting fields [10-12]. Substitutional doping is considered one of the most desirable methods for tuning the electronic structure of semiconductors and it is also used to improve its photocatalytic performance [10, 11, 13-15]. Aluminium (Al) at the Zn site is considered an energetically favorable dopant in the g-ZnO ML. The g-AZO has various advantages such as reasonable cost, ample resources, tunable bandgap, and high stability in hydrogen plasma [16-22]. Although there are many studies have been reported on the improvement of the photocatalytic performance of 2D semiconductors by tuning the band gap [11, 23]. However, the photocatalytic properties of g-AZO ML have not been reported yet. Therefore, in this work, we investigated the photocatalytic properties of g-AZO ML under the application of biaxial strain using hybrid DFT calculations.

II. Computational details

Here, all the DFT calculations were performed using the Quantum ATK package [24]. The exchange-correlation functionals are described using hybrid functional (HSE06) [25]. A Linear combination of atomic orbitals (LCAO) basis with an energy cut-off of 125 Hartree and grid sampling of 25×25×1.

The dopant formation energy of Al in the g-ZnO monolayer is calculated as [26, 27], using

$$E_{form} = E_{ZnO+Al} - E_{ZnO} + \mu_{Zn} - \mu_{Al},$$

https://doi.org/10.36375/prepare_u.iiche.a409

The E_{form} of the g-AZO ML is calculated as -2.98 eV [28], which is exothermic in nature.

III. Results and discussions

A. Atomic and Electronic Structure of Al-doped ZnO monolayer

Here, we have doped one Al atom in a ZnO monolayer (4×4×1 supercell size) corresponding to a 6.25% doping concentration of the Al atom. The schematic atomic structure of g-AZO ML is shown in Fig. 1. The lattice constant and bond length for g-AZO ML is given as a = 3.29 Å, and d_{Al-O} = 1.77 Å [17]. The electronic band structure of g-AZO ML with HSE06 functionals has been shown in Fig. 2 and it is direct (Γ- Γ) in nature with a bandgap (E_g) value equal to 3.8 eV [17, 29].

It is observed that by doping an Al atom in the ZnO ML, the Fermi level shift inside the conduction band minima (CBM) resulted in n-type doping.

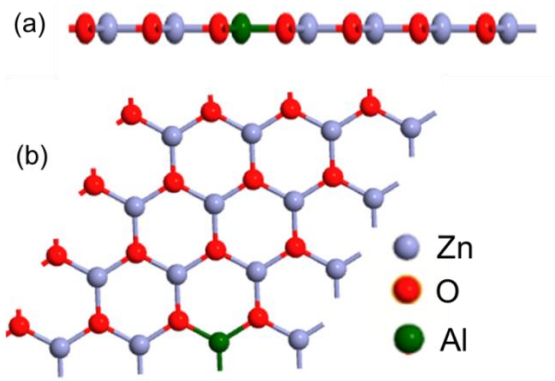

Fig. 1 (a) Side and (b) top view of the atomic structure of Al-doped g-ZnO monolayer,

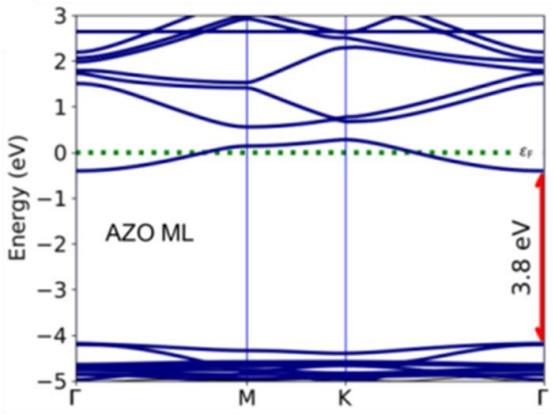

Fig. 2 Band structures of Al-doped ZnO ML obtained by HSE06 calculations.

B. Bandgap tunability of g-AZO monolayer under application of biaxial strain

Here, the effect of biaxial strain ($\varepsilon = \varepsilon_x = \varepsilon_y = (a_0 - a)/a \times 100\%$) on the electronic bandgap of the g-AZO ML is studied. The variations of bandgap under the application of varying biaxial strain from -10% to +10% are shown in Fig. 3. It is visible that the bandgap value linearly decreases with an increase in tensile strain from 0% to +9% and a slight increase at ε =+10% is observed. For compressive strain, the E_g value increases up to ε = -1% strain and then it starts decreasing continuously up to ε = -10%. We observed that the bandgap of g-AZO ML at +9% and +10% has decreased to 2.89 eV and 2.91 eV respectively, which satisfies the photocatalytic criteria for water splitting reaction [30].

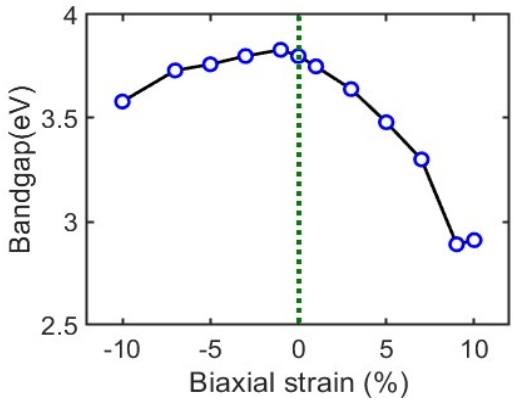

Fig. 3 Band gap of the g-AZO monolayer at different applied biaxial strains

C. Biaxial strain modulated optical spectra of g-AZO monolayer

The optical spectra of the g-AZO monolayer under varying biaxial strain are shown in Fig. 4. The absorption spectra at ε = 0% are shown by the black solid line. By increasing the tensile strain ε = 0% to +5%, a suppression of absorption spectra is observed in the UV and visible regions and it is shifted to red. However, a sharp peak is observed in the visible region at ε = +10% tensile strain (pink line). In the compressive strain up to ε = -5%, clampdown in UV and visible absorption have been observed with a blue shift. Interestingly, at ε = -10%, a sudden increase in absorption spectra occurs in the visible range.

https://doi.org/10.36375/prepare_u.iiche.a409

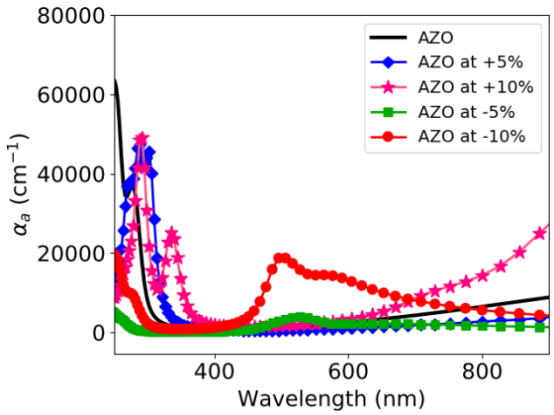

Fig. 4 Absorption spectra of the g-AZO monolayer with ε= ±5% and ±10%

D. Band edge positions of g-AZO monolayer under biaxial strain

Here, the band edge positions of g-AZO ML have been investigated by varying biaxial strain for analysis of photocatalytic performance. The band edge positions i. e. CBM, and VBM, under varying biaxial strain of the g-AZO monolayer, are shown in Fig. 5. It is noted that the g-AZO ML satisfies the band edge positions of CBM and VBM at unstrained conditions for water splitting. However, the bandgap energy of g-AZO ML at unstrained conditions exceeds bandgap of 3 eV which is not ideal for photocatalytic reaction. By applying biaxial tensile and compressive strain from -10% to +10%, the band edge positions of g-AZO ML have been tuned. The band edge positions of g-AZO ML initially reduces upto ε = +7% and then it started to increase. In the case of compressive strain, the band edge positions decrease continuously up to -9%. We found that the appropriate band edge positions for photocatalytic reaction have been observed at +9% and +10% tensile strain. At +9% and +10% tensile strain, the obtained CBM values are -4.41 eV, and -4.2 eV which are higher than H^+/H_2 (-4.44 eV) and the obtained VBM values are -7.3 eV, -7.11 eV which are lower than O_2/H_2O (-5.67 eV), respectively. The CBM level is located about 0.03 eV above the H^+/H^2 potential for +9% tensile strain. At +10% tensile strain, the CBM level increases to about 0.24 eV which is enough for hydrogen production. Meanwhile, the VBM level is always lower than the water oxidation potential (O_2/H_2O), and the oxidation capacity increases with the biaxial strain. The results show that the AZO ML has enough potential about 1.63 eV and 1.44 eV respectively for oxidation reaction at +9% and +10% tensile strain.

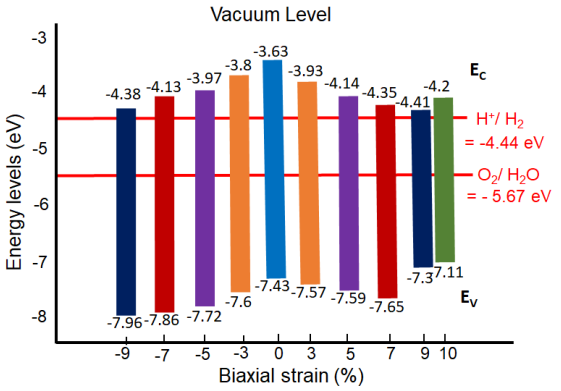

Fig. 5 CBM and VBM energy levels of g-AZO monolayer at unstrained and strained conditions.

Conclusion

In summary, the electronic structure and absorption spectra of g-AZO monolayer under varying biaxial strain have been studied by using hybrid DFT calculations for photocatalytic applications. Our results show that the g-AZO monolayer at ε = +9% and +10% has an appropriate bandgap, CBM, VBM positions for photocatalytic water splitting. Moreover, at ε = +10%, g-AZO ML shows good absorption in the visible region from 600 to 900 eV, which shows that biaxial strain can effectively modulate the photocatalytic performance of the g-AZO monolayer.

Acknowledgment

Divya Somvanshi thanks the DST INSPIRE Faculty Award (DST/INSPIRE/04/2017/000147) of the Government of India for the financial support.

References

[1] A. K. Singh, K. Mathew, H. L. Zhuang, and R. G. Hennig, "Computational Screening of 2D Materials for Photocatalysis," *The Journal of Physical Chemistry Letters*, vol. 6, pp. 1087-1098, 2015.

[2] P. Ganguly, M. Harb, Z. Cao, L. Cavallo, A. Breen, S. Dervin, *et al.*, "2D Nanomaterials for Photocatalytic Hydrogen Production," *ACS Energy Letters*, vol. 4, pp. 1687-1709, 2019.

https://doi.org/10.36375/prepare_u.iiche.a409

[3] S. Cho, J.-W. Jang, K.-H. Lee, and J. S. Lee, "Research Update: Strategies for efficient photoelectrochemical water splitting using metal oxide photoanodes," *APL Materials*, vol. 2, p. 010703, 2014.
[4] S. Hu and M. Zhu, "Ultrathin Two-Dimensional Semiconductors for Photocatalysis in Energy and Environment Applications," *ChemCatChem*, vol. 11, pp. 6147-6165, 2019.
[5] T. Hisatomi, J. Kubota, and K. Domen, "Recent advances in semiconductors for photocatalytic and photoelectrochemical water splitting," *Chemical Society Reviews*, vol. 43, pp. 7520-7535, 2014.
[6] Y. Ji, M. Yang, H. Dong, T. Hou, L. Wang, and Y. Li, "Two-dimensional germanium monochalcogenide photocatalyst for water splitting under ultraviolet, visible to near-infrared light," *Nanoscale*, vol. 9, pp. 8608-8615, 2017.
[7] B. Luo, G. Liu, and L. Wang, "Recent advances in 2D materials for photocatalysis," *Nanoscale*, vol. 8, pp. 6904-6920, 2016.
[8] Y. Li, Y.-L. Li, B. Sa, and R. Ahuja, "Review of two-dimensional materials for photocatalytic water splitting from a theoretical perspective," *Catalysis Science & Technology*, vol. 7, pp. 545-559, 2017.
[9] S. J. A. Moniz, S. A. Shevlin, D. J. Martin, Z.-X. Guo, and J. Tang, "Visible-light driven heterojunction photocatalysts for water splitting – a critical review," *Energy & Environmental Science*, vol. 8, pp. 731-759, 2015.
[10] H. Chen, C. Tan, K. Zhang, W. Zhao, X. Tian, and Y. Huang, "Enhanced photocatalytic performance of ZnO monolayer for water splitting via biaxial strain and external electric field," *Applied Surface Science*, vol. 481, pp. 1064-1071, 2019.
[11] T. Kaewmaraya, A. De Sarkar, B. Sa, Z. Sun, and R. Ahuja, "Strain-induced tunability of optical and photocatalytic properties of ZnO mono-layer nanosheet," *Computational Materials Science*, vol. 91, pp. 38-42, 2014.
[12] K. K. Korir, E. M. Benecha, F. O. Nyamwala, and E. B. Lombardi, "Tuning electronic structure of ZnO nanowires via 3d transition metal dopants for improved photo-electrochemical water splitting: An ab initio study," *Materials Today Communications*, vol. 26, p. 101929, 2021.
[13] I. Ahmad, E. Ahmed, and M. Ahmad, "The excellent photocatalytic performances of silver doped ZnO nanoparticles for hydrogen evolution," *SN Applied Sciences*, vol. 1, p. 327, 2019.
[14] D. Commandeur, J. McGuckin, and Q. Chen, "Hematite coated, conductive Y doped ZnO nanorods for high-efficiency solar water splitting," *Nanotechnology*, vol. 31, p. 265403, 2020.
[15] R. Dom, L. R. Baby, H. G. Kim, and P. H. Borse, "Enhanced Solar Photoelectrochemical Conversion Efficiency of ZnO:Cu Electrodes for Water-Splitting Application," *International Journal of Photoenergy*, vol. 2013, p. 928321, 2013.
[16] C.-H. Zhai, R.-J. Zhang, X. Chen, Y.-X. Zheng, S.-Y. Wang, J. Liu, *et al.*, "Effects of Al Doping on the Properties of ZnO Thin Films Deposited by Atomic Layer Deposition," *Nanoscale Research Letters*, vol. 11, p. 407, 2016.
[17] Q. Fan, J. H. Yang, Y. Yu, J. P. Zhang, and J. Cao, "Electronic Structure and Optical Properties of Al-doped ZnO from Hybrid Functional Calculations," *Chemical Engineering Transactions*, vol. 46, pp. 985-990, 2015.
[18] R. Mahdavi and S. S. A. Talesh, "Sol-gel synthesis, structural and enhanced photocatalytic performance of Al-doped ZnO nanoparticles," *Advanced Powder Technology*, vol. 28, pp. 1418-1425, 2017.
[19] F. Maldonado and A. Stashans, "Al-doped ZnO: Electronic, electrical and structural properties," *Journal of Physics and Chemistry of Solids*, vol. 71, pp. 784-787, 2010.
[20] R. Saniz, Y. Xu, M. Matsubara, M. N. Amini, H. Dixit, D. Lamoen, *et al.*, "A simplified approach to the band gap correction of defect formation energies: Al, Ga, and In-doped ZnO," *Journal of Physics and Chemistry of Solids*, vol. 74, pp. 45-50, 2013.
[21] Y.-F. Xu, H.-S. Rao, X.-D. Wang, H.-Y. Chen, D.-B. Kuang, and C.-Y. Su, "In situ formation of zinc ferrite modified Al-doped ZnO nanowire arrays for solar water splitting," *Journal of Materials Chemistry A*, vol. 4, pp. 5124-5129, 2016.
[22] X. Zhang, Y. Chen, S. Zhang, and C. Qiu, "High photocatalytic performance of high concentration Al-doped ZnO nanoparticles," *Separation and Purification Technology*, vol. 172, pp. 236-241, 2017.
[23] B. Sa, Y.-L. Li, J. Qi, R. Ahuja, and Z. Sun, "Strain Engineering for Phosphorene: The Potential Application as a Photocatalyst," *The Journal of Physical Chemistry C*, vol. 118, pp. 26560-26568, 2014.
[24] S. Smidstrup, T. Markussen, P. Vancraeyveld, J. Wellendorff, J. Schneider, T. Gunst, *et al.*, "QuantumATK: an integrated platform of electronic and atomic-scale modeling tools," *J. Condens. Matter Phys.*, vol. 32, p. 015901, 2019.
[25] J. Carmona-Espíndola, J. L. Gázquez, A. Vela, and S. B. Trickey, "Generalized Gradient Approximation Exchange Energy Functional with Near-Best Semilocal Performance," *J. Chem. Theory Comput.*, vol. 15, pp. 303-310, 2019.
[26] X. Zhao, P. Chen, and T. Wang, "Controlled electronic and magnetic properties of WSe2 monolayers by doping transition-metal atoms," *Superlattices and Microstructures*, vol. 100, pp. 252-257, 2016.
[27] S. Liu, S. Huang, H. Li, Q. Zhang, C. Li, X. Liu, *et al.*, "Tunable electronic behavior in 3d transition metal doped 2H-WSe2," *Physica E: Low-dimensional Systems and Nanostructures*, vol. 87, pp. 295-300, 2017.
[28] S. Chowdhury, P. Venkateswaran, and D. Somvanshi, "A systematic study on the electronic structure of 3d, 4d, and 5d transition metal-doped WSe2 monolayer," *Superlattices and Microstructures*, vol. 148, p. 106746, 2020.
[29] D. Sun, C. Tan, X. Tian, and Y. Huang. (2017, 2017/06//). Comparative Study on ZnO Monolayer Doped with Al, Ga and In Atoms as Transparent Electrodes. *Materials (Basel, Switzerland) 10(7)*. Available:
[30] S. Chowdhury, P. Venkateswaran, and D. Somvanshi, "Strain-dependent doping and optical absorption in Al-doped graphene-like ZnO monolayer," *Solid State Communications*, vol. 365, p. 115139, 2023.

https://doi.org/10.36375/prepare_u.iiche.a410

Characterization and Adsorption Performance Evaluation of Waste Char

Arka Sanyal[a], Manoj Kumar Sonthalia[b], Abhijit Kundu[c], Aparna Ray Sarkar*[d]

[a,b,c]*Undergraduate student, Department of Chemical Engineering, Heritage Institute of Technology, Chowbaga Road, Anandapur, East Kolkata Township, Kolkata, 700107, India*

[*d]*Assistant professor, Department of Chemical Engineering, Heritage Institute of Technology, Chowbaga Road, Anandapur, East Kolkata Township, Kolkata, 700107, India*

Abstract

Environmental threats such as global warming, soil contamination, ground water pollution and air pollutions are the penalties of the huge generation of wastes from industries and urban areas. Therefore, waste management has become an important issue. An effective waste management includes prevention, reuse, recycling, recovery and disposal of waste. Several technological approaches have been explored to attain any one of the processes. Waste to energy (WTE) conversion is well accepted. Pyrolysis is one such promising technology which can produce three different types of fuel such as, pyro-oil, char and gases from solid or liquid wastes. This pyro char can be used as a good adsorbent. On the other hand industrial effluent contain heavy metals like Lead (Pb), Arsenic (As), and Cadmium (Cd), as well as harmful anions like fluorides, nitrates, and sulphates, which cause extensive damage to our environment. Hence, treatment of industrial effluents is utmost important. In this present study, char material will be prepared from pyrolysis of waste materials and will be used for the liquid phase adsorption of Eosin y. Adsorption isotherm will be evaluated. Characterization of adsorbent will be done. The removal of pollutants from waste water solution using this adsorbent will be presented.

Keywords: Pyro char; adsorption isotherm; solid waste; wastewater treatment; industrial effluent treatment

1. Introduction

Electrical and Electronic Equipment (EEE) such as monitors, screens, lamps, temperature exchange equipments, telecommunication and information technology equipments, mobile parts etc. has been defined as E-wastes when extended to annihilation. The E-waste generation increases gradually due to the rapid technological change and growth which forces people, companies and institutes to replace the EEE very frequently. According to a recent survey only 17.4% of 53.6 X 10^6 metric tons of e-waste was recycled in 2019[1]. E-waste

https://doi.org/10.36375/prepare_u.iiche.a410

contains heavy metals, chloroflurocarbons and brominated flame retardants (BFR) which leads to drastic risk to the environment and human health[2]. However, there is a still dearth of effective technologies and infrastructure to recycle or treat or manage these E-wastes. Therefore, environmentally sound treatment methodologies are required in E-waste management sector.

Pyrolysis is a thermochemical process that involves the decomposition of organic materials, such as biomass, plastics, and rubber at a temperature of 300 to 1000^{o}C in the absence of oxygen. Under pyrolysis condition, these materials are decomposed into volatile gasses, liquids, and solid char. This method not only converts the waste materials in to high density fuels, it also recovers value added materials. on industrial waste water to remove impurities and an indirect path of E-waste minimization. The char which is obtained from pyrolysis of E-wastes has been used in this present study as an adsorbent. This way the E-waste can be reused in waste water treatment sector.

In this respect, this paper aims to present a treatment methodology which can be applied

Several studies, have been reported on the adsorption characteristics of the char obtained from pyrolysis of corn cobs [3]. But studies on adsorption characteristics using eosin y, have not been reported. In this present study the determination of adsorption isotherm of E-waste generated pyro-char material using eosin y dye Eosin y dye has been. The impurities removal efficiency of has been calculated. Waste water characterizations have been done. Pyro char is an inexpensive adsorbent that can remove heavier impurities and metals to a certain degree. This will certainly reduce the cost of treating effluents and make it economical for the interested parties.

2. Materials and methods

2.1 Chemicals

Analytical grade chemicals (Eosin y dye, NaOH) were acquired from Sigma Aldrich. Deionized waters were obtained from

https://doi.org/10.36375/prepare_u.iiche.a410

laboratory. Industrial wastewater sample was procured from the Sulphuric Acid Plant (SAP) of a fertilizer industry.

2.2 Synthesis of adsorbent from pyrolysis of char

E-waste specially Printed Circuit Boards (PCB) (computer motherboard, mini circuit of remote controls, smartphones, calculators, etc.) were collected from local shop near Ruby market. Collected e-wastes were shredded. Pyrolysis experiments were conducted of shredded PCB at around 550°C for 1 hour. The pyro-char obtained was set to cool down at room temperature. Pyro char was washed with conc. NaOH solution to wash away heavy metals remaining in the char.

2.3 Dye adsorption experiments

Batch adsorption tests were carried out in 100 mL Erlenmeyer flasks at room temperature (27◦C) containing Eosin y dye within 40 – 5 mg/L with a varying adsorbent dose of 7gm to 0.5 gm. The pH was set between 5 and 6. For pH adjustment, dropwise addition of NaOH or HCl solutions (1 or 0.1 M) was carried out. The PCB char adsorption isotherms were obtained after adsorbent–dye solution contact for 3 to 1 h, keeping constant the adsorbent dose. The same procedure was replicated for NaOH treated pyro char. Aqueous samples were filtered with Nylon Filters (0.90 µm), and the concentration of Eosin y in water was obtained by colorimeter (Chemiline CL610) at a wavelength of 570nm [4]. Adsorption experiments were carried out in triplicate, and the average value was represented. The relative standard deviation was lower than 5%.

Adsorption isotherms are carried out to evaluate the maximum adsorption capacity. Three isotherm models of linear isotherm (eqn. (1)), Langmuir isotherm (eqn. (2)), and Freundlich isotherm (eqn. (3)) are adopted for the non-linear fitting [5].

$$q = KC_e \quad (1)$$

$$q = \frac{q_0 C_e}{K_L + C_e} \quad (2)$$

$$q = K_f C_e^n \quad (3)$$

Where, C_e (mg/L) is the equilibrium concentration of dye, K is a constant, q is the concentration in the solid phase, q_0 is the maximum monolayer adsorption capacity, k_L is the Langmuir constant, k_f and n are constants.

2.4 Char characterizations

https://doi.org/10.36375/prepare_u.iiche.a410

XRD analysis of this pyro char was performed considering the range of 2θ values from 10 to 90. Surface charge analysis of the char was also done using Zetasizer 2000.

2.5 Adsorption studies of industrial effluent

Batch adsorption studies were carried out in 100 mL Erlenmeyer flasks at room temperature (27 °C) containing industrial effluent within 40 – 5 mg/L with an adsorbent dose of 0.5gm. The pH was set between 5 and 6. The PCB char adsorption experiment had adsorbent–waste water solution contact for 3hrs, keeping constant the adsorbent dose. The treated sample was measured for their TSS using a Systronics Digital Nephelo/Turbidity meter calibrated to zero using laboratory grade de-ionised water. Since the wastewater we obtained was mostly neutral with baseline level TDS, only the TSS change was observed and recorded for this specific experiment.

3.Results and discussions

3.1 Adsorption isotherm

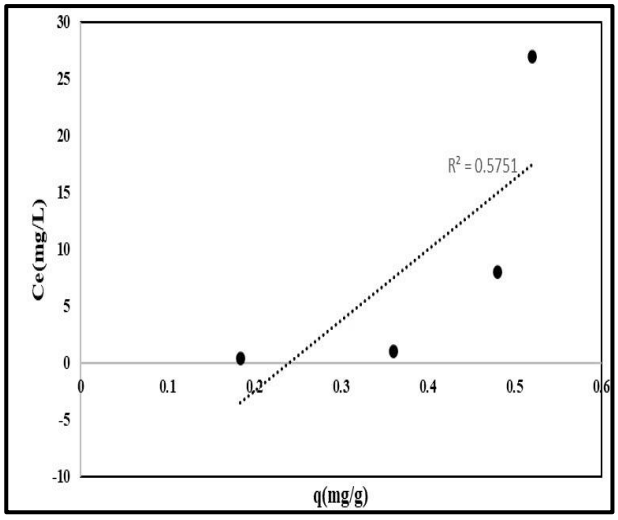

Figure 1(a): Linear Isotherm

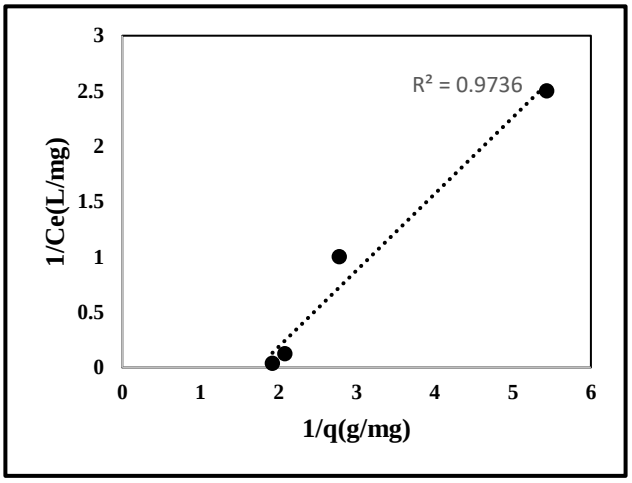

Figure 1(b): Langmuir Isotherm

https://doi.org/10.36375/prepare_u.iiche.a410

Experimental data for the dye adsorption isotherms in the PCB char are modeled using three models. Using these experimental data three different plots were constructed namely, Figure 1(a) (Linear model), Figure 1(b) (Langmuir isotherm) and Figure 1(c) (Freundlich isotherm). By tracking Ce vs q for Linear isotherm, 1/Ce vs 1/q for Langmuir isotherm, and log Ce vs log q for Freundlich isotherm are checked, if a straight line is obtained. According to these results, the correlation coefficient of the Linear isotherms is equal to 0.575, Langmuir model is equal to 0.973, and the Freundlich correlation coefficient of 0.575.

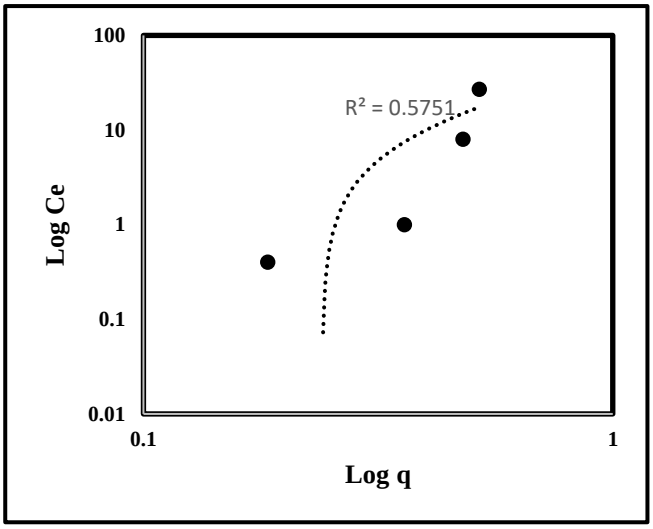

Figure1(c): Freundlich Isotherm

This means that the process of Eosin y adsorption by PCB char is perfectly described by Langmuir model. Table 1 represents the values of the adsorption equilibrium parameters according to the Langmuir model.

https://doi.org/10.36375/prepare_u.iiche.a410

Table 1: The values of the adsorption equilibrium parameters of Langmuir isotherm model

Sl. No.	Equilibrium parameters	Values
1.	Intercept	1.731
2.	q_o	0.577mg/g
3.	K_L	1.259
4.	R^2	0.973

Here, q_0 is the maximum dye adsorption capacity per gram of char, and K_L is the Langmuir constant. Both of these data are found out from the intercept and slope of the graph.

3.2 Adsorption kinetics

3.2.1 Effect of adsorbent load on dye removal:

Adsorption load has a major role in adsorption studies because it determines the adsorption capacity for a given initial concentration of dye. Experiments were conducted to understand the effect of PCB char on Eosin y taking initial dye concentration 40 mg/L. The adsorbent loads are varied from 0.5 to 7gm. Figure 2 shows the effect of adsorption load on percentage of dye removal.

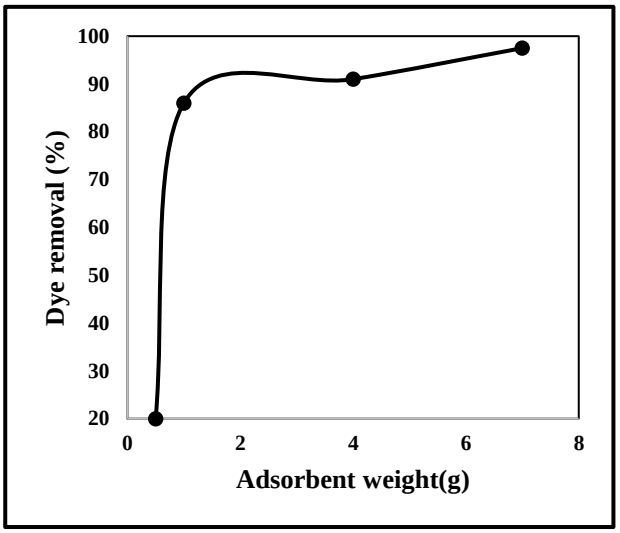

Figure 2: Dye removal vs Adsorbent

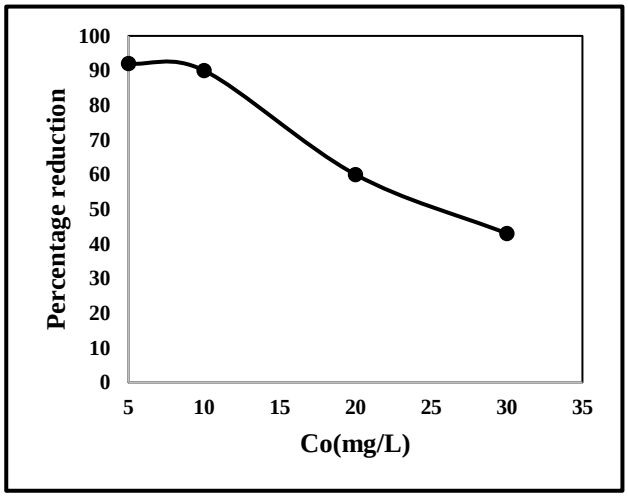

Figure 3: Percentage removal of dye vs initial concentration

It is clear from the figure that the removal rate of dye solution increased sharply as the adsorbent loads were increased. The maximum dye removal efficiency was 97.5% at a dosage of 7gm. The increased adsorbent load shares

https://doi.org/10.36375/prepare_u.iiche.a410

large surface area as well as exchangeable active sites.

3.2.2 Effect of initial dye concentration:

The dye concentration also plays a vital role in adsorption studies to evaluate the adsorbent capacity. In this study four different dye concentrations, 5, 10, 20 and 30 mg/l were selected to study the effect of the initial dye concentration on the adsorption of dye on PCB char. The other process parameters such as adsorbent load, temperature and pH were kept constant. The dye removal percentage is inversely related with the initial dye decreased as the initial dye concentrations were increased. The percentages of dye removal decreased from 92 to 43% as the initial dye

concentration. Figure 3 shows the effect of initial dye concentration on adsorption capacity. The percentage of dye removal

On the contrary, the surface charge of PCB char was found to be highly negative. The value of zeta potential is -9.494 mV. Since the Eosin y dye ions are positively charge, they gets attracted towards negative surface of the char. Additionally, increase in dye concentration, blocked the char pores and hindered effective adsorption. Therefore, dye removal decreased with increase in dye concentration.

3.2.3 Effect of contact time:

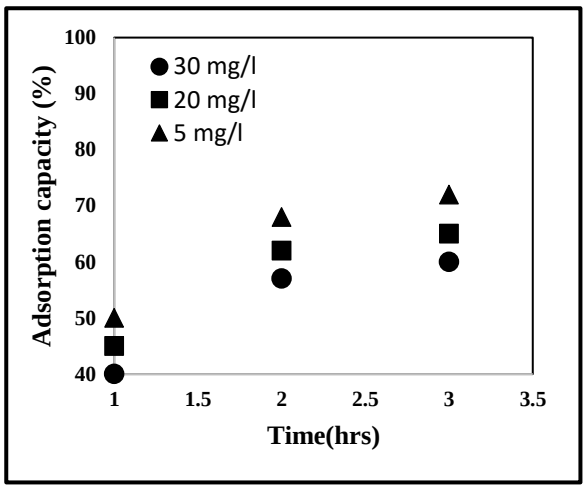

Figure 4: Adsorption capacity vs Time

Figure 4 illustrates the effect of contact time on adsorption capacity of PCB char. Three different experiments were conducted, 1, 2 and 3 hr and the effects were observed at different concentrations, 5, 20, 30 mg/l to investigate the adsorption capacity. The adsorbent load was kept constant. The result shows that the equilibrium time is independent on initial concentration of dye. Initially the adsorption capacity increased rapidly as all the vacant active sites are available. But after certain

https://doi.org/10.36375/prepare_u.iiche.a410

prolonged contact time equilibrium were reached due to the lack of free active sites availability.

3.3. XRD analysis of PCB char:

XRD analysis of the PCB pyro char sheds light on the overall crystallinity of the material and which compounds contribute towards its crystallinity. Figure 5 shows the shows the XRD spectrum for the char.

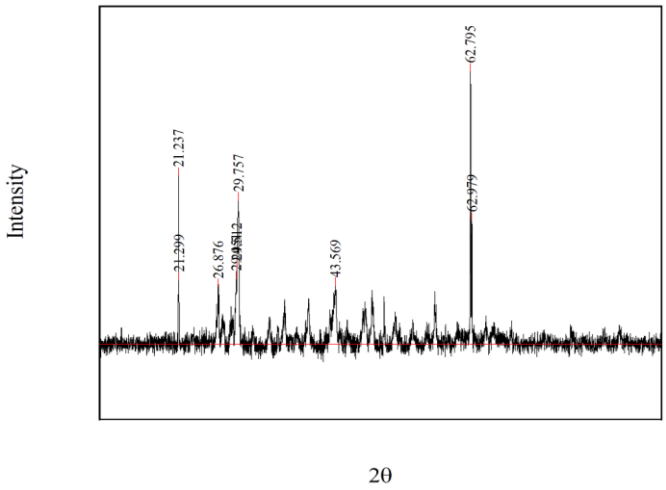

Figure 5: XRD data graph

From the figure peaks are evident at 2θ = 21^0, 29^0 and 62^0. The sharp peaks indicate crystallinity. The material is mostly amorphous. At 2θ= 63° and 21° the peaks resemble the presence of Silica. At 2θ= 43° contributes to the presence of Copper, and an unknown compound with empirical formula $Al_3Ca_{0.5}Si_3O_{11}$ presents itself at 2θ=29° [6][7][8][9]. Crystallinity index of the compound was found out to be 10.13%. This data reveals low crystallinity of pyro char.

3.4 Adsorption of Industry effluent:

A big part of cleaning up industrial effluent is removal of suspended solids. TSS(Total Suspended Solids) gives us an idea of turbidity of a solution. Table 2 shows that the turbidity decreases significantly after adsorption treatment. To put that into perspective, raw effluent passed through two filter papers has a turbidity value higher than that of treated effluent.

https://doi.org/10.36375/prepare_u.iiche.a410

Table 2: TSS values before and after adsorption

Samples	Turbidity (NTU)
Raw effluent	2.2
Treated effluent	1.2
Double filter paper	1.9

4. Conclusions:

From our study, the following conclusions can be drawn:

Pyro char obtained from pyrolyzing PCB, is an amorphous material with a surface charge of -9.494. All of which are great indicators for a good adsorbent. The negative surface charge explains the affinity towards eosin y dye, which is positively charged, and indicates a possibility for heavy metal ion removal.

The Pyro char follows Langmuir model isotherm for the adsorption of eosin y dye. This means that the adsorbate particles (here, eosin y molecules) form a monolayer over the exposed adsorbent surface, after which the adsorbent is saturated. As a result in this study; the percentage removal of dye decreases with increase in concentration of dye solution, the adsorbent becomes saturated. This also means, percentage removal of dye increases with increase is surface area of the adsorbent or in the case of our study, increase in the amount of adsorbent will result in an increased removal of dye molecules from the solution.

The Pyro char can effectively clear up turbidity from industrial effluent. In this study, effluent of Sulphuric Acid Plant was used with 2.2NTU TSS. After treating it with pyro char, TSS became 1.2NTU. At the same time, a comparative test by passing the raw effluent through two laboratory grade filter papers were done, the resulting TSS was 1.9NTU. Comparatively, pyro char provides an effective cleaning of industrial effluent.

Pyro char washed with conc. NaOH is unfit as an adsorbent. It gave us inconclusive results for the dye adsorption experiment.

These conclusions are quite valuable and thus prove that PCB pyro char can be used as a cheap and effective adsorbent for industrial effluent treatment.

Conflict of interests: The authors declare that they have no conflict of interest.

Appendix:

Ce	equilibrium concentration
K	a constant
q	concentration in the solid phase
q_0	maximum monolayer adsorption capacity
K_L	Langmuir constant
K_f	Freundlich constant
N	a constant
Co	Initial concentration
PCB	Printed Circuit Board
SAP	Sulphuric Acid Plant

References:

1. Forti, V., Bald´e, C.P., Kuehr, R., Bel, G., (2020). The global E-waste monitor (2020): quantities, flows, and the circular economy potential. United nations university (UNU)/United nations institute for training and research (UNITAR) – co-hosted J. Joo et al. 11 SCYCLE programme. In: International Telecommunication Union (ITU) & International Solid Waste Association (ISWA) (Bonn/Geneva/Rotterdam)
2. Yl¨ a-Mella, J., Poikela, K., Lehtinen, U., Tanskanen, P., Roman, ´ E., Keiski, R.L., Pongracz, ´ E., (2014). Overview of the WEEE Directive and its implementation in the Nordic Countries: national realisations and best practices. *J. Waste Manage. 2014, 457372.* https://doi.org/10.1155/2014/457372
3. El-Hendawy AN, Samra SE, Girgis BS. (2001). Adsorption characteristics of activated carbons obtained from corncobs. *Colloids and Surfaces A: Physicochemical and Engineering Aspects, 180, 3,* 209–221. https://doi.org/10.1016/S0927-7757(00)00682-8
4. Koegl M, Weiß C, Zigan L. (2020). Fluorescence Spectroscopy for Studying Evaporating Droplets Using

the Dye Eosin-Y. *Sensors*. *20 (21)*, 5985. https://doi.org/10.3390/s20215985

5. Salman MS. (2009). Removal of sulfate from waste water by activated carbon. *Al-Khwarizmi Engineering Journal*, *5*, *3*, 72-76. https://doi.org/10.1016/j.jenvman.2018.02.096
6. ONO H, DODBIBA G, FUJITA T. 2010. Copper Recovery from Printed Circuit Board by Carbonization. *International Journal of the Society of Materials Engineering for Resources*, *17 (1)*, 53-57. https://doi.org/10.5188/ijsmer.17.53
7. Shen Y, Chen X, Ge X, Chen M. (2018). Chemical pyrolysis of E-waste plastics: Char characterization. *Journal of environmental management*, *214*, 94-103. https://doi.org/10.1016/j.jenvman.2018.02.096
8. Khayyam Nekouei R, Pahlevani F, Golmohammadzadeh R, Assefi M, Rajarao R, Chen YH, Sahajwalla V. (2019). Recovery of heavy metals from waste printed circuit boards: statistical optimization of leaching and residue characterization. *Environmental Science and Pollution Research*, *26*, 24417-24429. https://doi.org/10.1007/s11356-019-05596-y
9. Khayyam Nekouei R, Maroufi S, Assefi M, Pahlevani F, Sahajwalla V. (2020). Thermal isolation of a clean alloy from waste slag and polymeric residue of electronic waste. *Processes*, *8(1)*, 53. https://doi.org/10.3390/pr8010053

https://doi.org/10.36375/prepare_u.iiche.a411

Preparation, Characterization and Application of Mixed Clay Based Low-Cost Ceramic Membrane in Treatment of Oil-in-Water Emulsions

Kanchapogu Suresh[a*], Amish Gour[a], Mukesh Kumar Yadav[b], Vidhi Jani[c],

[a*, a,b,c] Department of Chemical Engineering, Maulana Azad National Institute of Technology Bhopal-462003, India
*Corresponding author Dr. Kanchapogu Suresh, ksuresh@manit.ac.in, +91 755-405-1807

Abstract

Fly ash is a cost-effective alternative for preparing ceramic membranes but they are often weak for practical use. We have made different mixtures by taking different compositions of polyvinyl alcohol to improve mechanical strength at the same time preserving permeability. We tested 3 PVA concentrations from which sintered 10 ppm PVA solution treated at 1100 °C demonstrated optimal characteristics, featuring L_h (water permeability coefficient) of 9.19×10^{-6} (m^3/m^2 s kPa), 39% porosity, pore size of 1.029 µm, a flexural strength of 40 MPa, and testing with oil-in-water emulsions revealed a rejection rate exceeding 98%.

Keywords: Cost-effective; Fly ash; Pore-forming agent; Ceramic membrane; Wastewater.

1. Introduction

Ceramic membranes have gained widespread use in wastewater treatment due to their specific attributes, including high flux, antifouling properties, extended lifespan, and operational flexibility [1]. Primarily made from various raw ingredients such as kaolin, titania, alumina, and silica, zirconia. Generally, ceramic membranes exhibit exceptional mechanical, chemical and thermal stability in contrast to polymeric alternatives, enduring pressures and high temperature effectively. They are robust and can be cleaned using strong industrial chemicals without notable performance degradation [2]. Recent studies have emphasized cost reduction through the use of economical raw materials such as kaolin, clay, and fly ash, sintered at lower temperatures (1100°C). Kaolin, a widely available and cost-effective clay mineral, is commonly employed in ceramic membrane production [3].

While kaolin-based membranes dominate the literature, some scholars have explored using

fly ash as a free raw material to produce inorganic membranes, aiming to further reduce costs. However, fly ash-based membranes exhibit wider pores, lower porosity, and inferior strength compared to their kaolin-based counterparts. Combining fly ash and kaolin could yield cost-effective membranes with favorable physical and pore properties [4]. Despite this, there is a lack of published studies on inorganic membranes created from fly ash and kaolin mixtures.

This study evaluated the mechanical strength of fly ash ceramic membranes using a compression machine and assessed membrane chemical stability with Hydrochloric acid (0.1M) and Sodium Hydroxide over seven days. Surface characteristics were analyzed using a field emission scanning electron microscope [5]. Previous studies by Singh et al. (2020), Liu et al. (2019), Yu et al. (2018), Wang et al. (2018), and Zhao et al. (2016) emphasized the favorable attributes of fly ash-based ceramic membranes, such as exceptional mechanical strength, high water permeability, efficient contaminant removal, and long-term stability [6-10].

Despite advancements, certain research gaps remain, including evaluating the economic viability of large-scale water treatment using ceramic membranes. The cost-effectiveness of the fabrication process, encompassing material procurement, fabrication, and operation, requires further investigation. Additionally, limited knowledge exists regarding the performance of ceramic membranes under various water quality circumstances. Most current research focuses on ideal conditions, necessitating more studies on real-world scenarios with varying organic and inorganic impurities in wastewater. Efficient cleaning and regeneration techniques for fly ash-based ceramic membranes are also crucial to address fouling issues [11-12].

The objectives of this research are as follows:

a) Develop ceramic membranes from mixed clays using the uniaxial pressing method.

b) Characterize the fabricated ceramic membrane through Archimedes' principle, chemical analysis, mechanical testing, and SEM.

c) Apply the fabricated membrane for separating oil-in-water emulsions via dead-end microfiltration.

https://doi.org/10.36375/prepare_u.iiche.a411

2. Materials and Methods

2.1. Compounds Used

2.1.1. Fly Ash

Fly ash is a finely divided material that is produced as a byproduct from the combustion of coal in power plants and carried away by flue gases. This pulverized fuel ash contains mineral components such as silica, alumina, and calcium oxide. Its remarkable pozzolanic properties have made fly ash a valuable resource in the construction industry, enhancing the strength and durability of concrete. Beyond its role in construction, fly ash finds applications in diverse fields, including agriculture, road stabilization, and even as a raw material in the creation of ceramic membranes. Importantly, the utilization of fly ash in various industries contributes to sustainable practices by diverting a substantial waste stream away from landfills. The specific constituents of fly ash are influenced by the variety of coal, as illustrated in Table 1.

Table 1. Fly ash composition by coal type

Component	*Bituminous*	*Subbituminous*	*Lignite*
Al_2O_3 (%)	15-30	24-28	21-24
CaO (%)	5-10	10-20	20-35
Fe_2O_3 (%)	15-30	5-8	5-12
SiO_2 (%)	30-50	42-58	20-40
LOI (%)	0-10	0-2	0-6

2.1.2 .Quartz

Quartz, a resilient and crystalline mineral, is primarily composed of silica, also known as silicon dioxide. In this mineral, each oxygen atom is shared between two tetrahedra, forming a continuous framework of SiO_4 silicon-oxygen tetrahedra. This arrangement gives quartz its chemical formula, SiO_2. Following feldspar, quartz stands as the second most prevalent mineral in the Earth's continental crust. Both normal and high-temperature quartz are recognized as two chiral forms of this mineral [13].

2.1.3 .Kaolin

Aluminium silicate minerals, such as feldspar, undergo chemical weathering processes that lead to the creation of kaolinite, characterized as a soft and earthy mineral typically exhibiting a white color. The term "China clay" or "kaolin" is used to describe rocks with elevated concentrations of kaolinite and halloysite [13].

2.1.4 .Boric Acid

Orthoboric acid, with the chemical formula $B(OH)_3$, is a chemical compound composed of boron, oxygen, and hydrogen. It is alternatively known as trihydroxidoboron, hydrogen orthoborate, and boracic acid. Found naturally as the mineral sassolite, orthoboric acid is

commonly encountered in the form of colorless crystals or a white powder that readily dissolves in water. As a weak acid, it can engage in reactions with alcohols, yielding borate esters, along with the formation of various borate anions and salts.

2.1.5 .Calcium Carbonate

Calcium carbonate, identified by the chemical formula CaCO3, is a common compound found in nature. It is prevalent in rocks as the minerals calcite and aragonite, with limestone being a notable example. Limestone, a predominant type of sedimentary rock, is primarily constituted by calcite [13].

2.1.6 .Titanium Dioxide

Titanium dioxide, or TiO_2, functions as a versatile white pigment extensively employed in industries like paints, coatings, and cosmetics due to its outstanding light-scattering capabilities. It adds brightness and opacity to diverse products. Widely utilized in sunscreens for UV protection, titanium dioxide's inert and non-toxic characteristics make it a favored option in applications ranging from food coloring to photocatalysis.

2.2 .Method of membrane fabrication

The raw precursors used for the disc-shaped membrane from fly-ash are detailed in Table 2, and the specific quantities of each individual raw material are illustrated in Figure 1. Fly ash is collected from a power plant, and then it is sieved to remove impurities such as stones, metals, and other particles**.** The fly ash is then washed and dried to remove any impurities and moisture. A mixture is prepared by mixing fly ash, sodium metasilicate, quartz, kaolin, boric acid, calcium carbonate and titanium dioxide in a fixed ratio. Three solutions are prepared with different concentrations of PVA: 2 ppm for sample S1, 5 ppm for sample S2 and 10 ppm for sample S3 and water is added as binder to the mixture. The components are thoroughly mixed and kneaded to get a mixture of uniform composition [13]. The slurry is then placed in a casting mould and pressed under a pressure of 400 KN to obtain disc shaped membrane [13]. The membrane is first dried under sun for 24 hours. Then it is sintered in the muffle furnace in the following fashion [shown in Fig.2]: The programe of programmable furnance

1. To attain a temperature of 100°C, a time of 45 mins is set. The temperature of 100°C is held for a duration of 1440 mins (1day).
2. To attain a temperature of 200°C, a time span of 60 mins is provided. The

https://doi.org/10.36375/prepare_u.iiche.a411

temperature of 200°C is held for a duration of 1440 mins (1day).

3. To attain 1100°C of temperature, a time duration for 540 mins is provided. The attained temperature is held for 300 mins. The final obtained sintered membrane shown in Fig.3.

The systematic overall procedure followed for membrane preparation was depicted in Fig.4.

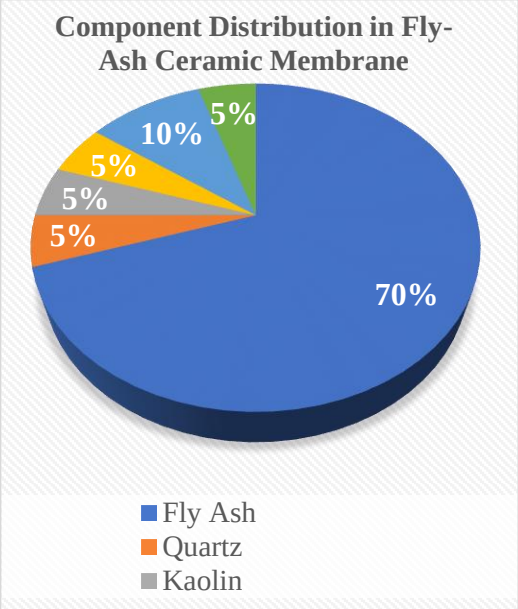

Figure 1: The distribution of components utilized in membrane

Figure 2: Sintering of membrane in muffle furnace

Figure 3: Ceramic Membrane after si ntering in muffle furnace

Table 2. Ingredients used for manufacturing of membranes S1, S2 and S3

Component	Weight (in grams)
Fly Ash	70
Quartz	5
Kaolin	5
Boric Acid	5
Calcium Carbonate	10
Titanium Dioxide	5

https://doi.org/10.36375/prepare_u.iiche.a411

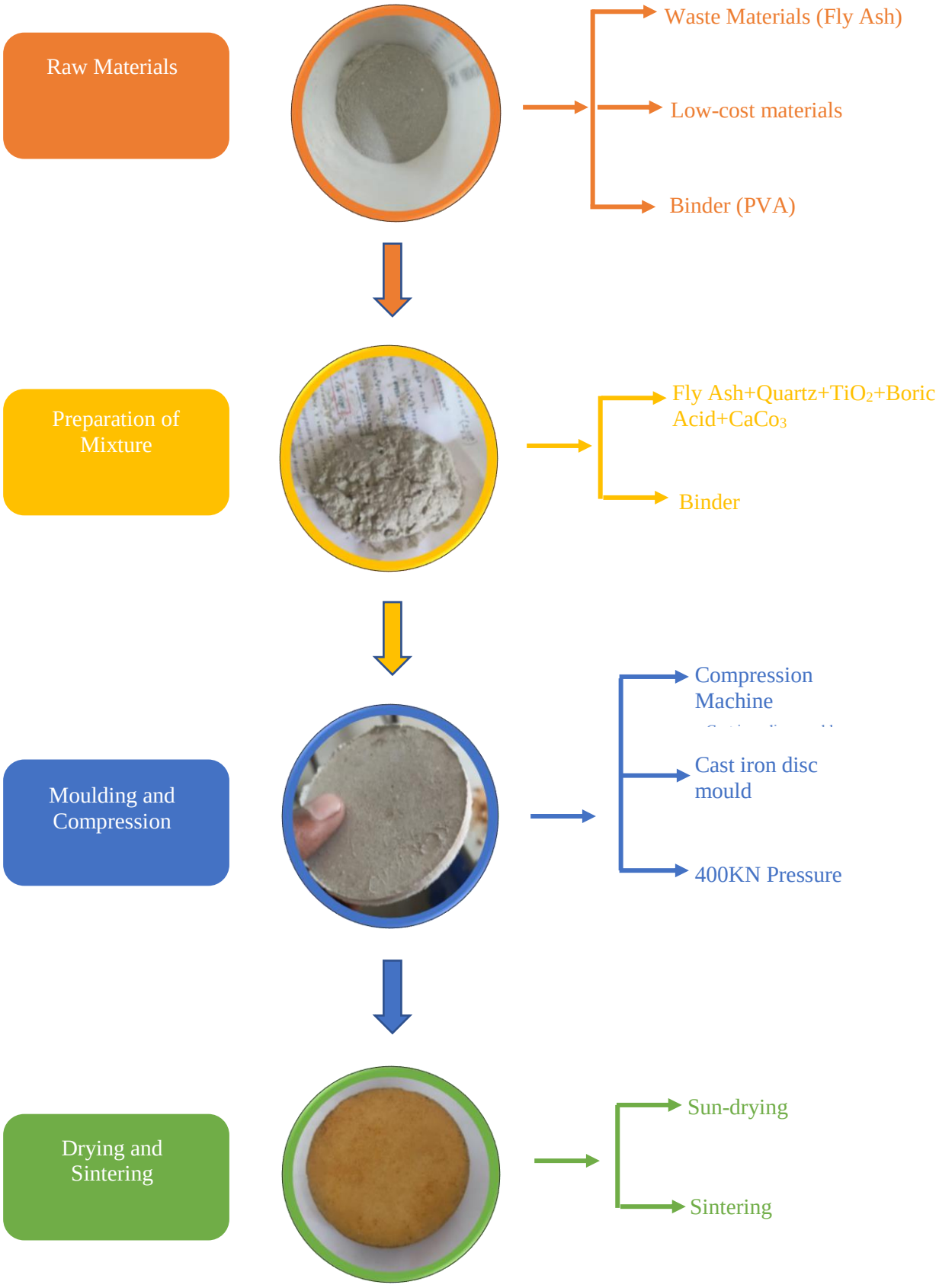

Figure 4: Process Chart for the Preparation of Ceramic Membrane

https://doi.org/10.36375/prepare_u.iiche.a411

3. Results and Discussion

3.1 .Porosity

The membranes are submerged in a water container for a duration of 24 hours, after which it is weighed, and the following equation (equation 1) is employed to calculate the porosity.

$$\text{Porosity} = \frac{w_2 - w_1}{w_2} \times 100 \ldots\ldots\ldots \text{Equation (1)}$$

Where w_1 is the weight of the membrane before experiment and w_2 is the weight of the membrane after experiment.

Porosity results for the three membranes are presented in Table 3.

Table 3. Porosity results through Archimedes principle for S1, S2 and S3

Membrane	Porosity	SEM Analysis Porosity
S1	20%	25
S2	24%	30
S3	39%	45

The membranes exhibit a maximum porosity of 39%.

3.2. Surface Morphology

The sintered membrane was analyzed using scanning electron microscopy (SEM), and the corresponding image is presented in Fig. 5. These images reveal the surface of the membrane, showing a rugged morphological structure. The SEM images verify that the membrane surface is devoid of cracks or pinholes, indicating a defect-free surface.

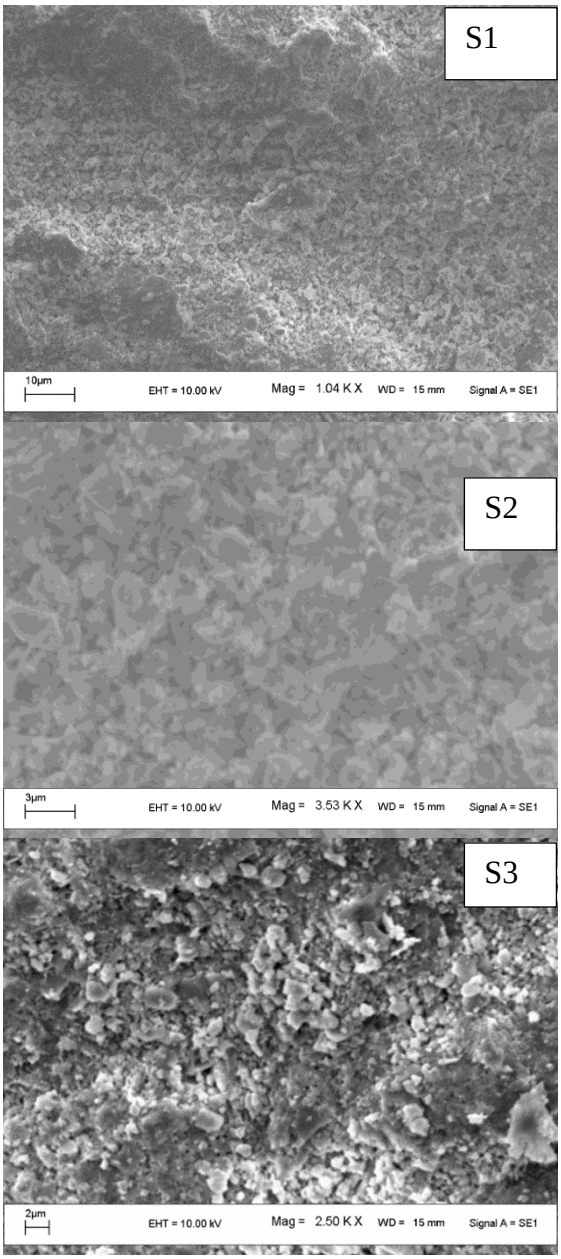

Figure 5: SEM micrograph of membrane S1, S2, S3 respectively

https://doi.org/10.36375/prepare_u.iiche.a411

Furthermore, the membranes' average pore diameter is determined through SEM image analysis by employing ImageJ software [14].

The membranes' S1, S2 and S3 pore size has been measured and reported as average value, represented as d_{avg}, is computed using the equation 2 below:

$$d_{avg} = \sqrt{\frac{\sum_{i=1}^{n} n_i d_i^2}{\sum_{i=1}^{n} n_i}} \quad \text{……Equation (2)}$$

d_{avg} represents the average pore diameter in micrometers (µm).

From SEM images, The membranes' S1, S2 and S3 pore size has been measured and reported as average values of 2.7 µm, 2 µm, and 1.59 µm, respectively.

3.3. Chemical stability

Membranes' chemical stability was evaluated by exposing them to acidic and basic environments by calculating individual membrane weight loss. The membranes were kept in strong acid (HCl) and base (NaOH) solutions for one week to assess their stability in acidic and basic environments. The weight loss in terms of the percentage of the membranes was determined by comparing their dry weights before and after exposure to the solutions using Equation 3. The resulting chemical stability data for the membranes are summarized in Table 4.

$$\text{Weight loss}(\%) = \frac{(W_1 - W_2)}{W_1} \times 100 \quad \text{Equation (3)}$$

Table 4. Observations for chemical stability of membranes S1, S2 and S3

Membrane	Initial weight (g) in		Final weight (g) in		Weight loss (%)	
	Acid	Base	Acid	Base	Acid	Base
S1	16.23	16.08	13.50	14.22	16.8	11.5
S2	16.52	15.95	12.15	14.11	26.4	11.5
S3	16.85	16.11	14.41	15.11	14.5	6

According to the findings, the membranes demonstrate superior corrosion resistance in alkaline conditions [13].

3.4. Mechanical strength

For effective utilization in ultra- and nanofiltration applications, a desirable ceramic

Figure 6: Sample placed in a Hydraulic Press

https://doi.org/10.36375/prepare_u.iiche.a411

membrane should possess high mechanical strength, ideally exceeding 30 MPa [4]. To mitigate errors, we subjected three membranes individually to examination in a hydraulic press, as illustrated in Figure 6.

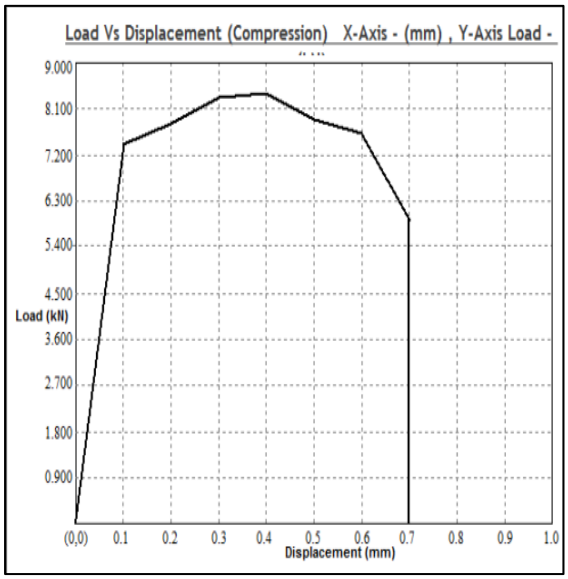

Figure 7[a]: Membrane S1, Yield Load(kN):5.92 Yield Stress (MPa):26.311

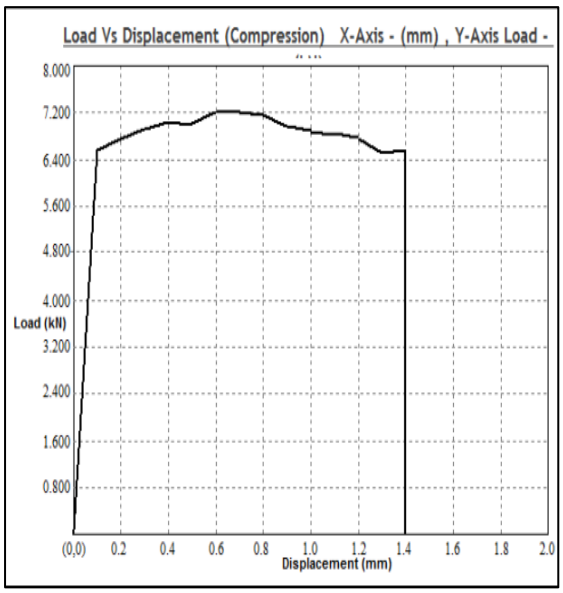

Figure 7[b]: Membrane S2, Yield Load (kN):6.52, Yield Stress (MPa):28.978

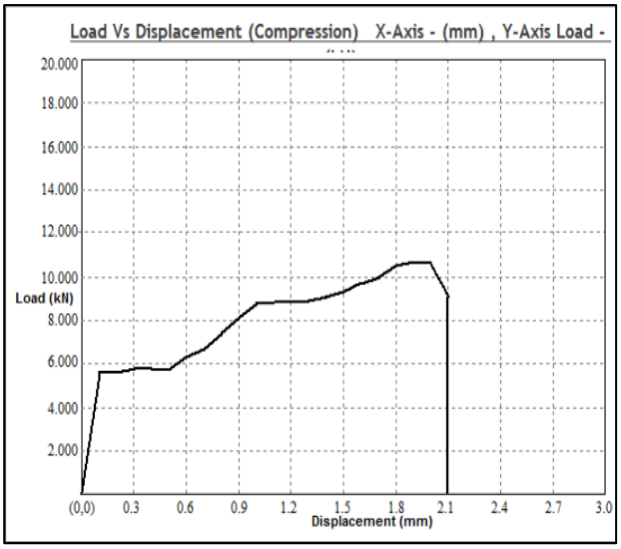

Figure 7[c]: Membrane S3, Yield Load (kN):8.84, Yield Stress (MPa):39.289

Figure 7: Mechanical strength of membrane through Universal Testing Machine (UTM).

From Fig 7. (a) To Fig.7. (c) The tested mechanical stability curve depicted through that the mechanical strength of the membrane was calculated. The strengths of membrane S1, S2 and S3 has been obtained as 26.311, 28.978 and 39.289 MPa, respectively.

3.5. TGA analysis of membranes (S1, S2, S3)

To investigate the thermal changes occurring during the sintering process, membrane ingredients were analysed through TGA instrument(Manufacturer: Netzsch, Model: STA449F3A00). Samples were undergone constant heating rate 10°C/min in the presence of argon gas as the carrier gas.

https://doi.org/10.36375/prepare_u.iiche.a411

The thermogravimetric analysis (TGA) results of membranes S1, S2 and S3 are depicted in Figure 8. The curves clearly indicate that the main source of weight loss is attributed to the transformation of calcium carbonate ($CaCO_3$) into carbon dioxide (CO_2). The porosity of the membrane is significantly influenced by the pathway of CO_2 gas release. Additionally, both membranes S2 and S3 exhibit a similar net weight loss of around 4% for the powder mixture. This observation indicates the membrane weight losses was due to various amounts of calcium carbonate and polyvinyl alcohol (PVA) present in the samples.

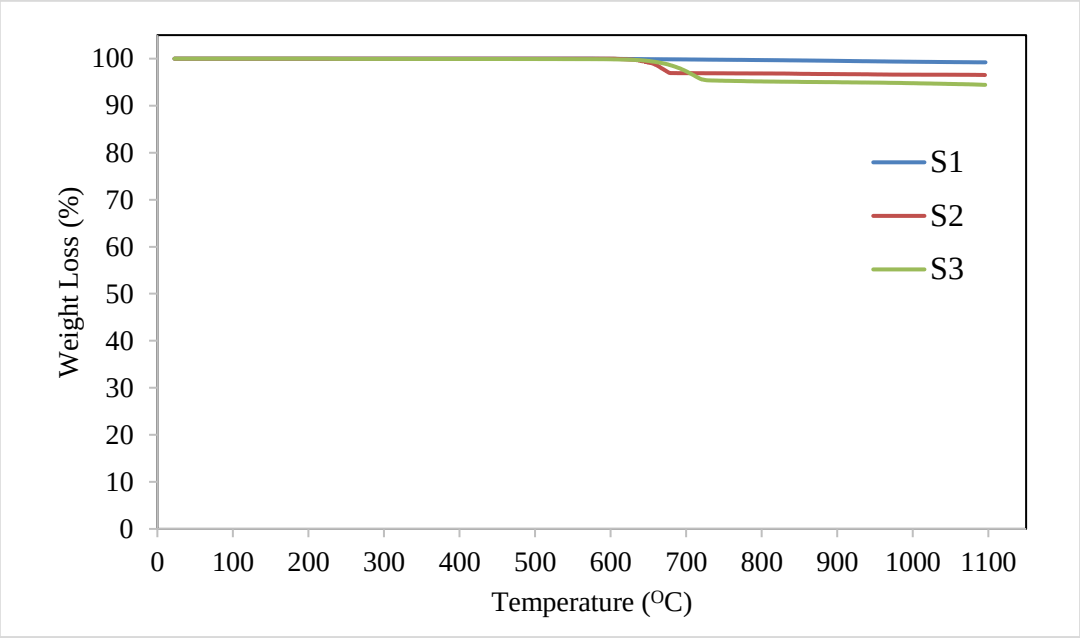

Figure 8: Thermogravimetric analysis of membrane samples mixtures (S1, S2 and S3)

Notably, minimal weight loss is observed across all samples at temperatures exceeding 800 °C, underscoring the need for a minimum sintering temperature higher than 800 °C. In the case of membranes S2 and S3, the significant decrease in mass in the powder mixture at temperatures below 800 °C is caused by the thermal decomposition of $CaCO_3$ and the evaporation of PVA. In contrast, the TGA plots obtained for the S1 membrane shows minimum weight loss because of the presence of lower quantity of PVA.

3.6. Water Permeation (S1, S2, S3)

The microfiltration setup used for water permeation and oil-in-water emulsion treatment was illustrated in Fig. 9. This contains Nitrogen cylinder, gas pressure regulator, pressure

https://doi.org/10.36375/prepare_u.iiche.a411

gauge, dead end filtration membrane module and bottom weighing balance on top it place a measuring cylinder to collect permeate with respect to time. Each of the fabricated membranes underwent characterization for their hydraulic permeability.

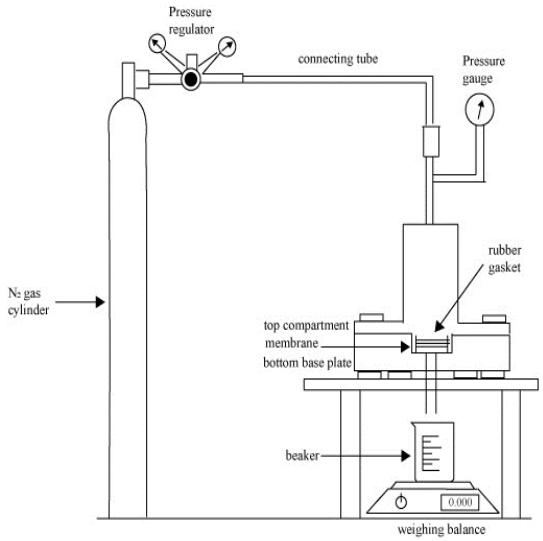

Figure 9: The dead end flow microfiltration setup

Pressure is applied within the range of 30 to 70 kPa, as illustrated in Figure 9 and the pure water flux of the membrane was calculated using Equation 4.

$$J_w = \frac{V_W}{A \times t} \quad \text{..... Equation (4)}$$

In the equation, A represents the area of the membrane used for filtration, t denotes the duration of filtration, V_W signifies the volume of collected water, and J_W is the water flux.

Figure 10 illustrates the relation between water flux and applied pressure and their variations on pure water flux at various applied pressures that was conducted through water permeation data. The slope of this plot provides the hydraulic permeability value L_h that follows the Darcy's law, same as described in Equation (5).

$$J_w = L_h \Delta P \quad \text{.....Equation (5)}$$

$$R = \left(\frac{8\,\mu_w\, L\, L_h \tau}{\varepsilon}\right)^{\frac{1}{2}} \text{.....Equation (6)}$$

In the equation (6), τ represents the tortuosity of the membrane (assumed as 1 for cylindrical pores), L_h denotes the pure hydraulic permeability, ε represents membrane porosity, R signifies the pore radius, L represents the length of the pore with l = 0.005 m, and μ_w denotes the viscosity of water at 25 °C.

The flux of the membranes is observed to be dependent on the applied pressure, increasing with higher applied pressures. The hydraulic permeability of membranes S1, S2, and S3 is calculated to be approximately 11.58×10^{-6}, 10.14×10^{-6}, and 9.19×10^{-6} (m^3/m^2 s Pa), respectively. Additionally, the average pore sizes of membranes S1, S2, and S3 are determined as 2.12 μm, 1.52 μm, and 1.029 μm, respectively.

https://doi.org/10.36375/prepare_u.iiche.a411

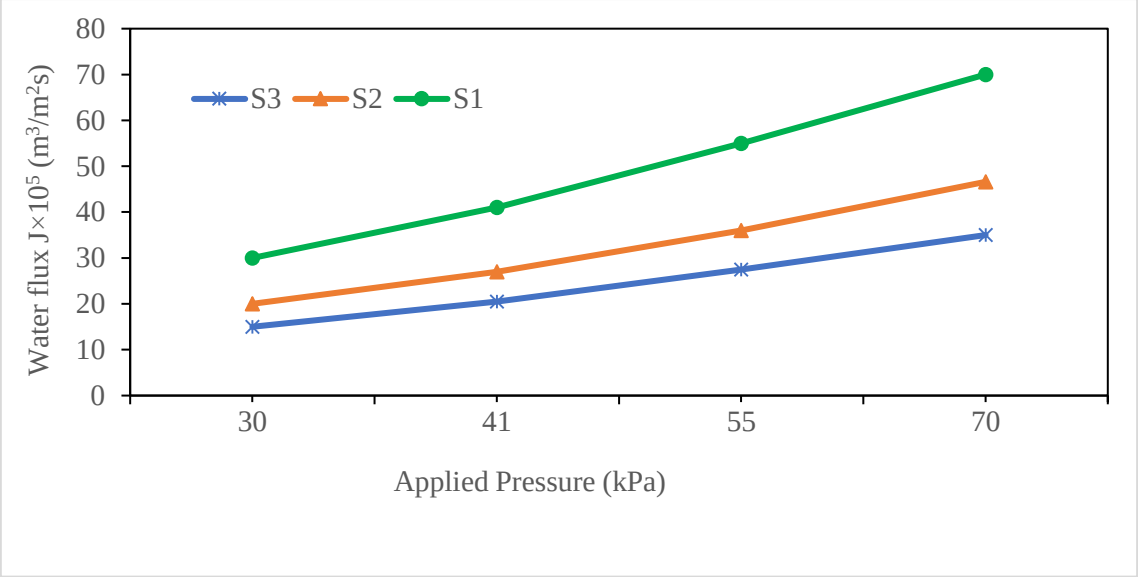

Figure 10: Changes in membrane hydraulic flu x under varying applied pressures.

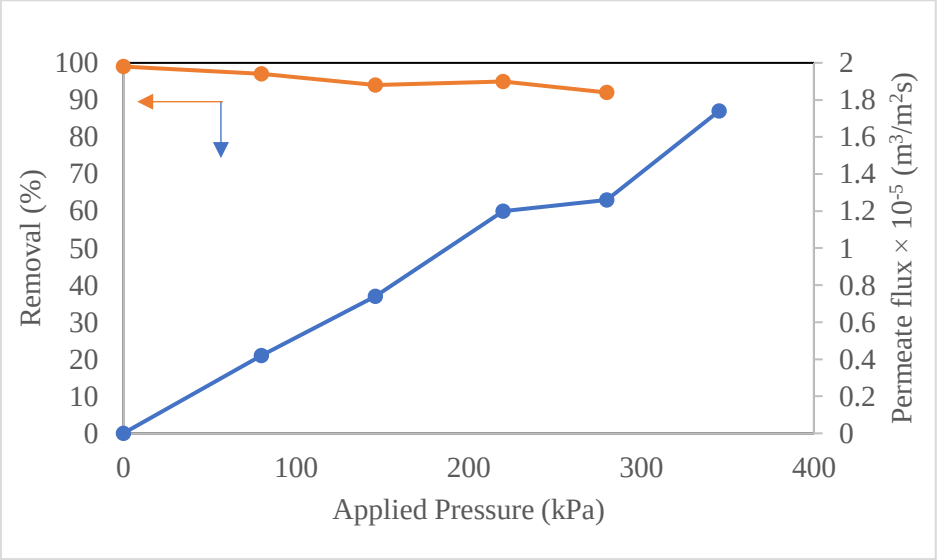

Figure 11: Observing the fluctuation in permeate flux and the oil removal percentage at various applied pressures for the S3 membrane.

Table 5. Comparison of the percentage of oil removal achieved by the membrane with that of other membranes.

Membrane material	Feed concentration (mg/L)	Pore Radius size (µm)	Removal (%)	References
α-Al_2O_3	100	2.1	55	Cui et al. [13]
Al_2O_3	600–11,000	0.16	98	Cui et al. [13]
α- Al_2O_3	150	0.1	61.4	Ebrahimi [15]
α- Al_2O_3/α- Al_2O_3	5,000	1.0	94.3	Yang et al. [16]
Membrane, S3	200	1.59	98	Present Study

https://doi.org/10.36375/prepare_u.iiche.a411

3.7. Oil-in-water emulsion treatment by using membrane S3

Among the crafted membranes, the one featuring the smallest pore size (S3) was specifically chosen for assessing its efficacy in separating oil-water emulsion. Figure 11 depicts the fluctuation in permeate flux and oil removal percentage across different applied pressures, (70 -250 kPa), the primary tested oil sample concentration was 200 mg/L. As expected, the permeation analysis data showed that the removal efficiency reduces with augment of applied pressure it owing to enhanced oil droplet wetting and coalescence, that caused passing of some oil droplets through the membrane with the permeate. These findings are consistent with previous studies [13,16]. Notably, the highest oil rejection rate of 98% is achieved at a relatively lower applied pressure of 70 kPa.

The rejection of oil is calculated using equation (7).

$$R = \left(1 - \frac{C_p}{C_f}\right) \times 100 \text{……..Equation (7)}$$

Where feed and permeate oil sample concentrations are represented by C_f and C_p respectively.

The driving force across the membrane was increased along enhanced various applied pressures (70-250 kPa) which was helpful to increase the permeate flux. Specifically, the S3 membrane shows significant variation primarily attributed to pore blocking and concentration polarization. In an industrial setting, membranes ideally should combine high purification efficiency with commendable permeate flux. Consequently, the prepared S3 membrane demonstrates superior oil rejection (98–96%) alongside favourable permeate flux. When compared to other membranes (as shown in Table 5). A comparative study concludes that the prepared membranes show better rejection and good permeate flux. Thus, the membrane (S3) derived from fly ash emerges as a promising solution for treating oily wastewater containing oil-in-water emulsions.

4. Conclusions

A range of economically efficient ceramic membranes has been effectively produced using various compositions of raw materials through the uni-axial dry compaction method. These prepared membranes, featuring diverse compositions, exhibit impressive mechanical strength ranging from 26.31 to 39.11 MPa.

When exposed to acid and alkali solutions, the membranes exhibit weight losses of 12% and 6%, respectively, indicating higher stability in alkaline environments. The average pore size of the membranes, determined to be 1.029 µm based on water flux data, is supported by SEM analysis, which measures it to be 1.59 µm. Notably, among all the membranes, S3 shows superior mechanical strength at 39.11 MPa with excellent chemical stability in both acid and base environments. Additionally, membrane S3 displays 39% porosity, water permeability of 9.19 × 10−6 m^3 /m^2 s Pa, and pore size of the membrane is measured at 1.029 µm. This membrane was used to treat oily wastewater with an initial concentration of 200 mg/L, achieving 98% oil removal with a flux 4.20 × 10 $^{-8}$ m^3/m^2 s at 80 kPa.

Acknowledgement-

The authors would like to extend our appreciation to the Civil and MME Departments of NIT Bhopal for their assistance in facilitating membrane formation and their support in conducting SEM analysis. The utilization of the UTM in this study was made possible through the generosity of the MME Department. Additionally, Authors extend our appreciation to the Chemical Engineering Department, NIT Bhopal for providing us with this valuable opportunity

References

1. Benito, J.M., Conesa, A., Rubio, F., & Rodriguez, M.A. (2005). Preparation and characterization of tubular ceramic membranes for treatment of oil emulsions. Journal of the European Ceramic Society, 25, 1895–1903. https://doi.org/10.1016/j.jeurceramsoc.2004.06.016
2. Yoshino, Y., Suzuki, T., Nair, B.N., Taguchi, H., & Itoh, N. (2005). Development of tubular substrates, silica based membranes and membrane modules for hydrogen separation at high temperature. Journal of Membrane Science, 267, 8–17. https://doi.org/10.1016/j.memsci.2005.05.020
3. Saffaj, N., Persin, M., Younsi, S.A., Albizane, A., Cretin, M., & Larbot, A. (2006). Elaboration and characterization of microfiltration and ultrafiltration membranes deposited on raw support prepared from natural Moroccan clay:

Application to filtration of solution containing dyes and salts. Applied Clay Science, 31, 110–119. https://doi.org/10.1016/j.clay.2005.07.002

4. Rawat, M., & Bulasara, V. K. (2018). Synthesis and characterization of low-cost ceramic membranes from fly ash and kaolin for humic acid separation, Korean Journal of Chemical Engineering, 35, 725-733. https://doi.org/10.1007/s11814-017-0316-6
5. Dong, Y., Hampshire, S., Zhou, J., Lin, B., Ji, Z., Zhang, X., & Meng, G. (2010). Recycling of fly ash for preparing porous mullite membrane supports with titania addition. Journal of Hazardous Materials, 180, 173–180. https://doi.org/10.1016/j.jhazmat.2010.04.010
6. Zou, D., Qiu, M., Chen, X., Drioli, E., & Fan, Y. (2019). One step co-sintering process for low-cost fly ash based ceramic microfiltration membrane in oil-in-water emulsion treatment. Separation and Purification Technology, 210, 511-520. https://doi.org/10.1016/j.seppur.2018.08.040
7. Sing, G., & Bulasara, V.K. (2015). Preparation of low-cost microfiltration membranes from fly ash. Desalination and Water Treatment, 53, 1204-1212. https://doi.org/10.1080/19443994.2013.855677
8. Vasanth, D., Uppaluri, R., & Pugazhenthi, G. (2011). Influence of Sintering Temperature on the Properties of Porous Ceramic Support Prepared by Uniaxial Dry Compaction Method Using Low-Cost Raw Materials for Membrane Applications. Separation Science and Technology, 46,1241–1249. https://doi.org/10.1080/01496395.2011.556097
9. Boudaira, B., Harabia, A., Bouzerara, F., & Condom, S. (2009). Preparation and characterization of microfiltration membranes and their supports using kaolin (DD2) and $CaCO_3$. Desalination and Water Treatment, 9, 142–148. https://doi.org/10.5004/dwt.2009.764
10. Mittal, P., Jana, S., & Mohanty, K. (2011). Synthesis of low-cost hydrophilic ceramic–

polymeric composite membrane for treatment of oily wastewater. Desalination, 282, 54–62. https://doi.org/10.1016/j.desal.2011.06.071

11. Dong, Y.C., Liu, X.Q., Ma, Q.L., & Meng, G.Y. (2006). Preparation of cordierite-based porous ceramic micro-filtration membranes using waste fly ash as the main raw material. Journal of Membrane Science, 285, 173–181. https://doi.org/10.1016/j.memsci.2006.08.032
12. Das, B., Chakraborty B., & Barkakati, P. (2017). Separation of oil from oily wastewater using low cost ceramic membrane. Korean Journal of Chemical Engineering, 34, 2559-2569. https://doi.org/10.1007/s11814-017-0185-z
13. Cui, J., Zhang, X., Liu, H., Liu, S., & Yeung, K.L. (2008). Preparation and application of zeolite/ceramic microfiltration membranes for treatment of oil contaminated water. Journal of Membrane Science, 325, 420–426. https://doi.org/10.1016/j.memsci.2008.08.015
14. Suresh, K., & Pugazhenthi, G. (2016). Development of ceramic membranes from low-cost clays for the separation of oil–water emulsion. Desalination and water treatment, 57, 1927-1939. https://doi.org/10.1080/19443994.2014.979445
15. Ebrahimi, M., Willershausen, D., Ashaghi, K.S., Engel, L., Placido, L., Mund, P., Bolduan, P., & Czermak, P. (2010). Investigations on the use of different ceramic membranes for efficient oil-field produced water treatment, Desalination, 250, 991–996. https://doi.org/10.1016/j.desal.2009.09.088
16. Yang, C., Zhang, G., Xu, N., & Shi, J. (1998). Preparation and application in oil–water separation of ZrO_2/α-Al_2O_3 MF membrane. Journal of Membrane Science, 142, 235–243. https://doi.org/10.1016/S0376-7388(97)00336-0

https://doi.org/10.36375/prepare_u.iiche.a412

Synthesis, characterization and degradation of Boron, Cerium and silver ternary doped titanium dioxide photocatalyst via EDTA citrate method using ampicillin antibiotic under Sunlight

Yash Mishra, Dr Hari Mahalingam
National Institute of technology Karnataka,Surathkal
(Department of Chemical Engineering)
yash250025@gmail.com

Abstract

Nowadays, we can see that in river water, traces of antibiotics can be found, which is an emerging problem. Also, pharmaceutical companies' wastewater contains antibiotic traces present in it in a significant amount which makes it an excellent experimental domain to work upon. Which is very harmful if taken by humans without its treatment, so to treat it as early as possible is very necessary, else the bacteria emerging in that water will be converted to superbugs and then curing the disease from that bacteria will be exceedingly difficult as they have resistive power to that antibiotic. For that, we have prepared a tri-doped photocatalyst by doping boron cerium and silver in a titanium dioxide structure. It can work under sunlight light because the presence of silver in this boron amount is increased so that it can satisfactorily degrade antibiotics. Cerium is for water disinfection in the further catalyst. Its amount was also increased. Then the characterization analysis was performed with the help of DLS analysis with the help of a nanoparticle size analyzer, and we got particle size in the range of 115 to 600 nanometer XRD analysis. We got a band gap Of 2.3 to 2.4 electron Volt.BET surface area analysis showed us a surface area of about 25 m2/g.So instead of the UVA lights now, it was performed under the sunlight and the degradation percent was increased significantly to approx 70 percent.

Keywords :-PhotoCatalyst, antibiotic, Ampicillin,Sunlight,EDTA Citrate Method,Ternary –doping

https://doi.org/10.36375/prepare_u.iiche.a412

INTRODUCTION

Rapid modernization were the most important contributors to water pollutants for the duration of the world. nowadays, pharmaceutical residues detected in the μg/L-ng/L variety in surface water,groundwater, and consuming water resources are considered as emerging contaminants due to the extended opportunity of improvement of superbugs. A recent newspaper article has pointed out the presence of superbugs in the river Ganga, a primary river in India. some other article has highlighted the pollution due to antibiotics in rivers everywhere in the international, with the concentrations often exceeding the threshold limits. nearly 90% of the antibiotics are excreted in their determined form from the human body, which subsequently reaches the sewage treatment plants . The considerable assets of antibiotic residues because of the anthropogenic activities are partially treated or untreated effluents from sewage treatment flowers, hospitals, and pharmaceutical manufacturing industries.Fluoroquinolones, carbapenems, and cephalosporins are the maximum generally said class of antibiotic residues in the effluent treatment vegetation of India. Ampicillin belongs to the fluoroquinolone magnificence of antibiotics, and they're used to treat a variety of bacterial infections. Their presence in water bodies has been suggested in the range of 5,000–31,000 μg/L and 251,000 μg/L, respectively . The predicted No-impact concentration-minimal Inhibitory concentration (PNEC-MIC) for the prevention of growing resistance is postulated based on the technique endorsed by Bengtsson-Palme and Larsson (2016) and by way of the Antimicrobial Resistance (AMR) Industry Alliance (2018). The PNEC for ampicillin is 0.4 μg/L . The capacity adverse results of those antibiotic residues are vegetation irrigated with contaminated water ends in bio-accumulation within the food chain (from the farm to the table and then into the human body), the aquatic existence is affected due to quandary of the mild penetration, sewage drains get clogged with the bacterial biofilms due to the accumulation/sorption of antibiotic residues onto the sewage sludge, and the switch of pathogenic (antibiotic-resistant) genes into wholesome microbes promote an growth in superbugs . therefore, there is a pressing want to deal with these wastewaters. diverse physical, chemical, and organic remedy methods like membrane strategies, reverse osmosis; activated carbon, chlorination; cardio, and anaerobic strategies had been in existence for the remedy of pharmaceutical wastewaters. The fundamental drawbacks of these remedy methods are clogging of membranes, carbon regeneration, obstacle of size exclusion range, disposal problems (physio-chemical remedy), biomass accumulation, sluggish technique, and requirement of long startup intervals (biological treatment). due to the poor degradability of antibiotics and the unsuitableness of wastewater remedy plants to deal with that pollution, there's

https://doi.org/10.36375/prepare_u.iiche.a412

a need for the improvement of opportunity sustainable remedy methods . Photocatalysis, with the potential to degrade the organic contaminants in water and wastewater, serves this cause . Semiconductor-based totally photocatalysis is one of the superior oxidation processes (AOPs) for the removal of organic contaminants via the generation of powerful oxidizing marketers [14]. TiO2 is the maximum broadly used photocatalyst as it's far effectively available, non-poisonous, chemically, and mechanically solid. but seen light usage because of the huge bandgap of 3.2 eV is a prime quandary. the usage of seen mild active photocatalysts is gaining importance in recent times, which may be executed through engineering the bandgap of semiconductors through doping. diverse metals (transition-Fe, Cu, Co, Zn, Mn, Mo, Ni, W; rare earth-Ce, Gd, European, Y; and others-Li, Ge, Si, Sn, Pb,) or non-metals (B, C, N,S, P) help in narrowing the bandgap for effective usage of visible light, and gives splendid chemical stability .it's miles glaring that the presence of rising pollution mainly antibiotic residues in water bodies and the ensuing linkage to the increasing antimicrobial resistance is of great challenge and on this context, it'd be suited to have a seen mild photocatalyst that is simultaneously effective for each photo-degradation in addition to disinfection. preserving this goal in mind, the dopants are narrowed down to cerium (Ce) and boron (B) for the reasons said below. uncommon-earth metallic doping like cerium results in the narrowing of the bandgap and promotes the adsorption capacity for this reason, enhancing photocatalytic hobby by way of providing better touch between pollutant and photocatalyst. Ce-TiO2 photocatalysts had been suggested for the degradation of phenol, chlorophenol, polyvinylpyrrolidone, and methylene blue and disinfection of Staphylococcus aureus. some of the various non-metal dopants, B ions occupy both the substitutional and interstitial lattice positions of TiO2, the former position facilitates in narrowing of the bandgap, introduction of new power ranges and transferring of the absorption part closer to visible light even as the latter role promotes effective electron-hollow separation and reduces the recombination rate. it's also a powerful disinfectant . B-TiO2 photocatalysts were suggested for the degradation of p-nitrophenol, Orange II azo dye, and disinfection of Staphylococcus aureus and Escherichia coli. other than those, photocatalytic degradation of antibiotics (ampicillin) and dyes (Rhodamine B, RhB) had been suggested via [25–27] the use of l. a./Cu/Ze trimetallic nano photocatalyst BiOBr/BiFeO3, and Sr/Ce/AC bimetallic nanocomposite respectively. numerous strategies for the synthesis of doped photocatalysts like sol-gel, hydrolysis, hydrothermal, solvothermal, and co-precipitation have been pronounced. The EDTA-citrate technique affords a higher catalyst yield and additionally improves the properties of the catalyst debris. EDTA forms a hoop structure with a maximum of the metallic ions and enables the molecular level of mixing. there's little or no or no literature on the synthesis of Ce-TiO2 ,Ag-TiO2 and B-TiO2 using this method. The photocatalytic degradation of ampicillin by means of TiO2 was studied , and a few researchers have mentioned the usage of doped TiO2, BiOBr and Fe debris . A summary of the research carried out on

https://doi.org/10.36375/prepare_u.iiche.a412

the photocatalytic degradation of ampicillin is provided in tables S9 - S10 of supplementary. in this manuscript, the photocatalytic degradation of ampicillin under sunlight with the use of a series of B,Ag and Ce-doped TiO2 photocatalysts synthesized by the EDTA-citrate approach has been finished at the side of the photocatalytic disinfection of E.coli. The precise stress MTCC 9541 used for the disinfection examination is remoted/derived from the river Ganga in view of the full-size antimicrobial resistance present in this river .

Materials

The following chemicals were used without further purification in the synthesis of the catalysts TiO2 (Degussa P25, 99.9% pure) from Evonik (Japan), Boric acid, EDA, citric acid and ammonia solution from Loba Chemie Pvt Ltd. (India), Cerium nitrate and silver nitrate from Sigma-Aldrich (India), Ampicillin from Sigma-Aldrich (USA). Distilled water was employed in the preparation of all solutions.

Synthesis of Nanoparticles

Two ternary doped TiO_2 catalysts were made using the modified sol-gel method employing EDTA & citric acid as the chelating and complexing agents respectively. A mole ratio of 1:1:1.5 being the ratio of metal ions to EDTA and citric acid was used in the synthesis. EDTA $C_{10}H_{16}N_2O_8$) solution was made using water and ammonia. Stoichiometric quantities of boric acid (H_3BO_3), cerium nitrate ($Ce(NO_3)_3{\cdot}6H_2O$), silver nitrate ($AgNO_3$), and titanium dioxide (TiO_2) in aqueous form was added to the solution & stirred. Then, solid citric acid ($C_6H_8O_7$) was added to the above mixture. Ammonia is used for adjusting the pH to 9, and the resulting mixture was agitated gently till an organometallic gel formed. Drying of the gel was done a laboratory oven at 150 °C for 24 h. The dried sample was finely crushed and subjected to calcination in a muffle furnace at 350 °C for 12 h, followed by calcining at 600 °C for 5 h. The powder thus obtained was stored in an air-tight bottle for further use. In this work, two ternary doped catalysts are synthesized and denoted as 2B-0.1Ce-0.06Ag-TiO_2, 2B-1Ce-0.06Ag-TiO_2.Due to the use of water as a solvent thus replacing the volatile organic solvents usually employed, the process can be considered as relatively green . It may be noted that Boron is an excellent disinfectant and cerium promotes the adsorption capability of the catalyst while silver has excellent antimicrobial properties and surface plasmon resonance enabling the catalysts functioning under visible or solar light. We wanted to examine in detail, the effect of increased amounts of cerium and silver in this work keeping the amount of boron dopant is constant.

LEACHING ANALYSIS :-

Leaching analysis were performed on both photo-catalyst to deduce the amount of dopants and titanium being leached while performing

https://doi.org/10.36375/prepare_u.iiche.a412

analysis.Results obtained are shown below

BORON RESULTS
2 B 1 CE 0.06 AG 0.54 PPM
2 B 0.1 CE 0.06 AG 0.29PPM

CERIUM RESULTS
2 B 1 CE 0.06 AG 0.04 PPM
2 B 0.1 CE 0.06 AG 0.00 PPm

TITANIUM RESULTS
2B 1 CE 0.06 AG 0.24 PPM
2 B 0.1 CE 0.06 AG 0.11 PPM

SILVER RESULTS
2B 1 CE 0.06 AG 0.00 PPM
2 B 0.1 CE 0.06 AG 0.00 PPM

XRD ANALYSIS :-

The XRD spectra of two doped photocatalysts are shown in below fig . As can be seen, the two spectra are nearly identical, confirming the correctness of the synthesis procedure. The peaks observed at □ = 24.5 and 47° indicate the anatase phase, while the slight rise immediately following this at about 29° suggests the presence of the cerium oxide (111) phase. Since silver ion is relatively large compared to titanium and cerium, besides being present in meagre amounts, the XRD spectra do not show the presence of silver. Boron is also not indicated.

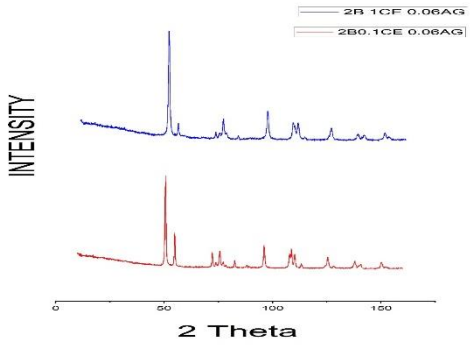

DRS ANALYSIS :-

Diffuse reflectance spectroscopy analysis was performed on the synthesized catalysts to obtain the band gap energy values as determined from the Tauc plot. In the analysis, TiO_2 is considered as an indirect semiconductor and the calculations are done on this basis. The formula used is

$$\alpha h\nu = A\left(h\nu - E_g\right)^{n/2} \quad (1)$$

where, E_g - band gap energy (eV), α - absorption coefficient, h - Planck's constant, ν - frequency of light, A - constant, n = 4 (for indirect transition). The plot of $(\alpha h\nu)^{1/2}$ versus (hν) energy determines the band gap energy values which is obtained by extrapolation of the linear portion of the curve to the x-axis. Relative to the band gap energy value of TiO_2 (3.4 eV) .

https://doi.org/10.36375/prepare_u.iiche.a412

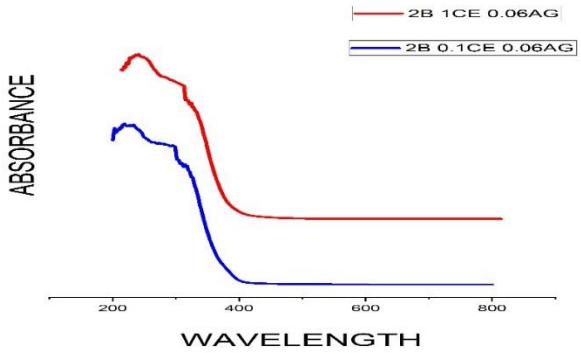

The characterization analysis results obtained from DRS analysis were used for plotting the graph of Absorbance Vs Energy

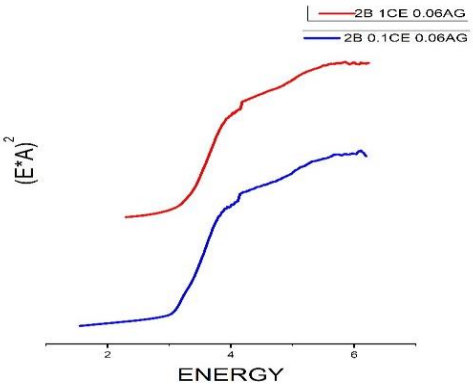

The characterization analysis results obtained from DRS analysis were used for plotting the graph of (E*A) ^2 vs energy.

CALIBRATION OF AMPICILLIN ANTIBIOTIC

The photocatalytic degradation of ampicillin under sunlight irradiation is used to evaluate the performance of TiO2 and the synthesized photocatalysts. A irradiation time of3 hours with a mean intensity of 200 ± 20 lx and a temperature of 28°C is used in the conduct of experiments. The volume is 200 mL of 10 mg/L, 20 mg/L, and 30 mg/L pollutant concentration (Ampicillin) and the catalyst loading is chosen as 1 g/L. The samples are kept in the dark for 30 minutes to attain complete adsorption before starting the illumination. Liquid samples are taken at regulartime intervals and filtered & centrifuged to remove the solid catalyst particles.

The percentage of Ampicillin was calculated according to the following equation:

Ampicillin degradation = (c0−c/c0× 100%)

where Co – Initial concentration,

C - Final concentration

The calibration analysis was performed for the ampicillin antibiotic with the help of UV Spectro photometer and the respective absorbance vs wavelength graph was plotted as shown in below figure and also absorbance Vs concentration graph was plotted for the

https://doi.org/10.36375/prepare_u.iiche.a412

ampicillin antibiotic as depicted in the second figure

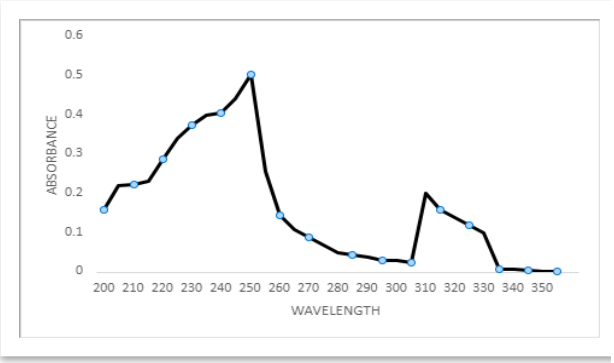

Fig :- Absorbance Vs Wavelength curve for Ampicillin Antibiotic

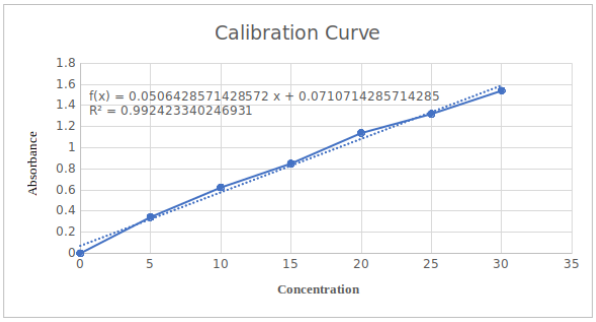

Fig Absorbance Vs Concentration graph for Ampicillin Antibiotic

DLS ANALYSIS :-

The particle size was more than the previously formed catalyst which is usual as the amount of boron is increased in the catalyst and also in comparison amonf gboth photo-catalyst second one was having more size since it has more amount of cerium content being doped.

As the graph below clearly shows the size of few nano particles is more than the desired value it is because the boron may not have doped correctly in the Ti-O2 or due to the formation of the agglomerates.

ATOMIC CONFRIGUATION :- 2B 0.1B 0.06AG

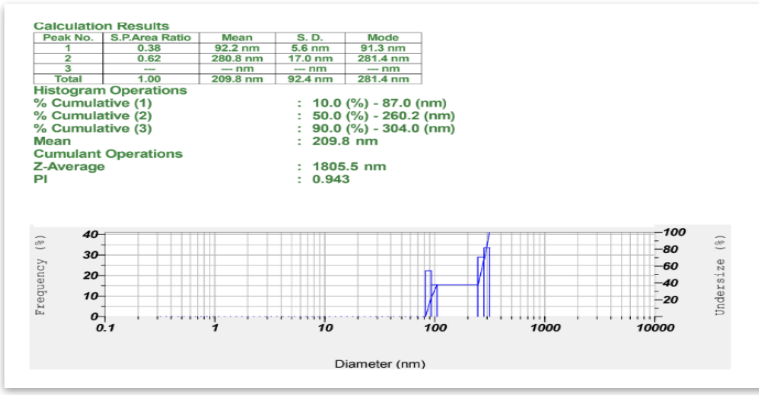

ATOMIC CONFRIGUATION:-2B 1B 0.06Ag-TiO2

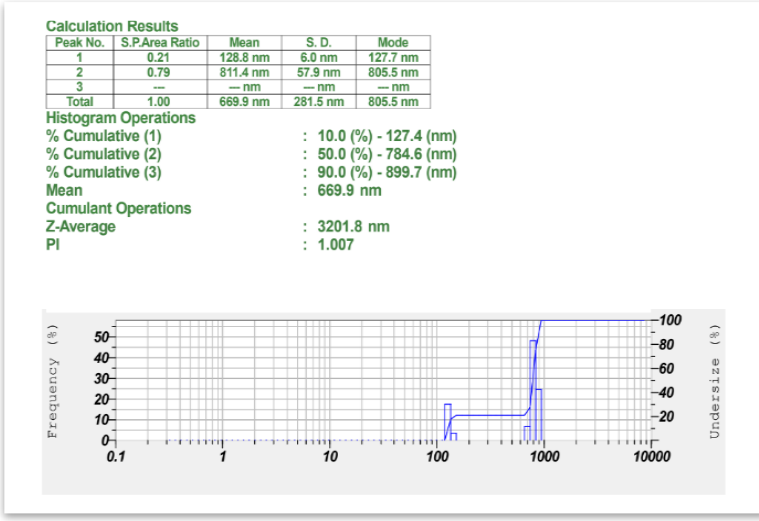

PARTICLE SIZE RESULTS

https://doi.org/10.36375/prepare_u.iiche.a412

2B 1 CE 0.06 AG	209.8 NM
2 B 0.1 CE 0.06 AG	669.8 NM

SEM Analysis

The surface morphologies of undoped TiO2, B-Ce-Ag-TiO2, and B-Ce-Ag samples are characterized by SEM and the images are shown below .No specific treatment is provided to the TiO2 sample prior to SEM analysis as it was commercially available. However, in the case of synthesized ternary doped catalysts prior to SEM analysis, they are sonicated for 10 min and then dried. The ternary doped photocatalyst particles appear as loosely packed irregular/elongated aggregates with a coarse surface, whereas TiO2 particles appear as closely packed small aggregates with a smooth surface. In the doped catalysts, a large number of nanoparticles are assembled to form aggregates on the primary particles. Higher agglomeration with an increase in the Ce dopant concentration can be attributed to the larger ionic radius of Ce than that of Ti, implying that it cannot enter the lattice of TiO2 and therefore, Ce peaks are observed in the XRD spectra However, an opposite trend of a decrease in agglomeration (as well as particle size) with an increase in boron dopant concentration was observed. The decrease in agglomeration and particle size can be attributed to the smaller ionic radius of B than that of Ti due SEM Images of the first ternary doped photo catalyst were analysed and best 4 images among them were selected.

SEM Results.

ATOMIC CONFRIGUATION:- 2B 0.1CE 0.06AG

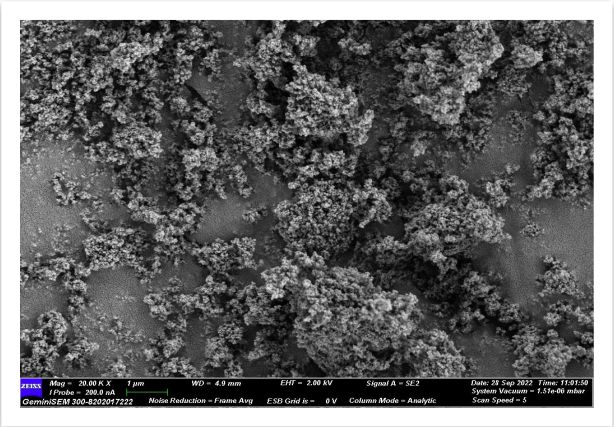

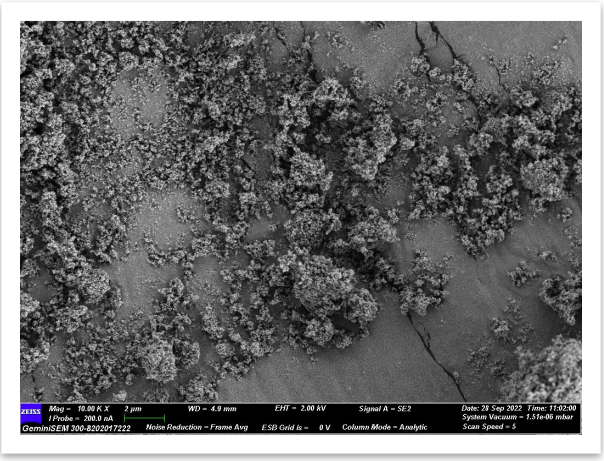

https://doi.org/10.36375/prepare_u.iiche.a412

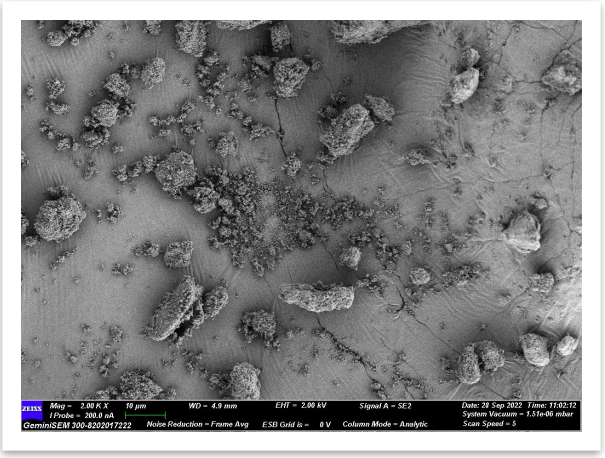

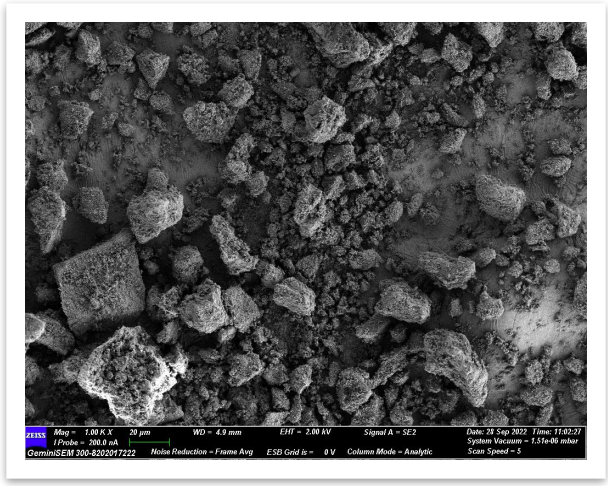

.

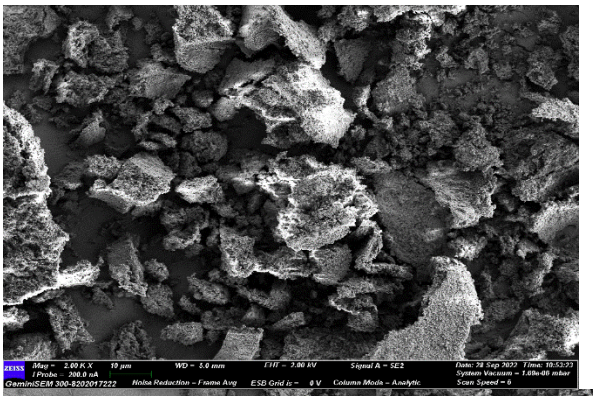

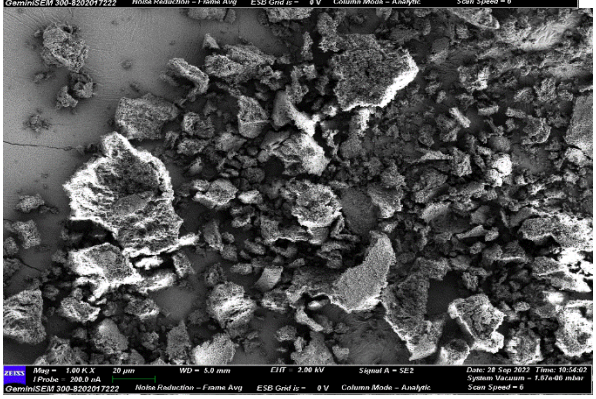

ATOMIC CONFRIGUATION :-2B 1CE 0.06AG

The images of the second photo catalyst were also analyzed and best 4 images were selected from them. Agglomerates can be seen in the below images

https://doi.org/10.36375/prepare_u.iiche.a412

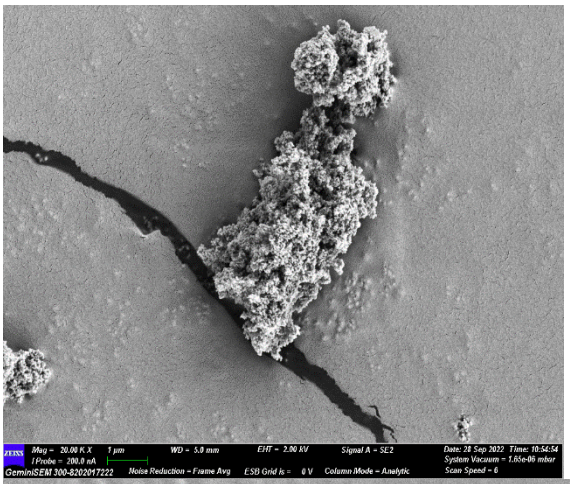

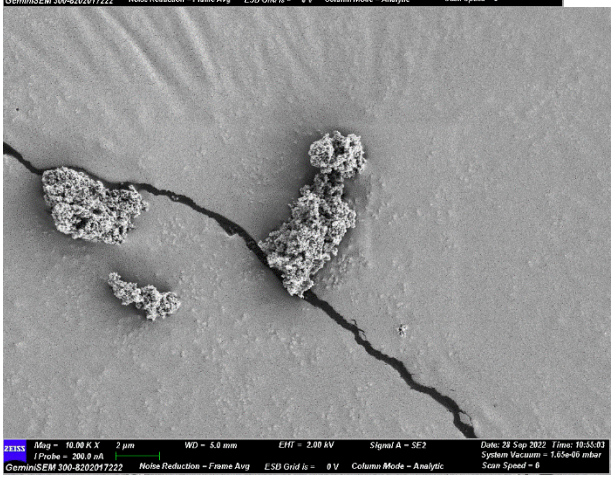

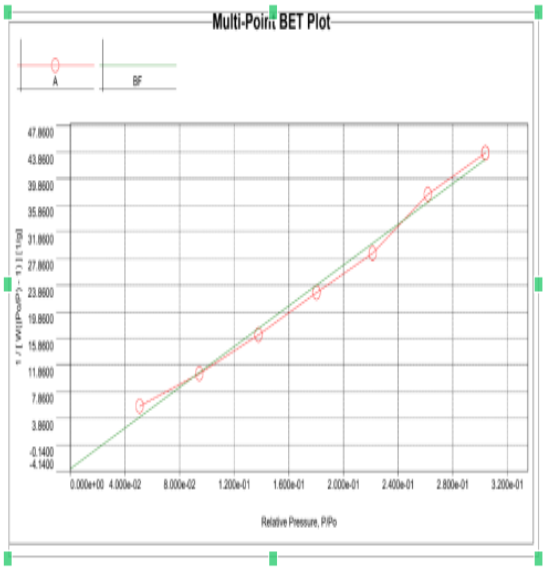

BET SURFACE AREA ANALYSIS: -

Langmuir and BET plot analysis gave the desired results. The pore size and pore volume were also found in the desired range.The outgas time was 6 hrs.The method used for the BET surface analysis is physisorption method. The model of the BET surface area which describes the quantity of adsorbed gas as a function of the relative pressure, p/po.In the BET suface area analysis we use the area per molecule for the calculation olf whole BET surface area.

GOT bet surface area as 23m^2/g.

RAMAN SPECTROSCOPY:-

Raman spectroscopy is employed to understand the crystal structure of the photocatalysts through vibrational modes, and the spectrum is depicted below. The anatase Raman modes in the undoped and doped samples are found at: Eg(1)-143 cm–1, Eg(2)-196 cm–1, Eg(3)-636 cm–1, B1g-396 cm–1, A1g + B1g-5176cm–1. The intensity of anatase Raman mode, especially Eg(1), is found to be higher in all the photocatalysts . It is noted that as in the XRD, here also, the boron peaks are not detectable.

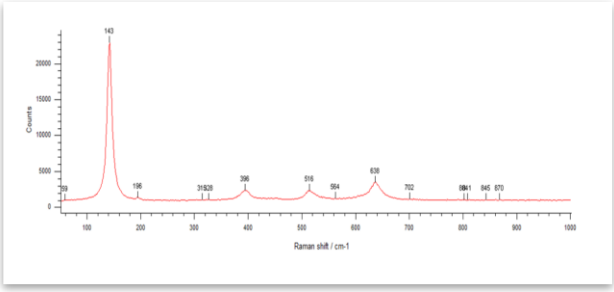

https://doi.org/10.36375/prepare_u.iiche.a412

DEGRADATION RESULTS:-

The degradation studies of ampicillin for best-performing ternary-doped photocatalysts, i.e., B2Ce1Ag0.1TiO2 and B2Ce0.1Ag0.06TiO2 were carried out under sunlight at room temperature. The degradation in the presence of TiO2 shows good results, whereas the remaining ternary-doped catalysts are not performed significantly under the sunlight. The results are shown below in the graphs.The graph above shows the degradation of ampicillin under sunlight in which the effect of photocatalytic degradation of ampicillin was studied at 10 ppm, 20 ppm, and 30 ppm using ternary-doped catalysts i.e., B2Ce1Ag0.1TiO2 and B2Ce0.1Ag0.06TiO2. To compare the ternary-doped catalyst performance with TiO2, the degradation study was carried out with TiO2. An optimum value is noticed for the co-doped catalyst from previously done research work, while an increasing trend is observed for the Ternary-doped catalysts. TiO2 showed almost 100% degradation at an optimum catalyst loading of 1g/l in 10ppm, 20ppm, and 30ppm concentrations of ampicillin. After placing the whole system of each concentration for 30min in dark conditions, the degradation was observed in 20% for 30ppm solution and 35% for 10ppm, and after 90min the ampicillin is almost degraded to 100% for all concentrations (10ppm, 20ppm, 30ppm). After 90 min, the degradation of ampicillin by TiO2 was more than 96%. For ternary-doped catalyst 2B-1Ce-0.1Ag-TiO2, after 30min of placing in dark conditions, the degradation was observed at a minimum of 16% at 50ppm and a maximum of 27% at 10ppm. After 120min of placing the whole system under sunlight, the degradation was observed at a minimum of 45% and a maximum of 68%. Among both photo catalyst one with more dopant concentration of cerium was best performing.

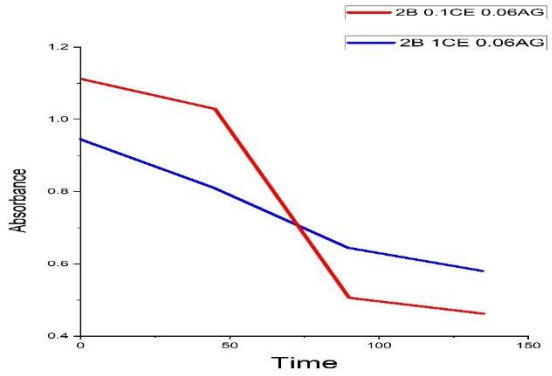

CONCLUSION: -

The solar light-driven photocatalytic degradation of ampicillin using B-TiO2, Ag-TiO2 and Ce-TiO2 has been carried out i

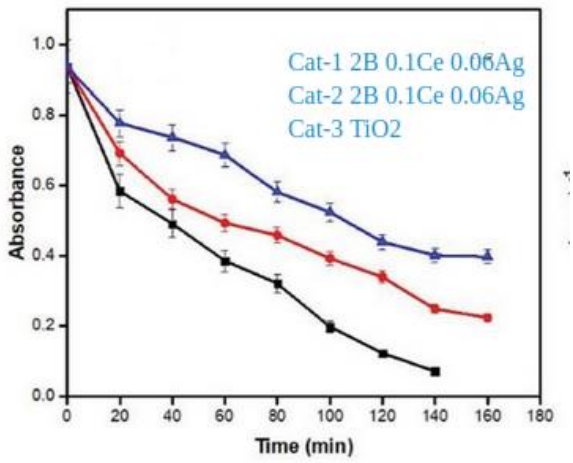

n this study. The photocatalysts synthesized by the EDTA-citrate method showed particle size in the nanoscale range and surface area in the field of 25 m2/g. T The XRD diffraction peaks of Ce suggest the presence of Ce on the surface of TiO2

due to its large radius, and the absence of prominent boron peaks indicates the uniform dispersion of B in TiO2. The bandgap values obtained are in the range of 2.4–2.7 eV, which suggests an introduction of a new energy level for effective charge separation and reduction of recombination. The enhancement in the photocatalytic activity of Ce-TiO2 and Ag-TiO2can be ascribed to the higher adsorption ability of these photocatalysts when compared with boron as the water adsorbed surface generates more hydroxyl radicals and acts as a photoexcited hole trap. An enhancement in the photocatalytic activity of B-TiO2 to the presence of B in the interstitial lattice position where there is a formation of a shallow level below the conduction band as confirmed from DRS, which reduces recombination and due to the presence of Ti3+, which acts as trapping sites of photogenerated electrons. The degradation of ampicillin is found to obey pseudo-first-order kinetics with high k values and R2, suggesting an increase in the rate of the reaction. The photocatalytic degradation of ampicillin has occurred mainly through decarboxylation, hydroxylation, defluorination, and transformation of the piperazine ring with an intact quinolone moiety which finally forms lower molecular weight/less harmful products. The absence/decrease in the intensity of the pollutants peak in the HPLC/LC-MS data validates their effective photo catalytic degradation under sunlight. However, the COD reduction in some photocatalysts was found to be lesser than the degradation observed through a spectrophotometer, which might be due to the formation of other, less harmful and stable organic compounds as observed in the LC-MS. The photocatalysts are found to be durable for up to three consecutive recycles. The trapping experiment results implied that the e– and OH are the dominant active species involved during the photocatalytic degradation of ampicillin. From the above analysis, one at. % Ce-TiO2 and one at. % B-TiO2 are found to be the best-performing photocatalysts, which can be due to the higher adsorption rates in cerium and interstitial lattice position of boron, along with a decrease in the bandgap. Their disinfection efficiencies (of the best-performing catalysts of degradation) are found to be in the range of 97–99.99%. Hence, these sunlight-active photocatalysts could be the facile and sustainable solution for the emerging problem of antimicrobial resistance. The immobilization of these photocatalysts onto suitable support may be employed for large-scale use in the near future to solve the looming environmental crisis.The pollutant named ampicillin was almost degarded about 70 percent.

References:-

[1] K. Kümmerer, Antibiotics in the aquatic environment – a review – part II,

Chemosphere 75 (2009) 435–441, https://doi.org/10.1016/j. Chemosphere.2008.12.006.

[2] C. Hai Wei, X. Hu Tang, J. Rong Liang, and S. Ying Tan, “Preparation, characterization

and photocatalytic activities of boron- and cerium-codoped TiO2,” Journal of

Environmental Sciences, vol. 19, no. 1, 2007, doi: 10.1016/S1001-0742(07)60015-1.

[3] G. B. Vieira, H. J. José, M. Peterson, V. Z. Baldissarelli, P. Alvarez, and R. de Fátima

Peralta Muniz Moreira, "CeO2/TiO2 nanostructures enhance adsorption and photocatalytic

degradation of organic compounds in aqueous suspension," J Photochem Photobiol A

Chem, vol. 353, pp. 325–336, 2018, doi: 10.1016/j.jphotochem.2017.11.045.

[4] J. Arun, V. Felix, M. J. Monica, and K. P. Gopinath, "Application of Nano-Photocatalysts

for Degradation and Disinfection of Wastewater," in Springer Briefs in Information

Systems, 2019, pp. 249–261. doi: 10.1007/978-3-030-02381-2_11.

[5] M. Manjunatha, P. R. Chandewar, and H. Mahalingam, "Exploring the Synergy of B, Ce

Dopants in Codoped Titanium Dioxide Multifunctional Photocatalysts for Antibiotic

Degradation and Microbial Disinfection Under Solar Light," physica status solidi (a), vol.

219, no. 3, p. 2100581, Feb. 2022, doi: 10.1002/pssa.202100581.

[6]. A.M. Deegan, B. Shaik, K. Nolan, K. Urell, M. Oelgemöller, J. Tobin, A. Morrissey,

Treatment options for wastewater effluents from pharmaceutical companies, Int. J.

Environ. Sci. Technol. 8 (2011) 649–666, https://doi.org/10.1007/BF03326250.

[7].D. Kanakaraju, B.D. Glass, M. Oelgemöller, Advanced oxidation process-mediated

removal of pharmaceuticals from water: a review, J. Environ. Manage. 219 (2018)

189–207, https://doi.org/10.1016/j.jenvman.2018.04.103.

[8].U. Riaz, S.M. Ashraf, J. Kashyap, Role of conducting polymers in enhancing TiO2-

based photocatalytic dye degradation: a short review, Polym. - Plast. Technol. Eng.

54 (2015) 1850–1870, https://doi.org/10.1080/03602559.2015.1021485

[9].G.B. Vieira, H.J. José, M. Peterson, V.Z. Baldissarelli, P. Alvarez, R. De Fátima

Peralta Muniz Moreira, CeO2/TiO2 nanostructures enhance adsorption and

photocatalytic degradation of organic compounds in aqueous suspension,

J. Photochem. Photobiol. A Chem. 353 (2018) 325–336, https://doi.org/10.1016/

j.jphotochem.2017.11.045.

[10].J. Reszczyńska, T. Grzyb, J.W. Sobczak, W. Lisowski, M. Gazda, B. Ohtani,

A. Zaleska, Visible light activity of rare earth metal doped (Er3+, Yb3+ or Er3+/Yb3

+) titania photocatalysts, Appl. Catal. B Environ. 163 (2015) 40–49, https://doi.

org/10.1016/j.apcatb.2014.07.010.

[11].Y. Wang, Y. Wu, H. Yang, X. Xue, Z. Liu, Doping TiO2 with boron or/and cerium

elements: effects on photocatalytic antimicrobial activity, Vacuum 131 (2016)

58–64, https://doi.org/10.1016/j.vacuum.2016.06.003.

[12].R. Jaiswal, N. Patel, A. Dashora, R. Fernandes, M. Yadav, R. Edla, R.S. Varma, D.

C. Kothari, B.L. Ahuja, A. Miotello, Efficient Co-B-codoped TiO2 photocatalyst for

degradation of organic water pollutant under visible light, Appl. Catal. B Environ.

183 (2016) 242–253, https://doi.org/10.1016/j.apcatb.2015.10.041

[13].G. Sharma, V.K. Gupta, S. Agarwal, S. Bhogal, M. Naushad, A. Kumar, F.J. Stadler,

Fabrication and characterization of trimetallic nano-photocatalyst for remediation

of ampicillin antibiotic, J. Mol. Liq. 260 (2018) 342–350, https://doi.org/

10.1016/j.molliq.2018.03.059.

[14].W.E.I. Chao-hai, T. Xin-hu, L. Jie-rong, T.A.N. Shu-ying, Preparation,

characterization and photocatalytic activities of boron- and cerium-codoped TiO2,

J. Environ. Sci. 19 (2004) 90–96.

[15] S. Das et al., "Disinfection of multidrug resistant escherichia coli by solar-photocatalysis

using fe-doped ZnO nanoparticles," Sci Rep, vol. 7, no. 1, pp. 1–14, 2017, doi:

10.1038/s41598-017-00173-0.

[16] S. Teixeira et al., "Photocatalytic degradation of recalcitrant micropollutants by reusable

Fe3O4/SiO2/TiO2 particles," J Photochem Photobiol A Chem, vol. 345, 2017, doi:

10.1016/j.jphotochem.2017.05.024.

[17] M. Manasa, P. R. Chandewar, and H. Mahalingam, "Photocatalytic degradation of

ciprofloxacin & norfloxacin and disinfection studies under solar light using boron &

cerium doped TiO2 catalysts synthesized by green EDTA-citrate method," Catal Today,

2020, doi: 10.1016/j.cattod.2020.03.018.

[18] P. Sekar, D. Sadanand Joshi, M. Manjunatha, and H. Mahalingam, "Enhanced disinfection

of E. faecalis and levofloxacin antibiotic degradation using tridoped B-Ce-Ag TiO2

photocatalysts synthesized by ecofriendly citrate EDTA complexing method,"

Environmental Science and Pollution Research, no. 0123456789, 2022, doi:

10.1007/s11356-022-19268-x.

https://doi.org/10.36375/prepare_u.iiche.a412

[19].G. Sharma, D.D. Dionysiou, S. Sharma, A. Kumar, A.H. Al-Muhtaseb, M. Naushad,

F.J. Stadler, Highly efficient Sr/Ce/activated carbon bimetallic nanocomposite for

photoinduced degradation of rhodamine B, Catal. Today 335 (2019) 437–451,

https://doi.org/10.1016/j.cattod.2019.03.063.

[20].F. Mikaeili, S. Topcu, G. Jodhani, P.-I. Gouma, Flame-Sprayed Pure and Ce-Doped

TiO2 Photocatalysts, Catalysts. 8 (2018) 342, https://doi.org/10.3390/

catal8090342.

https://doi.org/10.36375/prepare_u.iiche.a414

Intelligent Techniques for Wastewater Treatment: A Technical Review

Swati Sharma[a], Mita K. Dalal[b]

[a]*Department of Chemical Engineering, Sarvajanik College of Engineering & Technology, Surat 395001, India*
[b]*Department of Information Technology, Sarvajanik College of Engineering & Technology, Surat 395001, India*

Abstract

Industrial wastewater treatment is a crucial but challenging task. The perpetual chemical and bio-chemical reactions impart a great deal of complexity to the composition of industrial wastewaters. While conventional modeling approaches can handle linear processes, complex systems exhibiting non-stationary behavior can prove challenging. Machine learning techniques based on variants of Artificial Neural Networks, Bayesian approaches and Genetic Algorithms have proven promising for outlier detection, model generation and prediction in the field of wastewater treatment. In this context, intelligent techniques enable both feature extraction and application of suitable algorithms to datasets to obtain precise results. Inference mechanisms that support decision-making combined with visualization render machine learning algorithms as the most dependable techniques for analyzing various factors affecting wastewater treatment systems. Machine learning approaches are useful for data processing, real-time modeling and actionable inference for compliance with government norms for wastewater treatment. Moreover, machine learning algorithms have also been applied in wastewater treatment to optimize efficiency parameters.

This paper reviews the application of machine learning algorithms for data processing, modeling, parameter optimization, prediction, and decision-making for efficient management of wastewater treatment processes. The challenges and limitations of these approaches are also discussed.
Keywords: wastewater treatment; machine learning; algorithm; modeling; optimization

1. Introduction

Industrial wastewaters are teeming with a plethora of pollutants. Wastewater treatment process (WWTP) is a challenging task due to the complex dynamics of the perennial reactions taking place in the natural environment. This makes real-time prediction analysis more difficult than ever. Intelligent Machine Learning techniques such as Bayesian Learning [7, 21], Artificial Neural Networks (ANN) [4, 10, 14, 17, 19, 22, 24, 29], Support Vector Machines (SVM)[6], Decision Trees [20], Genetic Algorithms (GAs) [15] and Fuzzy Learning based methods [15-18] have proven effective in the generation of models that are applicable to a diverse range of applications in the field of water-quality monitoring, wastewater treatment as well as plant design for the same. For example, Bayesian inference methods have been applied

https://doi.org/10.36375/prepare_u.iiche.a414

to generate multi-objective water-quality models which can determine the sources of contamination in water, detect presence of pathogenic micro-organisms and suggest optimal placement of sensors for quality monitoring [1]. Likewise, ANNs can be trained to predict the concentrations of continuous valued attributes like suspended solids (SS) concentrations and biochemical oxygen demand (BOD) in wastewater plant effluent [15, 22]. ANNs can also be used to model nitrogen and phosphorous removal from wetlands constructed for wastewater treatment [2, 19] Further, ANNs are found to be suitable for modeling and prediction of chemical precipitation of heavy metals in mining industry wastewaters [26]. The use of ANNs in adsorption modeling helps to address the shortcomings in traditional adsorption models and thereby enable better predictions in various systems [2, 4]. Section II of the paper summarizes diverse intelligent methods for wastewater treatment found in literature.Section III of the paper discusses the major challenges faced by machine learning based methods when applied to the task of wastewater treatment. Finally, Section IV of the paper provides observations and concluding remarks regarding application of machine learning technology and tools to the challenging task of wastewater treatment.

2. Intelligent Techniques in Wastewater Treatment

Conventional mathematical modeling approaches are capable of demonstrating the water quality parameters which tend to change with time. This approach can very well handle linear processes but are subject to various limitations while handling unstationary behavioural patterns arising due to biological growth or algal growth in industrial wastewaters.

It is observed from Table 1 that ML based inductive learning approaches are helpful in monitoring the waste water treatment processes, minimize problems and also come up with efficient solutions to the problems being encountered in waste water treatment and management.

ML based algorithms can extract relevant features and can be used to train models which are capable of achieving better results in terms of accuracy and sensitivity [10]. AI based techniques can moreover pre-process and sample raw datasets, perform data smoothing and noise removal, identify outliers and train models and thus have emerged as versatile tools in managing day to day operations in WWTPs and rendering effluent of a better quality. As per the literature surveyed, it is evident that different AI based approaches offer a varied set of advantages. ANN serves to provide prediction and control models for parameters as BOD, COD and other organic pollutants and can thus be utilized in most wastewater applications [10, 28]. While GAs are known for their high versatility, they can also be used for the qualitative analysis of wastewater [15, 28]. PSO algorithms are highly flexible and can be used in optimization of wastewater treatment systems [31].

https://doi.org/10.36375/prepare_u.iiche.a414

Table 1: Intelligent approaches in wastewater treatment

Sr No.	Intelligent Modeling Approach	Parameters predicted	References
1.	BLS (Broad learning system) with MOPIO-OBLS :optimized MOPIO-OBLS and unoptimized OBLS	BOD_5	[8]
2.	Bayesian Networks for the analysis of MSBR	COD, Total Nitrogen and Total Phosphorous	[21]
3.	Multi-layer perceptron	BOD, COD, TSS	[3]
4.	Feedforward Neural Network, adaptive neuro-fuzzy inference system and SVM	BOD	[26]
5.	Adaptive neuro-fuzzy inference system and SVM	Prediction of removal of Kjeldahl Nitrogen	[23]
6.	ANN and SVM	Prediction of TSS and COD	[13]
7.	ANN and SVM	Prediction of TDS and COD	[11]
8.	ANN	COD and trace metals	[24]
9.	Recurrent Neural Network, Deep Neural Network	NO_2	[5]
10.	Time Stacked Broad Learning System	mechanism faults considered are sludge bulking, toxicity shock and inhabitation	[9]
11.	Multi-objective particle swarm optimization algorithm, Fuzzy neural network controller	dissolved oxygen and nitrate	[15]
12.	ANN & Response Surface Methodology	COD, TSS, TDS, TS	[27]

3. Major challenges for Intelligent Techniques

The complex dynamics of industrial wastewaters are best understood by AI tools and formulated into specific mathematical models. However, abrupt changes in process parameters may lead to incorrect results and inconclusive outputs, which in turn may pose a deterrent in decision making, minimize the accuracy of the model trained with selected data using AI tools and thereby affect the prediction accuracies required for operational performance. Far more reliable outputs can be achieved by appropriate selection of historical, real-time or raw data and adequate training of the models ordained for WWT tasks. Lack of robust security mechanisms may lead to crucial situations which warrant comprehensive management meticulous handling and operation of WWTPs.

The remarkable solutions offered by AI tools could be marred by cyber attacks, malware [28]. So in a nutshell, protection from cyber attacks, optimizing operational costs and energy consumptions and training data to capture complex situations would render AI tools more reliable and profitable.

Specifically, the challenges to intelligent techniques comprise, ‘sampling of data for training of the model’, ‘parameter tuning for ML based models’, ‘relevant feature

extraction' and 'interpretation and visualization of results', which are described next.

3.1 Sampling of data for training the ML model: The efficiency and generalization of any ML based model depends upon efficient sampling of data. In wastewater plants the consistency of the samples is usually not uniform across the collection grid. Hence, it is necessary to use optimal placement of sensors for collecting training samples from different acquisition points [7, 30]. Moreover, water quality could keep changing due to complex internal reactions and environmental effects. So, reliance should not be built upon a model trained using historical samples alone, but should be time-variant and dynamically adjusted using adaptive techniques [12, 22].

3.2 Parameter tuning for ML model: Machine Learning models often require tuning of configuration parameters [32, 33]. For instance, efficiency of Neural Networks based models for WWTP will also depend upon selection of activation function and tuning of hyper-parameters such as number of hidden layers, learning rate and number of epochs [32, 33]. Popular ML tools like WEKA facilitate iterative hyper-parameter tuning for model training which in turn helps to achieve acceptable accuracy and avoid over-fitting in the derived models [36].

3.3 Feature Extraction: In order to train an accurate model for WWTP, it is important to prioritize and extract the most relevant features from waste water. Deep learning methods have proven effective in this regard [24].

3.4 Interpretation and Visualization of Results: A trained ML model may be accurate in its predictions, however it may still remain difficult to interpret for humans. Some techniques like Decision Trees accord easy visual interpretation and can also be translated into rule sets, however this is difficult for ANN based models. Hence, domain experts may still be required to interpret the learned results from an ML model, thus limiting the scope for automation. Soft computing tools like MATLAB [34], TensorFlow [35] and WEKA [36] can assist in visualization of results to some extent.

4. Conclusion

The literature reviewed reiterates the fact that the use of intelligent techniques has emerged as a boon in the field of wastewater treatment. ML based intelligent techniques have proven versatile and more efficient in modeling various aspects of wastewater treatment compared to conventional methods. The increased ability of various modeling approaches to remove hazardous contaminants and predict wastewater quality is really commendable. It is expected that future research will further strive to work upon the existing limitations for more robust intelligent approaches for wastewater treatment and management.

Declaration of Interests: The authors declare no competing interests.

References

1. Ailamaki, A., Faloutsos, C., Fischbeck, P.S, Small, M.J., VanBriesen, J. (2003). An environmental sensor network to determine drinking water quality and security. *SIGMOD RECORD, 32.*

2. Akratos, C. S., Papaspyros I. N. E., Tsihrintzis, V. A. (2009). Artificial neural network use in ortho-phosphate and total phosphorus removal prediction in horizontal subsurface flow constructed wetlands. *Biosystems Engineering, 102,* 190-201. doi:10.1016/j.biosystemseng.2008.10.010

3. Arismendy, L., Cardenas, C., Gomez D., Maturana, A., Mejia, R., Quintero, M. C. G. (2020). Intelligent system for the predictive analysis of an industrial wastewater treatment process. *Sustainability, 12.* https://doi.org/10.3390/su12166348

4. Bahramian, M., Dereli, R. K., Zhao, W., Giberti, M., Casey, E. (2023). Data to intelligence: The role of data-driven models in wastewater treatment. *Expert Systems with Applications, 217,* 11945. https://doi.org/10.1016/j.eswa.2022.119453

5. Bakht, A., Nawaz, A., Lee, M., Lee, H. (2022). Ingredient analysis of biological wastewater using hybrid multi-stream deep learning framework. *Computers & Chemical Engineering, 168, 108038.* https://doi.org/10.1016/j.compchemeng.2022.108038

6. Bellamoli, F., Di Lorio, M., Vian, M., Melgani, F. (2023). Machine learning methods for anomaly classification in wastewater treatment plants. *Journal of Environmental Management, 344,* 118594. https://doi.org/10.1016/j.jenvman.2023.118594

7. Candelieri, A., Perego, R., Archetti, F. (2018). Bayesian optimization of pump operations in water distribution systems. *Journal of Global Optimization, 71,* 213. https://doi.org/10.1007/s10898-018-0641-2

8. Chang, P., Bao, X., Meng, F. C., Lu, R. W. (2023a). Multi-objective Pigeon-inspired Optimized feature enhancement soft-sensing model of Wastewater Treatment Process. *Expert Systems with Applications, 215*:119193 doi:10.1016/j.eswa.2022.119193

9. Chang, P., Xu, Y., Meng, F. C (2023b). Efficient fault monitoring in wastewater treatment processes with time stacked broad learning network. *Expert Systems with Applications, 233,* 120958. https://doi.org/10.1016/j.eswa.2023.120958

10. Cheng, T., Harrou F., Kadri, F., Sun, Y., Leiknes, T. (2020). Forecasting of Wastewater Treatment Plant Key Features Using Deep Learning-Based Models: A Case Study. *IEEE Access,* 8, 184475. doi: 10.1109/ACCESS.2020.3030820

11. Curteanu, S., Godini, K., Piuleac, C. G., Azarian, G., Rahmani, A. R., Butnariu, C. (2014). Electro-oxidation method applied for activated sludge treatment: experiment and simulation based on supervised machine learning methods. *Industrial Engineering Chemistry Research, 53*, 4902. doi: 10.1021/ie500248q

12. Fang, X., Zhai, Z., Xiong, R., Zhang, Li., Gao, B. (2022). LSTM-based Modelling for Coagulant Dosage Prediction in Wastewater Treatment Plant. 3rd International Conference on Artificial Intelligence in Electronics Engineering (AIEE 2022). Bangkok, Thailand, ACM, New York, NY, USA.

13. Guo, H., Jeong, K., Lim, J., Jo, J., Kim, Y. M., Park, J-p., Kim, J. H., Cho, K. H. (2015). Prediction of effluent concentration in a wastewater treatment plant using machine learning models. *Journal of Environment Science, 32*, 90. doi: 10.1016/j.jes.2015.01.007.

14. Hamed, M. M., Khalafallah, M. G., Hassanien, E. A. (2004). Prediction of wastewater treatment plant performance using artificial neural networks. *Environment Modelling & Software 19*, 919. https://doi:10.1016/j.envsoft.2003.10.005

15. Han, H-G., Zhang, L., Liu, H-X., Qiao, J-F. (2018). Multiobjective design of fuzzy neural network controller for wastewater treatment process. *Applied Soft Computing, 67*,467. https://doi.org/10.1016/j.asoc.2018.03.020

16. He, Y., Tang, C., Zhang, D., Liao, N. (2023). Assessing the effects of the influencing factors on industrial green competitiveness fusing fuzzy C-means, rough set and fuzzy artificial neural network methods. *Ecological Indicators, 147*, 109921. https://doi.org/10.1016/j.ecolind.2023.109921

17. Jana, D. K., Bhunia, P., Adhikary, S. D., Bej, B. (2022). Optimization of Effluents Using Artificial Neural Network and Support Vector Regression in Detergent Industrial Wastewater Treatment. *Cleaner Chemical Engineering, 3*, 100039. https://doi.org/10.1016/j.clce.2022.100039

18. Kambli, A., Modi, S. (2019). Fuzzy Neuro Approach to Water Management Systems ICMLSC '19: Proceedings of the 3rd International Conference on Machine Learning and Soft Computing. 215. https://doi.org/10.1145/3310986.3311026

19. Kiiza, C., Pan, S-q., Bockelmann-Evans B., Babatunde, A. (2020). Predicting pollutant removal in constructed wetlands using Artificial Neural Networks. *Water Science Engineering, 13*,14. https://doi.org/10.1016/j.wse.2020.03.005

20. Krovvidy, S., Wee, W. G. (1990). A knowledge based planning approach for waste water treatment system. 3rd International conference on Industrial and engineering applications of artificial intelligence and expert systems, Volume 2

21. Li, D., Yang, H. Z., Liang, X. F. (2013). Prediction analysis of a wastewater treatment system using a Bayesian network. *Environmental Modelling & Software,40,*140. http://dx.doi.org/10.1016/j.envsoft.2012.08.011

22. Liu, Y., Li, K., Huang, D. (2021). Prediction of Biochemical Oxygen Demand Based on VIP-PSO-Elman Model in Wastewater Treatment. ACM International Conference on Intelligent Computing and its Emerging Applications (ACM ICEA '21), Jinan, China. 3506502 https://doi.org/10.1145/3491396.3506502

23. Manu, D. S., Thalla, A. K. (2017). Artificial intelligence models for predicting the performance of biological wastewater treatment plant in the removal of Kjeldahl nitrogen from wastewater. *Applied water science,7*,3783. https://doi.org/10.1007/s13201-017-0526-4

24. Matheri, A. N., Ntuli, F., Ngila, J. C., Seodigeng, T., Zvinowanda, C. (2021). Performance prediction of trace metals and COD in wastewater treatment using artificial neural network. *Computers & Chemical Engineering, 149*, 107308. https://doi.org/10.1016/j.compchemeng.2021.107308

25. Mehrpour, P., Mirbagheri, S. A., Kavianimalayeri, M., Sayyahzadeh, A. H., Ehteshami, M. (2023). Experimental pH adjustment for different concentrations of industrial wastewater and modeling by Artificial Neural Network. *Environmental Technology & Innovation, 31*, 103212. https://doi.org/10.1016/j.eti.2023.103212

26. Nourani, V., Elkiran, G., Abba, S. I. (2018). Wastewater treatment plant performance analysis using artificial intelligence - an ensemble approach. *Water Science Technology, 78*, 2064. doi:10.2166/wst.2018.477

27. Rai, P. K., Kant, V., Sharma, R. K., Gupta, A. (2023). Process optimization for textile industry-based wastewater treatment via ultrasonic-assisted electrochemical processing. *Engineering Applications of Artificial Intelligence, 122*, 106162. https://doi.org/10.1016/j.engappai.2023.106162

28. Ray, S. S., Verma, R. K., Singh, A., Ganesapillai, M., Kwon, Y-N. (2023). A holistic review on how artificial intelligence has redefined water treatment and seawater desalination processes. *Desalination, 546*,

116221.
https://doi.org/10.1016/j.desal.2022.116221

29. R. Vijayabhanu, V. Radha (2012). Statistical Normalization Techniques for the Prediction of COD Level for an Anaerobic Wastewater Treatment Plant. Proceedings of the 2nd International Conference on Computational Science, Engineering and Information Technology (CCSEIT-12), Coimbatore, Tamilnadu, India.

30. Venkatasubramanian, N., Davis, C. A., Eguchi, R. T. (2020). Designing Community Based Intelligent Systems for Water Infrastructure Resilience. 3rd ACM SIGSPATIAL Workshop on Advances in Resilient and Intelligent Cities (ARIC'20), Seattle, WA, USA.
https://doi.org/10.1145/3423455.3430318

31. Yadav, A., Roy, S. M. (2023). An artificial neural network-particle swarm optimization (ANN-PSO) approach to predict the aeration efficiency of venturi aeration system. *Smart Agricultural Technology, 4, 100230*
https://doi.org/10.1016/j.atech.2023.100230

32. Mitchell, T. M. (1997). Machine Learning. McGraw-Hill, New York. (ISBN: 0070428077)

33. Jiawei, Han. and Micheline, Kamber. (2006). Data Mining: Concepts and Techniques, 2nd edition. Morgan Kaufmann Publishers.

34. MATLAB: https://in.mathworks.com/products/matlab.html

35. TensorFlow: https://www.tensorflow.org

36. WEKA: https://www.cs.waikato.ac.nz/ml/weka

https://doi.org/10.36375/prepare_u.iiche.a415

How does climate change impact water sources, affecting quality and availability, and what are the resulting consequences for water treatment and infrastructure?

[1]Rajarshi Ray, [2]Rupam Khowash, [3]Bidripta Mondal,[4]Saswata Saha

[1]Department of Chemical Engineering, Jadavpur University, Jadavpur, Kolkata [1]udayanbitan@gmail.com,[2] rupamkhowash@gmail.com, [3]bidripta35@gmail.com,[4]saswata.saha11@gmai.com

Abstract

This abstract addresses a critical research gap by examining the intricate relationship between climate change and wastewater systems, acknowledging their vulnerability to climate-induced effects. Despite being crucial for societal well-being, wastewater systems' susceptibility exposes communities to risks. This comprehensive study analyzes the diverse impacts of climate change on wastewater systems across different timeframes and dimensions.The research begins by evaluating the direct climate-related effects on various components of wastewater systems, including reticulated and on-site systems, and treatment plants. This assessment covers both urban and peri-urban contexts. The identified impacts center on three key themes: nuisance flooding leading to spills and odors, deteriorating water quality from uncontrolled discharges, and physical infrastructure damage.These impacts, both immediate and long-term, resonate widely across social, cultural, environmental, and economic realms. Asset loss disrupts communities, while compromised water quality triggers cascading effects on various aspects of society, environment, economy, and culture. Concurrently, public health risks and economic burdens arise from damages, lost production, and insurance claims. Given the complexity and severity of these impacts, the study considers their distribution among different groups and their manifestation in various contexts and locations. The paper concludes by offering guiding principles for local government decision-makers. These principles serve as a strategic framework for addressing the challenges posed by climate-induced impacts on wastewater systems.In summary, this research enhances our understanding of climate change's consequences for wastewater systems, emphasizing the need for proactive mitigation and adaptation strategies. By highlighting the interconnected nature of social, cultural, economic, and environmental implications, the study underscores the requirement for holistic approaches that ensure the resilience of wastewater systems in an ever-changing climate.

Index Terms— intricate relationship between climate change and wastewater systems, diverse impacts of climate change on wastewater systems, strategic framework for addressing challenges posed by climate-induced impacts

I. INTRODUCTION

Climate change poses a severe risk to both water sources and their treatment processes. This document delves into the "Influence of Climate Change on Water Sources and Treatment Procedures," shedding light on their susceptibilities. We analyze the direct impacts of climate change on these systems, highlighting issues such as nuisance flooding, declining water quality, and damage to infrastructure. These consequences have widespread implications, impacting communities, public health, and the economy. The document also examines how these impacts are distributed across different groups and contexts. It concludes by providing essential principles for local decision-makers to tackle these challenges and underscores the significance of comprehensive strategies for enhancing the resilience of water systems in the face of a changing climate.

II. PROBLEM STATEMENT

The growing repercussions of climate change present a substantial and complex obstacle to the durability and robustness of water sources and treatment techniques. This document seeks to thoroughly tackle the distinct ways in which climate change is impacting water systems, covering concerns like modified water quality,

heightened flooding, and infrastructure susceptibility. Through the identification and analysis of these challenges, our goal is to offer insight into the pressing requirement for efficient strategies and policies to adapt to and alleviate the impact of climate change on our crucial water resources and treatment procedures.

III. HYPOTHESIS

As our climate undergoes continuous changes, it is probable that water sources and treatment methods will face escalating difficulties. These challenges may encompass more frequent extreme weather events, changes in water quality, and increased vulnerability of infrastructure. The potential consequences of these challenges are anticipated to have far-reaching impacts, affecting the dependability of our water sources, public health, and economic stability. We emphasize the importance of implementing proactive measures for adaptation and mitigation to safeguard our water resources and ensure the resilience of treatment methods amid a shifting climate. By delving into the specific ways these issues manifest and are distributed, our research aims to offer valuable insights for the development of effective policies and practices in addressing the intricate impact of climate change on water systems.

IV. RESEARCH QUESTIONS

1. How does climate change directly affect the quality and availability of water sources, and what are the specific consequences of these changes on water treatment methods and infrastructure?
2. What are the potential public health risks and economic implications associated with the impact of climate change on water sources and treatment methods, and what strategies can be developed to mitigate these risks and enhance the resilience of water systems?

V. SIGNIFICANCE

Our research on the 'Impact of Climate Change on Water Sources and Treatment Methods' holds critical relevance across various key areas:

1. **Environmental Resilience:** Understanding how climate change affects water systems is crucial for environmental conservation. Changes in water sources can disrupt ecosystems, impacting biodiversity and aquatic health. Effective water treatment is essential for mitigating these impacts and ensuring the sustainability of natural resources.
2. **Public Health and Safety:** Clean and reliable water sources are fundamental to public health. Climate-related changes can compromise water quality, posing health risks from contamination and inadequate treatment. Addressing these challenges can contribute to safeguarding the health of communities.
3. **Economic Stability:** Reliable water sources and effective treatment methods are vital for economic activities like agriculture, industry, and tourism. Climate change-related disruptions in water availability and quality can lead to economic losses. Developing strategies to adapt to these changes can help maintain economic stability.
4. **Policy Development:** Our research informs policymakers and water management authorities about the urgent need for climate-resilient water systems. It contributes to the formulation of effective policies and regulations aimed at preserving water resources and safeguarding societal and environmental interests.
5. **Community Resilience:** Vulnerable communities are disproportionately affected by climate change impacts on water systems. Our research sheds light on how these impacts are distributed among different groups and regions, aiding in the development of equitable and inclusive adaptation strategies.
6. **Long-term Sustainability:** By exploring adaptation and mitigation strategies, our research contributes to long-term sustainability. This includes initiatives such as water conservation, infrastructure upgrades, and sustainable water management practices.
7. **Global Perspective:** Our research is part of the larger global effort to address the consequences of climate change. By adding to the knowledge on climate impacts on water systems, our work assists in the development of international strategies to combat climate change and its effects.

VI. LITERATURE REVIEW

- The impacts of climate change on waste water treatment methods depends on the geography of the location of interest.The following observations are taken from the research which firstly considered direct climate-related impacts on a range of wastewater system elements (including reticulated wastewater systems, on-site wastewater systems and treatment plants), in both urban and peri-urban settings in New Zealand. The following

discussion of impacts is focused on those which were identified as having medium to high severity. We acknowledge that impacts will be experienced differently depending on location around New Zealand due to geographical variation in climate and climate change.

A) Impacts on wastewater conveyance systems

-Climate change is impacting wastewater conveyance systems, which can be either combined (stormwater and wastewater in the same pipe) or separated (distinct pipes for stormwater and wastewater). These systems may use gravity for wastewater flow or employ pumps for pressurized or vacuum-based conveyance. The pipes in these systems must be flexible and durable to maintain proper sealing. Climate change is causing medium and high severity impacts on these systems, which require attention and adaptation to ensure their functionality and resilience in the face of changing environmental conditions.

B) *Impacts of increased rainfall on wastewater pipeline conveyance systems*

-Increased rainfall due to climate change has significant impacts on wastewater conveyance systems, particularly in terms of increased overflows, blockages, and breakages. This is mainly due to the higher rainfall intensity and extreme events leading to more inflow and infiltration (I&I) into wastewater networks. In combined systems, where stormwater and wastewater share the same pipes, there's a higher vulnerability to I&I, which can result in uncontrolled discharge of untreated wastewater during heavy rainfall. Separated systems are less vulnerable to I&I due to lower stormwater inflow volumes and tighter seals between joints, especially in newer systems. Pressure systems are less vulnerable to I&I because pressure loss affects system performance and can be quickly detected.As wet weather overflow events become more frequent and severe, there's an increased risk of environmental contamination. Climate change-related severe weather events can also lead to pipe damage due to flooding and erosion. Higher wind velocities associated with severe weather can cause blockages or damage, especially in combined systems, where debris accumulates in pump stations and screens. Wind damage to infrastructure like power lines can indirectly affect pressurized wastewater systems that rely on power for conveyance. Climate change impacts on wastewater conveyance systems require attention and adaptation to maintain functionality and prevent environmental contamination.

C) Impacts of reduced rainfall and increased temperature on wastewater pipeline conveyance systems

-Reduced rainfall and increased temperatures impact wastewater conveyance systems, causing issues like corrosion, odors, and blockages. Prolonged droughts and water restrictions reduce wastewater inflow and result in concentrated, high-strength wastewater with increased pollutant levels. This leads to higher risks of blockages, odors, and corrosion. Common blockage causes during droughts include fats, oils, greases, debris, solids deposition, and tree root intrusion. Low flows can lead to the release of odorous compounds like hydrogen sulfide due to increased anaerobic decomposition. These changes can threaten public health and the environment. Furthermore, reduced rainfall increases the risk of aquifer contamination as pollutant dilution decreases during infrequent recharge events.

D) Impacts of sea-level rise on wastewater pipeline conveyance systems

-Sea-level rise, storm surges, and coastal erosion can damage pipelines, impacting wastewater systems. Fully submerged gravity pipelines may cause sewer backups and coastal wastewater contamination. Rising sea levels can raise coastal water tables, affecting inland groundwater levels and leading to increased groundwater infiltration in older systems with cracks. This can result in salt-water intrusion, reduced conveyance capacities, and corrosion. In New Zealand, locations like South Dunedin are already experiencing these issues, with artificially low groundwater tables due to infiltration into the stormwater and wastewater network, leading to high salinity in the wastewater system during high tide.

E) Impacts of increased rainfall on treatment plants / processes

-Increased inflows and power outages are the most significant impacts on wastewater treatment plants (WWTPs). Higher rainfall leads to larger volumes of wastewater entering WWTPs due to flow from combined systems and inflow and infiltration (I&I). The increased flow dilutes the influent to the WWTP, affecting biological treatment processes and potentially deteriorating effluent quality. This is attributed to decreased detention times in treatment processes. Extended dry periods following increased rainfall can worsen these effects, causing biologic overloading and increased combined sewage overflow.

High flows can carry storm-related debris to WWTPs, potentially causing blockages or screen damage. High inflows can overwhelm the system, leading to bypasses that divert partially treated or untreated wastewater into the environment, posing health risks and contaminating water supplies.

https://doi.org/10.36375/prepare_u.iiche.a415

Stormy weather can increase the risk of power outages, disrupting WWTP operations and relying on backup generators. Additionally, storm-related road closures can hinder access to treatment plants.

F) Impacts of increased temperature extremes on treatment plants / processes
-Increased temperature extremes have significant impacts on wastewater treatment plants (WWTPs) and processes. Warmer temperatures can lead to changes in WWTP performance, increased odors, and alterations in wastewater composition, as malodorous compounds are produced in the wastewater network. The strength of wastewater, WWTP performance changes, and a higher likelihood of overflows can all contribute to increased odors, especially during warmer weather. Additionally, elevated temperatures can affect WWTP processes, as biological reactions occur faster in higher temperatures. The secondary treatment phase in WWTPs relies on these reactions, leading to reduced land requirements, enhanced conversion processes, increased removal efficiencies, and improved feasibility of certain treatment processes. For instance, in sludge digestion, less energy is needed to heat the sludge at higher ambient temperatures. However, processes like activated sludge and aerobic biofilm reactors are less temperature-dependent due to advanced technology and mechanization. Furthermore, a warmer climate can lead to higher evaporation rates, as warmer air can hold more water. This may result in stricter effluent discharge standards for WWTPs due to increased salinity in receiving water bodies.

Wastewater system element	Climate hazards / stressor				
	Increased rainfall	Reduced rainfall	Sea-level rise	Temperature	Wind
Wastewater conveyance (all types; separated and combined gravity and pressure)	• Increased overflows • Increased blockages and breakages	• Corrosion due to low flows resulting in increased concentration • Blockages or siltation when combined with increased temp, and reduced water use.	• Pipes float due to increased groundwater level causing cracking • Corrosion • Groundwater ingress leading to loss of functionality and capacity • Erosion/inundation causing damage to infrastructure	• Increased odours	• Increased blockages and breakages associated with rainfall events or storms
Pump stations	• Increased overflows • Increased blockages	• Corrosion due to low flows resulting in increased concentration	• Corrosion • Flotation • Inundation • Flooding causing a reduction in the service zone of the pump station	• Blockages due to user behaviour changes in hot weather (e.g. flushing of wet wipes)	• Increased blockages, breakages and outages associated with rainfall events or storms
WWTP – general	• Increased inflows leading to more frequent bypassing. • Storm related power outages and road closures	• Increased strength of influent risking breach of toxicity levels	• Flooding and infrastructure damage • Raised groundwater table preventing sludge management dewatering • Outfalls may be impacted • Increased pumping heads for outfalls	• Performance of biological systems, oxidation ponds and sludge management varies with temperature • Odours (due to higher temperatures)	• Increased blockages and breakages associated with rainfall events or storms
On-site wastewater	• Soakage performance affected when soils are waterlogged • Floatation of below ground chambers • Soil structure damage reducing soakage performance • Ecological changes to soakage fields	• Ecological changes to soakage fields	• Soakage performance affected when soils are waterlogged • Floatation of below ground chambers • Soil structure damage reducing soakage performance • Ecological changes to soakage fields	• Performance varies with temperature • Odours increase	

Key: High Severity | Medium Severity | Low Severity

[3]
IMPACT SUMMARY-
As well as the identified impacts of climate change, many existing problems with wastewater systems are likely to be exacerbated. Existing problems relate to aging infrastructure, poorly designed infrastructure, or infrastructure that is designed to meet outdated environmental or service standards (NIWA, MWH, GNS, & BRANZ, 2012). New Zealand on-site wastewater disposal systems are dominated by septic tanks, which generally treat effluent to a minimum standard. Many systems are ageing and while all systems require ongoing maintenance, it has been identified that in many cases this is not carried out (Ministry for the Environment, 2008c). Climate change impacts will potentially exacerbate existing issues with poor performing or poorly maintained systems. In order to characterise and further explore impacts and their implications, three main summary impact themes for wastewater have been developed and are listed below. These themes were chosen by grouping the impacts discussed for each of the wastewater system components above into similar types of impacts, termed 'impact themes'. The identified impact themes are:

- Wastewater nuisance flooding, spills and odour
- Water quality deterioration due to worsening impacts of wastewater discharges
- Damage to infrastructure leading to disruption to wastewater services.

- Climate change is a major challenge for water and sanitation services, impacting water supply and sanitation. Concerns include infrastructure damage, loss of water sources due to declining rainfall, and changes in water quality. Sanitation faces risks from floods and reduced carrying capacity of water bodies receiving wastewater. To mitigate these risks, measures of climate resilience should be integrated into water safety plans, and water resource management should be improved. Policy measures, especially in low-income settings, can help reduce risks by adopting technology and management changes.

Wastewater treatment contributes to greenhouse gas emissions. Addressing this can involve choices of treatment technologies, improving pumping efficiency, using renewable energy sources, and generating energy within the system, which can reduce emissions.

IMPACTS ON SURFACE WATER TREATMENT

Increased suspended solids loads in rivers can strain drinking water treatment systems, potentially necessitating significant upgrades. While coagulation can help adjust for higher suspended solids, there's a limit to the removal capacity, and the treatment works may need to be shut down if that limit is exceeded.

https://doi.org/10.36375/prepare_u.iiche.a415

Failure to shut down coagulation units promptly can result in suspended solids breakthrough into subsequent filtration units, causing clogging and underperformance, ultimately affecting the final water tanks and distribution system.

Water treatment units, especially in developing countries, may struggle with short-term changes in high suspended solids loads, leading to water quality failures. High suspended solids can also reduce the effectiveness of chlorination and other disinfection systems, posing elevated public health risks. One management response is to implement systems that can automatically shut down to prevent substantial breakthrough, which is common in high-income developed countries but less so in many developing countries.

Multistage filtration systems can be affected by increasing suspended solids loads and need improved controls and physical measures to manage sediment loads.

Rising temperatures can favor the survival and proliferation of pathogens in piped drinking water supplies, including those associated with biofilms, which can increase health risks. Climate change may also lead to increased risks of cyanobacterial blooms in water sources, particularly affecting health facilities that lack specific additional treatment for water. Decreasing flows can result in higher pollutant concentrations, while changes in temperature and precipitation can alter water composition, potentially increasing disinfection by-product precursors. Wildfires in dry areas can change nutrient concentrations and dissolved organic carbon, challenging water treatment.

Water sources that receive wastewater upstream of supply intakes face additional water quality challenges, with increasing pollutant concentrations as river flows decline. Combined sewer systems may pose greater risks during extreme rain events, leading to water quality deterioration. Population growth, urban development, and climate impacts are expected to exacerbate water quality challenges in the future.

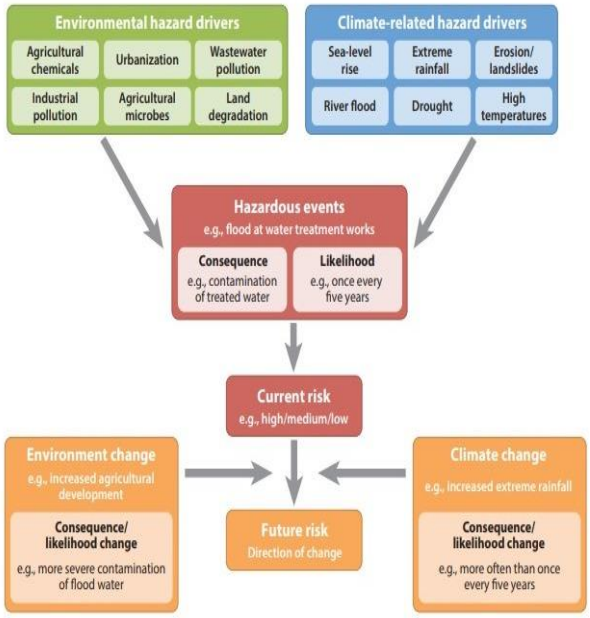

[4]

VII. METHODOLOGY

The research encompassed both a quantitative survey and qualitative interviews conducted with wastewater system managers, referred to as wastewater managers henceforth. The primary objective was to comprehend the experiences of wastewater managers with past storms, their preparatory, responsive, and recovery actions, the facilitating factors behind these actions, and their adaptation strategies to future climate change.

Quantitative Survey Design: The survey questions were meticulously crafted to evaluate several dimensions, including past storm experiences, risk perceptions related to future storms and climate change, characteristics of the wastewater system (e.g., size, location), organizational aspects (e.g., leadership, culture), and the broader context (e.g., public or political support, regulatory environment). The survey design drew insights from relevant theoretical literature on factors influencing adaptation actions, such as risk perceptions and organizational learning. To ensure measurement reliability and validity, a pilot test was conducted in October 2015 with feedback from wastewater managers not included in the final survey

sample, wastewater experts at CTDEEP, and experts in questionnaire design.

We received a total of 86 completed surveys, yielding a response rate of 65.6%.

Qualitative Interview Process: 29 wastewater managers were interviewed, selected from a stratified sample of survey respondents based on factors such as inland vs. coastal location, impact vs. no impact from past storms, and changes vs. no changes made. The interview protocol underwent testing with four wastewater managers, leading to refinements before initiating interviews with the final sample. The interviews, conducted by phone, delved into the nature and severity of past storm impacts, adaptive changes implemented, motivations for those changes, hindrances and facilitators, and perspectives on adaptation to future climate change.

Variable Construction and Survey Data Analysis: Dependent and independent variables were derived from survey questions. A binary dependent variable, "Changes," indicating whether changes were made to enhance wastewater system resilience, was created. Independent variables explored a range of factors influencing changes, including impact-related variables, risk exposure and perception, organizational factors, sociopolitical factors, and knowledge-related factors. These variables were analyzed using SPSS software, incorporating descriptive statistics, chi-square tests, independent samples t-test, and logistic regression to determine significant predictors of change.

Analysis of Interview Data: Interviews were recorded, transcribed, and analyzed using qualitative data analysis software NVIVO 11. Coding of transcripts was independently conducted by each coauthor, focusing on identifying changes made, motivating factors, hindrances and facilitators, and wastewater managers' perspectives on storms, changing storm patterns, climate change, and climate change adaptation. Anonymity was maintained, and survey data were reported in aggregated form.

This comprehensive data collection process aimed to provide a nuanced understanding of the intricate relationship between climate change and wastewater systems, addressing critical research gaps and informing proactive mitigation and adaptation strategies.

Our survey data reveals that a significant majority (78%) of wastewater managers implemented adaptive changes. Insights from interviews shed light on the nature of these changes. Approximately 30% of interviewees detailed low-cost, temporary adaptive measures undertaken to prepare for and cope with storm events. Examples include the fabrication and installation of temporary flood gates and flood-proofing doors ahead of storms. One respondent highlighted, "Our local machine shop made stop gates that we just drop in, and it holds back the water" (S24). Another mentioned, "We sealed the hatches as best we could using the foam that comes out in the can" (S15). Other measures involved purchasing and installing plugs for pump station vents to prevent flooding: "We started seeing water entering from vent holes, so we did get plugs, and have them to this day" (S09). Additional strategies included topping off fuel tanks and stockpiling fuel in anticipation of extended power outages.

Preparation and coping strategies extended beyond temporary modifications to equipment or structures. Interviewees highlighted short-term operational and staffing changes to navigate storm events successfully. For instance, adjustments were made to how wastewater treatment plants (WWTP) operated to maintain permit limits despite higher inflows during storms (S32). Some systems kept extra staff on call or on-site in preparation for storms, ensuring a timely response and avoiding workforce disruptions (S16, S14).

In addition to temporary adaptations, 62% of interviewees reported implementing permanent changes aimed at enhancing system resilience. These changes encompassed alterations to operational procedures, investments in ongoing training programs, and financial strategies such as saving more money to fund emergency repairs (DE18). Permanent physical changes were also made to improve resilience to extreme events, including sealing manholes to reduce rates of infiltration and buying new equipment such as pumps and generators designed to withstand flooding.

Furthermore, some systems invested in costly yet impactful changes, involving the redesign and reconstruction of entire WWTPs. These comprehensive overhauls, while entailing substantial financial investments, were deemed necessary by wastewater managers to fortify their facilities against the escalating challenges posed by extreme weather events (S12, S13, S21, S22).

Drivers of Change in Wastewater Systems

The statistical analysis of survey data, presented in Table 1, provides valuable insights into the factors influencing adaptive changes in wastewater systems. Managers who implemented changes demonstrated a higher average concern about future climate-related risks (mean concern 2.48 vs. mean concern 1.36) and specific concerns about climate change (median 2, "somewhat or greatly concerned" vs. 0, "not at all concerned") compared to those who did not initiate changes. The results further highlight the significance of local public support, strong organizational leadership, up-to-date technology, aging infrastructure, and empowerment in facilitating changes. Local political support and experiencing impacts from past storms were also found to be more helpful for managers implementing changes than those who did not.

Examining factors individually, various elements emerged as significant contributors. However, in a logistic regression controlling for other variables, the most crucial predictors of change were experiencing impacts from past storms, possessing strong organizational leadership, and expressing a higher average concern about future climate-related risks (see Table 2). These three predictors collectively accounted for 89% of the variance in the dependent variable "made changes."

Interview data complement these findings by offering nuanced insights into how impacts from past storms, leadership, and concern about future risks influence decisions to implement changes in wastewater systems. For instance, the majority of systems that made changes (78.6%) experienced disruptive and damaging impacts from past storms, such as significant flooding, high inflows, and lengthy power outages. These impactful events often motivated proactive changes, with interviewees emphasizing the importance of learning from past experiences and incorporating lessons into training and standard operating procedures.

Organizational leadership emerged as a critical factor, with two-thirds of systems making changes attributing their adaptability to empowered wastewater managers and a culture of continuous improvement within the organization. Managers empowered to make decisions and fostering a culture of continuous improvement tended to be proactive in implementing changes to address evolving conditions and demands on the system.

Concern about future climate-related risks, while not a universal driver of change, influenced some interviewees. Those expressing concerns about global warming or the potential impact of severe storms due to climate change were motivated to implement changes. However, others explicitly stated that future climate-related risk did not drive their decision-making, emphasizing the local and immediate relevance of their actions.

In summary, the data suggests a complex interplay of factors driving changes in wastewater systems, with a strong emphasis on learning from past experiences, empowered leadership, and varying degrees of concern about future climate-related risks.

Adaptation Strategies in Wastewater Management

Analysis of interview data sheds light on the adaptive measures undertaken by wastewater managers in response to climate-related challenges. Notably, 50% of managers who implemented changes aimed to enhance resiliency, fortifying their systems to withstand the most severe storm impacts recorded to date. Describing this focus on resiliency, one interviewee articulated it as "hardening facilities to increase survivability due to extreme weather events," coining it as the emerging concept of "resiliency" (S23). The strategies employed included elevating equipment previously affected by storms, such as generators, onto elevated platforms and sealing manholes or replacing sewer lines to minimize infiltration and inflow (I&I). While these measures represent incremental and reactive steps, they are primarily geared toward sustaining current capacities and ensuring compliance with regulatory requirements.

However, when specifically asked about adapting to climate change, responses varied among wastewater managers. Some expressed skepticism or a perception

of climate change impacts as irrelevant to their systems. For instance, one interviewee associated climate change with coastal issues and rising sea levels, emphasizing its seeming detachment from their inland system (S09). Others viewed climate change as a long-term concern that currently lacked direct relevance to their operations, unless it posed an immediate threat (S15).

Interestingly, around 30% of interviewees making changes acknowledged a willingness to adapt to a changing climate, but the impetus for their actions stemmed from new state regulations rather than a perceived direct impact of climate change. These regulations mandated wastewater systems receiving Clean Water Fund (CWF) funds to fortify infrastructure against severe weather events and anticipated climate change impacts. Compliance with these regulations involves adhering to specific flood protection levels outlined in TR-16 Guides for the Design of Wastewater Treatment Works. These guidelines dictate elevating critical equipment and structures to withstand either the 100-year storm plus three feet or the 500-year flood elevation. Wastewater managers with state-funded projects emphasized that the state regulations were the driving force behind their decisions to elevate infrastructure to the required levels.

This regulatory framework underscores the instrumental role of rules and regulations in prompting adaptation actions. The relationship observed aligns with existing literature emphasizing the compliance-driven nature of utilities when rules explicitly mandate the consideration of climate change impacts. Without such regulations, the likelihood of wastewater systems proactively adapting to climate change appears diminished.

The impacts of climate change on wastewater treatment are significant, mainly due to shifts in water distribution and the increasing frequency of extreme weather events. Climate-related changes, such as altered rainfall patterns, sea-level rise, and more intense storms, have profound effects on wastewater systems.

Wastewater treatment plants, designed for specific daily water volumes, face challenges during rapid stormwater influx. To prevent overwhelming the system, these plants may release untreated wastewater into the environment. With climate change leading to more frequent and intense rainstorms, the likelihood of untreated wastewater discharges on high-volume days increases.

The aftermath of extreme weather events exemplifies the havoc caused by the interaction of climate-related challenges and wastewater treatment limitations. Heavy rainfall during Sandy resulted in massive wastewater spills, with Washington experiencing a sewage overflow of 475 million gallons. Storm surges overwhelmed treatment facilities in various areas, causing plant failures and leading to a total of 11 billion gallons of untreated or partially treated wastewater flowing into water bodies and streets in the most affected states.

Climate change also poses a threat to septic systems, especially cesspools, which heavily rely on the surrounding soil for the removal of contaminants. As sea levels rise, groundwater in coastal areas may elevate, reducing the distance between septic systems and water sources and resulting in environmental contamination.

The vulnerability of septic systems is a global concern alone due to sea-level rise. Coastal regions with a high percentage of septic system usage, such as New England and Florida, face substantial challenges. Miami-Dade County, for instance, is already experiencing problems with 56% of households on septic systems, and this number is expected to rise to 64% by 2040. The destruction of coastal marshlands, vital for protecting communities from flooding, adds another layer to the environmental consequences of climate change on wastewater treatment.

Water and climate change are intricately connected, with the impacts of climate change manifesting through exacerbated floods, rising sea levels, shrinking ice fields, and the intensification of wildfires and droughts.

Yet, water itself can be a powerful tool in the fight against climate change. Sustainable water management plays a central role in enhancing the resilience of societies and ecosystems while simultaneously reducing carbon emissions. Every individual and household can contribute to this effort through their actions.

https://doi.org/10.36375/prepare_u.iiche.a415

In the accompanying images, Jiya and her seven-year-old daughter, Dipika, exhibit early symptoms of fluorosis. The installation of a solar De-fluoridation unit (DFU) plant by the Public Health Engineering Department, Government of Rajasthan, in their village (Sagwada) has provided them with sustained access to safe water. The Integrated Fluorosis Mitigation (IFM) approach, demonstrated by UNICEF, addresses areas with fluoride content exceeding 1.5mg per litre in drinking water. IFM focuses on ensuring a safe water supply through DFU units, providing calcium and vitamin C-rich food supplementation via anganwadi centers, and promoting kitchen gardens with market-friendly vitamin C-rich fruits and crops through horticultural and agricultural departments. This successful approach has been scaled up statewide by the Department of Health, Government of Rajasthan, through the National Program for Prevention and Control of Fluorosis (NPPCF) of the Ministry of Health, Government of India.

Explaining the issue, the link between water and climate change becomes evident. Extreme weather events are rendering water scarcer, more unpredictable, and more polluted, posing threats to sustainable development, biodiversity, and people's access to water and sanitation.

Flooding and rising sea levels contaminate land and water resources, damaging water and sanitation infrastructure. The rapid disappearance of glaciers, ice caps, and snow fields affects river systems, impacting freshwater regulation for large populations in lowland areas.

Droughts and wildfires destabilize communities, triggering unrest and migration. Destruction of vegetation exacerbates soil erosion, reducing groundwater recharge and increasing water scarcity and food insecurity.

The growing demand for water contributes to energy-intensive processes, degradation of carbon sinks like peatlands, and exacerbation of water scarcity through water-intensive agriculture.

The way forward involves placing water at the core of climate action plans. Sustainable water management aids adaptation to climate change by building resilience, protecting health, and mitigating climate change itself. Cooperation across borders is essential to balance water needs, and innovative financing for water resource management is crucial.

Sustainable, affordable, and scalable water solutions include improving carbon storage, protecting natural buffers like coastal mangroves, harvesting rainwater, adopting climate-smart agriculture, reusing wastewater, and harnessing groundwater sustainably. These strategies can attract investment, create jobs, and support governments in achieving water and climate goals.

Concerning climate change, water serves as both a valuable resource and a potential hazard. Its quality is fundamental for the well-being of the growing urban population and is indispensable for various economic activities, including peri-urban agriculture, food and beverage production, and industry. Nevertheless, extreme weather events such as excess precipitation or drought can pose hazards, leading to increased pollutant concentrations with adverse health effects, insufficient water flow for sewerage, and flood-related damage to physical assets.

Forecasts indicate future deficits in urban water supplies, impacting both availability and costs. Present decisions will significantly shape future water supply for industry, domestic use, and agriculture.

Major Findings:

- Climate change intensifies pressure on existing urban water systems, resulting in adverse effects on human health, economies, and the environment.
- Impacts encompass increased frequency of extreme weather events, large stormwater runoff volumes, rising sea levels, and alterations in surface water and groundwater.
- Urban water security, especially in lower-income countries, remains an ongoing challenge, with many cities struggling to provide basic services to residents, particularly those in informal settlements.
- As cities expand, demand for limited water resources will rise, compounded by the exacerbating effects of climate change.

- Water security challenges extend to peri-urban areas with acute resource pressure and overlapping governance issues.
- Existing governance systems often fail to adequately address climate change challenges due to a lack of coherent policy, limited technical capacity for adaptation planning, insufficient resources, coordination issues, and low political will and public interest.

Key Messages:

- Adaptation strategies for urban water resources must be tailored to each city based on local conditions, emphasizing the importance of understanding the local context.
- Acting promptly can minimize long-term negative impacts, with master planning anticipating changes over a timeframe exceeding fifty years.
- Finance and investment should prioritize low-regret options promoting water security and economic development, with flexible policies responsive to evolving information.
- Effective governance, coordination, and collaboration among various stakeholders and communities are crucial for adapting to changing climates.
- Cities should seek co-benefits in water management, considering low-carbon energy production and improved health through wastewater treatment.
- Investment strategies should employ life-cycle analysis, anaerobic reactors for energy conservation in wastewater treatment, avoidance of high-energy options where alternative sources exist, and the recovery of biogas produced by wastewater.

Identifying Risks: In the realm of wastewater treatment, biosolids management, and reuse operations, an unusual blend of warmer and drier summers poses challenges. The risk involves the potential for more extreme heat waves, dry spells, and increased drought risks, coupled with the complications of intensified rainfall events. Both extremes bring a spectrum of operational challenges, complicating the effects of climate change.

Assessing Vulnerability: Determining critical threshold levels for key influent and operating parameters during extremely dry and wet weather conditions is essential. The question arises: What conditions could lead to process failure without adaptive responses? Wastewater treatment, biosolids management, and reuse treatment plants are designed based on assumptions about flow rates, temperatures, and influent characteristics. With climate change, the increasing variability in the influent stream is a given, affecting various processes and potentially leading to anaerobic conditions and odor control issues.

Impact on Industrial Sources: These challenges extend to industrial sources, affecting both direct dischargers and those contributing waste to municipal wastewater systems. The additional operating challenges at municipal plants may influence future agreements regarding the timing and strength of waste flows into the system.

Anticipating Critical Thresholds: The changing landscape of operating conditions, characterized by more frequent dry spells and intense rainfall events, is already evident. However, the stochastic nature of these phenomena could result in more extreme events sooner than expected. While these impacts are gradually emerging, there is time to deploy adaptive responses.

Adapting to Challenges: To manage risks effectively, a vulnerability analysis of treatment, biosolids, and reuse facilities is crucial. Examining existing designs and operations helps identify weaknesses that could be stressed by sudden shifts in extreme operating conditions. Adapting to climate-induced challenges requires considering not only the process changes in wastewater treatment but also their potential impact on downstream biosolids and reuse facilities. Balancing the goals of water quality objectives and minimizing greenhouse gas emissions is a complex task that demands careful consideration.

Research Needs: To address these challenges, proposed research projects aim to quantify the magnitude of climate change impacts, develop new design and operating parameters for resilience, and comprehensively assess opportunities for optimization in wastewater treatment and resource recovery processes. These efforts highlight the importance of adapting to evolving climate conditions while minimizing environmental impacts.

https://doi.org/10.36375/prepare_u.iiche.a415

VIII. RESULTS

Let's break it down step by step:

Maintain and Restore Wetlands:

1. **Allow Coastal Wetlands to Migrate Inland:** This involves implementing setbacks, density restrictions, and land purchases to enable natural inland migration of coastal wetlands. It's a way to adapt to rising sea levels and changing coastal dynamics.
2. **Regional Sediment Management (RSM) Plan:** Developing a plan to manage sediment on a regional scale, ensuring the proper distribution and balance to support coastal ecosystems.
3. **Adaptive Stormwater Management Practices:** Promoting practices like natural buffers and proper culvert sizing to manage stormwater effectively, preventing erosion and habitat disruption.
4. **Rolling Easements:** Establishing easements that adapt to changing coastlines, allowing for flexibility in land use and protection.
5. **Identify and Protect Ecologically Significant Areas:** Recognizing and safeguarding critical areas such as nursery grounds, spawning grounds, and regions with high species diversity.
6. **Incorporate Wetland Protection into Infrastructure Planning:** Integrating wetland protection considerations into broader infrastructure planning processes, such as transportation and sewer utilities.

Maintain Sediment Transport:

1. **Preserve and Restore Vegetation in Coastal Ecosystems:** Ensuring the structural complexity and biodiversity of vegetation in tidal marshes, seagrass meadows, and mangroves are preserved and restored.
2. **Prohibit Hard Shore Protection:** Avoiding the use of hard protection methods to allow for natural coastal processes.
3. **Promote Wetland Accretion:** Introducing sediment to promote the growth and expansion of wetland areas.
4. **Remove Barriers to Tidal and Riverine Flow:** Removing dike structures to allow for natural tidal and riverine flow.
5. **Beach Nourishment and Groin Construction:** Adding sand to shorelines and constructing groins to manage sediment transport.

Preserve Coastal Land and Development:

1. **Permitting Rules for Hazardous Facilities:** Creating rules that restrict the location of landfills, hazardous waste dumps, and other potentially harmful facilities in vulnerable coastal areas.
2. **Consider Climate Change Impacts in Infrastructure Planning:** Integrating climate change considerations into the planning of new infrastructure.
3. **Integrated Coastal Zone Management (ICZM):** Adopting an integrated approach to achieve sustainability in coastal management.
4. **Land Acquisition and Exchange Programs:** Purchasing and exchanging coastal land for conservation purposes.
5. **Realignment of Engineering Structures:** Deliberately realigning structures affecting rivers, estuaries, and coastlines.

Use "Soft" Shoreline Maintenance:

1. **Composite Systems:** Integrating multiple methods like breakwater, sand fill, and vegetation to provide comprehensive shoreline protection.
2. **Create Dunes and Marshes:** Using natural features like dunes and marshes to stabilize coastlines.
3. **Increase Shoreline Setbacks:** Creating buffer zones between development and shorelines.
4. **Artificial Breakwaters and Planting Vegetation:** Installing structures and planting vegetation to dissipate wave action and protect shorelines.
5. **SAV (Sea Grass) Planting:** Stabilizing sediment and reducing erosion through the planting of sea grasses.

Use "Hard" Shoreline Maintenance:

1. **Fortify Dikes and Shorelines:** Strengthening dikes and shorelines through various methods like breakwaters, bulkheads, revetments, seawalls, and headland control.

Preserve Habitat:

1. **Adapt Protections of Important Zones:** Adjusting protections for critical habitats and biogeochemical zones as their locations change with climate.
2. **Connect Landscapes with Corridors:** Creating corridors to facilitate migrations and connectivity between landscapes.
3. **Design Estuaries with Dynamic Boundaries:** Adapting estuaries to have dynamic boundaries and buffers.
4. **Expand Planning Horizons:** Incorporating longer-term climate predictions into land use planning.
5. **Purchase Upland Development Rights:** Acquiring development rights in upland areas to protect them.
6. **Replicate Habitat Types:** Creating multiple areas with similar habitat types to spread risks associated with climate change.
7. **Retreat from Coastal Barriers:** Strategically retreating from and abandoning vulnerable coastal barriers.

Maintain Water Quality and Availability:

1. **Create Water Markets:** Transferring land and water from agricultural to community use through market mechanisms.
2. **Design New Coastal Drainage Systems:** Developing drainage systems that consider the coastal environment.
3. **Adaptive Stormwater Management Practices:** Implementing practices like removing impervious surfaces and replacing undersized culverts.
4. **Use Containment Areas:** Allocating and capping water withdrawal through containment areas.
5. **Incorporate Sea Level Rise into Infrastructure Planning:** Considering sea level rise in the planning of sewage systems and other infrastructure.
6. **Integrate Climate Change Scenarios into Water Supply Systems:** Incorporating climate change scenarios into the planning and management of water supply systems.
7. **Manage Water Demand:** Implementing measures such as water reuse, recycling, rainwater harvesting, and desalination to manage water demand.
8. **Plug Drainage Canals:** Preventing excessive drainage through the plugging of canals.

Use Integrated Water Resources Management (IWRM):

1. **Restore and Protect Ecosystems:** Prioritizing the restoration and protection of ecosystems, including fish and wildlife habitat.
2. **Increase Drinking Water Supply Reliability:** Enhancing the reliability of drinking water supply through coordinated management.
3. **Enhance Water Conservation:** Promoting measures to conserve water resources.
4. **Improve Storage and Use of Surface Water and Groundwater:** Managing the storage and utilization of both surface water and groundwater.
5. **Flood Hazard Mitigation:** Implementing measures to mitigate the risks of flooding.

Each of these strategies contributes to a comprehensive and adaptive approach to coastal and wetland management, considering the challenges posed by climate change and aiming for sustainable, resilient coastal ecosystems.

REFERENCES

[1] J. Hughes, K. Cowper-Heays, E. Olesson, R. Bell, A. Stroombergen, Impacts and implications of climate change on wastewater systems: A New Zealand perspective, Climate Risk Management (2020)

[2] Abbass, K., Qasim, M.Z., Song, H. *et al.* A review of the global climate change impacts, adaptation, and sustainable mitigation measures. *Environ Sci Pollut Res* **29**, 42539–42559 (2022).

[3] Impact of Climate changes.

[4] Hazardous Events.

https://doi.org/10.36375/prepare_u.iiche.a416

Optimization of Novel Symbiotic Bacteria in Algae Growth

Chelladurai Chellamboli[1*], Muthiah Perumalsamy[2], Udayar Kabil Dev[3]
[1] Research Scholar, Department of Chemical Engineering, National Institute of Technology, Tiruchirappalli, Tamil Nadu, India.

[2] Associate Professor, Department of Chemical Engineering, National Institute of Technology, Tiruchirappalli, Tamil Nadu, India.

[3]Student, Gnanamani College of Technology, Namakkal, Tamil Nadu, India

Corresponding author: Chelladurai Chellamboli, Department of Chemical Engineering, National Institute of Technology, Tiruchirappalli, Tamil Nadu, India. Email ID: c.chilambu@gmail.com, 9489799295

Abstract

In this study, a novel symbiotic bacterium (*Stenotrophomonas maltophilia)* was isolated from algae culture and cocultured with the abundant species *Chlorella pyrenoidosa* and *Scenedesmus abundans* in 3 N BBM+V medium under aseptic conditions. Furthermore, an optimization study was carried out to maximize the growth of the algae biomass. The independent parameters used to determine the bacterial inoculum concentration, pH of the medium, aeration rate of the culture system and other known parameters were temperature, light intensity, inoculum volume of algae and culture time. Thus, the effect of the bacterial inoculum concentration was studied by varying the concentration by 0, 2, 4, 6, 8 and 10%. The initial pH of the medium was changed by changing the medium pH via buffer solutions. The culture system aeration rate was the foremost important factor for determining the actual outcome of the product. Therefore, to determine the influence of the aeration rate in the system, different ranges of volumetric oxygen rates were tested: 90, 80, 70, 60, 50, 40, and 30%. The results showed that the optimal values for maximum biomass production were 8% bacterial inoculum concentration, 7% pH of the medium, and 90% aeration rate.

Keywords: Algae, *Chlorella pyrenoidosa*, *Scenedesmus abundans*, *Stenotrophomonas maltophilia*, Symbiotic, Lipid

https://doi.org/10.36375/prepare_u.iiche.a416

Introduction

The world's energy demand is currently the most important factor. Fossil fuels are typically used to meet this demand, but excessive use of these resources causes depletion and environmental problems. Evolving hazards from fossil fuel usage are one of the critical issues. However, the global energy demand has been satisfied by fossil fuels. The consumption of fossil fuel could continuously increase for global development, which was predicted in the global energy scenario in all yearly energy reports. Many remedies have been established to reduce fossil fuel emissions by monitoring and controlling emissions from industry and all powered vehicles and encouraging reforestation. This is a temporary solution, and moreover, several studies have reported that renewable energy can permanently overcome all these issues and suppress unsustainable energy usage. Additionally, greenhouse gas (GHG) emissions and global warming are causes of climate change (Hillet al. 2006). Renewable energy is identified as a sustainable energy source because of its greater benefits, because it fulfils the requirements of global energy demands, and because it is eco-friendly in nature and potentially carbon neutral (Demirbas 2009 and Hillet al. 2006).

A statistical review reported that the rate of world energy consumption from fossil fuel could decrease within 45 years (Rühl C 2008). Hence, there is a need to identify an alternative energy source for fossil fuel to reduce the excess shortages of petrol and diesel and minimize the hiking price of transport fuel. Several studies have shown that triacylglycerides (TAGs) are promising alternative energy sources for fossil fuels (Khan,et al., 2009). The production of biodiesel from biomass encourages the rural economy and is also eco-friendly in nature (Barnwal,et al., 2005). Hence, this research focused on the production of biofuel. Thus, roughly four energy generations have been established to harvest biofuel from food crops, nonfood crops, microorganisms, carbon capture and storage to meet those demands. Because it is easier to obtain and more effective than other sources for producing biofuel, extracting fuel from algae has garnered more attention than other types of extraction.

Microalgae are unicellular or multicellular photosynthetic microorganisms

with simple structures and multiple types of primary metabolites. Due to their simple structure, microalgae possess high potential. Generally, microalgae are composed of 6 to 52% proteins, 7 to 23% lipids, and 5 to 23% carbohydrates. Moreover, the protein content is relatively high in algae, which have a 10.2 C/N ratio. Studies have confirmed that certain algal species can stimulate 20−50% of the total TAG (TAG) in terms of cellular dry weight (Williams, et al., 2010). On the basis of algae cultivation, the open-pond microalgae cultivation system involves carbon dioxide (CO_2) utilization, which enriches the yield of biomass; e.g., one kilogram of dry algal biomass utilizes approximately 1.83 kg of CO_2 (Chisti 2007 and 2012).

There are numerous techniques developed in algae technology for biodiesel production. One of the available methodologies is to use a symbiotic bacterial technique for cultivating and producing algae for diesel. In general, natural ecosystems such as fresh and marine water ecosystems are partially occupied by microalgae. Even if these ecosystems are not in a purified condition, algae can still arise in natural ecosystems. An alga tends to cohabit with other microorganisms, and this technique is known as symbiosis culturing (Cole, 1982). Some microorganisms may lead to the suppression of algae growth through different functional parameters, such as physical or chemical factors. On the other hand, few organisms support each other through photosynthetic reactions. In this study, the growth of symbiotic algae–bacteria pairs was studied for biodiesel production. The basic concept encouraged by the symbiotic photosynthetic reaction is that the microalgae exhales oxygen to the environment and it inhales carbon dioxide in their life cycle process, whereas as the bacteria is having the behavior of liberating carbon dioxide into the surroundings and it consumes oxygen for their own cyclic activity (Munoz and Guieysse 2006). Therefore, a system is built to improve the interactions between both biosources, which results in improved cultivation.

In addition, algae produce hormones and organic and antibacterial components that are more useful for bacteria (Pratt et al. 1944). In industry, this method has been implemented in wastewater management and algae cultivation. However, many algae–bacteria interaction studies are theoretically based only. This study aimed to determine how to improve

the use of the symbiotic bacteria-algae technique for diesel fuel production. Generally, nutrients and changes in phosphate or nitrate concentrations promote algae growth. In this work, the symbiotic bacterium *Stenotrophomonas maltophilia*, which was isolated from an algal culture that was older than three months, was introduced. This particular species of bacteria strongly accelerates the growth of algae without requiring a long time. First, stable colonies were separated and subsequently subjected to algal growth; the most productive species was subsequently chosen, and its culture was identified via a molecular technique based on the 16S rRNA sequence.

Stenotrophomonas maltophilia belongs to the family *Xanthomonadaceae*. Formerly called *Pseudomonas maltophilia* or *Xanthomonas maltophilia, Stenotrophomonas maltophilia* is now recognized as the only species in the recently created genus *Stenotrophomonas*. On a range of bacteriological media, the nonfermentative gram-negative bacterium *Stenotrophomonas maltophilia* grows readily and is mostly found in the biosphere layer of the earth (Adegoke et al. 2017; Sherpa MT et al. 2020; Dunne et al. 1997). *Stenotrophomonas maltophilia* mostly infects humans, and other strains of this bacterium promote the growth of plants and the production of different proteins (Crossman et al. 2008; Jakobi et al. 1996; Sherpa et al. 2020). *Stenotrophomonas maltophilia* possesses a number of traits that make it potentially pathogenic, most notably, the capacity to secrete a broad variety of extracellular enzymes, including lipases, fibrolyses, and proteases, which may be crucial for colonization. Understanding the epidemiology of *Stenotrophomonas maltophilia* infection has improved the use of molecular typing systems (Gajdács et al. 2019; Brooke et al. 2021). Thus, *Stenotrophomonas maltophilia*, a kind of symbiotic bacterium, was identified from the algal culture.

An algal–bacteria symbiosis system has been used for natural purification systems in all water systems (Tang et al. 2016; Wang et al. 2008). Bacteria consume oxygen and release carbon dioxide (Munoz et al. 2003). However, in algae, carbon dioxide is utilized by microalgae, and oxygen is released into the environment or from water through photosynthetic activity (Muñoz and Guieysse, 2006). Hence, this alga–bacterium pair works

symbiotically. Therefore, a purified isolated symbiotic bacterial strain was sequentially coupled with different algal species to determine the symbiotic algae–bacteria growth behaviour for the production of biodiesel. Basically, algal cell division occurs through mitosis and meiosis until the end of nutrient starvation in the medium (Lodish et al. 2000, Chellamboli et al. 2014). In symbiotic technology, both algae and bacteria undergo mutualism, commensalism, and parasitism (Saravanan et al. 2021; Chia et al.2023). Numerous studies on the enhancement of algae growth, which may rely on artificial sources directly or indirectly, have been conducted, but the yield efficiency has not yet reached a level that is considered satisfactory. To address this restriction, a unique symbiotic bacterial strain was extracted from the algal culture, and its growth profile was examined in a variety of scenarios to produce biodiesel. Furthermore, the operating factors for algae cultured with symbiotic bacteria should be optimized.

Methodology

Preparation of symbiotic bacteria for the production of algae biodiesel

Initially, this study started with collecting samples/alga culture products after they had matured for three to four months. This algae culture was grown under nonaxenic conditions with good biomass production without additional nutrient supplementation or aeration. Therefore, to determine the culture status, the sample was checked for cross-contamination in the culture system. The microscopic analysis confirmed the presence of *Chlorella pyrenoidosa and Scenedesmus abundans* in the culture system. In addition, bacterial identification techniques such as the streak and pour plate methods were used to identify stable colonies that survived in the culture system. Several rounds of purification of two isolated pure colonies were carried out, and growth curves were plotted for the isolated colonies (white and yellow colonies), which had maximum absorbance values of 0.467 and 0.154, respectively, at 660 nm. Moreover, the isolated bacterial colonies were cocultured with a pure axenic culture of *Chlorella pyrenoidosa* and *Scenedesmus*.

This section focused on identifying the effects of independent parameters such as the bacterial inoculum concentration, the pH of the medium, and the aeration rate of the culture

system. Other known parameters, such as temperature, light intensity, inoculum volume of algae and culture time, were kept constant at 30°C, 13.5 μmoles/m^2/sec, 10% and 20 days for optimization studies. Thus, the effect of the bacterial inoculum concentration was studied by varying the concentration by 0, 2, 4, 6, 8 and 10%. Similarly, the initial pH of the medium varies from 4 to 9, and buffer solutions are used to vary the pH. The aeration rate of the culture system was the foremost important factor for determining the actual outcome of the product without the support of aeration, and it is difficult to establish cell divisions of bacteria as well as algae. Therefore, to determine the influence of the aeration rate in the system, different ranges of volumetric oxygen rates were tested: 90, 80, 70, 60, 50, 40, and 30%. Finally, the present study focused on the symbiotic bacterium *Stenotrophomonas maltophilia,* which was isolated from algae cultivation and subsequently used to increase the growth of algae.

Quantitative analysis

The most often employed techniques in this research are bacterial strain selection and screening, algal biomass quantification, cell disruption or pretreatment techniques, and lipid extraction. In addition, a detailed description of the analytical and quantification methods employed is provided. The obtained parameters were further optimized. Previously, the literature claimed that large-scale algae cultivation in open or closed reactors was carried out in well-equipped, established laboratories or industries; however, for initial investigations, Erlenmeyer flasks are adequate for establishing the necessary parameters, media, and other details.

Microbial isolation technique

Three techniques are available for the isolation of bacteria from culture. These methods include the streak, pour and spread plate methods (Erin R Sanders 2012). These three techniques were used for further study. Samples were withdrawn, and serial dilutions were performed. Several plating techniques have been used to identify stable organisms. Further isolated colonies were subjected to16S rRNA-based molecular analysis to determine the nomenclature of the bacteria**.**

Dry weight method

The gleaned cells were harvested from the culture system, and then, centrifugation was

performed to separate the algal cells from the solution at 5000 RPM for 10 min. The supernatant portion of the centrifuged culture was discarded, the precipitated or deposited algal cells were suspended in ammonium solution to wash out the residues, and the sample was subsequently dried at 104 °C for 24 hr to quantify the acquired biomass following **Eq. (1)**. (Chellamboli et al. 2014 and 2016).

$$\text{Dry weight of biomass} = \frac{[Finalweightofcrucible - Initialweightofcrucible]}{Culturevolume}\ \text{g/L} \quad (1)$$

Optical Density Method

The growth phases of the algal cultures were determined by measuring the absorbance at 660 nm with a UV-2600 Shimadzu, and the corresponding dry weight was calculated from the standard algal growth plot (Chellamboli et al. 2014 and 2016).

Lipid extraction

To determine the total lipid content in algae, several physical disruptions, such as osmotic shock treatment and solvent extraction processes, of intracellular activity were applied to isolate lipids from algae cells. The required amount of algal culture was harvested from the culture system subjected to ultrasonication at 25 kHz for 15 min at 25°C. The appropriate concentration of osmotic shock agent was applied to the aliquot culture by dissolving 0.1 g/ml NaCl in the cell culture mixture, followed by mixing n-hexane and methanol at a ratio of 7:3. The prepared sample was continuously shaken and incubated for 24 h at 100 RPM and 30°C. Furthermore, the sample was transferred to a separating funnel for phase separation. The upper layer was separated and consisted of n-hexane and dissolved lipid cells. The organic phase was removed to a preweighed crucible (W_1) and dried in a vacuum oven at 60°C for 24 h. Quantification of the mass of lipids was performed by calculating the difference between the initial weight (W_1) and the final weight of the dried lipid (W_2) via the formula given in **Eq. (2)** (Chellamboli et al. 2014 and 2016; GursongYoo et al. 2012).

$$\text{Lipid Yield (\%)} = \frac{weightofOilextracted}{weightofBiomass}\ x\ 100 \quad (2)$$

Results and Discussions

A pure bacterium was isolated, and symbiotic bacteria were identified for algae growth. Hence, the isolated symbiotic bacteria

were subjected to maternal culture by culturing pure *Stenotrophomonas maltophilia, Chlorella pyrenoidosa* and *Scenedesmus colonies* in nutrient broth (bacteria) and algae broth medium (algal species) under aseptic conditions. The prepared mother culture was used as a starter culture in the parameter optimization studies. The symbiotic bacteria were cocultured with algae in an enriched nutrient medium to satisfy the cell demand of both algae and bacterial cells, which were 3 N-BBM+V (bold basal medium supplemented with 3-fold nitrogen and vitamins). Therefore, this study also used 3 N-BBM+V media for the study of symbiotic bacteria and algae. Furthermore, optimization has been carried out for maximum growth of biomass production of microalgae in the presence of symbiotic bacteria (Guo and Tong, 2014).

Identification of symbiotic bacteria for algae growth

The growth of the symbiotic bacteria was carried out by measuring the optical density of the growth media at certain intervals (Krishnamurthy et al. 2021). Within 12 hours, the maximum ODs of white and yellow colonies were obtained, i.e., approximately 0.154 and 0.467, respectively. A lack of nutrients in the medium causes bacterial depletion, and the death phase was noted. The growth curves for both pure colonies are displayed in Fig. 1. A yellow colony was later chosen for further experimentation. The activity of symbiotic bacteria is required after twelve hours; this activity begins to support algae growth. In addition, two isolated algal colonies were cocultured. The outcomes of the experiment demonstrated that a yellow colony

https://doi.org/10.36375/prepare_u.iiche.a416

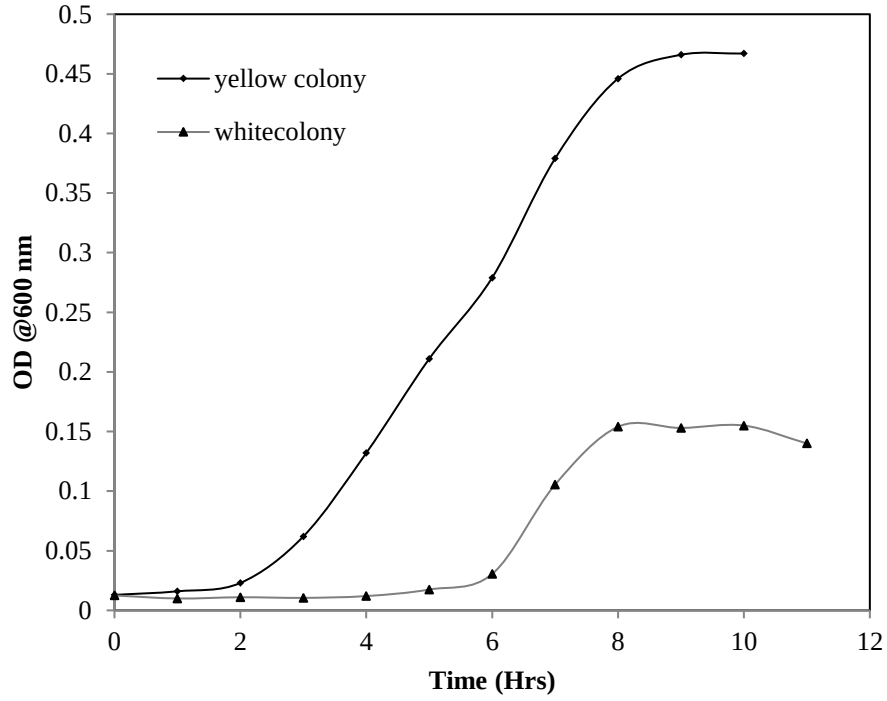

Fig. 1 Bacterial Growth curve for isolated species

bacterium improved the growth of the algal species. Thus, white colonies showed a non-supportive response to the growth of algae, which was neglected in the present study. Furthermore, gene sequence analysis was performed for the yellow bacteria that passed the screening.

Statistical analysis and optimization of the independent factors influencing the biomass and lipid production of symbiotic algae

Every experiment was carried out in triplicate, the data are presented as the average of three runs, and a P value of less than 0.05 indicates a significant effect. This study aimed to determine the operational conditions for the growth of algae supported by symbiotic bacteria. Therefore, symbiotic bacteria and algae coculture studies were initiated with media containing different inoculum (symbiotic bacteria) concentrations, aeration rates and initial pH values for mixed algae culture growth.

Dependence of pH on the production of biomass during algae-bacteria growth

When the initial pH of the nutrient medium was optimized, the growth response improved at pH values of 9, 7, and 5. The gradual progression of algal growth was

https://doi.org/10.36375/prepare_u.iiche.a416

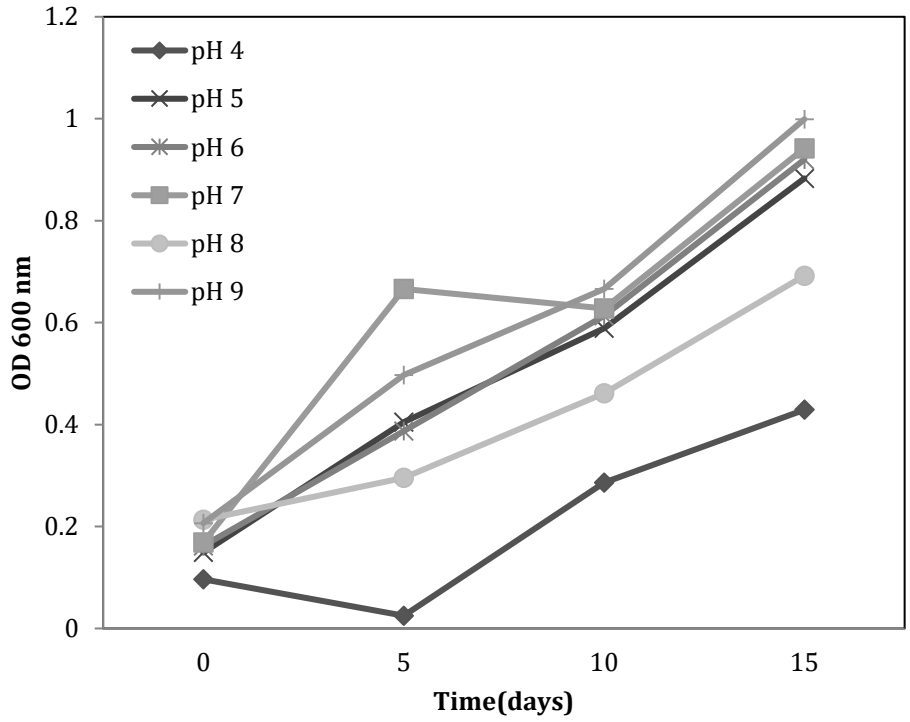

Fig.2 Growth responses of symbiotic bacteria and algae cultured in different pH

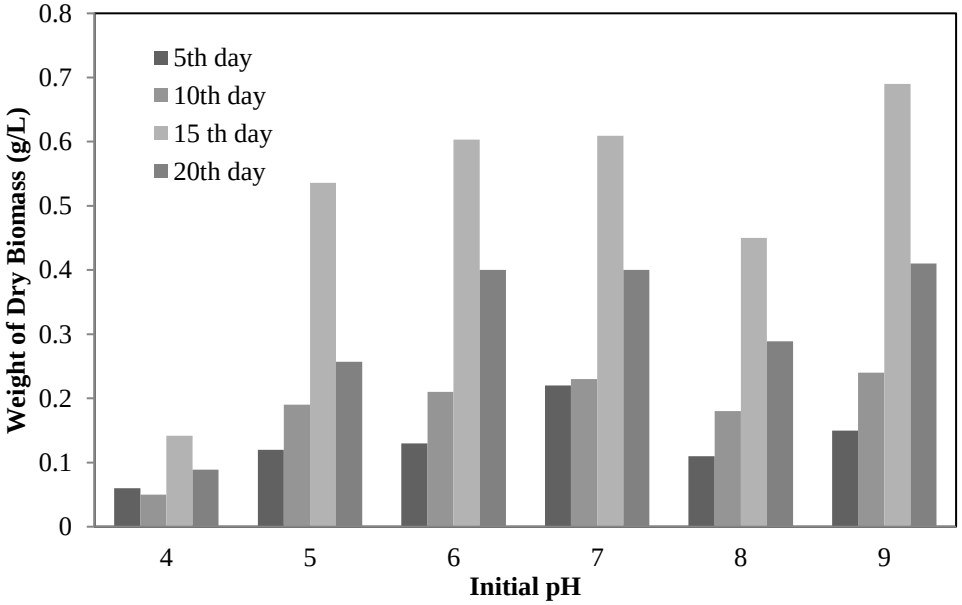

Fig.3 Effect of different initial pH of medium in biomass concentration of algae coculture with symbiotic bacteria

predicted by the optical density at 600 nm. The pH values of 4 and 8 gradually increase in the ranges shown in Fig. 2. The maximum dry biomasses obtained were 0.142, 0.536, 0.603, 0.609, 0.45, and 0.69 g/L for the 4, 5, 6, 7, 8 and 9 pH values, respectively, on the 15th day of the study, as shown in Fig. 3. An increase in pH has a positive effect on dry biomass, but

https://doi.org/10.36375/prepare_u.iiche.a416

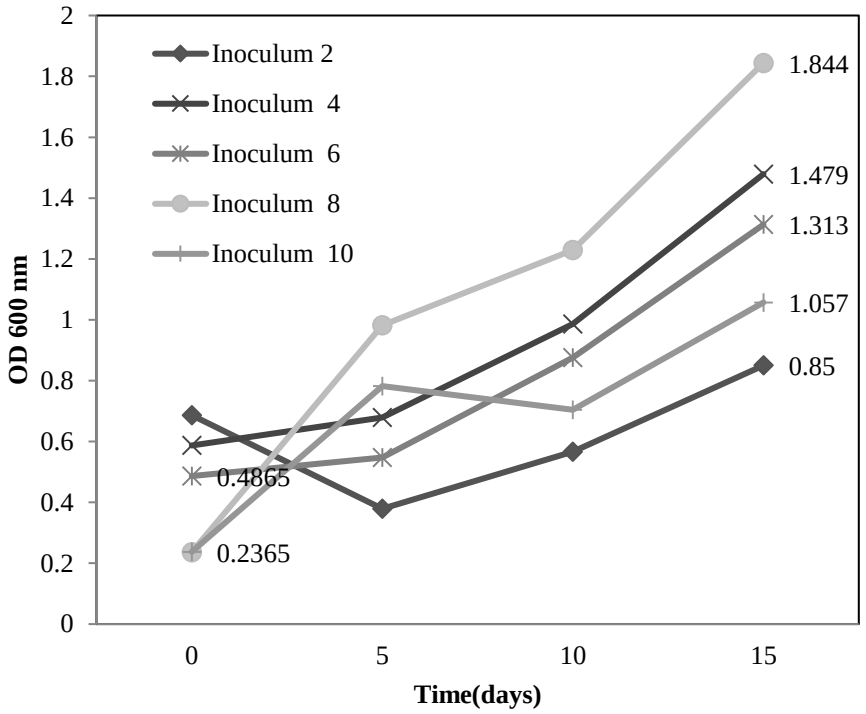

Fig.4 Growth response of mixed algae cultured inoculated in different ranges of bacterial concentration

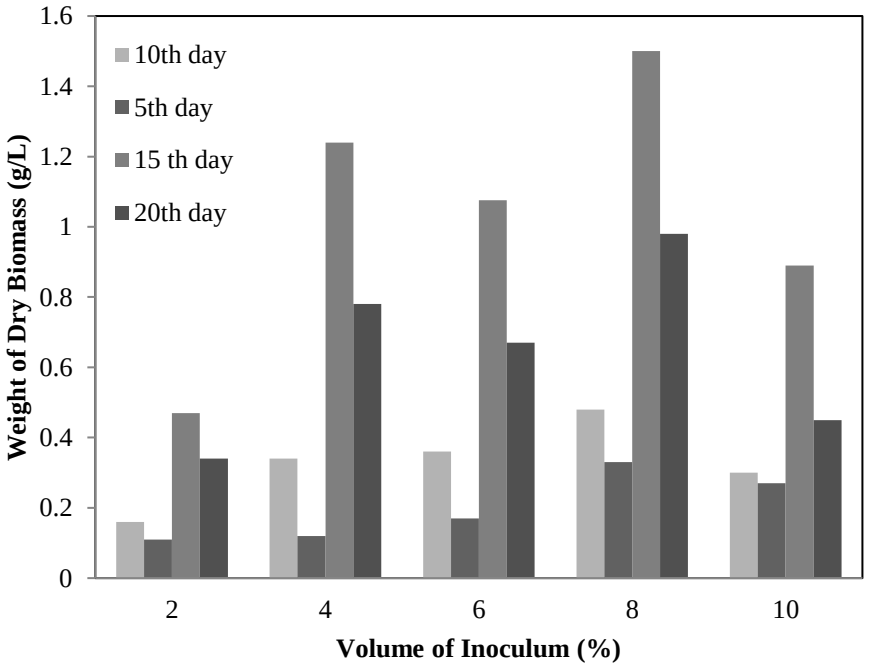

Fig.5 Effect of symbiotic bacteria in different inoculum concentration of algae biomass

a decrease in pH up to 9 results in the agglomeration or destruction of algae. For this reason, nutrient intake decreases, or the blockage of pores present in the cellular membrane acts as a hindering layer. Therefore, algae will be lost if the temperature is greater

than alkaline. In 2006, Travieso et al. reported that the highest algae biomass was 93–98 mg VSS_A/L d (37.2–39.2 g/m^2d) after cultivating algae-bacteria growth by utilizing wastewater. In 2022, Yu et al. reported that the maximum levels of NH^{4+}-N removal and algae growth were observed in cultures maintained at neutral pH 7-8. Conversely, the cultures kept below pH 8 showed better growth in terms of biomass. Therefore, pH plays a crucial role in the development of algae growth

Effect of inoculum concentration on the production of symbiotic bacteria and algae biomass

Fig. 4 shows the effect of different concentrations of bacterial inoculum on the growth of algae. Fig. 5 shows that an increase in the inoculum concentration of symbiotic bacteria did not increase the growth of algae beyond 10%. The inoculum concentrations of 2 and 10% bacteria fluctuated more strongly at the beginning of the experimental runs and later slowly increased the concentration of algae. Compared to the other treatments, 8% of the bacterial inoculum concentrations had a highly influential effect on the growth of algae from the first day onwards. The maximum dry biomass at 2, 4, 6, 8, and 10% inoculum concentrations for the symbiotic bacteria had responses of 0.47, 1.24, 1.076, 1.5, and 0.89 g/L of dry biomass, respectively, on the 15^{th} day of culture. A maximum dry biomass of 1.5 g/L was obtained at an inoculum concentration of 8%. Few bacteria may release algaecides during the growth phase while receiving signals from algae (Seyedsayamdostet al. 2011). Therefore, limiting bacteria was necessary for algae growth.

Effect of aeration rate on the production of biomass by symbiotic bacteria and algae

The effect of aeration rate on the growth of symbiotic bacteria has been studied. The maximum growth response occurred at 90 and 80% aeration, but the overpenetration of aeration in the algae culture led to evaporation or water loss. Therefore, the water loss must be controlled if a 90% aeration rate is used. The aeration rate will definitely improve the growth of algae, but due to the greater growth rate of bacteria, there will be a proliferation of plants utilizing nutrients. Additionally, the inhibition of algae growth may occur due to nutrient

https://doi.org/10.36375/prepare_u.iiche.a416

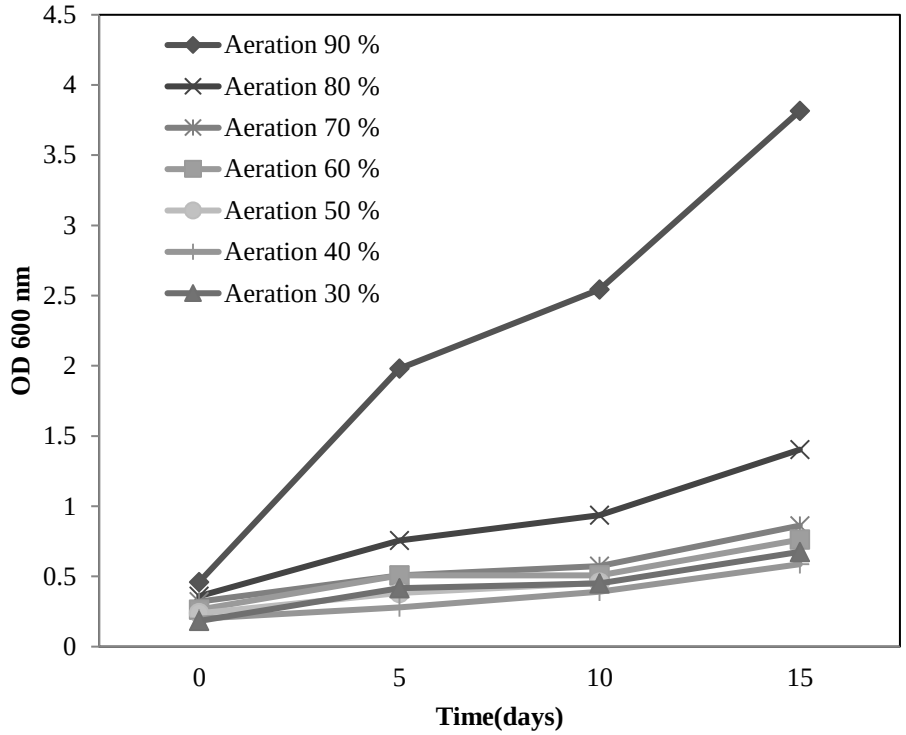

Fig. 6 Growth response of symbiotic bacteria and algae cultured in different aeration rate

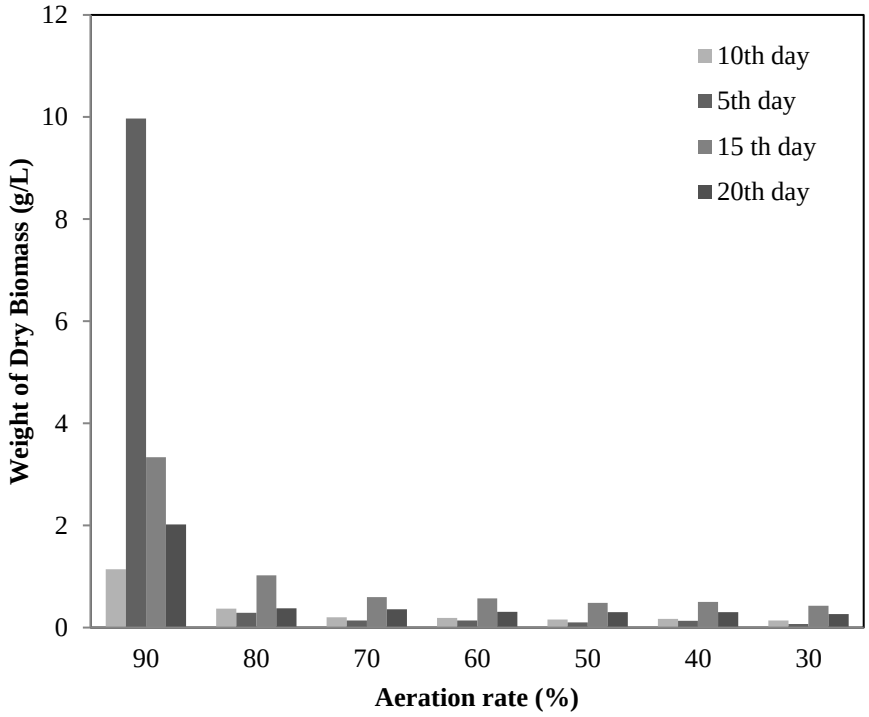

Fig.7 Impact of aeration rate in algae biomass coculture in symbiotic bacteria

shortages (Guo and Tong 2014). Hence, the study showed better growth development at a high aeration rate, as shown in Fig. 6. However, an increase in the aeration rate simultaneously increased the growth of the algae culture. Aeration at a rate < 60% was associated with

decreased growth compared to the other treatments. With different aeration rates, maximum biomass concentrations of 9.97 and 3.34 g/L were obtained for 90% aeration rates on the 5th and 15th days of culture, respectively, as shown in Fig. 7. The results were compared with those of algae culture with a minimum aeration rate of 30%, which produced a biomass of 0.43 g/L on the 15th day. In 2016, Tang reported that the most favorable aeration rate occurred within the reduction range to support the culture system.

Growth response of *Stenotrophomonas maltophilia* cultured with different combinations of algae

Furthermore, algal growth was affected by the culture treatment. The maximum and best growth response was observed for *Chlorella pyrenoidosa* cocultured with *Stenotrophomonas maltophilia*. Similarly, a better growth response was obtained in mixed algae coculture with symbiotic bacteria. Individually growing symbiotic bacteria were considered controls in this investigation. Compared to those of *Stenotrophomonas maltophilia, the growth of Chlorella pyrenoidosa*+ *Stenotrophomonas maltophilia, Scenedesmus abundans*+ *Stenotrophomonas maltophilia* and mixed algae + *Stenotrophomonas maltophilia* was 6.3, 3.54, and 5.04-fold greater, respectively, as shown in Fig. 8. A positive response was detected at biomass concentrations of 0.154, 0.43, 0.8, and 0.637 g/L for *Stenotrophomonas maltophilia, Chlorella pyrenoidosa* cocultured with *Stenotrophomonas maltophilia, Scenedesmus abundans* cocultured with *Stenotrophomonas maltophilia* and mixed algae cocultured with *Stenotrophomonas maltophilia* obtained on the 15th day of culture, respectively. After the 15th day, the growth of the algae decreased, as shown in Fig. 9. The biomass concentrations of *Chlorella pyrenoidosa* + *Stenotrophomonas maltophilia, Scenedesmus abundans*+ *Stenotrophomonas maltophilia* and mixed algae + *Stenotrophomonas maltophilia* were 2.79-, 5.19-, and 4.13-fold greater, respectively. There is evidence that more biomass was produced by *Scenedesmus abundans* cocultured with *Stenotrophomonas maltophilia.*

Effect of the symbiotic bacteria concentration on the lipid yield of the algae

https://doi.org/10.36375/prepare_u.iiche.a416

The effect of inoculum concentration on the lipid yield of the different cultures is shown in Fig. 10. Studies have shown that the maximum lipid concentration occurs within 8% of the inoculum concentration of symbiotic bacteria. Five different concentrations of inoculums taken at concentrations ranging from2, 4, 6, 8, and 10% were assessed for different cultivation combinations maintained in aseptic environments, and the study was carried out for 15 days. The results showed good biomass and lipid yields at an8% inoculum concentration. Increasing the symbiotic bacteria inoculum concentration led to better growth of the algae, but at a10% inoculum concentration, it resulted in a lower percentage of lipids. Moreover, the results showed that the influence of a high range of symbiotic bacteria concentrations leads to the over exhaustion of nutrient media, and a stressful environment will be encountered by bacteria and algae cells. Even a very small amount of incocula will not have lipid production due to insufficient inoculum cells. (Mohamed H et al. 2022)

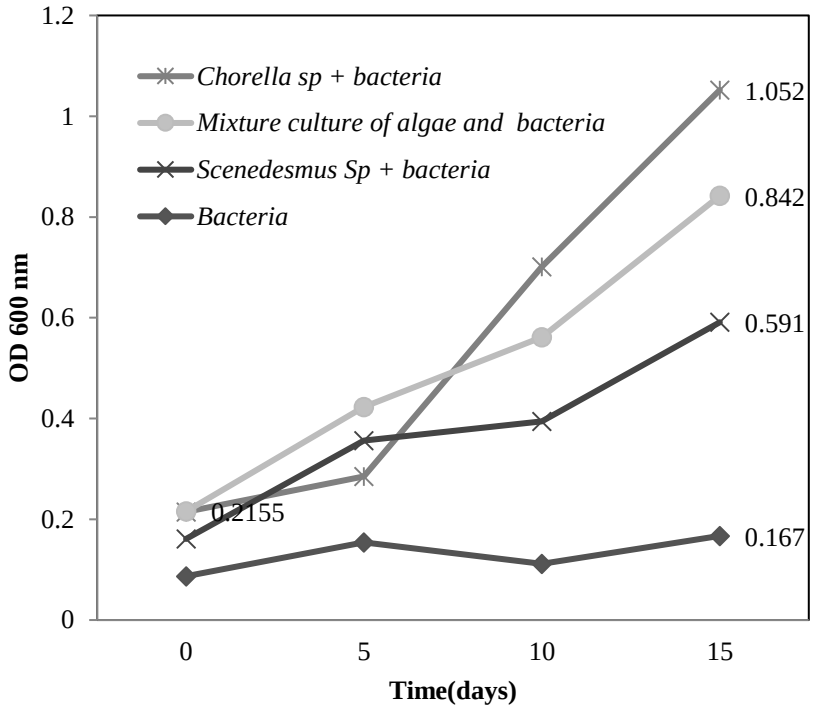

Fig.8 Growth response of different treatments i.e., *S. maltophilia, C. pyrenoidosa+ S. maltophilia, S. abundans+ S. maltophilia* and mixed algae + Symbiotic bacteria

https://doi.org/10.36375/prepare_u.iiche.a416

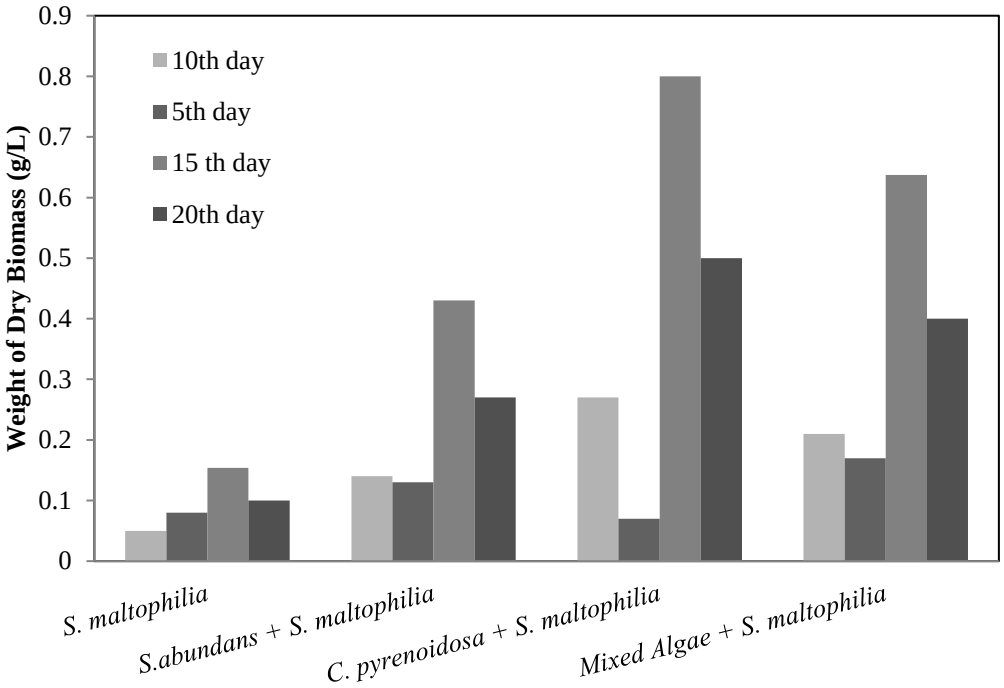

Fig.9 Influence of different treatment conditions such as *S. maltophilia, C. pyrenoidosa+ S. maltophilia, S. abundans+ S. maltophilia* and mixed algae + Symbiotic bacteria in biomass concentration

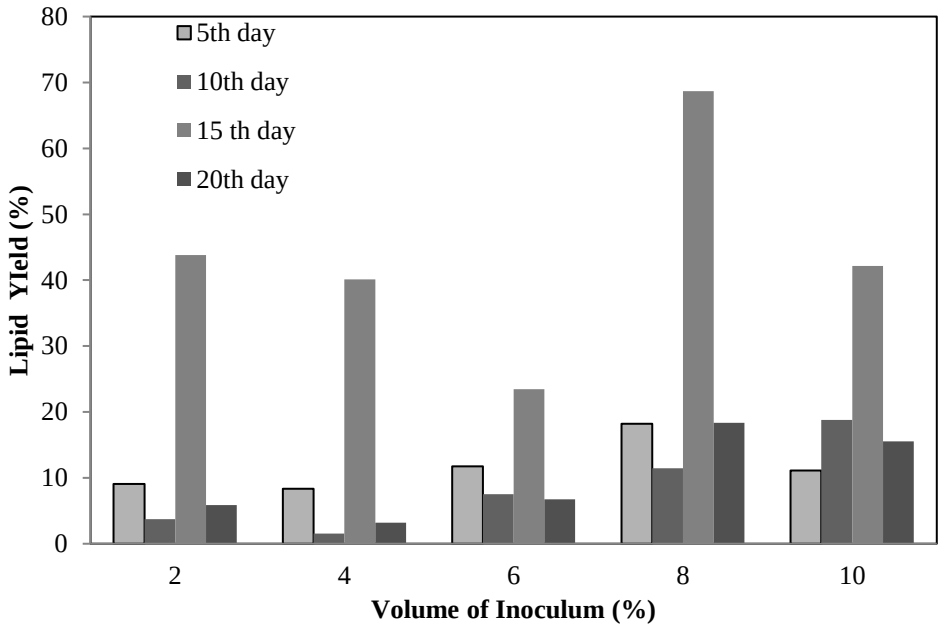

Fig.10 Stimulus of different inoculum (symbiotic bacteria) concentration in Lipid production

Response of lipid production during the growth of algae and symbiotic bacteria to varying pH values

After cultivation, the algae were cocultured with symbiotic bacteria at pH values ranging from 4 to 9 and incubated at 30 °C for 15 days, and the maximum lipid yields obtained

were 5.88±0.5, 47.71±0.9, 31.9±1.5, 48.59±1.0, 61.05±1.1, and 26.9±0.9% for the 4, 5, 6, 7, 8, and 9 pH groups, respectively, on the 15th day of culture, as shown in Fig. 11. The maximum lipid yield was attained at pH 8.

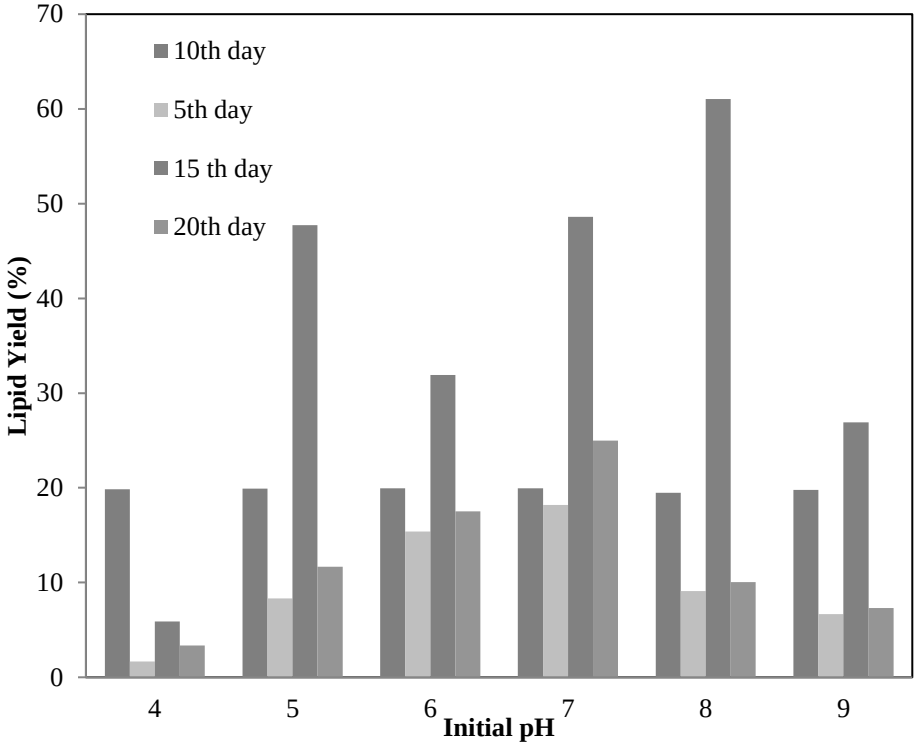

Fig.11 Effect of different initial pH in lipid production occurs in cocultured algae and symbiotic bacterial

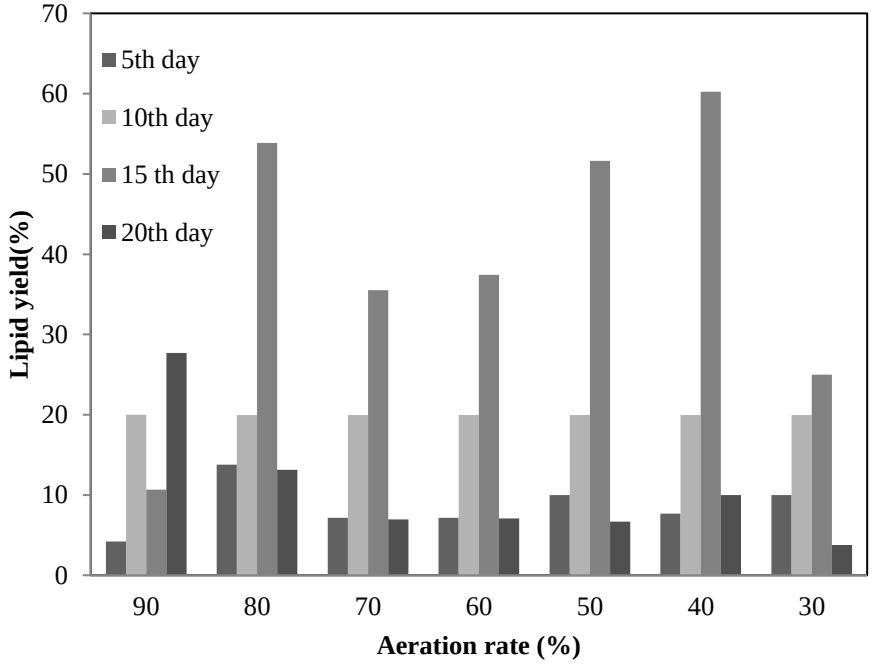

Fig.12 Influence of different aeration rate in lipid production for cocultured algae and symbiotic bacteria

https://doi.org/10.36375/prepare_u.iiche.a416

Influence of aeration rate on lipid production in symbiotic bacteria and algae

The effect of aeration rate on lipid yield in different cultures is shown in Fig. 12. A maximum lipid yield of 60.26% was observed at 40% aeration, i.e., 90, 80, 70, 60, 50, 40 and 30% aeration had 10.65±0.86, 53.85±0.56, 35.51±0.72, 37.41±0.58, 51.61±0.14, 60.26± 1.4 and 25±1.02%, respectively. Mostly, all culture systems require space for cell division and agitation to ensure a proper respiration rate and avoid agglomeration of microorganisms and algae cells. In the culture system, a basic range of 3/4th of the volume of the nutrient will be considered. A 40% decrease in aeration rate results in the maximum production of algal lipids. However, the maximum range of aeration rates results in an increase in the evaporation rate of nutrients from the system. Therefore, an excess aeration rate results in exhaustion of the liquid medium because the cells reach the death phase.

Impact of culture of *Stenotrophomonas maltophilia* on different algae cultures

The maximum lipid yields obtained from *Stenotrophomonas maltophilia, Chlorella pyrenoidosa*+ *Stenotrophomonas maltophilia, Scenedesmus abundans*+ *Stenotrophomonas maltophilia* and mixed algae + *Stenotrophomonas maltophilia* were 19.84±1.9, 40.32±1.13, 35.29±0.89, and 47.69%±1.68, respectively. *Chlorella pyrenoidosa*+ *Stenotrophomonas maltophilia, Scenedesmus abundans*+ *Stenotrophomonas maltophilia* and mixed algae + *Stenotrophomonas maltophilia* had better lipid yields for the different treatments, as shown in Fig. 13. From the study, it was concluded that the optimal concentration of 8% of the bacterial inoculum, pH 7 of the medium, and 90% aeration rate produced the maximum lipid yield.

https://doi.org/10.36375/prepare_u.iiche.a416

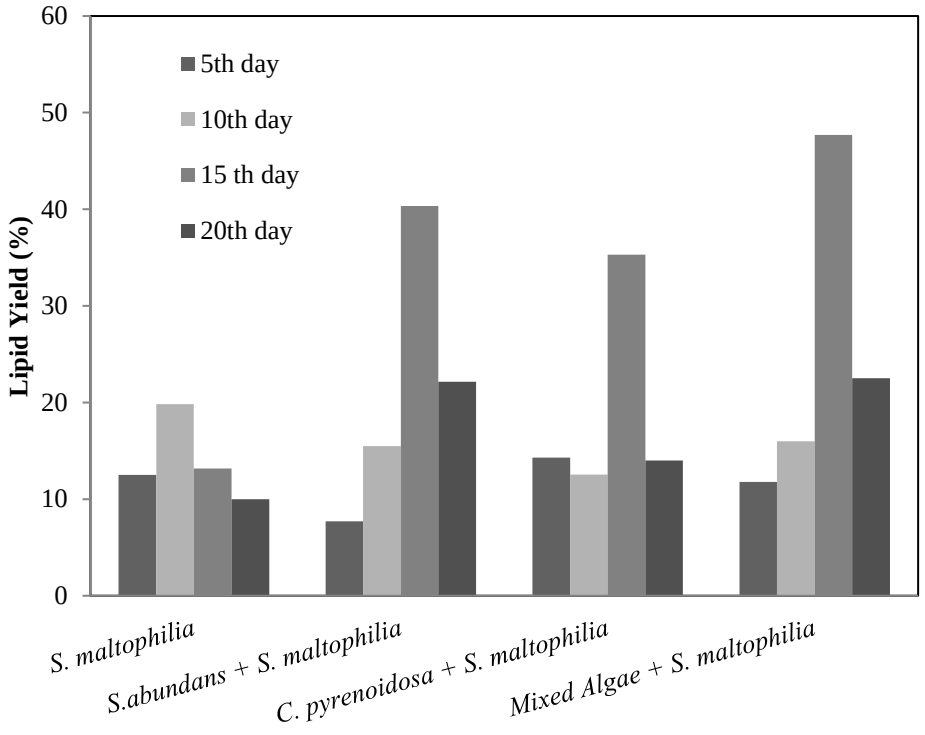

Fig.13 Response of different treatment conditions such as *S. maltophilia, C. pyrenoidosa+ S. maltophilia, S. abundans + S. maltophilia* and mixed algae + *S. maltophilia* in lipid production of biodiesel

Conclusion

Therefore, when *Stenotrophomonas maltophilia* was isolated and coupled with algae, better growth development was shown in the algae cells by symbiotic techniques. Different algal species were treated with symbiotic bacteria for biodiesel production. In this study, the culture conditions were optimized by varying the inoculum concentration of the symbiotic bacteria from 2 to 10%, the pH from 4 to 9 and the 30 to 30% (v/v) aeration rate. The results showed that the maximum lipid yield was obtained at an 8% bacterial inoculum concentration, a medium pH of 7, and a 90% aeration rate. Lipid production was obtained from different treatments, such as cultivation of *Stenotrophomonas maltophilia, Chlorella pyrenoidosa* + symbiotic bacteria, and *Scenedesmus abundans* + symbiotic bacteria, and from mixed cultures of both *Chlorella pyrenoidosa* and *Scenedesmus abundans* with symbiotic bacteria. Lipid yields of 13.16, 40.32, 35.29, and 47.69% were obtained for *Stenotrophomonas maltophilia, Chlorella pyrenoidosa* + symbiotic bacteria, *Scenedesmus abundans* + symbiotic bacteria and mixed cultures of both species with symbiotic bacteria, respectively.

https://doi.org/10.36375/prepare_u.iiche.a416

Acknowledgements

The authors are grateful to the National Institute of Technology, Trichy, for providing the necessary funds and facilities to carry out this research.

Author details

[1]Dr. C. Chellamboli, [2]Dr. M. Perumalsamy, [3]Udayar Kabil Dev, Bioseparation lab, Department of Chemical Engineering, National Institute of Technology, Tiruchirappalli – 620015, Tamil Nadu, India. Tel: 9489799295; Fax: +91-431-2500133; email:c.chilambu@gmail.com. The electronic supplementary information (ESI) is available: [The native format of the figures has also been uploaded].

References

Adegoke AA, Stenström TA, Okoh AI (2017) *Stenotrophomonas maltophilia* as an Emerging Ubiquitous Pathogen: Looking beyond Contemporary Antibiotic Therapy. Front. Microbiol 8: 2276.

Barnwal BK, Sharma MP (2005) Prospects of biodiesel production from vegetable oils in India. Renew Sust Energ Rev 9:363-398.

Brooke JS (2021) Advances in the Microbiology of *Stenotrophomonas maltophilia*. Clin. Microbiol. Rev 34: e0003019

Chellamboli C, Perumalsamy M (2014) Application of response surface methodology for optimization of growth and lipids in Scenedesmus abundans using batch culture system. RSC Advances 4 (42): 22129-2214.

Chellamboli C, Perumalsamy M (2016) Synergistic Effect of Hormones and Biosolids on Scenedesmus abundans for Eliciting Total Biolipids. Water Environment Research 88 (11): 2180-2190.

Chia SR, Ling Jing, Chia Wen Yi, Nomanbhay Saifuddin, Kurniawan Tonni Agustiono, Chew Kit Wayne (2023) Future bioenergy source by microalgae–bacteria consortia: a circular economy approach. Green Chem 25(22):8935-8949.

Chisti Y (2007) Biodiesel from microalgae. Biotech. Adv 25:294-306.

Chisti Y (2012) Raceways-based production of algal crude oil. In: Posten, C., Walter, C. (Eds.), Microalgal Biotechnology: Potential and Production. deGruyter, Berlin 113-146.

Cole JJ (1982) Interactions between bacteria and algae in aquatic ecosystems. Annu. Rev. Ecol. Evol. Syst 13: 291-314.

Crossman LC, Gould VC, Dow JM et al (2008) The complete genome, compar- ative and functional analysis of *Stenotrophomonas maltophilia* reveals an organism heavily shielded by drug resistance determinants. Genome Biol 9 (40), R74. https://doi.org/10.1186/gb-2008-9-4-r74.

Demirbas A (2009) Progress and recent trends in biodiesel fuels. Energy Convers Manage 50:14-34.

Dunne C, Crowley JJ, Moenne-Loccoz Y et al (1997) Biological control of pythiumultimum by *Stenotrophomonas maltophilia* W81 is mediated by an extracellular proteolytic activity. Microbiology 143:3921–3931. https://doi.org/10.1099/00221287-143-12-3921.

Gajdács M, Urbán E (2019) Prevalence and Antibiotic Resistance of *Stenotrophomonas maltophilia* in Respiratory Tract Samples: A 10-Year Epidemiological Snapshot.Health Serv. Res. Manag. Epidemiol 6:2333392819870774.

Guo Z, Yen Wah Tong (2014) The interactions between *Chlorella vulgaris* and algal symbiotic bacteria under photoautotrophic and photo heterotrophic conditions, *J Appl Phycol.*, 26(3), 1483-1492.

GursongYoo, Won-Kun Park, ChulWoong Kim, Yoon E Choi, Ji Won Yang (2012) Direct lipid extraction from wet *Chlamydomonas reinhardtii* biomass using osmotic shock. Bioresource Technology 123:717–722.

GursongYoo, Won-Kun Park, ChulWoong Kim, Yoon-E Choi, Ji-Won Yang (2012) Direct lipid extraction from wet *Chlamydomonasreinhardtii* biomass using osmotic shock. Bioresource Technology 123:717–722.

Hill J, Nelson E, Tilman D, Polasky S, Tiffany D (2006) Environmental, economic, and energetic costs and benefits of biodiesel and ethanol biofuels. *Proc. Natl Acad. Sci*., (USA), 103:11206-11210.

Jakobi M, Winkelmann G, Kaiser D et al (1996) Maltophilin: a new antifungal com- pound produced by *Stenotrophomonas maltophilia* R3089. J. Antibiot. (Tokyo) 49 (11):1101–1104 https://doi.org/10.7164/antibiotics.49.1101 .

Khan MS, Zaidi A, Wani PA, Ahemad M, Oves M (2009) Functional diversity among plant growth-promoting rhizobacteria. In: Khan MS, Zaidi A, Musarrat J (eds) Microbial strategies

for crop improvement. Springer, Berlin, 105-132.

Lodish H, Berk A, Zipursky SL et al (2000) Molecular CellBiology., 4th edn. W. H. Freeman, New York.

Mohamed H, Awad MF, Shah AM, Sadaqat B, Nazir Y, Naz T, Yang W, Song Y (2022) Coculturing of Mucor plumbeus and *Bacillus subtilis* bacterium as an efficient fermentation strategy to enhance fungal lipid and gamma-linolenic acid (GLA) production. Sci Rep. 2022 Jul 30;12(1):13111. doi: 10.1038/s41598-022-17442-2. PMID: 35908106; PMCID: PMC9338991

Munoz R, Guieysse B (2006) Algal-Bacterial Processes for the Treatment of Hazardous Contaminants: A Review. Water Res, 40:2799-2815.

Munoz R., Guieysse B, Mattiasson B. (2003) Phenanthrene biodegradation by an algal-bacterial consortium in two-phase partitioning bioreactors.Applied microbiology and biotechnology 61: 261-267.

Tang CC, Wei Zuo, Yu Tian, Ni Sun, Zhen-Wei Wang, Jun Zhang (2016) Effect of aeration rate on performance and stability of algal-bacterial symbiosis system to treat domestic wastewater in sequencing batch reactors. Bioresource Technology 222: 156-164.

Pratt R, Daniel TC, Eier JB, Gunnison JB et al (1944) Chlorellin. An antibacterial substance from Chlorella. Science 99:351-352.

Rühl C (2008) Bp statistical review of world energy. London*: BP*.

Sanders ER (2012) Aseptic Laboratory Techniques: Plating Methods. J Vis Exp (63):3064.

Saravanan, Senthil Kumar P, Sunita Varjani, Jeevanantham S, Yaashikaa PR, Thamarai P, Abirami B, Cynthia Susan George (2021) A review on algal-bacterial symbiotic system for effective treatment of wastewater. Chemosphere 271:129540.

Seyedsayamdost MR, Case RJ, Kolter R, Clardy J (2011) The Jekyll-and-Hyde chemistry of *Phaeobacter gallaeciensis*. Nat. Chem 3:331-335.

Sherpa MT, Sayak Das, IshfaqNabi Najar, Nagendra Thakur (2020) Draft genome sequence of *Stenotrophomonas maltophilia* strain P13 gives insight into its protease production and assessment of sulfur and nitrogen metabolism. Current Research in Microbial Sciences 2:100012

https://doi.org/10.36375/prepare_u.iiche.a416

Travieso L, Benítez F, Sánchez E, Borja R, Colmenarejo MF (2006) Production of Biomass (Algae-Bacteria) by Using a Mixture of Settled Swine and Sewage as Substrate. Journal of Environmental Science and Health, Part a, Toxic/Hazardous Substances and Environmental Engineering 41(3): 415-429.

Wang J, Zhang X, Chen Y, Sommerfeld M, Hu Q, (2008). Toxicity assessment of manufactured nanomaterials using the unicellular green alga Chlamydomonas reinhardtii.Chemosphere, *73*(7):1121-1128.

Williams PJB, Laurens LM (2010) Microalgae as biodiesel & biomass feedstocks: Review & analysis of the biochemistry, energetics & economics. Energ & Environ Sci 3(5):554-590.

Yu H, Kim J, Rhee C, Shin J, Shin SG Lee C (2022) Effects of Different pH Control Strategies on Microalgae Cultivation and Nutrient Removal from Anaerobic Digestion Effluent.Microorganisms 10*:*357.

https://doi.org/10.36375/prepare_u.iiche.a417

Effects of Indoor Plants on Occupants' Perceptions of Indoor Climate, Sick Building Syndrome (SBS), Emotional State, Self-Assessed Performance, and Overall Space Satisfaction: A Systematic Review

Mukesh Budaniya[a*] and Mani Sankar Dasgupta[a]
[1]Department of Mechanical Engineering, BITS Pilani, Pilani, 333031, India
*Email: mukesh.budaniyai@pilani.bits-pilani.ac.in

Abstract

This systematic review analyses the impact of indoor plants on various aspects of indoor environments and occupants' perceptions using bibliometric tools. The use of tool helps in identification, classification, and trend of research related to indoor plants effect on occupants' perception based on published manuscripts. Analysis brings out that a prominent number and quality publications from various research groups have offered evidence that indoor plants can have prominent impact on feelings of emotional states, self-assessed performance, and overall space satisfaction, as well as the impression of indoor climate. The published works encompassed scholarly articles, empirical studies, and surveys that examined the influence of indoor plants. However, some studies similarly did not find any benefits. While some others recommend careful consideration before placing indoor plant because doing so occupies functional space, require initial investment, augment maintenance cost, and also poses challenges with increased humidity, allergens, and the plants' own emission of volatile organic compounds. As a result, choosing to bring indoor plants require careful consideration. The corpus of research on the benefits of indoor plants for interior spaces and occupant perceptions is still lacking in conclusion. A few well-designed studies have been done to look at the effects of indoor plants on occupants in terms of temperature comfort, perception of air quality, sick building syndrome, emotional state, and task performance. To fully understand the impact of indoor plants on interior settings and occupant well-being, more research is necessary and a direction for future research is established through this manuscript using advanced analytical tools.

Keywords: *Indoor plants, bibliometry, air quality, thermal comfort, aesthetics, lighting, noise, Sick Building Syndrome (SBS), emotional state, performance.*

1. Introduction

The indoor environment quality (IEQ) is an major concern for the scientific community because people spend over 80–90% of their life indoors [1]. Numerous factors contribute to shaping the indoor environment within a building, such as indoor air quality (IAQ), thermal comfort, lighting, noise levels, etc.

In pursuit of a sustainable way to enhance the quality of the interior environment, researchers opted for a variety of indoor plants. Their explorations primarily centred around extensive studies probing the phytoremediation (plants use clean up polluted air) effects of plants, specifically targeting the reduction of particulate matter (PM) levels [2–7] and total volatile organic compounds (TVOCs). Commencing with closed chamber experiments in controlled environments [8–14], these studies subsequently transitioned into real-world settings [15–18]. However, the initial findings regarding the efficacy of passive potted plants towards reducing both PM and VOCs were

not promising [19,20]. Researchers inferred that achieving notable effects would necessitate a much larger quantity of plants within the indoor space.

To address this challenge of scale, researchers turned their attention to the concept of creating green walls [21]. This innovative approach presented the possibility of accommodating high number of plants that are an order of magnitude larger than what room floor can accommodate. Nevertheless, the implementation of green walls is notably more complicated than the straightforward placement of potted plants [22–24]. It involves a complex setup encompassing various elements such as regular monitoring, irrigation systems, structural support, and they often demand specialized knowledge or training. Moreover, researchers intended the integration of active airflow through these green walls to enhance their efficacy [25–27]. This necessitated the installation of fans alongside the green wall structure, further adding to the complexity of the setup and maintenance.

Lohr et al. [28] used hanging plants also and assessed productivity and stress level in presence and absence of plants and many later scholars have sought to understand their perceived benefits across various dimensions like indoor climate [29–34], sick building syndrome (SBS), emotional state [35–37], self-assessed performance [28,30,34,37,38], and overall space satisfaction. While reviewing the existing studies Bringslimark et al. [39] reported inconsistency in results in the aspects of benefits of indoor plants. Additionally, Han et al. [40] noted in their review that the most prominent effects of indoor plants on participants include heightened positive emotions and diminished negative feelings, with a subsequent reduction in physical discomfort. Further, work by Lee Bak Yeo [41] provide important insights regarding selection of indoor plant species keeping psychological and physiological benefits of plants.

The authors have not come across any recent review paper that has provided a comprehensive analysis of existing studies that proposed a holistic methodology for future researchers to adopt in order to achieve consistent and impartial outcomes. To address this research gap, we conducted a systematic review of available English articles focusing on the effects of indoor plants on occupants' comfort and psychological well-being. Standard bibliometric approaches are employed to comprehensively analyse high-quality journal papers that investigate the integration of indoor plants into indoor settings.

The objective of this review are to:

- Identify the key findings and trends in the literature related to the effects of indoor plants on indoor climate, occupant perceptions, and well-being.
- Critically evaluate the strengths and limitations of existing studies, addressing conflicting results and gaps in the current knowledge.

2. Methodology

To ensure a critical review of the existing literature, we employed a systematic approach to keyword selection. Our search strategy encompassed a range of terms related to occupant perception, indoor climate, and the influence of indoor plants. The keywords included: occupant perception, indoor climate, indoor air quality, thermal comfort, aesthetics, privacy, noise, Sick Building Syndrome (SBS), emotional state, and indoor plants. This broad selection is aimed at capturing a diverse area of the research landscape and facilitate an in-depth bibliometric analysis.

Based on these keywords we gathered a total 1467 articles from various database sources like Web of Science (WoS) and Scoups reported in the past four decades ranged from 1980 to 2023, after removing 315 duplicate articles. Using these collected articles, we generated the density keyword plot (Figure 1) using VOS viewer [42] served as a visual representation of

https://doi.org/10.36375/prepare_u.iiche.a417

the prevalence and interconnectedness of these keywords, providing insights into the landscape of existing literature.

Observations from the density plot highlighted the inclusion of studies related to phytoremediation, green walls, online surveys, photosynthesis, plant growth, biological control, medical research, bacteria, and also other topics beyond our intended scope. Recognizing the importance of refining our dataset for a more targeted review, we systematically excluded these undesirable papers from our analysis. This process ensured that the remaining articles aligned closely with the key theme of our investigation. Refer to figure 2 for a visual representation of the collecting and screening process.

The final selection include 20 articles, and was based on stringent inclusion criteria, including studies conducted with potted plants in laboratory or field settings, the presence of both control and treatment experiments, and a specific focus on indoor potted plants' effects on occupants' perceptions of their indoor environment and well-being. This selection criteria is aimed at ensuring the relevance, quality, and alignment of the chosen studies with our research objectives.

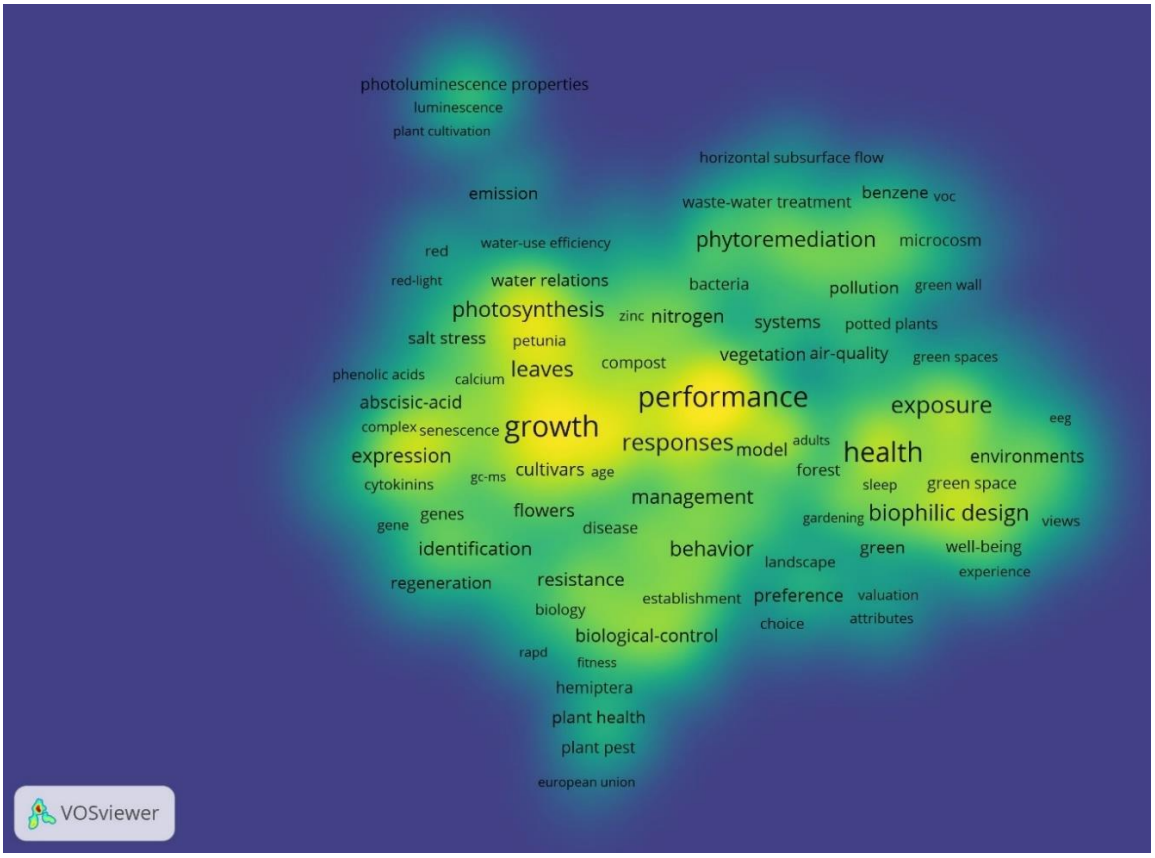

Fig. 1 The density map of frequently of appearance of keywords.

https://doi.org/10.36375/prepare_u.iiche.a417

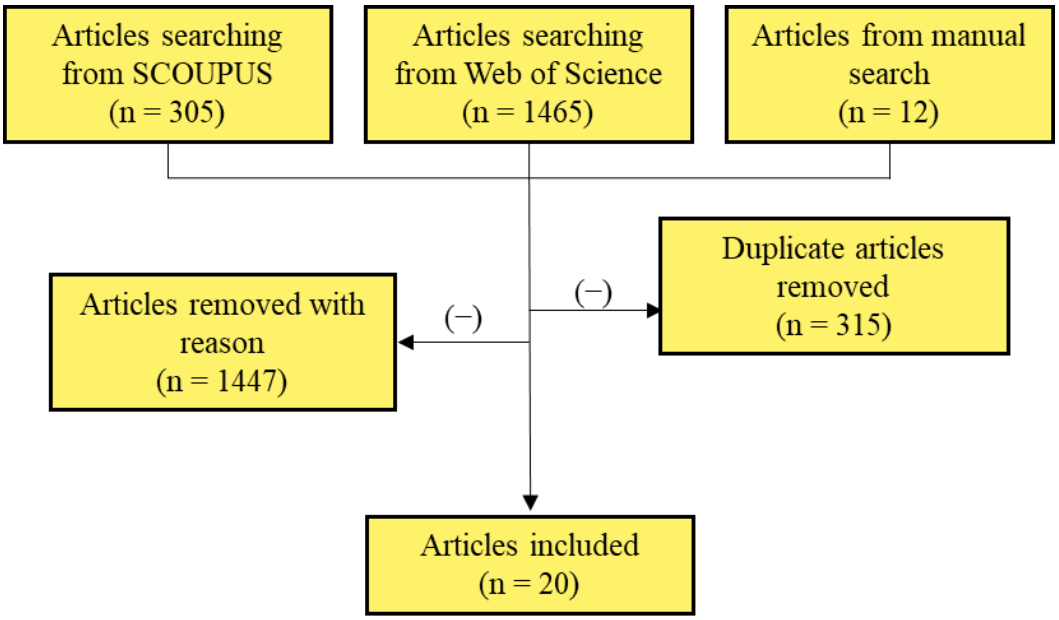

Fig. 2 Collecting and screening process of articles.

3. Results and discussions

3.1. Analysis of keyword frequencies in selected studies

The examination of keywords and their respective frequencies are extracted from the 20 shortlisted studies. This provided valuable insights on common themes and focus points in the field of indoor plants and their impact on the well-being of occupants. Figure 3 shows that "Indoor plants" [34,37,43–48] emerged as the most frequently mentioned keyword, highlighting a substantial focus on the general impact of indoor flora. Additionally, "People-plant interactions" [43,45] and "Human issues in horticulture" [28,43,45,49] surfaced as recurrent themes, indicating a considerable interest in understanding human experiences concerning indoor plants.

Keywords such as "Task performance," [31,44] "Productivity," [28,50] "Mood," [48,51] and "Mental fatigue" [45,48] underscored a notable interest in cognitive aspects, emotional states, and overall well-being influenced by indoor plants. Notably, "Educational building" [46,47] suggested specific research inquiries within educational settings, while "Indoor environment quality" [46,47] depicted an exploration of the overall indoor space quality. Furthermore, the frequencies of terms such as "Repeated measures" [46,52], and "Task reaction time" [34,43,46] pointed towards an experimental approach in assessing the impact of indoor plants on human performance.

These findings collectively highlight a multifaceted research landscape, indicating a substantial interest in understanding of the nuanced relationship between indoor plants, human experiences, and diverse environmental contexts. The prevalent keywords and their frequencies provide valuable insights into the key areas of focus within the literature, setting the stage for a comprehensive understanding of the impact of indoor plants on occupant well-being and indoor environment.

https://doi.org/10.36375/prepare_u.iiche.a417

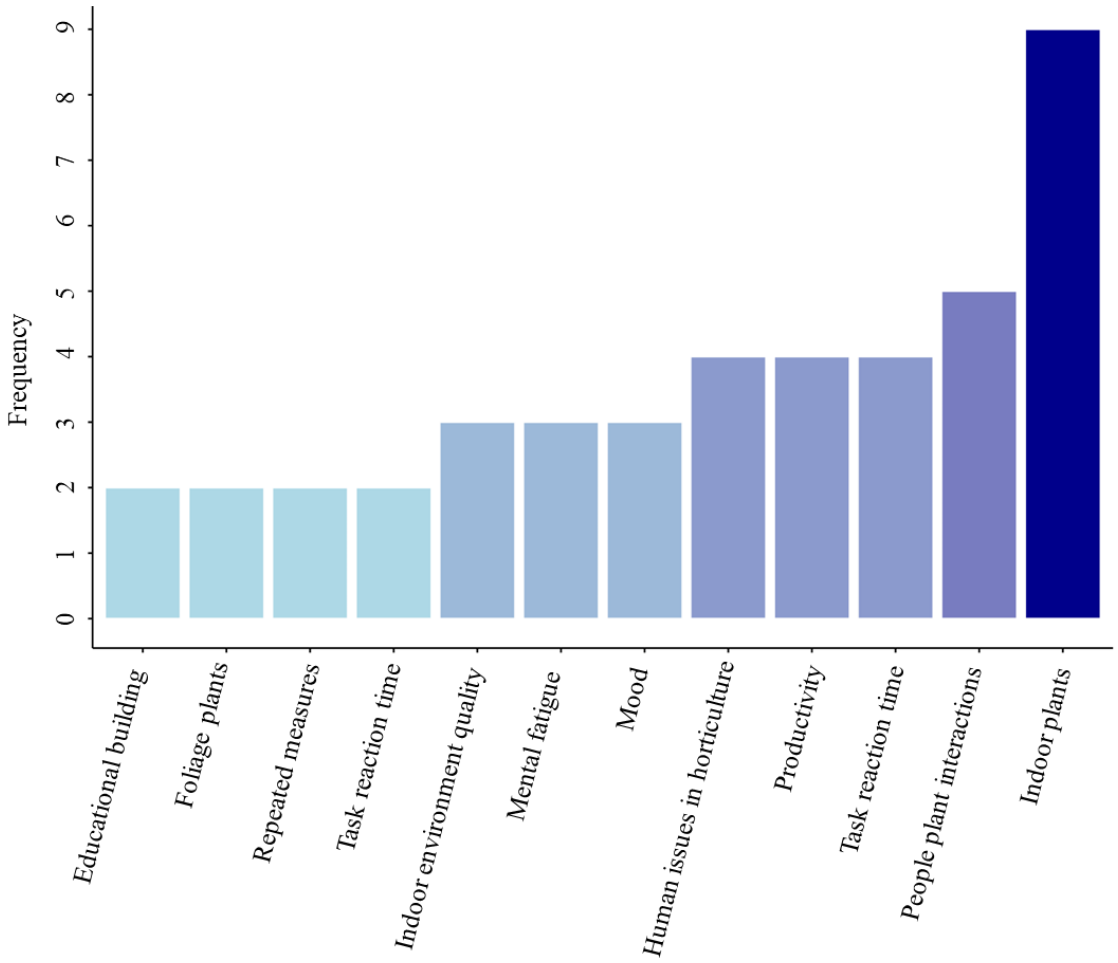

Fig. 3 Frequency of keywords used in twenty shortlisted studies.

3.2. Analysis of studies and citations

Figure 4 presents a compilation of studies on indoor plants and occupant well-being, along with their respective citation counts. The figure showcases a diverse range of studies spanning several decades, from as early as 1995 to recent publications in 2022. Each study is associated with a citation count, providing insights into its impact within the academic sphere. Upon analyzing figure 4, it becomes evident that some authors and studies consistently appear across multiple years. Works authored by S. Shibata et al. [44,48,53] span multiple years, so is by R.K. Raanaas'et al. [45,50] . The highest cited study includes by Larsen et al. [51] and M Niwuwenhuis [30] , and are influential within the dataset, in terems of their relevance relevance.

Recent studies, such as those by P. Archary et al. [34] , A. Thatcher et al. [54] , and S. Sugano et al. [55] , indicate ongoing research endeavors in the field. Additionally, the presence of multiple studies from the year 2021 underscores sustained interest and contributions during that period. The spred in publication years and citation counts among the compiled studies depicts an evolving landscape of research within the domain of indoor plants and occupant well-being. These findings highlight the diverse array of studies and their respective impacts, providing valuable insights into the historical evolution and contemporary relevance of research in this field.

In terms of Instutional affiliation of the prominent aiuthors, we find researchers from esteemed institution like Washington State University, Pullman; Toyohashi University of Technology, Japan; University of Malaya,

https://doi.org/10.36375/prepare_u.iiche.a417

Malaysia; Ajman University; University of the Witwatersrand, Johannesburg, South Africa; Bunkyo Women's University, Japan; Norwegian University of Life Sciences, Norway; Agricultural University of Norway; Delft University of Technology, The Netherlands; Waseda University, Japan; Vrije Universiteit Amsterdam, the Netherlands; Bunkyo Gakuin University, Japan; Kansas State University; Cardiff University; and the University of Michigan. All of these works enrich the ever-changing field of research in this area, adding some local preference and prominence.

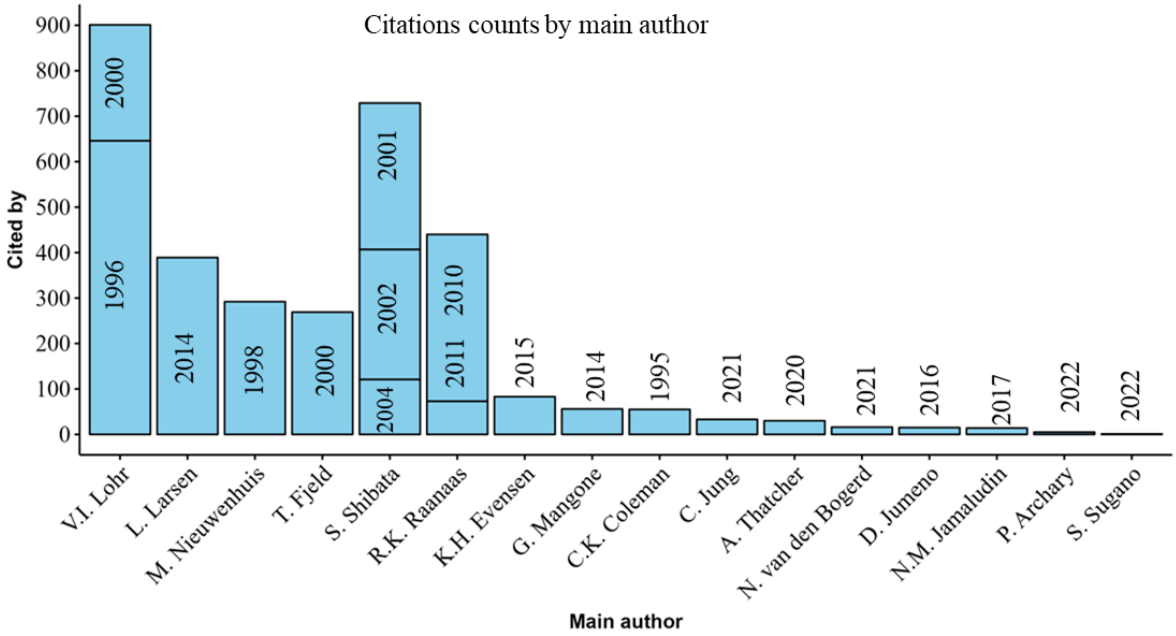

Fig. 4 Prominent authors and their citations

3.3. Geographic distribution of indoor plant studies

The analysis of indoor plant studies based on authors' and co-authors' countries reveals a diverse and global engagement in the research domain. A comprehensive examination of the dataset illustrates a broad geographic representation of studies on indoor plants and occupant well-being. Figure 5 indicate that studies originating from Japan, including works by D. Jumeno et al. [46] , S. Shibata et al. [53], stand out, indicating Japan's significant involvement and contributions to this field. Studies by authored T. Fjeld et al. [55], R.K. Raanaas et al. [45], and others, portray active participation in indoor plant research from Norway, often in collaboration with countries like Sweden and the USA. Concurrently, multiple studies from the USA, such as those by V.I. Lohr et al. [34], highlight the country's sustained engagement in this area of study. Moreover, contributions from regions like Malaysia, South Africa, United Arab Emirates, Netherlands, Canada, United Kingdom, and Indonesia reflect a global interest.

https://doi.org/10.36375/prepare_u.iiche.a417

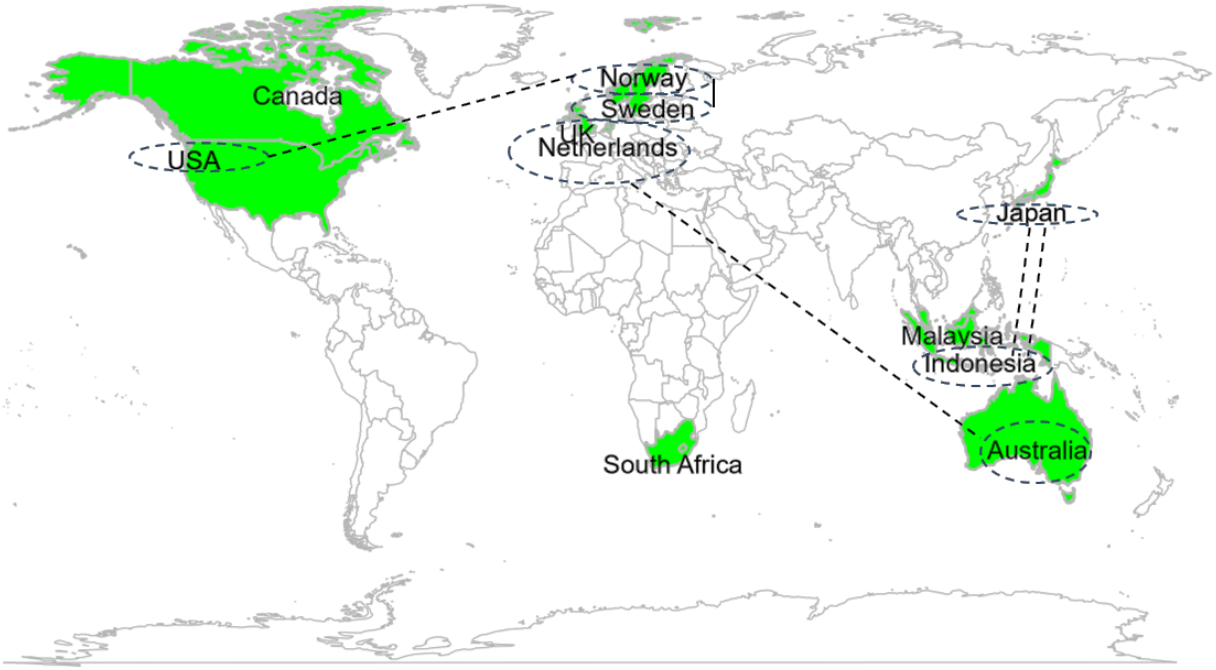

Fig. 5 Indoor plant studies by regions.

3.4. Diversity of plants used in indoor studies

Table 1 displays a diverse array of plants utilized in indoor studies related to occupant well-being. Certain plants have been commonly utilized in numerous investigations, however, there are others that are comparatively underrepresented in the dataset. Plants such as *Dracaena fragrans* (Janet Craig), *Epipremnum aureum* (Money plant), and *Schefflera arboricola* (Dwarf umbrella tree), emerge as the most frequently used species, each featured in six studies. Similarly, *Aglaonema* (Chinese Evergreen), and *Philodendron scandens* (Sweetheart Plant) have been employed in five studies, signifying their recurring presence in indoor plant-related research. Several other plant species, including *Spathiphyllum* (Lily), *Dracaena marginata* (Dragon tree), *Chamaedorea seifrizii* (Bamboo palm), among others, are featured in fewer studies, ranging from one to three instances, within the dataset. The dataset demonstrates a rich diversity of plant species utilized in indoor studies.

While certain plants like the Money plant and Dwarf umbrella tree are extensively explored, the inclusion of a variety of other plant species highlights the breadth of exploration in understanding the effects of diverse indoor plants on occupant well-being. The distribution of plant usage across studies emphasizes the importance of comprehensive assessments encompassing a wide range of plant species. The presence of several plant species offers researchers the chance to investigate a range of plant traits, taking into account elements such as visual appeal and the overall influence on indoor environmental quality and human well-being.

3.5. Investigated aspects in indoor plant studies

The analysis of various studies concerning effect of indoor plant reveals a multifaceted exploration across various domains. Trends of indoor plant studies in different directions can be seen in the table 2.

N.M. Jamaludin et al [34] reported a two-week long study with plants in a classroom's corners, in a non-controlled environment. The

research, resembling a laboratory-style design, sampled classroom students and reported that learning was not significantly affected by the presence or absence of plants. The young age of the students was suggested as a reason, indicating their limited susceptibility to indoor environmental qualities and health symptoms. The study did not provide information on effect size or p-values. In year 1996, V.I. Lohr et al. [28] conducted a between-group study in a computer lab, keeping plants in the periphery. Participants reported higher productivity, less stress, and feeling more attentiveness in presence of plants. However, the study did not report the effect size, and a 10% alpha level was chosen for analysis. Similarly, C. Jung et al. [47] conducted a between-group study in two classrooms with plants, sampling classroom students. The study duration in the running classroom was not specified. Students perceived fresher IAQ, reported fewer complaints of SBS symptoms, and demonstrated increased focus on learning. However, the study did not report the effect size.

R.K. Raanaas et al. [50] in year 2019, assessed the impact of an indoor plant on patients of coronary and pulmonary desease. They reported improved subjective well-being and overall improvements in physical and mental health during the program, while the addition of plants did not further enhance these benefits. In a separate a between-group study in the year 2010 also conducted in an office setting by Raanaas et al. [50], examining the impact of indoor plants, they did not provide information about environmental control. Performance was assessed three times during a one-hour session both with and without plant conditions. Participants in the plant condition exhibited improved performance from the first to the second assessment. However, neither group showed improvement from the Isecond to the third assessment. Furthermore, Evensen et al. [56] examined the restorative effects of indoor plants on participants with and without window conditions. The study included three experiment conditions: live plants, inanimate objects, and a control, all with and without a window view. The presence of plants resulted in greater perceived fascination. However, they did not report any significant performance improvement.

S. Shibata et al. [44,48,53] reported a series of studies: In 2001, they reported that plants had no impact on self-reported fatigue [48]. However, plants showed a greater stress-reducing effect during breaks compared to task performance. In 2002, their findings revealed that one plant had a significant positive effect on the performance of a creative task but not on a concentration task. The positioning of the plant in front of the participant had a greater impact than when it was positioned at the side [53]. In 2004, they found that self-reported mood significantly improved in the presence of plants, positive effects were more observed in females [44]. However, they did not provide a thorough analysis of the indoor circumstances in their trial. Thatcher et al. [38] conducted three studies, first a laboratory study and the other two field studies conducted at a call center setup. Laboratory study showed positive outcomes, howecer, those findings could not be observed in the their field studies. The field studies used various proxy measures of performance and well-being, productivity, physical and psychological health, work engagement, job satisfaction, and work environment. Notably, they have not reported the effect size in their analysis. Additionally, Larsen et al. (1998) [51] explored the impact of plant density (number of plants) on productivity, attitudes, and perceptions. Participants reported improved mood, appreciation for office decoration, and increased comfort when plants were present. However, productivity was reported to be lowest with the highest plant density, while moderate plant density yielded the highest productivity scores.

https://doi.org/10.36375/prepare_u.iiche.a417

Table 1: Trends of plant species used in research

Preferred by Author's → / Plant species ↓	V I lohr (1996)	D. Jumeno (2016)	N.M. Jamaludin (2017)	C. Jung (2021)	V I lohr (2000)	P Archary (2022)	S Shibata (2001)	R K Raanaas (2010)	S Shibata (2002)	T. Fjeld (1998)	G. Mangone (2014)	S Sugano (2022)	A. Thatcher (2011)	N. van den (2021)	S. Shibata (2004)	R K Raanaas (2011)	K.H. Evensen (2015)	C K Coleman (1995)
Dracaena fragrans (Janet Craig)	■		■				■		■	■			■	■				
Epipremnum aureum (Money plant)	■	■	■				■	■	■									
Aglaonema (Chinese Evergreen)	■				■		■			■					■	■		
Philodendron scandens (Sweetheart plant)	■				■		■			■					■	■		
Schefflera arboricola (Dwarf umbrella)		■						■					■		■	■		
Chamaedorea seifrizii (Bamboo palm)	■				■	■												
Dracaena marginata (dragon tree)	■									■		■						
Sansevieria (Snake plant)	■		■										■					
Spathiphyllum (Lily)		■	■															
Dracaena reflexa (Song of Jamaica)							■			■								
Dracaena surculosa (Spotted dracaena)							■			■								
Dypsis lutescens (Areca palm)				■														
Howea forsteriana (Paradise Palm)										■								
Livistona palm (Fountain Palm)													■					
Phycorapis Singaporensis (stick palm)							■											
Rhapis excelsa (lady palm)							■			■								
Ficus carica (Common fig)						■												
Aloevera (Burn plant)													■					
Anthurium (Flamingo flower)										■								
Asparagus (Satawar)										■								
Chlorophytum comosum (Spider)			■															
Dieffenbachia (dumb cane)													■					
Ficus elastica (Rubber fig)										■								
Ficus umbellata (Umbrella Tree Fig.)											■							
Liriope muscari (blue lily turf)							■											
Monstera (Swiss cheese plant)													■					
Polyscias fabian (Aralia Fabian)										■								
Strelitzia nicolai (wild banana)						■												
Tripogandra serrulata (Purple Scimitars)																		■
Zamioculcas (ZZ Plant)													■					
Syngonium podophyllum (Syngonium)	■																	
Scindapsus pictus (Argyraeus)	■																	
Hoya sp. (axplant)	■																	

C.K. Coleman, et al. [36] investigated influence of indoor plants on human stress in a classroom divided into three compartments to isolate treatments. Each compartment, having three participants, represented different conditions: one with a live foliage plant, another with a life-sized photo of the plant, and the third serving as a control with a metal stool. The experiment involved four stages, including the plant in front

of the subject, a photo of the plant, the stool alone, and a baseline with neither plant nor stool. However, due to the small number of participants, no significant conclusions could be drawn. D. Jumeno et al. [46] explored the impact of the number and size of indoor plants on perceived air quality, mood, attention, and productivity. Experimentation was carried out with two variations on the number of plants and three variations on the plant size. Findings indicats that rooms with 3 small and medium-sized plants provided the highest mood, while rooms with 1 small plant, 3 medium-sized plants, and 3 large plants returned the smallest reaction time. The room with 1 small plant exhibited the highest productivity, and the room with 3 small plants recorded the highest perceived air quality. Overall, the study concluded that the number of plants had a positive impact on subjects' mood, with larger numbers correlating with better mood.

Table 2: Trends of indoor plant studies in different directions

Study	Indoor climate (air quality, thermal comfort)	Performance	Working environment (aesthetics, privacy, illumination, and noise)	Emotional state	SBS
V.I. Lohr, et al. (1996) [28]		■		■	
D. Jumeno, et al. (2016) [46]	■	■	■	■	
N.M. Jamaludin, et al. (2017) [34]	■	■			■
C. Jung, et al. (2021) [47]	■	■			■
V.I. Lohr, et al. (2000) [49]	■				
P. Archary, et al. (2022) [57]		■		■	
S. Shibata, et al. (2001) [48]		■	■	■	■
R.K. Raanaas, et al. (2010) [45]					■
S. Shibata, et al. (2002) [53]		■		■	
T. Fjeld, et al. (1998) [55]					■
G. Mangone, et al. (2014) [31]	■				
S. Sugano, et al. (2022) [58]		■			
A. Thatcher, et al. (2020) [54]			■		
N. van den, et al (2021) [37]	■	■	■	■	
S. Shibata, et al. (2004) [44]		■		■	
R.K. Raanaas, et al. (2011) [50]		■			
K.H. Evensen, et al. (2015) [59]		■			
C.K. Coleman, et al. (1995) [36]				■	
M. Nieuwenhuis, et al. (2014) [30]	■	■	■		
L. Larsen, et al. (1998) [51]	■	■	■	■	

N. van den Bogerd et al. [37] conducted a quasi-experimental study and assessed the impact of introducing potted plants in a university library on students' well-being and performance. Although students preferred the room with plants, improvements in mood and cognitive performance were not observed. While students found the room with plants more attractive and comfortable, they did not report effect on mood and cognitive performance. M. Nieuwenhuis, et al. [30] conducted three experiments in large commercial offices in to explore the impact of plants. All three

experiments consistently reported positive impact on workers' well-being and productivity. G. Mangone, et al. (2014) [31] conducted a quasi-experiment to evaluate the impact of indoor plants on the thermal comfort of office workers in an office building. Thermal comfort improved by 1.79 to 1.95 times more when plants were present than they were not, findings suggest that incorporating a substantial quantity of plants in office buildings could contribute to reduced energy consumption that may be obtained by offsetting the air conditioning device.

T. Fjeld et al. [55] reported a study to investigate the impact of plants in office spaces on the health and discomfort symptoms of office workers. Participants responded a questionnaire covering neuropsychological, mucous membrane, and skin symptoms. In the with-plant condition, participants reported 23% lower score sum of symptoms, indicating a significant reduction in neuropsychological and mucous membrane symptoms. In addition, conditions related to cough, fatigue, and dry/hoarse throat were reduced by 37%, 30%, and 23% respectively. S. Sugano et al. [58] explored a mechanisms by which indoor plants improve human cognitive function. Thirty students participated in cognitive tasks across four desktop conditions: no objects, real plants, artificial plants, and books. Results revealed that viewing real plants led to lower cognitive effort and better restoration of attention capacity. Female participants, in particular, exhibited higher scores under the real plant condition compared to the no-object condition, indicating potential gender differences in the cognitive benefits of plants.

3.6. Limitations and future research

As recommendations for future research, it is crucial to develop standardized protocols considering some factors like: 1) Intention-to-treat analysis, 2) ensure demographic parity, 3) conduct a priori and post-hoc power calculation, 4) participant blinding to intervention, and 5) maintaining indoor conditions. Considering these limitations are crucial for conducting more unbiased researc

4. Conclusion

The scarcity of well-designed research articles in prominent databases, and concentration studies in a limited number of countries and a complete absence of standard publications from India, emphasizes the need for a more diverse and comprehensive global research effort. Additionally, non-inclusion of various social demographics among study groups creates challenges in achieving a complete understanding of the impacts of indoor potted plants on human occipants.

Furthermore, the absence of a study planned with a priori estimate of statistical power undermines the study's validity and dependability. The lack of participant blinding to interventions (indoor plant) introduces the potential for bias, and oversight in reporting specific indoor conditions further complicates nuanced interpretations of effects. The limited availability of studies, particularly in exploring multiple dimensions with holistic approach such as emotions, cognition, thermal comfort, and overall satisfaction with space influenced by indoor plants, highlights a gap in the current research landscape.

Acknowledgment

Authors thankful to Birla Institute of Technology and Science Pilani (Pilani Campus) for providing the sophisticated analytical instrumental facilities.

References

[1] N.E. Klepeis, W.C. Nelson, W.R. Ott, J.P. Robinson, A.M. Tsang, P. Switzer, J. V Behar, S.C. Hern, W.H. Engelmann, The national human activity pattern survey (NHAPS): a resource for assessing exposure to environmental pollutants, J. Expo. Sci. Environ. Epidemiol. 11 (2001) 231–252. https://doi.org/10.1038/sj.jea.7500165.

[2] T. Pettit, P.J. Irga, F.R. Torpy, Towards practical indoor air phytoremediation: a review, Chemosphere. 208 (2018) 960–974. https://doi.org/10.1016/j.chemosphere.2018.06.048.

[3] A. Aydogan, R. Cerone, Review of the effects of plants on indoor environments, Indoor Built Environ. 30 (2021) 442–460. https://doi.org/10.1177/1420326X19900213.

[4] A. Prigioniero, D. Zuzolo, Ü. Niinemets, C. Guarino, Nature-based solutions as tools for air phytoremediation: a review of the current knowledge and gaps, Environ. Pollut. 277 (2021) 116817. https://doi.org/10.1016/j.envpol.2021.116817.

[5] R.J. Leonard, C. McArthur, D.F. Hochuli, Particulate matter deposition on roadside plants and the importance of leaf trait combinations, Urban For. Urban Green. 20 (2016) 249–253. https://doi.org/10.1016/j.ufug.2016.09.008.

[6] S. Janhäll, Review on urban vegetation and particle air pollution - deposition and dispersion, Atmos. Environ. 105 (2015) 130–137. https://doi.org/10.1016/j.atmosenv.2015.01.052.

[7] V.I. Lohr, C.H. Pearson-Mims, Particulate matter accumulation on horizontal surfaces in interiors: Influence of foliage plants, Atmos. Environ. 30 (1996) 2565–2568. https://doi.org/10.1016/1352-2310(95)00465-3.

[8] N.R. Jeong, K.J. Kim, J.H. Yoon, S.W. Han, S. You, Evaluation on the potential of 18 species of indoor plants to reduce particulate matter, J. People, Plants, Environ. 23 (2020) 637–646. https://doi.org/10.11628/ksppe.2020.23.6.637.

[9] Y. Cao, F. Li, Y. Wang, Y. Yu, Z. Wang, X. Liu, K. Ding, Assisted deposition of PM2.5 from indoor air by ornamental potted plants, Sustain. 11 (2019) 1–10. https://doi.org/10.3390/su11092546.

[10] J. Ryu, J.J. Kim, H. Byeon, T. Go, S.J. Lee, Removal of fine particulate matter (PM2.5) via atmospheric humidity caused by evapotranspiration, Environ. Pollut. 245 (2019) 253–259. https://doi.org/10.1016/j.envpol.2018.11.004.

[11] J.-S.C. Bo-Kook Jang, Kyungtae Park, Sang Yeob Lee, Hamin Lee, Soo Ho Yeon, Boran Ji, Cheol Hee Lee, Screening of particulate matter reduction ability of 21 Indigenous Korean evergreen species for indoor use, Int. J. Environ. Res. Public Health. 18 (2021) 1–10. https://doi.org/10.3390/ijerph18189803.

[12] J.-W. Yoon, K.-C. Son, D.S. Yang, S.J. Kays, Removal of indoor tobacco smoke under light and dark conditions as affected by foliage plants, Korean J. Hortic. Sci. Technol. 27 (2009) 312–318.

[13] G.Y. Gong, J.S. Kang, K.J. Jeong, J.H. Jeong, J.G. Yun, Effect of several native moss plants on particulate matter, volatile organic compounds and air composition, J. People, Plants, Environ. 22 (2019) 31–38. https://doi.org/10.11628/ksppe.2019.22.1.031.

[14] S. Panyametheekul, T. Rattanapun, M. Ongwandee, Ability of artificial and live houseplants to capture indoor particulate matter, Indoor Built Environ. 27 (2018) 121–128. https://doi.org/10.1177/1420326X16671016.

[15] P.N. Pegas, C.A. Alves, T. Nunes, E.F. Bate-Epey, M. Evtyugina, C.A. Pio, Could houseplants improve indoor air quality in schools?, J. Toxicol. Environ. Heal. - Part A Curr. Issues. 75 (2012) 1371–1380. https://doi.org/10.1080/15287394.2012.721169.

[16] A.J. Ghazalli, C. Brack, X. Bai, I. Said, Alterations in use of space, air quality, temperature and humidity by the presence of vertical greenery system in a building corridor, Urban For. Urban Green. 32 (2018) 177–184. https://doi.org/10.1016/j.ufug.2018.04.015.

[17] T. Pettit, P.J. Irga, F.R. Torpy, The in situ pilot-scale phytoremediation of airborne VOCs and particulate matter with an active green wall, Air Qual. Atmos. Heal. 12 (2019) 33–44. https://doi.org/10.1007/s11869-018-0628-7.

[18] S.-H. Hong, J. Hong, J. Yu, Y. Lim, Study of the removal difference in indoor particulate matter and volatile organic compounds through the application of plants, Environ. Health Toxicol. 32 (2017) e2017006. https://doi.org/10.5620/eht.e2017006.

[19] M. Budaniya, A.C. Rai, Effectiveness of plants for passive removal of particulate matter is low in the indoor environment, Build. Environ. 222 (2022) 109384. https://doi.org/10.1016/j.buildenv.2022.109384.

[20] B.E. Cummings, M.S. Waring, Potted plants do not improve indoor air quality: a review and analysis of reported VOC removal efficiencies, J. Expo. Sci. Environ. Epidemiol. 30 (2020) 253–261. https://doi.org/10.1038/s41370-019-0175-9.

[21] X. Meng, L. Yan, F. Liu, A new method to improve indoor environment: combining the living wall with air-conditioning, Build. Environ. 216 (2022) 108981. https://doi.org/10.1016/j.buildenv.2022.108981.

[22] T. Pettit, P.J. Irga, P. Abdo, F.R. Torpy, Do the plants in functional green walls contribute to their ability to filter particulate matter?, Build. Environ. 125 (2017) 299–307. https://doi.org/10.1016/j.buildenv.2017.09.004.

[23] P.J. Irga, N.J. Paull, P. Abdo, F.R. Torpy, An assessment of the atmospheric particle removal efficiency of an in-room botanical biofilter system, Build. Environ. 115 (2017) 281–290. https://doi.org/10.1016/j.buildenv.2017.01.035.

[24] A.L. Morgan, F.R. Torpy, P.J. Irga, R. Fleck, R.L. Gill, T. Pettit, The botanical biofiltration of volatile organic compounds and particulate matter derived from cigarette smoke, Chemosphere. 295 (2022) 133942. https://doi.org/10.1016/j.chemosphere.2022.133942.

[25] M. Mannan, S.G. Al-Ghamdi, Active botanical biofiltration in built environment to maintain indoor air quality, Front. Built Environ. 7 (2021) 1–8. https://doi.org/10.3389/fbuil.2021.672102.

[26] F. Torpy, M. Zavattaro, Bench-study of green-wall plants for indoor air pollution reduction, J. Living Archit. 5 (2018) 1–15. https://doi.org/10.46534/jliv.2018.05.01.001.

[27] J. Sowa, J. Hendiger, M. Maziejuk, T. Sikora, L. Osuchowski, H. Kamińska, Potted plants as active and passive biofilters improving indoor air quality, IOP Conf. Ser. Earth Environ. Sci. 290 (2019). https://doi.org/10.1088/1755-1315/290/1/012150.

[28] V.I. Lohr, C.H. Pearson-Mims, G.K. Goodwin, Interior plants may improve worker productivity and reduce stress in a windowless environment, J. Environ. Hortic. 14 (1996) 97–100. https://doi.org/10.24266/0738-2898-14.2.97.

[29] D. Jumeno, H. Matsumoto, The effects of indoor foliage plants on perceived air quality, mood, attention, and productivity, J. Civ. Eng. Archit. Res. 3 (2016) 1359–1370.

[30] M. Nieuwenhuis, C. Knight, T. Postmes, S.A. Haslam, The relative benefits of green versus lean office space: three field experiments, J. Exp. Psychol. Appl. 20 (2014) 199–214. https://doi.org/10.1037/xap0000024.

[31] G. Mangone, S.R. Kurvers, P.G. Luscuere, Constructing thermal comfort: investigating the effect of vegetation on indoor thermal comfort through a four season thermal comfort quasi-experiment, Build. Environ. 81 (2014) 410–426. https://doi.org/10.1016/j.buildenv.2014.07.019.

[32] R. Elnaklah, I. Walker, S. Natarajan, Moving to a green building: indoor environment quality, thermal comfort and health, Build. Environ. 191 (2021) 107592. https://doi.org/10.1016/j.buildenv.2021.107592.

[33] J. Qin, C. Sun, X. Zhou, H. Leng, Z. Lian, The effect of indoor plants on human comfort, Indoor Built Environ. 23 (2014) 709–723. https://doi.org/10.1177/1420326X13481372.

[34] N.M. Jamaludin, N. Mahyuddin, F.W. Akashah, Assessment on indoor environmental quality (IEQ) with the application of potted plants in the classroom: case of university Malaya, J. Des. Built Environ. 17 (2017) 1–15. https://doi.org/10.22452/jdbe.vol17no2.1.

[35] D.L. Rich, Effects of exposure to nature and plants on cognition and mood: a cognitive psychology perspective, Cornell University, New York, 2007.

[36] C.K. Coleman, R.K. Mattson, Influences of foliage plants on human stress during thermal biofeedback training, Horttechnology. 5 (1995) 137–140. https://doi.org/10.21273/horttech.5.2.137.

[37] N. van den Bogerd, S.C. Dijkstra, S.L. Koole, J.C. Seidell, J. Maas, Greening the room: a quasi-experimental study on the presence of potted plants in study rooms on mood, cognitive performance, and perceived environmental quality among university students, J. Environ. Psychol. 73 (2021) 101557. https://doi.org/10.1016/j.jenvp.2021.10155

7.
[38] A. Thatcher, K. Adamson, L. Bloch, A. Kalantzis, Do indoor plants improve performance and well-being in offices? Divergent results from laboratory and field studies, J. Environ. Psychol. 71 (2020) 101487. https://doi.org/10.1016/j.jenvp.2020.101487.
[39] T. Bringslimark, T. Hartig, G.G. Patil, The psychological benefits of indoor plants: a critical review of the experimental literature, J. Environ. Psychol. 29 (2009) 422–433. https://doi.org/10.1016/j.jenvp.2009.05.001.
[40] K. Han, Effects of indoor plants on self-reported perceptions: a systemic review, Sustainability. 11 (2019) 4506. https://doi.org/https://doi.org/10.3390/su11164506.
[41] L.B. Yeo, Psychological And Physiological Benefits Of Plants In The Indoor Environment: A Mini And In-Depth Review, Int. J. Built Environ. Sustain. 8 (2020) 57–67. https://doi.org/10.11113/ijbes.v8.n1.597.
[42] N.J. Van Eck, L. Waltman, Manual VOSviewer, Univeristeit Leiden. (2021) 54.
[43] S. Sugano, M. Tazaki, H. Arai, K. Matsuo, S.I. Tanabe, Effects of indoor plants on occupants' cognitive functions: a systematic review, 17th Int. Conf. Indoor Air Qual. Clim. INDOOR AIR 2022. (2022).
[44] S. Shibata, N. Suzuki, Effects of an indoor plant on creative task performance and mood, Scand. J. Psychol. 45 (2004) 373–381. https://doi.org/10.1111/j.1467-9450.2004.00419.x.
[45] R.K. Raanaas, G.G. Patil, T. Hartig, Effects of an indoor foliage plant intervention on patient well-being during a residential rehabilitation program, HortScience. 45 (2010) 387–392. https://doi.org/10.21273/hortsci.45.3.387.
[46] D. Jumeno, H. Matsumoto, The effects of indoor foliage plants on perceived air quality, mood, attention, and productivity, J. Civ. Eng. Archit. Res. 3 (2016) 1359–1370.
[47] C. Jung, J. Awad, Improving the IAQ for Learning Efficiency with Indoor Plants in University Classrooms in Ajman, United Arab Emirates, (2021).
[48] S. Shibata, N. Suzuki, Effects of Indoor Foliage Plants on Subjects' Recovery from Mental Fatigue, N. Am. J. Psychol. 3 (2001) 385–396.
[49] V.I. Lohr, C.H. Pearson-Mims, Physical discomfort may be reduced in the presence of interior plants, Horttechnology. 10 (2000) 53–58. https://doi.org/10.21273/horttech.10.1.53.
[50] R.K. Raanaas, K.H. Evensen, D. Rich, G. Sjøstrøm, G. Patil, Benefits of indoor plants on attention capacity in an office setting, J. Environ. Psychol. 31 (2011) 99–105. https://doi.org/10.1016/j.jenvp.2010.11.005.
[51] L. Larsen, J. Adams, B. Deal, B.S. Kweon, E. Tyler, Plants in the workplace the effects of plant density on productivity, attitudes, and perceptions, Environ. Behav. 30 (1998) 261–281. https://doi.org/10.1177/001391659803000301.
[52] S.H. Park, R.H. Mattson, Effects of flowering and foliage plants in hospital rooms on patients recovering from abdominal surgery, Horttechnology. 18 (2008) 563–568. https://doi.org/10.21273/horttech.18.4.563.
[53] S. Shibata, N. Suzuki, Effects of the foliage plant on task performance and mood, J. Environ. Psychol. 22 (2002) 265–272. https://doi.org/10.1006/jevp.2002.0232.
[54] A. Thatcher, K. Adamson, L. Bloch, A. Kalantzis, Do indoor plants improve performance and well-being in offices? Divergent results from laboratory and field studies, J. Environ. Psychol. 71 (2020). https://doi.org/10.1016/j.jenvp.2020.101487.
[55] T. Fjeld, B. Veiersted, L. Sandvik, G. Riise, F. Levy, The effect of indoor foliage plants on health and discomfort symptoms among office workers, Indoor Built Environ. 7 (1998) 204–209. https://doi.org/10.1177/1420326X9800700404.
[56] K.H. Evensen, R.K. Raanaas, C.M. Hagerhall, M. Johansson, G.G. Patil, Restorative Elements at the Computer Workstation: A Comparison of Live Plants and Inanimate Objects With and Without Window View, Environ. Behav. 47 (2015) 288–303. https://doi.org/10.1177/0013916513499584.
[57] P. Archary, A. Thatcher, Affective and cognitive restoration: comparing the restorative role of indoor plants and guided meditation, Ergonomics. 65 (2022) 933–942. https://doi.org/10.1080/00140139.2021.2003873.
[58] S. Sugano, M. Tazaki, H. Arai, K. Matsuo, S. ichi Tanabe, Characteristics of eye movements while viewing indoor plants

and improvements in occupants' cognitive functions, Japan Archit. Rev. 5 (2022) 621–632. https://doi.org/10.1002/2475-8876.12284.

[59] K.H. Evensen, R.K. Raanaas, C.M. Hagerhall, M. Johansson, G.G. Patil, Restorative Elements at the Computer Workstation: A Comparison of Live Plants and Inanimate Objects With and Without Window View, Environ. Behav. 47 (2015) 288–303. https://doi.org/10.1177/0013916513499584.

https://doi.org/10.36375/prepare_u.iiche.a418

Replacement of coal by RDF (Refused Derived Fuel)

Soumyadip Das[a], Ritu Thakur[a], Subrata Dasgupta[a], Sankalan Das[a] , Biswajit Mandal[b], Sunil Baran Kuila[c*]

[a, b , c*]Department of Chemical Engineering, Haldia Institute of Technology, Haldia 721657, West Bengal, India.

*Sunil Baran Kuila, hithodche@gmail.com, 8972960394,

Abstract

Within Municipal Solid Waste (MSW) management, processing of several fractions that are combustible in nature but are not recyclable such as soiled paper, soiled cloth, contaminated plastics, multilayer, packaging materials, other packaging materials, pieces of leather, rubber, tyre, polystyrene (thermocol), wood etc. has remained a challenge and these fractions unwantedly ends up at landfill sites. These fractions can be processed and converted to refuse derived fuel (RDF), which carries significant calorific value, and can be utilized as alternative fuel in various industries in line with the principle of waste to wealth. The principle of RDF production is recovering quality fuel fractions from the waste, particularly through the removal of recyclable particles such as metal and glass, and converting the raw waste into a more usable form of fuel with uniform particle size and higher calorific value than raw MSW. For example, the broad specification of RDF suitable for the Indian cement plants is preferably having Moisture (< 20 %), average particle size (< 75 mm), calorific value (~ 3000 kcal/kg), Chlorine (< 0.7%), Sulphur (< 2%) and should be free of restricted items such as PVC, explosives, batteries, aerosol containers and bio-medical waste.

Keywords: *Refuse derived fuel; Garbage; Pellet; Moisture; Municipal Solid Waste.*

1. Introduction:

The recent growth of metropolitan populace along with societal and economic prosperity leading to higher energy demand and higher rate of wastage production due to accelerated populace growth. Thus, in order to meet the constant energy demand implementation of solid municipal waste material is indeed a promising feedstock for energy production. In a metropolitan region deposition of several types of municipal solid waste material gets deposited at lower elevated region, often termed as waste disposal area or waste repository. The technique or process is much economically feasible thus it is the most acceptable traditional or conventional method of waste management technique. On contradict of above-mentioned method accumulation of large amount of municipal solid waste material in combination with organic and non-degradable waste material leads to emission of hothouse gases, thus certain regulations must be stipulated in order to maintain socio, economic and environmental sustainability **[**Balasubramanian Karpana et al. 2012**]**. Henceforth the immediate search for a newly developed methodology is highly required to convert municipal solid waste materials into usable energy form **[**S., Kamyab et al. 2020**]**. Firstly, the solid municipal waste materials can be apartheid into combustive, non-combustive and moisture enriched materials. The combustive proportion of waste material is defined as refused derived fuel mainly consists of carbon enriched by-products includes several bio-degradable and

https://doi.org/10.36375/prepare_u.iiche.a418

non -biodegradable polymers likely polyethylene polymer and papers which contributes >50%-<80% as main components in RDF along with minor yields such as timber, textile material and biologically derived waste products [S., Kamyab et al. 2020, Ahmad Hajinezhad et al., Varun Singh Bundela et al.]. Figure 1 depicts different fractions of municipal waste materials. Henceforth, refused derived fuel in MSW may be a promising source of clean energy in the nearer future [S., Kamyab et al. 2020, J.E. Reed et al. 1983, Baharez Reza et al. 2013 , Constantinos S. Psomopoulos.2014]. The below pie-chart representation shows the recent municipal solid waste composition of India and specifying various components present in MSW [Constantinos S. Psomopoulos. 2014]. The other different methodologies other than RDF such as direct combustion process and bio-gasification.

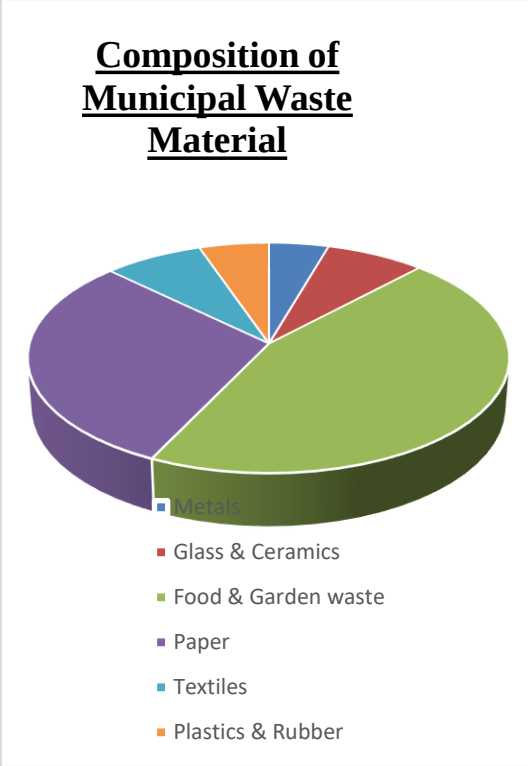

Fig. 1. Pie-Chart representation depicting percentage composition of MSW in India.

The granular forms of refused derived fuel are considered to be potent alternative over coal, since energy value (J/gm) or (J/m^3) of granules are higher in comparison with coal. It also referred to be sustainable form of energy which signifies environmental friendliness and highly competent over several fossil fuel relied industries [Balasubramanian Karpana et al 2021, Van Tubergen J et al. 2005]. Bio-gasification is an anoxygenic method responsible for methane emission which includes (>50%) of CH4 concentration. Later it has been evaluated 75 Watts of electrical energy can be synthesized per unit volume of methane gas by bio-gasification method using solidified municipal waste materials [Balasubramanian Karpana et al 2021, Archer E et al. 2005]. The direct combustion method involves explicit application of heat energy on solidified waste materials under oxygenic condition at >1073K (K-kelvin) which is responsible for emission of hothouse gases. It involves energy convalescence rate within >50% - <100% consisting mostly biodegradable waste materials. The recovered energy has several industrial applications likely for heating purpose or in industrial turbines [Balasubramanian Karpana et al 2021, A. Gendebien et al. 2003].

The above conversion methods from wastage materials to energy paves a way towards environmental sustainability. Among these conversion methods municipal solid waste is the most promising feedstock for energy extraction. It provides solution to waste management issues and provides environmental sustainability [S., Kamyab et all 2020 , Garg, A. et al. 2007]. In spite of having several energy extraction methods, gasification method is suitable technique in nearer future.

2. RDF

2.1. Preparation of Refused Derived Fuel (RDF)

Refuse-derived fuel (RDF) is a type of fuel produced from non-recyclable

https://doi.org/10.36375/prepare_u.iiche.a418

waste materials. The RDF preparation process follows following steps:

1. The process initializes by collecting non-recyclable waste materials such as plastics, paper, cardboard, textiles, and organic waste from various sources like households, industrial and commercial establishments. [Balasubramanian Karpana et al. 2021, S., Kamyab et al. 2020]
2. The collected waste undergoes some manual and mechanical methods to remove contaminants and recyclable materials to ensure that only suitable waste materials are used for RDF production.
3. After sorting, the remaining waste is shredded into smaller pieces to facilitate further processing. This can be done using industrial shredders. [Ahmad Hajinezhad et al.2016]
4. Depending on the moisture content of the waste, it may be necessary to dry it to reduce moisture levels. Lower moisture content improves the energy content of the RDF.
5. The shredded and dried waste is then compacted or pelletized to form RDF. This can be done by compressing the waste material into dense pellets or blocks using hydraulic presses.
6. It's crucial to ensure the quality of RDF by conducting regular quality control checks. This involves analyzing the composition, calorific value, and moisture content of the produced RDF to meet specific standards.
7. After that the RDF is stored in suitable containers or storage facilities before distribution to end-users, such as cement kilns, industrial boilers, or power plants. [Varun Singh Bundela et al. 2022]
8. RDF can be used as a fuel source in various applications. It can be burned in industrial furnaces, boilers, or even gasified to produce syngas for electricity generation or other energy purposes.
9. The production and use of RDF comply with local environmental regulations and emissions standards to minimize environmental impact.

The exact RDF preparation process may vary depending on local regulations, the specific waste materials available, and the intended end-use of the fuel. Additionally, technologies for RDF production continue to evolve, with an increasing focus on sustainability and resource recovery. [J.E. Reed et al. 1983]

2.2. Characteristics of RDF

The properties of RDF make it a lot different from fossil fuel and other fuels. Some of them are notably good for both environment and economics while others are not.

A few of the characteristic properties are listed below.

- The bulk density and the calorific value of RDF are comparatively lower than fossil fuels. The lower calorific value is a bit less economical for a country. **[**Baharez Reza et al. 2013**]**
- RDF also has a lower energy conversion efficiency and density.
- RDF is a heterogeneous composition that is it consists of matters of variable size, volatility, alkali content, heavy metal content, and inert material composition.
- These have partially lower combustion behavior. **[**Baharez Reza et al. 2013**]**

The chemical properties of RDF vary with the quantity and composition of MSW (Municipal Solid Waste). [Baharez Reza et al. 2013]

The feasible and desired chemical properties and characteristics of RDF; **[**Constantinos S. Psomopoulos 2014**]**

- Calorific Value – 11 to 18 MJ/kg
- Sulphur content – 0.3 to 0.8 % wt.

https://doi.org/10.36375/prepare_u.iiche.a418

- Chlorine content – 1.0 to 1.8 % wt.
- Moisture content – below 30 % wt.
- Ash content – 11 to 21 % wt.
- Carbon content – above 50 % wt.
- Humidity – below 25% wt.

The below graphical representation has been plotted to study comparison analysis with RDF and other conventional fuel sources and coal related with calorific value and proximate study respectively [Van Tubergen J et al. 2005, Archer E et al. 2005, A. Gendebien et al. 2003, Garg, A. et al. 2007, D. MVW Lechtenberg; 2008, Mustafa Kara. 2017].

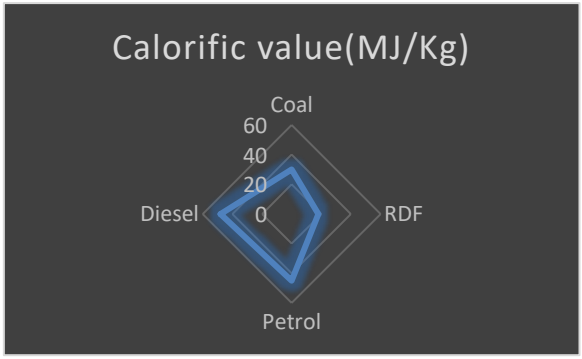

Fig.2. Comparison plot of RDF with conventional fuel on basis of calorific value

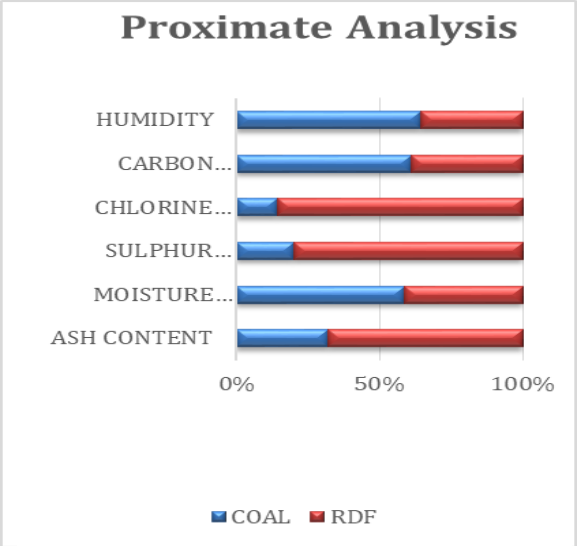

Fig.3. Comparison chart of RDF vs Coal on basis of proximate analysis.

RDF is produced in the course of Mechanical Biological Treatment (MBT) of wastes or Biological Drying Process of wastes [Rada EC and Andreottoala G 2012, Archer E et al. 2005]. The waste is basically decomposed from organic parts and recyclable solid wastes that mainly include metals, papers, plastic etc. and hence RDF is prepared [D. MVW Lechtenberg; 2008, Mustafa Kara. 2017].

Refuse-derived fuel represents a significant quantity of energy. Recovery of part of this energy content in a form with high value, i.e., fuel oil, would also reduce a growing environmental problem. The wide variety of plastics found in the RDF that are produced originally from crude oil can be thermally cracked into fuels or petrochemicals [R.C. Poller 1980, W. Kaminsky and H. Roessler 1992].

The calorific value of RDF is comparatively lower than coal but the cost of coal is much higher than RDF. This makes RDF a better substitute of coal as the former one is environment friendly [Ganesh Thirugnanam 2013].

3. Challenges and it's utilization

RDF upon combustion leads to a very minimum number of pollutants. As a result of which it has a widespread application in several domains and industries. Refused derived fuel has been in use in industries not only in India but also in several other parts of the world.

RDF is acknowledged for its cost-saving benefits, particularly visible in European nations with modern waste collection and disposal infrastructure, paired with elevated disposal expenses. Typically, roughly 55% of carbon dioxide emissions during cement clinker manufacture occur from the transformation of limestone (CaCO3) into lime (CaO). Additionally, roughly 40% of the emissions occur from the combustion processes needed for commencing the reaction at a temperature of 1450°C. RDF

coupled with other fuel sources can significantly reduce carbon emission from cement industry [Mustafa Kara, 2012].

Certainly RDF, or refuse-derived fuel, can undergo extra processing to obtain consistent size (60–100 mesh) and weight, coupled with an enhanced energy density. This makes it a viable input for pyrolysis or co-combustion in a typical power plant. The considerable energy content inside refuse-derived fuel presents a viable resource. Extracting a portion of this energy in the form of high-value fuel oil not only addresses environmental problems but also provides an attractive option for resource recovery through the pyrolysis of polymeric wastes to generate liquid hydrocarbons [Lin, K. S. et al 1999].

RDF can replace coal in power plant boilers, functioning as a substitute for both firewood and furnace oil in the combustion process. RDF has also been found to be immensely useful in the generation of electricity. There has been examples of implementation and utilisation of RDF in electricity generation in many parts of India. In the context of Vellore District, around 120 metric tons of solid garbage is produced daily. From this, it is possible to generate 30 metric tons of Refuse-Derived Fuel (RDF) daily, resulting in the generation of roughly 2.5 megawatts of power each day. Notably, Arcot has established a self-sufficient program where a 30-kilovolt generator is deployed to manufacture electricity from municipal solid trash, generating 265 to 285 units per day. This electricity output can illuminate around 100-150 street lights in Arcot [Thirugnanam, Ganesh & Prakasam, Vignesh 2013].

To comprehend the benchmark practices of municipal solid waste (MSW) management in India, data was gathered from various organizations, and a subset was chosen for in-depth analysis by various research scholars. A case study has been done on a company named Shalivahana (MSW) Green Energy Ltd. [S (MSW)GEL]. Located in Rebladevpally Village, (near Sultanabad) Karimnagar District, Telangana. They are using OFMSW as a feed material with a capacity of 225 TPD RDF plant capacity and 12 MW power generation capacity these two are main commercial products of this company [Ghosh, A et al. 2022].

RDF plants have been found to have some environmental impact, including the potential for global warming, the creation of non-methane volatile organic compounds, the potential for NOx-corrected photooxidative creation, the potential for acidification, and the potential for nutrification, despite their high market demand and numerous success stories [CPCB Bulletin 2016, Reza, B et al. 2013]. In addition, field surveys on RDF reveal that it has a high social approval rate and a medium to high economic aspect [PlanningCommission, G. 2015]. India's current situation, as shown by case studies, highlights the presence of many RDF plants. Thus, employing RDF followed by pyrolysis or gasification is suggested as a sustainable approach, depending on the desired outcome [Ghosh, A et al. 2022].

Now, focusing on India's current scenario describes the generation of municipal solid waste is around 62–65 million tonnes and by 2031, it is estimated to be 130 million tonnes [Sharma, P. et al. 2022, Urban, S. B. 2018, N. K. Gupta 2016]. Given the current worldwide context and the close proximity of Indian cement facilities, it is projected that approximately 13,600 tonnes of Refuse Derived Fuel (RDF) could be accessible daily, amounting to roughly 4.96 million tonnes annually [Sharma, P. et al. 2022, Urban, S. B. 2018]. The Ministry of Housing and Urban Affairs (MoHUA) has formulated guidelines for Indian RDF Grading, which are determined by the quality of refused derived fuel [Sharma, P.

et al. 2022, Urban, S. B. 2018]. Nevertheless, the utilization of refused derived fuel is subject to certain constraints, with one key factor being TSR (Thermal Substitution Rate), which denotes the proportion of traditional fossil fuel heat substituted by alternative fuels. Reports indicate that certain cement plants in Europe have attained a TSR of 80–100% by incorporating RDF into the calciner. However, it's important to note limitations such as the occurrence of hot spots and elevated carbon monoxide emissions [Sharma, P. et al. 2022, Abbas, T. 2018]. In India, just 59 out of 148 integrated cement plants engage in co-processing waste, primarily within the calciner [Sharma, P. et al. 2022, Saxena, A. et al. 2019, Kumr S. and Verma R. 2021]. Several studies have indicated that RDF contributes merely 0.6% to the overall 4% TSR. Only a handful of cement plants have achieved a TSR exceeding 15% [Sharma, P. et al. 2022]. Recently, only two cement plants in India have installed a kiln bypass, resulting in a TSR operating percentage of 30%, with RDF serving as the primary alternative fuel in the calciner [Sharma, P. et al. 2022]. During operational phases, various constraints have been noted, including subpar waste quality, low calorific value, inadequate segregation, elevated chloride content, fluctuations in costs, flaws in system design, deficient characterization facilities, and operational challenges [Sharma, P. et al. 2022]. A report outlines numerous challenges concerning pre-processing and co-processing encountered by Indian cement plants during the utilization of RDF [Sharma, P. et al. 2022, Sharma, P. et al. 2019, Kukreja, K. et al. 2019, Kukreja, K. & Mohapatra, B. N. et al. 2019]. Another report underscores significant challenges faced by Dalmia Cement Ltd.-Dalmiapuram during RDF utilization, including a lower heating value of 1800 kcal/kg with 25% moisture content and odor issues [Sharma, P. et al. 2022, ajamohan, R. et al. 2017]. Elevated chloride content emerges as a prevalent challenge in RDF operational procedures. Consequently, particularly in India, the cement industry seeks alternative thermochemical treatment options to address these challenges. Research indicates that two other thermochemical treatment technologies, namely Pyrolysis and gasification, offer potential solutions, enabling waste reduction and significant savings of land from landfills [Sharma, P. et al. 2022]. To ensure the sustainability of society, a clear differentiation between pyrolysis and gasification has been emphasized. Gases released from the pyrolysis process often go unutilized, contributing to pollution. Research suggests that the commercial viability of this process may face challenges in obtaining approval from pollution control boards due to pollution concerns, potentially leading to increased costs for pollution mitigation. Additionally, proper storage facilities are necessary for the utilization of pyrolytic oil, incurring additional expenses for users. Numerous authors have conducted waste characterization using analytical equipment [. Mehta, A., & Rao, S. 2023, Miskolczi, N. et al. 2010, Cozzani, V. et al. 1995, Fang, D. et al. 2021, Chen, X. et al. 2019]. A report also indicates a high tar content in gas products. Therefore, while the RDF pyrolysis process can be utilized at the laboratory scale to develop kinetic models and determine product yields, it may not be suitable for larger scale or commercial purposes. In contrast, gasification presents several advantages. It generates primarily syngas, which can be directly burned in the calciner/kiln without requiring gas cleaning. Hence, gasification emerges as a viable waste treatment technology for converting solid waste into clean gaseous fuel, with impurities removed from the pyro-processing system [Sharma, P. et al. 2022, Kusz, B. et al. 2022]. Since the gasification process enables the production of syngas which signifies better ignition quality inside

the calciner as compared to directly putting the pellets of solid waste material inside it. The gasification process also fixes up a challenge related to klink system the consistent contribution to hydrogen due shift reaction induces the increment of calorific value of syngas thus providing better efficiency of clinker as it also mitigates the accumulation of ash inside the clinker [Sharma, P. et al. 2022]. In India, an RDF gasification plant was established in Pune with the aim of generating 10 MW of power; however, technical issues prevented the plant from becoming operational [Sharma, P. et al. 2022, Singh, A. and Patel, R. 2023]. Cement plants encountering obstacles in increasing TSR beyond 15–20% stand to gain from gasification technology. Integration of gasification with the cement industry can facilitate the attainment of the 25% TSR target within the specified timeframe. The Indian government has established a goal of achieving 100 million tonnes of coal gasification by 2030, with an investment of Rs 0.4 trillion [Sharma, P. et al. 2022, Kumar, S., and Gupta, P. 2023, Dr. M. M. Kutty 2019]. Upon the implementation of gasified coal utilization in the cement sector, it will encourage the co-gasification of coal and waste, offering the benefit of enhanced syngas quality [Sharma, P. et al. 2022].

4. Conclusion

Recent technological advancements, coupled with an effective waste management system, play a pivotal role in realizing sustainable development objectives. This study examines the present status of refused derived fuel (RDF) in India, exploring its implementation, production methods, and accompanying case studies to grasp its challenges and future potential. RDF finds extensive use across various industries, primarily in cement production. However, challenges such as economic viability, waste sorting, and societal awareness, compounded by the absence of decision-making support systems in waste management, persist. The research also underscores the optimal production processes within the cement industry to enhance Thermal Substitution Rates (TSR). Gasification emerges as the most suitable method for RDF implementation in this context. Such primary research endeavors are deemed crucial for countries like India, aiding in the identification and mitigation of sustainability barriers within the broader system.

Acknowledgement

We are grateful to everyone who contributed to this work. We are particularly grateful to Prof. Sunil Baran Kuila (Professor and Head of the Chemical Engineering Department) and Prof. Biswajit Mondal for their invaluable guidance and insights throughout the course of this research. In addition, we'd also like to thank our friends and coworkers for their ongoing encouragement and constructive feedback. Lastly, we want to convey our heartfelt gratitude to our families for their unwavering encouragement and compassion.

References:

1. Balasubramanian Karpana, Abdul Aziz Abdul Ramana,∗,Mohamed Kheireddine Taieb Aroua Waste-to-energy: Coal-like refuse derived fuel from hazardous waste and biomass mixture Department of Chemical Engineering, Faculty of Engineering, University of Malaya, 50603, Kuala Lumpur, Malaysia b Centre for Carbon Dioxide Capture and Utilization, School of Science and Technology, Sunway University, 47500, Petaling Jaya, Selangor, Malaysia.

2. S., Kamyab, H., Pham, Q.B., Yadav, S., Bhattacharyya, S., Yadav, V.K., Bach, Q.-V.,2020. A review on municipal solid waste

as a renewable source for waste-to-energy project in India: c

3. Utilization of Refuse-Derived Fuel (RDF) from Urban Waste as an Alternative Fuel for Cement Factory: a Case Study Ahmad Hajinezhad*, Emad Ziaee Halimehjani, Mojtaba Tahani (2016) Faculty of New Sciences and Technologies, University of Tehran, Tehran, Iran

4. The Role Of Rdf In Place Of Coal Varun Singh Bundela, Dr. Arun Patel PhD Research Scholar, Professor department of Civil engineering Vedica Institute of Technology Civil engineering department RKDF University Airport by pass road Gandhi nagar Bhopal Madhya Pradesh India (2022)

5. J.E. Reed, J.L. Conrad, C.D. Price, "Co-firing of Refuse-Derived Fuel (RDF) with natural Gas, in a Cement Kiln", National Technical Information Service, March (1983). Book.

6. Baharez Reza, Atousa Soltani, Rajeev Ruparathna, Rehan Sadiq, Kasun Hewage. "Environmental and economic aspects of production and utilization of RDF as alternative fuel in cement plants: A case study of Metro Vancouver Waste Management." 2013 Elsevier B.V. http://dx.doi.org/10.1016/j.resconrec.2013.10.009

7. Constantinos S. Psomopoulos. "Residue Derived Fuels as an Alternative Fuel for the Hellenic Power Generation Sector and their Potential for Emissions Reduction". · September 2014 DOI: 10.3934/energy.2014.3.321

8. Van Tubergen J, Glorius T, Waeyenbergh E, Classification of Solid Recovered Fuels, European Recovered Fuel Organisation, 2005.

9. Archer E, Baddeley A, Klein A, et al. (2005) Mechanical-Biological-Treatment: A Guide for Decision Makers Processes, Policies and Markets (Juniper Consultancy Services Ltd.)

10. A. Gendebien, A. Leavens, K. Blackmore, A. Godley, K. Lewin, K.J. Whiting and R. Davis (2003) European Commission – Directorate General Environment, Refuse Derived Fuel, Current Practice and Perspectives (B4-3040/2000/306517/Mar/E3), Final Report, 2003.

11. Garg, A., Smith, R., Hill, D., Simms, N., & Pollard, S. (2007). Wastes as co-fuels: the policy framework for solid recovered fuel (SRF) in Europe, with UK implications. Facts and Figures, European Recovered Fuel Organisation (Erfo) (2007).

12. D. MVW Lechtenberg; 2008. Www.lechtenberg-partner.de. Mermod AY, Dömbekci B. Emission trading applications in the European Union and the case of Turkey as an emerging market. International Journal of Energy Sector Management 2011; 5:345–60

13. Mustafa Kara. "Environmental and economic advantages associated with the use of RDF in cement kilns." 09 October 2017; DOI: 10.1016/j.resconrec.2012.06.011

14. Rada EC, Andreottoala G (2012). "RDF/SRF which perspective for its future in EU. Waste Manage" 32(6): 1059–1060

15. Archer E, Baddeley A, Klein A, et al. (2005) Mechanical-Biological-Treatment: A Guide for Decision Makers Processes, Policies and Markets (Juniper Consultancy Services Ltd.)

16. R.C. Poller, Reclamation of waste plastics and rubber: recovery of materials and energy, J. Chem. Tech. Biotechnol. 30 1980 152–160. Ž . w x

17. W. Kaminsky, H. Roessler, Olefins from wastes, CHEMTECH 22 1992 108–113

18. Ganesh Thirugnanam. "Refuse Derived Fuel To Electricity". September 2013.

19. Mustafa Kara, "Environmental and economic advantages associated with the use of RDF in cement kilns, Resources, Conservation

and Recycling “, Volume 68,2012, Pages 21-28, ISSN 0921-3449, https://doi.org/10.1016/j.resconrec.2012.06.011.(https://www.sciencedirect.com/science/article/pii/S0921344912001097)

20. Kuen-Song Lin, H. Paul Wang, S.-H. Liu, Ni-Bin Chang, Y.-J. Huang, H.-C. Wang, “Pyrolysis kinetics of refuse-derived fuel”, Fuel Processing Technology 60 1999 103–110.

21. Thirugnanam, Ganesh & Prakasam, Vignesh. (2013). “Refuse Derived Fuel to Electricity”. International Journal of Engineering Research & Technology.

22. Ghosh, A., Debnath, B., Ghosh, S. K., Das, B., & Sarkar, J. P. (2018). Sustainability analysis of organic fraction of municipal solid waste conversion techniques for efficient resource recovery in India through case studies. *Journal of Material Cycles and Waste Management*, *20*, 1969-1985.

23. Mehta, A., & Rao, S. (2023). Sustainability challenges in pyrolysis and gasification: Environmental and economic implications. Journal of Waste Management and Sustainability, 14(2), 45-58. https://doi.org/10.1016/j.wms.2023.03.004

24. Reza, B., Soltani, A., Ruparathna, R., Sadiq, R., & Hewage, K. (2013). Environmental and economic aspects of production and utilization of RDF as alternative fuel in cement plants: A case study of Metro Vancouver Waste Management. *Resources, Conservation and Recycling*, *81*, 105-114.

25. Planning Comission Report (2014) Report of the task force on waste to energy (vol I) (in the context of integrated MSW management). Government of India. http://planningcommission.nic.in/reports/genrep/rep_wte1205.pdf. Accessed 11 May 2017

26. Sharma, P., Sheth, P. N., & Mohapatra, B. N. (2022). Recent progress in refuse derived fuel (RDF) co-processing in cement production: direct firing in kiln/calciner vs process integration of RDF gasification. *Waste and Biomass Valorization*, *13*(11), 4347-4374.

27. Ministry of housing and urban afairs Government of India: Guidelines on usage of refuse derived fuel in various industries (2018). pp. 13–14. http://cpheeo.gov.in/upload/5bda791e5afb3SBMRDFBook.pdf.

28. N. K. Gupta Central pollution control board: Guidelines for Pre-Processing and Co-Processing of Hazardous and Other Wastes in Cement Plant as per H&OW(M & TBM) Rules, 2016 2017. p. 1–34
29. Abbas, T.: Michalis Akritopoulos, Calciner challenges, in World cement. (2018).
30. Saxena, A., Chaturvedi, S., Ojha, P., Agarwal, S., Mittal, A.,Sharma, P., Ahamad, G., Mazumdar, R., Arora, V., Kalyani, K.Anupam, Singh, B., Kukreja, K., Ahmed, R., Bohra, A. Kaura,P.: Compendium The Cement Industry India. National council for cement and building materials, India. pp. 251–260 (2019)
31. Kumr S. and Verma R. (2021) Confederation of Indian industry: status paper on alternate fuel usage in Indian cement industry (2018). pp. 1–2. http://www.ciiwasteexchange.org/doc/afr2018.pdf.
32. Confederation of Indian Industry: Energy benchmarking for Indian cement industry (2019).
33. Sharma, P., Sheth, P. Mohapatra, B.N.: Waste to energy: issues,opportunities and challenges for RDF utilization in Indian cement industry. Proceedings of the 7th International Conference on Advances in Energy Research. pp. 891–900. Springer, Mumbai (2019). https://doi.org/10.1007/978-981-15-5955-6_84
34. Kukreja, K., Anupam, Sharma, P. Bhatnagar, S.: Handling of Multi type Alternative Fuels: A Challenge and

Opportunity for Cement Plant in 16th NCB International Seminar on Cement, Concrete and Building Materials. (2019): New Delhi
35. Kukreja, K., Mohapatra, B. N. Saxena, A.: Transfer chute design for solid alternative fuels. Indian cement review, May ed. (2019). 52–53.
36. ajamohan, R., Vinayagamurthi, K., Kumar, R.A.K.: Alternative fuel & raw material: our journey with in-house systems—a glimpse. In: 15th NCB International Seminar on Cement, Concrete and Building Materials (2017): New Delhi
37. Miskolczi, N., Buyong, F., Williams, P.T.: Thermogravimetric analysis and pyrolysis kinetic study of Malaysian refuse derived fuels. J. Energy Instit. 83, 125–132 (2010). https://doi.org/10.1179/014426010X12759937396632
38. Cozzani, V., Petarca, L., Tognotti, L.: Devolatilization and pyrolysis of refuse derived fuels: characterization and kinetic modelling by a thermogravimetric and calorimetric approach. Fuel 74,903–912 (1995). https://doi.org/10.1016/0016-2361(94)00018-M
39. Fang, D., He, F., Xie, J.: Pyrolysis characteristics and mechanism of hydrocarbon compounds for RDF. Fullerenes, Nanotubes and Carbon Nanostruct. 29, 13–20 (2021). https://doi.org/10.1080/1536383X.2020.1803287
40. Chen, X., Xie, J., Mei, S., He, F., Yang, H.: RDF pyrolysis by TG-FTIR and Py-GC/MS and combustion in a double furnaces reactor. J. Therm. Anal. Calorim. 136, 893–902 (2019). https://doi.org/10.1007/s10973-018-7694-9
41. Kusz, B., Kardaś, D., Heda, Ł, Trawiński, B.: Pyrolysis of RDF and catalytic decomposition of the produced tar in a char bed secondary reactor as an efcient source of syngas. Processes 10,90 (2022). https://doi.org/10.3390/pr10010090
42. Singh, A., & Patel, R. (2023). Challenges in RDF gasification: A case study of Pune's 10 MW plant. Journal of Renewable Energy Studies, 12(4), https://doi.org/10.5678/jrenenergystud.2023.004 energy, S.c.o.: Power generation from municipal solid waste.
43. Kumar, S., & Gupta, P. (2023). Enhancing TSR in cement plants through gasification technology: A strategic approach. Journal of Clean Energy Technologies, 11(3), https://doi.org/10.1016/j.jcet.2023.0301 IEA.:100 MT Coal Gasification Target by 2030—Policies.: https://www.iea.org/policies/12931-100-mt-coal-gasification-target-by-2030. Accessed 27 Aug 2021
44. Dr. M. M. Kutty India, G.o.: Five Year Vision Document 2019–2024 Group III—Resources.

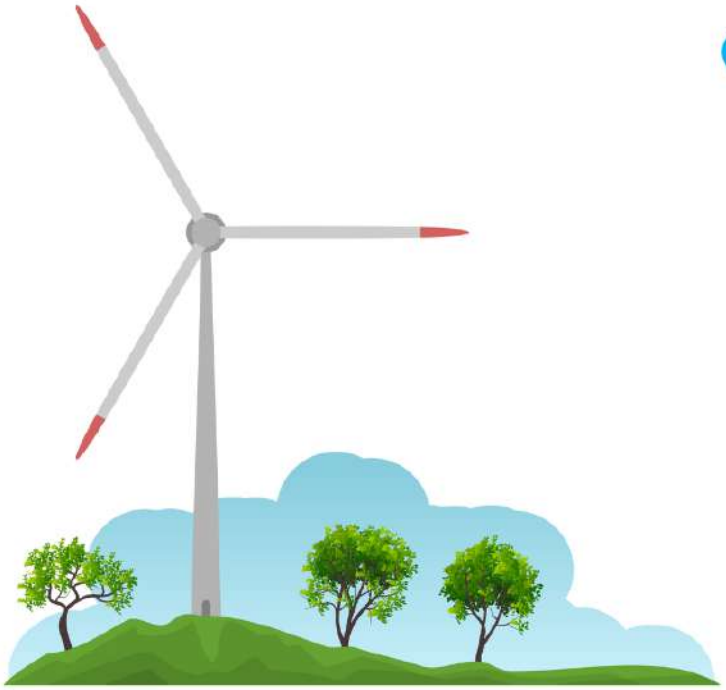

Published By:
Indian Institute of Chemical Engineers
Dr. H.L. Roy Building, Raja S.C. Mullick Road,
Jadavpur University Campus, Kolkata - 700032

Email: iichehq@iiche.org.in, chemcon2023@iiche.org.in
website: https://www.iiche.org.in/